Mixed Schur–Weyl duality in quantum information

Dmitry Andreevich Grinko

Mixed Schur–Weyl duality in quantum information

ILLC Dissertation Series DS-2025-02

Institute for Logic, Language and Computation

For further information about ILLC-publications, please contact

Institute for Logic, Language and Computation
Universiteit van Amsterdam
Science Park 107
1098 XG Amsterdam
phone: +31-20-525 6051
e-mail: illc@uva.nl
homepage: http://www.illc.uva.nl/

The research presented in this doctoral thesis was supported by Netherlands Organization for Scientific Research (NWO) through Vidi grant (Project No. VI.Vidi.192.10).

Printed and bound by Ipskamp Printing

ISBN: 978–94–6473–674–8

Mixed Schur-Weyl duality in quantum information

ACADEMISCH PROEFSCHRIFT

ter verkrijging van de graad van doctor
aan de Universiteit van Amsterdam
op gezag van de Rector Magnificus
prof. dr. ir. P.P.C.C. Verbeek
ten overstaan van een door het College voor Promoties ingestelde commissie,
in het openbaar te verdedigen in de Agnietenkapel
op maandag 3 februari 2025, te 14.00 uur

door Dmitry Andreevich Grinko
geboren te Sjachtarsk

Promotiecommissie

Promotor:	prof. dr. H.M. Buhrman	Universiteit van Amsterdam
Copromotor:	dr. M. Ozols	Universiteit van Amsterdam
Overige leden:	prof. dr. R. Renner	ETH Zürich
	prof. dr. M. Walter	Ruhr-Universität Bochum
	prof. dr. E.M. Opdam	Universiteit van Amsterdam
	dr. J. Zuiddam	Universiteit van Amsterdam
	prof. dr. R.M. de Wolf	Universiteit van Amsterdam

Faculteit der Natuurwetenschappen, Wiskunde en Informatica

to my family and teachers

List of publications

The results presented in this thesis are based on the following articles. Co-authorship in alphabetically ordered papers is shared equally. In papers [GBO23a] and [GBO23b], where authors are not listed alphabetically, the principal author appears first.

1. [GO22] Dmitry Grinko and Maris Ozols. "Linear programming with unitary-equivariant constraints". *Communications in Mathematical Physics* 405.12 (2024), p. 278. DOI: 10.1007/s00220-024-05108-1. arXiv: 2207.05713
   Contributed talks at TQC 2022, QIP 2023

2. [All+23] Rene Allerstorfer, Matthias Christandl, Dmitry Grinko, Ion Nechita, Maris Ozols, Denis Rochette, and Philip Verduyn Lunel. "Monogamy of highly symmetric states". *arXiv preprint* (2023). arXiv: 2309.16655
   Contributed talk at QIP 2024

3. [GBO23a] Dmitry Grinko, Adam Burchardt, and Maris Ozols. "Gelfand–Tsetlin basis for partially transposed permutations, with applications to quantum information". *arXiv preprint* (2023). arXiv: 2310.02252
   Contributed talk at QIP 2024

4. [GBO23b] Dmitry Grinko, Adam Burchardt, and Maris Ozols. "Efficient quantum circuits for port-based teleportation". *arXiv preprint* (2023). arXiv: 2312.03188
   Contributed talk at TQC 2024

The author has additionally co-authored the following articles, which are not included in this thesis.

1. [BGVW24] Harry Buhrman, Dmitry Grinko, Philip Verduyn Lunel, and Jordi Weggemans. "Permutation tests for quantum state identity". *arXiv preprint* (2024). arXiv: 2405.09626
   Contributed talk at TQC 2024

2. [GU24] Dmitry Grinko and Roope Uola. "On compatibility of binary qubit measurements". *arXiv preprint* (2024). arXiv: 2407.07711

3. [AGKH24] Mirko Arienzo, Dmitry Grinko, Martin Kliesch, and Markus Heinrich. "Bosonic randomized benchmarking with passive transformations". *arXiv preprint* (2024). arXiv: 2408.11111

4. [SGSV24] Eddie Schoute, Dmitry Grinko, Yiğit Subaşı, and Tyler Volkoff. "Quantum programmable reflections". *arXiv preprint* (2024). arXiv: 2411.03648

Contents

Acknowledgments

First and foremost, I would like to express my deepest gratitude to my supervisor, Māris Ozols. I am incredibly fortunate to have been your PhD student. You are the ideal combination of a scientist, organiser, and mentor. I truly appreciate the countless hours we spent tackling problems together. Those moments were immensely productive for my growth as a researcher, and I am profoundly grateful for them. I appreciate your patience, guidance, and support throughout my PhD journey. Your encouragement was particularly invaluable during the challenging times of the COVID-19 pandemic and the war in Ukraine, especially in my homeland, Donbass. I would also like to sincerely thank my co-supervisor, Harry Buhrman, for your support during difficult times, advice, and insightful discussions.

I am deeply honoured to have such an esteemed committee. I thank Eric Opdam, Renato Renner, Michael Walter, Ronald de Wolf, and Jeroen Zuiddam for agreeing to serve on my committee, carefully reading my thesis, and providing feedback.

My PhD journey would not have been possible without my exceptional co-authors: Adam Burchardt, Denis Rochette, Eddie Schoute, Harry Buhrman, Ion Nechita, Jordi Weggemans, Marcus Heinrich, Martin Kliesch, Matthias Christandl, Māris Ozols, Mirko Arienzo, Philip Verduyn Lunel, René Allerstorfer, Roope Uola, Tyler Volkoff, and Yiğit Subaşı. It is a privilege to have each of you as part of my academic journey.

I would especially like to acknowledge Adam Burchardt, Denis Rochette, Philip Verduyn Lunel, René Allerstorfer, and Jordi Weggemans for the enjoyable and productive problem-solving sessions we had. Thanks go to Marcus Heinrich for inviting me to collaborate on bosonic randomised benchmarking. Moreover, I was fortunate to participate in the Los Alamos Summer School, where I had the pleasure of working with Yiğit Subaşı, Eddie Schoute, and Tyler Volkoff. I am also grateful to Sam Slezak and Touheed Anwar Atif for our engaging discussions, and to the school's organisers, Marco Cerezo and Lukasz Cincio, for making my participation possible.

Many thanks to Matthias Christandl, Ion Nechita, Michał Studziński, and Mio Murao for their kind invitations and for organising my academic visits. Each of these visits was not only highly productive but also genuinely memorable.

Special thanks to Tudor Giurgica-Tiron for our inspiring discussions—I have learned a lot from you. I would also like to express my sincere gratitude to my amazing collaborators with whom I am working on other projects not mentioned in this thesis: Adrián Solymos, Amira Abbas, Chaithanya Rayudu, Cunlu Zhou, Francesco Anna Mele, Francisco Escudero Gutiérrez, Jiani Fei, Jun Takahashi, Kevin Thompson, Ludovico Lami, Marek Mozrzymas, Martin Larroca, Michał Studziński, Michał Horodecki, Mio Murao, Nunzia Cerrato, Ojas Parekh, Piotr Kopszak, Satoshi Yoshida, Sydney Timmerman, Tomasz Młynik, Vladyslav Visnevskyi, Vojtěch Havlíček, and Zoltán Zimborás.

I thank my paranymphs, Adam Burchardt and Philip Verduyn Lunel. Adam, you are an

exceptional friend and companion in tackling scientific challenges, and I have learned so much from your problem-solving approach and expertise. Your support and scientific partnership have been truly invaluable. Philip, thank you very much for your friendship, for our joint work, guidance in navigating life in the Netherlands, and for bringing laughter and positivity along the way.

I would also like to thank my long-term officemates René, Quinten, Mani, and Philip. Sharing an office with all of you has been a great pleasure. Thank you, Sebas and Joran, for the enjoyable skiing trip we shared. Additionally, special thanks to Sebas for your friendship, for your help on various occasions, and for always creating a positive atmosphere.

Moreover, I appreciate and cherish the fantastic community at QuSoft. Warm thanks to all QuSofters, including Adam Burchardt, Ailsa Robertson, Akshay Ramachandran, Ake Köhne, Amira Abbas, Anna Luchnikova, Arghavan Safavi-Naini, Arie Soeteman, Arjan Cornelissen, Chris Cade, Christian Schaffner, Daan Planken, Davi Castro-Silva, Filippo Girardi, Florian Speelman, Francisco Escudero Gutiérrez, Freek Witteveen, Galina Pass, Garazi Muguruza Lasa, Gina Muuss, Harold Nieuwboer, Harry Buhrman, Ido Niesen, Jana Sotáková, Jelena Mackeprang, Jeroen Zuiddam, Jiri Minar, John van de Wetering, Jonas Helsen, Jordi Weggemans, Jop Briet, Joppe Stokvis, Joran van Apeldoorn, Junqiao Lin, Kareljan Schoutens, Koen Groenland, Koen Leijnse, Krystal Guo, Léo Colisson, Llorenç Escolà Farràs, Lorenzo Grevink, Luca D'Alessandro, Ludovico Lami, Lynn Engelberts, Marc Farreras Bartra, Manideep Mamindlapally, Māris Ozols, Marten Folkertsma, Maxim van den Berg, Mehrdad Tahmasbi, Michael Walter, Niels Neumann, Nikhil Mande, Peter van der Gulik, Philip Verduyn Lunel, Poojith Umesh Rao, Quinten Tupker, René Allerstorfer, Ronald de Wolf, Salvatore Tirone, Sarah Meng Li, Sebastian Zur, Sebastiaan Verschoor, Seenivasan Hariharan, Simona Etinski, Stacey Jeffrey, Subhasree Patro, Tony Gómez Pérez, Victor Land, Yanlin Chen, Yaroslav Herasymenko, and Zongbo Bao. Thank you all for creating such a welcoming environment—I could not have asked for better colleagues.

My sincere thanks also go to QuSoft directors—Harry Buhrman, Kareljan Schoutens, and Christian Schaffner—for their excellent leadership and for fostering a relaxed yet highly productive research environment. QuSoft is truly a unique and inspiring place, and I feel privileged to be a part of it. I am also grateful for the administrative support by Peter van Ormondt and Ewout Arends from ILLC, as well as Doutzen Amba, Susanne van Dam, and Carla van Asperen from CWI.

Besides QuSoft, I would like to express my gratitude for the brief yet fruitful discussions I have had on various occasions with Adam Wills, Antonio Anna Mele, Aram Harrow, Chi-Fang Chen, Eunou Lee, Faedi Loulidi, Felix Huber, Giulio Chiribella, Hari Krovi, Jordan Docter, Jürg Fröhlich, Libor Caha, Marco Túlio Quintino, Michał Oszmaniec, Michael Ragone, Min-Hsiu Hsieh, Nicolas Brunner, Nicolas Gisin, Paweł Horodecki, Pavel Sekatski, Quynh Nguyen, Robert König, Sadra Boreiri, Sang-Jun Park, Sergey Bravyi, Sergii Strelchuk, Steven Flammia, Tatsuki Odake, and Wataru Yokojima.

In the final months of my PhD, I had the opportunity to undertake an internship at Phasecraft. I am sincerely grateful to the team for this unique and enriching experience. I particularly thank Raul Santos, Laura Clinton, Charles Derby, and Filippo Gambetta for their collaboration. It was a pleasure to work alongside and engage in discussions with Max Hunter Gordon, Marcos Crichigno, Ieva Čepaitė, Lana Mineh, Jan Lukas Bosse, Joel Klassen, Toby Cubitt, Ashley Montanaro, and other members of the team.

As the saying goes, "It takes a village to raise a child", and I cannot finish without mentioning people who helped me grow as a scientist before my PhD journey. Among the most significant influences in my life are the people who inspired my passion for science: my school teachers. I extend my deepest gratitude to Alexander Nikolaevich Zhukov, who introduced me to the beauty of physics and the art of scientific reasoning. I am equally thankful to Tatiana

Vladimirovna Sokolova for fostering my mathematical mindset, and to Grigory Alexandrovich Ivanov and Dmitry Anatolyevich Alexandrov for their mentorship and for teaching me how to tackle complex problems. Dear teachers, this thesis is dedicated to you.

Next, I wish to thank my university professors who inspired me and my mentors who guided me throughout my bachelor's and master's studies in Moscow, Zurich, and Geneva: Oleg Alexandrovich Sudakov, Dmitry Arkadyevich Pritykin, Roman Viktorovich Konstantinov, Elena Evgenyevna Nokhrina, Alexander Semenovich Holevo, Lídia del Rio, Renato Renner, Gianni Blatter, Gian Michele Graf, Will Merry, Anton Yurevich Alexeev, and Stanislav Konstantinovich Smirnov. I especially thank Lídia del Rio and Anton Yurevich Alexeev for their support during challenging times.

I thank my friends, whom I am fortunate to have in my life: Gleb Poshin, Mikhail Karasikov, Anton Permenev, Polina Shichkova, Vlad Dyachenko, Sasha Eroshenko, Ilya Gukov, Slava Matunin, Aleksey Surdyaev, David Aznaurov, Sasha Sherbina, Aleksey Oskolkov, Igor Sokolov, Benjamin Strittmatter, Nikita Astrakhantsev, Anna Efimova, Alberto Rolandi, Aleksey Lunkin, Javid Javadzade, Albina Galiullina, Airat Galiullin, Ivan Kulesh, Natalia Nudga, and many more.

Finally, and most importantly, I dedicate this thesis to my family. The love and support of my parents, Oxana and Andrey; my brother, Kirill; my grandparents, Vera and Dmitry, and Valentina and Mikhail; and my uncle, Andrey, have profoundly shaped who I am today. Special thanks to my parents, particularly my mother, Oxana, for their unwavering love, effort, and constant encouragement—without you, this PhD thesis would not have been possible.

I dedicate this work especially to my dear wife, Ira. Your love, care, and incredible sense of humour are a continuous source of warmth, comfort, and inspiration for me. Meeting you five years ago, avoiding the two-body problem and walking this journey together have been my greatest fortune.

Amsterdam — Dmitry Grinko
December, 2024

Chapter 1

Introduction

> The Universe is an enormous direct product of representations of symmetry groups.
>
> *Steven Weinberg*

Symmetry plays a fundamental role in mathematics and physics. For example, in classical mechanics, thanks to Noether's theorem, symmetry is responsible for conservation laws. At the same time, symmetry is also the focus of a major area of mathematics—representation theory, whose applications range from physics to biology, chemistry and the arts. "Symmetry argument" is a common problem solving technique both in physics and mathematics: observing the symmetries inherent to a problem often allows simplifying the problem. In the absence of symmetry, difficult problems can often be made more tractable by assuming some form of symmetry. Generally speaking, the more symmetry a problem has the more tractable it is.

Quantum mechanics, formally established in 1925 with Werner Heisenberg's breakthrough article [Hei25], has transformed our fundamental understanding of nature and led to new technologies. As quantum theory approaches its 100th anniversary, it continues to pose significant scientific challenges. In particular, questions regarding the quantum nature of information and the computational foundations of quantum theory were largely overlooked during the field's early development. However, the current computation and information era naturally led people to ask questions about the nature of quantum information. Interest in quantum information theory has surged since the late 1980s, and with the discovery of Shor's algorithm in 1995, interest in quantum computing exploded. Today, quantum information and quantum computing are thriving research areas, with many open questions that demand more developed mathematical tools.

On the mathematical side, representation theory has played a crucial role in the development of quantum mechanics throughout the 20th century, particularly in the study of symmetries, conservation laws, and the classification of quantum systems. Its ability to reveal hidden structures has had profound impacts, from understanding atomic spectra to the formulation of the Standard Model. The broad goal of this thesis is to extend representation-theoretic techniques to quantum information and computation. More concretely, we study in detail and apply a certain generalisation of an important representation-theoretic tool, Schur–Weyl duality, to a broader setting that naturally arises in quantum information theory.

Schur–Weyl duality

The unitary group of symmetries plays a special role in the context of quantum mechanics and quantum information, and, for systems consisting of many identical parts, the unitary symmetry becomes intertwined with permutational symmetry. This intimate connection between unitary and permutation groups acting on several identical quantum systems is expressed via the so-called *Schur–Weyl duality*. In its simplest form, it states that the two-qubit *singlet state* $|\psi^-\rangle := (|01\rangle - |10\rangle)/\sqrt{2}$ is the unique (up to a global phase) state that is invariant under identical local unitary rotations: $(U \otimes U)|\psi^-\rangle = \det(U)|\psi^-\rangle$ for any $U \in \mathrm{U}_2$, as well as the unique anti-symmetric state: $\mathrm{SWAP}|\psi^-\rangle = -|\psi^-\rangle$. A similar dual characterisation in terms of unitary and permutational symmetries applies not only to $|\psi^-\rangle$ but also its orthogonal complement, allowing to decompose the whole two-qubit space $\mathbb{C}^2 \otimes \mathbb{C}^2$ into invariant subspaces. This duality extends also to $(\mathbb{C}^d)^{\otimes n}$ where each of the n systems has dimension d.

More formally, Schur–Weyl duality states that unitary and permutation actions are mutual centralisers within the algebra of linear transformations on $(\mathbb{C}^d)^{\otimes n}$. This means that the algebra generated by the action of U_d is the commutant of the permutation action of S_n, and vice versa. This duality provides a powerful tool for understanding the representation theory of both groups and has numerous applications in various branches of mathematics and physics.

A natural situation where Schur–Weyl duality arises in quantum information is when dealing with many copies of some quantum state ρ. The total state $\rho^{\otimes n}$ is then invariant under permutations and transforms in a straightforward way under simultaneous unitary basis change on each of the n systems. This scenario is very common in quantum information theory where Schur–Weyl duality has become an important tool [Har05; Bot16]. It has also found numerous applications in the design and analysis of quantum algorithms where weak Schur sampling [CHW07] and quantum Schur transform [Har05; BCH06; KS18; Kro19] play an important role [Wri16]. Specific quantum algorithmic tasks where Schur–Weyl duality is used include quantum spectrum [KW01a] and entropy [AISW20] estimation, quantum spectrum testing [OW15], state tomography [Key06; HHJWY17; OW16; OW17], and quantum majority vote [BLMMO22].

Mixed Schur–Weyl duality

The classic Schur–Weyl duality admits various generalisations [Ber12; MS14; Ben96; Ben+94; Dot08]. We are particularly interested in the setting referred to as *mixed Schur–Weyl duality*. In this setting, we consider the action $U^{\otimes n} \otimes \bar{U}^{\otimes m}$ on the space $(\mathbb{C}^d)^{\otimes n+m}$. The $(n+m)$-tensors in this space are called *mixed*[1] because they have two types of indices: some are acted upon by U while others by $\bar{U}$ [Hal96; Nik07]. The commutant of this action is known as *walled Brauer algebra* and the concrete matrix representation of it on $(\mathbb{C}^d)^{\otimes n+m}$ is called *partially transposed permutation matrix algebra*. The regular Schur–Weyl duality is then the special case when either $n = 0$ or $m = 0$. We are interested in the general case of arbitrary n, m and local dimension d.

The most common scenario is when either $n = 1$ or $m = 1$. Such symmetry naturally occurs in many quantum tasks with a single input or a single output system, such as asymmetric quantum cloning [Cer00; NPR21; NPR23], port-based teleportation [IH08; MSSH18; SSMH17; Led22; Chr+21; SMK22; SS23b; FTH23; WHS23], quantum majority vote [BLMMO22], or U_d-covariant quantum error correction [KL21; KL22]. It also occurs in situations that involve a partial transpose on a single system, such as in entanglement detection [EW01; COS18; Hub21].

[1] This has nothing to do with the notion of mixed states in quantum mechanics.

Group equivariance

Another place where mixed Schur–Weyl duality appears is in studies of quantum transformations of states that preserve symmetry. Such quantum transformations are called *quantum channels*. A quantum channel Φ is called *G-covariant*, for some group G, if there exist two unitary representations of G, ϕ_{in} and ϕ_{out}, such that $\Phi\big(\phi_{\text{in}}(g)\,\rho\,\phi_{\text{in}}(g)^\dagger\big) = \phi_{\text{out}}(g)\,\Phi(\rho)\,\phi_{\text{out}}(g)^\dagger$, for any group element $g \in G$ and state ρ. The structure of group-covariant quantum channels can be much simpler than the structure of general channels [MSD17]. For example, while perfect universal programming of general quantum channels is impossible [NC97], covariant channels can be programmed [GBW21], even in infinite dimensions [GW21]. Group covariance is important in many contexts. Let us briefly illustrate two that are less obvious: quantum error correction and machine learning.

Group covariance is particularly important in the context of quantum error correction and fault tolerance. Many quantum error correcting codes are covariant with respect to the Clifford group and thus allow for simple or so-called "transversal" implementation of Clifford gates. An even higher degree of symmetry, namely possessing a universal set of transversal gates, would be ideal for devising schemes that can manipulate encoded quantum data. However, codes with such continuous symmetries are ruled out by the well-known Eastin–Knill theorem [EK09]. The interplay between continuous symmetries and quantum error correction has received revived attention in the context of holography and quantum gravity, where an approximate version of the Eastin–Knill theorem was recently established [Fai+20]. Group-covariant quantum codes with continuous symmetries are also closely related to the notion of quantum reference frames [HNPS21; YMRCW22].

A special case of group covariance is *equivariance*, which means that the representations ϕ_{in} and ϕ_{out} are either identical or related to each other in some simple way. Intuitively, equivariance says that applying some transformation on the input is equivalent to applying the same transformation on the output. This is a natural condition that occurs in many contexts. For example, in machine learning, the structure of neural networks should respect the symmetries of the problem at hand, such as translations and rotations when dealing with images. Such group-equivariant neural networks can have substantially increased expressive capacity without the need to increase their number of parameters [Coh21; CW16; BBCV21]. In particular, unitary-equivariant neural networks that capture the symmetries of many-body quantum systems have recently found applications in quantum chemistry [Qia+22]. More generally, coordinate-independent convolutional networks on Riemannian manifolds require equivariance under local gauge transformations [WFVW21].

In quantum machine learning, group-equivariant convolutional quantum circuits have been proposed to speed up learning of quantum states [ZLLSK23]. In general, equivariant gatesets can be used to exploit symmetry in variational quantum algorithms [Mey+23]. A general framework for group-invariant and equivariant quantum machine learning was recently outlined in [Lar+22].

A particularly natural special case of group covariance is *local unitary equivariance*, which corresponds to the case when Φ is a quantum channel from n to m systems, each of dimension d, the symmetry group G is the full unitary group U_d, and the two unitary representations are given by $\phi_{\text{in}}(U) := U^{\otimes n}$ and $\phi_{\text{out}}(U) := U^{\otimes m}$. In other words, applying the same unitary $U \in \mathrm{U}_d$ on each of the n input systems of Φ is equivalent to applying U on each of the m output systems. This is precisely the setting of mixed Schur–Weyl duality.

Symmetries with general values of $n > 1$ and $m > 1$ correspond to scenarios with multiple input and output systems [Key02, Section 7], such as quantum state purification [KW01b] and cloning [SIGA05; Fan+14], multiport-based teleportation [KMSH21; SMKH22; MSK21]. Such symmetries also occur in situations that involve the partial transpose on several systems, such as the extendability problem [JV13; JSZ22], entanglement detection [BCS20; BSH24], or

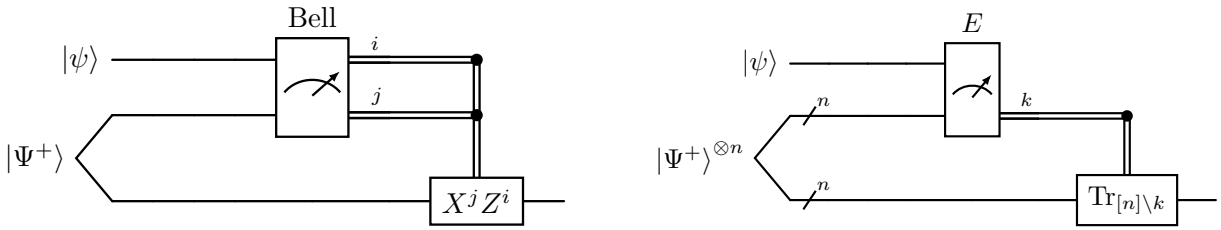

Figure 1.1: Standard teleportation (left) and port-based teleportation (right) represented as quantum circuits. In standard teleportation Alice has a qubit state $|\psi\rangle$ and one half of the maximally entangled state $|\Psi^+\rangle$; the other half is with Bob. Alice performs a Bell measurement on her qubits and sends the two outcome bits i, j to Bob. Bob then performs a correction operation by applying a product of Pauli unitaries X^jZ^i. In port-based teleportation, Bob shares with Alice n copies of the $|\Psi^+\rangle$ state. Alice performs a joint measurement E on all her qubits and obtains an outcome $k \in [n]$. Upon receiving the measurement outcome k from Alice, Bob simply discards (or "traces out") all systems except for the k-th one (this is denoted by $\mathrm{Tr}_{[n]\setminus k}$), where the teleported state is to be found without the need for any correction operations.

universality of qudit gate sets [SMZ22; DS23; SS23a]. Universality of quantum circuits with two-local U_d-equivariant gates has recently been considered in [Mar22; HLM21; MLH24] from the perspective of conservation laws. Finally, this class of symmetries is also of independent interest in high-energy physics [KR07; Can11] and the study of quantum spin systems [Rya21; BRR23].

Port-based teleportation

One of the examples mentioned above where mixed Schur–Weyl duality appears is *port-based teleportation* (PBT). Before we describe port-based teleportation, let us remind the standard teleportation protocol.

Quantum teleportation is a fundamental protocol within quantum information theory, allowing an unknown quantum state to be transferred between parties without the state's physical transmission. First proposed by Bennett et al. in 1993 [Ben+93], the classic protocol involves Alice and Bob, who share an entangled qubit pair. Alice then performs a joint Bell-state measurement on her qubit and the qubit she wishes to teleport. After that, she sends the outcome to Bob through a classical communication channel. Based on the information provided by Alice, Bob applies a specific unitary operation to his qubit to reconstruct the original quantum state, see Fig. 1.1.

Port-based teleportation (PBT) is an interesting variant of teleportation that was proposed by Ishizaka and Hiroshima in 2008 [IH08]. PBT eliminates the need for Bob to perform any corrective operations after receiving Alice's classical message. Instead, Alice and Bob share multiple entangled qubit pairs, known as "ports". Alice performs a measurement that entangles her input state with all her qubits and then sends the measurement result to Bob. Bob, upon receiving this information, selects one of his qubits from the entangled ports as the teleported state without needing to apply any further transformations, see Fig. 1.1.

A downside of PBT is that the teleportation implemented in this way cannot be perfect, while standard teleportation achieves perfect transmission of the state. PBT also requires much more entanglement resources compared to the standard protocol. However, as the amount of shared entanglement grows, the quality of PBT improves and becomes arbitrarily close to perfect. PBT offers a solution for teleportation in situations where performing conditional operations is impractical or when a "correction-free" teleportation is desired. Such situation arises in the study of non-local quantum computations and a quantum cryptographic primitive

called quantum position verification.

The theoretical underpinnings of port-based teleportation are closely connected to the mixed Schur–Weyl duality. However, efficient construction of quantum circuits for this task was a long-standing open problem. That is why the tools we developed for mixed Schur–Weyl duality enabled us to make progress on construction of efficient quantum algorithms for PBT.

1.1 Summary of the results

This thesis makes several contributions to the understanding and application of mixed Schur–Weyl duality in quantum information and quantum computing. Our main contributions are as follows.

1. We find an explicit action of the generators of the matrix algebra of partially transposed permutations in the Gelfand–Tsetlin basis of all irreducible representations, see Theorem 3.7.1. This algebra appears naturally in the context of mixed Schur–Weyl duality, and explicit knowledge of its action is crucial for applications in quantum information and computing.

2. We adapt existing constructions of primitive and primitive central idempotents to the matrix algebra of partially transposed permutations in Section 3.6. Our main technical result here is Theorem 3.6.6, which adapts Jucys–Murphy elements of the walled Brauer algebra to the matrix algebra of partially transposed permutations.

3. We introduce and develop an efficient quantum circuit for the mixed quantum Schur transform in Theorem 4.3.1. Mixed quantum Schur transform is a key element to allow applications of mixed Schur–Weyl duality in quantum computing. The main new ingredient of the mixed quantum Schur transform is the dual Clebsch–Gordan transform, which we implement as a quantum circuit in Theorem 4.4.1.

4. We construct efficient quantum algorithms for port-based teleportation in Theorem 5.1.1, thus solving a long-standing open problem. The key idea is the realisation of the Naimark dilation theorem in the Hilbert space comprised of paths of the Bratteli diagram of the matrix algebra of partially transposed permutations, see Section 5.3.

5. We apply mixed Schur–Weyl duality to symmetry reduction of certain semidefinite optimisation problems. We show that a class of SDPs with unitary equivariance symmetry can be reduced to linear programs whose size does not depend on the local dimension d, see Theorem 6.3.4. As a step towards generalisation of this result, we also describe in Section 6.4 how a certain class of SDPs can be simplified without additional symmetry assumptions, see Theorem 6.4.2.

6. As an application of our symmetry reduction framework, we show how to simplify different SDPs with unitary equivariance symmetry, allowing new insights into previously unsolved problems, such as transposition of unknown unitaries (see Section 6.5.4).

7. We study the monogamy of entanglement for quantum states respecting unitary, mixed unitary, and orthogonal symmetries, obtaining new results on the extendibility of these states, see Theorem 7.1.1. In particular, we obtain the full extendibility region for qubit Brauer states, see Theorem 7.1.2

These contributions advance the understanding of mixed Schur–Weyl duality and its applications in quantum information and computing and have implications for the design and analysis of quantum algorithms and protocols involving unitary symmetries. We now provide an overview of the chapters.

1.2 Overview of the thesis

Chapter 2 sets the stage by introducing the notation, the basics of quantum information, semidefinite programming, and the representation theory of groups and algebras. We describe the basics of the module-theoretic language and introduce the key notions of Gelfand–Tsetlin bases and Bratteli diagrams. We also introduce the basics of the representation theory of symmetric groups, and unitary and general linear groups. This chapter describes the fundamentals of Schur–Weyl duality, which serves as a basis for our generalisation in the next chapter.

Chapter 3 describes the representation theory of the partially transposed permutation matrix algebra and introduces the mixed Schur–Weyl duality, which is a generalisation of Schur–Weyl duality. Our main result in this chapter is the explicit formula for the action of the partially transposed permutation matrix algebra generators in the Gelfand–Tsetlin basis. This result extends the Gelfand–Tsetlin basis for the symmetric group, also known as the Young–Yamanouchi basis. The chapter also includes the construction of primitive and primitive central idempotents in this basis. Overall, this chapter is central to the whole thesis, building a foundation for the next chapters.

Chapter 4 constructs quantum circuits for the mixed Schur transform by using Clebsch–Gordan transforms as the main building block. Quantum mixed Schur transform is a new primitive in quantum information, which did not exist before our work [GBO23a] and an independent work [Ngu23], which constructs the same quantum circuits. Thus, our work fills an important gap in the literature. We present two different encodings of the Gelfand–Tsetlin basis, which we call "standard" and "Yamanouchi". The first encoding is less space-efficient but provides a more convenient possibility to implement more complicated unitary operations, while the second encoding is more space-efficient but may not be optimal for implementing certain quantum operations. We hope that our work will allow for a deeper understanding of previously unsolved problems and will find a range of new applications within quantum information theory. One example of such an application is port-based teleportation, which we describe in the next chapter.

Chapter 5 presents efficient quantum algorithms for all port-based teleportation protocols, thus solving a long-standing open problem. Building on previous chapters that study mixed Schur transform and partially transposed permutation matrix algebras, this chapter presents efficient quantum algorithms for both probabilistic and deterministic PBT protocols. Two encoding schemes are used: one with $\widetilde{O}(n)$ time complexity and $\widetilde{O}(n)$ space complexity, and another with $\widetilde{O}(n^2)$ time complexity but reduced $\widetilde{O}(1)$ space complexity for constant local dimension and precision. It also includes the construction of efficient circuits for preparing optimal resource states for probabilistic PBT. Overall, this chapter presents the culmination of years of research into PBT, achieving significant advancement in the field of quantum information by providing the first known efficient algorithms for this teleportation method. By closing this long-standing gap, we pave the way towards practical implementation of PBT protocols.

Chapter 6 discusses unitary-equivariant linear and semidefinite programming. This chapter provides a general framework to reduce unitary-equivariant SDP problems into simpler ones and, by leveraging additional symmetry assumptions, transforming them into much simpler linear programs that can be solved more efficiently. The reduction process is made possible by using results from mixed Schur–Weyl duality and a compact parameterisation of the solution space via walled Brauer algebra diagrams. The chapter illustrates practical applications of this framework in quantum information theory, including tasks like determining the principal eigenvalue of a quantum state, quantum majority vote, asymmetric cloning, and transposition of a black-box unitary. Overall, this chapter presents a powerful method for solving a large class of optimisation problems in quantum information and beyond, offering both theoretical insights and practical tools for reducing the complexity of semidefinite programs.

Chapter 7 focuses on a fundamental notion in quantum information theory—monogamy of entanglement. Monogamy limits the degree to which different particles may share entanglement with each other. This chapter studies a particular aspect of monogamy called "extendibility" for highly symmetric quantum states on the complete graph. We go beyond the original mixed Schur–Weyl duality and explore applications of the full Brauer algebra in our setting. The Brauer algebra is larger than the walled Brauer algebra and appears in the Schur–Weyl duality for the orthogonal groups. This chapter explores the extendibility problem for three classes of symmetric quantum states: Werner, isotropic, and Brauer states. For each class, we determine the amount of bipartite entanglement that a global state can possess if all its two-party marginals are identical and belong to the given class. We address this question by formulating the problem as a semidefinite program (SDP), which we solve using tools from representation theory and SDP duality. One of the key contributions of this chapter is the derivation of the exact maximum values for projections onto the maximally entangled state and the antisymmetric Werner state. This chapter also introduces the notion of G-extendibility for symmetric states, generalising previous results in the area of quantum state extendibility.

Chapter 2

Preliminaries

Representation theory is a branch of mathematics that studies abstract algebraic structures by representing their elements as linear transformations of vector spaces. This approach allows us to study complicated abstract algebraic objects within the context of easy-to-understand linear algebra, providing deep insights into their structure.

This chapter summarises the basics of the representation theory of finite groups and associative algebras. The aim here is to present the necessary representation-theoretic facts concisely and introduce relevant notions needed for further chapters. We assume knowledge of standard definitions such as groups, algebras, and knowledge of linear algebra, complex analysis, basic topology and differential geometry.

We start this chapter by introducing the notation, basics of quantum information theory and semidefinite programming, which we will use throughout this thesis.

We base our exposition on the following books on quantum information [NC10; Wat18] and representation theory [FH91; GW98; Sag13; Eti+11; CR62; DK12; VK92; Kir08].

2.1 Notation

In this thesis, we consider only finite-dimensional complex Hilbert spaces $\mathcal{H} \cong \mathbb{C}^d$, where d is the dimension of the space. Most of the time, we only need a vector space structure of a Hilbert space, so we refer to $\mathcal{H}$ simply as $\mathbb{C}^d$. We will often use the abbreviation $[d] := \{1, \ldots, d\}$.

The set of all $\mathbb{K}$-linear maps between two vector spaces V, W over field $\mathbb{K}$ is denoted by $\mathrm{Hom}_{\mathbb{K}}(V, W)$, and if $W = V$, we speak of the set of *endomorphisms* $\mathrm{End}_{\mathbb{K}}(V) := \mathrm{Hom}_{\mathbb{K}}(V, V)$. This notation is mostly used to highlight the underlying field. In this thesis, we mostly consider the field $\mathbb{K} = \mathbb{C}$. Therefore we usually drop the subscript and simply write $\mathrm{End}(V) \equiv \mathrm{End}_{\mathbb{C}}(V)$ and $\mathrm{Hom}(V, W) \equiv \mathrm{Hom}_{\mathbb{C}}(V, W)$. $\mathrm{End}(V)$ is a space of linear transformations of V. Equivalently, $\mathrm{End}(\mathbb{C}^d)$ denotes the set of all complex $d \times d$ matrices.

We denote by U_d all *unitary* matrices on $\mathbb{C}^d$, i.e., all $U \in \mathrm{End}(\mathbb{C}^d)$ such that $U^\dagger U = I$, where I is the identity matrix on $\mathbb{C}^d$. A complex $d \times d$ matrix H is *Hermitian* if $H^\dagger = H$, where $H^\dagger := \bar{H}^\mathsf{T}$ is the *conjugate transpose* of H. The collection of all Hermitian matrices acting on $\mathcal{H}$ is denoted by $\mathrm{Herm}(\mathcal{H})$. For a Hermitian matrix $H \in \mathrm{Herm}(\mathcal{H})$, we use the notation $H \succeq 0$ to indicate that H is *positive semidefinite*, i.e. $\langle\psi|H|\psi\rangle \geqslant 0$ for all $|\psi\rangle \in \mathcal{H}$. A Hermitian matrix $\Pi \succeq 0$ is a *projector* if $\Pi^2 = \Pi$.

To discuss the complexity of classical and quantum algorithms the *big-O* notation is often used. If $f(n)$ and $g(n)$ are functions defined for large values of n, writing $f(n) = O(g(n))$ is formally equivalent to $\exists\, C > 0$, $n_0 \geqslant 0$ such that $f(n) \leqslant Cg(n)$ for all $n \geqslant n_0$. We also often use the notation $\mathrm{poly}(n)$ and $\mathrm{polylog}(n)$ to mean $\mathrm{poly}(n) = O(n^k)$ and $\mathrm{polylog}(n) = O(\log^k n)$ for some constant $k \geqslant 0$, respectively. Moreover, we also use *soft-O* notation $\widetilde{O}(f(n))$ to mean $\widetilde{O}(f(n)) :=$

$O(f(n)\log^k f(n))$ for some constant $k \geqslant 0$. Occasionally, we can also hide polylog dependence of some additionally specified parameters into $\widetilde{O}$, slightly abusing this notation. Finally, we sometimes use $f(n)\operatorname{polylog} g(n,m,\dots)$ as abbreviation for $O(f(n)\operatorname{polylog} g(n,m,\dots))$ for brevity and for highlighting which parameters appear inside the logarithm.

2.2 Quantum information

In this section, we review basic notions and concepts of quantum information, which we need throughout the thesis. For more background on quantum information theory see [NC10; Wat18].

Quantum states

In quantum theory, the state of a physical system is described by a vector in a complex Hilbert space $\mathcal{H}$. *Pure quantum states* are unit vectors $|\psi\rangle \in \mathcal{H}$, where the unit norm condition is $\|\psi\| = \langle\psi|\psi\rangle = 1$. For several physical systems, their combined state space is described by the *tensor product* of their Hilbert spaces, e.g., $\mathcal{H}_1 \otimes \mathcal{H}_2$.

More generally, in quantum information, a quantum state can be described by a *density matrix* ρ, which is a positive semidefinite operator on $\mathcal{H}$ with trace $\operatorname{Tr}(\rho) = 1$. Density matrices describe *mixed states*, which formalise a physical intuition about classical uncertainty in preparing pure states, or, in other words, they correspond to probabilistic mixtures of pure states. The density matrix of a pure state $|\psi\rangle$ is $\rho = |\psi\rangle\langle\psi|$. For a mixed state, $\rho = \sum_i p_i|\psi_i\rangle\langle\psi_i|$, where $\{|\psi_i\rangle\}_i$ are pure states and $\{p_i\}$ are probabilities with $p_i \geqslant 0$ and $\sum_i p_i = 1$. We denote by $\mathrm{D}(\mathcal{H})$ the set of all density matrices on $\mathcal{H}$.

Evolution of states

The evolution of a closed quantum system is described by unitary operators. This unitary evolution of density matrices is given by $\rho \mapsto U\rho U^\dagger$. However, unitary evolution is a mathematical idealisation. Interactions with an external environment lead to transformations of quantum states that cannot be described solely by unitary operators. Therefore, in quantum information, the most general form of evolution is given by the notion of *quantum channel*. Let $\mathcal{H}_{\mathrm{in}} := \mathbb{C}^{d_{\mathrm{in}}}$ and $\mathcal{H}_{\mathrm{out}} := \mathbb{C}^{d_{\mathrm{out}}}$ be finite-dimensional complex Hilbert spaces. A *quantum channel* $\Phi\colon \operatorname{End}(\mathcal{H}_{\mathrm{in}}) \to \operatorname{End}(\mathcal{H}_{\mathrm{out}})$ is a completely positive and trace-preserving linear map. *Complete positivity* means that, for any reference space $\mathcal{H}_{\mathrm{ref}}$ and state $\rho \in \mathrm{D}(\mathcal{H}_{\mathrm{in}} \otimes \mathcal{H}_{\mathrm{ref}})$, we have $(\Phi \otimes \mathrm{I}_{\mathrm{ref}})(\rho) \succeq 0$ where $\mathrm{I}_{\mathrm{ref}}$ denotes the identity channel on $\mathcal{H}_{\mathrm{ref}}$. *Trace preservation* means that $\operatorname{Tr}\big(\Phi(\rho)\big) = \operatorname{Tr}(\rho)$, for all $\rho \in \mathrm{D}(\mathcal{H}_{\mathrm{in}})$.

Quantum channels could be expressed via several equivalent ways. One way is to express them using the Kraus operators $\{K_i\}$, where each K_i is a linear operator $K_i\colon \mathcal{H}_{\mathrm{in}} \to \mathcal{H}_{\mathrm{out}}$ such that $\Phi(\rho) = \sum_i K_i\rho K_i^\dagger$ and $\sum_i K_i^\dagger K_i = I_{\mathcal{H}_{\mathrm{in}}}$. The condition $\sum_i K_i^\dagger K_i = I_{\mathcal{H}_{\mathrm{in}}}$ ensures that the map is trace-preserving, i.e., $\operatorname{Tr}(\Phi(\rho)) = \operatorname{Tr}(\rho)$. Another equivalent way to describe quantum channels is via *Stinespring dilation* as $\Phi(\rho) = \operatorname{Tr}_{\mathcal{H}_{\mathrm{e}}}(V\rho V^\dagger)$, where V is some *isometry* operator $\operatorname{End}(\mathcal{H}_{\mathrm{in}}) \to \operatorname{End}(\mathcal{H}_{\mathrm{out}} \otimes \mathcal{H}_{\mathrm{e}})$ for some environment system $\mathcal{H}_{\mathrm{e}}$, i.e. $V^\dagger V = I_{\mathcal{H}_{\mathrm{in}}}$, and $\operatorname{Tr}_{\mathcal{H}_{\mathrm{e}}}$ is the *partial trace* over $\mathcal{H}_{\mathrm{e}}$.

For this thesis, the most useful characterisation of a quantum channel is via its *Choi matrix* $X^\Phi \in \operatorname{End}(\mathcal{H}_{\mathrm{in}} \otimes \mathcal{H}_{\mathrm{out}})$ defined as

$$X^\Phi := \sum_{i,j=1}^{d_{\mathrm{in}}} |i\rangle\langle j| \otimes \Phi\big(|i\rangle\langle j|\big) \tag{2.1}$$

where $\{|1\rangle, \ldots, |d_{\text{in}}\rangle\}$ is an orthonormal basis for $\mathcal{H}_{\text{in}}$. The action of Φ on $\rho \in \mathrm{D}(\mathcal{H}_{\text{in}})$ can be recovered from its Choi matrix X^Φ as follows:

$$\Phi(\rho) = \mathrm{Tr}_{\mathcal{H}_{\text{in}}}\left[X^\Phi(\rho^\mathsf{T} \otimes I_{\text{out}})\right]. \tag{2.2}$$

A given matrix $X \in \mathrm{End}(\mathcal{H}_{\text{in}} \otimes \mathcal{H}_{\text{out}})$ describes a quantum channel if and only if

$$X \succeq 0, \qquad \mathrm{Tr}_{\mathcal{H}_{\text{out}}}(X) = I_{\text{in}}. \tag{2.3}$$

Quantum measurements

To extract classical information from a quantum system, a *quantum measurement* is performed. The most general measurement in quantum mechanics is known as *positive operator-valued measure* (POVM), which is a set $E := \{E_k\}_{k=1}^n$ of positive semidefinite operators $E_k \succeq 0$ on a given Hilbert space $\mathcal{H}$ that sum to the identity matrix: $\sum_{k=1}^n E_k = I_{\mathcal{H}}$. The *Born rule* postulates the outcome probabilities of this measurement: upon measuring state ρ the classical outcome $k \in [n]$ is obtained with probability $\mathrm{Tr}(\rho E_k)$.

An important simpler subclass of measurements are *projective measurements*: $\Pi := \{\Pi_i\}_{i=1}^n$ is a *projection-valued measure* (PVM) on a given Hilbert space $\mathcal{H}$ if $\sum_{i=1}^n \Pi_i = I_{\mathcal{H}}$ and Π_i is an orthogonal projection, i.e. $\Pi_i^2 = \Pi_i = \Pi_i^\dagger \succeq 0$, for every $i \in [n]$.

If $\{\Pi_i\}_{i=1}^n$ is a PVM then for every pair $i, j \in [n]$, $i \neq j$ the projectors Π_i and Π_j are mutually orthogonal, i.e. $\Pi_i\Pi_j = \delta_{i,j}\Pi_i$. Indeed, take any vector $|v\rangle \in \mathrm{im}(\Pi_i) \subseteq \mathcal{H}$ where $\mathrm{im}(\Pi_i)$ denotes the image of Π_i. Since $\sum_j \Pi_j = I_{\mathcal{H}}$ we have $1 + \sum_{j\neq i}\langle v|\Pi_j|v\rangle = 1$. Therefore, since each Π_j is positive semidefinite it must be that $\langle v|\Pi_j|v\rangle = 0$ for every $j \neq i$, which implies $\Pi_i\Pi_j = \delta_{i,j}\Pi_i$. The converse is also true: if every pair of operators in a given POVM is mutually orthogonal then this POVM is a PVM.

Finally, we recall a particular instance of Stinespring dilation—the *Naimark dilation theorem*. This fundamental result states that any POVM can be represented as a PVM on a larger Hilbert space. This theorem allows any generalised measurement to be realised as a standard projective measurement in an extended space, which is particularly useful in quantum information theory and construction of quantum algorithms. However, finding an explicit Naimark dilation, which is easy to implement on a quantum computer can be a highly non-trivial task.

2.3 Semidefinite programming

Semidefinite programming is an important subfield of optimisation [WSV12] that has numerous applications in quantum information theory [ST22; Wat18]. A typical formulation of a *semidefinite program* (SDP) has the form [WSV12, Section 1.1]

$$\begin{aligned} \sup_X \quad & \mathrm{Tr}(C^\mathsf{T}X) \\ \text{s.t.} \quad & \mathrm{Tr}(A_i^\mathsf{T}X) = b_i, \quad \forall i \in [m], \\ & X \succeq 0, \end{aligned} \tag{2.4}$$

where X is a symmetric real matrix variable, C and A_i are constant symmetric real matrices, and b_i are real constants.[1] A special case of SDPs are *linear programs* (LPs) which correspond to the case when all matrices involved are diagonal. Any LP can be formulated in the standard form

$$\begin{aligned} \sup_x \quad & c^\mathsf{T}x \\ \text{s.t.} \quad & a_i^\mathsf{T}x = b_i, \quad \forall i \in [m], \\ & x \geqslant 0, \end{aligned} \tag{2.5}$$

[1] This formulation can be extended to complex numbers, i.e., X, C, A_i could be Hermitian matrices.

where x is a real vector variable, c and a_i are constant real vectors, and b_i are real constants. In practice, LPs are much faster to solve than SDPs. Therefore, being able to reduce a given SDP to an LP under additional symmetry assumptions is often desirable. We will encounter such a scenario in Chapter 6.

A fundamental idea in optimisation theory is that of *weak duality*: for a given *primal problem*, there is an associated *dual problem*. For example, for the primal SDP (2.4) we can write a *Lagrangian* [BV04]:

$$L(X, \lambda) := \operatorname{Tr}(C^{\mathsf{T}} X) + \sum_{i=1}^{m} \lambda_i (b_i - \operatorname{Tr}(A_i^{\mathsf{T}} X)), \tag{2.6}$$

where $\lambda_i \in \mathbb{R}$ are real *Lagrange multipliers*. Note that the problem (2.4) is equivalent to $\sup_{X \succeq 0} \inf_{\lambda \in \mathbb{R}^m} L(X, \lambda)$.

The *Min-Max principle* states that

$$\sup_{X \succeq 0} \inf_{\lambda \in \mathbb{R}^m} L(X, \lambda) \leqslant \inf_{\lambda \in \mathbb{R}^m} \sup_{X \succeq 0} L(X, \lambda), \tag{2.7}$$

therefore it is natural to define the *dual problem* of the primal problem (2.4) as $\inf_{\lambda \in \mathbb{R}^m} \sup_{X \succeq 0} L(X, \lambda)$, which is equivalent to

$$\begin{aligned} \inf_{\lambda} \quad & \sum_{i=1}^{m} \lambda_i b_i \\ \text{s.t.} \quad & \sum_{i=1}^{m} \lambda_i A_i - C \succeq 0, \\ & \lambda \in \mathbb{R}^m. \end{aligned} \tag{2.8}$$

Weak duality is based on Eq. (2.7) and asserts that $p^* \leqslant d^*$, where p^* and d^* are the optimal values of primal and dual problems, respectively. If equality holds, then we say that *strong duality* holds. There exist sufficient conditions for strong duality, such as *Slater's condition*, see [BV04; Wat18].

2.4 Representations of finite groups

Basic definitions

We start by defining a concept of representation which, intuitively, one should imagine as a "shadow" of the group G onto the space of linear transformations.

2.4.1. Definition (Representation). Let G be a finite group. A *representation* of G on a vector space V over field $\mathbb{K}$ is a homomorphism $R : G \to \operatorname{End}(V)$. In other words, the map R is such that

$$R(gh) = R(g)R(h) \quad \forall g, h \in G. \tag{2.9}$$

Abusing the notation, we could also specify a representation by mentioning a pair (R, V) or the map R or the space V only. The dimension of V is called the *degree* of the representation. We also refer to $|G|$ as the *size* of the group G. In the following, we always assume the ground field $\mathbb{K} = \mathbb{C}$ for all vector spaces, unless otherwise specified. Next, we define a concept of *intertwiner*.

2.4.2. Definition (Intertwiner). Let (R_1, V) and (R_2, W) be two representations of G. The linear map $\phi : V \to W$ is called an *intertwiner* or *G-homomorphism* if for every $g \in G$:

$$\phi R_1(g) = R_2(g)\phi. \tag{2.10}$$

The set of all G-homomorphisms between V and W is denoted by $\mathrm{Hom}_G(V, W)$. In particular, if $W = V$ then we denote $\mathrm{End}_G(V) := \mathrm{Hom}_G(V, V)$.

2.4.3. Example (Trivial Representation). The simplest representation is the *trivial representation*, where every group element is mapped to the identity matrix of a one-dimensional vector space. Formally, $R(g) = 1$ for all $g \in G$.

2.4.4. Example (Left-Regular and Right-Regular Representations). The *left-regular representation* $L\colon G \to \mathrm{End}(\mathbb{C}^{|G|})$ acts on an $|G|$-dimensional vector space with the basis $\{|g\rangle \mid g \in G\}$. $\mathbb{C}^{|G|}$ is commonly denoted by

$$\mathbb{C}\mathrm{G} := \mathrm{span}_{\mathbb{C}}\{|g\rangle \mid g \in G\}. \tag{2.11}$$

Each group element $h \in G$ acts by permuting these basis vectors: $L(h)|g\rangle = |hg\rangle$. Similarly, the *right-regular representation* $R\colon G \to \mathrm{End}(\mathbb{C}^{|G|})$ is defined on $\mathbb{C}\mathrm{G}$ such that each $h \in G$ acts as $R(h)|g\rangle = |gh^{-1}\rangle$. It is easy to see that these actions commute with each other.

The most important definition in this theory is that of *irreducible representation*.

2.4.5. Definition (Irreducible Representation). A representation R of G in V is *irreducible* if V does not have proper non-zero invariant subspaces under the action of G. That is, there is no subspace $W \subseteq V$ (other than $\{0\}$ and V itself) such that $R(g)W \subseteq W$ for all $g \in G$.

We will call irreducible representations simply *irreps* most of the time. Intuitively, irreducible representations for group representations are like primes for natural numbers, and we would like to understand how different representations decompose into simple pieces – the irreducible representations. The set of labels of all irreducible representations of G is usually denoted by

$$\widehat{G} := \{\lambda \mid V_\lambda \text{ is irreducible representation of } G\}. \tag{2.12}$$

Burnside's theorem provides a useful way to understand what "irreducibility" means.

2.4.6. Theorem (Burnside [LR04]). *Suppose $R : G \to \mathrm{GL}(V)$ is an irreducible representation of G, then*

$$\mathrm{span}_{\mathbb{C}}\{R(g) \mid g \in G\} = \mathrm{End}(V). \tag{2.13}$$

We can construct new representations by taking *direct sum* and *tensor product*. Namely, for two representations (R_1, V_1), (R_2, V_2) we can define

1. Direct sum: $R : G \to \mathrm{End}(V_1 \oplus V_2)$, for every $g \in G$

$$R(g) := R_1(g) \oplus R_2(g), \tag{2.14}$$

2. Tensor product: $R : G \to \mathrm{End}(V_1 \otimes V_2)$, for every $g \in G$

$$R(g) := R_1(g) \otimes R_2(g). \tag{2.15}$$

Fundamental results

A fundamental fact about finite group representations over $\mathbb{C}$ is that every representation is *completely reducible* in the following sense:

2.4.7. THEOREM (Maschke's theorem). *An arbitrary representation V over $\mathbb{C}$ of a finite group G decomposes into a direct sum of irreducible representations.*

Maschke's theorem implies, in particular, that left-regular representation of G can be decomposed into irreducibles.

2.4.8. THEOREM. *Let G be a finite group. The left-regular representation $\mathbb{C}$G is completely reducible and*

$$\mathbb{C}\mathrm{G} \cong \bigoplus_{\lambda \in \widehat{G}} V_\lambda \otimes V_\lambda^*, \tag{2.16}$$

where V_λ^* is a multiplicity space of the left-regular action, which can be indentified with the right-regular representation of G.

One of the key technical results that permeates across all representation theory is *Schur's lemma*, which puts stringent restrictions on the classes of maps different irreducible representations can have.

2.4.9. THEOREM (Schur's Lemma). *Let V and W be irreducible representations of G. If $\phi : V \to W$ is a G-homomorphism, then ϕ is either an isomorphism or zero. If $V = W$, then any endomorphism $\phi : V \to V$ commuting with all $R(g)$ for $g \in G$ is a scalar multiple of the identity map.*

To study how representations decompose into irreps, the concept of a character is very handy.

2.4.10. DEFINITION (Character). The *character* of a representation $R : G \to \mathrm{GL}(V)$ is the function $\chi : G \to \mathbb{C}$ defined by

$$\chi(g) := \mathrm{Tr}[R(g)] \quad \text{for every } g \in G, \tag{2.17}$$

where Tr denotes the trace of a matrix. We say that χ is *irreducible* whenever R is.

Character theory is a powerful tool to study the decomposition of a given representation into irreps because they have several important properties:

- $\chi(g)$ is a *class function*, i.e. it is constant on the conjugacy classes[2] of the group G;
- the character of the direct sum $R_\lambda \oplus R_\mu$ of two representations is the sum of their characters: $\chi_{\lambda\oplus\mu} = \chi_\lambda + \chi_\mu$;
- the character of the tensor product $R_\lambda \otimes R_\mu$ of two representations is the product of their characters: $\chi_{\lambda\otimes\mu} = \chi_\lambda \cdot \chi_\mu$.

2.4.11. THEOREM (Character Orthogonality Relations). *Let $\chi_1, \chi_2, \ldots, \chi_n$ be the complete set of irreducible characters of G. Then the following orthogonality relations hold:*

$$\frac{1}{|G|}\sum_{g\in G} \chi_i(g)\overline{\chi_j(g)} = \delta_{ij}, \qquad \frac{1}{|G|}\sum_{i=1}^{n} \chi_i(g)\overline{\chi_i(h)} = \delta_{g,h}, \tag{2.18}$$

where δ is the Kronecker delta.

[2]Two elements a and b of a group G are *conjugate* if there exists an element $g \in G$ such that $a = gbg^{-1}$. This is an equivalence relation and its equivalence classes are called *conjugacy classes*.

The information about characters is usually stored in a *character table*. The character table of a finite group G is a square matrix where rows correspond to the irreducible characters and columns correspond to the conjugacy classes of G.

Character orthogonality relations can be generalised to orthogonality relations between matrix entries of the corresponding representations. This very important result, relating two arbitrary unitary irreps R_λ and R_μ, is call *Schur Orthogonality Relations*:

2.4.12. THEOREM (Schur Orthogonality Relations). *For two arbitrary unitary irreducible representations of G, $R_\lambda : G \to \mathrm{End}(V_\lambda)$ and $R_\mu : G \to \mathrm{End}(V_\mu)$, their matrix elements satisfy the following orthogonality relations:*

$$\frac{1}{|G|}\sum_{g\in G} R_\lambda(g)_{ij}\overline{R_\mu(g)_{kl}} = \frac{1}{d_\lambda}\delta_{\lambda\mu}\delta_{ik}\delta_{jl}, \tag{2.19}$$

where d_λ is the dimension of the irrep V_λ, $R_\lambda(g)_{ij}$ and $R_\mu(g)_{kl}$ are the (i,j)-th and (k,l)-th elements of the matrices $R_\lambda(g)$ and $R_\mu(g)$, respectively.

Character and Schur orthogonality relations have several important consequences in representation theory. They imply that any class function on G can be expressed as a linear combination of irreducible characters. They also allow the construction of orthogonal projectors onto the isotypic components of representations. Specifically, for a given representation $R : G \to \mathrm{End}(V)$ the *isotypic projector* $R(\varepsilon_\lambda)$ onto irreducible representations V_λ, appearing inside representation V, is given by

$$R(\varepsilon_\lambda) = \frac{d_\lambda}{|G|}\sum_{g\in G}\chi_\lambda(g^{-1})R(g), \tag{2.20}$$

where d_λ is the dimension of the irrep λ. It projects onto all irreducible components within the representation R. The image of this projection inside the space V is usually called *isotypic component* λ.

It is useful to think about ε_λ as a formal linear combination in the *group algebra* $\mathbb{C}G$ (see Example 2.5.8):

$$\varepsilon_\lambda = \frac{d_\lambda}{|G|}\sum_{g\in G}\chi_\lambda(g^{-1})g. \tag{2.21}$$

This provides an example of *primitive central idempotent*. We describe this notion in more detail in Section 2.7.2.

2.5 Modules of finite-dimensional associative algebras

Representation theory of finite-dimensional associative algebras is a logical generalisation of the representation theory of finite groups. We have already seen an example of an algebra constructed from a group – the group algebra, which we defined as the left-regular representation in Example 2.4.4. However, the representation theory is richer in the case of finite-dimensional associative algebras. Unlike finite group representation theory over $\mathbb{C}$, representations of algebras over $\mathbb{C}$ are not completely reducible. That gives rise to different types of modules. Key objectives in this field include classifying simple and indecomposable modules, understanding projective and injective modules, and studying extensions between modules. However, for applications in quantum information, one is usually interested in finite-dimensional matrix $*$-algebras, which are semisimple. Because of this, we will not need all the complicated machinery developed in the field of finite-dimensional associative algebras. More background on finite-dimensional algebras and their modules can be found in [DK12; Cox12].

Basic definitions

We start with the basic definition of an associative algebra.

2.5.1. Definition (Associative Algebra). An *associative algebra* $\mathcal{A}$ over a field $\mathbb{K}$ is a vector space over $\mathbb{K}$ equipped with a bilinear multiplication operation $\cdot : \mathcal{A}\times\mathcal{A} \to \mathcal{A}$ that is associative:

$$(a \cdot b) \cdot c = a \cdot (b \cdot c) \quad \text{for all} \quad a, b, c \in \mathcal{A}. \tag{2.22}$$

We also assume that $\mathcal{A}$ has a multiplicative identity e[3] such that $e \cdot a = a \cdot e = a$ for all $a \in \mathcal{A}$.

In the following, we usually drop the adjective "associative" most of the time. Similar to Cayley's theorem for groups, any algebra over $\mathbb{K}$ is isomorphic to a subalgebra of the full matrix algebra $\mathrm{End}(\mathbb{K}^{\dim \mathcal{A}})$. Indeed, the action of $\mathcal{A}$ on any basis of $\mathcal{A}$ produces a matrix algebra that is analogous to the left-regular representation of a group.

A *subalgebra* $\mathcal{B} \subseteq \mathcal{A}$ is a vector subspace of $\mathcal{A}$ which is closed under multiplication operation. An important class of subalgebras are *ideals*.

2.5.2. Definition (Ideal). An *ideal* I of an algebra $\mathcal{A}$ is a vector subspace $I \subseteq \mathcal{A}$ such that for every $a \in \mathcal{A}$ and $x \in I$, both $a \cdot x \in I$ and $x \cdot a \in I$.

If V is a vector space, a *matrix algebra* $\mathcal{A}$ on V is a linear subspace of $\mathrm{End}(V)$ that is closed under matrix multiplication. The *centraliser* or *commutant* of a matrix algebra $\mathcal{A}$ in $\mathrm{End}(V)$ is the set of all matrices acting on V that commute with $\mathcal{A}$:

$$\mathrm{End}_{\mathcal{A}}(V) := \{B \in \mathrm{End}(V) \mid [A, B] = 0 \text{ for every } A \in \mathcal{A}\}, \tag{2.23}$$

where $[A, B] := AB - BA$ denotes the *commutator* of A and B.

If $\mathcal{A}$ and $\mathcal{B}$ are general abstract algebras, $\varphi\colon \mathcal{A} \to \mathcal{B}$ is an *algebra embedding* if φ is an injective homomorphism. The embedding is *unity-preserving* if $\varphi(e_{\mathcal{A}}) = e_{\mathcal{B}}$. We write $\mathcal{A} \hookrightarrow \mathcal{B}$ to mean that such embedding exists (in such case one can intuitively think of $\mathcal{A}$ as a subalgebra of $\mathcal{B}$). Similar to matrix algebras, we can define the notion of centraliser for abstract algebras.

2.5.3. Definition (Centraliser and Center). If $\mathcal{B} \subseteq \mathcal{A}$ then we denote by $\mathcal{Z}_{\mathcal{B}}(\mathcal{A})$ the *centraliser* of $\mathcal{B}$ in $\mathcal{A}$:

$$\mathcal{Z}_{\mathcal{B}}(\mathcal{A}) := \{a \in \mathcal{A} \mid ab = ba \text{ for every } b \in \mathcal{B}\}. \tag{2.24}$$

If $\mathcal{B} = \mathcal{A}$ in the above definition then $\mathcal{Z}(\mathcal{A}) := \mathcal{Z}_{\mathcal{A}}(\mathcal{A})$ is known as the *center* of the algebra $\mathcal{A}$.

A *representation* of $\mathcal{A}$ is a homomorphism $R : \mathcal{A} \to \mathrm{End}_{\mathbb{K}}(V)$, where V is a finite-dimensional vector space over $\mathbb{K}$. This means that each element $a \in \mathcal{A}$ is mapped to a linear transformation $R(a) \in \mathrm{End}_{\mathbb{K}}(V)$ such that

$$R(ab) = R(a)R(b) \quad \text{for all} \quad a, b \in \mathcal{A}. \tag{2.25}$$

However, usually in the context of algebras the equivalent word "module" is used. The words "representation" and "module" are essentially synonyms.

2.5.4. Definition (Module). An $\mathcal{A}$-*module* M is a vector space over $\mathbb{K}$ along with an action of $\mathcal{A}$ on M:

$$\cdot : \mathcal{A} \times M \to M, \qquad (a, m) \mapsto a \cdot m,$$

satisfying the following properties:

[3] Sometimes, we simply write 1 instead of e.

1. $(a+b)\cdot m = a\cdot m + b\cdot m$,
2. $a\cdot(m+n) = a\cdot m + a\cdot n$,
3. $(ab)\cdot m = a\cdot(b\cdot m)$,
4. $e\cdot m = m$.

Given a subalgebra $\mathcal{A}$ of an algebra $\mathcal{B}$ and a $\mathcal{B}$-module V, its *restriction* to the subalgebra $\mathcal{A}$ is the module V with action coming from $\mathcal{A}$ only. We denote such $\mathcal{A}$-module by $\mathrm{Res}^{\mathcal{B}}_{\mathcal{A}}V$.

A *submodule* of an $\mathcal{A}$-module M is a subspace W of M such that $a\cdot w \in W$ for all $w\in W$ and $a\in\mathcal{A}$. (Note that W is an $\mathcal{A}$-module in its own right.) For example, M and $\{0\}$ are trivial submodules of an $\mathcal{A}$-module M. If an $\mathcal{A}$-module M has submodules W_1 and W_2 such that $M = W_1\oplus W_2$ as a vector space then we say that M is the direct sum of W_1 and W_2. A module V is *indecomposable* if it is not the direct sum of two non-zero submodules, and is *decomposable* otherwise.

As in the context of finite groups, we can define "simple" representations, which we will call *simple modules*. A module which decomposes into simple modules is *semisimple* – this is an analogue of the concept of complete reducibility in the context of groups.

2.5.5. Definition (Simple and Semisimple Modules). Let $\mathcal{A}$ be a finite-dimensional algebra over a field $\mathbb{K}$. A *simple* $\mathcal{A}$-module is a non-zero finite-dimensional[4] $\mathcal{A}$-module M such that the only submodules of M are $\{0\}$ and M itself. An $\mathcal{A}$-module M is said to be *semisimple* if it is a direct sum of simple $\mathcal{A}$-modules.

A "representation" of an algebra is called a "module", and the adjective "irreducible" is usually replaced by "simple". We will use both terminologies interchangeably. The former is used more often in the group context, while the latter is used in the context of algebras. We denote the set of all simple $\mathcal{A}$-modules by $\widehat{\mathcal{A}}$.

To characterise algebras which only have semisimple modules, we need a concept of *Jacobson radical*. The Jacobson radical is also known as simply the radical of the algebra, and it plays a crucial role in the representation theory of finite-dimensional algebras, allowing to distinguish between "easy" semisimple algebras and "non-easy" non-semisimple algebras.

2.5.6. Definition (Jacobson Radical). Let $\mathcal{A}$ be a finite-dimensional algebra over a field $\mathbb{K}$. The Jacobson radical of $\mathcal{A}$, denoted by $\operatorname{rad}\mathcal{A}$, is the intersection of all maximal left ideals of $\mathcal{A}$. Equivalently, it is the set of all elements $a\in\mathcal{A}$ such that $e+ax$ is invertible for all $x\in\mathcal{A}$.

In the following, we always assume that the ground field $\mathbb{K}=\mathbb{C}$ unless specified otherwise.

2.5.7. Theorem. *Let $\mathcal{A}$ be a finite-dimensional algebra over $\mathbb{C}$. It is semisimple as left $\mathcal{A}$-module if and only if* $\operatorname{rad}\mathcal{A} = 0$.

A basic example of a semisimple algebra is the group algebra of a finite group G over a field $\mathbb{K}$, where the characteristic of $\mathbb{K}$ does not divide the order of the group G – this is basically a restatement of Maschke's theorem.

2.5.8. Example (Group algebra). The *group algebra* $\mathbb{C}G$ is constructed from a group G and a field $\mathbb{C}$. It consists of formal sums $\sum_{g\in G} a_g g$ with $a_g\in\mathbb{C}$, and multiplication extends linearly from the group operation:

$$\Big(\sum_{g\in G} a_g g\Big)\Big(\sum_{h\in G} b_h h\Big) = \sum_{g,h\in G}(a_g b_h)(gh) = \sum_{t\in G}\Big(\sum_{g\in G} a_g b_{g^{-1}t}\Big)t. \tag{2.26}$$

[4]Usually, the requirement is that the module should be *finitely generated*. However, for the purposes of this thesis it is enough to consider finite-dimensional modules.

Another important class of semisimple algebras relevant to quantum information are *matrix $*$-algebras* over $\mathbb{C}$. Formally, *$*$-algebra* is defined as follows:

2.5.9. Definition ($*$-algebra). A *$*$-algebra* is a finite-dimensional associative algebra $\mathcal{A}$ over $\mathbb{C}$, equipped with an involution $* : \mathcal{A} \to \mathcal{A}$, which satisfies the following properties for all $a, b \in \mathcal{A}$ and $k \in \mathbb{C}$:

1. $(a+b)^* = a^* + b^*$,
2. $(ka)^* = \overline{k}a^*$,
3. $(ab)^* = b^*a^*$,
4. $(a^*)^* = a$.

A *matrix $*$-algebra* is a matrix algebra, where the $*$ operation is the conjugate transpose $\dagger$. An example would be the algebra of block-diagonal matrices:

2.5.10. Example (Matrix $*$-algebra). Let V and W be vector spaces. Then

$$\mathcal{A} = \left\{ \begin{pmatrix} A & 0 \\ 0 & B \end{pmatrix} \;\middle|\; A \in \mathrm{End}(V),\, B \in \mathrm{End}(W) \right\} \tag{2.27}$$

is a matrix $*$-algebra. It is a subalgebra of the full matrix algebra $\mathrm{End}(V \oplus W)$.

An example of a non-semisimple matrix algebra is the upper triangular matrix algebra:

2.5.11. Example (Non-semisimple matrix algebra).

$$\mathcal{A} = \left\{ \begin{pmatrix} a & b & c \\ 0 & d & 0 \\ 0 & 0 & f \end{pmatrix} \;\middle|\; a, b, c, d, f \in \mathbb{C} \right\}. \tag{2.28}$$

Intuitively, being closed under the $\dagger$ operation forbids the existence of "upper triangular" matrix algebras as the one above. This is formalised in the following statement:

2.5.12. Lemma. *Every finite-dimensional matrix $*$-algebra is semisimple.*

Fundamental results

A crucial difference between the representation theory of finite groups and algebras is that for algebras there can be reducible but indecomposable modules in the following sense:

2.5.13. Definition. Let $\mathcal{A}$ be a finite-dimensional associative algebra over a field $\mathbb{K}$. A module M over $\mathcal{A}$ is called *indecomposable* if it cannot be expressed as a direct sum of two non-zero submodules. In other words, M is indecomposable if for every decomposition $M = M_1 \oplus M_2$ where M_1 and M_2 are submodules of M, we have either $M_1 = 0$ or $M_2 = 0$.

The *Krull–Schmidt Theorem* proves that indecomposable modules are elementary building blocks of modules of algebras in the following sense:

2.5.14. Theorem (Krull–Schmidt). *A finite-dimensional module over a finite-dimensional associative algebra decomposes uniquely (up to isomorphism and order) into a direct sum of indecomposable modules.*

Returning to the semisimple world, for the special case $\mathbb{K} = \mathbb{C}$ relevant for this thesis the *Wedderburn–Artin theorem* provides a classification of semisimple algebras.

2.5.15. THEOREM (Wedderburn–Artin). *A finite-dimensional semisimple algebra $\mathcal{A}$ over $\mathbb{C}$ is isomorphic to a direct sum of matrix algebras over $\mathbb{C}$:*

$$\mathcal{A} \cong \bigoplus_{\lambda \in \widehat{\mathcal{A}}} \operatorname{End}(V_\lambda), \tag{2.29}$$

where each V_λ is a simple $\mathcal{A}$-module.

This isomorphism is very useful since it allows us to think of an abstract semisimple algebra $\mathcal{A}$ as an algebra of block-diagonal matrices, a perspective that we will repeatedly use. Note that Theorem 2.5.15 implies

$$\dim \mathcal{A} = \sum_{\lambda \in \widehat{\mathcal{A}}} d_\lambda^2 \tag{2.30}$$

which is analogous to the dimension formula for irreducible representations of groups. Another way to look at Theorem 2.5.15 is to view $\mathcal{A}$ itself as left-regular representation of $\mathcal{A}$, so the statement of the Wedderburn–Artin theorem is equivalent to complete reducibility of this left-regular representation.

Similar to finite groups, Schur's lemma also holds for algebras. Namely, if M and N are simple modules over an algebra $\mathcal{A}$, then any $\mathcal{A}$-module homomorphism $f : M \to N$ is either zero or an isomorphism.

2.6 Young diagrams and tableaux

Now we would like to take a step back from discussing purely representation-theoretic basics to introduce some fundamental combinatorial objects, which are needed to talk about representations of symmetric groups S_n and unitary groups U_d.

A *partition* $\lambda \vdash n$ of an integer $n \geqslant 0$ is a tuple of integers $\lambda = (\lambda_1, \dots, \lambda_d)$ such that $\lambda_1 \geqslant \dots \geqslant \lambda_d \geqslant 0$ and $\lambda_1 + \dots + \lambda_d = n$. We denote by $\ell(\lambda) = \max\{k \mid \lambda_k > 0\}$ the *length* of λ. We use the notation $\lambda \vdash_d n$ to indicate that $\lambda \vdash n$ and $\ell(\lambda) \leqslant d$. A partition $\lambda \vdash n$ can be graphically represented as a *Young diagram*—a collection of n *cells* arranged in $\ell(\lambda)$ rows with λ_i of them in the i-th row. For example,

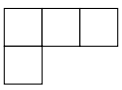

(2.31)

represents the partition $\lambda = (3, 1)$. Note that the same Young diagram could, for example, also refer to $\lambda = (3, 1, 0, 0)$. The *size* $|\lambda|$ of Young diagram is the number of boxes n. We call $\mu = (\mu_1, \dots, \mu_{d'})$ a *subpartition* of $\lambda = (\lambda_1, \dots, \lambda_d)$, and write $\mu \subseteq \lambda$ if $d' \leqslant d$ and $\mu_i \leqslant \lambda_i$ for $i = 1, \dots, d'$.

The *conjugate* or *transpose* of the partition λ, denoted λ', is the partition corresponding to transposing the Young diagram representing λ. E.g. if $\lambda = (3, 1)$ then

$\lambda =$ 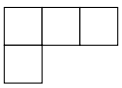 and $\lambda' =$ 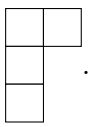 . (2.32)

Sometimes we use column notation to represent partitions. For example, a partition $\lambda = (3, 2)$ could be written as $\lambda = (2^2, 1^1)$.

Any cell $u \in \lambda$ of a Young diagram λ can be specified by its row and column coordinates i and j. The *content* of cell $u = (i, j)$ is

$$\operatorname{cont}(u) := j - i. \tag{2.33}$$

For example, the cells of the Young diagram $(5,3,3)$ have the following content:

$$\begin{array}{|c|c|c|c|c|}\hline 0 & 1 & 2 & 3 & 4 \\ \hline -1 & 0 & 1 \\ \cline{1-3} -2 & -1 & 0 \\ \cline{1-3}\end{array} \quad . \tag{2.34}$$

Note that content is constant on diagonals of λ and indicates how far each diagonal is from the main one. Content increases by one when going right or up, and decreases by one when going left or down. The *axial distance* (also known as *hook* or *Manhattan distance*) from cell $u = (i, j)$ to $v = (i', j')$ in a Young diagram is

$$r(u, v) := \mathrm{cont}(v) - \mathrm{cont}(u) = (j' - j) - (i' - i). \tag{2.35}$$

For example, the axial distance from cell u to all other cells in the Young diagram $(5,3,3)$ is as follows:

$$\begin{array}{|c|c|c|c|c|}\hline -1 & u & 1 & 2 & 3 \\ \hline -2 & -1 & 0 \\ \cline{1-3} -3 & -2 & -1 \\ \cline{1-3}\end{array} \quad . \tag{2.36}$$

For a Young diagram λ, a cell $u \in \lambda$ is called *removable* if the diagram $\lambda \setminus u$ obtained by removing the cell u from λ is a valid Young diagram. In the literature, removable cells are also called *corners* of a given Young diagram. Similarly, a cell $u \notin \lambda$ is called *addable* if the diagram $\lambda \cup u$ obtained by adding the cell u to λ is a valid Young diagram. The set of all removable cells of λ is denoted by $\mathrm{RC}(\lambda)$, while the set of all addable cells by $\mathrm{AC}(\lambda)$. We also need to define a subset $\mathrm{AC}_d(\lambda) \subseteq \mathrm{AC}(\lambda)$ of addable cells to a Young diagram λ that do not increase the length of λ beyond d:

$$\mathrm{AC}_d(\lambda) := \{a \in \mathrm{AC}(\lambda) \mid \ell(\lambda \cup a) \leqslant d\}. \tag{2.37}$$

For example, the Young diagram $\lambda = (5,3,3)$ (shown in gray) has two removable cells: $r_1 = (1,5)$, $r_2 = (3,3)$, and three addable cells (shown in white): $a_1 = (1,6)$, $a_2 = (2,4)$, $a_3 = (4,1)$:

$$\begin{array}{|c|c|c|c|c|c|}\hline \multicolumn{4}{|c|}{\multirow{2}{*}{}} & & r_1 & a_1 \\ \cline{5-6} \multicolumn{3}{|c|}{} & a_2 \\ \cline{4-4} \multicolumn{2}{|c|}{} & r_2 \\ \cline{3-3} a_3 \\ \cline{1-1}\end{array} \quad . \tag{2.38}$$

The addable cell a_3 is omitted from $\mathrm{AC}_3(\lambda)$.

A *Young tableau* T of shape $\lambda \vdash n$ is a Young diagram with cells filled with some natural numbers. A *standard Young tableau* T of shape $\lambda \vdash n$ is obtained by filling the cells of the Young diagram λ with numbers from $[n] := \{1, \ldots, n\}$ strictly increasing downwards across the rows and to the right across the columns. For example,

$$T = \begin{array}{|c|c|c|}\hline 1 & 2 & 3 \\ \hline 4 \\ \cline{1-1}\end{array}, \qquad S = \begin{array}{|c|c|c|}\hline 1 & 2 & 4 \\ \hline 3 \\ \cline{1-1}\end{array}, \qquad Q = \begin{array}{|c|c|c|}\hline 1 & 3 & 4 \\ \hline 2 \\ \cline{1-1}\end{array} \tag{2.39}$$

are all standard Young tableaux of shape $\lambda = (3,1)$. The set of all standard Young tableaux of a given shape λ is denoted as $\mathrm{SYT}(\lambda)$. According to the famous *hook length formula* [Sag13],

$$|\mathrm{SYT}(\lambda)| = \frac{(\lambda_1 + \cdots + \lambda_d)!}{\prod_{u \in \lambda} h(u)} \tag{2.40}$$

where $h(u)$ denotes the *hook length* of cell u (the number of cells in λ either to the right of u or below u, including u itself). The same value can also be obtained by the following alternative formula [Sag13]:

$$|\mathrm{SYT}(\lambda)| = \frac{(\lambda_1 + \cdots + \lambda_d)!}{\tilde{\lambda}_1! \cdots \tilde{\lambda}_d!} \prod_{1 \leqslant i < j \leqslant d} (\tilde{\lambda}_i - \tilde{\lambda}_j) \tag{2.41}$$

where $\tilde{\lambda}_i := \lambda_i + d - i$.

Notice that any standard Young tableau $T \in \mathrm{SYT}(\lambda)$ of shape $\lambda \vdash n$ can be represented as a tuple or sequence of $n+1$ Young diagrams:

$$T = (T^0, \ldots, T^n) \equiv T^0 \to T^1 \to \cdots \to T^n, \tag{2.42}$$

such that $T^i \vdash i$, $T^i \subseteq T^{i+1}$, and $T^n = \lambda$. Indeed, T^i is obtained from the Young diagram $\lambda \vdash n$ by keeping only those cells of T whose symbols are in $[i]$. For example, the Young tableau T from Eq. (2.39) is represented by the following sequence of Young diagrams:

$$T = \Big(\varnothing\,,\ \ydiagram{1},\ \ydiagram{2},\ \ydiagram{3},\ \ydiagram{3,1}\Big). \tag{2.43}$$

This sequence can be thought of as a path in a so-called Bratteli diagram (see Fig. 2.1), a concept which we will discuss in Section 2.7.

Another way to label such path T is via *Yamanouchi word* by recording a row where you add a box at a given step. For example, the Yamanouchi word corresponding to the path T from Eq. (2.43) is $(1, 1, 1, 2)$.

Consider a standard Young tableau $T \in \mathrm{SYT}(\lambda)$ of shape $\lambda \vdash n$ and an arbitrary permutation $\pi \in \mathrm{S}_n$. We will denote by πT the tableau obtained by permuting cell fillings of T according to π. For example, the Young tableaux T, S, Q presented in Eq. (2.39) are related in the following way: $S = (34)T$, $Q = (23)S = (234)T$, where $(34), (23), (234) \in \mathrm{S}_4$. Note that πT is not necessarily a standard tableau, e.g., consider $(14)T$.

Given a standard Young tableau T, we define

$$\mathrm{cont}_i(T) := \mathrm{cont}(T^{(i)} \setminus T^{(i-1)}). \tag{2.44}$$

This is simply the content of the cell of T containing i. Moreover, we define $r_i(T)$ to be the hook distance between the cells containing i and $i+1$, i.e.,

$$r_i(T) := \mathrm{cont}_{i+1}(T) - \mathrm{cont}_i(T). \tag{2.45}$$

A *semistandard Young tableau* M of shape λ and entries in $[d]$ is obtained by filling the cells of the Young diagram λ with symbols from $[d]$, strongly increasing downwards across the rows and weakly increasing to the right across the columns. For example,

$$M_1 = \begin{array}{|c|c|c|}\hline 1 & 1 & 1 \\ \hline 2 \\ \cline{1-1}\end{array}\,, \qquad M_2 = \begin{array}{|c|c|c|}\hline 1 & 1 & 2 \\ \hline 2 \\ \cline{1-1}\end{array}\,, \qquad M_3 = \begin{array}{|c|c|c|}\hline 1 & 2 & 2 \\ \hline 2 \\ \cline{1-1}\end{array} \tag{2.46}$$

are all semistandard Young tableau of shape $\lambda = (3, 1)$ with entries in $[2]$. We will denote the set of all semistandard Young tableaux of shape λ and entries in $[d]$ by $\mathrm{SSYT}(\lambda, d)$. According to the well-known *Weyl dimension formula* [Lou08, eq. (11.46)] and *hook-content formula*,

$$|\mathrm{SSYT}(\lambda, d)| = \prod_{1 \leqslant i < j \leqslant d} \frac{\lambda_i - \lambda_j + j - i}{j - i} = \frac{\prod_{u \in \lambda} (d + \mathrm{cont}(u))}{\prod_{u \in \lambda} h(u)}. \tag{2.47}$$

Recording the number of times each number appears in tableau M gives a sequence known as the *weight* of M, denoted as $w(M)$:

$$w(M)_i := \text{“the number of } i\text{'s in tableau } M\text{”}. \tag{2.48}$$

For example, the tableaux presented in Eq. (2.46) have weights $(3,1)$, $(2,2)$, and $(1,3)$, respectively. We can extend the notion of weight also to tuples of natural numbers. The *weight* $w(x) = w(x_1, \dots, x_k)$ of a sequence $x = (x_1, \dots, x_k)$ records the number of times each natural number appears in it. For example,

$$(1,2,2,2), \qquad (2,1,2,2), \qquad (2,2,1,2), \qquad (2,2,2,1) \tag{2.49}$$

are all sequences of weight $w(M) = (1,3)$.

2.7 Gelfand–Tsetlin basis

Now we would like to address the following question: are there algebras $\mathcal{A}$ for which one can define a "canonical" basis for all simple $\mathcal{A}$-modules? By "canonical" here we mean some natural construction, which depends on arbitrary, "mathematically unmotivated" choices as little as possible. It turns out that this question has a particularly nice answer when there exists a family of subalgebras with a certain restriction property. This is formalised in the following definition which is motivated by the canonical example of the sequence $\mathbb{C}\mathrm{S}_0 \hookrightarrow \mathbb{C}\mathrm{S}_1 \hookrightarrow \cdots \hookrightarrow \mathbb{C}\mathrm{S}_n$ of symmetric group algebras considered by Okounkov and Vershik in [OV96; VO05]. They re-derive the classic representation theory of S_n in what is now called the *Okounkov–Vershik approach*. We review the key elements of this approach in a more general setting of semisimple algebras presented in [DLS18].

2.7.1 Bratteli diagram

We start with a key definition of multiplicity-free family.

2.7.1. Definition (Definition 1.1 in [DLS18]). A family $\mathcal{A}_0, \dots, \mathcal{A}_n$ of finite-dimensional semisimple[5] algebras over $\mathbb{C}$ is *multiplicity-free* if the following axioms hold:

(a) $\mathcal{A}_0 \cong \mathbb{C}$.

(b) For each k, there is a unity-preserving algebra embedding $\mathcal{A}_k \hookrightarrow \mathcal{A}_{k+1}$.

(c) The restriction of a simple $\mathcal{A}_k$-module to $\mathcal{A}_{k-1}$ is isomorphic to a direct sum of pairwise non-isomorphic simple $\mathcal{A}_{k-1}$-modules. We say that in that case the restriction from $\mathcal{A}_k$ to $\mathcal{A}_{k-1}$ is *multiplicity-free*.

Given a multiplicity-free family of algebras, one can create a graph that shows how different simple modules of these algebras restrict to their subalgebras. We denote by V_λ a simple $\mathcal{A}$-module corresponding to $\lambda \in \widehat{\mathcal{A}}$. The dimension of this module is denoted by $d_\lambda := \dim V_\lambda$. We can represent the multiplicity-free restrictions among $\mathcal{A}_k$ by a directed acyclic graph known as Bratteli diagram [Bra72].

2.7.2. Definition. Let $\mathcal{A}_0, \dots, \mathcal{A}_n$ be a multiplicity-free family of algebras. Its *Bratteli diagram* $\mathscr{A}$[6] is a directed acyclic graph whose vertices are the isomorphism classes $\bigsqcup_{k=0}^{n} \widehat{\mathcal{A}}_k$ of simple $\mathcal{A}_k$-modules. There is an edge $\lambda \to \mu$ from vertex $\lambda \in \widehat{\mathcal{A}}_k$ to vertex $\mu \in \widehat{\mathcal{A}}_{k+1}$ if and only

[5] In [DLS18] the algebras are also required to be *split*. However, since we consider only algebras over $\mathbb{C}$, which is an algebraically closed field, in our setting all algebras are automatically split.

[6] Throughout the thesis we mainly use different letters $\mathscr{Y}, \mathscr{B}, \mathscr{A}$ to refer to different Bratteli diagrams corresponding to different algebras, which should be clear from a given context: $\mathscr{Y}$ corresponds to symmetric group algebras, $\mathscr{B}$ corresponds to walled Brauer algebras and $\mathscr{A}$ corresponds to partially transposed permutation matrix algebras. In this chapter, we refer to $\mathscr{A}$ as an abstract Bratteli diagram.

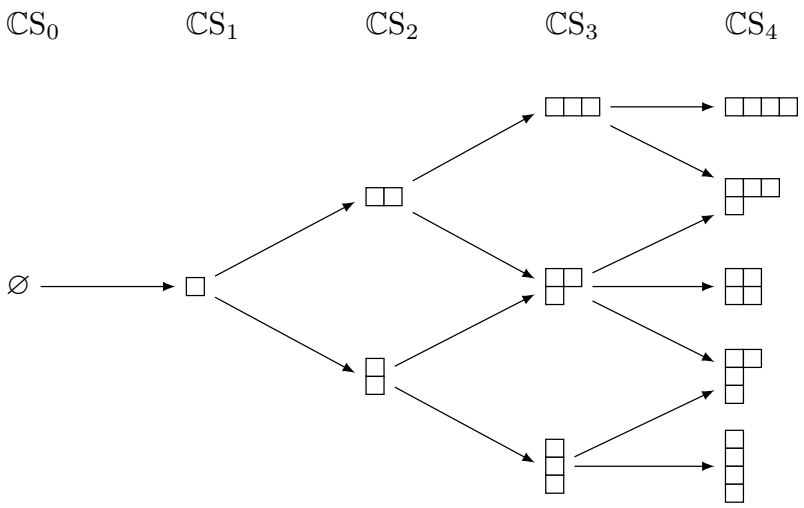

Figure 2.1: The Bratteli diagram $\mathscr{Y}$ for the family of symmetric group algebras $\mathbb{C}S_0 \hookrightarrow \mathbb{C}S_1 \hookrightarrow \mathbb{C}S_2 \hookrightarrow \mathbb{C}S_3 \hookrightarrow \mathbb{C}S_4$, also known as Young's lattice. The vertices at level k are labelled by Young diagrams $\lambda \vdash k$ corresponding to all non-isomorphic irreducible representations of $\mathbb{C}S_k$.

if V_λ is isomorphic to a direct summand of $\mathrm{Res}^{\mathcal{A}_{k+1}}_{\mathcal{A}_k} V_\mu$, the restriction of V_μ to the subalgebra $\mathcal{A}_k$. We call $\widehat{\mathcal{A}}_k$ the k-th *level* of the Bratteli diagram. We denote the unique vertex in $\widehat{\mathcal{A}}_0$ by $\varnothing$ and call it the *root*, while $\widehat{\mathcal{A}}_n$ are called *leaves*.

An example of a Bratteli diagram for the multiplicity-free family of semisimple symmetric group algebras $\mathbb{C}S_k$ [OV96] is shown in Fig. 2.1; it is also called the *Young lattice* or the *Young graph* (see [Sag13]).

Paths[7] in the Bratteli diagram play an important role in the representation theory of the corresponding algebras, so we will introduce some notation for them. If λ and μ are two vertices at levels $i < j$ of the Bratteli diagram $\mathscr{A}$, we will denote the set of all paths from λ to μ by

$$\mathrm{Paths}_{i,j}(\lambda, \mu, \mathscr{A}). \tag{2.50}$$

We will denote the set of all paths starting at the root $\varnothing$ and terminating at vertex λ at level j by

$$\mathrm{Paths}_j(\lambda, \mathscr{A}) := \mathrm{Paths}_{0,j}\big(\varnothing, \lambda, \mathscr{A}\big). \tag{2.51}$$

When $j = n$, i.e., λ is a leaf, we will abbreviate this to

$$\mathrm{Paths}(\lambda, \mathscr{A}) := \mathrm{Paths}_n(\lambda, \mathscr{A}). \tag{2.52}$$

Finally, we use $\mathrm{Paths}(\mathscr{A})$ to denote the set of all paths in the Bratteli diagram $\mathscr{A}$. If the Bratteli diagram $\mathscr{A}$ is clear from a given context, we often drop $\mathscr{A}$ in the notation and simply write $\mathrm{Paths}_{i,j}(\lambda, \mu)$, $\mathrm{Paths}_j(\lambda)$, $\mathrm{Paths}(\lambda)$.

An arbitrary path $T = (T^0, \dots, T^n)$ in the Bratteli diagram can be *decomposed* at level $i \in \{0, \dots, n\}$ as $T = T_1 \to T_2$ where $T_1 = (T^0, \dots, T^i)$ and $T_2 = (T^{i+1}, \dots, T^n)$ belong to $\mathrm{Paths}_i(T^i)$ and $\mathrm{Paths}_{i+1,n}(T^{i+1}, T^n)$, respectively.

Finally, we often use notation $\mu \colon \lambda \to \mu$ as a summation index to mean that a given sum ranges over all vertices μ which are connected to the vertex λ on a previous level in a given Bratteli diagram.

[7] By a "path" we always mean a *directed path*, i.e., a path that traverses edges only in the allowed direction (from lower to higher levels).

2.7.2 Idempotents

In this section, we summarize the [DLS18] algorithm for finding the primitive central idempotents of any multiplicity-free family of algebras.

2.7.3. Definition. An *idempotent* ε in the algebra $\mathcal{A}$ is an element with the property $\varepsilon^2 = \varepsilon$. Two idempotents $a, b \in \mathcal{A}$ are said to be *orthogonal* if $ab = ba = 0$. A *central* idempotent $\varepsilon \in \mathcal{A}$ is an idempotent that commutes with every element $a \in \mathcal{A}$, i.e., $\varepsilon a = a\varepsilon$.

Certain types of idempotents are extremely useful for studying the representation theory of a given algebra. We define them as follows.

2.7.4. Definition. A *primitive idempotent* is an idempotent that cannot be written as a sum of two non-zero orthogonal idempotents. A *primitive central idempotent* is a central idempotent that cannot be written as a sum of two non-zero orthogonal central idempotents.

If algebra $\mathcal{A}$ is semisimple, due to Wedderburn's theorem (Theorem 2.5.15) we have the isomorphism

$$\mathcal{A} = \bigoplus_{\lambda \in \widehat{\mathcal{A}}} \varepsilon_\lambda \mathcal{A} \cong \bigoplus_{\lambda \in \widehat{\mathcal{A}}} \operatorname{End}(V_\lambda) \tag{2.53}$$

where ε_λ are the *primitive central idempotents* of $\mathcal{A}$ and the first direct sum should be understood as a decomposition of the left-regular representation of $\mathcal{A}$. The primitive central idempotents ε_λ are in one-to-one correspondence with simple $\mathcal{A}$-modules labeled by $\lambda \in \widehat{\mathcal{A}}$ and provide a resolution of the unit element of the algebra $\mathcal{A}$: $\sum_{\lambda \in \widehat{\mathcal{A}}} \varepsilon_\lambda = 1$.

2.7.3 Gelfand–Tsetlin subalgebra

Let $\mathcal{A}_0, \dots, \mathcal{A}_n$ be a multiplicity-free family of algebras (see Definition 2.7.1) with Bratteli diagram $\mathscr{A}$. We can now define a certain basis for the direct sum $\bigoplus_{\lambda \in \widehat{\mathcal{A}}_n} V_\lambda$ of all simple $\mathcal{A}_n$-modules, where each element of the basis corresponds to a path in the Bratteli diagram $\mathscr{A}$. This basis can be obtained by choosing any leaf $\lambda \in \widehat{\mathcal{A}}_n$ and considering the restriction $\operatorname{Res}^{\mathcal{A}_n}_{\mathcal{A}_{n-1}} V_\lambda$ of the corresponding simple $\mathcal{A}_n$-module V_λ to $\mathcal{A}_{n-1}$, which according to Definition 2.7.1 is multiplicity-free. This restriction can then be iterated further along any path in the Bratteli diagram towards the root $\varnothing$ that corresponds to the one-dimensional algebra $\mathcal{A}_0 \cong \mathbb{C}$. Doing this along all $\operatorname{Paths}(\lambda)$ between $\varnothing$ and λ results in a decomposition of the chosen simple $\mathcal{A}_n$-module V_λ into one-dimensional simple $\mathcal{A}_0$-modules. Repeating this procedure for all leaves $\lambda \in \widehat{\mathcal{A}}_n$ produces the *Gelfand–Tsetlin basis* of $\bigoplus_{\lambda \in \widehat{\mathcal{A}}_n} V_\lambda$:

$$\big\{ |T\rangle \;\big|\; T \in \operatorname{Paths}(\mathscr{A}) \big\}. \tag{2.54}$$

These vectors are labeled by elements of $\operatorname{Paths}(\mathscr{A})$ since each sequence of restrictions corresponds to some leaf-root path in the Bratteli diagram.

Now we would like to explicitly construct primitive idempotents inside $\mathcal{A}_n$ which project onto the Gelfand–Tsetlin basis. To do that we need to look at the maximal commutative subalgebras of $\mathcal{A}_k$. Due to Eq. (2.53) one can think of them as subalgebras of diagonal matrices, carrying the information about the projectors onto the Gelfand–Tsetlin basis. This motivates the following definition.

2.7.5. Definition. For each $k \in [n]$, the corresponding *Gelfand–Tsetlin subalgebra* is

$$\mathcal{X}_k := \langle \mathcal{Z}(\mathcal{A}_1), \dots, \mathcal{Z}(\mathcal{A}_k) \rangle \subseteq \mathcal{A}_k \tag{2.55}$$

where $\mathcal{Z}(\mathcal{A}_i)$ denotes the center of the subalgebra $\mathcal{A}_i$.

Note that $\mathcal{X}_1 \subseteq \cdots \subseteq \mathcal{X}_n$. The Gelfand–Tsetlin subalgebra $\mathcal{X}_k$ is a maximal commutative subalgebra of $\mathcal{A}_k$, see Proposition 1.1 of [OV96; VO05]. We will later find a particular set of generators for $\mathcal{X}_k$, known as *Jucys–Murphy elements*, which will help us to construct the primitive central idempotents of $\mathcal{A}_n$.

For each path $T = T^0 \to T^1 \to \cdots \to T^n \in \mathrm{Paths}(\mathscr{A})$ in the Bratteli diagram, set

$$\varepsilon_T := \varepsilon_{T^1}\varepsilon_{T^2}\cdots\varepsilon_{T^n} \tag{2.56}$$

where ε_{T^i} are the primitive central idempotents of $\mathcal{A}_i$, see Eq. (2.53). Note that ε_T is an element of the Gelfand–Tsetlin subalgebra $\mathcal{X}_n$ since $\varepsilon_{T^i} \in \mathcal{Z}(\mathcal{A}_i)$ for each i.

2.7.6. Proposition (Proposition 1.6 and Corollary 1.7 in [DLS18]). *The collection* $\{\varepsilon_T \mid T \in \mathrm{Paths}(\mathscr{A})\}$ *is a family of orthogonal primitive idempotents in* $\mathcal{A}_n$ *that sums to the identity* 1 *and is a basis for the Gelfand–Tsetlin subalgebra* $\mathcal{X}_n$*. Moreover, the primitive central idempotents of* $\mathcal{A}_n$ *are given by*

$$\varepsilon_\lambda = \sum_{T \in \mathrm{Paths}(\lambda)} \varepsilon_T. \tag{2.57}$$

Using the isomorphism in Eq. (2.53), the primitive idempotents ε_T correspond to the projectors $|T\rangle\langle T|$ onto the Gelfand–Tsetlin basis vectors $|T\rangle \in \bigoplus_{\lambda \in \widehat{\mathcal{A}}_n} V_\lambda$.

2.7.4 Jucys–Murphy elements

In this section, we define a certain nice set of elements of the algebra $\mathcal{A}_k$ that generate the Gelfand–Tsetlin subalgebra $\mathcal{X}_k$. They are commonly known as Jucys–Murphy elements.

2.7.7. Definition (Definition 3.1 in [DLS18]). Let $\mathcal{A}_0, \ldots, \mathcal{A}_n$ be a multiplicity-free family of algebras and let $\mathcal{X}_1, \ldots, \mathcal{X}_n$ be their Gelfand–Tsetlin subalgebras. Let $J_1, \ldots, J_n$ be a sequence of elements in $\mathcal{A}_n$ such that $J_k \in \mathcal{X}_k$ for each $k \in [n]$. This sequence is

(a) *additively central* if $J_1 + \cdots + J_k \in \mathcal{Z}(\mathcal{A}_k)$ for all $k \in [n]$,

(b) *separating* if $\mathcal{X}_k = \langle J_1, \ldots, J_k \rangle$ for all $k \in [n]$.

It is a *Jucys–Murphy sequence* if it is both additively central and separating.

Since $J_1, \ldots, J_n \in \mathcal{X}_n$ and $\{\varepsilon_T : T \in \mathrm{Paths}(\mathscr{A})\}$ is a basis of $\mathcal{X}_n$ due to Proposition 2.7.6, we can expand each J_k as a linear combination of ε_T.

2.7.8. Definition. For a given sequence $J_1, \ldots, J_n$ with $J_k \in \mathcal{X}_k$, we define a tuple called *weight vector* $c_T = (c_T(1), \ldots, c_T(n))$ where each $c_T(k) \in \mathbb{C}$ is such that for all $k \in [n]$

$$J_k = \sum_{T \in \mathrm{Paths}(\mathscr{A})} c_T(k)\varepsilon_T. \tag{2.58}$$

Sometimes in the literature the tuple c_T is also called *content vector*. Note that under the isomorphism in Eq. (2.53) $\{c_T(k) \mid T \in \mathrm{Paths}(\mathscr{A})\}$ are the eigenvalues of J_k. An important observation regarding the $c_T(k)$ is that the value of $c_T(k)$ does not depend on the whole path T but only on the vertices T^k and T^{k-1}, see Lemma 3.9 in [DLS18], which is a consequence of the property (a) in Definition 2.7.7. This means that the number $c_T(k)$ can be assigned to the edge $T^{k-1} \to T^k$ in the Bratteli diagram and we can equivalently write

$$c_{T^{k-1} \to T^k} := c_T(k). \tag{2.59}$$

2.7.5 Algorithm for computing idempotents

We now have all ingredients to state the [DLS18] algorithm for computing primitive central and canonical primitive pairwise orthogonal idempotents of any multiplicity-free family $\mathcal{A}_0, \dots, \mathcal{A}_n$ of semisimple finite-dimensional algebras.

Following [DLS18], we assign to each edge $\lambda \to \mu$ between levels $k-1$ and k of the Bratteli diagram an *interpolating polynomial* $P_{\lambda\to\mu}$ of $x \in \mathcal{A}_k$ defined as

$$P_{\lambda\to\mu}(x) := \prod_{\tilde{\mu}\,:\,\lambda\to\tilde{\mu}\neq\mu} \frac{x - c_{\lambda\to\tilde{\mu}}}{c_{\lambda\to\mu} - c_{\lambda\to\tilde{\mu}}}, \tag{2.60}$$

where the product is over all edges $\lambda \to \tilde{\mu}$ (other than $\lambda \to \mu$) outgoing from the vertex λ. According to their main result [DLS18, Theorem 3.11], the primitive central idempotents of $\mathcal{A}_k$ can be computed recursively for any $k \in [n]$ and $\mu \in \widehat{\mathcal{A}}_k$ as follows:

$$\varepsilon_\mu = \sum_{\lambda\,:\,\lambda\to\mu} P_{\lambda\to\mu}(J_k)\varepsilon_\lambda, \tag{2.61}$$

where the sum is over all edges $\lambda \to \mu$ incoming into μ and $J_1, \dots, J_n$ is a Jucys–Murphy sequence for the algebras $\mathcal{A}_0, \dots, \mathcal{A}_n$. The base case of the recursion is $\varepsilon(\varnothing) = 1$. According to [DLS18, Theorem 3.8], the canonical primitive idempotents corresponding to the Gelfand–Tsetlin basis can be found by substituting Eq. (2.60) into Eq. (2.56):

$$\varepsilon_T = \prod_{k=1}^{n} P_{T^{k-1}\to T^k}(J_k) = \prod_{k=1}^{n} \prod_{\mu\,:\,T^{k-1}\to\mu\neq T^k} \frac{J_k - c_{T^{k-1}\to\mu}}{c_{T^{k-1}\to T^k} - c_{T^{k-1}\to\mu}} \tag{2.62}$$

where $T = T^0 \to T^1 \to \cdots \to T^n$ is a path in the Bratteli diagram.

To summarize, using these formulas requires the following data about the family $\mathcal{A}_0, \dots, \mathcal{A}_n$:

1. the Bratteli diagram of $\mathcal{A}_0, \dots, \mathcal{A}_n$,
2. a Jucys–Murphy sequence $J_1, \dots, J_n$ for $\mathcal{A}_0, \dots, \mathcal{A}_n$,
3. the scalars $c_T(k)$ for all $k \in [n]$ and paths $T \in \mathrm{Paths}(\mathscr{A})$ in the Bratteli diagram.

2.7.6 Matrix units

Matrix units generalise the notion of primitive idempotents ε_T for $T \in \mathrm{Paths}(\mathscr{A})$. Namely, for every $T, S \in \mathrm{Paths}(\lambda, \mathscr{A})$ of every $\lambda \in \widehat{\mathcal{A}}_n$ we can construct elements $E_{T,S} \in \mathcal{A}_n$ such that under the isomorphism of Theorem 2.5.15 we have

$$E_{T,S} \cong \bigoplus_{\mu\in\widehat{\mathcal{A}}_n} \delta_{\lambda,\mu}|T\rangle\langle S|, \tag{2.63}$$

and correspondingly they provide a nice basis for the algebra $\mathcal{A}_n$

$$\mathcal{A}_n = \mathrm{span}_{\mathbb{C}}\{E_{T,S} \mid T, S \in \mathrm{Paths}(\lambda, \mathscr{A}),\ \lambda \in \widehat{\mathcal{A}}_n\} \tag{2.64}$$

whose elements satisfy

$$E_{T,S}E_{T',S'} = \delta_{S,T'}E_{T,S'}, \qquad \sum_{T\in\mathrm{Paths}(\mathscr{A})} E_{T,T} = 1. \tag{2.65}$$

Note that we can choose $E_{T,T} = \varepsilon_T$.

2.8 Representation theory of S_n

Now we have all necessary ingredients and we are ready to summarize the representation theory of S_n, which is crucial for the rest of this thesis. The representation theory of the symmetric group is widely used and has a long history [Sag13; Rut48; CST10; How22].

Formally, the symmetric group is defined as follows:

2.8.1. Definition. Let $n \geqslant 1$. The *symmetric group* S_n can be presented with identity 1 and generators σ_i for $i \in \{1, \dots, n-1\}$ with relations:

$$\sigma_i^2 = 1, \qquad \sigma_i\sigma_{i+1}\sigma_i = \sigma_{i+1}\sigma_i\sigma_{i+1}, \qquad \sigma_i\sigma_j = \sigma_j\sigma_i \quad (|i-j| > 1). \tag{2.66}$$

One should think that σ_i correspond to permutations of elements i and $i+1$ in the set $\{1, \dots, n\}$. We use the notation (i, j) to label a permutation $i \mapsto j$, $j \mapsto i$, so that $\sigma_i = (i, i+1)$. More generally, we use the *cycle notation* $(a, b, \dots, f)$ to mean $a \mapsto b \mapsto \dots \mapsto f \mapsto a$.

It is better to think about the elements of S_n as diagrams, with group multiplication corresponding to concatenation of diagrams. For example, a permutation $(1, 4, 5, 3, 2) \in \mathrm{S}_5$ corresponds to

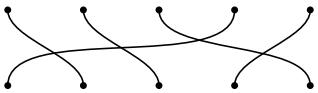

(2.67)

Irreducible representations of S_n, or equivalently simple modules of $\mathbb{C}\mathrm{S}_n$, are classified by partitions $\lambda \vdash n$:

$$\widehat{\mathbb{C}\mathrm{S}_n} = \{\lambda \vdash n\}. \tag{2.68}$$

One way to see this is via the *Okounkov–Vershik* approach [OV96], the general aspects of which we outlined in Section 2.7. It is common to call the corresponding simple modules V_λ *Specht modules*. The characters of Specht modules are given by the Murnaghan–Nakayama rule [Sag13], which is a somewhat involved combinatorial formula that we will not present here. A basis of Specht modules can be labelled by standard Young tableaux, which we introduced in Section 2.6. In particular, the dimension d_λ of a Specht module corresponding to a partition $\lambda \vdash n$ is given by the *hook length formula* (see Eq. (2.40)):

$$d_\lambda = |\mathrm{SYT}(\lambda)| = \frac{n!}{\prod_{u \in \lambda} h(u)}. \tag{2.69}$$

The symmetric group S_n has a natural action on the tensor product space $(\mathbb{C}^d)^{\otimes n}$ that permutes the n tensor factors. This so-called *tensor representation* of S_n is given by a map $\psi_n^d : \mathbb{C}\mathrm{S}_n \to \mathrm{End}((\mathbb{C}^d)^{\otimes n})$ that acts as

$$\psi_n^d(\pi)\big(|x_1\rangle \otimes \cdots \otimes |x_n\rangle\big) := |x_{\pi^{-1}(1)}\rangle \otimes \cdots \otimes |x_{\pi^{-1}(n)}\rangle \tag{2.70}$$

for every $\pi \in \mathrm{S}_n$ and $x = (x_1, \dots, x_n) \in [d]^n$. The image of $\mathbb{C}\mathrm{S}_n$ under ψ_n^d gives rise to an important quotient algebra of $\mathbb{C}\mathrm{S}_n$ – the *permutation matrix algebra*

$$\mathcal{A}_n^d := \psi_n^d(\mathbb{C}\mathrm{S}_n). \tag{2.71}$$

We will often abuse the notation and simply write ψ instead of ψ_n^d. It is important to observe that ψ_n^d has a non-trivial kernel when the local dimension d is smaller than n. For this reason we will often have to make a distinction between small and large local dimensions d.

2.8.2. Example (Unfaithfulness of ψ_3^d). $\psi_3^d\big(\sum_{\pi \in \mathrm{S}_3} \mathrm{sign}(\pi)\pi\big)$ vanishes when $d = 2$. Namely, any string $x = (x_1, x_2, x_3) \in [2]^3$ has two positions $i \neq j$ such that $x_i = x_j$. Therefore, for each $\pi \in \mathrm{S}_3$ there is $\pi' \in \mathrm{S}_3$ with $\mathrm{sign}(\pi) = -\mathrm{sign}(\pi')$ such that $\pi x = \pi' x$, meaning $\psi_3^d\big(\sum_{\pi \in \mathrm{S}_3} \mathrm{sign}(\pi)\pi\big)|x_1, x_2, x_3\rangle = 0$. In contrast, it does not vanish when $d \geqslant 3$.

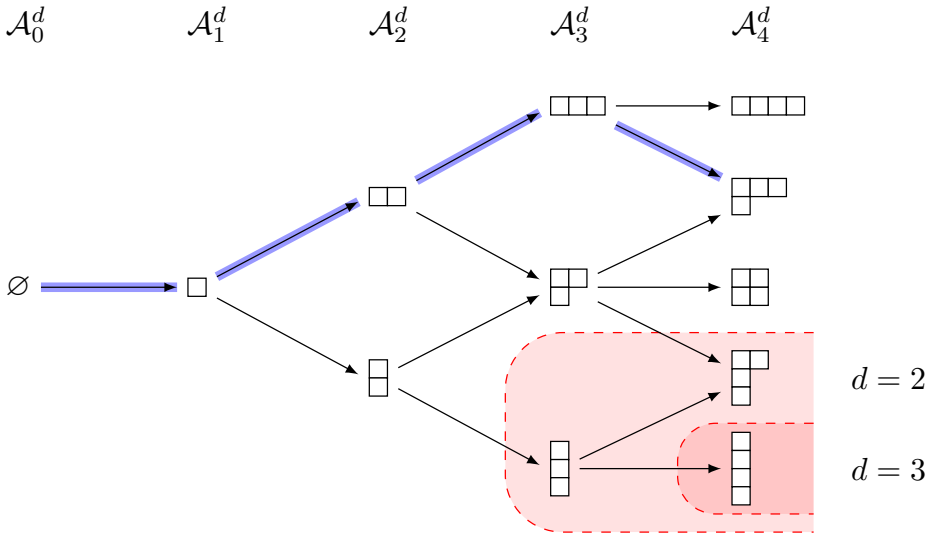

Figure 2.2: The Bratteli diagram for the permutation matrix algebras $\mathcal{A}_0^d \hookrightarrow \mathcal{A}_1^d \hookrightarrow \mathcal{A}_2^d \hookrightarrow \mathcal{A}_3^d \hookrightarrow \mathcal{A}_4^d$ defined in Eq. (2.71) when $d \geqslant 4$ is the same as Young's lattice in Fig. 2.1. When $d = 2$ or $d = 3$, vertices with Young diagrams containing more than d rows are removed. We have highlighted the path corresponding to sequence (2.43) and terminating at leaf $\lambda = (3, 1)$.

This unfaithfulness is reflected in the fact that the irreps of $\mathcal{A}_n^d$ are different from those of $\mathbb{C}\mathrm{S}_n$:

$$\widehat{\mathcal{A}}_n^d = \{\lambda \vdash n \mid \ell(\lambda) \leqslant d\}. \tag{2.72}$$

The Bratteli diagram for $\mathbb{C}\mathrm{S}_0 \hookrightarrow \mathbb{C}\mathrm{S}_1 \hookrightarrow \cdots \hookrightarrow \mathbb{C}\mathrm{S}_n$ is known as *Young's lattice*, see Figs. 2.1 and 2.2. A path T in this Bratteli diagram can also be viewed as a *standard Young tableau*. Jucys–Murphy elements of $\mathbb{C}\mathrm{S}_n$ [Juc74; Mur81] are

$$J_k := \begin{cases} 0 & \text{if } k = 1, \\ \sum_{i=1}^{k-1} (i, k) & \text{if } 2 \leqslant k \leqslant n, \end{cases} \tag{2.73}$$

where (i, k) is the transposition of elements i and k. Moreover, it turns out that the entries of the weight vector c_T are simply given by the contents, see Eq. (2.44), of the Young tableau T:

$$c_T(k) = \mathrm{cont}_k(T), \tag{2.74}$$

thus motivating the name "content vector" for the weight vector c_T in Definition 2.7.8. The Bratteli diagram of $\mathcal{A}_n^d$ is closely related to the Young's lattice and can be obtained by removing vertices which violate the condition $\ell(\lambda) \leqslant d$. The Bratteli diagrams for the symmetric groups and permutation matrix algebras are presented in Fig. 2.2.

There are three commonly used forms for irreducible representations of the symmetric group [Rut48] (see Table 2.1 for examples):

1. *Young's natural form* provides invertible matrices with integer entries (i.e., in $\mathbb{Z}$),
2. *Young's seminormal form* provides invertible matrices with rational entries (i.e., in $\mathbb{Q}$),
3. *Young's orthogonal form* (also known as *Young–Yamanouchi basis*) provides real orthogonal matrices whose entries are square roots of rational numbers (i.e., in $\pm\sqrt{\mathbb{Q}_{\geqslant 0}}$).

The basis change between Young's seminormal and orthogonal forms is diagonal and corresponds to normalisation, while the basis change between seminormal and natural forms is triangular [AH21].

The action of S_n on paths of the Bratteli diagram is given by the following famous result:

$\pi \in \mathrm{S}_3$	e	$\sigma_2\sigma_1$	$\sigma_1\sigma_2$	σ_1	$\sigma_1\sigma_2\sigma_1$	σ_2
Diagram of π						
$R_{\mathrm{nat}}(\pi)$	$\begin{pmatrix} 1 & 0 \\ 0 & 1 \end{pmatrix}$	$\begin{pmatrix} -1 & -1 \\ 1 & 0 \end{pmatrix}$	$\begin{pmatrix} 0 & 1 \\ -1 & -1 \end{pmatrix}$	$\begin{pmatrix} 1 & 0 \\ -1 & -1 \end{pmatrix}$	$\begin{pmatrix} -1 & -1 \\ 0 & 1 \end{pmatrix}$	$\begin{pmatrix} 0 & 1 \\ 1 & 0 \end{pmatrix}$
$R_{\mathrm{semi}}(\pi)$	$\begin{pmatrix} 1 & 0 \\ 0 & 1 \end{pmatrix}$	$\begin{pmatrix} -1/2 & -3/2 \\ 1/2 & -1/2 \end{pmatrix}$	$\begin{pmatrix} -1/2 & 3/2 \\ -1/2 & -1/2 \end{pmatrix}$	$\begin{pmatrix} 1 & 0 \\ 0 & -1 \end{pmatrix}$	$\begin{pmatrix} -1/2 & -3/2 \\ -1/2 & 1/2 \end{pmatrix}$	$\begin{pmatrix} -1/2 & 3/2 \\ 1/2 & 1/2 \end{pmatrix}$
$R_{\mathrm{orth}}(\pi)$	$\begin{pmatrix} 1 & 0 \\ 0 & 1 \end{pmatrix}$	$\begin{pmatrix} -1/2 & -\sqrt{3}/2 \\ \sqrt{3}/2 & -1/2 \end{pmatrix}$	$\begin{pmatrix} -1/2 & \sqrt{3}/2 \\ -\sqrt{3}/2 & -1/2 \end{pmatrix}$	$\begin{pmatrix} 1 & 0 \\ 0 & -1 \end{pmatrix}$	$\begin{pmatrix} -1/2 & -\sqrt{3}/2 \\ -\sqrt{3}/2 & 1/2 \end{pmatrix}$	$\begin{pmatrix} -1/2 & \sqrt{3}/2 \\ \sqrt{3}/2 & 1/2 \end{pmatrix}$

Table 2.1: Young's natural, seminormal, and orthogonal form (denoted by R_{nat}, R_{semi}, and R_{orth}, respectively) for the two-dimensional irrep  of the symmetric group S_3.

2.8.3. Theorem (Young–Yamanouchi basis). *For any irrep $\lambda \in \widehat{\mathbb{C}\mathrm{S}_n}$, a transposition σ_i acts on a given path $T \in \mathrm{Paths}(\lambda, \mathscr{Y})$ as follows:*

$$\psi_\lambda(\sigma_i)\,|T\rangle = \frac{1}{r_i(T)}\,|T\rangle + \sqrt{1 - \frac{1}{r_i(T)^2}}\,|\sigma_i T\rangle \qquad \text{for } i \neq n, \tag{2.75}$$

where $\sigma_i T$ denotes the path T with vertex T^i at level i replaced by $T^{i-1} \cup (T^{i+1} \setminus T^i)$.

An example of this theorem in action is presented in the last row of Table 2.1. Somewhat confusingly, for historical reasons this basis can be referred to by three different names: "Young's orthogonal form", "Young–Yamanouchi basis", and "Gelfand–Tsetlin basis".

Finally, we mention that the primitive idempotents from Section 2.7.5 corresponding to the Young–Yamanouchi basis are *Young symmetrisers*, see [DLS18; Sag13]. Young symmetrisers historically were constructed before the general algorithm in Section 2.7.5 was developed.

2.9 Representation theory of GL_d and U_d.

In this section, we summarize the representation theory of complex *general linear groups* GL_d and *unitary groups* U_d, which are defined as follows:

$$\mathrm{GL}_d := \{g \in \mathrm{End}(\mathbb{C}^d) \mid \det g \neq 0\}, \tag{2.76}$$

$$\mathrm{U}_d := \{g \in \mathrm{GL}_d \mid gg^\dagger = I\}. \tag{2.77}$$

There are two important subgroups inside both of them: *special linear* SL_d and *special unitary groups* SU_d, which are defined as

$$\mathrm{SL}_d := \{g \in \mathrm{GL}_d \mid \det g = 1\}, \tag{2.78}$$

$$\mathrm{SU}_d := \{g \in \mathrm{U}_d \mid \det g = 1\}. \tag{2.79}$$

Complex general linear group GL_d and special linear group SL_d both can be seen from different viewpoints as *real Lie groups*, or *complex Lie groups*, or *linear algebraic groups*. These three structures highlight different nature of the group seen as a real smooth manifold, a complex-analytic manifold, or an affine algebraic variety, respectively. Correspondingly, this group can

be studied through the lens of differential geometry or via algebraic geometry. In contrast, both U_d and SU_d, which are important subgroups of GL_d, are only real Lie groups, since the complex conjugation in their definition obstructs them to be complex Lie groups or linear algebraic groups. We are not going to review the corresponding theories in full detail, since it is a hopeless task for the thesis format. We merely summarize the main aspects of their representation theory.

Topology

Topologically, GL_d is connected, not simply connected and non-compact. SL_d is connected, simply connected and non-compact. U_d is connected, not simply connected and compact; it can be seen as maximal compact subgroup of GL_d. SU_d is compact and simply connected Lie group; it can be seen as maximal compact subgroup of SL_d.

Categories of Representations

Before delving into the representation theory of these groups, it is crucial to distinguish between different categories of representations: *continuous*, *smooth*, *analytic*, and *algebraic*. For a Lie group G, a representation $\phi : G \to \mathrm{End}(V)$ is called

- *continuous* if the map ϕ is continuous with respect to the given topology on G,
- *smooth* if ϕ is infinitely differentiable,
- *analytic* if ϕ is real-analytic if G is a real Lie group, or complex-analytic if G is a complex Lie group,
- *algebraic* if G is an algebraic group and ϕ is a morphism of algebraic varieties; that is, the matrix entries of $\phi(g)$ are rational functions in the entries of g.

For compact Lie groups like U_d and SU_d, all finite-dimensional continuous representations are automatically smooth and analytic due to the compactness and smooth manifold structure of these groups. In contrast, for GL_d, which is a complex algebraic group, we are particularly interested in *algebraic representations*, where the action is given by polynomial or rational functions. In this thesis, we focus on finite-dimensional representations, primarily smooth and algebraic ones, as they are the most relevant for the study of GL_d, SL_d, U_d, and SU_d.

Lie algebras and highest weights

Representation theory of Lie groups and linear algebraic groups is intimately connected with representation theory of their *Lie algebras*. The Lie algebra $\mathfrak{g}$, defined as the tangent space at the identity element of its associated Lie group G, carries a bilinear operation known as the *Lie bracket*.

2.9.1. Definition (Lie algebra). A *Lie algebra* over $\mathbb{C}$ is a vector space $\mathfrak{g}$ together with a binary operation called the *Lie bracket*, denoted by

$$[\cdot, \cdot] : \mathfrak{g} \times \mathfrak{g} \to \mathfrak{g}, \tag{2.80}$$

which satisfies the following properties for all $x, y, z \in \mathfrak{g}$:

1. bilinearity: $[ax + by, z] = a[x, z] + b[y, z], \quad \forall a, b \in \mathbb{C}$,
2. antisymmetry: $[x, y] = -[y, x]$,

3. Jacobi identity: $[x,[y,z]]+[y,[z,x]]+[z,[x,y]]=0$.

Assume G is a connected reductive linear algebraic group (such as GL_d) with Lie algebra $\mathfrak{g}$. To study a representation $R\colon G\to\mathrm{End}(V)$ of a Lie group G, by analogy with Definition 2.7.5, it is natural to understand how a given representation R restricts to *maximal abelian subgroup* T of a *maximal compact subgroup* of G. T is called a *torus* of G and its Lie algebra is denoted by $\mathfrak{t}$ with complexification $\mathfrak{h}$. We can naturally restrict the action of $\mathfrak{g}$ on V to that of $\mathfrak{h}$ to obtain a *weight* decomposition of V:

$$V=\bigoplus_{\omega\in L}V_\omega, \tag{2.81}$$

where $L\subseteq\mathfrak{h}^*$ is a *weight lattice* and $\mathfrak{h}^*:=\mathrm{Hom}(\mathfrak{h},\mathbb{C})$. The classification of irreducible representations of Lie groups relies on the concept of *highest weights*. Intuitively, highest weights are special weights that label the "top" or "dominant" state in an irreducible representation, from which all other (lower) weights are generated by applying lowering operators in the Lie algebra, see [FH91] for more details.

For the group GL_d, the highest weights are elements $\lambda=(\lambda_1,\dots,\lambda_d)\in\mathbb{Z}^d$ satisfying $\lambda_1\geqslant\lambda_2\geqslant\cdots\geqslant\lambda_d$. These weights classify the irreducible representations, often referred to as *Weyl modules* W_λ:

$$\widehat{\mathrm{GL}}_d=\{\lambda=(\lambda_1,\dots,\lambda_d)\in\mathbb{Z}^d\mid\lambda_1\geqslant\lambda_2\geqslant\cdots\geqslant\lambda_d\}. \tag{2.82}$$

In the context of polynomial representations, the highest weights correspond to partitions (Young diagrams) with at most d parts:

$$\widehat{\mathrm{GL}}_d\big|_{\mathrm{poly}}=\{\lambda\vdash n\mid\ell(\lambda)\leqslant d,n\in\mathbb{Z}_{\geqslant0}\}. \tag{2.83}$$

Here, it is customary to pad partitions with zeros to the right, ensuring that each λ consists of exactly d integers. We provide some examples of common irreps of GL_d.

2.9.2. Example (Defining representation). Highest weight $\lambda=(1,0,\dots,0)$ corresponds to Young diagram $\square$ and labels the following irrep $\phi_\square\colon\mathrm{GL}_d\to\mathrm{End}(\mathbb{C}^d)$ for every $g\in\mathrm{GL}_d$:

$$\phi_\square(g):=g. \tag{2.84}$$

2.9.3. Example (Dual of the defining representation). Highest weight $\lambda=(0,0,\dots,-1)$, which we label by $\bar{\square}$, corresponds to the following irrep $\phi_{\bar\square}\colon\mathrm{GL}_d\to\mathrm{End}(\mathbb{C}^d)$ for every $g\in\mathrm{GL}_d$:

$$\phi_{\bar\square}(g):=(g^{-1})^{\mathsf{T}}. \tag{2.85}$$

2.9.4. Example (Determinant irrep). Highest weight $\lambda=(1,1,\dots,1)=(1^d)$ corresponds to the following irreducible representation:

$$\phi_{(1^d)}(g):=\det(g). \tag{2.86}$$

Moreover, for GL_d any rational representation $\mu\in\widehat{\mathrm{GL}}_d$ is of the form $\mu=\det^k\cdot\lambda$ for certain $k\in\mathbb{Z}$ and $\lambda\in\widehat{\mathrm{GL}}_d\big|_{\mathrm{poly}}$.

Similarly, the irreducible representations of U_d and SU_d are also classified by highest weights:

$$\widehat{\mathrm{U}}_d=\{\lambda=(\lambda_1,\dots,\lambda_d)\in\mathbb{Z}^d\mid\lambda_1\geqslant\lambda_2\geqslant\cdots\geqslant\lambda_d\}, \tag{2.87}$$

$$\widehat{\mathrm{SU}}_d=\{\lambda=(\lambda_1,\dots,\lambda_{d-1})\in\mathbb{Z}^{d-1}\mid\lambda_1\geqslant\lambda_2\geqslant\cdots\geqslant\lambda_{d-1}\geqslant0\}. \tag{2.88}$$

Lie Algebra Representations and Gelfand–Tsetlin Bases

Simple modules of the Lie algebra $\mathfrak{gl}_d$ correspond to the Weyl modules W_λ of the group GL_d. Although constructing explicit actions of GL_d in a Gelfand–Tsetlin basis is challenging, it is more manageable to construct such bases for simple modules of $\mathfrak{gl}_d$. In Section 2.9.2, we discuss the Gelfand–Tsetlin basis for these modules.

The Gelfand–Tsetlin basis arises from a combinatorial object known as *Gelfand–Tsetlin pattern*, which provides a convenient way to label basis vectors in the representation spaces of $\mathfrak{gl}_d$ and GL_d. Each valid Gelfand–Tsetlin pattern corresponds to a basis vector in the Weyl module W_λ. This combinatorial approach provides a powerful tool for studying representations of $\mathfrak{gl}_d$ and, by extension, GL_d through the exponential map. By constructing the Gelfand–Tsetlin basis for the Lie algebra $\mathfrak{gl}_d$, we effectively construct it for the group GL_d as well.

2.9.1 Gelfand–Tsetlin patterns

It turns out that the family $\mathrm{GL}_1 \hookrightarrow \mathrm{GL}_2 \hookrightarrow \cdots \hookrightarrow \mathrm{GL}_{d-2} \hookrightarrow \mathrm{GL}_d$ is multiplicity-free [VK92], meaning that we can label the Gelfand–Tsetlin basis for this family as a tuple

$$(\mathbf{m}_1, \mathbf{m}_2, \ldots, \mathbf{m}_{d-1}, \mathbf{m}_d),$$

where $\mathbf{m}_i$ is a highest weight for GL_i. We can arrange this tuple into a *Gelfand–Tsetlin pattern* M of shape λ and length d, which is represented by a triangular table with d rows and i integers in the i-th row (when counted from the bottom):

$$M = \begin{bmatrix} m_{1,d} & & m_{2,d} & & \cdots & & m_{d-1,d} & & m_{d,d} \\ & m_{1,d-1} & & & \cdots & & & m_{d-1,d-1} & \\ & & \ddots & & \vdots & & \iddots & & \\ & & & m_{1,2} & & m_{2,2} & & & \\ & & & & m_{1,1} & & & & \end{bmatrix} = \begin{bmatrix} \mathbf{m}_d \\ \mathbf{m}_{d-1} \\ \vdots \\ \mathbf{m}_2 \\ \mathbf{m}_1 \end{bmatrix}, \tag{2.89}$$

where $\mathbf{m}_j := (m_{1,j}, \ldots, m_{j,j}) \in \mathbb{Z}^j$ denotes the j-th row of M. The entries $m_{i,j}$ of M are subject to the following constraints: the top row of M is equal to λ, i.e., $\mathbf{m}_d = (m_{1,d}, \ldots, m_{d,d}) = (\lambda_1, \ldots, \lambda_d)$, and all entries $m_{i,j}$ satisfy the so-called *interlacing* or *in-betweenness* condition:

$$m_{i,j} \geqslant m_{i,j-1} \geqslant m_{i+1,j} \quad \text{for all} \quad 1 \leqslant i < j \leqslant d. \tag{2.90}$$

We will write $\mathbf{m}_{j-1} \sqsubseteq \mathbf{m}_j$ as a shorthand for the interlacing relations (2.90) between vectors $\mathbf{m}_{j-1}$ and $\mathbf{m}_j$. Then all constraints on $m_{i,j}$ can be concisely summarised as

$$\mathbf{m}_1 \sqsubseteq \mathbf{m}_2 \sqsubseteq \ldots \sqsubseteq \mathbf{m}_d. \tag{2.91}$$

We denote by $M_{[k]}$ a smaller Gelfand–Tsetlin pattern which consists of the first k rows of the original pattern M:

$$M_{[k]} := \begin{bmatrix} \mathbf{m}_k \\ \vdots \\ \mathbf{m}_1 \end{bmatrix}. \tag{2.92}$$

We will denote the set of all Gelfand–Tsetlin patterns of shape λ and length d by $\mathrm{GT}(\lambda, d)$ or simply by $\mathrm{GT}(\lambda)$, since we will always assume that λ is padded to the rank d of the corresponding Lie group GL_d. However, sometimes it will be important to highlight d and we will use notation $\mathrm{GT}(\lambda, d)$ in that cases.

For any partition λ of length d, the Gelfand–Tsetlin patterns $\mathrm{GT}(\lambda)$ are in one-to-one correspondence with semistandard Young tableaux $\mathrm{SSYT}(\lambda)$:

$$m_\lambda := \dim W_\lambda = |\mathrm{GT}(\lambda)| = |\mathrm{SSYT}(\lambda)|, \tag{2.93}$$

where we assumed $m_{i,j} \geqslant 0$ for every entry of the Gelfand–Tsetlin pattern $M \in \mathrm{GT}(\lambda)$. Indeed, for any tableau $T \in \mathrm{SSYT}(\lambda)$ let $m_{i,j}$ be the number of symbols from $[j]$ in the i-th row of T. Equivalently, $\mathbf{m}_j \subseteq \lambda$ is the shape of the subtableau of T formed by entries less than or equal to j. Then Eq. (2.89) constitutes the Gelfand–Tsetlin pattern of tableau T. For example, the Gelfand–Tsetlin patterns corresponding to the semistandard Young tableaux in Eq. (2.46) are

$$M_1 = \begin{bmatrix} 3 & & 1 \\ & 3 & \end{bmatrix}, \qquad M_2 = \begin{bmatrix} 3 & & 1 \\ & 2 & \end{bmatrix}, \qquad M_3 = \begin{bmatrix} 3 & & 1 \\ & 1 & \end{bmatrix}, \tag{2.94}$$

which are in fact all Gelfand–Tsetlin patterns $\mathrm{GT}(\lambda)$ for $\lambda = (3,1)$. Conversely, given any Gelfand–Tsetlin pattern M, the corresponding semistandard tableau T has shape $\lambda = \mathbf{m}_d$ given by the d-th row of M, while the filling of the i-th row of T can be deduced from the i-th diagonal of M. Indeed, $m_{i,j} - m_{i,j-1}$ is the number of j's in the i-th row of T.

The *weight* of Gelfand–Tsetlin pattern M consists of differences of consecutive row sums:

$$w(M) := \big(w(\mathbf{m}_1), w(\mathbf{m}_2) - w(\mathbf{m}_1), \dots, w(\mathbf{m}_d) - w(\mathbf{m}_{d-1})\big) \quad \text{where} \quad w(\mathbf{m}_j) := \sum_{i=1}^{j} m_{i,j}. \tag{2.95}$$

Notice that the weight of a Gelfand–Tsetlin pattern coincides with the weight (2.48) of the corresponding semistandard Young tableaux. For example, patterns (2.94) have weights $(3,1)$, $(2,2)$, and $(1,3)$, respectively.

2.9.2 Gelfand–Tsetlin basis for $\mathfrak{gl}_d$

The Lie algebra of GL_d turns out to be the full matrix algebra:

$$\mathfrak{gl}_d = \mathrm{End}(\mathbb{C}^d). \tag{2.96}$$

The matrices $E_{ik} := |i\rangle\langle k|$, $1 \leqslant i,k \leqslant d$, form a basis of the Lie algebra $\mathfrak{gl}_d$. They satisfy the following commutation relations:

$$[E_{ik}, E_{js}] = 0 \quad \text{if} \quad i \neq s, \quad k \neq j, \tag{2.97}$$
$$[E_{ik}, E_{kk}] = E_{ik} \quad \text{if} \quad i \neq k, \tag{2.98}$$
$$[E_{ik}, E_{ki}] = E_{ii} - E_{kk}. \tag{2.99}$$

The explicit action of the generators E_{ik} on the Weyl modules W_λ was obtained by Gelfand and Tsetlin [GT50]. They showed that the following explicit formulas satisfy the commutation relations in Eqs. (2.97) to (2.99):

2.9.5. Theorem (p. 363 of [VK92]). *Consider the Weyl module W_λ with the basis labelled by Gelfand–Tsetlin patterns $M \in \mathrm{GT}(\lambda)$. Let $\ell_{p,q} := m_{p,q} - p$ and set*

$$a^j_{p-1} = \left(\frac{\prod_{i=1}^{p} (\ell_{i,p} - \ell_{j,p-1}) \prod_{i=1}^{p-2} (\ell_{i,p-2} - \ell_{j,p-1} - 1)}{\prod_{i \neq j} (\ell_{i,p-1} - \ell_{j,p-1})(\ell_{i,p-1} - \ell_{j,p-1} - 1)} \right)^{1/2}, \tag{2.100}$$

$$b^j_{p-1} = \left(\frac{\prod_{i=1}^{p} (\ell_{i,p} - \ell_{j,p-1} + 1) \prod_{i=1}^{p-2} (\ell_{i,p-2} - \ell_{j,p-1})}{\prod_{i \neq j} (\ell_{i,p-1} - \ell_{j,p-1})(\ell_{i,p-1} - \ell_{j,p-1} + 1)} \right)^{1/2}. \tag{2.101}$$

Denote the Gelfand–Tsetlin pattern M in which $m_{j,p-1}$ is replaced with $m_{j,p-1} \pm 1$ by $M^{\pm j}_{p-1}$. Then the Gelfand–Tsetlin formulas for the action of the operators $E_{p-1,p}$, $E_{p,p-1}$, $2 \leqslant p \leqslant d$, and E_{pp}, $1 \leqslant p \leqslant d$, are as follows:

$$E_{p-1,p}|M\rangle = \sum_{j=1}^{p} a^j_{p-1}|M^{+j}_{p-1}\rangle, \tag{2.102}$$

$$E_{p,p-1}|M\rangle = \sum_{j=1}^{p} b^j_{p-1}|M^{-j}_{p-1}\rangle, \tag{2.103}$$

$$E_{p,p}|M\rangle = \left(\sum_{i=1}^{p} m_{i,p} - \sum_{j=1}^{p-1} m_{j,p-1}\right)|M\rangle. \tag{2.104}$$

The other operators $E_{p,q}$ are obtained with the help of relations Eqs. (2.97) to (2.99).

2.9.3 Tensor product decompositions

Understanding how tensor products of irreducible representations decompose into direct sums of irreducible representations is a fundamental aspect of the representation theory of GL_d. This decomposition is governed by combinatorial coefficients known as *Littlewood–Richardson coefficients*. In this section, we introduce these coefficients and discuss their role in the representation theory of GL_d.

Let W_λ and W_μ be two Weyl modules of GL_d corresponding to highest weights λ and μ of polynomial representations of GL_d. Their tensor product $W_\lambda \otimes W_\mu$ is, in general, a reducible representation of GL_d. It decomposes into a direct sum of irreducible representations as follows:

$$W_\lambda \otimes W_\mu \cong \bigoplus_{\nu \vdash_d |\lambda|+|\mu|} W_\nu \otimes \mathbb{C}^{c^\nu_{\lambda\mu}}, \tag{2.105}$$

where the sum is over all partitions ν of size $|\nu| = |\lambda| + |\mu|$, and $c^\nu_{\lambda\mu} \in \mathbb{Z}_{\geqslant 0}$ are the Littlewood–Richardson coefficients. When $c^\nu_{\lambda\mu} = 0$ the convention is that the corresponding irrep W_ν does not appear as a direct summand in Eq. (2.105). The precise statement on how to compute general Littlewood–Richardson coefficients can be found in [FH91]. Importantly for our thesis, in the special case when μ is a single row or column there is a simple formula for $c^\nu_{\lambda\mu}$ known as *Pieri's Rule*.

2.9.6. Theorem (Pieri's Rule [FH91]). *If μ has only one row, i.e. $\mu = (n)$, the Littlewood–Richardson coefficient $c^\nu_{\lambda\mu} = 1$ if the Young diagram ν can be obtained from λ by adding n boxes such that no two of them are added in the same column; otherwise $c^\nu_{\lambda\mu} = 0$. Similarly, if μ' has only one column, i.e. $\mu' = (1^n)$, then $c^\nu_{\lambda\mu} = 1$ if the Young diagram ν can be obtained from λ by adding n boxes such that no two of them are added in the same row; otherwise $c^\nu_{\lambda\mu} = 0$.*

Equation (2.105) only refers to the multiplicities in the decomposition of the tensor product. However, how can we find an explicit basis change achieving this decomposition when given Gelfand–Tsetlin bases in the Weyl modules W_λ and W_μ? The answer is given in the form of *Clebsch–Gordan coefficients*, also known as *Wigner coefficients* [BL68]. The transformation $\mathrm{CG}_{\lambda,\mu}$ achieving this is called *Clebsch–Gordan transform*: for any $g \in \mathrm{GL}_d$,

$$\mathrm{CG}_{\lambda,\mu}\big(R_\lambda(g) \otimes R_\mu(g)\big)\,\mathrm{CG}^\dagger_{\lambda,\mu} = \bigoplus_{\nu \vdash_d |\lambda|+|\mu|} R_\nu(g) \otimes I_{c^\nu_{\lambda\mu}}, \tag{2.106}$$

where R_λ, R_μ, R_ν are the corresponding irreps of GL_d. The Clebsch–Gordan coefficients, which are matrix entries of a Clebsch–Gordan transform $\mathrm{CG}_{\lambda,\mu}$, can be obtained from Eqs. (2.102)

to (2.104) for matrix elements of $\mathfrak{gl}_d$ generators in the Gelfand–Tsetlin basis [VK92]. In Section 4.A.1, we describe a special class of Clebsch–Gordan coefficients for GL_d (or equivalently for U_d) corresponding to arbitrary λ and $\mu = (1, 0, \dots, 0)$ or $\mu = (0, \dots, 0, -1)$.

2.10 Schur–Weyl duality

Schur–Weyl duality reveals a connection between the general linear group GL_d and the symmetric group S_n through their actions on tensor spaces $(\mathbb{C}^d)^{\otimes n}$. This duality was first established by Issai Schur in [Sch27]. Schur's original motivation was to understand the decomposition of tensor powers of the standard representation of GL_d into irreducible components. He discovered that the actions of GL_d and S_n on the tensor space $(\mathbb{C}^d)^{\otimes n}$ commute and that their centralisers are mutual centralisers within the matrix algebra $\mathrm{End}((\mathbb{C}^d)^{\otimes n})$. This means that the algebra generated by the action of GL_d is the commutant of the group algebra $\mathbb{C}\mathrm{S}_n$ acting via permutation of tensor factors, and vice versa.

Hermann Weyl later expanded upon Schur's work in the 1930s, incorporating it into the broader context of Lie group representations and invariant theory. Weyl recognised the significance of this duality in understanding the representation theory of classical groups and utilised it extensively in [Wey46]. The Schur–Weyl duality not only provides a clear framework for decomposing tensor spaces into irreducible representations but also establishes a bridge between the representation theories of finite groups and continuous groups.

Over the years, the Schur–Weyl duality has been generalised and extended to various settings, including quantum groups and Hecke algebras. The duality also plays a crucial role in theoretical physics, particularly in quantum mechanics and quantum information theory, where it aids in the analysis of symmetries and entanglement in multi-particle systems. For more background, see [FH91; GW98; Eti+11; Har05].

One way to view Schur–Weyl duality is through the lens of the *double centraliser theorem*, see [Eti+11, Theorem 4.54].

2.10.1. Theorem (Double centraliser). *Let V be a finite-dimensional vector space over $\mathbb{C}$, and let $\mathcal{A} \subseteq \mathrm{End}(V)$ be a matrix subalgebra of the full matrix algebra on V. Then the double commutant of $\mathcal{A}$ satisfies:*

$$\mathcal{A} = \mathcal{A}'', \tag{2.107}$$

where $\mathcal{A}' := \mathrm{End}_{\mathcal{A}}(V)$ is the commutant of $\mathcal{A}$ in $\mathrm{End}(V)$, and $\mathcal{A}'' = (\mathcal{A}')'$.

To proceed, we need to define the action of GL_d on tensor space. A natural way for GL_d to act on $(\mathbb{C}^d)^{\otimes n}$ is by applying an identical operator on each tensor factor. This is captured by the *tensor representation* $\phi_n^d \colon \mathrm{GL}_d \to \mathrm{End}((\mathbb{C}^d)^{\otimes n})$ defined as

$$\phi_n^d(U) := U^{\otimes n}, \tag{2.108}$$

for all $U \in \mathrm{GL}_d$. Let us denote the algebra generated by the image of U_d under ϕ_n^d by

$$\mathcal{U}_n^d := \mathrm{span}_{\mathbb{C}}\{\phi_n^d(U) \,|\, U \in \mathrm{U}_d\}. \tag{2.109}$$

It turns out that we could have instead considered the span over GL_d, SU_d or SL_d instead of U_d—the result would not change.

2.10.2. Lemma. *Let ϕ_n^d be the map from Eq. (2.108) and $\mathcal{U}_n^d$ the algebra defined in Eq. (2.109). Then*

$$\mathcal{U}_n^d = \mathrm{span}_{\mathbb{C}}\{\phi_n^d(U) \,|\, U \in \mathrm{GL}_d\} = \mathrm{span}_{\mathbb{C}}\{\phi_n^d(U) \,|\, U \in \mathrm{SL}_d\} = \mathrm{span}_{\mathbb{C}}\{\phi_n^d(U) \,|\, U \in \mathrm{SU}_d\}. \tag{2.110}$$

Proof:
For the purposes of the proof, we label

$$\mathcal{SU}_n^d := \operatorname{span}_{\mathbb{C}}\{\phi_n^d(U) \mid U \in \mathrm{SU}_d\}, \qquad \mathcal{GL}_n^d := \operatorname{span}_{\mathbb{C}}\{\phi_n^d(U) \mid U \in \mathrm{GL}_d\}. \tag{2.111}$$

From $\mathrm{SU}_d \subset \mathrm{U}_d \subset \mathrm{GL}_d$ we easily see that

$$\mathcal{SU}_n^d \subseteq \mathcal{U}_n^d \subseteq \mathcal{GL}_n^d. \tag{2.112}$$

We need to show the inverse inclusions in Eq. (2.112) to obtain the desired result.

Firstly, any $U \in \mathrm{U}_d$ can be written as $U = e^{i\theta}V$ for some $V \in \mathrm{SU}_d$ and $\theta \in \mathbb{R}$. It means that $\phi_n^d(U) = \phi_n^d(e^{i\theta}V) = e^{in\theta}V^{\otimes n} = e^{in\theta}\phi_n^d(V)$, so we can rewrite any linear combination of $\phi_n^d(U)$ as a linear combination of $\phi_n^d(V)$ for special unitaries V. That shows $\mathcal{U}_n^d \subseteq \mathcal{SU}_n^d$.

Secondly, we would like to write $M^{\otimes n}$ for arbitrary $M \in \mathrm{GL}_d$ as a linear combination of $U^{\otimes n}$ for $U \in \mathrm{U}_d$. To show that it is possible we present the argument from [Aub18]. Without loss of generality, we can take $M \in \mathrm{GL}_d$ to have the following singular value decomposition:

$$M = \sum_{i=1}^{d} s_i |e_i\rangle\langle f_i|, \tag{2.113}$$

where $\{|e_i\rangle\}_{i=1}^d$ and $\{|f_i\rangle\}_{i=1}^d$ are some orthonormal bases of $\mathbb{C}^d$, and $0 < s_i < 1$ for every $i \in [d]$. Cauchy's formula tells us that for $|s| < 1$ we have the following contour integral

$$s = \frac{1}{2\pi i} \oint_{\Gamma} z \, \frac{\mathrm{d}z}{z - s}, \tag{2.114}$$

where Γ denotes the unit circle in the complex plane $\mathbb{C}$. By defining

$$U_{z_1,\ldots,z_d} := \sum_{i=1}^{d} z_i |e_i\rangle\langle f_i| \tag{2.115}$$

and using Cauchy's formula together with Fubini's theorem,

$$M^{\otimes n} = \sum_{i_1=1}^{d} \cdots \sum_{i_n=1}^{d} s_{i_1} \ldots s_{i_n} |e_{i_1}, \ldots, e_{i_n}\rangle\langle f_{i_1}, \ldots, f_{i_n}| \tag{2.116}$$

$$= \sum_{i_1,\ldots,i_n=1}^{d} \frac{1}{(2\pi i)^n} \oint_{\Gamma^n} z_{i_1} \ldots z_{i_n} \, \frac{\mathrm{d}z_{i_1}}{z_{i_1} - s_{i_1}} \cdots \frac{\mathrm{d}z_{i_n}}{z_{i_n} - s_{i_n}} |e_{i_1}, \ldots, e_{i_n}\rangle\langle f_{i_1}, \ldots, f_{i_n}| \tag{2.117}$$

$$= \frac{1}{(2\pi i)^n} \oint_{\Gamma^n} U_{z_1,\ldots,z_d}^{\otimes n} \, \frac{\mathrm{d}z_{i_1}}{z_{i_1} - s_{i_1}} \cdots \frac{\mathrm{d}z_{i_n}}{z_{i_n} - s_{i_n}}, \tag{2.118}$$

which shows that $\mathcal{GL}_n^d \subseteq \mathcal{U}_n^d$.

Finally, since $\mathrm{SU}_d \subset \mathrm{SL}_d \subset \mathrm{GL}_d$ and $\mathcal{SU}_n^d = \mathcal{GL}_n^d = \mathcal{U}_n^d$ then $\mathcal{U}_n^d = \operatorname{span}_{\mathbb{C}}\{\phi_n^d(U) \mid U \in \mathrm{SL}_d\}$ as well. □

Recall from Eq. (2.71) that $\mathcal{A}_n^d$ denotes the permutation matrix algebra on n qudits of dimension d, and recall from Eq. (2.23) that $\operatorname{End}_{\mathcal{A}_n^d}((\mathbb{C}^d)^{\otimes n})$ denotes the centraliser of $\mathcal{A}_n^d$ in $\operatorname{End}((\mathbb{C}^d)^{\otimes n})$, i.e., all matrices in $\operatorname{End}((\mathbb{C}^d)^{\otimes n})$ that commute with $\mathcal{A}_n^d$. One way to state the Schur–Weyl duality is that $\mathcal{U}_n^d$ is the centraliser of $\mathcal{A}_n^d$, and vice versa.

2.10.3. THEOREM (Schur–Weyl duality). *The algebra $\mathcal{U}_n^d$ is the centraliser algebra of $\mathcal{A}_n^d$ in* $\mathrm{End}((\mathbb{C}^d)^{\otimes n})$ *and vice versa, i.e.,*

$$\mathcal{U}_n^d = \mathrm{End}_{\mathcal{A}_n^d}((\mathbb{C}^d)^{\otimes n}), \qquad \mathcal{A}_n^d = \mathrm{End}_{\mathcal{U}_n^d}((\mathbb{C}^d)^{\otimes n}). \tag{2.119}$$

Moreover, when $d \geqslant n$ the representation ψ_n^d is faithful, i.e., $\mathcal{A}_n^d \cong \mathbb{C}\mathrm{S}_n$.

Equivalently, in more practical terms we can reformulate this statement as follows: there exists a Schur transform *unitary U_{Sch} such that for every $\sigma \in \mathrm{S}_n$ and $u \in \mathrm{U}_d$:*

$$U_{\mathrm{Sch}}\, \phi_n^d(u)\, U_{\mathrm{Sch}}^\dagger = \bigoplus_{\lambda \in \widehat{\mathcal{A}}_n^d} I_\lambda \otimes \phi_\lambda(u), \qquad U_{\mathrm{Sch}}\, \psi_n^d(\sigma)\, U_{\mathrm{Sch}}^\dagger = \bigoplus_{\lambda \in \widehat{\mathcal{A}}_n^d} \psi_\lambda(\sigma) \otimes I_\lambda, \tag{2.120}$$

where $\phi_\lambda \colon \mathrm{U}_d \to \mathrm{End}(W_\lambda)$ and $\psi_\lambda \colon \mathrm{S}_n \to \mathrm{End}(V_\lambda)$ are irreps of U_d and S_n respectively, i.e. V_λ is a Specht module and W_λ is a Weyl module. In other words, the vector space $(\mathbb{C}^d)^{\otimes n}$ seen as a representation of $\mathcal{A}_n^d \times \mathcal{U}_n^d$ decomposes into its irreducible rperesentations as

$$(\mathbb{C}^d)^{\otimes n} \simeq \bigoplus_{\lambda \in \widehat{\mathcal{A}}_n^d} V_\lambda \otimes W_\lambda. \tag{2.121}$$

Note that Eq. (2.121) implies to following remarkable combinatorial identity:

$$d^n = \sum_{\lambda \vdash_d n} d_\lambda m_\lambda. \tag{2.122}$$

The Schur transform U_{Sch} plays important role in quantum information. We explain the construction of U_{Sch} in Chapter 4 where U_{Sch} appears as a special case of *mixed Schur transform*. To get a feeling how U_{Sch} looks like, let's consider the simplest non-trivial case.

2.10.4. EXAMPLE ($n = 2$ and $d = 2$). Since $\mathrm{S}_2 = \{e, (12)\}$, the algebra $\mathcal{A}_2^2$ is generated correspondingly by the identity matrix and SWAP:

$$\mathcal{A}_2^2 := \left\{ x \begin{pmatrix} 1 & 0 & 0 & 0 \\ 0 & 1 & 0 & 0 \\ 0 & 0 & 1 & 0 \\ 0 & 0 & 0 & 1 \end{pmatrix} + y \begin{pmatrix} 1 & 0 & 0 & 0 \\ 0 & 0 & 1 & 0 \\ 0 & 1 & 0 & 0 \\ 0 & 0 & 0 & 1 \end{pmatrix} \,\middle|\, x, y \in \mathbb{C} \right\}, \tag{2.123}$$

whereas $\mathcal{U}_2^2$ is generated by tensor squares of unitary matrices:

$$\mathcal{U}_2^2 := \mathrm{span}_{\mathbb{C}} \left\{ \begin{pmatrix} a & b \\ c & d \end{pmatrix} \otimes \begin{pmatrix} a & b \\ c & d \end{pmatrix} \,\middle|\, \begin{pmatrix} a & b \\ c & d \end{pmatrix} \in \mathrm{U}(2) \right\}. \tag{2.124}$$

Using the two-qubit Schur transform [Har05, p. 121]

$$U_{\mathrm{Sch}} := \begin{pmatrix} 0 & 1/\sqrt{2} & -1/\sqrt{2} & 0 \\ 1 & 0 & 0 & 0 \\ 0 & 1/\sqrt{2} & 1/\sqrt{2} & 0 \\ 0 & 0 & 0 & 1 \end{pmatrix}, \tag{2.125}$$

we can simultaneously block-diagonalize both algebras:

$$U_{\mathrm{Sch}} \mathcal{A}_2^2 U_{\mathrm{Sch}}^{\mathsf{T}} = \left\{ \left(\begin{array}{c|ccc} x-y & 0 & 0 & 0 \\ \hline 0 & x+y & 0 & 0 \\ 0 & 0 & x+y & 0 \\ 0 & 0 & 0 & x+y \end{array} \right) \,\middle|\, x, y \in \mathbb{C} \right\}, \tag{2.126}$$

$$U_{\mathrm{Sch}} \mathcal{U}_2^2 U_{\mathrm{Sch}}^{\mathsf{T}} = \mathrm{span}_{\mathbb{C}} \left\{ \left(\begin{array}{c|ccc} ad-bc & 0 & 0 & 0 \\ \hline 0 & a^2 & \sqrt{2}ab & b^2 \\ 0 & \sqrt{2}ac & ad+bc & \sqrt{2}bd \\ 0 & c^2 & \sqrt{2}cd & d^2 \end{array} \right) \,\middle|\, \begin{pmatrix} a & b \\ c & d \end{pmatrix} \in \mathrm{U}(2) \right\}. \tag{2.127}$$

These algebras centralize each other since

$$U_{\mathrm{Sch}}\mathcal{A}_2^2 U_{\mathrm{Sch}}^{\mathsf{T}} = \mathbb{C} \oplus \mathbb{C}I_3, \qquad U_{\mathrm{Sch}}\mathcal{U}_2^2 U_{\mathrm{Sch}}^{\mathsf{T}} = \mathbb{C} \oplus \mathrm{End}(\mathbb{C}^3), \tag{2.128}$$

where the second equality follows from Burnside's theorem 2.4.6 since the 3×3 block in Eq. (2.127) is irreducible.

Chapter 3

Mixed Schur–Weyl duality

In this chapter, we present a generalisation of Schur–Weyl duality, commonly referred to as mixed Schur–Weyl duality, which plays an important role in various contexts within quantum information theory. This duality relates the walled Brauer algebra to a centraliser of a natural unitary group action on a mixed tensor space. The natural action of the walled Brauer algebra on tensor spaces gives rise to the partially transposed permutation matrix algebra, serving as a matrix representation of the diagrammatic walled Brauer algebra. In this chapter, we focus on the representation theory of the partially transposed permutation matrix algebra.

Our main technical result is the derivation of an explicit formula for the action of the walled Brauer algebra generators within the Gelfand–Tsetlin basis of the partially transposed permutation matrix algebra. This result extends the well-known Gelfand–Tsetlin basis for the symmetric group, also referred to as Young's orthogonal form or the Young–Yamanouchi basis. Furthermore, we provide a construction of both primitive and primitive central idempotents within the Gelfand–Tsetlin basis for partially transposed permutation matrix algebras.

The results in this chapter are based on [GO24; GBO23a].

3.1 Introduction

The main focus of this chapter is a variant of Schur–Weyl duality, known as *mixed Schur–Weyl duality*, which is equally important in quantum information as Schur–Weyl duality but has received less attention due to its more complicated nature. The simplest instance of mixed Schur–Weyl duality is for two qubits. Here, instead of the anti-symmetric singlet state $|\psi^-\rangle$ which one considers in Schur–Weyl duality, we single out the canonical maximally entangled state $|\phi^+\rangle := (|00\rangle + |11\rangle)/\sqrt{2}$. This state is invariant under the following unitary action $(U \otimes \bar{U})|\phi^+\rangle = |\phi^+\rangle$ for any $U \in \mathrm{U}_2$. In addition, $\mathrm{SWAP}^\Gamma|\phi^+\rangle = 2|\phi^+\rangle$ where $\mathrm{SWAP}^\Gamma = 2|\phi^+\rangle\langle\phi^+|$ denotes the partial transpose of SWAP. Similarly, the three-dimensional orthogonal complement of $|\phi^+\rangle$ is also invariant under the action of both $U \otimes \bar{U}$ and SWAP^Γ. Mixed Schur–Weyl duality generalises this observation by partitioning $(\mathbb{C}^d)^{n+m}$ into subspaces that are invariant under the unitary action $U^{\otimes n} \otimes \bar{U}^{\otimes m}$ and the matrix algebra $\mathcal{A}^d_{n,m}$ of partially transposed permutations that are transposed only on the last m systems [Koi89; Ben+94; Hal96; Nik07]. In particular, $[\mathcal{A}^d_{n,m}, U^{\otimes n} \otimes \bar{U}^{\otimes m}] = 0$ for all $U \in \mathrm{U}_d$. The usual Schur–Weyl duality corresponds to the special case when either $n = 0$ or $m = 0$.

Mixed Schur–Weyl duality appears in a variety of contexts, particularly in scenarios with multiple input and output systems such as quantum state purification [KW01b] and cloning [SIGA05; Fan+14; NPR21], port-based [MSSH18; SSMH17; Led22; Chr+21; SMK22] and multi-port-based teleportation [KMSH21; SMKH22; MSK21], and quantum algorithmic applications [BLMMO22]. This symmetry also occurs in situations that involve the partial transpose

on several systems, such as in entanglement detection [BCS20; BSH24], universality of qudit gate sets [SMZ22; DS23; SS23a], and U_d-equivariant quantum circuits [HLM21; ZLLSK23]. It is also relevant in high-energy physics [KR07; Can11].

Partially transposed permutations can be easily visualised as diagrams. The set of all partially transposed permutation diagrams under composition forms the *walled Brauer algebra* $\mathcal{B}^d_{n,m}$. The walled Brauer algebra $\mathcal{B}^d_{n,m}$ is a restricted version of the full Brauer algebra [Bra37], and a prominent example of a diagram algebra, which has been widely studied [Tur89; Koi89; Ben+94; Ben96; Nik07; Bul20] (see [Koe08] for a survey on Brauer and other diagram algebras). The characters of the walled Brauer algebra were first derived by Halverson [Hal96] (see also [Nik07]). Mixed Schur–Weyl duality was established in [Koi89; Ben+94], where the matrix algebra $\mathcal{A}^d_{n,m}$ of partially transposed permutations was first introduced.

The representation theory of walled Brauer algebras has been strongly influenced by representation theory of symmetric group algebras, which correspond to the special case when either $n = 0$ or $m = 0$.

In the context of quantum information, Young's orthogonal form is by far the most useful since it provides unitary matrices that can readily be used as operations in a quantum computer. In particular, irreps of this form are produced by the quantum Schur transform [Har05; Ber12]. Our goal in this chapter is to extend Young's orthogonal form from the symmetric group to the matrix algebra $\mathcal{A}^d_{n,m}$. In Chapter 4, we derive the corresponding mixed Schur transform that decomposes mixed tensor representation of $\mathcal{A}^d_{n,m}$ into irreps of this form.

While the diagrammatic walled Brauer algebra $\mathcal{B}^d_{n,m}$ is well studied, its matrix representation $\mathcal{A}^d_{n,m}$ has received much less attention. A key difficulty in studying $\mathcal{A}^d_{n,m}$ is the fact that it is a quotient of the walled Brauer algebra, and hence has a rather complicated description in terms of the walled Brauer diagrams. In addition, since $\mathcal{B}^d_{n,m}$ is not semisimple when $d < n + m - 1$ [CDDM08], it can be difficult to obtain results for $\mathcal{B}^d_{n,m}$ and then transfer them to $\mathcal{A}^d_{n,m}$ (which is always semisimple).

Our strategy hinges on the close connection between the walled Brauer algebra $\mathcal{B}^d_{n,m}$ and the group algebra $\mathbb{C}(\mathrm{S}_n \times \mathrm{S}_m)$ corresponding to its two symmetric subgroups. We will make use of the fact that $\mathcal{B}^d_{n,m}$ is generated by diagrams $\sigma_1, \ldots, \sigma_{n+m-1}$ [Nik07] shown in Eq. (3.10), where σ_i $(i \neq n)$ are *transpositions* of consecutive systems i and $i+1$ which generate $\mathrm{S}_n \times \mathrm{S}_m$, while the remaining generator σ_n *contracts* systems n and $n+1$ (see Definition 3.2.2 for more details). The matrix algebra $\mathcal{A}^d_{n,m}$ is generated by a matrix representation of these generators.

Results

Our main result in this chapter is Theorem 3.7.1, which provides an explicit construction of all irreducible representations of $\mathcal{A}^d_{n,m}$, the matrix algebra of partially transposed permutations on $n+m$ qudits. We provide a formula that allows to evaluate the irrep matrix entries on each of the generators, which by homomorphism and linearity fully determines the irrep on the rest of the algebra.

An important feature of our construction is that it provides irrep matrix entries in the Gelfand–Tsetlin basis. This basis has a recursive definition and hence is automatically adapted to a natural sequence of subalgebras obtained by including the generators σ_i one by one. This guarantees that the generators have a particularly sparse representation and gives a conceptually simple way to pinpoint their non-zero entries and describe their action.

3.1.1. Theorem (Qualitative statement of Theorem 3.7.1). *When evaluated on one of the generators, any irreducible representation of the matrix algebra $\mathcal{A}^d_{n,m}$ has the following form:*

- *Transpositions σ_i $(i \neq n)$ are represented by a direct sum of 1×1 and 2×2 blocks, where each 1×1 block is equal to ± 1, while for each 2×2 block there is a constant $r \in \mathbb{Z}$ such*

that the block is equal to

$$\begin{pmatrix} \frac{1}{r} & \sqrt{1-\frac{1}{r^2}} \\ \sqrt{1-\frac{1}{r^2}} & -\frac{1}{r} \end{pmatrix}, \tag{3.1}$$

which is an orthogonal reflection. The exact signs and values of r can be inferred from Young's orthogonal form for symmetric groups.

- *The contraction σ_n is represented by a direct sum of rank-1 matrices with eigenvalue d.*

When $n = 0$ or $m = 0$, our formula reduces to the well-known Young's orthogonal form for the symmetric group, see Theorem 2.8.3.

A concrete example of how all irreps of $\mathcal{A}^3_{3,2}$ look like in the Gelfand–Tsetlin basis is provided in Table 3.1. The main idea of the proof is that, thanks to this being the Gelfand–Tsetlin basis, we already know from Young's orthogonal form how all generators (except for the contraction σ_n) are supposed to act. We made an educated guess for the matrix representation of σ_n and verified that it indeed works. This requires checking that the matrix representations of all generators satisfy the walled Brauer algebra relations stated in Definition 3.2.2.

The second main result of this chapter is a construction of idempotents for the matrix algebra $\mathcal{A}^d_{n,m}$, which we adapt from Section 2.7. The main technical ingredient for this construction is Theorem 3.6.6.

Related work

Young's natural representation for the walled Brauer algebra has been constructed by Nikitin [Nik07], while Young's orthogonal form for the full Brauer algebra is described in [Naz96]. In addition, [ST17] has obtained a seminormal form for the q-deformed version of the walled Brauer algebra. However, taking the "classical" $q \to 1$ limit of their construction and renormalising the resulting basis vectors to obtain the corresponding orthogonal form is non-trivial. Moreover, their construction only works for semisimple walled Brauer algebras $\mathcal{B}^d_{n,m}$, so the problem of adapting their construction to $\mathcal{A}^d_{n,m}$ is still open. Motivated by applications to quantum information, previously the algebra $\mathcal{A}^d_{n,m}$ was studied in [ZKW07; SHM13; MHS14; MSH18] for the $m = 1$ case. Some aspects of it were also studied for general m in [SMKH22; MSK21]. In particular, [SMKH22] constructs the same action as in our Theorem 3.7.1, but not for very restricted class of irreducible representations. In this sense, our work generalises that of [SMKH22].

3.2 Walled Brauer algebra

Let $n, m \geqslant 0$ be integers and $d \in \mathbb{C}$ arbitrary[1]. The *walled Brauer algebra* $\mathcal{B}^d_{n,m}$ consists of formal complex linear combinations of diagrams, where each diagram has two rows of $n + m$ nodes each and a vertical *wall* between the first n and the last m nodes [Tur89; Koi89; Ben+94; Ben96; Nik07; Bul20]. All nodes are connected in pairs, and any two connected nodes are either on the same side of the wall and in different rows, or the other way around. For example, the following diagram

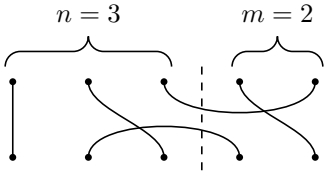

(3.2)

[1] We will later require $d \geqslant 2$ to be an integer as well.

belongs to $\mathcal{B}^d_{3,2}$. The addition in $\mathcal{B}^d_{n,m}$ is defined by simply adding the respective coefficients in the two formal linear combinations. Multiplication of two diagrams corresponds to their *concatenation* by identifying the bottom row of the first diagram with the top row of the second diagram. Any loops that may have appeared in this process are erased and the resulting diagram is multiplied by the scalar $d^{\#\text{loops}}$:

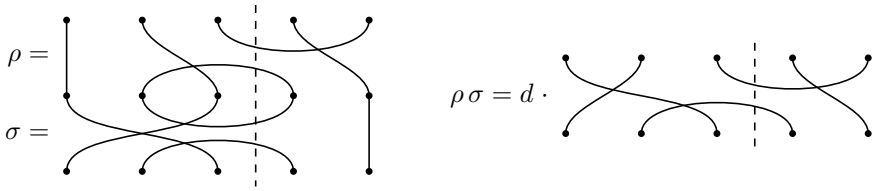

(3.3)

where parameter d of a walled Brauer algebra $\mathcal{B}^d_{n,m}$ explicitly appear. Multiplication of diagrams extends by linearity to multiplication in a walled Brauer algebra $\mathcal{B}^d_{n,m}$.

The walled Brauer algebra $\mathcal{B}^d_{n,m}$ itself is a subalgebra of the so-called full *Brauer algebra* $\mathcal{B}^d_{n+m}$ that is defined similarly but without the wall and with no restrictions on which pairs of nodes can be connected [Bra37]. This algebra was originally introduced by Richard Brauer for studying Schur–Weyl-like dualities of orthogonal and symplectic groups.

For any diagram $\sigma \in \mathcal{B}^d_{n,m}$, the *partial transpose* σ^Γ is obtained by exchanging the last m nodes of both rows (i.e., the nodes on the right-hand side of the wall):

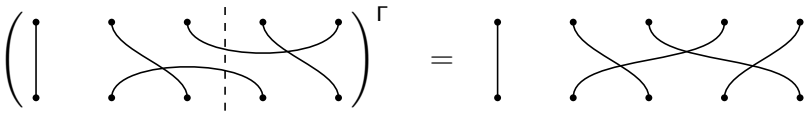

(3.4)

Note that $\sigma \in \mathcal{B}^d_{n,m}$ is a walled Brauer algebra diagram if and only if $\sigma^\Gamma \in \mathrm{S}_{n+m}$. In particular, $\dim(\mathcal{B}^d_{n,m}) = (n+m)!$ since $(\mathcal{B}^d_{n,m})^\Gamma = \mathbb{C}\mathrm{S}_{n+m}$ as vector spaces.

The walled Brauer algebra carries the natural structure of a $*$-algebra. The star operation on diagrams is defined by exchanging the bottom nodes with the top nodes:

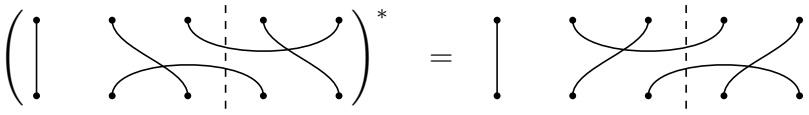

(3.5)

Walled Brauer algebras have a natural notion of trace and partial trace, resembling a similar notion for matrix algebras. The *trace* $\mathrm{Tr}\colon \mathcal{B}^d_{n,m} \to \mathbb{C}$ of a walled Brauer algebra diagram σ is defined as

$$\mathrm{Tr}(\sigma) := d^{\mathrm{loops}(\sigma)}, \tag{3.6}$$

where $\mathrm{loops}(\sigma)$ denotes the number of loops formed by connecting all nodes in the top row of σ to the corresponding nodes in the bottom row. This definition is extended to the whole of $\mathcal{B}^d_{n,m}$ by linearity. For any subset $S \subseteq [n+m]$, the corresponding *partial trace* $\mathrm{Tr}_S\colon \mathcal{B}^d_{n,m} \to \mathcal{B}^d_{n',m'}$ is defined similarly, except we connect only those pairs of nodes in σ that are indicated by S:

$$\mathrm{Tr}_S(\sigma) := d^{\mathrm{loops}_S(\sigma)}\sigma', \tag{3.7}$$

where $\mathrm{loops}_S(\sigma)$ denotes the number of loops formed in this way and $\sigma' \in \mathcal{B}^d_{n',m'}$ denotes the smaller diagram left after erasing the loops. Note that $n+m = n'+m'+|S|$ where $n' := n - |S \cap [n]|$ and $m' := m - |(S-n) \cap [m]|$.

3.2.1. Example. The trace of a diagram in $\mathcal{B}^d_{4,1}$:

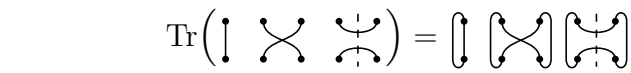

(3.8)

The partial trace of the same diagram over $S = \{2,3,4\}$:

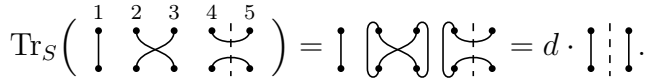

(3.9)

Note that the group algebra of the permutation group $\mathrm{S}_n \times \mathrm{S}_m$ forms a subalgebra of the walled Brauer algebra $\mathcal{B}^d_{n,m}$ consisting only of those diagrams where no edge goes through the wall. In fact, the two algebras are isomorphic when $n = 0$ or $m = 0$, i.e., $\mathbb{C}\mathrm{S}_n \cong \mathcal{B}^d_{n,0} \cong \mathcal{B}^d_{0,n}$ for any value of d.

The walled Brauer algebra $\mathcal{B}^d_{n,m}$ is generated by *transpositions* σ_i that swap the i-th and $(i+1)$-th node of the two rows, where $i \in \{1, \dots, n+m-1\} \setminus \{n\}$, and a *contraction* σ_n between the n-th and $(n+1)$-th node within each row. For example, $\mathcal{B}^d_{2,2}$ is generated by

$\sigma_1 =$ 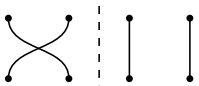

$\sigma_2 =$ 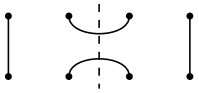

$\sigma_3 =$ 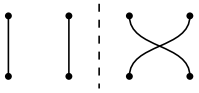 (3.10)

One can also define $\mathcal{B}^d_{n,m}$ abstractly in terms of relations between its generators [Nik07; BS12].

3.2.2. Definition. Let $n, m \geqslant 0$ be integers and $d \in \mathbb{C}$. The *walled Brauer algebra* $\mathcal{B}^d_{n,m}$ is a finite-dimensional associative algebra over $\mathbb{C}$ generated by $\sigma_1, \dots, \sigma_{n+m-1}$ subject to the following relations:

$$\text{(a) } \sigma_i^2 = 1 \ (i \neq n), \quad \text{(b) } \sigma_i\sigma_{i+1}\sigma_i = \sigma_{i+1}\sigma_i\sigma_{i+1} \ (i \neq n-1, n), \quad \text{(c) } \sigma_i\sigma_j = \sigma_j\sigma_i \ (|i-j| > 1), \tag{3.11}$$

$$\text{(d) } \sigma_n^2 = d\sigma_n, \qquad \text{(e) } \sigma_n\sigma_{n\pm1}\sigma_n = \sigma_n, \qquad \text{(f) } \sigma_n\sigma_i = \sigma_i\sigma_n \ (i \neq n \pm 1), \tag{3.12}$$

$$\text{(g) } \sigma_n\sigma_{n+1}\sigma_{n-1}\sigma_n\sigma_{n-1} = \sigma_n\sigma_{n+1}\sigma_{n-1}\sigma_n\sigma_{n+1}, \tag{3.13}$$

$$\text{(h) } \sigma_{n-1}\sigma_n\sigma_{n+1}\sigma_{n-1}\sigma_n = \sigma_{n+1}\sigma_n\sigma_{n+1}\sigma_{n-1}\sigma_n. \tag{3.14}$$

Sometimes, we could refer to the contraction generator σ_n as $\bar{\sigma}_n$ to highlight that it has some horizontal strands.

More generally, we define $\sigma_{i,j} \equiv (i,j)$ to be the transposition between i-th and j-th node, which acts as identity on other $n+m-2$ nodes. Similarly, we define $\overline{\sigma}_{i,j} \equiv \overline{(i,j)}$ to be the contraction between i-th and j-th node, which acts as identity on other $n+m-2$ nodes.

In the quantum information context, the generator σ_n can be thought as "unnormalised EPR state projector". We can generalise this and introduce special elements $\tau_k \in \mathcal{B}^d_{n,m}$ defined formally as

$$\tau_k := \prod_{i=0}^{k-1} \overline{(n-i, n+1+i)}, \tag{3.15}$$

which intuitively represent k copies of "unnormalised EPR projector". They represented by diagrams with k contractions located near the wall, i.e

$\tau_k \ =$ 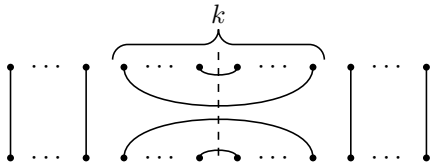

(3.16)

3.3 Matrix algebra of partially transposed permutations

Fix the integer $d \geqslant 2$. We now consider a matrix representation of the walled Brauer algebra $\mathcal{B}^d_{n,m}$ by extending Eq. (2.70) from a tensor representation of S_p to a *mixed tensor* representation $\psi^d_{n,m} \colon \mathcal{B}^d_{n,m} \to \mathrm{End}((\mathbb{C}^d)^{\otimes n} \otimes (\mathbb{C}^d)^{\otimes m})$ of $\mathcal{B}^d_{n,m}$. Denoting the nodes in the first row of a diagram $\sigma \in \mathcal{B}^d_{n,m}$ by $1, \ldots, n+m$ and in the second row by $\underline{1}, \ldots, \underline{n+m}$, the action of $\psi^d_{n,m}(\sigma)$ on the standard basis tensors of $(\mathbb{C}^d)^{\otimes n} \otimes (\mathbb{C}^d)^{\otimes m}$ is given by

$$\psi^d_{n,m}(\sigma)\big(|x_1\rangle \otimes \cdots \otimes |x_{n+m}\rangle\big) = \sum_{1 \leqslant x_{\underline{1}}, \ldots, x_{\underline{n+m}} \leqslant d} \sigma^{x_1,\ldots,x_{n+m}}_{x_{\underline{1}},\ldots,x_{\underline{n+m}}} |x_{\underline{1}}\rangle \otimes \cdots \otimes |x_{\underline{n+m}}\rangle, \tag{3.17}$$

for all $x_1, \ldots, x_{n+m} \in \{1, \ldots, d\}$, where the coefficients are given by

$$\sigma^{x_1,\ldots,x_{n+m}}_{x_{\underline{1}},\ldots,x_{\underline{n+m}}} := \begin{cases} 1 & \text{if } x_r = x_s \text{ for all connected pairs of vertices} \\ & r, s \in \{1, \ldots, n+m, \underline{1}, \ldots, \underline{n+m}\} \text{ of } \sigma, \\ 0 & \text{otherwise.} \end{cases} \tag{3.18}$$

Equivalently,

$$\sigma^{x_1,\ldots,x_{n+m}}_{x_{\underline{1}},\ldots,x_{\underline{n+m}}} = \prod_{(r,s) \in \sigma} \delta_{x_r, x_s}, \tag{3.19}$$

where the product is over all pairs (r, s) of nodes that are connected in σ.

3.3.1. Example. According to Eqs. (3.17) and (3.19),

$\langle x_1, \ldots, x_5| \, \psi^d_{3,2}\Big($ 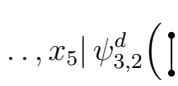 $\Big) \, |y_1, \ldots, y_5\rangle =$ 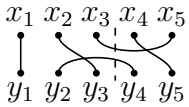 (3.20)

$$= \delta_{x_1,y_1} \delta_{x_2,y_3} \delta_{x_3,x_5} \delta_{x_4,y_5} \delta_{y_2,y_4} \tag{3.21}$$

for any choice of $x_1, \ldots, x_5 \in [d]$ and $y_1, \ldots, y_5 \in [d]$.

A crucial fact about the matrix $\psi^d_{n,m}(\sigma)$ representing a diagram σ is that its partial traces are related to those of the diagram. Namely, for any $\sigma \in \mathcal{B}^d_{n,m}$ and $S \subseteq [n+m]$,

$$\mathrm{Tr}(\psi^d_{n,m}(\sigma)) = \mathrm{Tr}(\sigma), \qquad \mathrm{Tr}_S(\psi^d_{n,m}(\sigma)) = \psi^d_{n',m'}(\mathrm{Tr}_S(\sigma)), \tag{3.22}$$

where the diagrammatic traces $\mathrm{Tr}(\sigma)$ and $\mathrm{Tr}_S(\sigma)$ are defined in Eqs. (3.6) and (3.7), respectively. We formally establish these two identities in Section 3.A.1.

Similar to Eq. (2.71), we denote the image of $\mathcal{B}^d_{n,m}$ under $\psi^d_{n,m}$ by

$$\mathcal{A}^d_{n,m} := \psi^d_{n,m}(\mathcal{B}^d_{n,m}) \cong \mathcal{B}^d_{n,m} / \ker \psi^d_{n,m}. \tag{3.23}$$

This is known as *matrix algebra of partially transposed permutations* as it is generated by permutation matrices on $n+m$ qudit registers, partially transposed on the last m registers. Recall that the *partial transpose* $\Gamma \colon \mathrm{End}((\mathbb{C}^d)^{\otimes n+m}) \to \mathrm{End}((\mathbb{C}^d)^{\otimes n+m})$ is defined as $(M \otimes N)^\Gamma := M \otimes N^\mathsf{T}$, for all $M \in \mathrm{End}((\mathbb{C}^d)^{\otimes n})$ and $N \in \mathrm{End}((\mathbb{C}^d)^{\otimes m})$. This operation can be used to relate the maps $\psi^d_{n,m}$ and ψ^d_{n+m} defined in Eqs. (2.70) and (3.17), respectively:

$$\psi^d_{n,m}(\sigma) = \Big(\psi^d_{n+m}\big(\sigma^\Gamma\big)\Big)^\Gamma, \tag{3.24}$$

where σ^Γ denotes the partial transpose of the diagram $\sigma \in \mathcal{B}^d_{n,m}$, see Eq. (3.4). Hence, as vector spaces, the algebras $\mathcal{A}^d_{n,m}$ and $\mathcal{A}^d_{n+m}$ are related as follows:

$$\mathcal{A}^d_{n,m} = \big(\mathcal{A}^d_{n+m}\big)^\Gamma. \tag{3.25}$$

However, because of different product operations, the two algebras are not isomorphic.

3.3.2. Example (Transposition versus contraction). When $n = 2$ and $m = 0$, the only non-trivial element of $\mathcal{B}^d_{2,0}$ is the transposition $\sigma_1 = (12)$. Its matrix version acts as

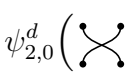

$$\psi^d_{2,0}(\quad) \colon |i\rangle|j\rangle \mapsto |j\rangle|i\rangle, \tag{3.26}$$

for all $i, j \in \{1, \dots, d\}$, since the diagram is encoded by $\sigma^{i,j}_{k,l} = \delta_{i,l}\delta_{j,k}$. More generally, any diagram that represents a permutation (i.e., has no edges across the wall) simply translates into the corresponding permutation of the tensor factors.

When $n = m = 1$, the only non-trivial element of $\mathcal{B}^d_{1,1}$ is the contraction of 1 and 2. The corresponding matrix acts as

$$\psi^d_{1,1}(\quad) \colon |i\rangle|j\rangle \mapsto \delta_{i,j} \sum_{k=1}^{d} |k\rangle|k\rangle, \tag{3.27}$$

for all $i, j \in \{1, \dots, d\}$, since $\sigma^{i,j}_{k,l} = \delta_{i,j}\delta_{k,l}$ in this case. In particular, when $d = 2$,

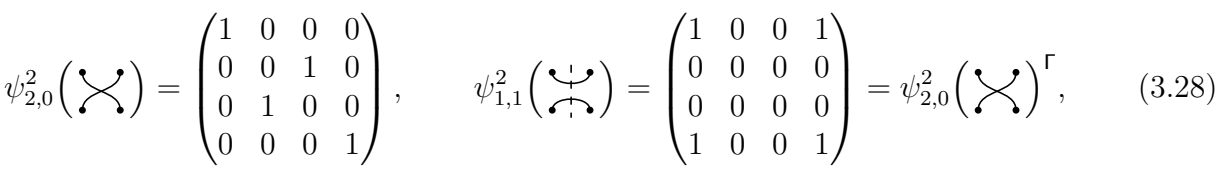

$$\psi^2_{2,0}(\quad) = \begin{pmatrix} 1 & 0 & 0 & 0 \\ 0 & 0 & 1 & 0 \\ 0 & 1 & 0 & 0 \\ 0 & 0 & 0 & 1 \end{pmatrix}, \qquad \psi^2_{1,1}(\quad) = \begin{pmatrix} 1 & 0 & 0 & 1 \\ 0 & 0 & 0 & 0 \\ 0 & 0 & 0 & 0 \\ 1 & 0 & 0 & 1 \end{pmatrix} = \psi^2_{2,0}(\quad)^{\Gamma}, \tag{3.28}$$

which are known as the SWAP operator and the unnormalised projector onto the canonical maximally entangled state.

3.4 Mixed Schur–Weyl duality

The mixed Schur–Weyl duality is concerned with the action of U_d and $\mathcal{B}^d_{n,m}$ on the mixed tensor product space $(\mathbb{C}^d)^{\otimes n} \otimes (\mathbb{C}^d)^{\otimes m}$ where $n, m \geqslant 0$. The $m = 0$ case is equivalent to the usual Schur–Weyl duality discussed in Section 2.10 while the $n = 0$ case is isomorphic to it. As a generalisation of Eq. (2.108), consider the natural representation $\phi^d_{n,m} \colon \mathrm{U}_d \to \mathrm{End}((\mathbb{C}^d)^{\otimes n+m})$ of U_d defined as

$$\phi^d_{n,m}(U) := U^{\otimes n} \otimes \bar{U}^{\otimes m} \tag{3.29}$$

for all $U \in \mathrm{U}_d$, where the entry-wise complex conjugate $\bar{U}$ is the dual of the defining representation. Similar to Eq. (2.109), let

$$\mathcal{U}^d_{n,m} := \mathrm{span}_{\mathbb{C}}\{\phi^d_{n,m}(U) \mid U \in \mathrm{U}_d\}. \tag{3.30}$$

We are particularly interested in the matrix algebra $\mathrm{End}_{\mathcal{U}^d_{n,m}}((\mathbb{C}^d)^{\otimes n} \otimes (\mathbb{C}^d)^{\otimes m})$, i.e., the centraliser of the natural U_d action on $(\mathbb{C}^d)^{\otimes n} \otimes (\mathbb{C}^d)^{\otimes m}$, which captures the unitary equivariance condition. The following result generalises Theorem 2.10.3 to the mixed tensor product space $(\mathbb{C}^d)^{\otimes n} \otimes (\mathbb{C}^d)^{\otimes m}$ and says that $\mathrm{End}_{\mathcal{U}^d_{n,m}}((\mathbb{C}^d)^{\otimes n} \otimes (\mathbb{C}^d)^{\otimes m})$ is equal to the matrix algebra $\mathcal{A}^d_{n,m}$ of partially transposed permutations and, when $d \geqslant n + m$, isomorphic to the walled Brauer algebra $\mathcal{B}^d_{n,m}$.

3.4.1. Theorem (Mixed Schur–Weyl duality [Koi89; Ben+94]). *The algebra $\mathcal{U}^d_{n,m}$ is the centraliser algebra of $\mathcal{A}^d_{n,m}$ in $\mathrm{End}((\mathbb{C}^d)^{\otimes n} \otimes (\mathbb{C}^d)^{\otimes m})$ and vice versa, i.e.,*

$$\mathcal{U}^d_{n,m} = \mathrm{End}_{\mathcal{A}^d_{n,m}}((\mathbb{C}^d)^{\otimes n} \otimes (\mathbb{C}^d)^{\otimes m}), \qquad \mathcal{A}^d_{n,m} = \mathrm{End}_{\mathcal{U}^d_{n,m}}((\mathbb{C}^d)^{\otimes n} \otimes (\mathbb{C}^d)^{\otimes m}). \tag{3.31}$$

Moreover, when $d \geqslant n + m$ the representation $\psi^d_{n,m}$ is faithful, i.e., $\mathcal{A}^d_{n,m} \cong \mathcal{B}^d_{n,m}$.

The simplest non-trivial instance of this duality is illustrated in Example 3.4.2 below. It is similar to Example 2.10.4, except here the second system of $\mathcal{U}_{1,1}^2$ and $\mathcal{A}_{1,1}^2$ is subject to the dual action of U_d and the partial transpose, respectively.

3.4.2. Example ($n = m = 1$ and $d = 2$). The algebra $\mathcal{A}_{1,1}^2$ is generated by the identity matrix and the matrix $\psi_{1,1}^d\left(\begin{smallmatrix}\cdot & \cdot\\ \cdot & \cdot\end{smallmatrix}\right)$ given in Eq. (3.28):

$$\mathcal{A}_{1,1}^2 := \left\{ x \begin{pmatrix} 1&0&0&0\\0&1&0&0\\0&0&1&0\\0&0&0&1 \end{pmatrix} + y \begin{pmatrix} 1&0&0&1\\0&0&0&0\\0&0&0&0\\1&0&0&1 \end{pmatrix} \,\middle|\, x, y \in \mathbb{C} \right\}. \tag{3.32}$$

Note from Eq. (2.123) that $\mathcal{A}_{1,1}^2 = (\mathcal{A}_{2,0}^2)^\Gamma$. We can describe $\mathcal{U}_{1,1}^2$ by introducing the dual representation: for any invertible matrix M, let $M^* := (M^{-1})^\mathsf{T}$. Note that $M^* = \bar{M}$ when M is unitary and, for a general M, the entries of M^* are rational functions in the entries of M. In particular,

$$\begin{pmatrix} a & b\\ c & d \end{pmatrix}^* = \frac{1}{ad-bc} \begin{pmatrix} d & -c\\ -b & a \end{pmatrix} \tag{3.33}$$

for any $a, b, c, d \in \mathbb{C}$ such that $ad - bc \neq 0$. The algebra $\mathcal{U}_{1,1}^2$ is then given by

$$\mathcal{U}_{1,1}^2 := \mathrm{span}_{\mathbb{C}} \left\{ \begin{pmatrix} a & b\\ c & d \end{pmatrix} \otimes \begin{pmatrix} a & b\\ c & d \end{pmatrix}^* \,\middle|\, \begin{pmatrix} a & b\\ c & d \end{pmatrix} \in \mathrm{U}_2 \right\}. \tag{3.34}$$

Using the dual two-qubit Schur transform [BLMMO22]

$$U := \begin{pmatrix} 1/\sqrt{2} & 0 & 0 & 1/\sqrt{2}\\ 0 & -1 & 0 & 0\\ 1/\sqrt{2} & 0 & 0 & -1/\sqrt{2}\\ 0 & 0 & 1 & 0 \end{pmatrix}, \tag{3.35}$$

we can simultaneously block-diagonalize both algebras:

$$U\mathcal{A}_{1,1}^2 U^\mathsf{T} = \left\{ \left(\begin{array}{c|ccc} x+2y & 0 & 0 & 0\\ \hline 0 & x & 0 & 0\\ 0 & 0 & x & 0\\ 0 & 0 & 0 & x \end{array}\right) \,\middle|\, x, y \in \mathbb{C} \right\}, \tag{3.36}$$

$$U\mathcal{U}_{1,1}^2 U^\mathsf{T} = \mathrm{span}_{\mathbb{C}} \left\{ \frac{1}{ad-bc} \left(\begin{array}{c|ccc} ad-bc & 0 & 0 & 0\\ \hline 0 & a^2 & \sqrt{2}ab & b^2\\ 0 & \sqrt{2}ac & ad+bc & \sqrt{2}bd\\ 0 & c^2 & \sqrt{2}cd & d^2 \end{array}\right) \,\middle|\, \begin{pmatrix} a & b\\ c & d \end{pmatrix} \in \mathrm{U}_2 \right\}. \tag{3.37}$$

These algebras centralize each other since

$$U\mathcal{A}_{1,1}^2 U^\mathsf{T} = \mathbb{C} \oplus \mathbb{C} I_3, \qquad U\mathcal{U}_{1,1}^2 U^\mathsf{T} = \mathbb{C} \oplus \mathrm{End}(\mathbb{C}^3). \tag{3.38}$$

While this appears identical to Eq. (2.128), the decompositions of $\mathcal{A}_{n,m}^d$ and $\mathcal{U}_{n,m}^d$ are generally very different for $d > 2$ from those of $\mathcal{A}_{n+m}^d$ and $\mathcal{U}_{n+m}^d$, see Section 3.6.

3.4.3. Remark. Theorem 3.4.1 can also be seen as an instance of the Double Centraliser Theorem 2.10.1. Indeed, we can rephrase it as follows: as a representation of $\mathcal{A}_{n,m}^d \times \mathcal{U}_{n,m}^d$, the space $(\mathbb{C}^d)^{\otimes n} \otimes (\mathbb{C}^d)^{\otimes m}$ decomposes as

$$(\mathbb{C}^d)^{\otimes n} \otimes (\mathbb{C}^d)^{\otimes m} \cong \bigoplus_{\lambda \in \widehat{\mathcal{A}}_{n,m}^d} V_\lambda \otimes W_\lambda, \tag{3.39}$$

where V_λ are simple modules of $\mathcal{A}^d_{n,m}$ and W_λ are simple modules of $\mathcal{U}^d_{n,m}$. This automatically implies the following combinatorial identity:

$$d^{n+m} = \sum_{\lambda \in \widehat{\mathcal{A}}^d_{n,m}} d_\lambda m_\lambda, \tag{3.40}$$

where $d_\lambda = \dim V_\lambda$ and $m_\lambda = \dim W_\lambda$.

The distinction between $\mathcal{A}^d_{n,m}$ and $\mathcal{B}^d_{n,m}$ is crucial if one is interested in small dimensions $d < n+m$ since the two algebras are not isomorphic in this case. For example, the algebra $\mathcal{A}^d_{n,m}$ is always semisimple because $\mathcal{U}^d_{n,m}$ is known to be semisimple from the representation theory of Lie groups [Eti+11, Theorem 4.66], so its commutant $\mathcal{A}^d_{n,m}$ must also be semisimple by the Double Centraliser Theorem 2.10.1. However, $\mathcal{B}^d_{n,m}$ is not semisimple for integer $d < n+m-1$ [CDDM08].

One of our main technical results is the determination of primitive central idempotents of the matrix algebras $\mathcal{A}^d_{n,m}$, see Section 3.6, which will play a central role in our results in Chapter 6 on optimisation with unitary-equivariant constraints.

3.5 Mixed Young diagrams, tableaux and staircases

In this section, we introduce combinatorial notions analogous to Young diagrams and tableaux that can be used to describe paths in the Bratteli diagram for the algebra $\mathcal{A}^d_{n,m}$ later. First, let us first describe three equivalent ways of representing a pair of Young diagrams.

A *mixed Young diagram* of length d is a pair of Young diagrams $\lambda = (\lambda_l, \lambda_r)$ of total length at most d: $\ell(\lambda_l)+\ell(\lambda_r) \leqslant d$. Equivalently, we can represent λ by combining the diagrams $\lambda_l \in \mathbb{Z}^d_{\geqslant 0}$ and $\lambda_r \in \mathbb{Z}^d_{\geqslant 0}$ into a single *staircase* $\widetilde{\lambda} \in \mathbb{Z}^d$ obtained by subtracting from $\lambda_l = (\lambda_{l,1}, \ldots, \lambda_{l,d})$ the reverse of $\lambda_r = (\lambda_{r,1}, \ldots, \lambda_{r,d})$ [Ste87]:

$$\widetilde{\lambda} := \big(\lambda_{l,1} - \lambda_{r,d},\ \lambda_{l,2} - \lambda_{r,d-1},\ \ldots,\ \lambda_{l,d} - \lambda_{r,1}\big). \tag{3.41}$$

Intuitively, the staircase $\widetilde{\lambda}$ corresponds to rotating the diagram λ_r by 180 degrees and attaching it at the bottom of λ_l (see Fig. 3.1). Since $\ell(\lambda_l) + \ell(\lambda_r) \leqslant d$, this operation is reversible and one can easily recover λ_l and λ_r from the staircase $\widetilde{\lambda}$. Finally, a third way of representing the same concept is via *walled concatenation* $(\hat{\lambda}, s)$ where $s := \lambda_{r,1}$ and $\hat{\lambda}$ is a Young diagram of shape

$$\hat{\lambda} := \lambda_{r,1} + \widetilde{\lambda} = \big(\lambda_{r,1} + \lambda_{l,1} - \lambda_{r,d},\ \lambda_{r,1} + \lambda_{l,2} - \lambda_{r,d-1},\ \ldots,\ \lambda_{r,1} + \lambda_{l,d-1} - \lambda_{r,2},\ \lambda_{l,d}\big). \tag{3.42}$$

This diagram corresponds to shifting the staircase $\widetilde{\lambda}$ to the right by $\lambda_{r,1}$ boxes so that all its entries become non-negative. Equivalently, we can obtain $\hat{\lambda}$ by adding $\lambda_{r,1}$ columns of d boxes on the left of λ_l and then removing the diagram λ_r (rotated by 180 degrees) from the bottom of these columns (see Fig. 3.1). This process is reversible, so we can easily convert $(\hat{\lambda}, s)$ back into the pair of diagrams (λ_l, λ_r) or the staircase $\widetilde{\lambda}$. Mixed Young diagrams, walled concatenations, and staircases are three equivalent ways of thinking about the same combinatorial object, see Fig. 3.1. Throughout the chapter, we will use the same symbol λ to denote either of these three concepts, depending on the convenience in a given context.

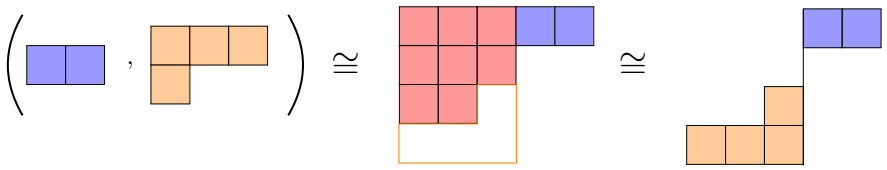

Figure 3.1: Three equivalent ways of representing a pair of Young diagrams: as a mixed Young diagram $\lambda = (\lambda_l, \lambda_r)$, as a staircase $\widetilde{\lambda}$, or as a walled concatenation $(\hat{\lambda}, \lambda_{r,1})$. Here the total length of all tableaux is $d = 4$.

Recall from Eq. (2.42) that a sequence of Young diagrams can be interpreted as a standard Young tableau. Similarly, for any shape $\lambda = (\lambda_l, \lambda_r)$, where $\lambda_l \vdash n - k$ and $\lambda_r \vdash m - k$ for some $n, m \geqslant 0$ and $k \geqslant 0$ such that $0 \leqslant k \leqslant \min(n, m)$, we define a *mixed standard Young tableau* T of length d as a sequence $(T^0, T^1, T^2, \ldots, T^{n+m})$ of mixed Young diagrams such that each T^i has length d and

1. $T^0 := (\varnothing, \varnothing)$ and $T^{n+m} := \lambda = (\lambda_l, \lambda_r)$,
2. if $n \geqslant i \geqslant 1$ then $T_l^{i-1} \subseteq T_l^i$ with $|T_l^{i-1}| + 1 = |T_l^i|$ and $T_r^{i-1} = T_r^i = \varnothing$,
3. if $n + m \geqslant i > n$ then either
   (a) $T_l^i \subseteq T_l^{i-1}$ with $|T_l^i| + 1 = |T_l^{i-1}|$ and $T_r^{i-1} = T_r^i$, or
   (b) $T_r^{i-1} \subseteq T_r^i$ with $|T_r^{i-1}| + 1 = |T_r^i|$ and $T_l^{i-1} = T_l^i$.

This sequence corresponds to a path in a certain Bratteli diagram (see Section 3.6 for more details).

Similar to Eq. (2.43), we can translate a sequence T of mixed Young diagrams into what is essentially a pair of standard tableaux, thus justifying calling T a *mixed standard Young tableau*. The first n steps of this translation build up the left tableau following the same procedure as described in Section 2.6. The remaining steps either build up the right tableau in the same way or add secondary entries to the left tableau indicating at which steps the corresponding boxes are removed. For example, when $n = 3$, $m = 2$, and $k = 1$, the sequence

$$T = \big((\varnothing, \varnothing), (\ydiagram{1}, \varnothing), (\ydiagram{2}, \varnothing), (\ydiagram{3}, \varnothing), (\ydiagram{2}, \varnothing), (\ydiagram{2}, \ydiagram{1})\big) \tag{3.43}$$

corresponds to the following pair of tableau:

$$T = \Big(\begin{array}{|c|c|c|}\hline 1 & 2 & 3{,}4 \\ \hline \end{array}\,, \begin{array}{|c|}\hline 5 \\ \hline \end{array}\Big). \tag{3.44}$$

This is a mixed Young tableau of shape $\lambda = ((2), (1))$ since the left tableau has only two boxes remaining. Similarly to Section 2.6, for any permutation $\pi \in \mathrm{S}_n \times \mathrm{S}_m$ we will write πT to denote the tableau obtained by permuting the cell fillings of T according to π.

In the following section, we summarise a method for constructing primitive central idempotents of multiplicity-free family of walled Brauer algebras which we described in Section 2.7.

3.6 Idempotents for the matrix algebras $\mathcal{A}_{n,m}^d$

In this section, we provide the necessary ingredients for applying the [DLS18] framework, presented in Section 2.7, to the partially transposed permutation matrix algebras $\mathcal{A}_{n,m}^d$. Our main technical contribution is Theorem 3.6.6 which shows that Jucys–Murphy elements of partially

transposed permutation matrix algebras can be obtained from Jucys–Murphy elements of walled Brauer algebras, even when the corresponding walled Brauer algebras are not semisimple.

Consider the following multiplicity-free family of walled Brauer algebras:

$$\mathbb{C} \cong \mathcal{B}^d_{0,0} \hookrightarrow \mathcal{B}^d_{1,0} \hookrightarrow \cdots \hookrightarrow \mathcal{B}^d_{n,0} \hookrightarrow \mathcal{B}^d_{n,1} \hookrightarrow \cdots \hookrightarrow \mathcal{B}^d_{n,m}, \tag{3.45}$$

where the embeddings correspond to adding on the right of the diagram an extra pair of nodes that are connected with a vertical line. For the sake of brevity, let us denote this family by $\mathcal{B} := (\mathcal{B}_0, \ldots, \mathcal{B}_{n+m})$ where

$$\mathcal{B}_k := \begin{cases} \mathbb{C} & \text{if } k = 0, \\ \mathcal{B}^d_{k,0} & \text{if } 1 \leqslant k \leqslant n, \\ \mathcal{B}^d_{n,k-n} & \text{if } n+1 \leqslant k \leqslant n+m. \end{cases} \tag{3.46}$$

Sometimes we want to highlight the dependence on local dimension, so we can refer to $\mathcal{B}_k$ as $\mathcal{B}^d_k$.

Similarly, let $\mathcal{A} := (\mathcal{A}_0, \ldots, \mathcal{A}_{n+m})$ where, for every $k \in \{0, \ldots, n+m\}$,

$$\mathcal{A}_k := \psi^d_{n,m}(\mathcal{B}_k) \subseteq \mathrm{End}((\mathbb{C}^d)^{\otimes n} \otimes (\mathbb{C}^d)^{\otimes m}) \tag{3.47}$$

is the corresponding partially transposed permutation matrix algebra and $\psi^d_{n,m}$ is the map from Eq. (3.17). Note that $\mathcal{A}_{k-1}$ is the subalgebra of $\mathcal{A}_k$ that consists of all matrices of the form $M \otimes I_d$ for some M. We will later also write $\mathcal{A}^d_k \cong \mathcal{A}_k$ when we want to highlight the dependence on local dimension d.

For every $k \in [n+m]$, let

$$\mathcal{X}^{\mathcal{B}}_k := \langle \mathcal{Z}(\mathcal{B}_1), \ldots, \mathcal{Z}(\mathcal{B}_k) \rangle, \qquad \mathcal{X}^{\mathcal{A}}_k := \langle \mathcal{Z}(\mathcal{A}_1), \ldots, \mathcal{Z}(\mathcal{A}_k) \rangle \tag{3.48}$$

denote the Gelfand–Tsetlin subalgebras of $\mathcal{B}$ and $\mathcal{A}$, respectively, see Definition 2.7.5.

Bratteli diagram for walled Brauer algebras

The simple modules of the walled Brauer algebra $\mathcal{B}^d_{n,m}$ are labeled by pairs of Young diagrams (λ_l, λ_r) where λ_l and λ_r are partitions of $n-k$ and $m-k$ for some $0 \leqslant k \leqslant \min(n,m)$ [BO20]:

$$\widehat{\mathcal{B}}^d_{n,m} = \big\{ \lambda = (\lambda_l, \lambda_r) \;\big|\; 0 \leqslant k \leqslant \min(n,m),\ \lambda_l \vdash n-k,\ \lambda_r \vdash m-k \big\}. \tag{3.49}$$

The Bratteli diagram $\mathscr{B}$ (see Definition 2.7.2) for the family $\mathcal{B}$ of walled Brauer algebras is defined as follows. The only vertex at level $k = 0$ is the root $(\varnothing, \varnothing)$.[2] For any $k \in [n+m]$, the vertices at level k are given by $\widehat{\mathcal{B}}_k$, see Eqs. (3.46) and (3.49). For any pair of adjacent levels $k-1$ and k where $k \in [n+m]$, an edge $\lambda \to \mu$ between $\lambda \in \widehat{\mathcal{B}}_{k-1}$ and $\mu \in \widehat{\mathcal{B}}_k$ is present if and only if

1. $k \leqslant n$ and the diagram μ is obtained from λ by adding one cell to the diagram λ_l,
2. $k > n$ and μ is obtained from λ by either adding a cell to λ_r or removing a cell from λ_l.

For example, the Bratteli diagram for the multiplicity-free family ending with $\mathcal{B}^d_{2,2}$ is given in Fig. 3.2.

By construction, the number of paths from the root vertex to any leaf λ in the Bratteli diagram is equal to the dimension of the corresponding simple module of $\mathcal{B}^d_{n,m}$.

[2] Here we use $(\varnothing, \varnothing)$ instead of $\varnothing$ for the root of the Bratteli diagram of the walled Brauer algebra because the irreducible representations of this algebra are labeled by pairs of Young diagrams.

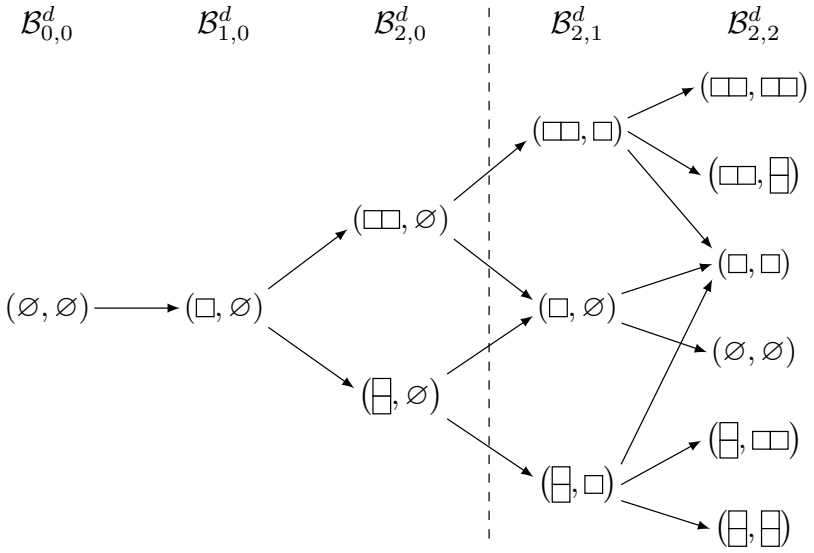

Figure 3.2: Bratteli diagram associated to the multiplicity-free family $\mathbb{C} \cong \mathcal{B}^d_{0,0} \hookrightarrow \mathcal{B}^d_{1,0} \hookrightarrow \mathcal{B}^d_{2,0} \hookrightarrow \mathcal{B}^d_{2,1} \hookrightarrow \mathcal{B}^d_{2,2}$ of walled Brauer algebras when they are semisimple.

Jucys–Murphy elements and content vectors

If $d \in \mathbb{C}$ is such that the walled Brauer algebras $\mathcal{B}^d_{n,m}$ are semisimple, their Jucys–Murphy elements are given by [BS12; SS15; JK20]

$$J^{\mathcal{B}}_k := \begin{cases} 0 & \text{if } k = 1, \\ \sum_{i=1}^{k-1} (i,k) & \text{if } 2 \leqslant k \leqslant n, \\ \sum_{i=n+1}^{k-1} (i,k) - \sum_{i=1}^{n} \overline{(i,k)} + d & \text{if } n+1 \leqslant k \leqslant n+m, \end{cases} \tag{3.50}$$

where (i,k) is the transposition of elements i and k, and $\overline{(i,k)}$ is the corresponding contraction. When the walled Brauer algebra is not semisimple, we still define $J^{\mathcal{B}}_k$ via the above formula.

Let $T \in \mathrm{Paths}(\mathscr{B})$ be an arbitrary root-leaf path in the Bratteli diagram of $\mathcal{B}^d_{n,m}$ and let $T^{k-1} \to T^k$ where $k \in [n+m]$ denote an edge on this path. Recall from Eq. (3.49) that each vertex T^k of T is labeled by some bipartition (λ_l, λ_r). The number $c_{T^{k-1} \to T^k}$ introduced in Definition 2.7.8 and Eq. (2.59) that corresponds to this edge is calculated via the following rule [BO20; JK20]:

1. if $1 \leqslant k \leqslant n$ and T^k is obtained from T^{k-1} by adding a cell (i,j) to the left diagram in the bipartition T^{k-1} then

$$c_{T^{k-1} \to T^k} = j - i \equiv \mathrm{cont}(T^k_l \setminus T^{k-1}_l),$$

2. if $n+1 \leqslant k \leqslant n+m$ and T^k is obtained from T^{k-1} by removing a cell (i,j) from the left diagram in the bipartition T^{k-1} then

$$c_{T^{k-1} \to T^k} = i - j \equiv -\mathrm{cont}(T^{k-1}_l \setminus T^k_l),$$

3. if $n+1 \leqslant k \leqslant n+m$ and T^k is obtained from T^{k-1} by adding a cell (i,j) to the right diagram in the bipartition T^{k-1} then

$$c_{T^{k-1} \to T^k} = j - i + d \equiv \mathrm{cont}(T^k_r \setminus T^{k-1}_r) + d.$$

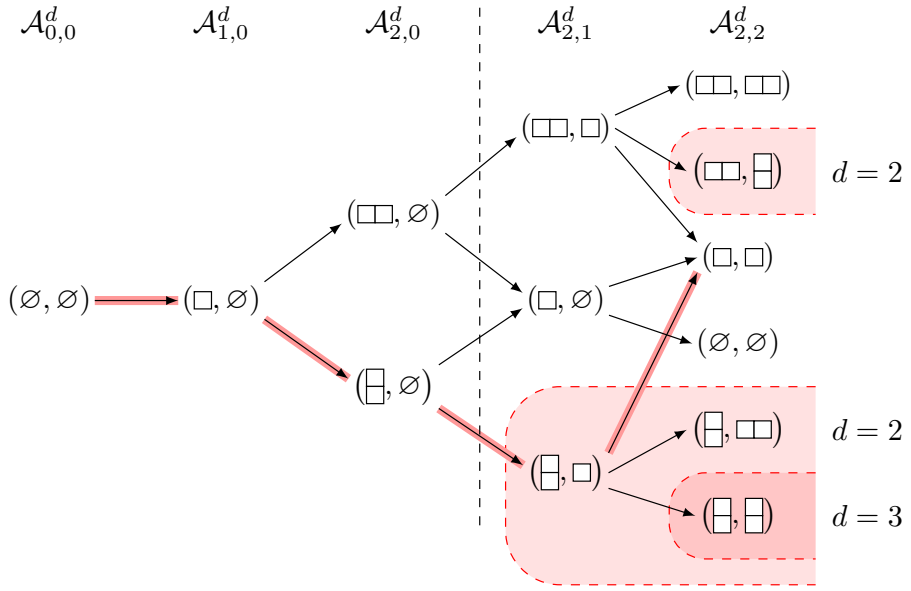

Figure 3.3: Bratteli diagram associated to the multiplicity-free family $\mathbb{C} \cong \mathcal{A}^d_{0,0} \hookrightarrow \mathcal{A}^d_{1,0} \hookrightarrow \mathcal{A}^d_{2,0} \hookrightarrow \mathcal{A}^d_{2,1} \hookrightarrow \mathcal{A}^d_{2,2}$ of partially transposed permutation matrix algebras for different values of the local dimension d. When $d \geqslant 4$, this diagram coincides with that of the walled Brauer algebras (see Fig. 3.2). However, for small values of d (i.e., $d = 2$ and $d = 3$) the diagram has to be modified by removing the designated vertices. Note that removing the vertex $(\begin{smallmatrix}\square\\\square\end{smallmatrix},\square)$ when $d = 2$ eliminates the highlighted path from the root $(\varnothing,\varnothing)$ to the leaf $(\square,\square)$, which decreases the dimension of the corresponding simple $\mathcal{A}^d_{2,2}$-module $V_{(\square,\square)}$ by one, i.e., $\dim V_{(\square,\square)} = 4$ if $d > 2$ while $\dim V_{(\square,\square)} = 3$ if $d = 2$.

Since these formulas are very similar to the definition of the *content* $j-i$ of a cell (i,j) in a Young tableau, see Eq. (2.33), it motivates us to introduce a notion of *walled content* of a cell containing i in T similar to Eq. (2.44). Namely, for a given path $T = (T^0, \dots, T^{n+m}) \in \mathrm{Paths}(\mathscr{B})$ we define

$$\mathrm{wcont}_i(T) := \begin{cases} \mathrm{cont}(T^i_l \setminus T^{i-1}_l) & \text{if } i \leqslant n, \\ \mathrm{cont}(T^i_r \setminus T^{i-1}_r) + d & \text{if } i > n \text{ and } T^i_l = T^{i-1}_l, \\ -\mathrm{cont}(T^{i-1}_l \setminus T^i_l) & \text{if } i > n \text{ and } T^i_r = T^{i-1}_r. \end{cases} \tag{3.51}$$

This definition is chosen so that for any $k \in [n+m]$

$$c_{T^{k-1} \to T^k} = \mathrm{wcont}_k(T). \tag{3.52}$$

For example, the path T given in Eqs. (3.43) and (3.44) has the following values of walled content: $\mathrm{wcont}_1(T) = 0$, $\mathrm{wcont}_2(T) = 1$, $\mathrm{wcont}_3(T) = 2$, $\mathrm{wcont}_4(T) = -2$, $\mathrm{wcont}_5(T) = d$.

We refer to the full vector of walled contents as $c_T := (\mathrm{wcont}_1(T), \dots, \mathrm{wcont}_{n+m}(T))$.

Adapting the Bratteli diagram from $\mathcal{B}^d_{n,m}$ to $\mathcal{A}^d_{n,m}$

According to [Ben+94, Theorem 1.11], the simple modules of the $\mathcal{A}^d_{n,m}$ are labeled by pairs of Young diagrams (λ_l, λ_r) where λ_l and λ_r are partitions of $n-k$ and $m-k$ for some $0 \leqslant k \leqslant \min(n,m)$ with additional constraint:

$$\widehat{\mathcal{A}}^d_{n,m} = \big\{\lambda = (\lambda_l, \lambda_r) \;\big|\; 0 \leqslant k \leqslant \min(n,m),\ \lambda_l \vdash n-k,\ \lambda_r \vdash m-k,\ \ell(\lambda_l) + \ell(\lambda_r) \leqslant d\big\}. \tag{3.53}$$

The Bratteli diagram $\mathscr{A}$ for the family of partially transposed permutation matrix algebras $\mathcal{A}$ can be obtained from the Bratteli diagram $\mathscr{B}$ for semisimple walled Brauer algebras $\mathcal{B}$ by

removing all vertices (λ_l, λ_r) that violate the condition $\ell(\lambda_l) + \ell(\lambda_r) \leqslant d$. Note that along with the removed vertices we also remove their incident edges. For example, Fig. 3.3 shows how Fig. 3.2 should be adapted for small values of d.

Depending on the local dimension d we may need to remove some vertices that are not leaves of the diagram, which in turn can decrease the number of root-leave paths, thus affecting the dimension of V_λ (see Fig. 3.3). In particular, a dimension

$$d_\lambda := \dim V_\lambda = |\mathrm{Paths}(\lambda, \mathscr{A})| \tag{3.54}$$

of the simple $\mathcal{A}_n$-module V_λ generally depends on the local dimension d.

Adapting Jucys–Murphy elements and content vectors to $\mathcal{A}^d_{n,m}$

The Jucys–Murphy elements for semisimple walled Brauer algebras $\mathcal{B}$, given in Eq. (3.50), can be used in the algorithm from Section 2.7.5 to find the primitive central idempotents $\varepsilon^{\mathcal{B}}_\lambda$ and canonical primitive idempotents $\varepsilon^{\mathcal{B}}_T$ of $\mathcal{B}^d_{n,m}$. In this section, we show how this procedure can be adapted to the partially transposed permutation matrix algebras $\mathcal{A}^d_{n,m}$. To construct the primitive central idempotents $\varepsilon^{\mathcal{A}}_\lambda$ and canonical primitive idempotents $\varepsilon^{\mathcal{A}}_T$ of $\mathcal{A}^d_{n,m}$, we can use the modified Bratteli diagram from Section 3.6, and it only remains to adapt the Jucys–Murphy elements and content vectors from $\mathcal{B}^d_{n,m}$ to $\mathcal{A}^d_{n,m}$. Below we show that we can use lifted versions of Jucys–Murphy elements of $\mathcal{B}^d_{n,m}$ and their content vectors for that purpose.

Throughout this section we set for every $k \in [n+m]$

$$J^{\mathcal{A}}_k := \psi^d_{n,m}(J^{\mathcal{B}}_k) \in \mathcal{A}^d_{n,m}, \tag{3.55}$$

where $J^{\mathcal{B}}_k$ are the Jucys–Murphy elements of $\mathcal{B}$ given in Eq. (3.50) and $\psi^d_{n,m}$ is the map from Eq. (3.17). To establish that $J^{\mathcal{A}}_1, \dots, J^{\mathcal{A}}_{n+m}$ is a Jucys–Murphy sequence for $\mathcal{A}^d_{n,m}$, we need to show that it is both additively central and separating (see Definition 2.7.7).

3.6.1. Lemma. *The sequence $J^{\mathcal{A}}_1, \dots, J^{\mathcal{A}}_{n+m}$ is additively central in $\mathcal{A}^d_{n,m}$.*

Proof:
For any $k \in [n+m]$, one can verify that the Jucys–Murphy elements $J^{\mathcal{B}}_k$ defined in Eq. (3.50) satisfy $J^{\mathcal{B}}_k \in \mathcal{X}^{\mathcal{B}}_k$ and $J^{\mathcal{B}}_1 + \dots + J^{\mathcal{B}}_k \in \mathcal{Z}(\mathcal{B}_k)$ [JK20]. Since $\psi^d_{n,m}$ is a homomorphism, $\psi^d_{n,m}\big(\mathcal{Z}(\mathcal{B}_k)\big) \subseteq \mathcal{Z}(\mathcal{A}_k)$ and hence $\psi^d_{n,m}(\mathcal{X}^{\mathcal{B}}_k) \subseteq \mathcal{X}^{\mathcal{A}}_k$. Therefore $J^{\mathcal{A}}_k = \psi^d_{n,m}(J^{\mathcal{B}}_k) \in \psi^d_{n,m}(\mathcal{X}^{\mathcal{B}}_k) \subseteq \mathcal{X}^{\mathcal{A}}_k$ and the sequence $J^{\mathcal{A}}_1, \dots, J^{\mathcal{A}}_{n+m}$ is additively central in $\mathcal{A}^d_{n,m}$. □

3.6.2. Lemma. *For any $T \in \mathrm{Paths}(\mathscr{A})$ in the Bratteli diagram of $\mathcal{A}^d_{n,m}$,*

$$(J^{\mathcal{A}}_1 + \dots + J^{\mathcal{A}}_{n+m})\, \varepsilon^{\mathcal{A}}_T = \big(\mathrm{cont}(\lambda_l) + \mathrm{cont}(\lambda_r) + d \cdot |\lambda_r|\big)\, \varepsilon^{\mathcal{A}}_T \tag{3.56}$$

where $\varepsilon^{\mathcal{A}}_T$ is the corresponding canonical primitive idempotent of $\mathcal{A}^d_{n,m}$, $\lambda = (\lambda_l, \lambda_r) = T^{n+m}$ is the last vertex of the path T, $\mathrm{cont}(\lambda)$ is the total content of all cells of the Young diagram λ and $|\lambda|$ is the number of cells in λ.

Proof:
See Appendix 3.A.2 for proof. Our proof is reminiscent of [BS12, Lemma 2.3], which is a similar statement for the walled Brauer algebras. □

3.6.3. Corollary. *For any $k \in [n+m]$ and $T \in \mathrm{Paths}(\mathscr{A})$, $J^{\mathcal{A}}_k \varepsilon^{\mathcal{A}}_T = \mathrm{wcont}_k(T) \varepsilon^{\mathcal{A}}_T$ where $\mathrm{wcont}_k(T)$ is the notion of content for the walled Brauer algebra $\mathcal{B}^d_{n,m}$, see Eq. (3.51).*

Proof:
Let $T^{[k]} := T^0 \to T^1 \to \cdots \to T^k$ denote the first k edges of the path T. Recall from Eq. (2.56) that the canonical primitive idempotents of $\mathcal{A}$ are given by

$$\varepsilon^{\mathcal{A}}_{T^{[k]}} = \varepsilon^{\mathcal{A}}_{T^1}\varepsilon^{\mathcal{A}}_{T^2}\cdots\varepsilon^{\mathcal{A}}_{T^k}. \tag{3.57}$$

Each value of k effectively corresponds to truncating the Bratteli diagram to a certain n and m. Thus Lemma 3.6.2 with appropriate n and m allows us to compute the eigenvalue of $J^{\mathcal{A}}_1 + \cdots + J^{\mathcal{A}}_k$ for two consecutive $\varepsilon^{\mathcal{A}}_{T^k}$:

$$(J^{\mathcal{A}}_1 + \cdots + J^{\mathcal{A}}_k)\,\varepsilon^{\mathcal{A}}_{T^{[k]}} = \big(\mathrm{cont}(T^k_l) + \mathrm{cont}(T^k_r) + d\cdot|T^k_r|\big)\,\varepsilon^{\mathcal{A}}_{T^{[k]}}, \tag{3.58}$$
$$(J^{\mathcal{A}}_1 + \cdots + J^{\mathcal{A}}_{k-1})\,\varepsilon^{\mathcal{A}}_{T^{[k-1]}} = \big(\mathrm{cont}(T^{k-1}_l) + \mathrm{cont}(T^{k-1}_r) + d\cdot|T^{k-1}_r|\big)\,\varepsilon^{\mathcal{A}}_{T^{[k-1]}}. \tag{3.59}$$

Multiplying both equations with the primitive central idempotents of $\mathcal{A}$ ranging from $\varepsilon^{\mathcal{A}}_{T^k}$ to $\varepsilon^{\mathcal{A}}_{T^{n+m}}$ transforms the subscripts T^k and T^{k-1} into $T^{n+m} = T$:

$$(J^{\mathcal{A}}_1 + \cdots + J^{\mathcal{A}}_k)\,\varepsilon^{\mathcal{A}}_{T} = \big(\mathrm{cont}(T^k_l) + \mathrm{cont}(T^k_r) + d\cdot|T^k_r|\big)\,\varepsilon^{\mathcal{A}}_{T}, \tag{3.60}$$
$$(J^{\mathcal{A}}_1 + \cdots + J^{\mathcal{A}}_{k-1})\,\varepsilon^{\mathcal{A}}_{T} = \big(\mathrm{cont}(T^{k-1}_l) + \mathrm{cont}(T^{k-1}_r) + d\cdot|T^{k-1}_r|\big)\,\varepsilon^{\mathcal{A}}_{T}. \tag{3.61}$$

Subtracting these two equations we get

$$J^{\mathcal{A}}_k\varepsilon^{\mathcal{A}}_T = \Big(\mathrm{cont}(T^k_l) - \mathrm{cont}(T^{k-1}_l) + \mathrm{cont}(T^k_r) - \mathrm{cont}(T^{k-1}_r) + d\cdot\big(|T^k_r| - |T^{k-1}_r|\big)\Big)\,\varepsilon^{\mathcal{A}}_T. \tag{3.62}$$

If $k \leqslant n$ then $T^k_r = T^{k-1}_r = \varnothing$ and $\mathrm{cont}(T^k_l) - \mathrm{cont}(T^{k-1}_l) = j - i$, where (i, j) is the location where adding a cell to the Young diagram T^{k-1}_l transforms it into T^k_l. If $k > n$ then there are two cases. If $T^k_r = T^{k-1}_r$ then $\mathrm{cont}(T^k_l) - \mathrm{cont}(T^{k-1}_l) = i - j$ because the cell (i, j) is removed from T^{k-1}_l. If $T^k_l = T^{k-1}_l$ then $\mathrm{cont}(T^k_l) - \mathrm{cont}(T^{k-1}_l) = j - i$ and $\mathrm{size}(T^k_r) - \mathrm{size}(T^{k-1}_r) = 1$, where (i, j) is the location where adding a cell to the Young diagram T^{k-1}_r transforms it into T^k_r. In either case,

$$J^{\mathcal{A}}_k\varepsilon^{\mathcal{A}}_T = \mathrm{wcont}_k(T)\varepsilon^{\mathcal{A}}_T, \tag{3.63}$$

where $\mathrm{wcont}_k(T)$ is exactly the notion of content for the walled Brauer algebra $\mathcal{B}^d_{n,m}$ as defined in Eq. (3.51). □

3.6.4. Lemma. *If $S, T \in \mathrm{Paths}(\mathscr{A})$ are two paths in the Bratteli diagram of $\mathcal{A}^d_{n,m}$ then $S = T$ if and only if $c_S = c_T$.*

Proof:
The forward direction is obvious. For the reverse implication, assume that $S \neq T$ and $c_S = c_T$. We consider two cases depending on the first location $k \in [n + m]$ where the two paths differ, i.e., $S^k \neq T^k$ while $S^{k-1} = T^{k-1} =: (\lambda_l, \lambda_r)$.

If $k \leqslant n$, we can only add cells to the Young diagram λ_l, so let (i, j) and (i', j') denote the two possible locations. It follows from Corollary 3.6.3 that $c_T(k) = j - i$ and $c_S(k) = j' - i'$, and hence $j - i = j' - i'$. Since any Young diagram has at most one location on any diagonal where a new cell can be added, $(i, j) = (i', j')$ and therefore $S^k = T^k$.

If $k > n$, the condition $c_T(k) = c_S(k)$ can be satisfied only if we assume (without loss of generality) that $c_T(k) = i^l - j^l$ and $c_S(k) = j^r - i^r + d$, implying that $i^l + i^r = j^l + j^r + d$ for the removed cell (i^l, j^l) of λ_l and the added cell (i^r, j^r) of λ_r. In particular, $i^l + i^r = j^l + j^r + d \geqslant d + 2$ since $j^l > 0$ and $j^r > 0$. On the other hand, the total length of the two diagrams satisfies $\ell(\lambda_l) + \ell(\lambda_r) \leqslant d$, which implies that $i^l + i^r \leqslant d$, a contradiction. □

3.6.5. Corollary. *The sequence $J_1^{\mathcal{A}}, \dots, J_{n+m}^{\mathcal{A}}$ is separating in $\mathcal{A}$.*

Proof:
This follows from Lemma 3.6.4 and Proposition 3.5 of [DLS18]. □

3.6.6. Theorem. *$J_1^{\mathcal{A}}, \dots, J_{n+m}^{\mathcal{A}}$ is a Jucys–Murphy sequence for $\mathcal{A}$.*

Proof:
This follows from Lemma 3.6.1 and Corollary 3.6.5. □

Theorem 3.6.6 establishes that the operators $J_k^{\mathcal{A}}$, which were obtained in Eq. (3.55) by lifting the Jucys–Murphy sequence $J_k^{\mathcal{B}}$ of the walled Brauer algebras $\mathcal{B}_{n,m}^d$ to the matrix algebras $\mathcal{A}_{n,m}^d$, are indeed Jucys–Murphy elements of $\mathcal{A}_{n,m}^d$. Furthermore, Corollary 3.6.3 shows that the content vectors of the two families of algebras agree.

Primitive idempotents of $\mathcal{A}_{n,m}^d$

We have now established the three ingredients required to apply the [DLS18] algorithm to the partially transposed matrix algebras $\mathcal{A}_{n,m}^d$:

1. the Bratteli diagram for $\mathcal{A}$ is obtained by truncating the Bratteli diagram of $\mathcal{B}$,
2. the Jucys–Murphy elements of $\mathcal{A}$ are obtained by applying $\psi_{n,m}^d$ to the Jucys–Murphy elements of $\mathcal{B}$ given in Eq. (3.50),
3. the content vectors of $\mathcal{A}$ agree with those of $\mathcal{B}$ and are given in Section 3.6.

This allows us to use the algorithm described in Section 2.7.5 to compute the primitive central idempotents and canonical primitive idempotents of $\mathcal{A}$.

A major advantage of this approach is that the entire computation can be performed by employing linear combinations of diagrams instead of actual matrices (i.e., staying within the diagrammatic walled Brauer algebra $\mathcal{B}_{n,m}^d$ rather than working in the matrix algebra $\mathcal{A}_{n,m}^d$). This results in a diagrammatic representation of an idempotent of $\mathcal{A}_{n,m}^d$ as a preimage of the actual idempotent under $\psi_{n,m}^d$. More explicitly, the primitive central idempotents of $\mathcal{A}_{n,m}^d$ can be computed iteratively as

$$\varepsilon_\mu^{\mathcal{A}} := \sum_{\lambda\,:\,\lambda\to\mu} \psi_{n,m}^d\left(P_{\lambda\to\mu}(J_k^{\mathcal{B}})\right)\varepsilon_\lambda^{\mathcal{A}}, \tag{3.64}$$

where the polynomials $P_{\lambda\to\mu}$ from Eq. (2.60) are evaluated for the Bratteli diagram of the family $\mathcal{A}$ described in Section 3.6. Similarly to Eq. (2.62), canonical primitive idempotents ε_T are adapted to the matrix algebras $\mathcal{A}$ as follows:

$$\varepsilon_T^{\mathcal{A}} = \psi_{n,m}^d\left(\prod_{k=1}^{n+m}\prod_{\mu\,:\,\lambda_{k-1}\to\mu\neq\lambda_k}\frac{J_k^{\mathcal{B}} - c_{\lambda_{k-1}\to\mu}}{c_{\lambda_{k-1}\to\lambda_k} - c_{\lambda_{k-1}\to\mu}}\right), \tag{3.65}$$

where the second product runs over edges in the Bratteli diagram $\mathscr{A}$ of the family $\mathcal{A}$.

This representation of idempotents is more compact compared to the naive one when d is large, and easily amenable to further fast diagrammatic calculations. This allows to significantly lower the computational complexity of various tasks within the partially transposed permutation matrix algebra, as illustrated later in Chapter 6.

3.7 Gelfand–Tsetlin basis for partially transposed permutations

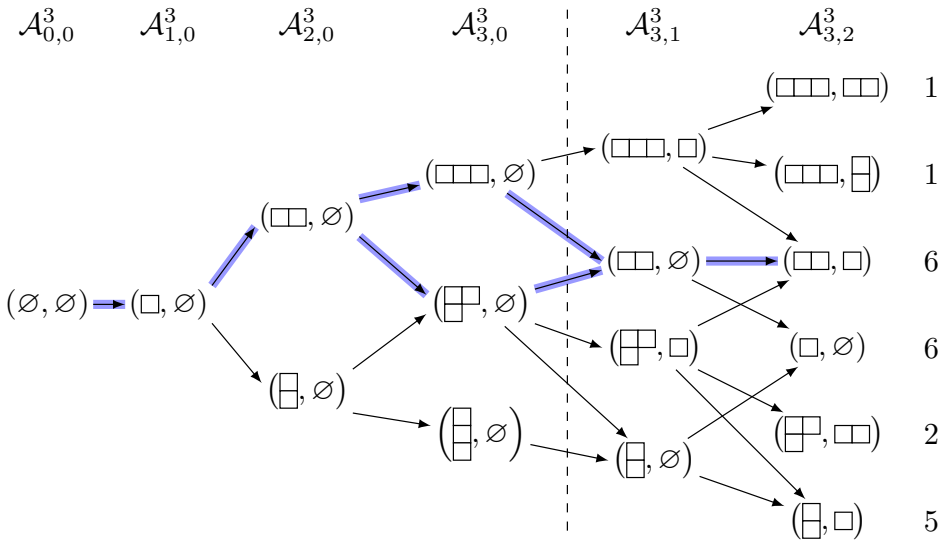

Figure 3.4: The Bratteli diagram associated with the family (3.67) of partially transposed permutation matrix algebras when $n = 3$, $m = 2$, and local dimension $d = 3$. For a chosen path $T = \big((\varnothing,\varnothing),(\square,\varnothing),(\square\square,\varnothing),(\square\square\square,\varnothing),(\square\square,\varnothing),(\square\square,\square)\big)$, we have highlighted in blue the set $\mathcal{M}(T)$ of all paths that agree with T everywhere except for level n. For each leaf, we have indicated the number of paths from the root to that leaf, which coincides with the dimension of the corresponding irrep.

Now we are ready to state our main result of this chapter. Recall from Section 3.6 that the irreducible representations of $\mathcal{A}^d_{n,m}$ are labelled by the following set of mixed Young diagrams (λ_l, λ_r):

$$\widehat{\mathcal{A}}^d_{n,m} := \Big\{ \lambda = (\lambda_l, \lambda_r) \;\Big|\; 0 \leqslant k \leqslant \min(n,m),\ \lambda_l \vdash n-k,\ \lambda_r \vdash m-k,\ \ell(\lambda_l)+\ell(\lambda_r) \leqslant d \Big\}, \quad (3.66)$$

which corresponds to the following multiplicity-free family of algebras:

$$\mathcal{A}^d_{0,0} \hookrightarrow \mathcal{A}^d_{1,0} \hookrightarrow \cdots \hookrightarrow \mathcal{A}^d_{n,0} \hookrightarrow \mathcal{A}^d_{n,1} \hookrightarrow \cdots \hookrightarrow \mathcal{A}^d_{n,m}. \quad (3.67)$$

The set of paths $\mathrm{Paths}(\lambda)$ in the Bratteli diagram of the family Eq. (3.67) correspond precisely to the set of mixed standard Young tableaux of shape λ (see Section 3.5). For example, Fig. 3.4 shows the Bratteli diagram for the sequence (3.67) ending with algebra $\mathcal{A}^3_{3,2}$.

For any $\lambda \in \widehat{\mathcal{A}}^d_{n,m}$, we will denote the corresponding irrep by

$$\psi_\lambda \colon \mathcal{A}^d_{n,m} \to \mathrm{End}(V_\lambda) \quad \text{where} \quad V_\lambda := \mathbb{C}^{\mathrm{Paths}(\lambda)}. \quad (3.68)$$

Our main technical result, Theorem 3.7.1, provides an explicit formula for $\psi_\lambda(\sigma_i)$, for any generator σ_i of $\mathcal{A}^d_{n,m}$. This effectively describes how the matrix algebra $\mathcal{A}^d_{n,m}$ acts on the Gelfand–Tsetlin basis vectors $|T\rangle$, where T is any root-leaf path in the corresponding Bratteli diagram. Before presenting our formula, we introduce some auxiliary notation.

We define the *walled axial distance* between cells containing i and $i+1$ in $T \in \mathrm{Paths}(\lambda)$ as

$$r_i(T) := \mathrm{wcont}_{i+1}(T) - \mathrm{wcont}_i(T). \quad (3.69)$$

The walled axial distance has a simple combinatorial interpretation. Indeed, $r_i(T)$ is the axial distance between cells containing i and $i+1$ in a staircase representation $\widetilde{T}$ of a mixed Young diagram T, see Fig. 3.1 and Eq. (3.44).

Furthermore, if $T^{n-1} = T^{n+1}$ we denote by

$$\mathcal{M}(T) := \{(T^0, \dots, T^{n-1}, \mu, T^{n+1}, \dots, T^{n+m}) \in \mathrm{Paths}(T^{n+m}) \mid \mu \in \widehat{\mathcal{A}}^d_{n,0}\} \tag{3.70}$$

and $\mathcal{M}(T) := \varnothing$ otherwise. The set of all paths in the Bratteli diagram differing from T only at the n-th level (see Fig. 3.4 for an example). For a given path T, we define a cell a_T, containing both numbers n and $n+1$ in the mixed Young tableau T, formally as

$$a_T := \begin{cases} T^n_l \setminus T^{n-1}_l & \text{if } T^{n-1} = T^{n+1}, \\ \varnothing & \text{otherwise,} \end{cases} \tag{3.71}$$

where T^k_l denotes the left diagram in $T^k = (T^k_l, T^k_r)$. With this notation at hand, we can state our main technical result.

3.7.1. Theorem (Gelfand–Tsetlin basis for $\mathcal{A}^d_{n,m}$). *For any $\lambda \in \widehat{\mathcal{A}}^d_{n,m}$, the following representation $\psi_\lambda \colon \mathcal{A}^d_{n,m} \to \mathrm{End}\big(\mathbb{C}^{\mathrm{Paths}(\lambda)}\big)$ is an irreducible representation of $\mathcal{A}^d_{n,m}$. Given a generator σ_i of $\mathcal{A}^d_{n,m}$, $i = 1, \dots, n+m-1$, the matrix $\psi_\lambda(\sigma_i)$ acts on the Gelfand–Tsetlin basis vectors $|T\rangle$ with $T \in \mathrm{Paths}(\lambda)$ as follows:*

$$\psi_\lambda(\sigma_i)\,|T\rangle = \frac{1}{r_i(T)}\,|T\rangle + \sqrt{1 - \frac{1}{r_i(T)^2}}\,|\sigma_i T\rangle, \qquad \text{for } i \neq n, \tag{3.72}$$

$$\psi_\lambda(\sigma_n)\,|T\rangle = c(T)\,|v_T\rangle, \quad |v_T\rangle := \sum_{T' \in \mathcal{M}(T)} c(T')\,|T'\rangle, \qquad \text{for } i = n, \tag{3.73}$$

where $r_i(T)$ is the walled axial distance defined in Eq. (3.69), $\sigma_i T$ denotes the mixed standard Young tableau T with cell fillings permuted according to σ_i (see Section 3.5), and the coefficient $c(T) \geqslant 0$ is given by

$$c(T) := \sqrt{\big(d + \mathrm{cont}(a_T)\big)\frac{\prod_{c \in \mathrm{RC}(T^{n-1}_l)}\big(\mathrm{cont}(a_T) - \mathrm{cont}(c)\big)}{\prod_{a \in \mathrm{AC}(T^{n-1}_l) \setminus a_T}\big(\mathrm{cont}(a_T) - \mathrm{cont}(a)\big)}} = \sqrt{\frac{m_{T^n}}{m_{T^{n-1}}}}, \tag{3.74}$$

where a_T is defined in Eq. (3.71), RC/AC are the sets of removable/addable cells, and $m_{T^n}, m_{T^{n-1}}$ are dimensions of the corresponding Weyl modules.

Table 3.1 provides an example of how Theorem 3.7.1 can be used to compute all irreps of $\mathcal{A}^3_{3,2}$ using the Bratteli diagram shown in Fig. 3.4. Note, that the second equality in Eq. (3.74) is immediate consequence of Lemmas 3.7.4 and 3.7.5.

Our proof is similar in spirit to that of [ST17]. However, they described a *seminormal* basis for the *quantum* walled Brauer algebra, while we consider *orthonormal* basis of the usual walled Brauer algebra.

Before we start the proof, let's recall the defining relations for the walled Brauer algebra.

3.7.2. Definition. Let $n, m \geqslant 0$ be integers and $d \in \mathbb{C}$. The *walled Brauer algebra* $\mathcal{B}^d_{n,m}$ is a finite-dimensional associative algebra over $\mathbb{C}$ generated by $\sigma_1, \dots, \sigma_{n+m-1}$ subject to the following relations:

$$\text{(a) } \sigma_i^2 = 1 \ (i \neq n), \quad \text{(b) } \sigma_i\sigma_{i+1}\sigma_i = \sigma_{i+1}\sigma_i\sigma_{i+1} \ (i \neq n-1, n), \quad \text{(c) } \sigma_i\sigma_j = \sigma_j\sigma_i \ (|i-j| > 1), \tag{3.11}$$

$$\text{(d) } \sigma_n^2 = d\sigma_n, \qquad \text{(e) } \sigma_n\sigma_{n\pm1}\sigma_n = \sigma_n, \qquad \text{(f) } \sigma_n\sigma_i = \sigma_i\sigma_n \ (i \neq n \pm 1), \tag{3.12}$$

$$\text{(g) } \sigma_n\sigma_{n+1}\sigma_{n-1}\sigma_n\sigma_{n-1} = \sigma_n\sigma_{n+1}\sigma_{n-1}\sigma_n\sigma_{n+1}, \tag{3.13}$$

$$\text{(h) } \sigma_{n-1}\sigma_n\sigma_{n+1}\sigma_{n-1}\sigma_n = \sigma_{n+1}\sigma_n\sigma_{n+1}\sigma_{n-1}\sigma_n. \tag{3.14}$$

	$(\ydiagram{3},\ydiagram{2})$	$(\ydiagram{3},\ydiagram{1,1})$	$(\ydiagram{2},\ydiagram{2})$	$(\ydiagram{1},\varnothing)$	$(\ydiagram{2,2},\ydiagram{2})$	$(\ydiagram{2,1},\ydiagram{1})$
σ_1	(1)	(1)	$\begin{pmatrix} -1 & 0 & 0 & 0 & 0 & 0 \\ 0 & -1 & 0 & 0 & 0 & 0 \\ 0 & 0 & 1 & 0 & 0 & 0 \\ 0 & 0 & 0 & 1 & 0 & 0 \\ 0 & 0 & 0 & 0 & 1 & 0 \\ 0 & 0 & 0 & 0 & 0 & 1 \end{pmatrix}$	$\begin{pmatrix} -1 & 0 & 0 & 0 & 0 & 0 \\ 0 & -1 & 0 & 0 & 0 & 0 \\ 0 & 0 & -1 & 0 & 0 & 0 \\ 0 & 0 & 0 & 1 & 0 & 0 \\ 0 & 0 & 0 & 0 & 1 & 0 \\ 0 & 0 & 0 & 0 & 0 & 1 \end{pmatrix}$	$\begin{pmatrix} -1 & 0 \\ 0 & 1 \end{pmatrix}$	$\begin{pmatrix} -1 & 0 & 0 & 0 & 0 \\ 0 & -1 & 0 & 0 & 0 \\ 0 & 0 & -1 & 0 & 0 \\ 0 & 0 & 0 & 1 & 0 \\ 0 & 0 & 0 & 0 & 1 \end{pmatrix}$
σ_2	(1)	(1)	$\begin{pmatrix} \frac{1}{2} & 0 & \frac{\sqrt{3}}{2} & 0 & 0 & 0 \\ 0 & \frac{1}{2} & 0 & \frac{\sqrt{3}}{2} & 0 & 0 \\ \frac{\sqrt{3}}{2} & 0 & -\frac{1}{2} & 0 & 0 & 0 \\ 0 & \frac{\sqrt{3}}{2} & 0 & -\frac{1}{2} & 0 & 0 \\ 0 & 0 & 0 & 0 & 1 & 0 \\ 0 & 0 & 0 & 0 & 0 & 1 \end{pmatrix}$	$\begin{pmatrix} -1 & 0 & 0 & 0 & 0 & 0 \\ 0 & \frac{1}{2} & 0 & \frac{\sqrt{3}}{2} & 0 & 0 \\ 0 & 0 & \frac{1}{2} & 0 & \frac{\sqrt{3}}{2} & 0 \\ 0 & \frac{\sqrt{3}}{2} & 0 & -\frac{1}{2} & 0 & 0 \\ 0 & 0 & \frac{\sqrt{3}}{2} & 0 & -\frac{1}{2} & 0 \\ 0 & 0 & 0 & 0 & 0 & 1 \end{pmatrix}$	$\begin{pmatrix} \frac{1}{2} & \frac{\sqrt{3}}{2} \\ \frac{\sqrt{3}}{2} & -\frac{1}{2} \end{pmatrix}$	$\begin{pmatrix} -1 & 0 & 0 & 0 & 0 \\ 0 & \frac{1}{2} & 0 & \frac{\sqrt{3}}{2} & 0 \\ 0 & 0 & \frac{1}{2} & 0 & \frac{\sqrt{3}}{2} \\ 0 & \frac{\sqrt{3}}{2} & 0 & -\frac{1}{2} & 0 \\ 0 & 0 & \frac{\sqrt{3}}{2} & 0 & -\frac{1}{2} \end{pmatrix}$
σ_3	(0)	(0)	$\begin{pmatrix} 0 & 0 & 0 & 0 & 0 & 0 \\ 0 & 0 & 0 & 0 & 0 & 0 \\ 0 & 0 & \frac{4}{3} & 0 & \frac{2\sqrt{5}}{3} & 0 \\ 0 & 0 & 0 & 0 & 0 & 0 \\ 0 & 0 & \frac{2\sqrt{5}}{3} & 0 & \frac{5}{3} & 0 \\ 0 & 0 & 0 & 0 & 0 & 0 \end{pmatrix}$	$\begin{pmatrix} \frac{1}{3} & \frac{2\sqrt{2}}{3} & 0 & 0 & 0 & 0 \\ \frac{2\sqrt{2}}{3} & \frac{8}{3} & 0 & 0 & 0 & 0 \\ 0 & 0 & 0 & 0 & 0 & 0 \\ 0 & 0 & 0 & 0 & 0 & 0 \\ 0 & 0 & 0 & 0 & \frac{4}{3} & \frac{2\sqrt{5}}{3} \\ 0 & 0 & 0 & 0 & \frac{2\sqrt{5}}{3} & \frac{5}{3} \end{pmatrix}$	$\begin{pmatrix} 0 & 0 \\ 0 & 0 \end{pmatrix}$	$\begin{pmatrix} \frac{1}{3} & \frac{2\sqrt{2}}{3} & 0 & 0 & 0 \\ \frac{2\sqrt{2}}{3} & \frac{8}{3} & 0 & 0 & 0 \\ 0 & 0 & 0 & 0 & 0 \\ 0 & 0 & 0 & 0 & 0 \\ 0 & 0 & 0 & 0 & 0 \end{pmatrix}$
σ_4	(1)	(-1)	$\begin{pmatrix} \frac{1}{2} & \frac{\sqrt{3}}{2} & 0 & 0 & 0 & 0 \\ \frac{\sqrt{3}}{2} & -\frac{1}{2} & 0 & 0 & 0 & 0 \\ 0 & 0 & \frac{1}{2} & \frac{\sqrt{3}}{2} & 0 & 0 \\ 0 & 0 & \frac{\sqrt{3}}{2} & -\frac{1}{2} & 0 & 0 \\ 0 & 0 & 0 & 0 & \frac{1}{5} & \frac{2\sqrt{6}}{5} \\ 0 & 0 & 0 & 0 & \frac{2\sqrt{6}}{5} & -\frac{1}{5} \end{pmatrix}$	$\begin{pmatrix} -1 & 0 & 0 & 0 & 0 & 0 \\ 0 & \frac{1}{2} & \frac{\sqrt{3}}{2} & 0 & 0 & 0 \\ 0 & \frac{\sqrt{3}}{2} & -\frac{1}{2} & 0 & 0 & 0 \\ 0 & 0 & 0 & \frac{1}{2} & \frac{\sqrt{3}}{2} & 0 \\ 0 & 0 & 0 & \frac{\sqrt{3}}{2} & -\frac{1}{2} & 0 \\ 0 & 0 & 0 & 0 & 0 & 1 \end{pmatrix}$	$\begin{pmatrix} 1 & 0 \\ 0 & 1 \end{pmatrix}$	$\begin{pmatrix} 1 & 0 & 0 & 0 & 0 \\ 0 & \frac{1}{4} & \frac{\sqrt{15}}{4} & 0 & 0 \\ 0 & \frac{\sqrt{15}}{4} & -\frac{1}{4} & 0 & 0 \\ 0 & 0 & 0 & \frac{1}{4} & \frac{\sqrt{15}}{4} \\ 0 & 0 & 0 & \frac{\sqrt{15}}{4} & -\frac{1}{4} \end{pmatrix}$

Table 3.1: Example of Theorem 3.7.1 in action: the matrices $\psi_\lambda(\sigma_i)$ in the Gelfand–Tsetlin basis for all irreducible representations ψ_λ and generators σ_i of the matrix algebra $\mathcal{A}^3_{3,2}$. Rows correspond to generators σ_i, and columns correspond to irrep labels $\lambda = (\lambda_l, \lambda_r)$. Note that irreps with $|\lambda_l| = 3$ and $|\lambda_r| = 2$ vanish on the contraction σ_3 since they are irreps of $\mathrm{S}_3 \times \mathrm{S}_2$. The Bratteli diagram for $\mathcal{A}^3_{3,2}$ is shown in Fig. 3.4.

Proof:
We will prove the theorem in several steps. First, we check that such action defines a representation of $\mathcal{A}^d_{n,m}$ by checking the relations in Eq. (3.11) for transpositions. The relations for transpositions in Eq. (3.72) are defined in the same way as the Young–Yamanouchi basis of the symmetric group [Rut48]. It is essentially folklore knowledge today, however, we still provide the proof for completeness. Next, we check the relations in Eqs. (3.12) to (3.14) for the contraction σ_n. Finally, we prove that such representation is irreducible. For simplicity, we will write σ instead of $\psi_\lambda(\sigma)$ for any $\sigma \in \mathcal{A}^d_{n,m}$. Note, that our further analysis will hold for all irreps $\lambda \in \mathcal{A}^d_{n,m}$ and all paths $T \in \mathrm{Paths}(\lambda, \mathscr{A})$, which we fix at the start of the arguments.

(a) To verify $\sigma_i^2 = 1$, consider the action of σ_i on the invariant subspaces V_T for each $T \in \mathrm{Paths}(\lambda)$ defined as

$$V_T := \mathrm{span}\{|T\rangle, |\sigma_i T\rangle\}. \tag{3.75}$$

It is clear from Eq. (3.72) that the matrix $\sigma_i|_{V_T}$ of this action is

$$\sigma_i\big|_{V_T} = \begin{pmatrix} \frac{1}{r_i(T)} & \sqrt{1-\frac{1}{r_i(T)^2}} \\ \sqrt{1-\frac{1}{r_i(T)^2}} & -\frac{1}{r_i(T)} \end{pmatrix}, \tag{3.76}$$

meaning that trivially $(\sigma_i|_{V_T})^2 = 1$. Since that holds for every $T \in \mathrm{Paths}(\lambda)$, then $\sigma_i^2 = 1$ holds.

(b) To verify $(\sigma_i\sigma_{i+1})^3 = 1$, consider for every $T \in \mathrm{Paths}(\lambda)$ the action of $\sigma_i\sigma_{i+1}$ (according to Eq. (3.72)) on the invariant vector space

$$V_T := \mathrm{span}\{|T\rangle, |\sigma_i T\rangle, |\sigma_{i+1}\sigma_i T\rangle, |\sigma_i\sigma_{i+1}\sigma_i T\rangle, |(\sigma_{i+1}\sigma_i)^2 T\rangle, |\sigma_i(\sigma_{i+1}\sigma_i)^2 T\rangle\}. \tag{3.77}$$

Now if we define

$$a := r_i(T), \quad b := r_i(\sigma_{i+1}\sigma_i T), \quad c := r_i\big((\sigma_{i+1}\sigma_i)^2 T\big), \tag{3.78}$$

then the action of σ_i and σ_{i+1} on the V_T in the above basis is given by the following matrices:

$$\sigma_i\big|_{V_T} = \begin{pmatrix} \frac{1}{a} & \sqrt{1-\frac{1}{a^2}} & 0 & 0 & 0 & 0 \\ \sqrt{1-\frac{1}{a^2}} & -\frac{1}{a} & 0 & 0 & 0 & 0 \\ 0 & 0 & \frac{1}{b} & \sqrt{1-\frac{1}{b^2}} & 0 & 0 \\ 0 & 0 & \sqrt{1-\frac{1}{b^2}} & -\frac{1}{b} & 0 & 0 \\ 0 & 0 & 0 & 0 & \frac{1}{c} & \sqrt{1-\frac{1}{c^2}} \\ 0 & 0 & 0 & 0 & \sqrt{1-\frac{1}{c^2}} & -\frac{1}{c} \end{pmatrix}, \tag{3.79}$$

$$\sigma_{i+1}\big|_{V_T} = \begin{pmatrix} \frac{1}{c} & 0 & \sqrt{1-\frac{1}{c^2}} & 0 & 0 & 0 \\ 0 & \frac{1}{b} & 0 & 0 & \sqrt{1-\frac{1}{b^2}} & 0 \\ \sqrt{1-\frac{1}{c^2}} & 0 & -\frac{1}{c} & 0 & 0 & 0 \\ 0 & 0 & 0 & \frac{1}{a} & 0 & \sqrt{1-\frac{1}{a^2}} \\ 0 & \sqrt{1-\frac{1}{b^2}} & 0 & 0 & -\frac{1}{b} & 0 \\ 0 & 0 & 0 & \sqrt{1-\frac{1}{a^2}} & 0 & -\frac{1}{a} \end{pmatrix}. \tag{3.80}$$

Taking into account the fact $b = a + c$, it is easy to verify that $(\sigma_i|_{V_T}\sigma_{i+1}|_{V_T})^3 = 1$. Since this holds for any $T \in \mathrm{Paths}(\lambda)$, it must be $(\sigma_i\sigma_{i+1})^3 = 1$.

(c) Finally, to verify the relation $\sigma_i\sigma_j = \sigma_j\sigma_i$ for $(|i-j| > 1)$ just note, that $\sigma_i\sigma_j T = \sigma_j\sigma_i T$ and

$$a := r_i(\sigma_j T) = r_i(T), \quad b := r_j(\sigma_i T) = r_j(T). \tag{3.81}$$

It means that on V_T defined for every $T \in \mathrm{Paths}(\mathscr{A})$ as

$$V_T := \mathrm{span}\{|T\rangle, |\sigma_i T\rangle, |\sigma_j T\rangle, |\sigma_j\sigma_i T\rangle\} \tag{3.82}$$

σ_i and σ_j have a tensor product structure:

$$\sigma_i\big|_{V_T} = \begin{pmatrix} \frac{1}{a} & \sqrt{1-\frac{1}{a^2}} & 0 & 0 \\ \sqrt{1-\frac{1}{a^2}} & -\frac{1}{a} & 0 & 0 \\ 0 & 0 & \frac{1}{a} & \sqrt{1-\frac{1}{a^2}} \\ 0 & 0 & \sqrt{1-\frac{1}{a^2}} & -\frac{1}{a} \end{pmatrix} = I_2 \otimes \begin{pmatrix} \frac{1}{a} & \sqrt{1-\frac{1}{a^2}} \\ \sqrt{1-\frac{1}{a^2}} & -\frac{1}{a} \end{pmatrix}, \tag{3.83}$$

$$\sigma_j\big|_{V_T} = \begin{pmatrix} \frac{1}{b} & 0 & \sqrt{1-\frac{1}{b^2}} & 0 \\ 0 & \frac{1}{b} & 0 & \sqrt{1-\frac{1}{b^2}} \\ \sqrt{1-\frac{1}{b^2}} & 0 & -\frac{1}{b} & 0 \\ 0 & \sqrt{1-\frac{1}{b^2}} & 0 & -\frac{1}{b} \end{pmatrix} = \begin{pmatrix} \frac{1}{b} & \sqrt{1-\frac{1}{b^2}} \\ \sqrt{1-\frac{1}{b^2}} & -\frac{1}{b} \end{pmatrix} \otimes I_2, \tag{3.84}$$

and consecutively $\sigma_i|_{V_T}\sigma_j|_{V_T} = \sigma_j|_{V_T}\sigma_i|_{V_T}$. Therefore, $\sigma_i\sigma_j = \sigma_j\sigma_i$ when $|i-j|>1$.

(d) For each $T \in \mathrm{Paths}(\lambda)$ there is an invariant subspace $V_T := \mathrm{span}\{|T'\rangle \mid T' \in \mathcal{M}(T)\}$. If $\mathcal{M}(T) = \varnothing$, then we assume $V_T := \mathrm{span}\{|T\rangle\}$. Note that $\||v_T\rangle\|_2^2 = d$, according to Lemma 3.7.6. Moreover, it is easy to see from the definition that $\sigma_n|_{V_T} = |v_T\rangle\langle v_T|$. From this it is obvious $(\sigma_n|_{V_T})^2 = d\cdot\sigma_n|_{V_T}$, and that implies $\sigma_n^2 = d\cdot\sigma_n$.

(f) To check $\sigma_n\sigma_i = \sigma_i\sigma_n$ $(i \neq n\pm 1)$, we define subspaces

$$W_T := \mathrm{span}\{|T'\rangle \mid T' \in \mathcal{M}(T)\cup\mathcal{M}(\sigma_i T)\}, \qquad V_T := \mathrm{span}\{|T'\rangle \mid T' \in \mathcal{M}(T)\}. \tag{3.85}$$

If $\sigma_i T$ is not valid mixed Young tableau, then $W_T \cong V_T$ and $\sigma_i\big|_{W_T}$ acts by scalar multiplication on W_T, so it obviously commutes with $\sigma_n\big|_{W_T}$. Now assume that $\sigma_i T$ is valid mixed Young tableau, then $W_T \cong V_T \otimes \mathrm{span}\{|1\rangle, |\sigma_i\rangle\}$. In that case, we have a similar tensor product structure as in the case of transpositions making these generators commute. Namely, since $r_i(T) = r_i(T')$ for every $T' \in \mathcal{M}(T)$ then we have

$$\sigma_n\big|_{W_T} = |v_T\rangle\langle v_T|\big|_{V_T} \otimes I_2, \tag{3.86}$$

$$\sigma_i\big|_{W_T} = I_{|\mathcal{M}(T)|} \otimes \begin{pmatrix} \frac{1}{r_i(T)} & \sqrt{1-\frac{1}{r_i(T)^2}} \\ \sqrt{1-\frac{1}{r_i(T)^2}} & -\frac{1}{r_i(T)} \end{pmatrix}. \tag{3.87}$$

Therefore $\sigma_n\sigma_i = \sigma_i\sigma_n$ $(i \neq n\pm 1)$ holds.

(e) Now let's first check the relation $\sigma_n\sigma_{n-1}\sigma_n = \sigma_n$. Note that we can conveniently write the generator σ_n in terms of the matrix units $E_{S,T}$ of $\mathcal{A}_{n,m}^d$. To make our notation more compact, we introduce the convention $E_T^S := E_{S,T}$.

$$\sigma_n = \sum_{\mu\in B(\lambda)} \sum_{\nu\in C(\lambda,\mu)} \sum_{\substack{S_1\in\mathrm{Paths}_{n-2}(\nu) \\ S_2\in\mathrm{Paths}_{n+1,n+m}(\mu,\lambda) \\ \theta,\theta'\in D(\lambda,\mu,\nu)}} c(\mu,\theta)c(\mu,\theta')E_{S_1\to(\nu,\mu,\theta,\mu)\to S_2}^{S_1\to(\nu,\mu,\theta',\mu)\to S_2}, \tag{3.88}$$

where we highlighted that coefficients do not depend on paths T fully:

$$c(\mu,\theta) := c(T) \text{ for arbitrary } T \in \mathrm{Paths}(\lambda) : T^{n-1} = T^{n+1} = \mu, T^n = \theta. \tag{3.89}$$

Moreover, we introduced specific sets of vertices in the Bratteli diagram $\mathscr{A}$:

$$B(\lambda) := \{\mu \in \widehat{\mathcal{A}}_{n-1,0}^d \mid \exists T \in \mathrm{Paths}(\lambda) : T^{n-1} = T^{n+1} = \mu\}, \tag{3.90}$$

$$C(\lambda,\mu) := \{\nu \in \widehat{\mathcal{A}}_{n-2,0}^d \mid \exists T \in \mathrm{Paths}(\lambda) : T^{n-1} = T^{n+1} = \mu, T^{n-2} = \nu\}, \tag{3.91}$$

$$D(\lambda,\mu,\nu) := \{\theta \in \widehat{\mathcal{A}}_{n,0}^d \mid \exists T \in \mathrm{Paths}(\lambda) : T^{n-1} = T^{n+1} = \mu, T^{n-2} = \nu, T^n = \theta\}. \tag{3.92}$$

Using the above notation, we can write generator σ_{n-1} in terms of the matrix units E^S_T, specifically highlighting only the relevant ones,

$$\sigma_{n-1} = \sum_{\mu\in B(\lambda)} \sum_{\nu\in C(\lambda,\mu)} \sum_{\substack{S_1\in \mathrm{Paths}_{n-2}(\nu)\\ S_2\in \mathrm{Paths}_{n+1,n+m}(\mu,\lambda)\\ \theta\in D(\lambda,\mu,\nu)}} f(\nu,\mu,\theta) E^{S_1\to(\nu,\mu,\theta,\mu)\to S_2}_{S_1\to(\nu,\mu,\theta,\mu)\to S_2} + \dots, \tag{3.93}$$

where we also highlight dependence of $r_{n-1}(T)$ only on certain nodes of a given path T:

$$f(\nu,\mu,\theta) := \frac{1}{r_{n-1}(T)} \text{ for arbitrary } T\in \mathrm{Paths}(\lambda) : T^{n-2}=\nu, T^{n-1}=\mu, T^n=\theta. \tag{3.94}$$

In Eq. (3.93) we do not write terms with the matrix units which multiply to zero with the matrix units from the sum of Eq. (3.88). We also abuse the notation by forgetting that ν,μ,θ are actually pairs of Young diagrams: we only refer to the left diagrams by dropping the subscript l. Using Eqs. (3.88) and (3.93) we can deduce by direct multiplication, that $\sigma_n\sigma_{n-1}\sigma_n = \sigma_n$ is equivalent to

$$\sum_{\theta\in D(\lambda,\mu,\nu)} f(\nu,\mu,\theta)\cdot c(\mu,\theta)^2 = 1 \tag{3.95}$$

for every $\mu\in B(\lambda)$, $\nu\in C(\lambda,\mu)$, $S_1\in\mathrm{Paths}(\nu)$, $S_2\in\mathrm{Paths}(\mu,\lambda)$. Let $c := \mu\setminus\nu$ be the cell containing $n-1$, it is a corner cell of μ, i.e. $c\in\mathrm{RC}(\mu)$. Let also $a := \theta\setminus\mu$, then Eq. (3.95) is equivalent to

$$\sum_{a\in\mathrm{AC}(\mu)} \frac{d+\mathrm{cont}(a)}{\mathrm{cont}(a)-\mathrm{cont}(c)} \frac{\prod_{v\in\mathrm{RC}(\mu)}(\mathrm{cont}(a)-\mathrm{cont}(v))}{\prod_{v\in\mathrm{AC}(\mu)\setminus a}(\mathrm{cont}(a)-\mathrm{cont}(v))} = 1 \tag{3.96}$$

for every $\mu\in B(\lambda)$ and $c\in\mathrm{RC}(\mu)$. By rewriting the previous formula as

$$d\cdot\sum_{a\in\mathrm{AC}(\mu)} \frac{\prod_{w\in\mathrm{RC}(\mu)\setminus c}(\mathrm{cont}(a)-\mathrm{cont}(w))}{\prod_{v\in\mathrm{AC}(\mu)\setminus a}(\mathrm{cont}(a)-\mathrm{cont}(v))} + \sum_{a\in\mathrm{AC}(\mu)} \mathrm{cont}(a) \frac{\prod_{w\in\mathrm{RC}(\mu)\setminus c}(\mathrm{cont}(a)-\mathrm{cont}(w))}{\prod_{v\in\mathrm{AC}(\mu)\setminus a}(\mathrm{cont}(a)-\mathrm{cont}(v))} = 1,$$

and using Lemma 3.7.8 we conclude that Eq. (3.95) holds, finishing the proof of $\sigma_n\sigma_{n-1}\sigma_n=\sigma_n$. Similar proof also works for the second relation $\sigma_n\sigma_{n+1}\sigma_n=\sigma_n$ which we do not repeat here.

(g) Finally, checking the relations in Eq. (3.13) is the same in spirit as for (e), but more cumbersome. Observe that relation (g) could we written in terms of $\tau_2 = \sigma_n\sigma_{n+1}\sigma_{n-1}\sigma_n$ from Eq. (3.15) as

$$\tau_2\sigma_{n-1} = \tau_2\sigma_{n+1}. \tag{3.97}$$

So we need to understand how τ_2 acts in the Gelfand–Tsetlin basis. Let's first write the generators in terms of matrix units:

$$\sigma_n = \sum_{\substack{\mu\in B(\lambda)\\ (\nu_1,\nu_2)\in C(\lambda,\mu)}} \sum_{\substack{S_1\in\mathrm{Paths}_{n-2}(\nu_1)\\ S_2\in\mathrm{Paths}_{n+2,n+m}(\nu_2,\lambda)\\ \theta,\theta'\in D(\lambda,\nu_2,\mu,\nu_1)}} c(\mu,\theta)c(\mu,\theta') E^{S_1\to(\nu_1,\mu,\theta',\mu,\nu_2)\to S_2}_{S_1\to(\nu_1,\mu,\theta,\mu,\nu_2)\to S_2} \tag{3.98}$$

$$\sigma_{n-1} = \sum_{\substack{\mu\in B(\lambda)\\ (\nu_1,\nu_2)\in C(\lambda,\mu)}} \sum_{\substack{S_1\in\mathrm{Paths}_{n-2}(\nu_1)\\ S_2\in\mathrm{Paths}_{n+2,n+m}(\nu_2,\lambda)\\ \theta\in D(\lambda,\nu_2,\mu,\nu_1)}} \Big(f_{n-1}(\nu_1,\mu,\theta) E^{S_1\to(\nu_1,\mu,\theta,\mu,\nu_2)\to S_2}_{S_1\to(\nu_1,\mu,\theta,\mu,\nu_2)\to S_2} + \\ + \sqrt{1-f^2_{n-1}(\nu_1,\mu,\theta)}\, E^{S_1\to(\nu_1,\mu^{\nu_1}_\theta,\theta,\mu,\nu_2)\to S_2}_{S_1\to(\nu_1,\mu,\theta,\mu,\nu_2)\to S_2} \Big) + \dots \tag{3.99}$$

$$\sigma_{n+1} = \sum_{\substack{\mu\in B(\lambda)\\ (\nu_1,\nu_2)\in C(\lambda,\mu)}} \sum_{\substack{S_1\in\mathrm{Paths}_{n-2}(\nu_1)\\ S_2\in\mathrm{Paths}_{n+2,n+m}(\nu_2,\lambda)\\ \theta\in D(\lambda,\nu_2,\mu,\nu_1)}} \Big(f_{n+1}(\theta,\mu,\nu_2) E^{S_1\to(\nu_1,\mu,\theta,\mu,\nu_2)\to S_2}_{S_1\to(\nu_1,\mu,\theta,\mu,\nu_2)\to S_2} + \\ + \sqrt{1-f^2_{n+1}(\theta,\mu,\nu_2)}\, E^{S_1\to(\nu_1,\mu,\theta,\mu^{\theta}_{\nu_2},\nu_2)\to S_2}_{S_1\to(\nu_1,\mu,\theta,\mu,\nu_2)\to S_2} \Big) + \dots \tag{3.100}$$

where notation $\mu_\theta^{\nu_1}$ (or $\mu_{\nu_2}^{\theta}$) is a shorthand for μ' which appears at the index $n-1$ (or $n+1$) of the corresponding mixed tableau $\sigma_{n-1}T$ (or $\sigma_{n+1}T$), where $T = S_1 \to (\nu_1, \mu, \theta, \mu, \nu_2) \to S_2$; we also use the notation similar to the case (e):

$$
\begin{aligned}
B(\lambda) &:= \{\mu \in \widehat{\mathcal{A}}^d_{n-1,0} \,|\, \exists\, T \in \mathrm{Paths}(\lambda) : T^{n-1} = T^{n+1} = \mu\},\\
C(\lambda,\mu) &:= \{(\nu_1,\nu_2) \in \widehat{\mathcal{A}}^d_{n-2,0} \times \widehat{\mathcal{A}}^d_{n,2} \,|\, \exists\, T \in \mathrm{Paths}(\lambda) : T^{n-2} = \nu_1, T^{n\pm1} = \mu, T^{n+2} = \nu_2\}\\
D(\lambda,\nu_2,\mu,\nu_1) &:= \{\theta \in \widehat{\mathcal{A}}^d_{n,0} \,|\, \exists\, T \in \mathrm{Paths}(\lambda) : T^{n-2} = \nu_1, T^{n\pm1} = \mu, T^{n+2} = \nu_2, T^n = \theta\},\\
c(\mu,\theta) &:= c(T) \text{ for arbitrary } T \in \mathrm{Paths}(\lambda) \text{ s.t. } T^{n-1} = T^{n+1} = \mu,\ T^n = \theta,\\
f_{n-1}(\nu_1,\mu,\theta) &:= \frac{1}{r_{n-1}(T)} \text{ for arbitrary } T \in \mathrm{Paths}(\lambda) : T^{n-2} = \nu_1, T^{n-1} = \mu, T^n = \theta,\\
f_{n+1}(\mu,\theta,\nu_2) &:= \frac{1}{r_{n+1}(T)} \text{ for arbitrary } T \in \mathrm{Paths}(\lambda) : T^{n} = \theta, T^{n+1} = \mu, T^{n+2} = \nu_2.
\end{aligned}
$$

Let's now analyse how τ_2 looks like in the Gelfand–Tsetlin basis. Assume $\nu_1 \neq \nu_2$ in the previous expressions. In that case, $\sigma_{n-1}\mu \neq \sigma_{n+1}\mu$. Therefore the only terms, which survive after mulpityling four different matrix units in the expansion of $\sigma_n\sigma_{n+1}\sigma_{n-1}\sigma_n$, are as follows:

$$
c(\mu,\theta')c(\mu,\theta'') \sum_{\theta \in D(\lambda,\nu_2,\mu,\nu_1)} c^2(\mu,\theta) f_{n-1}(\nu_1,\mu,\theta) f_{n+1}(\theta,\mu,\nu_2) E^{S_1\to(\nu_1,\mu,\theta',\mu,\nu_2)\to S_2}_{S_1\to(\nu_1,\mu,\theta'',\mu,\nu_2)\to S_2}, \tag{3.101}
$$

where for brevity we omitted the sums over $\mu, \nu_1, \nu_2, \theta', \theta'', S_1, S_2$. However, from Lemma 3.7.7 it follows by a similar technique which was used to show Eq. (3.95) from Lemma 3.7.8 that

$$
\sum_{\theta \in D(\lambda,\nu_2,\mu,\nu_1)} c^2(\mu,\theta) f_{n-1}(\nu_1,\mu,\theta) f_{n+1}(\theta,\mu,\nu_2) = 0, \tag{3.102}
$$

It is crucial that $\nu_1 \neq \nu_2$, which allows to use Lemma 3.7.8. therefore τ_2 acts as zero on paths of the form $S_1 \to (\nu_1, \mu, \theta, \mu, \nu_2) \to S_2$, where $\nu_1 \neq \nu_2$.

Now assume $\nu := \nu_1 = \nu_2$. We would like to understand how τ_2 acts on paths of the form $T := S_1 \to (\nu, \mu, \theta, \mu, \nu) \to S_2$. It is easy to see that any path $T' := S_1 \to (\nu, \mu', \theta', \mu', \nu) \to S_2$ could be produced upon the action of τ_2 on $S_1 \to (\nu, \mu, \theta, \mu, \nu) \to S_2$, where $\mu = \nu \cup a$, $\mu' = \nu \cup a'$ for $a, a' \in \mathrm{AC}_d(\nu)$, and $\theta = \mu \cup a$ for $a \in \mathrm{AC}_d(\mu)$, and $\theta' = \mu' \cup a'$ for $a' \in \mathrm{AC}_d(\mu')$. Let's calculate the diagonal elements $\langle T|\tau_2|T\rangle$. Taking into account $f_{n-1}(\nu,\mu,\theta') = f_{n+1}(\theta',\mu,\nu)$ we can write

$$
\begin{aligned}
\langle T|\tau_2|T\rangle &= c^2(\mu,\theta) \sum_{\theta' \in D(\lambda,\nu,\mu,\nu)} c^2(\mu,\theta') f_{n-1}(\nu,\mu,\theta') f_{n+1}(\theta',\mu,\nu) &(3.103)\\
&= c^2(\mu,\theta) \sum_{a \in \mathrm{AC}_d(\mu)} c^2(\mu,\mu\cup a) f^2_{n-1}(\nu,\mu,\mu\cup a). &(3.104)
\end{aligned}
$$

By defining the cell $x := \mu \setminus \nu$, we can transform the sum in the expression above into

$$
\begin{aligned}
&\sum_{a \in \mathrm{AC}(\mu)} \frac{d+\mathrm{cont}(a)}{(\mathrm{cont}(a)-\mathrm{cont}(x))^2} \frac{\prod_{v\in\mathrm{RC}(\mu)}(\mathrm{cont}(a)-\mathrm{cont}(v))}{\prod_{v\in\mathrm{AC}(\mu)\setminus a}(\mathrm{cont}(a)-\mathrm{cont}(v))} =\\
&\quad= \sum_{a \in \mathrm{AC}(\mu)} \frac{d+\mathrm{cont}(a)}{\mathrm{cont}(a)-\mathrm{cont}(x)} \frac{\prod_{v\in\mathrm{RC}(\mu)\setminus x}(\mathrm{cont}(a)-\mathrm{cont}(v))}{\prod_{v\in\mathrm{AC}(\mu)\setminus a}(\mathrm{cont}(a)-\mathrm{cont}(v))} =\\
&\quad= \sum_{a \in \mathrm{AC}(\mu)\cup x} (d+\mathrm{cont}(a)) \frac{\prod_{v\in\mathrm{RC}(\mu)\setminus x}(\mathrm{cont}(a)-\mathrm{cont}(v))}{\prod_{v\in(\mathrm{AC}(\mu)\cup x)\setminus a}(\mathrm{cont}(a)-\mathrm{cont}(v))} -\\
&\qquad - (d+\mathrm{cont}(x)) \frac{\prod_{v\in\mathrm{RC}(\mu)\setminus x}(\mathrm{cont}(x)-\mathrm{cont}(v))}{\prod_{v\in\mathrm{AC}(\mu)}(\mathrm{cont}(x)-\mathrm{cont}(v))} = \frac{m_\mu}{m_\nu},
\end{aligned} \tag{3.105}
$$

where in the last equality we observed that the first term is zero due to Lemma 3.7.8 and the second negative term is $\frac{m_\mu}{m_\nu}$ due to Lemmas 3.7.4 and 3.7.5. This shows

$$\langle T|\tau_2|T\rangle = c^2(\mu,\theta)\frac{m_\mu}{m_\nu} = \frac{m_\theta}{m_\mu}\frac{m_\mu}{m_\nu} = \frac{m_\theta}{m_\nu}. \tag{3.106}$$

By a similar argument, we can deduce that

$$\langle T'|\tau_2|T\rangle = \frac{\sqrt{m_{\theta'}m_\theta}}{m_\nu}. \tag{3.107}$$

Now observing that $\langle T'|\tau_2(\sigma_{n-1}-\sigma_{n+1})|T\rangle = 0$ for every $T, T' \in \mathrm{Paths}(\lambda, \mathscr{A})$ is easy. Indeed, since matrix elements $\langle T'|\tau_2|T\rangle$ do not depend on the nodes μ' and μ at levels $n-1$ and $n+1$ of paths T' and T, we can always collect the terms such that they cancel due to relation $f_{n-1}(\nu,\mu,\theta) = f_{n+1}(\theta,\mu,\nu)$. Similar proof also works for the relation (h) in Definition 3.2.2, which we do not repeat here.

Finally, we need to show the irreducibility of our representation. Due to Lemma 3.7.3 the spectrum of Jucys–Murphy elements in our basis coincides with the canonical definition of the action of Jucys–Murphy elements in the Gelfand–Tsetlin basis, see Corollary 3.6.3. Since Jucys–Murphy elements generate a maximal commutative subalgebra of $\mathcal{A}^d_{n,m}$ their action uniquely determines the basis. Therefore our basis coincides with the Gelfand–Tsetlin basis for $\mathcal{A}^d_{n,m}$, which is originally defined for irreducible representations. □

3.7.3. Lemma. *The action of Jucys–Murphy elements $J_k^{\mathcal{A}}$ of the algebra $\mathcal{A}^d_{n,m}$ is diagonal in the Gelfand–Tsetlin basis and the spectrum is given by the walled content* $\mathrm{wcont}_k(T)$. *More formally, for every $\lambda \in \widehat{\mathcal{A}}^d_{n,m}$ and every $T \in \mathrm{Paths}(\lambda, \mathscr{A})$*

$$\psi_\lambda(J_k^{\mathcal{A}})|T\rangle = \mathrm{wcont}_k(T)|T\rangle \tag{3.108}$$

Proof:
For $k \leqslant n$ this is just a statement of the same result for the symmetric group, e.g. see [OV96; VO05]. In the following, we drop the index $\mathcal{A}$ and ψ_λ, and we simply write $J_k := \psi_\lambda(J_k^{\mathcal{A}})$. Moreover, we will drop ψ_λ everywhere for brevity, but one should remember that all calculations should be done within fixed irrep λ for all $\lambda \in \widehat{\mathcal{A}}^d_{n,m}$. The proof for that case can be done by induction by exploiting the relation $J_{k+1} = \sigma_k J_k \sigma_k + \sigma_k$. The base of the induction is trivial. Now using the induction step we can immediately see that

$$\begin{aligned}
J_{k+1}|T\rangle &= (\sigma_k J_k \sigma_k + \sigma_k)|T\rangle = (\sigma_k J_k + 1)\sigma_k|T\rangle && (3.109)\\
&= (\sigma_k J_k + 1)\Big(\tfrac{1}{r_k(T)}|T\rangle + \sqrt{1-\tfrac{1}{r_k(T)^2}}|\sigma_k T\rangle\Big) && (3.110)\\
&= \tfrac{1}{r_k(T)}|T\rangle + \sqrt{1-\tfrac{1}{r_k(T)^2}}|\sigma_k T\rangle + && (3.111)\\
&\qquad + \sigma_k\Big(\tfrac{\mathrm{wcont}_k(T)}{r_k(T)}|T\rangle + \mathrm{wcont}_k(\sigma_k T)\sqrt{1-\tfrac{1}{r_k(T)^2}}|\sigma_k T\rangle\Big)\\
&= \Big(\tfrac{\mathrm{wcont}_k(T)}{r_k(T)}+1\Big)\Big(\tfrac{|T\rangle}{r_k(T)} + \sqrt{1-\tfrac{1}{r_k(T)^2}}|\sigma_k T\rangle\Big) + && (3.112)\\
&\qquad + \mathrm{wcont}_k(\sigma_k T)\sqrt{1-\tfrac{1}{r_k(T)^2}}\Big(-\tfrac{|\sigma_k T\rangle}{r_k(T)} + \sqrt{1-\tfrac{1}{r_k(T)^2}}|T\rangle\Big)\\
&= \Big(\tfrac{1}{r_k(T)} + \tfrac{\mathrm{wcont}_k(T)-\mathrm{wcont}_{k+1}(T)}{r_k(T)^2} + \mathrm{wcont}_{k+1}\Big)|T\rangle + && (3.113)\\
&\qquad + \sqrt{1-\tfrac{1}{r_k(T)^2}}\Big(1 + \tfrac{\mathrm{wcont}_k(T)-\mathrm{wcont}_{k+1}(T)}{r_k(T)}\Big)|\sigma_k T\rangle\\
&= \mathrm{wcont}_k(T)|T\rangle, && (3.114)
\end{aligned}$$

where we used that $\mathrm{wcont}_k(\sigma_k T) = \mathrm{wcont}_{k+1}(T), r_k(\sigma_k T) = -r_k(T)$ and $r_k(T) = \mathrm{wcont}_{k+1}(T) - \mathrm{wcont}_k(T)$.

Similarly, for $k \geqslant n+1$ we have a similar relation $J_{k+1} = \sigma_k J_k \sigma_k + \sigma_k$ and the same argument holds, assuming that $J_{n+1}|T\rangle = \mathrm{wcont}_{n+1}(T)|T\rangle$. However, for $k = n+1$ we need to prove the claim separately.

To show the claim for $k = n+1$, recall that $J_{n+1} = d - \rho$, where

$$\rho := \sum_{i=1}^{n} (i,n)\sigma_n(i,n) \tag{3.115}$$

and (i,n) is a transposition between sites i and n with the convention $(n,n) := 1$. Without loss of generality assume that $m = 1$. Note that since J_{n+1} commutes with $\mathcal{A}^d_{n,0}$, J_{n+1} must be diagonal in the Gelfand–Tsetlin basis and it has the same eigenvalues for every path T which goes through a given vertex μ at the level n in the Bratteli diagram. Therefore, we now assume $T \in \mathrm{Paths}(\lambda, \mathcal{A})$ has the property $T^n = \mu$. There are two cases:

1. If $\lambda_r = (1)$, then there is no mobile cell in T and the action of σ_n is zero, meaning that $J_{n+1}|T\rangle = d|T\rangle$ which is consistent with $J_{n+1}|T\rangle = \mathrm{wcont}_{n+1}(T)|T\rangle$ for that case.

2. If $\lambda_r = \varnothing$, then for every $T \in \mathrm{Paths}(\lambda)$ with $T^n = \mu$ we can write:

$$\langle T|\rho|T\rangle = \frac{1}{d_\mu} \sum_{\substack{T\in\mathrm{Paths}(\lambda)\\ T^n=\mu}} \langle T|\rho|T\rangle = \frac{1}{d_\mu} \sum_{\substack{T\in\mathrm{Paths}(\lambda)\\ T^n=\mu}} \sum_{i=1}^{n} \langle T|(i,n)\sigma_n(i,n)|T\rangle \tag{3.116}$$

$$= \frac{1}{d_\mu} \sum_{i=1}^{n} \sum_{\substack{T\in\mathrm{Paths}(\lambda)\\ T^n=\mu}} \langle T|(i,n)\Bigg(\sum_{\substack{S\in\mathrm{Paths}(\lambda)\\ S^n=\mu\\ S^{n-1}=\lambda}} |v_S\rangle\langle v_S| \Bigg)(i,n)|T\rangle \tag{3.117}$$

$$= \frac{1}{d_\mu} \sum_{i=1}^{n} \sum_{\substack{T,S\in\mathrm{Paths}(\lambda)\\ T^n=S^n=\mu\\ S^{n-1}=\lambda}} |\langle v_S|(i,n)|T\rangle|^2 \tag{3.118}$$

$$= \frac{1}{d_\mu} \sum_{i=1}^{n} \sum_{\substack{T,S\in\mathrm{Paths}(\lambda)\\ T^n=S^n=\mu\\ S^{n-1}=\lambda}} c(S)^2 \cdot |\langle S|(i,n)|T\rangle|^2. \tag{3.119}$$

Now let's denote $c(\lambda,\mu) := c(S)$ to indicate that $c(S)$ does not depend on the full path S but only on the two nodes λ, μ belonging to S.

$$\langle T|\rho|T\rangle = \frac{c(\lambda,\mu)^2}{d_\mu} \sum_{i=1}^{n} \sum_{\substack{T,S\in\mathrm{Paths}(\lambda)\\ T^n=S^n=\mu\\ S^{n-1}=\lambda}} |\langle S|(i,n)|T\rangle|^2 \tag{3.120}$$

$$= \frac{c(\lambda,\mu)^2}{d_\mu} \sum_{i=1}^{n} \sum_{\substack{S\in\mathrm{Paths}(\lambda)\\ S^n=\mu\\ S^{n-1}=\lambda}} \langle S|(i,n)\Bigg(\sum_{\substack{T\in\mathrm{Paths}(\lambda)\\ T^n=\mu}} |T\rangle\langle T| \Bigg)(i,n)|S\rangle \tag{3.121}$$

$$= \frac{c(\lambda,\mu)^2}{d_\mu} \sum_{i=1}^{n} \sum_{\substack{S\in\mathrm{Paths}(\lambda)\\ S^n=\mu\\ S^{n-1}=\lambda}} \langle S|\Bigg(\sum_{\substack{T\in\mathrm{Paths}(\lambda)\\ T^n=\mu}} |T\rangle\langle T| \Bigg)(i,n)^2|S\rangle, \tag{3.122}$$

where in the last step we used that (i, n) commutes with $\varepsilon_\mu := \sum_{T:\, T^n=\mu} |T\rangle\langle T|$ since ε_μ is a primitive central idempotent in $\mathcal{A}^d_{n,0}$. Therefore,

$$\langle T|\rho|T\rangle = \frac{c(\lambda,\mu)^2}{d_\mu} \sum_{i=1}^{n} \sum_{\substack{T,S\in \mathrm{Paths}(\lambda)\\ T^n=S^n=\mu\\ S^{n-1}=\lambda}} |\langle S|T\rangle|^2 \tag{3.123}$$

$$= \frac{c(\lambda,\mu)^2}{d_\mu} \cdot n \cdot d_\lambda = n \cdot \frac{d_\lambda}{d_\mu} \cdot \frac{m_\mu}{m_\lambda} = d + \mathrm{cont}(\mu \setminus \lambda), \tag{3.124}$$

where in Eq. (3.124) we used Lemmas 3.7.4 and 3.7.5. Therefore,

$$\begin{aligned} \langle T|J_{n+1}|T\rangle &= d - \langle T|\rho|T\rangle = -\mathrm{cont}(\mu \setminus \lambda) \\ &= -\mathrm{cont}(T^n \setminus T^{n+1}) = \mathrm{wcont}_{n+1}(T). \end{aligned} \tag{3.125}$$

□

Auxiliary Lemmas

3.7.4. Lemma. *For every $\mu \vdash n$ and $\lambda \vdash n-1$, such that λ is obtained be adding a cell to μ and $\ell(\mu) \leqslant d$ and $\ell(\lambda) \leqslant d$,*

$$d + \mathrm{cont}(\mu \setminus \lambda) = n \cdot \frac{d_\lambda}{d_\mu} \cdot \frac{m_\mu}{m_\lambda}, \tag{3.126}$$

where d_λ and m_λ are dimensions of the Specht module λ and the Weyl module λ respectively.

Proof:
Use the hook length formula (2.40) for d_λ and the hook-content formula (2.47) for m_λ:

$$n \cdot \frac{d_\lambda}{d_\mu} \cdot \frac{m_\mu}{m_\lambda} = n \cdot \frac{\frac{(n-1)!}{\prod_{u\in\lambda} h(u)}}{\frac{n!}{\prod_{u\in\mu} h(u)}} \cdot \frac{\frac{\prod_{u\in\mu}(d+\mathrm{cont}(u))}{\prod_{u\in\mu} h(u)}}{\frac{\prod_{u\in\lambda}(d+\mathrm{cont}(u))}{\prod_{u\in\lambda} h(u)}} = d + \mathrm{cont}(\mu \setminus \lambda). \tag{3.127}$$

□

3.7.5. Lemma (Eqs. (1.6) and (1.8) in [Kos03]). *For every $\mu \vdash n$ and $\lambda \vdash n-1$, such that λ is obtained be adding a cell x to μ, i.e. $x := \mu \setminus \lambda$. Then there holds*

$$n \cdot \frac{d_\lambda}{d_\mu} = \frac{\prod_{a\in \mathrm{AC}(\lambda)\setminus x}(\mathrm{cont}(x) - \mathrm{cont}(a))}{\prod_{c\in \mathrm{RC}(\lambda)}(\mathrm{cont}(x) - \mathrm{cont}(c))} = -\frac{\prod_{a\in \mathrm{AC}(\mu)}(\mathrm{cont}(x) - \mathrm{cont}(a))}{\prod_{c\in \mathrm{RC}(\mu)\setminus x}(\mathrm{cont}(x) - \mathrm{cont}(c))} \tag{3.128}$$

where d_λ is the dimension of the symmetric group irrep λ.

3.7.6. Lemma. *For every T such that $\mathcal{M}(T) \neq \varnothing$ there holds $\||v_T\rangle\|_2^2 = d$.*

Proof:
Denote $\lambda := T_l^{n-1}$ and use Lemmas 3.7.4 and 3.7.5:

$$\||v_T\rangle\|_2^2 = \sum_{S\in\mathcal{M}(T)} c(S)^2 = \sum_{a\in \mathrm{AC}_d(\lambda)} \frac{m_{\lambda\cup a}}{m_\lambda} = d, \tag{3.129}$$

where the last equality is due to Pieri's rule for the irreps of the unitary group. □

3.7.7. Lemma ([War79; LB70; CL96]). *For each integer $k \geqslant 0$ and distinct $x_1, x_2, \ldots, x_n \in \mathbb{C}$ we have*

$$\sum_{i=1}^{n} \frac{x_i^k}{\prod_{i \neq j}(x_i - x_j)} = h_{k-n+1}(x_1, \ldots, x_n), \tag{3.130}$$

where h_r is complete r-homogeneous symmetric polynomial, which is defined as $h_r = 0$ for $r < 0$ and $h_0 = 1$.

Proof:
Consider the rational function

$$f(z) = \frac{z^k}{\prod_{j=1}^{n}(z - x_j)}. \tag{3.131}$$

The function $f(z)$ has simple poles at $z = x_i$ for $i = 1, 2, \ldots, n$. At each pole $z = x_i$, the residue can be easily evaluated as

$$\operatorname{Res}_{z=x_i} f(z) = \lim_{z \to x_i} (z - x_i) f(z) = \frac{x_i^k}{\prod_{j \neq i}(x_i - x_j)}. \tag{3.132}$$

Summing over all residues at finite poles, we get

$$\sum_{i=1}^{n} \operatorname{Res}_{z=x_i} f(z) = \sum_{i=1}^{n} \frac{x_i^k}{\prod_{j \neq i}(x_i - x_j)}. \tag{3.133}$$

By the Cauchy's residue theorem, the sum of all residues, including the residue at infinity, is zero:

$$\sum_{i=1}^{n} \operatorname{Res}_{z=x_i} f(z) + \operatorname{Res}_{z=\infty} f(z) = 0 \quad \Longrightarrow \quad \sum_{i=1}^{n} \frac{x_i^k}{\prod_{j \neq i}(x_i - x_j)} = -\operatorname{Res}_{z=\infty} f(z). \tag{3.134}$$

To find $\operatorname{Res}_{z=\infty} f(z)$, expand $f(z)$ as $z \to \infty$:

$$f(z) = z^{k-n} \prod_{j=1}^{n} \Big(1 - \frac{x_j}{z}\Big)^{-1}. \tag{3.135}$$

Using absolute convergence of the geometric series for the function $g(t) = (1 - t)^{-1}$ together with the generating function for complete homogeneous symmetric polynomials h_r [Mac98], we can expand the product in the previous formula into the following series:

$$\prod_{j=1}^{n} \Big(1 - \frac{x_j}{z}\Big)^{-1} = \sum_{r=0}^{\infty} h_r(x_1, \ldots, x_n) z^{-r}. \tag{3.136}$$

Therefore,

$$f(z) = z^{k-n} \sum_{r=0}^{\infty} h_r(x_1, \ldots, x_n) z^{-r} = \sum_{r=0}^{\infty} h_r(x_1, \ldots, x_n) z^{k-n-r}. \tag{3.137}$$

The residue at infinity is minus the coefficient of z^{-1} in this expansion. Set $k - n - r = -1$, which gives $r = k - n + 1$. Thus,

$$\operatorname{Res}_{z=\infty} f(z) = -h_{k-n+1}(x_1, \ldots, x_n). \tag{3.138}$$

Combining the results, we obtain

$$\sum_{i=1}^{n} \frac{x_i^k}{\prod_{j \neq i}(x_i - x_j)} = h_{k-n+1}(x_1, \ldots, x_n). \tag{3.139}$$

□

3.7.8. Lemma. *For every Young diagram λ and arbitrary $c \in \mathrm{RC}(\lambda)$ the following holds:*

$$\sum_{x \in \mathrm{AC}(\lambda)} \frac{\prod_{w \in \mathrm{RC}(\lambda)\setminus c}(\mathrm{cont}(x) - \mathrm{cont}(w))}{\prod_{v \in \mathrm{AC}(\lambda)\setminus x}(\mathrm{cont}(x) - \mathrm{cont}(v))} = 0, \tag{3.140}$$

$$\sum_{x \in \mathrm{AC}(\lambda)} \mathrm{cont}(x) \frac{\prod_{w \in \mathrm{RC}(\lambda)\setminus c}(\mathrm{cont}(x) - \mathrm{cont}(w))}{\prod_{v \in \mathrm{AC}(\lambda)\setminus x}(\mathrm{cont}(x) - \mathrm{cont}(v))} = 1 \tag{3.141}$$

Proof:
Note that the degree of the numerator as polynomial in $\mathrm{cont}(x)$ is $|AC(\mu)| - 2$ in the first case and $|AC(\mu)| - 1$ in the second case. Now just apply Lemma 3.7.7 with $n = |AC(\mu)|$ and variables being $\{\mathrm{cont}(x) \mid x \in \mathrm{AC}(\mu)\}$. □

3.A Appendix

3.A.1 Lifting traces from $\mathcal{B}^d_{n,m}$ to $\mathcal{A}^d_{n,m}$

Representing the elements of the matrix algebra $\mathcal{A}^d_{n,m}$ as preimages of diagrams under $\psi^d_{n,m}$ is particularly useful when computing traces and partial traces of $\psi^d_{n,m}(\sigma)$ for any $\sigma \in \mathcal{B}^d_{n,m}$. The following two propositions relate the matrix traces of $\psi^d_{n,m}$ to the diagrammatic traces of σ defined in Eqs. (3.6) and (3.7).

3.A.1. PROPOSITION. *For any $\sigma \in \mathcal{B}^d_{n,m}$,*

$$\mathrm{Tr}(\psi^d_{n,m}(\sigma)) = \mathrm{Tr}(\sigma). \tag{3.142}$$

In particular, when σ is a single diagram,

$$\mathrm{Tr}(\psi^d_{n,m}(\sigma)) = d^{\mathrm{loops}(\sigma)} \tag{3.143}$$

where $\mathrm{loops}(\sigma)$ *is the number of loops created by connecting all pairs of opposite vertices of σ.*

Proof:
To establish Eq. (3.142), it suffices to consider only the case when σ is a single diagram since the general case follows by linearity. Using Eqs. (3.17) and (3.19),

$$\begin{aligned}
\mathrm{Tr}(\psi^d_{n,m}(\sigma)) &= \sum_{x_1,\ldots,x_{n+m}\in[d]} \left(\langle x_1| \otimes \cdots \otimes \langle x_{n+m}|\right) \psi^d_{n,m}(\sigma) \left(|x_1\rangle \otimes \cdots \otimes |x_{n+m}\rangle\right) && (3.144)\\
&= \sum_{\substack{x_1,\ldots,x_{n+m}\in[d]\\ x_{\underline{1}},\ldots,x_{\underline{n+m}}\in[d]}} \sigma^{x_1,\ldots,x_{n+m}}_{x_{\underline{1}},\ldots,x_{\underline{n+m}}} \prod_{k\in[n+m]} \delta_{x_k,x_{\underline{k}}} && (3.145)\\
&= \sum_{\substack{x_1,\ldots,x_{n+m}\in[d]\\ x_{\underline{1}},\ldots,x_{\underline{n+m}}\in[d]}} \prod_{(r,s)\in\sigma} \delta_{x_r,x_s} \prod_{k\in[n+m]} \delta_{x_k,x_{\underline{k}}} && (3.146)\\
&= d^{\mathrm{loops}(\sigma)}. && (3.147)
\end{aligned}$$

The last equality follows by partitioning the product of delta functions into closed loops and observing that all indices on a given loop must have the same value. The final value agrees with the diagrammatic definition of $\mathrm{Tr}(\sigma)$ in Eq. (3.6). □

The following generalisation allows to graphically compute the partial trace $\mathrm{Tr}_S(\psi^d_{n,m}(\sigma))$ for any subset of systems $S \subseteq [n+m]$.

3.A.2. PROPOSITION. *For any $\sigma \in \mathcal{B}^d_{n,m}$ and subset $S \subseteq [n+m]$,*

$$\mathrm{Tr}_S\big(\psi^d_{n,m}(\sigma)\big) = \psi^d_{n',m'}(\mathrm{Tr}_S(\sigma)) \tag{3.148}$$

where $\mathrm{Tr}_S(\sigma)$ is defined in Eq. (3.7) and n' and m' denote the number of leftover systems on both sides of the wall. In particular, when σ is a single diagram,

$$\mathrm{Tr}_S\big(\psi^d_{n,m}(\sigma)\big) = d^{\mathrm{loops}_S(\sigma)}\psi^d_{n',m'}(\sigma^S) \tag{3.149}$$

where σ^S denotes the diagram σ with opposite pairs of nodes that belong to S contracted, and $\mathrm{loops}_S(\sigma)$ *is the number of loops formed in this process.*

Proof:
By linearity, it suffices to establish the result for any diagram $\sigma \in \mathcal{B}^d_{n,m}$. Note from Eq. (3.17) that

$$\psi^d_{n,m}(\sigma) = \sum_{\substack{l_1,\dots,l_{n+m}\in[d]\\ l_{\underline{1}},\dots,l_{\underline{n+m}}\in[d]}} \sigma^{l_1,\dots,l_{n+m}}_{l_{\underline{1}},\dots,l_{\underline{n+m}}} |l_{\underline{1}}\rangle\langle l_1| \otimes \cdots \otimes |l_{\underline{n+m}}\rangle\langle l_{n+m}| = \sum_{l,\underline{l}\in[d]^{n+m}} \sigma^l_{\underline{l}}\, |\underline{l}\rangle\langle l| \tag{3.150}$$

where $l = (l_1, \dots, l_{n+m})$ and $\underline{l} = (l_{\underline{1}}, \dots, l_{\underline{n+m}})$. Letting $\bar{S} := [n+m] \setminus S$, we can generalize Eq. (3.144) as follows:

$$\begin{aligned}
\mathrm{Tr}_S(\psi^d_{n,m}(\sigma)) &= \sum_{i\in[d]^S} \big(\langle i|_S \otimes I_{\bar{S}}\big)\, \psi^d_{n,m}(\sigma)\, \big(|i\rangle_S \otimes I_{\bar{S}}\big) && (3.151)\\
&= \sum_{i\in[d]^S} \big(\langle i|_S \otimes I_{\bar{S}}\big)\Big(\sum_{l,\underline{l}\in[d]^{n+m}} \sigma^l_{\underline{l}}\, |\underline{l}\rangle\langle l|\Big)\big(|i\rangle_S \otimes I_{\bar{S}}\big) && (3.152)\\
&= \sum_{i\in[d]^S} \sum_{l,\underline{l}\in[d]^{n+m}} \sigma^l_{\underline{l}} \Big(\prod_{k\in S} \delta_{x_k,l_{\underline{k}}}\delta_{l_k,x_k}\Big)\Big(\bigotimes_{k\in\bar{S}} |l_{\underline{k}}\rangle\langle l_k|_k\Big) && (3.153)\\
&= \sum_{l,\underline{l}\in[d]^{n+m}} \sigma^l_{\underline{l}} \Big(\prod_{k\in S} \delta_{l_{\underline{k}},l_k}\Big)\Big(\bigotimes_{k\in\bar{S}} |l_{\underline{k}}\rangle\langle l_k|_k\Big), && (3.154)
\end{aligned}$$

where we eliminated the sum over i in the last equality by noting that

$$\sum_{x_k\in[d]} \delta_{x_k,l_{\underline{k}}}\delta_{l_k,x_k} = \delta_{l_{\underline{k}},l_k} \tag{3.155}$$

for all $k \in S$. Substituting the definition of $\sigma^l_{\underline{l}}$ from Eq. (3.19) we get

$$\begin{aligned}
\mathrm{Tr}_S(\psi^d_{n,m}(\sigma)) &= \sum_{l,\underline{l}\in[d]^{n+m}} \Big(\prod_{(r,s)\in\sigma} \delta_{l_r,l_s}\Big)\Big(\prod_{k\in S} \delta_{l_k,l_{\underline{k}}}\Big)\Big(\bigotimes_{k\in\bar{S}} |l_{\underline{k}}\rangle\langle l_k|_k\Big) && (3.156)\\
&= d^{\mathrm{loops}_S(\sigma)} \sum_{l',\underline{l}'\in[d]^{\bar{S}}} \Big(\prod_{(u,v)\in\sigma^S} \delta_{l'_u,l'_v}\Big)|\underline{l}'\rangle\langle l'|, && (3.157)
\end{aligned}$$

where the second equality is obtained by using a generalisation of Eq. (3.155) to contract the chains of delta functions along all loops and paths. This collapses the sum from $[d]^{n+m}$ to $[d]^{\bar{S}}$ and reduces the product to run over edges (u, v) in the remaining smaller diagram σ^S. Using Eqs. (3.19) and (3.150) in reverse,

$$\begin{aligned}
\mathrm{Tr}_S(\psi^d_{n,m}(\sigma)) &= d^{\mathrm{loops}_S(\sigma)} \sum_{l',\underline{l}'\in[d]^{\bar{S}}} (\sigma^S)^{l'}_{\underline{l}'} |\underline{l}'\rangle\langle l'| && (3.158)\\
&= d^{\mathrm{loops}_S(\sigma)} \psi^d_{n',m'}(\sigma^S) && (3.159)\\
&= \psi^d_{n',m'}(\mathrm{Tr}_S(\sigma)), && (3.160)
\end{aligned}$$

where we used Eq. (3.7) that defines the diagrammatic partial trace $\mathrm{Tr}_S(\sigma)$. □

Finally, note from Eq. (3.150) that we can also easily evaluate the trace of $\psi^d_{n,m}(\sigma)$ with any elementary rank-1 standard basis matrix $|i\rangle\langle j|$ for any $i, j \in [d]^{n+m}$:

$$\mathrm{Tr}\big(\psi^d_{n,m}(\sigma)\, |i\rangle\langle j|\big) = \sigma^i_j, \tag{3.161}$$

where σ^i_j is given in Eq. (3.19). The partial trace $\mathrm{Tr}_S\big(\psi^d_{n,m}(\sigma)\, |i\rangle\langle j|\big)$ can be evaluated similarly.

3.A.2 Proof of Lemma 3.6.2

3.6.2. Lemma. *For any $T \in \mathrm{Paths}(\mathscr{A})$ in the Bratteli diagram of $\mathcal{A}^d_{n,m}$,*

$$(J^{\mathcal{A}}_1 + \cdots + J^{\mathcal{A}}_{n+m})\, \varepsilon^{\mathcal{A}}_T = \big(\mathrm{cont}(\lambda_l) + \mathrm{cont}(\lambda_r) + d \cdot |\lambda_r|\big)\, \varepsilon^{\mathcal{A}}_T \tag{3.56}$$

where $\varepsilon^{\mathcal{A}}_T$ is the corresponding canonical primitive idempotent of $\mathcal{A}^d_{n,m}$, $\lambda = (\lambda_l, \lambda_r) = T^{n+m}$ is the last vertex of the path T, $\mathrm{cont}(\lambda)$ is the total content of all cells of the Young diagram λ and $|\lambda|$ is the number of cells in λ.

Proof:
We will use the correspondence between a path T and a pair (τ, L) of a tableaux $\tau = (\tau^l, \tau^r)$ of shape (λ_l, λ_r) and a tuple L of pairs of numbers from the set $[n+m]$, see Theorem 1.11 of [Ben+94]. For this proof we assume $T := \lambda_1 \to \lambda_2 \to \ldots \to \lambda_{n+m-1} \to \lambda$ and $\psi := \psi^d_{n,m}$, see Eq. (3.17). Moreover, we will use upper "left" and "right" letters, i.e. $\lambda_k = (\lambda^l_k, \lambda^r_k)$.

It follows from Lemma 3.6.1 that $J^{\mathcal{A}}_1 + \cdots + J^{\mathcal{A}}_{n+m} \in \mathcal{Z}(\mathcal{A}_{n+m})$. Therefore it is enough to consider how this sum acts on any vector in the isotypic component $V_\lambda \otimes W_\lambda$ corresponding to the simple module labeled by $\lambda = (\lambda_l, \lambda_r) \in \widehat{\mathcal{A}}^d_{n,m}$ in the mixed Schur–Weyl duality, see Eq. (3.39). In particular, we can take a maximal vector

$$|t_{\tau,L}\rangle := \psi(y_\tau \bar{\sigma}_L)|\beta_{\tau,L}\rangle \in (\mathbb{C}^d)^{\otimes n} \otimes (\mathbb{C}^d)^{\otimes m} \tag{3.162}$$

from [Ben+94, Definition 2.4], where $y_\tau \in \mathbb{C}(\mathrm{S}_n \times \mathrm{S}_m) \subseteq \mathcal{B}^d_{n,m}$ is the *Young symmetriser* for the tableaux τ, $\bar{\sigma}_L \in \mathcal{B}^d_{n,m}$ is a diagram that contracts all pairs in L. The Young symmetriser y_τ is defined as $y_\tau := y_{\tau^l} y_{\tau^r}$, the product of standard Young symmetrisers y_{τ^l} and y_{τ^r}, see [Ben+94, Eq. 2.2]. The Young symmetrisers y_{τ^l} and y_{τ^r} are products of *column* and *row symmetrisers* (the terms which correspond to *column* and *row groups* in [Ben+94, Eq. 2.2]). The standard basis vector $|\beta_{\tau,L}\rangle \in (\mathbb{C}^d)^{\otimes n} \otimes (\mathbb{C}^d)^{\otimes m}$ is defined as follows:

$$|\beta_{\tau,L}\rangle := |u_1\rangle \otimes \cdots \otimes |u_n\rangle \otimes |u_{n+1}\rangle \otimes \cdots \otimes |u_{n+m}\rangle \tag{3.163}$$

where each $u_i \in [d]$ and we distinguish two cases: if $1 \leqslant i \leqslant n$ then

$$u_i := \begin{cases} j & \text{if } i \text{ belongs to the } j\text{-th row of } \tau^l, \\ 1 & \text{if } i \in L, \end{cases} \tag{3.164}$$

while if $n+1 \leqslant i \leqslant n+m$ then

$$u_i := \begin{cases} d-j+1 & \text{if } i \text{ belongs to the } j\text{-th row of } \tau^r, \\ 1 & \text{if } i \in L. \end{cases} \tag{3.165}$$

Recall that $J^{\mathcal{A}}_1 + \cdots + J^{\mathcal{A}}_{n+m} \in \mathcal{Z}(\mathcal{A}_{n+m})$, so

$$\big(J^{\mathcal{A}}_1 + \cdots + J^{\mathcal{A}}_{n+m}\big)|t_{\tau,L}\rangle = \psi(y_\tau \bar{\sigma}_L)\big(J^{\mathcal{A}}_1 + \cdots + J^{\mathcal{A}}_{n+m}\big)|\beta_{\tau,L}\rangle. \tag{3.166}$$

Since $J^{\mathcal{A}}_k := \psi(J^{\mathcal{B}}_k)$ and ψ is a homomorphism, we can use the definition of $J^{\mathcal{B}}_k$ from Eq. (3.50) to write the right-hand side more explicitly:

$$\psi\Big(y_\tau \bar{\sigma}_L \Big(\sum_{\substack{1 \leqslant i < j \leqslant n \text{ or} \\ n+1 \leqslant i < j \leqslant n+m}} \sigma_{i,j} - \sum_{\substack{1 \leqslant i \leqslant n \\ n+1 \leqslant j \leqslant n+m}} \bar{\sigma}_{i,j} + d \cdot m \Big)\Big)|\beta_{\tau,L}\rangle. \tag{3.167}$$

To simplify this, we evaluate all expressions of the form $\psi(y_\tau \bar{\sigma}_L \sigma_{i,j})|\beta_{\tau,L}\rangle$ and $\psi(y_\tau \bar{\sigma}_L \bar{\sigma}_{i,j})|\beta_{\tau,L}\rangle$, where we distinguish between transpositions $\sigma_{i,j}$ and contractions $\bar{\sigma}_{i,j}$ which can be located in three possible positions relative to L:

1. $i \notin L$, $j \notin L$,
2. $i \in L$, $j \notin L$ or $i \notin L$, $j \in L$,
3. $i \in L$, $j \in L$.

We now proceed to consider each of these six cases separately (we will write *(1)* and *(1̄)* to distinguish between the cases with $\sigma_{i,j}$ and $\bar{\sigma}_{i,j}$).

Case (1): $\sigma_{i,j}$ with $i \notin L$, $j \notin L$. There are two sub-cases:

(a) If i and j are in the same row of either τ^l or τ^r, the row symmetriser of y_τ does not change the resulting vector, i.e., $\psi(y_\tau \sigma_{i,j})|\beta_{\tau,L}\rangle = \psi(y_\tau)|\beta_{\tau,L}\rangle$. Since $\bar{\sigma}_L$ and y_τ commute,

$$\psi(y_\tau \bar{\sigma}_L \sigma_{i,j})|\beta_{\tau,L}\rangle = |t_{\tau,L}\rangle. \tag{3.168}$$

(b) If i and j are in different rows of either τ^l or τ^r, we denote the corresponding row numbers by r_i and r_j. In this case the row symmetriser of y_τ acting on $\psi(\sigma_{i,j})|\beta_{\tau,L}\rangle$ produces a product of two "W states" at positions defined by the rows r_i and r_j of $\tau^{l/r}$ with the numbers i and j swapped. The column antisymmetriser of y_τ will then kill most terms, leaving only the terms with basis vectors $|r_i\rangle, |r_j\rangle$ in positions within the same column. There are $\lambda^{l/r}_{\max\{r_i,r_j\}}$ such terms, where $\lambda^{l/r}_{\max\{r_i,r_j\}}$ is the size of the smallest of the two rows r_i, r_j within the corresponding left or right tableaux $\tau^{l/r}$. After this operation the resulting vector acquires a minus sign and a different factor compared to $\psi(y_\tau)|\beta_{\tau,L}\rangle$:

$$\psi(y_\tau \sigma_{i,j})|\beta_{\tau,L}\rangle = -\frac{\psi(y_\tau)|\beta_{\tau,L}\rangle}{\lambda^{l/r}_{\max\{r_i,r_j\}}}. \tag{3.169}$$

Again, since $\bar{\sigma}_L$ and y_τ commute,

$$\psi(y_\tau \bar{\sigma}_L \sigma_{i,j})|\beta_{\tau,L}\rangle = -\frac{1}{\lambda^{l/r}_{\max\{r_i,r_j\}}}|t_{\tau,L}\rangle. \tag{3.170}$$

Case (1̄): $\bar{\sigma}_{i,j}$ with $i \notin L$, $j \notin L$. In this case $\psi(\bar{\sigma}_{i,j})|\beta_{\tau,L}\rangle$ can only be non-zero when $u_i = u_j$, which is equivalent to $r_i = d - r_j + 1$. Thus $r_i + r_j = d + 1$. But since $r_i + r_j \leqslant \ell(\lambda_l) + \ell(\lambda_r) \leqslant d$,

$$\psi(y_\tau \bar{\sigma}_L \bar{\sigma}_{i,j})|\beta_{\tau,L}\rangle = 0. \tag{3.171}$$

Case (2): $\sigma_{i,j}$ with $i \in L$, $j \notin L$ or $i \notin L$, $j \in L$. Without loss of generality we can assume that $i \in L$ and $j \notin L$. There are two sub-cases:

(a) If $u_j = 1$ then $\psi(\bar{\sigma}_L \sigma_{i,j})|\beta_{\tau,L}\rangle = \psi(\bar{\sigma}_L)|\beta_{\tau,L}\rangle$. This happens when $j \in \tau^l$ and $r_j = 1$ or $j \in \tau^r$ and $r_j = d$. Therefore

$$\psi(y_\tau \bar{\sigma}_L \sigma_{i,j})|\beta_{\tau,L}\rangle = |t_{\tau,L}\rangle. \tag{3.172}$$

(b) If $u_j \neq 1$ then $\psi(\bar{\sigma}_L \sigma_{i,j})|\beta_{\tau,L}\rangle = 0$ because $\psi(\bar{\sigma}_L)$ would annihilate the vector $\psi(\sigma_{i,j})|\beta_{\tau,L}\rangle$. Therefore

$$\psi(y_\tau \bar{\sigma}_L \sigma_{i,j})|\beta_{\tau,L}\rangle = 0. \tag{3.173}$$

Case (2̄): $\bar{\sigma}_{i,j}$ with $i \in L$, $j \notin L$ or $i \notin L$, $j \in L$. Assume again that $i \in L$ and $j \notin L$. There are two sub-cases:

(a) If $u_j = 1$ then

$$\psi(\bar{\sigma}_L\bar{\sigma}_{i,j})|\beta_{\tau,L}\rangle = \psi(\bar{\sigma}_L)\left(|\beta_{\tau,L}\rangle + \sum_{k=2}^{d}\big(\cdots\otimes|k\rangle\otimes\cdots\otimes|k\rangle\otimes\cdots\big)\right), \tag{3.174}$$

where the basis vectors labeled by k are in positions i and j. But since $j \notin L$ all vectors $\cdots\otimes|k\rangle\otimes\cdots\otimes|k\rangle\otimes\cdots$ for $k \geqslant 2$ are annihilated by $\bar{\sigma}_L$. Therefore in this case

$$\psi(y_\tau\bar{\sigma}_L\bar{\sigma}_{i,j})|\beta_{\tau,L}\rangle = |t_{\tau,L}\rangle. \tag{3.175}$$

(b) If $u_j \neq 1$ then $\psi(\bar{\sigma}_{i,j})|\beta_{\tau,L}\rangle = 0$ and therefore

$$\psi(y_\tau\bar{\sigma}_L\bar{\sigma}_{i,j})|\beta_{\tau,L}\rangle = 0. \tag{3.176}$$

Case (3): $\sigma_{i,j}$ with $i \in L$, $j \in L$. Since i and j must belong together either to τ^l or τ^r, they cannot belong simultaneously to one pair of L. Since $u_i = u_j = 1$, it follows that $\psi(\sigma_{i,j})|\beta_{\tau,L}\rangle = |\beta_{\tau,L}\rangle$ and therefore

$$\psi(y_\tau\bar{\sigma}_L\sigma_{i,j})|\beta_{\tau,L}\rangle = |t_{\tau,L}\rangle. \tag{3.177}$$

Case ($\bar{3}$): $\bar{\sigma}_{i,j}$ with $i \in L$, $j \in L$. In contrast to the previous case, two sub-cases can occur:

(a) If i and j belong to the same pair in L then

$$\psi(\bar{\sigma}_L\bar{\sigma}_{i,j})|\beta_{\tau,L}\rangle = \psi(\bar{\sigma}_L)\left(\sum_{k=1}^{d}\big(\cdots\otimes|k\rangle\otimes\cdots\otimes|k\rangle\otimes\cdots\big)\right) = d\cdot\psi(\bar{\sigma}_L)|\beta_{\tau,L}\rangle, \tag{3.178}$$

where the basis vectors labeled by k are in positions i and j. Therefore

$$\psi(y_\tau\bar{\sigma}_L\bar{\sigma}_{i,j})|\beta_{\tau,L}\rangle = d\cdot|t_{\tau,L}\rangle. \tag{3.179}$$

(b) If i and j belong to different pairs in L then similarly to the previous case we can write

$$\psi(\bar{\sigma}_L\bar{\sigma}_{i,j})|\beta_{\tau,L}\rangle = \psi(\bar{\sigma}_L)\left(\sum_{k=1}^{d}\big(\cdots\otimes|k\rangle\otimes\cdots\otimes|k\rangle\otimes\cdots\big)\right), \tag{3.180}$$

where the basis vectors labeled by k are in positions i and j. But now since the positions i and j are not contracted with each other by $\psi(\bar{\sigma}_L)$, we will not acquire a factor of d:

$$\psi(y_\tau\bar{\sigma}_L\bar{\sigma}_{i,j})|\beta_{\tau,L}\rangle = |t_{\tau,L}\rangle. \tag{3.181}$$

Collecting everything together and separating the sums in Eq. (3.167) according to the cases above, we arrive at the following expression:

$$\begin{aligned}\left(J_1^{\mathcal{A}}+\cdots+J_{n+m}^{\mathcal{A}}\right)|t_{\tau,L}\rangle &= \psi\left(y_\tau\bar{\sigma}_L\left(\sum_{\substack{1\leqslant i<j\leqslant n\text{ or}\\ n+1\leqslant i<j\leqslant n+m}}\sigma_{i,j}-\sum_{\substack{1\leqslant i\leqslant n\\ n+1\leqslant j\leqslant n+m}}\bar{\sigma}_{i,j}+d\cdot q\right)\right)|\beta_{\tau,L}\rangle\\ &= \underbrace{\sum_{\substack{1\leqslant i<j\leqslant n\text{ or}\\ n+1\leqslant i<j\leqslant n+m}}|t_{\tau,L}\rangle}_{\text{case (1a)}}+\underbrace{\sum_{\substack{1\leqslant i<j\leqslant n\text{ or}\\ n+1\leqslant i<j\leqslant n+m}}|t_{\tau,L}\rangle}_{\text{case (2a)}}+\underbrace{\sum_{\substack{1\leqslant i<j\leqslant n\text{ or}\\ n+1\leqslant i<j\leqslant n+m}}|t_{\tau,L}\rangle}_{\text{case (3)}}+d\cdot q\\ &\quad-\underbrace{\sum_{\substack{1\leqslant i<j\leqslant n\text{ or}\\ n+1\leqslant i<j\leqslant n+m}}\frac{|t_{\tau,L}\rangle}{\lambda^{l/r}_{\max\{r_i,r_j\}}}}_{\text{case (1b)}}-\underbrace{\sum_{\substack{1\leqslant i\leqslant n\\ n+1\leqslant j\leqslant n+m}}|t_{\tau,L}\rangle}_{\text{case }(\bar{2}\text{a})}-\underbrace{\sum_{\substack{1\leqslant i\leqslant n\\ n+1\leqslant j\leqslant n+m}}d\cdot|t_{\tau,L}\rangle}_{\text{case }(\bar{3}\text{a})}-\underbrace{\sum_{\substack{1\leqslant i\leqslant n\\ n+1\leqslant j\leqslant n+m}}|t_{\tau,L}\rangle}_{\text{case }(\bar{3}\text{b})}.\end{aligned} \tag{3.182}$$

To simplify this we need to do some counting. Counting all possible pairs within each row of τ gives us

$$\sum_{\substack{1\leqslant i<j\leqslant n \text{ or} \\ n+1\leqslant i<j\leqslant n+m \\ \text{case (1a)}}} |t_{\tau,L}\rangle = \left(\sum_{i=1}^{\ell(\lambda_l)} \binom{\lambda_i^l}{2} + \sum_{i=1}^{\ell(\lambda_r)} \binom{\lambda_i^r}{2}\right) |t_{\tau,L}\rangle. \tag{3.183}$$

Pairing i and j across different rows gives us:

$$\sum_{\substack{1\leqslant i<j\leqslant n \text{ or} \\ n+1\leqslant i<j\leqslant n+m \\ \text{case (1b)}}} \frac{|t_{\tau,L}\rangle}{\lambda^{l/r}_{\max\{r_i,r_j\}}} = \left(\sum_{i=1}^{\ell(\lambda_l)} \lambda_i^l(i-1) + \sum_{i=1}^{\ell(\lambda_r)} \lambda_i^r(i-1)\right) |t_{\tau,L}\rangle. \tag{3.184}$$

Note that for a single diagram λ it is true that

$$\sum_{i=1}^{\ell(\lambda)} \binom{\lambda_i}{2} - \sum_{i=1}^{\ell(\lambda)} \lambda_i(i-1) = \operatorname{cont}(\lambda), \tag{3.185}$$

therefore

$$\sum_{\substack{1\leqslant i<j\leqslant n \text{ or} \\ n+1\leqslant i<j\leqslant n+m \\ \text{case (1a)}}} |t_{\tau,L}\rangle - \sum_{\substack{1\leqslant i<j\leqslant n \text{ or} \\ n+1\leqslant i<j\leqslant n+m \\ \text{case (1b)}}} \frac{|t_{\tau,L}\rangle}{\lambda^{l/r}_{\max\{r_i,r_j\}}} = (\operatorname{cont}(\lambda_l) + \operatorname{cont}(\lambda_r))\, |t_{\tau,L}\rangle. \tag{3.186}$$

Next, simple combinatorics gives us

$$\sum_{\substack{1\leqslant i<j\leqslant n \text{ or} \\ n+1\leqslant i<j\leqslant n+m \\ \text{case (2a)}}} |t_{\tau,L}\rangle = \sum_{\substack{1\leqslant i\leqslant n \\ n+1\leqslant j\leqslant n+m \\ \text{case (2a)}}} |t_{\tau,L}\rangle = \left(\lambda_1^l \cdot |L| + \lambda_d^r \cdot |L|\right) |t_{\tau,L}\rangle, \tag{3.187}$$

$$\sum_{\substack{1\leqslant i<j\leqslant n \text{ or} \\ n+1\leqslant i<j\leqslant n+m \\ \text{case (3)}}} |t_{\tau,L}\rangle = \sum_{\substack{1\leqslant i\leqslant n \\ n+1\leqslant j\leqslant n+m \\ \text{case (3b)}}} |t_{\tau,L}\rangle = 2 \cdot \binom{|L|}{2} |t_{\tau,L}\rangle, \tag{3.188}$$

so the corresponding sums cancel each other. Finally,

$$\sum_{\substack{1\leqslant i\leqslant n \\ n+1\leqslant j\leqslant n+m \\ \text{case (3a)}}} d \cdot |t_{\tau,L}\rangle = d \cdot |L| \cdot |t_{\tau,L}\rangle. \tag{3.189}$$

Using $m - |L| = |\lambda_r|$ and combining everything together gives us the desired result:

$$\left(J_1^{\mathcal{A}} + \cdots + J_{n+m}^{\mathcal{A}}\right) |t_{\tau,L}\rangle = (\operatorname{cont}(\lambda_l) + \operatorname{cont}(\lambda_r) + d \cdot |\lambda_r|)\, |t_{\tau,L}\rangle. \tag{3.190}$$

Since $J_1^{\mathcal{A}} + \cdots + J_{n+m}^{\mathcal{A}} \in \mathcal{Z}(\mathcal{A}_{n+m})$ and $\varepsilon_T^{\mathcal{A}} |t_{\tau,L}\rangle = |t_{\tau,L}\rangle$, we can draw the same conclusion for $\varepsilon_T^{\mathcal{A}}$:

$$\left(J_1^{\mathcal{A}} + \cdots + J_{n+m}^{\mathcal{A}}\right) \varepsilon_T^{\mathcal{A}} = (\operatorname{cont}(\lambda_l) + \operatorname{cont}(\lambda_r) + d \cdot |\lambda_r|)\, \varepsilon_T^{\mathcal{A}} \tag{3.191}$$

which completes the proof. □

Chapter 4

Quantum circuits for mixed Schur transform

In this chapter, we describe how to generalise the Schur transform to tensors of mixed unitary symmetry, resulting in the *mixed Schur transform*. We develop an efficient quantum circuit for the mixed Schur transform. An important feature of the mixed Schur transform is that it produces the Gelfand–Tsetlin basis for partially transposed permutations, which has useful applications in quantum information and computing. The essential novel component enabling the construction of the quantum mixed Schur transform is the efficient dual Clebsch–Gordan transform, for which we provide a comprehensive description. Additionally, we provide a matrix product state representation of the mixed Schur–Weyl basis vectors. For constant local dimension, this yields an efficient classical algorithm for computing any entry of the mixed quantum Schur transform unitary.

This chapter is based on [GBO23a].

4.1 Introduction

Schur–Weyl duality is particularly useful in quantum information, where one often needs to deal with many identical copies of a quantum state or to apply the same unitary to many systems in parallel. Its algorithmic manifestation, the quantum Schur transform and the related Clebsch–Gordan transform, can be efficiently implemented [BCH06; Har05; KS18; Kro19; WS23] and have many applications [Wri16; Har05], such as quantum spectrum [KW01a] and entropy estimation [AISW20], quantum state tomography [Key06; HHJWY17; OW16; OW17], black-box inversion of an unknown qubit unitary [YSM23a], and quantum majority vote [BLMMO22]. Some applications do not require the full quantum Schur transform but only a weaker form called weak Schur sampling [CM23].

Motivated by the wide range of applications of the quantum Schur transform, in this chapter we investigate the *mixed quantum Schur transform* which can be used both to block-diagonalize the matrix algebra $\mathcal{A}_{n,m}^{d}$ as well as to prepare the Gelfand–Tsetlin basis vectors. More specifically, in Lemma 4.2.1 of Section 4.2.1 we show that the rows of the mixed quantum Schur transform (or the Schur basis states) admit a matrix product state representation with bond dimension $(n+m)^{O(d^2)}$. This means that, for a constant local dimension d, we can compute the matrix entries of the mixed Schur transform in polynomial time. In addition, Theorem 4.3.1 of Section 4.3 provides an efficient quantum circuit with $\widetilde{O}((n+m)d^4)$ gates for computing the mixed Schur transform on a quantum computer. In particular, this transform produces the Gelfand–Tsetlin basis from Theorem 3.7.1 on the walled Brauer algebra register. The key new ingredient that allows us to generalise the standard quantum Schur transform from [BCH06] to the mixed setting is the construction of an efficient dual Clebsch–Gordan transform in Theorem 4.4.1. Finally, we note that related independent work [Ngu23] constructs the same quantum

circuits for mixed Schur transform as in our Theorem 4.3.1.

4.2 Mixed Schur transform

Recall from Theorem 3.4.1 that there is a *mixed Schur transform* unitary $U_{\mathrm{Sch}(n,m)}$ that simultaneously block-diagonalises the actions of U_d and $\mathcal{B}^d_{n,m}$ on the tensor space:

$$U_{\mathrm{Sch}(n,m)} \colon (\mathbb{C}^d)^{\otimes n+m} \to \bigoplus_{\lambda \in \widehat{\mathcal{A}}^d_{n,m}} V_\lambda \otimes W_\lambda. \tag{4.1}$$

It maps the computational basis to a new basis composed of irreducible representations of $\mathcal{A}^d_{n,m}$ and U_d:

$$U_{\mathrm{Sch}(n,m)}\ \psi^d_{n,m}(\sigma)\ U^\dagger_{\mathrm{Sch}(n,m)} = \bigoplus_{\lambda \in \widehat{\mathcal{A}}^d_{n,m}} \psi_\lambda(\sigma) \otimes I_{m_\lambda}, \qquad \forall \sigma \in \mathcal{B}^d_{n,m}, \tag{4.2}$$

$$U_{\mathrm{Sch}(n,m)}\ \phi^d_{n,m}(U)\ U^\dagger_{\mathrm{Sch}(n,m)} = \bigoplus_{\lambda \in \widehat{\mathcal{A}}^d_{n,m}} I_{d_\lambda} \otimes \phi_\lambda(U), \qquad \forall U \in \mathrm{U}_d, \tag{4.3}$$

where $\psi^d_{n,m}$ and $\phi^d_{n,m}$ are defined in Eqs. (3.17) and (3.29), ψ_λ is described in Theorem 3.7.1, and ϕ_λ is the Weyl module λ of the unitary group U_d.

Recall from Chapter 3 that we can choose the bases of V_λ and W_λ to be of Gelfand–Tsetlin type[1] and label them by paths $T \in \mathrm{Paths}(\lambda, \mathscr{A})$ and Gelfand–Tsetlin patterns $M \in \mathrm{GT}(\lambda)$, respectively:

$$V_\lambda := \mathrm{span}_{\mathbb{C}}\{|T\rangle \mid T \in \mathrm{Paths}(\lambda, \mathscr{A})\}, \tag{4.4}$$

$$W_\lambda := \mathrm{span}_{\mathbb{C}}\{|M\rangle \mid M \in \mathrm{GT}(\lambda)\}. \tag{4.5}$$

When $m = 0$ we can equivalently think of T and M as a standard and a semistandard Young tableau, respectively (see Sections 2.6 and 2.9.1). For general values of n, m, one can interpret T as a mixed standard Young tableau (see Section 3.5) while M can still be interpreted as a semistandard tableau by adding an appropriate constant to all entries of the Gelfand–Tsetlin pattern so that they become non-negative. Note that the irrep label $\lambda \in \widehat{\mathcal{A}}^d_{n,m}$ is implicit in both T and M. Indeed, it can be recovered from the final vertex of the path T as well as from the first row of the pattern M. Hence, we can treat the output space in Eq. (4.1) as a formal linear span of all pairs (T, M):

$$\bigoplus_{\lambda \in \widehat{\mathcal{A}}^d_{n,m}} V_\lambda \otimes W_\lambda = \mathrm{span}_{\mathbb{C}}\big\{|(T,M)\rangle \;\big|\; \lambda \in \widehat{\mathcal{A}}^d_{n,m}, T \in \mathrm{Paths}(\lambda, \mathscr{A}), M \in \mathrm{GT}(\lambda)\big\}. \tag{4.6}$$

Note that because of the direct sum over λ the output space of $U_{\mathrm{Sch}(n,m)}$ does *not* have a tensor product structure, i.e., one should not treat $|(T,M)\rangle$ as $|T\rangle \otimes |M\rangle$. Nevertheless, for each individual λ the corresponding subspace $\mathbb{C}^{d_\lambda} \otimes \mathbb{C}^{m_\lambda}$ is indeed a tensor product.

[1] Note that mixed Schur transform, defined as a transformation (4.1) which simultaneously decomposes $(\mathbb{C}^d)^{\otimes n+m}$ into irreducible modules of $\mathcal{A}^d_{n,m}$ and U_d, is not uniquely defined. Indeed, an arbitrary change of basis within the modules V_λ and W_λ does not affect the decomposition (4.1). On the other hand, such a change of basis within the modules is the only degree of freedom for the Schur transform. In this thesis, we make a specific choice of bases and present the mixed Schur transform for the Gelfand–Tsetlin bases corresponding to the sequence (3.67) of subalgebras of $\mathcal{A}^d_{n,m}$ and the sequence $\mathrm{U}_1 \hookrightarrow \cdots \hookrightarrow \mathrm{U}_d$ of subgroups of the unitary group U_d. For $d = 2$, it can be seen as a consecutive composition of spin-$\frac{1}{2}$ particles into a system with well-defined global spin.

We would like to find an efficient way of computing the mixed Schur transform matrix entries

$$\langle (T, M)|\, U_{\mathrm{Sch}(n,m)}\, |x_1, \ldots, x_{n+m}\rangle. \tag{4.7}$$

Here the rows are labeled by pairs (T, M), where $T \in \mathrm{Paths}(\lambda, \mathscr{A})$ and $M \in \mathrm{GT}(\lambda)$ for all choices of $\lambda \in \widehat{\mathcal{A}}^d_{n,m}$, while the columns are labeled by strings $x_1, \ldots, x_{n+m} \in [d]$.[2] The matrix entries (4.7) can be arranged into a matrix as follows:

$$U_{\mathrm{Sch}(n,m)} = \sum_{\lambda \in \widehat{\mathcal{A}}^d_{n,m}} \sum_{\substack{T \in \mathrm{Paths}(\lambda) \\ M \in \mathrm{GT}(\lambda)}} \sum_{x_1, \ldots, x_{n+m} \in [d]} \langle (T, M)|\, U_{\mathrm{Sch}(n,m)}\, |x_1, \ldots, x_{n+m}\rangle \cdot |(T, M)\rangle\langle x_1, \ldots, x_{n+m}|. \tag{4.8}$$

In particular, the mixed quantum Schur transform of any standard basis vector $|x_1, \ldots, x_{n+m}\rangle$ is

$$U_{\mathrm{Sch}(n,m)}\, |x_1, \ldots, x_{n+m}\rangle = \sum_{\lambda \in \widehat{\mathcal{A}}^d_{n,m}} \sum_{\substack{T \in \mathrm{Paths}(\lambda) \\ M \in \mathrm{GT}(\lambda)}} \langle (T, M)|\, U_{\mathrm{Sch}(n,m)}\, |x_1, \ldots, x_{n+m}\rangle \cdot |(T, M)\rangle, \tag{4.9}$$

while the Schur basis vectors $\langle (T, M)|$ can be expressed in the standard basis as

$$\langle (T, M)| U_{\mathrm{Sch}(n,m)} = \sum_{x_1, \ldots, x_{n+m} \in [d]} \langle (T, M)|\, U_{\mathrm{Sch}(n,m)}\, |x_1, \ldots, x_{n+m}\rangle \cdot \langle x_1, \ldots, x_{n+m}|. \tag{4.10}$$

The most common way of implementing the regular $m = 0$ Schur transform is by a sequence of Clebsch–Gordan transforms [BCH06; Har05; KS18]. The basic idea is to view the space $(\mathbb{C}^d)^{\otimes n}$ as tensor product of n defining representations $W_{\square}$ of U_d and sequentially decompose this tensor product by including one new system at a time, see Section 2.9.3. This approach can be generalised to any $m \geqslant 0$ in a straightforward way by incorporating *dual Clebsch–Gordan transforms* for an inductive decomposition of

$$(\mathbb{C}^d)^{\otimes n+m} \cong W_{\square} \otimes \ldots \otimes W_{\square} \otimes W_{\bar{\square}} \otimes \ldots \otimes W_{\bar{\square}} \tag{4.11}$$

where $W_{\bar{\square}}$ denotes the dual of the defining representation. We can derive an explicit formula for the matrix entries of the mixed quantum Schur transform obtained in this fashion.

We start with a single qudit in state $|x_1\rangle$ where $x_1 \in [d]$. At each step $k = 2, \ldots, n + m$ we use the Clebsch–Gordan transform $\mathrm{CG}^{(k)} \in \mathrm{U}_{d^k}$ to couple the output state from the previous iteration with an additional qudit in state $|x_k\rangle$ where $x_k \in [d]$. The input and output spaces of $\mathrm{CG}^{(k)}$ can be decomposed as follows:

$$\mathrm{CG}^{(k)} : \left(\bigoplus_{\lambda \in \widehat{\mathcal{A}}^d_{k-1}} V_\lambda \otimes W_\lambda \right) \otimes \mathbb{C}^d \to \bigoplus_{\mu \in \widehat{\mathcal{A}}^d_k} V_\mu \otimes W_\mu, \tag{4.12}$$

where we are using the single-subscript convention for the sequence of algebras $\mathcal{A}^d_k$ from Eq. (3.47). For any path $T = (T^0, \ldots, T^{k-1})$ and pattern $M \in \mathrm{GT}(T^{k-1})$ the action of $\mathrm{CG}^{(k)}$ is defined as

$$\mathrm{CG}^{(k)} \Big(|(T, M)\rangle \otimes |x_k\rangle \Big) := \sum_{\mu :\, T^{k-1} \to \mu} \sum_{\substack{N \in \mathrm{GT}(\mu) \\ w(N) = w(M) + w(x_k)}} c^{x_k}_{N,M} |(T \to \mu, N)\rangle, \tag{4.13}$$

[2] Note that Eq. (4.1) describes a passive transformation that changes the coordinate system from the computational basis vectors into the basis labeled by tuples (T, M). As the number of such tuples matches the dimension of $(\mathbb{C}^d)^{\otimes n+m}$, it can be seen as a transformation of $(\mathbb{C}^d)^{\otimes n+m}$ onto itself, after applying any bijection between the tuples (T, M) and the computational basis vectors. As such, the Schur transform is a unitary transformation (also active transformation).

where $\mu\colon T^{k-1} \to \mu$ means that μ can be reached from T^{k-1} by one step in the Bratteli diagram $\mathscr{A}$, and $c^{x_k}_{N,M}$ are the so-called *Clebsch–Gordan coefficients* (see Section 4.A.1 for an explicit formula). The mixed quantum Schur transform $U_{\mathrm{Sch}(n,m)}$ is given by a cascade of $n+m-1$ Clebsch–Gordan transforms:

$$U_{\mathrm{Sch}(n,m)} = \mathrm{CG}^{(n+m)} \cdot \Big(\mathrm{CG}^{(n+m-1)} \otimes I\Big) \cdots \Big(\mathrm{CG}^{(3)} \otimes I^{\otimes n+m-3}\Big) \cdot \Big(\mathrm{CG}^{(2)} \otimes I^{\otimes n+m-2}\Big). \tag{4.14}$$

In particular, the usual Schur transform satisfies $U_{\mathrm{Sch}(k,0)} = \mathrm{CG}^{(k)}\big(U_{\mathrm{Sch}(k-1,0)} \otimes I\big)$ where $k = 2, \ldots, n$.

Let us use Eq. (4.14) to derive an explicit formula for the matrix entries of the mixed quantum Schur transform. For an arbitrary path $T = (T^0, \ldots, T^{n+m}) \in \mathrm{Paths}(\lambda)$ and Gelfand–Tsetlin pattern $M \in \mathrm{GT}(\lambda)$, we get from Eqs. (4.13) and (4.14) that

$$\langle (T, M)|\, U_{\mathrm{Sch}(n,m)}\, |x_1, \ldots, x_{n+m}\rangle = \langle M|\, \mathrm{CG}^{x_{n+m}}_{T^{n+m}T^{n+m-1}} \cdots \mathrm{CG}^{x_2}_{T^2T^1} |x_1\rangle \tag{4.15}$$

where $|M\rangle$ is a Gelfand–Tsetlin basis vector of the unitary group irrep corresponding to the staircase λ, and $\mathrm{CG}^{x_k}_{T^kT^{k-1}}$ for $k = 2, \ldots, n+m$ are rectangular matrices with rows labeled by $N \in \mathrm{GT}(T^k)$ and columns labeled by $M \in \mathrm{GT}(T^{k-1})$, with the corresponding matrix entry equal to the Clebsch–Gordan coefficient:

$$\langle N|\, \mathrm{CG}^{x_k}_{T^kT^{k-1}} |M\rangle := c^{x_k}_{N,M}. \tag{4.16}$$

Hence, according to Eq. (4.15), any matrix entry of $U_{\mathrm{Sch}(n,m)}$ can be computed by applying a sequence of matrices onto $|x_1\rangle$. The complexity of this computation depends on the dimensions of the matrices $\mathrm{CG}^{x_k}_{T^kT^{k-1}}$.

In practice, one can take advantage of the fact that the matrices $\mathrm{CG}^{x_k}_{T^kT^{k-1}}$ are block-diagonal. By tracking which blocks contribute non-trivially to a given $\langle (T, M)|$, Eq. (4.15) can be modified as follows:

$$\langle (T, M)|\, U_{\mathrm{Sch}(n,m)}\, |x_1, \ldots, x_{n+m}\rangle = \langle M|\, \mathrm{CG}^{x_{n+m}, w(x_{n+m-1}, \ldots, x_1)}_{T^{n+m}T^{n+m-1}} \cdots \mathrm{CG}^{x_2}_{T^2T^1} |x_1\rangle, \tag{4.17}$$

where $\mathrm{CG}^{x_k, w(x_{k-1}, \ldots, x_1)}_{T^kT^{k-1}}$ are submatrices of $\mathrm{CG}^{x_k}_{T^kT^{k-1}}$ with rows labeled only by $N \in \mathrm{GT}(T^k)$ of weight $w(N) = w(x_k, \ldots, x_1)$ and columns labeled only by $M \in \mathrm{GT}(T^{k-1})$ of weight $w(M) = w(x_{k-1}, \ldots, x_1)$.

4.2.1 MPS representation of mixed Schur basis vectors

Notice that Eq. (4.15) presents the Schur basis vectors $|(T, M)\rangle$ as matrix product states (MPS) with bond dimensions given by $m_{T^k} = \dim W_{T^k} = |\,\mathrm{GT}(T^k)|$, see Fig. 4.1. For fixed local dimension d, the bond dimensions m_{T^k} are upper-bounded by $(n+m)^{O(d^2)}$. This can be easily seen by counting the number of Gelfand–Tsetlin patterns $\mathrm{GT}(T^k)$. Indeed, for any pair of Young diagrams $\lambda = (\lambda_l, \lambda_r)$ of size $|\lambda_l| \leqslant n$, $|\lambda_r| \leqslant m$ and satisfying $\ell(\lambda_l) + \ell(\lambda_r) \leqslant d$, the corresponding set of Gelfand–Tsetlin patterns $\mathrm{GT}(\lambda)$ consists of entries m_{ij} which must satisfy $-m \leqslant m_{ij} \leqslant n$. As the number of entries is $d(d+1)/2$, the size of the set $\mathrm{GT}(\lambda)$ can be upper bounded by $(n+m)^{O(d^2)}$. Note that the length of the MPS is $n+m$. As a consequence, for fixed local dimension d the computational complexity of computing $\langle (T, M)|\, U_{\mathrm{Sch}(n,m)}\, |x_1, \ldots, x_{n+m}\rangle$ is upper bounded by

$$(n+m)^{O(d^2)}. \tag{4.18}$$

Note that the complexity of computing the entries of the matrices $\mathrm{CG}^{x_k}_{T^kT^{k-1}}$ (see Section 4.A.1) is absorbed into the above bound. Thus, we have established the following result.

4.2.1. Lemma (MPS representation of mixed Schur basis vectors). *The mixed Schur basis vectors $U^\dagger_{\mathrm{Sch}(n,m)}|(T,M)\rangle$ (or rows of the mixed quantum Schur transform matrix $U_{\mathrm{Sch}(n,m)}$) admit a matrix product state representation with bond dimension $(n+m)^{O(d^2)}$. Hence, the matrix entries of the mixed Schur transform $U_{\mathrm{Sch}(n,m)}$ can be computed in time $(n+m)^{O(d^2)}$. In particular, for constant local dimension d, this is polynomial in system size $n+m$.*

Notice that Eq. (4.17) provides a more refined approach for computing the entries of vectors $|(T,M)\rangle$ in the computational basis, although it is no longer an MPS as the choice of consecutive matrices $\mathrm{CG}^{x_k,w(x_{k-1},\ldots,x_1)}_{T^kT^{k-1}}$ does not depend only on x_k. The matrices in this product are of size $|\{M \in \mathrm{GT}(T^k) \mid w(M) = w(x_1,\ldots,x_k)\}|$, i.e., the number of Gelfand–Tsetlin patterns with a given weight $w(x_1,\ldots,x_k)$. This is known as *Kostka number* $K_{T^k,w(x_1,\ldots,x_k)}$ and it depends on two integer partitions: T^k and $w(x_1,\ldots,x_k)$. Clearly, the matrices in Eq. (4.17) are smaller than those in Eq. (4.15), however, we do not get an asymptotic improvement in the upper bound. As before, $K_{T^k,w(x_1,\ldots,x_k)}$ can be upper bounded by $(n+m)^{O(d^2)}$, which leads to the same upper bound (4.18).

It is convenient to use tensor network notation to represent the Clebsch–Gordan tensors. Let us assume λ and μ are staircases that differ only by one box. We will denote by $\mathrm{CG}^+_{\mu,\lambda}$, $\mathrm{CG}^-_{\lambda,\mu}$ the Clebsch–Gordan tensors corresponding to matrices $\mathrm{CG}^x_{\mu,\lambda}$, $\mathrm{CG}^x_{\lambda,\mu}$, respectively:

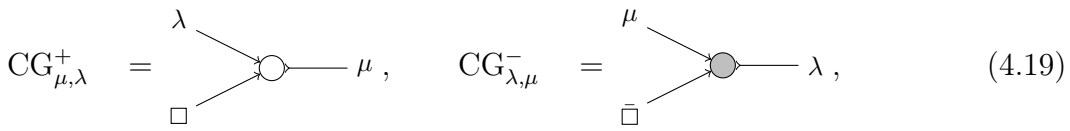

(4.19)

where the circles represent the corresponding tensors and the arrows represent two incoming and one outgoing irreps, labeled by staircases that differ only by one box (adding a box for CG^+ and removing for CG^-).

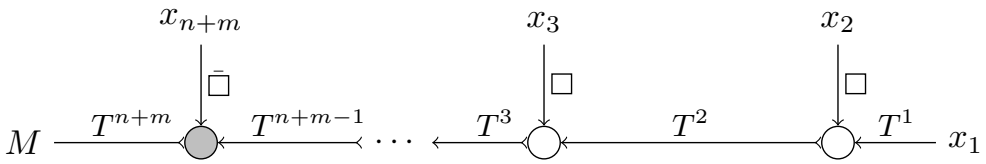

Figure 4.1: Tensor network representation of the state $U^\dagger_{\mathrm{Sch}(n,m)}|(T,M)\rangle$ defined in Eq. (4.10) as a matrix product state by using Eq. (4.15). The tensors $\mathrm{CG}^{\pm}_{T^kT^{k-1}}$ (depicted as white circles for $k \leqslant n$ and gray circles for $k > n$) have three indices. The matrices $\mathrm{CG}^{x_k}_{T^kT^{k-1}}$ from Eq. (4.16) are obtained from tensor $\mathrm{CG}^{\pm}_{T^kT^{k-1}}$ by fixing the index corresponding to $x_k \in [d]$, indicating the computational basis state $|x_k\rangle$. The bond dimensions $m_{T^k} = \dim W_{T^k} = |\mathrm{GT}(T^k)|$ are equal to the number of Gelfand–Tsetlin patterns of shape T^k. Asymptotically the maximal value of m_{T^k} for different k is upper bounded by $(n+m)^{O(d^2)}$.

4.2.2 Mixed Schur transform achieves the Gelfand–Tsetlin basis

By construction [VK92], the Clebsch–Gordan transform (4.13) achieves the Gelfand–Tsetlin basis of the unitary group on the unitary group registers W_λ in Eq. (4.1). As a consequence, the same holds also for the mixed Schur transform (4.14). However, it is also true that the mixed Schur transform yields the Gelfand–Tsetlin basis of the algebra $\mathcal{A}^d_{n,m}$ in the relevant registers V_λ. We prove this in Theorem 4.2.2 by showing that the matrix elements of the contraction generator σ_n in the mixed Schur basis coincide with the matrix elements in the Gelfand–Tsetlin basis from Theorem 3.7.1.

Because the Clebsch–Gordan transform CG^k from Eqs. (4.12) and (4.13) acts only on the unitary irrep registers upon adding a qudit $\mathbb{C}^d$, we get for every $\sigma \in \mathcal{A}^d_{k-1}$

$$\mathrm{CG}^{(k)}\left(\left(\bigoplus_{\mu\in\widehat{\mathcal{A}}^d_{k-1}} \psi_\mu(\sigma)\otimes I_{m_\mu}\right)\otimes I_d\right)\mathrm{CG}^{(k)\dagger} = \bigoplus_{\lambda\in\widehat{\mathcal{A}}^d_k}\left(\bigoplus_{\substack{\mu\in\widehat{\mathcal{A}}^d_{k-1}\\ \mu:\,\mu\to\lambda}} \psi_\mu(\sigma)\right)\otimes I_{m_\lambda}. \tag{4.20}$$

We see that the CG^k does not change the action inside the registers V_λ, meaning that it is naturally implementing a subalgebra-adapted basis, namely a Gelfand–Tsetlin basis of $\mathcal{A}^d_{n,m}$. However, there is still a degree of freedom of choosing phases for the Gelfand–Tsetlin basis vectors. In [Jor09; Har05] it was argued that our choice of the Clebsch–Gordan transforms CG^k implements exactly the same Gelfand–Tsetlin basis in the $\mathcal{A}^d_{n,m}$ register of the mixed Schur–Weyl duality as in Theorem 3.7.1 for the permutation generators σ_i, $i \neq n$. For the contraction generator $\sigma_n \in \mathcal{A}^d_{n,m}$ this can be proved by directly contracting two tensor networks from Fig. 4.1 corresponding to two different paths $S, T \in \mathrm{Paths}(\lambda, \mathscr{A})$ for every $\lambda \in \widehat{\mathcal{A}}^d_{n,m}$.

4.2.2. Theorem. *Consider the contraction generator $\sigma_n \in \mathcal{A}^d_{n,m}$. For every $\lambda \in \widehat{\mathcal{A}}^d_{n,m}$, $S, T \in \mathrm{Paths}(\lambda, \mathscr{A})$, and $M \in \mathrm{GT}(\lambda)$ we find*

$$\langle (S,M)|U_{\mathrm{Sch}(n,m)}\sigma_n U^\dagger_{\mathrm{Sch}(n,m)}|(T,M)\rangle = \begin{cases} \dfrac{\sqrt{m_{T^n} m_{S^n}}}{m_{T^{n-1}}} & \text{if } S,T \in \mathcal{M}(T) \\ 0 & \text{otherwise} \end{cases}, \tag{4.21}$$

where $\mathcal{M}(T)$, defined in Eq. (3.70), denotes the set of all paths that coincide with T, except possibly at level n, and satisfy $T^{n-1} = T^{n+1}$.

Proof:
The proof is crucially based on the following fact relating $\mathrm{CG}^+_{\mu,\lambda}$ and the dual $\mathrm{CG}^-_{\lambda,\mu}$ Clebsch–Gordan tensors [VK95, Eq. (10), p. 289]:

$$\mathrm{CG}^-_{\lambda,\mu} = \sqrt{\frac{m_\lambda}{m_\mu}}\,\mathrm{CG}^+_{\mu,\lambda}\,. \tag{4.22}$$

We also need to use the following orthogonality identities for Clebsch–Gordan tensors:

Note that left relation is also valid for CG^+ tensors. Now we can evaluate the matrix entries of σ_n by applying the above contraction rules for (dual) Clebsch–Gordan tensors to contract the

following expression:

$$m_{T^{n+m}}\langle (S,M)|U_{\mathrm{Sch}(n,m)}\sigma_n U^\dagger_{\mathrm{Sch}(n,m)}|(T,M)\rangle = \sum_{M\in \mathrm{GT}(T^{n+m})} \langle (S,M)|U_{\mathrm{Sch}(n,m)}\sigma_n U^\dagger_{\mathrm{Sch}(n,m)}|(T,M)\rangle =$$

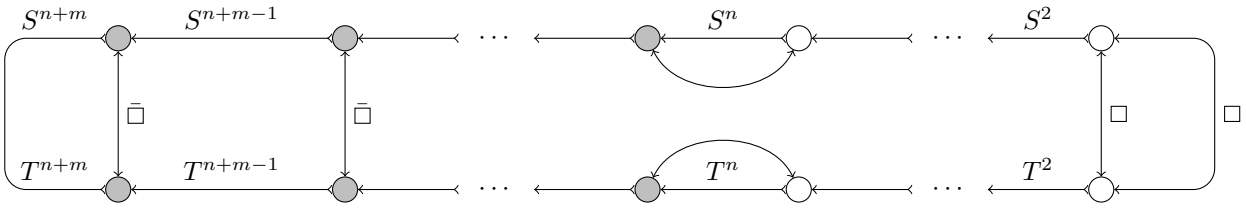

$$= \delta_{S^1,T^1}\cdots\delta_{S^{n-1},T^{n-1}}\delta_{S^{n+1},T^{n+1}}\cdots\delta_{S^{n+m},T^{n+m}}\frac{m_{T^{n+m}}}{m_{T^{n+1}}}\cdot$$

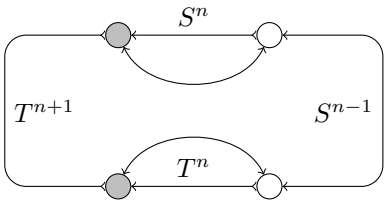

Canceling the $m_{T^{n+m}}$ term from both sides and using Eq. (4.22) and the orthogonality properties of Clebsch–Gordan tensors gives us

$$\begin{aligned}\langle (S,M)|U_{\mathrm{Sch}(n,m)}\sigma_n U^\dagger_{\mathrm{Sch}(n,m)}|(T,M)\rangle &= \delta_{S^1,T^1}\ldots\delta_{S^{n-1},T^{n-1}}\delta_{S^{n+1},T^{n+1}}\ldots\delta_{S^{n+m},T^{n+m}}\cdot\\ &\cdot\frac{1}{m_{T^{n+1}}}\sqrt{\frac{m_{T^{n+1}}}{m_{T^n}}}\sqrt{\frac{m_{T^{n+1}}}{m_{S^n}}}\frac{m_{S^n}}{m_{T^{n-1}}}\frac{m_{T^n}}{m_{T^{n-1}}}\delta_{T^{n-1},T^{n+1}}m_{T^{n+1}}\\ &= \delta_{S^1,T^1}\ldots\delta_{S^{n-1},T^{n-1}}\delta_{S^{n+1},T^{n+1}}\ldots\delta_{S^{n+m},T^{n+m}}\delta_{T^{n-1},T^{n+1}}\frac{\sqrt{m_{T^n}m_{S^n}}}{m_{T^{n-1}}},\end{aligned} \tag{4.23}$$

which is exactly what we claimed. □

A similar result can be proven for diagrams τ_k from Eq. (3.15), which was also obtained in [SMKH22] for restricted class of irreps.

The knowledge of explicit action of the generators of $\mathcal{A}^d_{n,m}$ in the Gelfand–Tsetlin basis is useful for quantum computing applications. For example, it yields the efficient quantum circuit for port-based teleportation derived in Chapter 5. Equation (4.14) suggests not only a way of classically computing the matrix entries of the mixed quantum Schur transform unitary but also a quantum circuit for implementing the corresponding isometry (we will use the same notation for both). In the next section, we describe a quantum circuit which implements this basis transformation.

4.3 Quantum circuits for mixed Schur transforms

In this section, we describe a quantum circuit that implements the mixed quantum Schur transform. It is more precise to think of it as an isometry $U_{\mathrm{Sch}(n,m)}$:

$$U_{\mathrm{Sch}(n,m)}\colon (\mathbb{C}^d)^{\otimes n+m} \to \overbrace{\mathbb{C}^{\widehat{\mathcal{A}}^d_2}\otimes\cdots\otimes\mathbb{C}^{\widehat{\mathcal{A}}^d_{n+m-1}}\otimes\underbrace{\mathbb{C}^{\widehat{\mathcal{A}}^d_{n+m}}}_{M}}^{T}\otimes\overbrace{\mathbb{C}^{\widehat{\mathrm{U}}^{n+m}_{d-1}}\otimes\cdots\otimes\mathbb{C}^{\widehat{\mathrm{U}}^{n+m}_1}}^{M_{[d-1]}}, \tag{4.24}$$

where the first $n+m-1$ registers of the output correspond to a path $T\in\mathrm{Paths}(\lambda,\mathscr{A})$ labeling the corresponding irreps of $\mathcal{A}^d_k$, the last d registers correspond to a Gelfand–Tsetlin pattern $M\in\mathrm{GT}(\lambda)$ for some $\lambda\in\widehat{\mathcal{A}}^d_{n,m}$, and $\widehat{\mathrm{U}}^{n+m}_k$ is the set of staircases of bounded size, labeling the irreps of the group U_k. One should think of $\widehat{\mathrm{U}}^{n+m}_k$ as the set of all allowed values of the k-th

row $\mathbf{m}_k$ in all possible Gelfand–Tsetlin patterns $M \in \mathrm{GT}(\lambda)$. The last vertex T^{n+m} of the path T coincides with the top row $\mathbf{m}_d$ of the Gelfand–Tsetlin pattern M, i.e., $T^{n+m} = \mathbf{m}_d = \lambda$; this explains the overlap between T and M in Eq. (4.24). More precisely, for every integer $n \in [n+m]$ and $k \in [d]$, we define the set $\widehat{\mathrm{U}}_k^l$ of staircases as the labels of the following irreps of U_k:

$$\widehat{\mathrm{U}}_k^l := \begin{cases} \left\{\lambda \in \widehat{\mathrm{U}}_k \,\middle|\, |\lambda_l| + |\lambda_r| \leqslant l\right\} & l < n+m \text{ or } k < d, \\ \widehat{\mathcal{A}}_{n+m}^d & l = n+m \text{ and } k = d. \end{cases} \tag{4.25}$$

The output of the mixed quantum Schur transform in Eq. (4.24) has tensor product structure both for storing the path $T \in \mathrm{Paths}(\lambda, \mathscr{A})$ as well as the Gelfand–Tsetlin pattern $M \in \mathrm{GT}(\lambda)$. The natural way of interpreting the rows of a general Gelfand–Tsetlin pattern $M = (\mathbf{m}_d, \mathbf{m}_{d-1}, \mathbf{m}_{d-2}, \ldots, \mathbf{m}_1) \in \mathrm{GT}(\mathbf{m}_d)$ is to use the staircase notation for each row. This means that one should think of the quantum states $|M\rangle$ as

$$|M\rangle := |\mathbf{m}_d\rangle \otimes |\mathbf{m}_{d-1}\rangle \otimes \cdots \otimes |\mathbf{m}_2\rangle \otimes |\mathbf{m}_1\rangle. \tag{4.26}$$

Moreover, it is useful to define a shorthand notation $M_{[k]}$ to indicate only the bottom k rows of the Gelfand–Tsetlin pattern M. The corresponding quantum state for any $k \in [d]$ is

$$|M_{[k]}\rangle := |\mathbf{m}_k\rangle \otimes |\mathbf{m}_{k-1}\rangle \otimes \cdots \otimes |\mathbf{m}_1\rangle. \tag{4.27}$$

Each row $\mathbf{m}_k$ of the Gelfand–Tsetlin pattern M can be stored as the tensor product of k integers $m_{i,k}$, each having absolute value no more than $n+m$:

$$|\mathbf{m}_k\rangle := |m_{1,k}\rangle \otimes |m_{k-1,k}\rangle \otimes \cdots \otimes |m_{k,k}\rangle. \tag{4.28}$$

Thus, the total number of qubits required to store $\mathbf{m}_k$ scales as $O(k \log(n+m))$. The total number of registers containing the entries $m_{i,k}$ for all rows $\mathbf{m}_k$ within M is $\frac{d(d+1)}{2}$. Consequently, the total number of qubits required to store M is $O(d^2 \log(n+m))$.

There are two options for encoding the paths $T \in \mathrm{Paths}(\lambda, \mathscr{A})$. For the first encoding, notice from Eq. (4.24) that a path T can be stored as a tensor product state

$$|T\rangle := |T^2\rangle \otimes \cdots \otimes |T^{n+m}\rangle, \tag{4.29}$$

where we have suppressed the registers $|T^0\rangle$ and $|T^1\rangle$ since they are one-dimensional ($T^0 = \varnothing$ and $T^1 = \square$ for any path T). T^{n+m} represents the irrep label, which we usually denote by $\lambda = T^{n+m}$. We call Eq. (4.29) the *standard encoding* of $|T\rangle$.

We also consider another more space-efficient isometry implementing the mixed quantum Schur transform which uses an alternative encoding for T. Notice that for a given path $T = (T^0, \ldots, T^{n+m}) \in \mathrm{Paths}(\Lambda, \mathscr{A})$, the vertex T^i is uniquely determined by the previous vertex T^{i-1} and the row number y_i of the added (or removed) box $T^i \setminus T^{i-1}$. The sequence $(y_1, \ldots, y_{n+m})$ is called the *Yamanouchi word* of path T. Since $y_i \in [d]$ for each i, encoding a path T as a sequence of y_i instead of T^i is more space-efficient. Indeed, each y_i can be stored directly in the i-th input qudit without requiring additional memory, while storing each T^i takes $O(d \log(n+m))$ additional qubits and thus $O((n+m)d \log(n+m))$ auxiliary qubits for T in total. We call this more efficient encoding of the mixed Schur transform the *Yamanouchi encoding*:

$$U_{\mathrm{Sch}(n,m)} \colon (\mathbb{C}^d)^{\otimes n+m} \to \overbrace{\underbrace{\mathbb{C}^d \otimes \cdots \otimes \mathbb{C}^d}_{(y_2,\ldots,y_{n+m})}}^{T_y} \otimes \overbrace{\mathbb{C}^{\widehat{\mathcal{A}}_{n+m}^d} \otimes \mathbb{C}^{\widehat{\mathrm{U}}_{d-1}^{n+m}} \otimes \cdots \otimes \mathbb{C}^{\widehat{\mathrm{U}}_1^{n+m}}}^{M_{[d-1]}}. \tag{4.30}$$

More specifically, we store a path $T \in \mathrm{Paths}(\mathscr{A})$ as the following tensor product state:

$$|T_y\rangle := |y_2\rangle \otimes \cdots \otimes |y_{n+m-1}\rangle \otimes |y_{n+m}\rangle \otimes |\lambda\rangle, \tag{4.31}$$

where the first register $|y_1\rangle$ is suppressed since it is one-dimensional ($y_1 = 1$ for any path). While the Yamanouchi encoding is more space-efficient, it makes certain operations less time-efficient. For example, to recover the i-th vertex T^i of a path T, one needs to perform a certain computation on $y_2, \dots, y_i$ stored in the first $i-1$ registers of $|T_y\rangle$, as opposed to directly looking up the i-th register $|T^i\rangle$ in the standard encoding (4.29).

Now we are ready to present our construction of the mixed quantum Schur transform, which is a slight modification of the original quantum Schur transform [BCH06; Har05] for the classical Schur–Weyl duality (i.e., the $m = 0$ case of our formalism). The original quantum Schur transform involves a cascade of Clebsch–Gordan isometries CG_d^+ (see Fig. 4.4), where each isometry implements one of the unitary Clebsch–Gordan transforms CG^k from Eq. (4.12). The only modification we make to the original construction is to replace CG_d^+ by a similarly defined *dual Clebsch–Gordan isometry* CG_d^- in the second half of the circuit (see Fig. 4.2). This immediately leads to the following result which agrees with [BCH06; Har05] in the $m = 0$ case.

4.3.1. Theorem (Mixed quantum Schur transform). *The mixed quantum Schur transform for block-diagonalising the algebra $\mathcal{A}_{n,m}^d$ has a quantum circuit with gate and time complexity $(n+m)d^4 \operatorname{polylog}(d, n, m, 1/\epsilon)$, where d is the local dimension, and n and m are the parameters of $\mathcal{A}_{n,m}^d$. Moreover, it can be implemented using two different encodings of the Gelfand–Tsetlin basis of $\mathcal{A}_{n,m}^d$ with the following auxiliary space complexity:*

1. *standard encoding: $(n+m+d)d \operatorname{polylog}(d, n, m, 1/\epsilon)$ auxiliary qubits (see Fig. 4.2),*
2. *Yamanouchi encoding: $d^2 \operatorname{polylog}(d, n, m, 1/\epsilon)$ auxiliary qubits (see Fig. 4.3).*

Proof:
The proof is by explicit construction, which we have already mentioned: we just need to apply the (dual) Clebsch–Gordan transformations sequentially, one-by-one, see Fig. 4.2.

The main new building block of the mixed quantum Schur transform circuit is the dual Clebsch–Gordan isometry CG_d^-. It can be obtained by a small modification of the usual CG_d^+ isometry, which can be taken directly from [BCH06; Har05]. While both isometries have the same structure, their representation-theoretic interpretations are slightly different: CG_d^+ is used when $k \leqslant n$ to add a new box to T_l^{k-1}, producing a new diagram T_l^k, while CG_d^- is used when $k > n$, either to remove a box from T_l^{k-1} or to add a box to T_r^{k-1}. In the staircase notation from Section 3.5, this is equivalent to adding a box to the staircase T^{k-1} when $k \leqslant n$ and removing a box when $k > n$. We describe efficient quantum circuits for both isometries in a unified way in Section 4.4. We show that their complexity is $\operatorname{poly}(d) \operatorname{polylog}(d, n, m, 1/\epsilon)$, where ϵ is the desired error. A more precise calculation shows that, in fact, their complexity is $d^4 \operatorname{polylog}(d, n, m, 1/\epsilon)$ [Ngu23]. This follows from Theorem 4.4.1, where we need to set the desired precision to be $\epsilon/(n+m)$, since there are $n+m$ quantum Clebsch–Gordan isometries in the mixed quantum Schur transform. Overall, this leads to the $(n+m)d^4 \operatorname{polylog}(n, m, d, 1/\epsilon)$ gate and time complexities for the mixed quantum Schur transform $U_{\mathrm{Sch}(n,m)}$.

The Yamanouchi encoding essentially uses the same circuit as in the standard encoding, see Fig. 4.3. The only difference is how we store paths $T \in \mathrm{Paths}(\mathscr{A})$. This slightly affects the implementation of the Clebsch–Gordan isometries $\mathrm{CG}_d^\pm$, which we describe in Theorem 4.4.1.

The auxiliary qubit count is as follows. To store $M \in \mathrm{GT}(\lambda)$ for every $\lambda \in \mathcal{A}_{n,m}^d$, we need a quantum register with $O(d^2)$ qudits, each of dimension $O(n+m)$, to store each entry of the Gelfand–Tsetlin pattern M (this register is initialised to $|\mathbf{0}\rangle$ in Figs. 4.2 and 4.3). This gives an additional $O(d^2 \log(n+m))$ qubits. In the standard encoding, we have a register that stores all nodes of the path T as staircases. Each staircase requires at most $O(d \log(n+m))$ qubits, so the full path T would require $O((n+m)d \log(n+m))$ additional qubits. Together with the additional memory requirement needed to implement Clebsch–Gordan transforms $d^2 \operatorname{polylog}(d, (n+m)/\epsilon)$ (see Theorem 4.4.1), this gives the claimed auxiliary space complexity. □

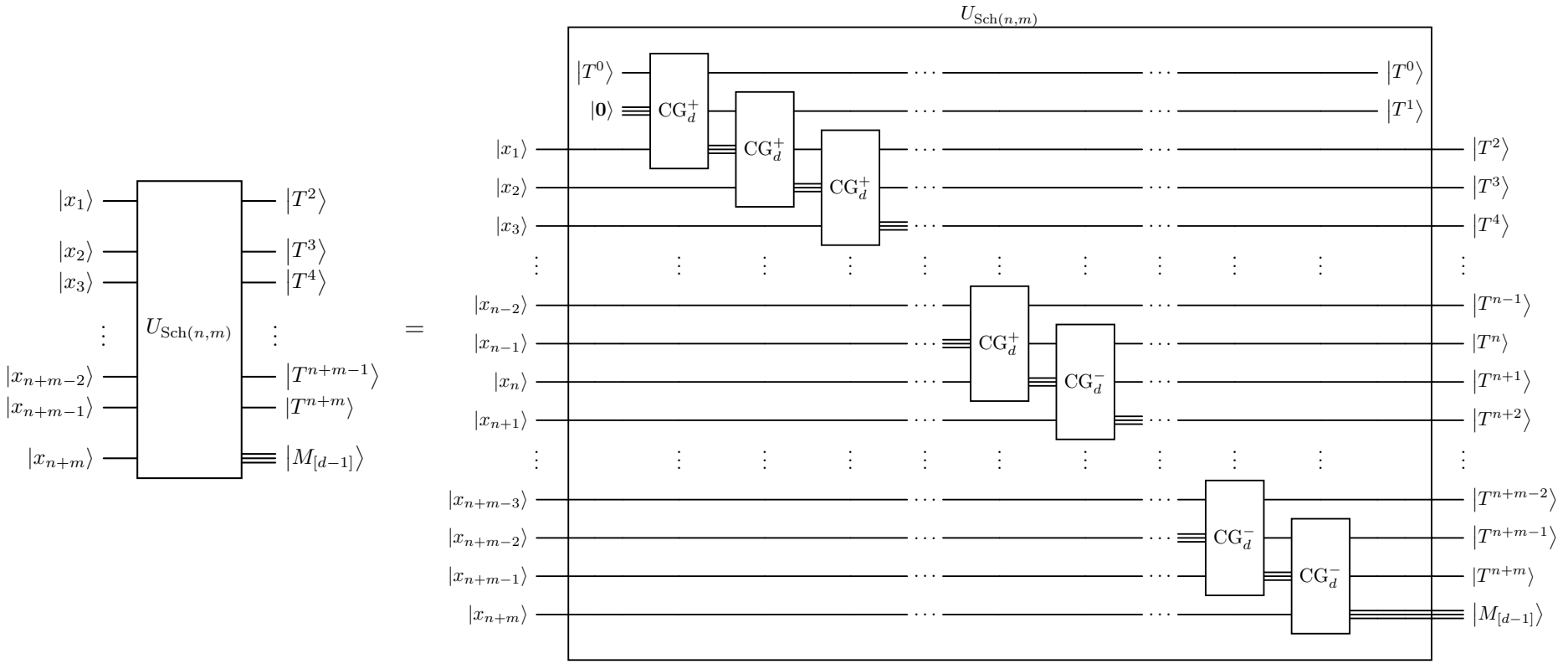

Figure 4.2: Schematic depiction of the mixed quantum Schur transform $U_{\mathrm{Sch}(n,m)}$ and its implementation by a cascade of Clebsch–Gordan transforms $\mathrm{CG}_d^{\pm}$. Note that we switch from CG_d^+ to CG_d^- starting at input $|x_{n+1}\rangle$. Also note that the two topmost registers $|T^0\rangle, |T^1\rangle$ on the right are one-dimensional, i.e., their values are always fixed to $|T^0\rangle = |(\varnothing, \varnothing)\rangle$ and $|T^1\rangle = |(\square, \varnothing)\rangle$, so we suppress them in $U_{\mathrm{Sch}(n,m)}$. The state $|\mathbf{0}\rangle$ initialises the Gelfand–Tsetlin pattern register, consisting of $O(d^2 \log(n+m))$ auxiliary qubits. Moreover, each $|T^i\rangle$ register requires $O(d \log(n+m))$ additinal qubits so that the total overhead for all staircases T^i is $O(d(n+m)\log(n+m))$. Finally, there is a space overhead for implementing $\mathrm{CG}_d^{\pm}$, which we describe in Theorem 4.4.1 and Lemma 4.4.2.

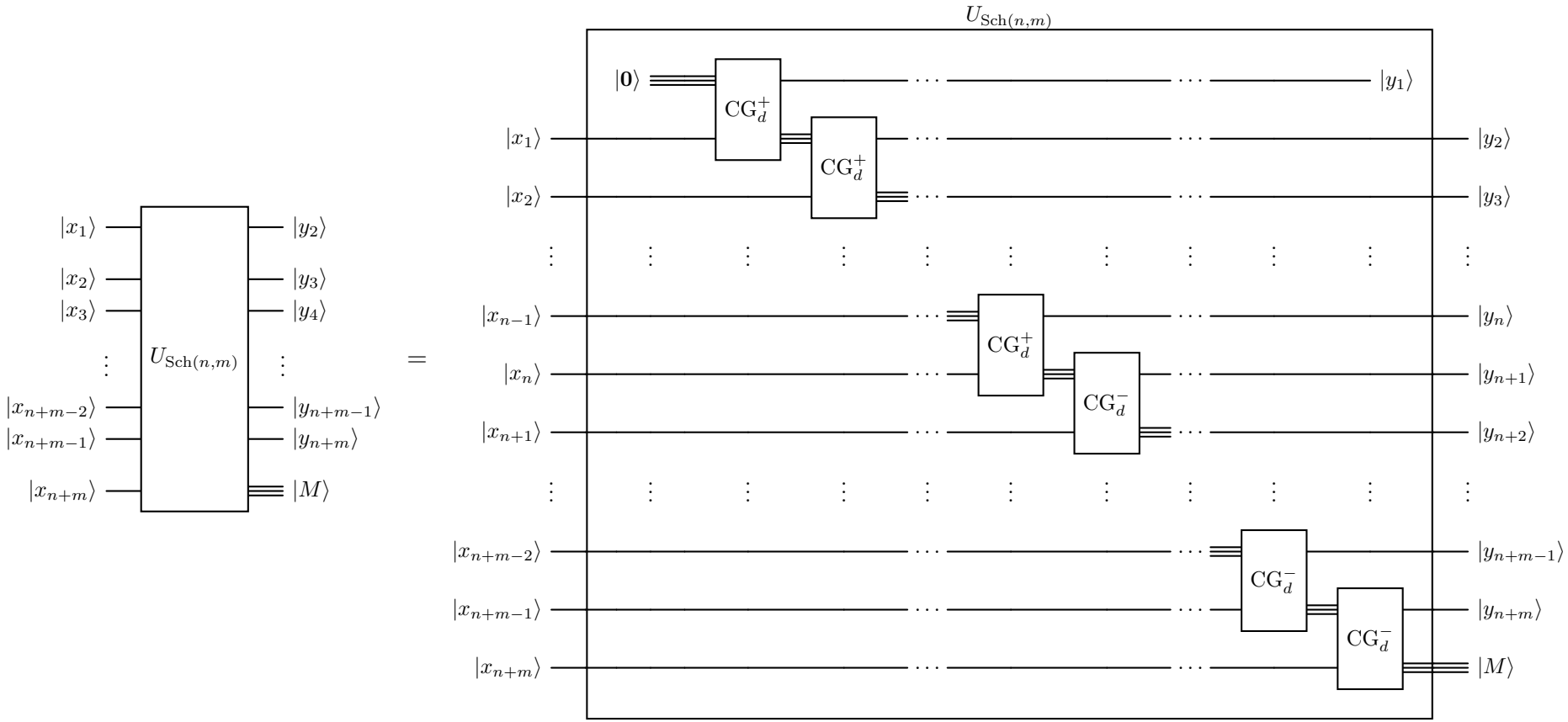

Figure 4.3: Mixed quantum Schur transform $U_{\mathrm{Sch}(n,m)}$ in Yamanouchi encoding from Eq. (4.31). Note that the topmost register $|y_1\rangle$ on the right is one-dimensional, i.e., its value is always fixed to $|y_1\rangle = |1\rangle$, so we suppress it in $U_{\mathrm{Sch}(n,m)}$. The Clebsch–Gordan transforms $\mathrm{CG}_d^{\pm}$ are specified in Fig. 4.7 and are implemented in Fig. 4.8 via reduced Wigner operators. The state $|\mathbf{0}\rangle$ initialises the Gelfand–Tsetlin pattern register, consisting of $O(d^2 \log(n+m))$ auxiliary qubits. Moreover, there is a space overhead for implementing $\mathrm{CG}_d^{\pm}$, which we describe in Theorem 4.4.1 and Lemma 4.4.2.

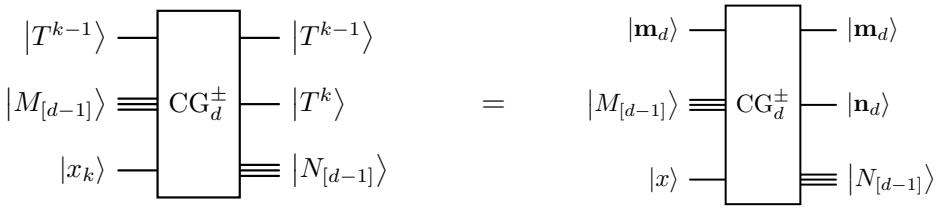

Figure 4.4: Input and output registers of the Clebsch–Gordan isometry $\mathrm{CG}_d^{\pm}$ which appears in Fig. 4.2. Here T^{k-1} and T^k denote the incoming and outgoing unitary group irreps (they are denoted by λ and μ in Eq. (4.12)). Moreover, $T^{k-1} = \mathbf{m}_d$ is the first row of a Gelfand–Tsetlin pattern M of length d whose remaining rows $M_{[d-1]}$ are encoded by the tensor product state $|M_{[d-1]}\rangle := |\mathbf{m}_{d-1}\rangle \cdots |\mathbf{m}_1\rangle$. Similarly, $T^k = \mathbf{n}_d$ is the first row of a Gelfand–Tsetlin pattern N of length d whose remaining rows $N_{[d-1]}$ are encoded by $|N_{[d-1]}\rangle := |\mathbf{n}_{d-1}\rangle \cdots |\mathbf{n}_1\rangle$.

4.4 Quantum Clebsch–Gordan transform

In this section, we describe a recursive quantum circuit of complexity $\mathrm{poly}(d)\,\mathrm{polylog}(d, n, m, 1/\epsilon)$ for Clebsch–Gordan isometries $\mathrm{CG}_d^{\pm}$. The only difference between CG_d^{-} and CG_d^{+} is the formulas for their matrix entries and the labeling scheme of their input and output basis vectors. Our construction is based on [BCH06; Har05] and can be seen as a consequence of the fact that both the usual and the dual Clebsch–Gordan coefficients can be expressed as products of *reduced Wigner coefficients*[3], see Section 4.A.1.

Let us fix an arbitrary level $k = 2, \ldots, n+m$ in the Bratteli diagram of $\mathcal{A}_{n,m}^d$, which is the same as fixing a position in the cascade of Clebsch–Gordan transforms in Fig. 4.2. Then for any $x \in [d]$ and $\mathbf{n}_d, \mathbf{m}_d \in \widehat{\mathrm{U}}_d^n$, we define

$$C_{\mathbf{n}_d,\mathbf{m}_d}^{x,\pm} |M_{[d-1]}\rangle := \sum_{N \in \mathrm{GT}(\mathbf{n}_d, d)} c_{N,M}^{x,\pm} |N_{[d-1]}\rangle \tag{4.32}$$

where $c_{N,M}^{x,\pm}$ are defined in Section 4.A.1 and $\pm$ refers to either dual or usual Clebsch–Gordan coefficients. The operators $C_{\mathbf{n}_d,\mathbf{m}_d}^{x,\pm}$ defined above are essentially the same as the classical matrices $C_{T^j,T^{j-1}}^{x_j}$ defined in Eq. (4.16). Now we can define the quantum Clebsch–Gordan transforms $\mathrm{CG}_d^{\pm}$, which are quantum analogues of CG^k from Eq. (4.12), as

$$\mathrm{CG}_d^{\pm} |\mathbf{m}_d\rangle |M_{[d-1]}\rangle |x\rangle := |\mathbf{m}_d\rangle \sum_{\mathbf{n}_d \,:\, \mathbf{m}_d \to_{\pm} \mathbf{n}_d} |\mathbf{n}_d\rangle \big(C_{\mathbf{n}_d,\mathbf{m}_d}^{x,\pm} |M_{[d-1]}\rangle \big), \tag{4.33}$$

where the notation $\mathbf{n}_d : \mathbf{m}_d \to_{\pm} \mathbf{n}_d$ means that we obtain a staircase $\mathbf{n}_d$ by either adding or removing a box from the staircase $\mathbf{m}_d$, depending on the chosen $\mathrm{CG}_d^{\pm}$ Clebsch–Gordan transform. More explicitly, we can write

$$\mathrm{CG}_d^{\pm} = \sum_{x \in [d]} \sum_{\mathbf{m}_d, \mathbf{n}_d \in \widehat{\mathrm{U}}_d^{n+m}} \sum_{\substack{M \in \mathrm{GT}(\mathbf{m}_d, d) \\ N \in \mathrm{GT}(\mathbf{n}_d, d)}} c_{N_{[d]}, M_{[d]}}^{x,\pm} |\mathbf{m}_d, \mathbf{n}_d, N_{[d-1]}\rangle\langle \mathbf{m}_d, M_{[d-1]}, x|. \tag{4.34}$$

Our goal is to recursively implement $\mathrm{CG}_d^{\pm}$ in terms of $\mathrm{CG}_{d-1}^{\pm}$. Using Eq. (4.34) we can easily write the Clebsch–Gordan transform for $d-1$:

$$\mathrm{CG}_{d-1}^{\pm} = \sum_{x \in [d-1]} \sum_{\mathbf{m}_{d-1}, \mathbf{n}_{d-1} \in \widehat{\mathrm{U}}_{d-1}^{n+m}} \sum_{\substack{M \in \mathrm{GT}(\mathbf{m}_{d-1}, d-1) \\ N \in \mathrm{GT}(\mathbf{n}_{d-1}, d-1)}} c_{N_{[d-1]}, M_{[d-1]}}^{x,\pm} |\mathbf{m}_{d-1}, \mathbf{n}_{d-1}, N_{[d-2]}\rangle\langle \mathbf{m}_{d-1}, M_{[d-2]}, x|. \tag{4.35}$$

[3] In [BCH06; Har05] this fact is proved from the first principles based on the Wigner–Eckart theorem. In our approach, the starting point is the fact that Clebsch–Gordan coefficients can be expressed as products of reduced Wigner coefficients, see [VK92]. Consequently, we try to keep the notation from [VK92], see Section 4.A.1.

Recall from Section 4.A.1 that for every $k \in [d]$ and Gelfand–Tsetlin patterns of length $k-1$,

$$c^{k,\pm}_{N_{[k-1]},M_{[k-1]}} := \delta_{N_{[k-1]},M_{[k-1]}}. \tag{4.36}$$

Moreover, for any symbol $x \in [k]$, staircases $\mathbf{m}_k, \mathbf{n}_k \in \widehat{\mathrm{U}}_k^{n+m}$, and Gelfand–Tsetlin patterns $M \in \mathrm{GT}(\mathbf{m}_k, k)$, $N \in \mathrm{GT}(\mathbf{n}_k, k)$ the following recursive identity holds:

$$c^{x,\pm}_{N_{[k]},M_{[k]}} = \big(z^{\pm}\big)^{\mathbf{m}_k,\mathbf{n}_k}_{\mathbf{m}_{k-1},\mathbf{n}_{k-1}} \cdot c^{x,\pm}_{N_{[k-1]},M_{[k-1]}}. \tag{4.37}$$

Moreover, note that

$$\begin{aligned}
&|\mathbf{m}_d, \mathbf{n}_d, N_{[d-1]}\rangle\langle \mathbf{m}_d, M_{[d-1]}, x| = |\mathbf{m}_d, \mathbf{n}_d, \mathbf{n}_{d-1}, N_{[d-2]}\rangle\langle \mathbf{m}_d, \mathbf{m}_{d-1}, M_{[d-2]}, x| \\
&\quad = \big(|\mathbf{m}_d, \mathbf{n}_d, \mathbf{n}_{d-1}\rangle\langle \mathbf{m}_d, \mathbf{m}_{d-1}, \mathbf{n}_{d-1}| \otimes I\big) \cdot \big(I \otimes |\mathbf{m}_{d-1}, \mathbf{n}_{d-1}, N_{[d-2]}\rangle\langle \mathbf{m}_{d-1}, M_{[d-2]}, x|\big),
\end{aligned} \tag{4.38}$$

which implies

$$\begin{aligned}
&c^{x,\pm}_{N_{[d]},M_{[d]}} |\mathbf{m}_d, \mathbf{n}_d, N_{[d-1]}\rangle\langle \mathbf{m}_d, M_{[d-1]}, x| \\
&\quad = \Big(\big(z^{\pm}\big)^{\mathbf{m}_d,\mathbf{n}_d}_{\mathbf{m}_{d-1},\mathbf{n}_{d-1}} |\mathbf{m}_d, \mathbf{n}_d, \mathbf{n}_{d-1}\rangle\langle \mathbf{m}_d, \mathbf{m}_{d-1}, \mathbf{n}_{d-1}| \otimes I\Big) \cdot \\
&\qquad\qquad \cdot \big(c^{x,\pm}_{N_{[d-1]},M_{[d-1]}} I \otimes |\mathbf{m}_{d-1}, \mathbf{n}_{d-1}, N_{[d-2]}\rangle\langle \mathbf{m}_{d-1}, M_{[d-2]}, x|\big).
\end{aligned} \tag{4.39}$$

Together, these observations allow us to rewrite Eq. (4.34) as

$$\mathrm{CG}^{\pm}_d = \sum_{x\in[d]} \sum_{\mathbf{m}_d,\mathbf{n}_d \in \widehat{\mathrm{U}}_d^{n+m}} \sum_{\substack{M\in \mathrm{GT}(\mathbf{m}_d,d) \\ N\in \mathrm{GT}(\mathbf{n}_d,d)}} |\mathbf{m}_d, \mathbf{n}_d, N_{[d-1]}\rangle\langle \mathbf{m}_d, M_{[d-1]}, x| \tag{4.40}$$

$$= \sum_{x\in[d]} \sum_{\substack{\mathbf{m}_d,\mathbf{n}_d \in \widehat{\mathrm{U}}_d^{n+m} \\ \mathbf{m}_{d-1},\mathbf{n}_{d-1} \in \widehat{\mathrm{U}}_{d-1}^{n+m}}} \sum_{\substack{M\in \mathrm{GT}(\mathbf{m}_{d-1},d-1) \\ N\in \mathrm{GT}(\mathbf{n}_{d-1},d-1)}} \Big(\big(z^{\pm}\big)^{\mathbf{m}_d,\mathbf{n}_d}_{\mathbf{m}_{d-1},\mathbf{n}_{d-1}} |\mathbf{m}_d, \mathbf{n}_d, \mathbf{n}_{d-1}\rangle\langle \mathbf{m}_d, \mathbf{m}_{d-1}, \mathbf{n}_{d-1}| \otimes I\Big) \cdot$$
$$\cdot \big(c^{x,\pm}_{N_{[d-1]},M_{[d-1]}} I \otimes |\mathbf{m}_{d-1}, \mathbf{n}_{d-1}, N_{[d-2]}\rangle\langle \mathbf{m}_{d-1}, M_{[d-2]}, x|\big) \tag{4.41}$$

$$= \left(\sum_{\substack{\mathbf{m}_d,\mathbf{n}_d \in \widehat{\mathrm{U}}_d^{n+m} \\ \mathbf{m}_{d-1},\mathbf{n}_{d-1} \in \widehat{\mathrm{U}}_{d-1}^{n+m}}} \big(z^{\pm}\big)^{\mathbf{m}_d,\mathbf{n}_d}_{\mathbf{m}_{d-1},\mathbf{n}_{d-1}} |\mathbf{m}_d, \mathbf{n}_d, \mathbf{n}_{d-1}\rangle\langle \mathbf{m}_d, \mathbf{m}_{d-1}, \mathbf{n}_{d-1}| \otimes I \right) \cdot \tag{4.42}$$
$$\cdot \left(I \otimes \sum_{x\in[d]} \sum_{\mathbf{m}_{d-1},\mathbf{n}_{d-1} \in \widehat{\mathrm{U}}_{d-1}^{n+m}} \sum_{\substack{M\in \mathrm{GT}(\mathbf{m}_{d-1},d-1) \\ N\in \mathrm{GT}(\mathbf{n}_{d-1},d-1)}} c^{x,\pm}_{N_{[d-1]},M_{[d-1]}} |\mathbf{m}_{d-1}, \mathbf{n}_{d-1}, N_{[d-2]}\rangle\langle \mathbf{m}_{d-1}, M_{[d-2]}, x| \right)$$

$$= \big(C^{\pm}_d \otimes I\big) \cdot \big(I \otimes \widetilde{\mathrm{CG}}^{\pm}_{d-1}\big), \tag{4.43}$$

where we introduced the following two operators:

$$C^{\pm}_d := \sum_{\substack{\mathbf{m}_d,\mathbf{n}_d \in \widehat{\mathrm{U}}_d^{n+m} \\ \mathbf{m}_{d-1},\mathbf{n}_{d-1} \in \widehat{\mathrm{U}}_{d-1}^{n+m}}} \big(z^{\pm}\big)^{\mathbf{m}_d,\mathbf{n}_d}_{\mathbf{m}_{d-1},\mathbf{n}_{d-1}} |\mathbf{m}_d, \mathbf{n}_d, \mathbf{n}_{d-1}\rangle\langle \mathbf{m}_d, \mathbf{m}_{d-1}, \mathbf{n}_{d-1}|, \tag{4.44}$$

$$\widetilde{\mathrm{CG}}^{\pm}_{d-1} := \sum_{x\in[d]} \sum_{\mathbf{m}_{d-1},\mathbf{n}_{d-1} \in \widehat{\mathrm{U}}_{d-1}^{n+m}} \sum_{\substack{M\in \mathrm{GT}(\mathbf{m}_{d-1},d-1) \\ N\in \mathrm{GT}(\mathbf{n}_{d-1},d-1)}} c^{x,\pm}_{N_{[d-1]},M_{[d-1]}} |\mathbf{m}_{d-1}, \mathbf{n}_{d-1}, N_{[d-2]}\rangle\langle \mathbf{m}_{d-1}, M_{[d-2]}, x|$$
$$= \mathrm{CG}^{\pm}_{d-1} + \sum_{\mathbf{m}_{d-1} \in \widehat{\mathrm{U}}_{d-1}^{n+m}} \sum_{M\in \mathrm{GT}(\mathbf{m}_{d-1},d-1)} |\mathbf{m}_{d-1}, \mathbf{m}_{d-1}, M_{[d-2]}\rangle\langle \mathbf{m}_{d-1}, M_{[d-2]}, d|, \tag{4.45}$$

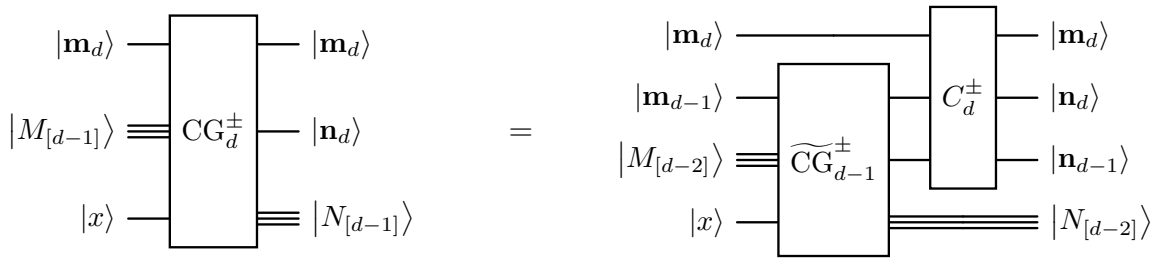

Figure 4.5: Schematic recursive implementation of the $\mathrm{CG}_d^{\pm}$ isometry. The registers $|M_{[d-1]}\rangle$ and $|N_{[d-1]}\rangle$ on the left-hand side should be understood as tensor products $|M_{[d-1]}\rangle = |\mathbf{m}_{d-1}\rangle|M_{[d-2]}\rangle$ and $|N_{[d-1]}\rangle = |\mathbf{n}_{d-1}\rangle|N_{[d-2]}\rangle$.

Figure 4.6: Schematic circuit for the $C_d^{\pm}$ isometry from Eq. (4.44). For the controlled isometry $C_{\mathbf{m}_d,\mathbf{n}_{d-1}}^{\pm}$ from Eq. (4.47) we drop the indices for brevity and refer to it simply by $\tilde{C}_d^{\pm}$.

where the last term corresponds to $x = d$. We can translate Eq. (4.43) into a quantum circuit shown in Fig. 4.5. This procedure can be continued recursively on the parameter d. Doing this accurately requires careful treatment of the auxiliary and input qudit $|x\rangle$, which we explain in detail in the next section.

Note from Eq. (4.44) that $C_d^{\pm}$ is a controlled operation acting on the middle register:

$$C_d^{\pm} = \sum_{\mathbf{m}_d \in \widehat{\mathbb{U}}_d^{n+m}} \sum_{\mathbf{n}_{d-1} \in \widehat{\mathbb{U}}_{d-1}^{n+m}} |\mathbf{m}_d\rangle\langle\mathbf{m}_d| \otimes C_{\mathbf{m}_d,\mathbf{n}_{d-1}}^{\pm} \otimes |\mathbf{n}_{d-1}\rangle\langle\mathbf{n}_{d-1}|, \tag{4.46}$$

where we define $C_{\mathbf{m}_d,\mathbf{n}_{d-1}}^{\pm}$ as

$$C_{\mathbf{m}_d,\mathbf{n}_{d-1}}^{\pm} := \sum_{\mathbf{m}_{d-1} \in \widehat{\mathbb{U}}_{d-1}^{n+m}} \sum_{\mathbf{n}_d \in \widehat{\mathbb{U}}_d^{n+m}} \left(z^{\pm}\right)_{\mathbf{m}_{d-1},\mathbf{n}_{d-1}}^{\mathbf{m}_d,\mathbf{n}_d} |\mathbf{n}_d\rangle\langle\mathbf{m}_{d-1}|. \tag{4.47}$$

We can think of $C_d^{\pm}$ as the quantum circuit shown in Fig. 4.6. Crucially, *reduced Wigner operator* $C_{\mathbf{m}_d,\mathbf{n}_{d-1}}^{\pm}$ is a $(d+1) \times (d+1)$ unitary matrix. Unitarity of $C_{\mathbf{m}_d,\mathbf{n}_{d-1}}^{\pm}$ follows from the orthogonality relations in [VK92, p. 369, Eqs. (8) and (9)], see also Section 4.A.1. The operator $C_{\mathbf{m}_d,\mathbf{n}_{d-1}}^{\pm}$ admits an efficient implementation as a quantum circuit because the reduced Wigner coefficients $(z^{\pm})_{\mathbf{m}_{d-1},\mathbf{n}_{d-1}}^{\mathbf{m}_d,\mathbf{n}_d}$ are efficiently computable, see Eqs. (4.53) to (4.56). From these formulas, we see that computing the reduced Wigner coefficients to accuracy ϵ has complexity $\mathrm{poly}(d, \log(n), \log(m), \log(1/\epsilon))$. Therefore, the complexity of implementing the operator $C_d^{\pm}$ to accuracy ϵ is $\mathrm{poly}(d, \log(n), \log(m), \log(1/\epsilon))$. This is based on the standard method to compile unitary gates from [NC10, Section 4.5]. So we get basically the same complexity as in [BCH06; Har05]. In the next section, we do a more careful unraveling of this recursive construction and a more precise counting of the gate and space complexity of the $C_d^{\pm}$ transformation. For brevity, we will drop the indices in $C_{\mathbf{m}_d,\mathbf{n}_{d-1}}^{\pm}$ and refer to it by $\tilde{C}_d^{\pm}$ thus slightly abusing the notation.

Quantum circuits for Clebsch–Gordan transforms

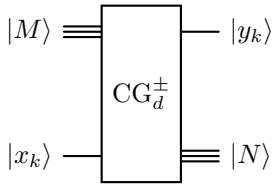

Figure 4.7: Clebsch–Gordan transforms $\mathrm{CG}^{\pm}$ in Yamanouchi encoding accept as input a Gelfand–Tsetlin pattern M and a standard basis vector x_k. They output an updated Gelfand–Tsetlin pattern M and the Yamanouchi symbol y_k indicating the row of the staircase $\mathbf{m}_d$ where a box was added or removed.

In this section, we explain in greater detail how to implement the quantum Clebsch–Gordan transforms based on the scheme outlined in the previous section, both for the standard and the Yamanouchi encoding of the $\mathcal{A}^d_{n,m}$ register introduced at the beginning of Section 4.3. We can unravel the recursion from Fig. 4.5 until the end to get a circuit for the Clebsch–Gordan transform in the Yamanouchi encoding, see Figs. 4.7 and 4.8. Careful accounting for the number of gates, depth and memory in Fig. 4.8 results in Theorem 4.4.1. We note that a similar result was also obtained independently in [Ngu23].

4.4.1. Theorem. *Consider the Clebsch–Gordan isometries* $\mathrm{CG}_d^{\pm}$ *that decompose the tensor product of an irrep* $\lambda = (\lambda_l, \lambda_r)$*, where* $|\lambda_l| \leqslant n$ *and* $|\lambda_r| \leqslant m$*, with the defining irrep* $\square$ *or the dual of the defining irrep* $\bar{\square}$*. The gate and depth complexities of implementing* $\mathrm{CG}_d^{\pm}$ *are* $d^4\,\mathrm{polylog}(d, n, m, 1/\epsilon)$*, where* ϵ *is the desired precision. The number of auxiliary qubits needed is* $d^2\,\mathrm{polylog}(d, 1/\epsilon)$ *for the Yamanouchi encoding, see Eq.* (4.31)*, and* $O(d^2\,\mathrm{polylog}(d, 1/\epsilon) + d\log(n+m))$ *for the standard encoding, see Eq.* (4.29)*.*

Proof:
We first analyse the circuit for the reduced Wigner operators $C_d^{\pm}$ in Fig. 4.8 in the Yamanouchi encoding. They start with a $\tilde{C}_d^{\pm}$ gate. Using Eqs. (4.47) and (4.53) to (4.56), and taking $K = d\,\mathrm{polylog}(d, n, m)$ in Lemma 4.4.2, the complexity of implementing the $\tilde{C}_d^{\pm}$ operator controlled from registers $\mathbf{m}_d, \mathbf{n}_{d-1}$ is $d^3\,\mathrm{polylog}(d, n, m, 1/\epsilon')$, where ϵ' is the desired precision.

According to Lemma 4.4.2, the memory requirement is $d^2\,\mathrm{polylog}(d, 1/\epsilon')$. Note that we can reuse the same auxiliary register to implement all $C_k^{\pm}$ gates sequentially for all $k \in [d]$.

Next, implementing the controlled addition/subtraction gate "$\pm$" within $C_d^{\pm}$ requires $O(d^2)$ gates. Therefore, if we sum the complexities for all d gates $C_k^{\pm}$ with $k \in [d]$, we get the total complexity $d^4\,\mathrm{polylog}(d, n, m, 1/\epsilon')$, where ϵ' is the precision for each $C_k^{\pm}$ gate. To implement the full circuit with precision ϵ we have to set $\epsilon' \leqslant \epsilon/d$. Therefore the total gate and depth complexity for implementing $\mathrm{CG}_d^{\pm}$ is $d^4\,\mathrm{polylog}(d, n, m, 1/\epsilon)$. The memory requirement in Yamanouchi encoding is simply $d^2\,\mathrm{polylog}(d, 1/\epsilon)$.

In standard encoding, we need to have $O(d\log(n+m))$ more qubits to store the full staircase instead of just the Yamanouchi symbol y_k. We can classically obtain a staircase T^{k-1} from the registers $|y_k\rangle$ and $\mathbf{n}_d$ in Fig. 4.8. This operation does not affect the full depth and gate complexity, but requires $O(d\log(n+m))$ additional qubits to what is already required for Yamanouchi encoding. □

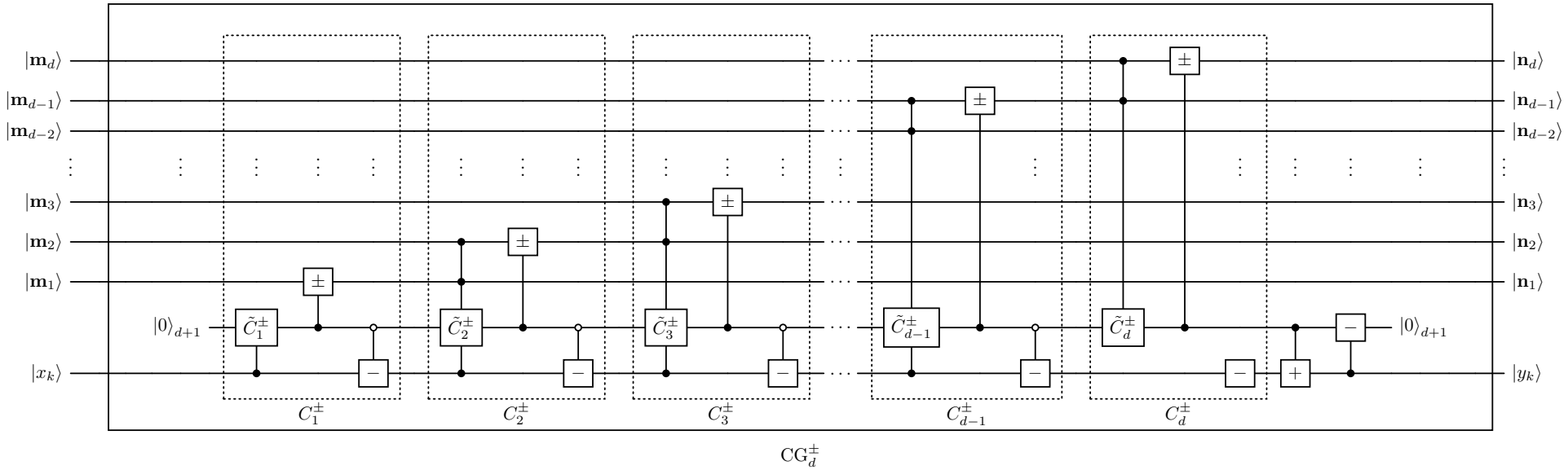

Figure 4.8: Iterative structure of the Clebsch–Gordan transforms $\mathrm{CG}^{\pm}$. We store the rows $\mathbf{m}_i$ of a Gelfand–Tsetlin pattern M in separate quantum registers: $|M\rangle = |\mathbf{m}_d\rangle|\mathbf{m}_{d-1}\rangle \ldots |\mathbf{m}_2\rangle|\mathbf{m}_1\rangle$. The construction of $\tilde{C}_k^{\pm}$ gates for $k \in [d]$ is based on Lemma 4.4.2, and the total complexity is summarised in Theorem 4.4.1.

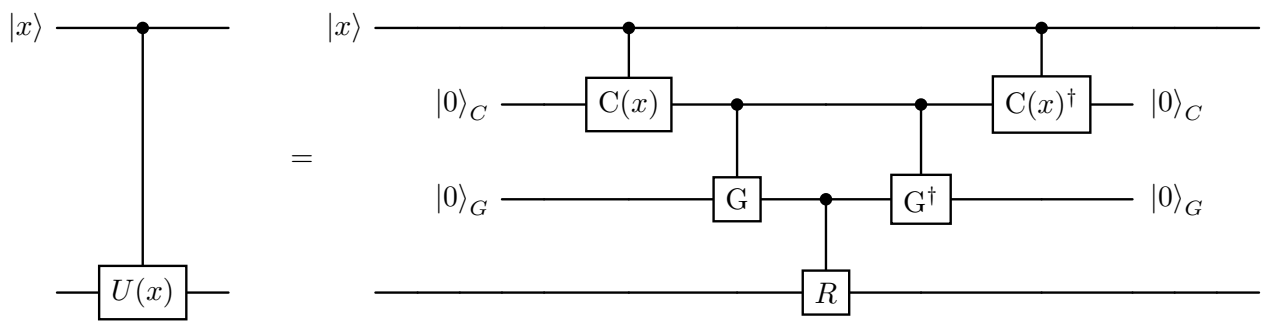

Figure 4.9: Illustration for Lemma 4.4.2. To implement a unitary $U(x)$ whose matrix entries depend on another register $|x\rangle$, we use the circuit on the right-hand side. The register C is for coherent classical computation of the matrix entries $U_{ij}(x)$ of $U(x)$, which is denoted by a controlled C(x) gate. The register G is for coherent classical computation of the Givens rotation angles in the gate decomposition of $U(x)$ based on the matrix entries already computed in the register C. This computation is denoted by a controlled G gate. Finally, unitary operation R implements the Givens rotations computed in the register G. Note that this gate does not explicitly depend on classical data x anymore.

4.4.2. Lemma. *Consider a $d \times d$ unitary matrix $U(x)$ whose entries $U_{ij}(x)$ depend on a tuple of integers x. Assume that each entry $U_{ij}(x)$ can be computed classically to a precision ϵ' with complexity $K \operatorname{polylog}(1/\epsilon')$.*

Then $\sum_x |x\rangle\langle x| \otimes U(x)$, i.e., the unitary U controlled on the register $|x\rangle$, can be implemented with gate and depth complexity $d^2 K \operatorname{polylog}(d, 1/\epsilon)$, where ϵ is the desired precision. Moreover, the implementation requires $d^2 \operatorname{polylog}(d, 1/\epsilon)$ auxiliary qubits.

4.4.3. Remark. The motivation for this lemma comes from the $\tilde{C}_k^{\pm}$ gates in Fig. 4.8. In particular, we know that each entry of $\tilde{C}_k^{\pm}$ depends only on $\mathbf{m}_k$ and $\mathbf{n}_{k-1}$, which are tuples of integers. These entries have exact formulas involving $O(d)$ arithmetical operations, see Eqs. (4.53) to (4.56). Integer entries in these formulas are of order $O(n+m+d)$, so computing them classically would require $K = d \operatorname{polylog}(d, n, m)$ in the setting of Lemma 4.4.2, so performing this calculation to some precision ϵ' on a quantum computer with quantum arithmetic operations would require $K \operatorname{polylog}(1/\epsilon') = d \operatorname{polylog}(d, n, m, 1/\epsilon')$ gates.

Proof:
To implement a gate $U(x)$ controlled on $|x\rangle$, we will use two additional registers C and G to coherently run a reversible classical circuit, see Fig. 4.9, that first evaluates the matrix entries $U_{ij}(x)$ of $U(x)$ and then computes the gate decomposition of $U(x)$ into Givens rotations. Thus we need to carefully count the gate and memory complexity of evaluating $U_{ij}(x)$ for all $i, j \in [d]$ (indicated by the operation C(x) in Fig. 4.9) and the subsequent gate decomposition (indicated by the operation G in Fig. 4.9). We analyse Fig. 4.9 step by step:

1. By assumption, classical reversible circuit description of the evaluation of $U_{ij}(x)$ requires $K \operatorname{polylog}(1/\epsilon')$ gates for every $i, j \in [d]$, where ϵ' is the desired precision. Consequently, we can implement this classical computation as a quantum circuit with the same complexity $K \operatorname{polylog}(1/\epsilon')$. Here we assume that our quantum gateset allows to implement the classical computation exactly. Since we need to compute d^2 entries of U, the total gate and depth complexity of the operation C in Fig. 4.9 is $d^2 K \operatorname{polylog}(1/\epsilon')$.[4] We need to have $d^2 \log(1/\epsilon')$ qubits in register C to store each entry to precision ϵ'.

[4] If there is a clever way to parallelise this computation—for example, by reusing intermediate computation steps—then the gate and depth complexity could be reduced.

2. Next we use the standard method based on Givens rotations [NC10, Section 4.5] to decompose the $d \times d$ unitary $U(x)$ whose classical description is stored in register C into a sequence of $d^2 \operatorname{polylog}(d, 1/\epsilon)$ gates, where ϵ is the desired precision for implementing $U(x)$. This computation, which we denote by G in Fig. 4.9, is again purely classical and can be implemented as quantum circuit straightforwardly. It has gate and depth complexity $d^2 \operatorname{polylog}(d, 1/\epsilon)$ and requires $d^2 \operatorname{polylog}(d, 1/\epsilon)$ qubits in register G to store the obtained decomposition.

3. Next according to Fig. 4.9 we apply the obtained gate decomposition stored in the register G on the original target register of $U(x)$. This operation, which we denote by R, is controlled from the register G. It has gate complexity $d^2 \operatorname{polylog}(d, 1/\epsilon)$ and does not require any additional memory. Here we assume that the choice of our gateset includes arbitrary single qubit rotations. We can also use Solovay–Kitaev theorem to compile Givens rotations to other gatesets, but this does not change asymptotic complexity $d^2 \operatorname{polylog}(d, 1/\epsilon)$.

4. Finally, we undo both classical computations G and C.

Note, that we need to have $\epsilon' \leqslant \epsilon/2d^2$ so that we can guarantee ϵ-precise approximation of U: the precision of entries obtained by $\mathrm{C}(x)$ operation should be high enough for the gate decomposition obtained by the G operation in Fig. 4.9. Combining everything, we see that the total gate and depth complexity of the circuit is $d^2 K \operatorname{polylog}(d, 1/\epsilon)$ and the auxiliary registers C and G require $d^2 \operatorname{polylog}(d, 1/\epsilon)$ qubits. □

4.5 Discussion

We have developed efficient quantum circuits for Clebsch–Gordan transforms, which naturally led to an efficient quantum algorithm for the mixed Schur transform. Our mixed Schur transform achieves the Gelfand–Tsetlin basis for partially transposed permutations.

The results presented in this chapter lay the groundwork for Chapter 5, where the mixed Schur transform will play a crucial role in developing efficient quantum algorithms for port-based teleportation. We anticipate that the mixed Schur transform will prove useful in contexts involving unitary equivariant channels, as their Choi matrices naturally belong to the algebra $\mathcal{A}^d_{n,m}$. We will begin exploring this direction of research in Chapter 6.

One immediate practical question that remains open is the explicit gate decomposition of the Clebsch–Gordan transform in Theorem 4.4.1. This theorem is grounded in Lemma 4.4.2, which provides a theoretical guarantee based on standard unitary decomposition methods. While these methods offer polynomial asymptotic guarantees, they do not directly address the issue of explicit gate decomposition and circuit optimisation. This raises a natural question: can we derive *practical* quantum circuits for Clebsch–Gordan transforms that match the asymptotic complexity scaling outlined in Theorem 4.4.1?

In [Har05], a conjecture was proposed that the gate complexity of the quantum Schur transform could scale logarithmically with d. We expect this conjecture to hold naturally for the mixed Schur transform as well.

Finally, we note that our construction of dual Clebsch–Gordan transforms straightforwardly generalises to Clebsch–Gordan transforms that decompose the tensor product of Weyl modules λ and μ, where λ is an arbitrary module and $\mu = (k, 0, \ldots, 0)$ or $\mu = (0, \ldots, 0, -k)$ or $\mu = (1^k)$. This is because, in these specific cases, "easy" expressions for Clebsch–Gordan coefficients are available, see [VK92]. However, it remains an open problem to find exact expressions for arbitrary Clebsch–Gordan coefficients. Solving this problem would allow us to build new mixed Schur transforms via different coupling schemes. For example, instead of the sequential

application of the Clebsch–Gordan transforms described in this chapter, we could construct a tree-like coupling between arbitrary irreps of U_d.

4.A Appendix

4.A.1 Clebsch–Gordan coefficients

This section summarises formulas from [VK92, Chapter 18] for evaluating the Clebsch–Gordan coefficients of U_d which are matrix entries of transformations $\mathrm{CG}^{\pm}_{\mu,\lambda}$ from Eq. (4.19). Recall from Section 2.9.1 that a Gelfand–Tsetlin pattern $M \in \mathrm{GT}(\lambda)$ is a column vector

$$M = \begin{bmatrix} \mathbf{m}_d \\ \vdots \\ \mathbf{m}_1 \end{bmatrix}, \tag{4.48}$$

where $\mathbf{m}_n = (m_{1,n}, \ldots, m_{n,n})$ are row vectors of non-decreasing integers subject to interlacing relations (2.90). For any row $\mathbf{m}_n$ and integer $i \in \{1, \ldots, n\}$, we denote by $\mathbf{m}_n^{\pm i}$ the vector $\mathbf{m}_n$ with entry $m_{i,n}$ replaced by $m_{i,n} \pm 1$. Let us fix any symbol $x \in [d]$. We define Gelfand–Tsetlin patterns M^+ and M^- by modifying the top $d - x + 1$ rows of M as follows:

$$M = \begin{bmatrix} \mathbf{m}_d \\ \vdots \\ \mathbf{m}_x \\ \mathbf{m}_{x-1} \\ \vdots \\ \mathbf{m}_1 \end{bmatrix}, \qquad M^+ = \begin{bmatrix} \mathbf{m}_d^{+i_d} \\ \vdots \\ \mathbf{m}_x^{+i_x} \\ \mathbf{m}_{x-1} \\ \vdots \\ \mathbf{m}_1 \end{bmatrix}, \qquad M^- = \begin{bmatrix} \mathbf{m}_d^{-i_d} \\ \vdots \\ \mathbf{m}_x^{-i_x} \\ \mathbf{m}_{x-1} \\ \vdots \\ \mathbf{m}_1 \end{bmatrix}, \tag{4.49}$$

for some integers $i_x, \ldots, i_d$ where $1 \leqslant i_j \leqslant j$. Intuitively, this means that the semistandard tableau M^+ is obtained from M by adding a box containing x in the row i_x, and then consecutively bumping the entries j from row i_j downwards the tableau.

For any $x \in [d]$, the Gelfand–Tsetlin patterns corresponding to x and its dual are defined as follows:

$$X^+ := \begin{bmatrix} 1\,0\,0\ldots0\,0\,0 \\ 1\,0\,0\ldots0\,0 \\ \cdots\cdots\cdots \\ 1\,0\ldots0 \\ 0\ldots0 \\ \cdots \\ 0\,0 \\ 0 \end{bmatrix} \begin{matrix} d \\ d-1 \\ \cdots \\ x \\ x-1 \\ \cdots \\ 2 \\ 1 \end{matrix}, \qquad X^- := \begin{bmatrix} 0\,0\,0\ldots0\,0\,-1 \\ 0\,0\,0\ldots0\,-1 \\ \cdots\cdots\cdots \\ 0\,0\cdots-1 \\ 0\ldots0 \\ \cdots \\ 0\,0 \\ 0 \end{bmatrix} \begin{matrix} d \\ d-1 \\ \cdots \\ x \\ x-1 \\ \cdots \\ 2 \\ 1 \end{matrix}. \tag{4.50}$$

Now we can define the Clebsch–Gordan coefficients $c^{x,\pm}_{M^\pm,M}$ uniformly as

$$c^{x,\pm}_{M^\pm,M} := c^{X^\pm}_{M^\pm,M}, \tag{4.51}$$

where $c^{X^\pm}_{M^\pm,M}$ is the product of *reduced Wigner coefficients*:

$$c^{X^\pm}_{M^\pm,M} = \prod_{n=x+1}^{d} \left(\begin{array}{cc|c} \mathbf{m}_n & \mathbf{x}_n^\pm & \mathbf{m}_n^{\pm i_n} \\ \mathbf{m}_{n-1} & \mathbf{x}_{n-1}^\pm & \mathbf{m}_{n-1}^{\pm i_{n-1}} \end{array} \right). \tag{4.52}$$

The *reduced Wigner coefficients* [Har05, p. 152] are also known as *reduced Clebsch–Gordan coefficients* or *scalar factors* [VK92, p. 385] and are defined as follows. We take two consecutive rows $\mathbf{m}_n$ and $\mathbf{m}_{n-1}$ $(1 < n \leqslant d)$ of a Gelfand–Tsetlin pattern M and modify them at positions $1 \leqslant i \leqslant n$ and $1 \leqslant j \leqslant n-1$. The corresponding reduced Wigner coefficients are

$$\left(\begin{array}{cc|c} \mathbf{m}_n & (1,\mathbf{0}_{n-1}) & \mathbf{m}_n^{+i} \\ \mathbf{m}_{n-1} & (0,\mathbf{0}_{n-2}) & \mathbf{m}_{n-1} \end{array}\right) = \left|\frac{\prod_{j=1}^{n-1}(\ell_{j,n-1}-\ell_{i,n}-1)}{\prod_{j\neq i}(\ell_{j,n}-\ell_{i,n})}\right|^{1/2}, \tag{4.53}$$

$$\left(\begin{array}{cc|c} \mathbf{m}_n & (1,\mathbf{0}_{n-1}) & \mathbf{m}_n^{+i} \\ \mathbf{m}_{n-1} & (1,\mathbf{0}_{n-2}) & \mathbf{m}_{n-1}^{+j} \end{array}\right) = S(i,j)\left|\frac{\prod_{k\neq j}(\ell_{k,n-1}-\ell_{i,n}-1)\prod_{k\neq i}(\ell_{k,n}-\ell_{j,d-1})}{\prod_{k\neq i}(\ell_{k,n}-\ell_{i,n})\prod_{k\neq j}(\ell_{k,n-1}-\ell_{j,n-1}-1)}\right|^{1/2}, \tag{4.54}$$

$$\left(\begin{array}{cc|c} \mathbf{m}_n & (\mathbf{0}_{n-1},-1) & \mathbf{m}_n^{-i} \\ \mathbf{m}_{n-1} & (\mathbf{0}_{n-2},0) & \mathbf{m}_{n-1} \end{array}\right) = \left|\frac{\prod_{j=1}^{n-1}(\ell_{j,n-1}-\ell_{i,n})}{\prod_{j\neq i}(\ell_{j,n}-\ell_{i,n})}\right|^{1/2}, \tag{4.55}$$

$$\left(\begin{array}{cc|c} \mathbf{m}_n & (\mathbf{0}_{n-1},-1) & \mathbf{m}_n^{-i} \\ \mathbf{m}_{n-1} & (\mathbf{0}_{n-2},-1) & \mathbf{m}_{n-1}^{-j} \end{array}\right) = S(i,j)\left|\frac{\prod_{k\neq j}(\ell_{k,n-1}-\ell_{i,n})\prod_{k\neq i}(\ell_{k,n}-\ell_{j,n-1}+1)}{\prod_{k\neq i}(\ell_{k,n}-\ell_{i,n})\prod_{k\neq j}(\ell_{k,n-1}-\ell_{j,n-1}+1)}\right|^{1/2}. \tag{4.56}$$

where $\mathbf{0}_n$ denotes a row vector with n zeros, $\ell_{k,s} := m_{k,s}-k$, $S(i,j) := 1$ if $i \leqslant j$ and $S(i,j) := -1$ if $i > j$.

More explicitly, the Clebsch–Gordan coefficient $c^{x,+}_{M^+,M}$ is equal to the product of the reduced Wigner coefficients obtained by cutting the Gelfand–Tsetlin patterns M, x and $M^{\pm}$ into pairs of consecutive rows:

$$c^{x,+}_{M^+,M} = \left(\begin{array}{cc|c} \mathbf{m}_x & (1,\mathbf{0}) & \mathbf{m}_x^{+i_x} \\ \mathbf{m}_{x-1} & (0,\mathbf{0}) & \mathbf{m}_{x-1} \end{array}\right) \cdot \prod_{n=x+1}^{d}\left(\begin{array}{cc|c} \mathbf{m}_n & (1,\mathbf{0}) & \mathbf{m}_n^{+i_n} \\ \mathbf{m}_{n-1} & (1,\mathbf{0}) & \mathbf{m}_{n-1}^{+i_{n-1}} \end{array}\right). \tag{4.57}$$

On the other hand, for arbitrary M^+ which is not of the form (4.49), Clebsch–Gordan coefficient $c^{x,+}_{M^+,M} = 0$. A dual Clebsch–Gordan coefficient $c^{x,-}_{M^-,M}$ is given by the product of dual reduced Wigner coefficients:

$$c^{x,-}_{M^-,M} = \left(\begin{array}{cc|c} \mathbf{m}_x & (\mathbf{0},-1) & \mathbf{m}_x^{-i_x} \\ \mathbf{m}_{x-1} & (\mathbf{0},0) & \mathbf{m}_{x-1} \end{array}\right) \cdot \prod_{n=x+1}^{d}\left(\begin{array}{cc|c} \mathbf{m}_n & (\mathbf{0},-1) & \mathbf{m}_n^{-i_n} \\ \mathbf{m}_{n-1} & (\mathbf{0},-1) & \mathbf{m}_{n-1}^{-i_{n-1}} \end{array}\right). \tag{4.58}$$

On the other hand, for arbitrary M^-, M which is not of the form (4.49), dual Clebsch–Gordan coefficient $c^{x,-}_{M^-,M} = 0$.

We can summarize the above definitions succinctly as follows. We can define Clebsch–Gordan coefficients $c^{x,\pm}_{N_{[k]},M_{[k]}} = 0$ for arbitrary $k \in [d]$, $\lambda \in \widehat{\mathrm{U}}_k$, $N_{[k]}, M_{[k]} \in \mathrm{GT}(\lambda,k)$, $x \in [k]$ recursively as

$$c^{x,\pm}_{N_{[k]},M_{[k]}} = \left(z^{\pm}\right)^{\mathbf{m}_k,\mathbf{n}_k}_{\mathbf{m}_{k-1},\mathbf{n}_{k-1}} \cdot c^{x,\pm}_{N_{[k-1]},M_{[k-1]}}, \tag{4.59}$$

where for every $k \in [d]$ and Gelfand–Tsetlin patterns of length $k-1$ we define

$$c^{k,\pm}_{N_{[k-1]},M_{[k-1]}} := \delta_{N_{[k-1]},M_{[k-1]}}, \tag{4.60}$$

and the coefficients $(z^{\pm})^{\mathbf{m}_k,\mathbf{n}_k}_{\mathbf{m}_{k-1},\mathbf{n}_{k-1}}$ are defined for $\mathbf{m}_{k-1} \sqsubseteq \mathbf{m}_k$ and $\mathbf{n}_{k-1} \sqsubseteq \mathbf{n}_k$ as

$$\left(z^{+}\right)^{\mathbf{m}_k,\mathbf{n}_k}_{\mathbf{m}_{k-1},\mathbf{n}_{k-1}} := \begin{cases} \left(\begin{array}{ccc|c} \mathbf{m}_k & (1,\mathbf{0}) & \mathbf{m}_k^{+i} \\ \mathbf{m}_{k-1} & (1,\mathbf{0}) & \mathbf{m}_{k-1}^{+j} \end{array}\right) & \mathbf{n}_k = \mathbf{m}_k^{+i},\ \mathbf{n}_{k-1} = \mathbf{m}_{k-1}^{+j},\ i \in [k],\ j \in [k-1] \\ \left(\begin{array}{ccc|c} \mathbf{m}_k & (1,\mathbf{0}) & \mathbf{m}_k^{+i}, \\ \mathbf{m}_{k-1} & (0,\mathbf{0}) & \mathbf{m}_{k-1} \end{array}\right) & \mathbf{n}_k = \mathbf{m}_k^{+i} \text{ for some } i \in [k],\ \mathbf{n}_{k-1} = \mathbf{m}_{k-1} \\ 1 & & \mathbf{m}_k = \mathbf{n}_k,\ \mathbf{m}_{k-1} = \mathbf{n}_{k-1}, \\ 0 & & \text{otherwise} \end{cases} \tag{4.61}$$

and

$$\left(z^{-}\right)^{\mathbf{m}_k,\mathbf{n}_k}_{\mathbf{m}_{k-1},\mathbf{n}_{k-1}} := \begin{cases} \left(\begin{array}{ccc|c} \mathbf{m}_k & (\mathbf{0},-1) & \mathbf{m}_k^{-i} \\ \mathbf{m}_{k-1} & (\mathbf{0},-1) & \mathbf{m}_{k-1}^{-j} \end{array}\right) & \mathbf{n}_k = \mathbf{m}_k^{-i},\ \mathbf{n}_{k-1} = \mathbf{m}_{k-1}^{-j},\ i \in [k], j \in [k-1] \\ \left(\begin{array}{ccc|c} \mathbf{m}_k & (\mathbf{0},-1) & \mathbf{m}_k^{-i}, \\ \mathbf{m}_{k-1} & (\mathbf{0},0) & \mathbf{m}_{k-1} \end{array}\right) & \mathbf{n}_k = \mathbf{m}_k^{-i} \text{ for some } i \in [k],\ \mathbf{n}_{k-1} = \mathbf{m}_{k-1} \\ 1 & & \mathbf{m}_k = \mathbf{n}_k,\ \mathbf{m}_{k-1} = \mathbf{n}_{k-1}, \\ 0 & & \text{otherwise} \end{cases} \tag{4.62}$$

and if either $\mathbf{m}_{k-1} \sqsubseteq \mathbf{m}_k$ or $\mathbf{n}_{k-1} \sqsubseteq \mathbf{n}_k$ is not satisfied then we define $(z^{\pm})^{\mathbf{m}_k,\mathbf{n}_k}_{\mathbf{m}_{k-1},\mathbf{n}_{k-1}} := 0$.

Chapter 5

Efficient quantum algorithms for port-based teleportation

Port-based teleportation (PBT) is a variant of quantum teleportation that, unlike the canonical quantum teleportation protocol by Bennett et al. [Ben+93], does not require a correction operation on the teleported state. Since its introduction by Ishizaka and Hiroshima in 2008 [IH08], no efficient implementation of PBT was known. We close this long-standing gap by building on our results on representations of partially transposed permutation matrix algebras and mixed quantum Schur transform from Chapters 3 and 4. We construct efficient quantum algorithms for probabilistic and deterministic PBT protocols on n ports of arbitrary local dimension, both for EPR and optimised resource states. We describe two constructions based on different encodings of the Gelfand–Tsetlin basis for n qudits: a standard encoding that achieves $\widetilde{O}(n)$ time and $\widetilde{O}(n)$ space complexity, and a Yamanouchi encoding that achieves $\widetilde{O}(n^2)$ time and $\widetilde{O}(1)$ space complexity, both for constant local dimension and target error. We also describe efficient circuits for preparing the optimal resource states.

This chapter is based on [GBO23a; GBO23b].

5.1 Introduction

Quantum teleportation is a cornerstone of quantum information [Ben+93] (we have described it briefly already in Chapter 1, see Fig. 1.1). However, one potentially undesirable feature of the original teleportation protocol is that the receiving party needs to perform a correction operation on the received state. *Port-based teleportation* (PBT) gets around this limitation [IH08; IH09]. In PBT, Alice and Bob share an entangled resource state distributed among n quantum systems called *ports* on each side. To teleport an unknown quantum state, Alice measures it together with her share of the ports. The measurement outcome, which she communicates to Bob, indicates the port on Bob's side to which the state has been teleported. Bob does not need to perform any correction operation but simply retrieves the state from the correct port. Each of the quantum systems involved has a fixed *local dimension* d.

Our current understanding of PBT protocols is very detailed thanks to a long sequence of works [IH08; IH09; BK11; Ish15; SSMH17; MSSH18; Led22; Chr+21]. In particular, [SSMH17; MSSH18] were the first to obtain exact formulas for the asymptotic performance of PBT. The resource requirements for PBT have been studied further in [SMK22; SS23b]. The original PBT protocol has subsequently been extended to multi-port teleportation [SMKH22; KMSH21; MSK21] where several systems are teleported simultaneously.

A crucial feature of port-based teleportation is unitary equivariance, meaning that applying any unitary on Alice's input state is equivalent to applying the same unitary to all of Bob's ports.

Due to unitary equivariance, PBT can be seen as a concrete example of an approximate universal programmable quantum processor [IH08]. The quantum no-programming theorem [NC97; GBW21; YRC20] implies that unitarily equivariant PBT protocols with a finite-dimensional resource state can only achieve approximate teleportation. Nevertheless, certain PBT protocols are asymptotically faithful in the limit of a large number of ports.

PBT has diverse applications in non-local quantum computation and quantum communication [BK11; Buh+16; May22] with applications to quantum position verification [ABSL22; ABMSL23], channel discrimination [PLLP19], channel simulation [PBP21], and holography in high-energy physics [May19; May22].

Types of PBT protocols

The two main types of PBT protocols considered are *probabilistic exact* (pPBT) and *deterministic inexact* (dPBT) [SSMH17; MSSH18; Led22]. "Exact" means that the protocol achieves perfect entanglement fidelity $F = 1$, while "inexact" means that $F < 1$. "Probabilistic" refers to the fact that the protocol has some non-zero probability of failure, while "deterministic" highlights no possibility of failure, i.e., the average success probability of the protocol is $p_{\text{succ}} = 1$.[1] Besides pPBT and dPBT, one can also consider *probabilistic inexact* protocols that interpolate between pPBT and dPBT. One concrete example is minimal PBT (mPBT) which is a modified version of dPBT [SS23b].

Two types of resource states for PBT are typically considered: n pairs of maximally entangled states and an arbitrary optimised state; we call these the *EPR resource state* and the *optimised resource state*, respectively. Depending on the application, Alice's measurement is chosen either to maximize the entanglement fidelity F (in dPBT) or the average success probability p_{succ} (in pPBT). While the optimised resource states are different for deterministic and probabilistic protocols, the optimal measurement for optimised states turns out to be the same in both cases. Table 5.1 summarises the four main types of PBT protocols and their optimal fidelity and probability of success.

Resource state	Protocol type	
	Deterministic inexact (dPBT)	Probabilistic exact (pPBT)
EPR	$F = 1 - O(1/n)$ $p_{\text{succ}} = 1$	$F/p_{\text{succ}} = 1$ $p_{\text{succ}} = 1 - O(1/\sqrt{n})$
Optimised	$F = 1 - O(1/n^2)$ $p_{\text{succ}} = 1$	$F/p_{\text{succ}} = 1$ $p_{\text{succ}} = 1 - O(1/n)$

Table 5.1: Summary of different flavours of PBT protocols. Rows correspond to EPR and optimised resource states while columns correspond to deterministic (dPBT) [SSMH17; MSSH18; Led22; Chr+21] and probabilistic (pPBT) [SSMH17; Chr+21] protocols. Two figures of merit are used: the average success probability p_{succ} and the entanglement fidelity F (normalised by the success probability p_{succ}) as functions of the number of ports n, ignoring the dependence on the local dimension d. Cell colors correspond to different optimal POVMs: ☐ is the standard PGM E defined in Eqs. (5.4) and (5.17), ☐ is the dPBT POVM $E^{\star}$ defined in Eqs. (5.18) and (5.19) and ☐ is the POVM $E^{\star}$ defined in Eqs. (5.20) and (5.26).

[1] For brevity, in the rest of this chapter we will drop the terms "exact" and "inexact" in these cases since deterministic PBT protocols with finite resources are always inexact, and exact protocols cannot be deterministic due to [NC97]. Of course, there is still a possibility of having probabilistic inexact protocols.

Summary of our results

While analytic expressions for the optimal measurement operators in PBT were known [SSMH17; MSSH18; Led22], efficient quantum circuits that implement them were not known until our work. Our main result provides explicit quantum circuits for implementing PBT and analyses their complexity.

5.1.1. Theorem. *The measurements for all types of PBT protocols (deterministic/probabilistic and with optimised/EPR resource state) can be implemented in two ways with the following time and space complexities:*

1. *standard encoding:* $nd^4 \operatorname{polylog}(d, n, 1/\epsilon)$ *time and* $(n+d)d \operatorname{polylog}(d, n, 1/\epsilon)$ *space,*
2. *Yamanouchi encoding:* $n^2 d^4 \operatorname{polylog}(d, n, 1/\epsilon)$ *time and* $d^2 \operatorname{polylog}(d, n, 1/\epsilon)$ *space,*

where n is the number of ports, d is the dimension of the teleported quantum state, and ϵ is the target error. In both cases, the total gate complexity is the same: $n^2 d^4 \operatorname{polylog}(d, n, 1/\epsilon)$.

The setting of port-based teleportation is naturally suited for using the representation theory of the matrix algebra $\mathcal{A}^d_{n,1}$ of partially transposed permutations, see Chapter 3. It is natural to work in the Gelfand–Tsetlin basis, which can be achieved by applying the mixed quantum Schur transform, see Chapter 4. Therefore, to prove Theorem 5.1.1 we first explain how to rewrite PBT measurements in the Gelfand–Tsetlin basis in Sections 5.2.2 and 5.2.3 based on representation theory of partially transposed permutations (Theorem 3.7.1) and mixed quantum Schur transform (Theorem 4.3.1). Next, we explain how to construct explicitly Naimark dilations of PBT measurements in Sections 5.2.4 and 5.3. Finally, we use these ingredients to construct efficient quantum algorithms for PBT in standard encoding in Sections 5.4.1 to 5.4.4 and Yamanouchi encoding in Section 5.5 together with their respective complexity analysis.

We highlight that our construction works also for a large class of generic PBT protocols, see Section 5.4.3. Moreover, we construct efficient quantum circuits for preparing optimised states for probabilistic PBT protocols in Section 5.6. The question of preparing efficiently optimised resource states for deterministic PBT is left open.

Related work

Our initial result for standard PGM from [GBO23a] was obtained independently and simultaneously with [FTH23], which solves the problem for dPBT protocols with different methods. Another independent work [WHS23] tackles specifically the qubit case for all PBT protocols. In contrast to [WHS23], we solve the problem for dPBT and pPBT protocols for arbitrary local dimensions in full generality, achieving better time complexities. On the technical side, both results [FTH23; WHS23] construct their PBT protocols by using general techniques of block encodings and amplitude amplification, while our construction requires neither technique and is based on the phase estimation primitive. This leads to more practical circuits and more appealing theoretical analysis. These features of our constructions are enabled by proper use of the representation theory of partially transposed permutation matrix algebras via the Gelfand–Tsetlin basis which we developed in Chapter 3. Moreover, logarithmic space qubit Schur transforms described in [KS18; WS23] inspired our Yamanouchi encoding construction presented in Section 5.5.

Finally, a relevant work [DJR04] discusses general methods for Naimark's dilations of rank one covariant POVMs. Our work analyses specific multi-rank covariant POVMs used in PBT and does not employ the techniques used in [DJR04]. However, the ideas presented in [DJR04] could be useful in understanding and generalising our construction.

5.2 Preliminaries

5.2.1 PBT measurement and figures of merit

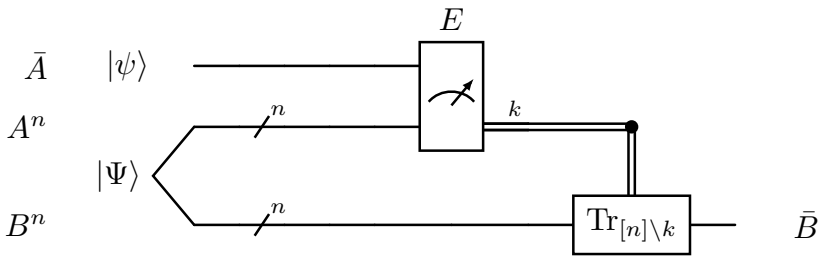

Figure 5.1: Quantum circuit representation of port-based teleportation protocols. A resource state $|\Psi\rangle$ on registers $A_1, \ldots, A_n, B_1, \ldots, B_n$ is used for teleportation between Alice's register $\bar{A}$ and Bob's register $\bar{B}$. To achieve teleportation Alice has to run a measurement E.

In this section, we briefly describe the general setting of PBT and the relevant figures of merit. In a PBT protocol two parties, Alice and Bob, share a resource state distributed among n quantum systems called ports, each of local dimension d. We denote Alice's ports by $A_1, \ldots, A_n$ and Bob's ports by $B_1, \ldots, B_n$. Alice has an additional $(n+1)$-th register $\bar{A}$ on her side that contains an unknown input state $|\psi\rangle_{\bar{A}} \in \mathbb{C}^d$ that she must teleport to Bob (see Fig. 5.1).

The main ingredient of every PBT protocol is a measurement or POVM E that is performed by Alice on all her registers $A_1, \ldots, A_n, \bar{A}$. The rest of the protocol consists of Alice transmitting the measurement outcome to Bob who uses it to locate the teleported state on one of his ports.

In dPBT, Alice's measurement has n outcomes and the outcome $k \in [n]$ indicates the port where Bob should find the teleported state $|\psi\rangle$. Probabilistic protocols, such as mPBT and pPBT, have an additional outcome $k = 0$ corresponding to the failure of the teleportation task.

We can describe a general PBT protocol in terms of a quantum channel $\mathcal{N}$ (see Fig. 5.1):

$$\mathcal{N}_{\bar{A}\to\bar{B}}(\rho) := \sum_{k=1}^{n} \mathrm{Tr}_{A^n\bar{A}B'_k}\Big[\Big((\sqrt{E_k})_{A^n\bar{A}} \otimes I_{B^n}\Big)(\Psi_{A^nB^n} \otimes \rho_{\bar{A}})\Big(\sqrt{E_k}_{A^n\bar{A}} \otimes I_{B^n}\Big)\Big], \tag{5.1}$$

where $A^n := A_1 \ldots A_n$ and $B^n := B_1 \ldots B_n$ denote Alice's and Bob's ports, $B'_k := B^n \setminus B_k$ denotes all of Bob's ports but the k-th, $\Psi_{A^nB^n}$ is the resource state shared between Alice and Bob, $\rho_{\bar{A}}$ is the state to be teleported, and E_k are Alice's POVM operators. Note that the sum in Eq. (5.1) omits the value $k = 0$, hence $\mathcal{N}$ is trace-decreasing if Alice's POVM contains a failure operator $E_0 \neq 0$.

The following two figures of merit are commonly used for characterising the performance of PBT. The *entanglement fidelity* of the protocol is given by

$$F := \mathrm{Tr}\Big[\Phi^+_{\bar{B}R}(\mathcal{N}_{\bar{A}\to\bar{B}} \otimes I_R)\big[\Phi^+_{\bar{A}R}\big]\Big] \tag{5.2}$$

where $\Phi^+_{\bar{A}R}$ denotes the two-qudit maximally entangled state between $\bar{A}$ and a reference system R. The *average success probability* is given by

$$p_{\mathrm{succ}} := \mathrm{Tr}\big[\mathcal{N}_{\bar{A}\to\bar{B}}(I/d)\big], \tag{5.3}$$

which can be less than 1 since in general $\mathcal{N}$ is trace-decreasing.

One can formulate semidefinite optimisation problems for maximising entanglement fidelity F (for dPBT) or average success probability p_{succ} (for pPBT) for general local dimension d.

That has been done, and optimal measurements together with optimal resource states were obtained [SSMH17; MSSH18; Led22].

In the next section, we describe these optimal measurements for different types of PBT [SSMH17; MSSH18; Led22; SS23b] in the mixed Schur basis (or, equivalently, the Gelfand–Tsetlin basis). The key role in optimal POVM constructions is played by a special type of POVM called *pretty good measurement* (PGM) [HW94]. We describe this *standard PGM* in Section 5.2.2. In Section 5.2.3, we describe optimal measurements for dPBT and pPBT using the standard PGM from Section 5.2.2.

5.2.2 The standard PGM

The fundamental POVM for PBT protocols is of a pretty good measurement type. We denote this POVM by $E = \{E_k\}_{k=0}^n$ and call it the *standard PGM* for PBT. It is used in mPBT for both types of resource states [SS23b] and it is defined as follows:

$$\begin{aligned} E_k &:= \rho^{-1/2}\rho_k\rho^{-1/2} \text{ for every } k \in [n], \\ E_0 &:= I - \sum_{k=1}^n E_k, \\ \rho &:= \sum_{k=1}^n \rho_k, \quad \rho_k := \pi^k \sigma_n \pi^{-k}, \end{aligned} \tag{5.4}$$

where ρ^{-1} is the generalised inverse of ρ, and

$$\pi := \sigma_1\sigma_2\ldots\sigma_{n-2}\sigma_{n-1} \in \mathcal{A}_{n,1}^d \tag{5.5}$$

is the cyclic shift permutation $(1\,2\,\ldots\,n)$ on the first n systems, and $\sigma_n \in \mathcal{A}_{n,1}^d$ is the contraction between systems n and $n+1$ (it corresponds to the unnormalised projection onto the maximally entangled state between them). Since ρ commutes with $\mathcal{A}_{n,0}^d$ and thus with π, the POVM elements E_k for $k \in [n]$ can be written as

$$E_k = \pi^k E_n \pi^{-k} \quad \text{where} \quad E_n = \rho^{-1/2}\sigma_n\rho^{-1/2}, \tag{5.6}$$

hence the standard PGM is group-covariant [DJR04] with respect to the cyclic group on n elements.

The key to finding an efficient implementation of the measurement (5.4) is expressing the operators E_k in the Gelfand–Tsetlin basis or, equivalently, in the mixed Schur basis, see Chapters 3 and 4. This requires deriving an explicit formula for $\psi_\Lambda(E_k)$ for any irrep $\Lambda \in \widehat{\mathcal{A}}_{n,1}^d$.[2] Let's express ρ operator in the mixed Schur basis first.

Since ρ coincides with the shifted *Jucys–Murphy element* $d - J_{n+1}$ of $\mathcal{A}_{n,1}^d$, its spectrum can be easily computed, see Lemma 3.7.3. More concretely, ρ is nonzero and diagonal in the Gelfand–Tsetlin basis of each irrep $(\lambda, \varnothing) \in \widehat{\mathcal{A}}_{n,1}^d$:

$$\psi_{(\lambda,\varnothing)}(\rho) = \sum_{a \in \mathrm{AC}_d(\lambda)} \big(d + \mathrm{cont}(a)\big)\Pi_{\lambda,a}, \tag{5.7}$$

$$\Pi_{\lambda,a} := \sum_{S \in \mathrm{Paths}_n(\lambda \cup a, \not\square)} |S \to (\lambda,\varnothing)\rangle\langle S \to (\lambda,\varnothing)|, \tag{5.8}$$

[2] In this chapter, we usually write Λ to label an irrep of $\mathcal{A}_{n,1}^d$. Throughout the chapter we use λ or μ to refer to the left Young diagram of Λ, i.e. we usually assume $\Lambda = (\lambda, \varnothing)$ or $\Lambda = (\mu, \square)$.

and $\psi_{(\mu,\square)}(\rho) = 0$ for every $(\mu,\square) \in \widehat{\mathcal{A}}^d_{n,1}$. In particular, $E_0 E_k = 0$ for every $k \in [n]$ or, more precisely, we have for every $k \in [n]$:

$$\psi_{(\mu,\square)}(E_k) = 0 \text{ for every } (\mu,\square) \in \widehat{\mathcal{A}}^d_{n,1}, \qquad \psi_{(\lambda,\varnothing)}(E_0) = 0 \text{ for every } (\lambda,\varnothing) \in \widehat{\mathcal{A}}^d_{n,1}. \tag{5.9}$$

Next, due to Eq. (3.73) the generator σ_n in the Gelfand–Tsetlin basis of any irrep $(\lambda,\varnothing) \in \widehat{\mathcal{A}}^d_{n,1}$ can be written as

$$\psi_{(\lambda,\varnothing)}(\sigma_n) = \sum_{S \in \mathrm{Paths}_{n-1}(\lambda,\mathscr{A})} |v_{S,\lambda}\rangle\langle v_{S,\lambda}|, \tag{5.10}$$

$$|v_{S,\lambda}\rangle := \sum_{a \in \mathrm{AC}_d(\lambda)} \sqrt{\frac{m_{\lambda\cup a}}{m_\lambda}}\, |S \to (\lambda \cup a) \to (\lambda,\varnothing)\rangle \tag{5.11}$$

and $\psi_{(\mu,\square)}(\sigma_n) = 0$ for every $(\mu,\square) \in \widehat{\mathcal{A}}^d_{n,1}$. Also note that due to Lemma 3.7.4 for every $\lambda \vdash_d n-1$ and $a \in \mathrm{AC}(\lambda)$ we have

$$n \cdot \frac{d_\lambda}{m_\lambda} \cdot \frac{m_{\lambda\cup a}}{d_{\lambda\cup a}} = d + \mathrm{cont}(a). \tag{5.12}$$

Using Eqs. (5.7), (5.10) and (5.12), we can rewrite E_n from Eq. (5.6) in the Gelfand–Tsetlin basis of irrep $\Lambda = (\lambda,\varnothing) \in \widehat{\mathcal{A}}^d_{n,1}$ as follows:

$$\psi_{(\lambda,\varnothing)}(E_n) = \psi_{(\lambda,\varnothing)}(\rho^{-1/2}\sigma_n\rho^{-1/2}) \tag{5.13}$$

$$= \sum_{S \in \mathrm{Paths}_{n-1}(\lambda,\mathscr{A})} \big(\psi_{(\lambda,\varnothing)}(\rho)\big)^{-1/2} |v_{S,\lambda}\rangle\langle v_{S,\lambda}| \big(\psi_{(\lambda,\varnothing)}(\rho)\big)^{-1/2} \tag{5.14}$$

$$= \sum_{S \in \mathrm{Paths}_{n-1}(\lambda,\mathscr{A})} |w_{S,\lambda}\rangle\langle w_{S,\lambda}|, \tag{5.15}$$

where for $\lambda \vdash_d n-1$ and $S \in \mathrm{Paths}_{n-1}(\lambda,\mathscr{A})$ we defined a vector $|w_{S,\lambda}\rangle$ in the irrep $(\lambda,\varnothing) \in \widehat{\mathcal{A}}^d_{n,1}$ as

$$|w_{S,\lambda}\rangle := \sum_{a \in \mathrm{AC}_d(\lambda)} \sqrt{\frac{d_{\lambda\cup a}}{n \cdot d_\lambda}} |S \to (\lambda \cup a) \to (\lambda,\varnothing)\rangle. \tag{5.16}$$

Summarising everything above, we can write the standard PGM E in the Gelfand–Tsetlin basis for every irrep $\Lambda \in \widehat{\mathcal{A}}^d_{n,1}$ and every $k \in [n]$ as follows:

$$\psi_\Lambda(E_0) = \begin{cases} I & \text{if } \Lambda = (\mu,\square), \\ 0 & \text{if } \Lambda = (\lambda,\varnothing), \end{cases} \qquad \psi_\Lambda(E_k) = \begin{cases} 0 & \text{if } \Lambda = (\mu,\square), \\ \psi_{(\lambda,\varnothing)}(\pi^k E_n \pi^{-k}) & \text{if } \Lambda = (\lambda,\varnothing), \end{cases} \tag{5.17}$$

$$\psi_{(\lambda,\varnothing)}(E_n) = \sum_{S \in \mathrm{Paths}_{n-1}(\lambda,\mathscr{A})} |w_{S,\lambda}\rangle\langle w_{S,\lambda}|, \quad |w_{S,\lambda}\rangle = \sum_{a \in \mathrm{AC}_d(\lambda)} \sqrt{\frac{d_{\lambda\cup a}}{n \cdot d_\lambda}} |S \to (\lambda \cup a) \to (\lambda,\varnothing)\rangle.$$

5.2.3 POVMs for deterministic and probabilistic PBT

We are now ready to describe the optimal POVMs for dPBT and pPBT from [SSMH17; MSSH18; Led22] in the Gelfand–Tsetlin basis. They are closely related to the standard PGM E from Eq. (5.4).

POVM for deterministic PBT

In the case of deterministic PBT there is no failure outcome corresponding to $k = 0$. The optimal POVMs for optimised and EPR resource states turn out to be the same [Led22; MSSH18] and are closely related to the standard PGM E from Eqs. (5.4) and (5.17). This POVM $E^{\text{☆}} = \{E_k^{\text{☆}}\}_{k=1}^n$ is defined as follows:

$$E_k^{\text{☆}} := E_k + \frac{E_0}{n}, \tag{5.18}$$

and in the Gelfand–Tsetlin basis for every irrep $\Lambda \in \widehat{\mathcal{A}}_{n,1}^d$ and every $k \in [n]$ it is given as

$$\psi_\Lambda(E_k^{\text{☆}}) = \begin{cases} \dfrac{I}{n} & \text{if } \Lambda = (\mu, \square) \text{ where } \mu \vdash_{d-1} n, \\ \psi_{(\lambda,\varnothing)}(E_k) & \text{if } \Lambda = (\lambda, \varnothing) \text{ where } \lambda \vdash_d n-1, \end{cases} \tag{5.19}$$

where $\psi_{(\lambda,\varnothing)}(E_k)$ are given in Eq. (5.17).

Generic PBT measurements

To describe measurements for pPBT, we first need to explain how one can parameterize *generic* PBT POVMs. Thanks to [Chr+21, Propositions 1.7 and 3.4] and [YKSQM24, Appendix B], we can motivate the following definition: a *generic* PBT measurement $E^\star = \{E_k^\star\}_{k=0}^n$ is defined in the Gelfand–Tsetlin basis as follows for $k \in [n]$:

$$E_k^\star := \sqrt{G} E_k^{\text{☆}} \sqrt{G}, \quad E_0^\star := I - G, \quad I \succeq G \succeq 0 \tag{5.20}$$

for some choice of $G \in \mathcal{A}_{n,1}^d$ such that G commutes with $\mathcal{A}_{n,0}^d$. Equivalently, $G \in \mathcal{A}_{n,1}^d$ is a diagonal matrix in the Gelfand–Tsetlin basis:

$$\psi_\Lambda(G) := \begin{cases} g_\mu I & \text{if } \Lambda = (\mu, \square) \text{ where } \mu \vdash_{d-1} n, \\ \sum_{a \in \mathrm{AC}_d(\lambda)} g_{\lambda,a} \Pi_{\lambda,a} & \text{if } \Lambda = (\lambda, \varnothing) \text{ where } \lambda \vdash_d n-1, \end{cases} \tag{5.21}$$

where the projectors $\Pi_{\lambda,a}$ are defined in Eq. (5.7). Diagonal entries of matrices $\psi_\Lambda(G)$

$$g_{\lambda,a} := \langle S \to (\lambda, \varnothing) | \psi_{(\lambda,\varnothing)}(G) | S \to (\lambda, \varnothing) \rangle, \tag{5.22}$$

$$g_\mu := \langle T \to (\mu, \square) | \psi_{(\mu,\square)}(G) | T \to (\mu, \square) \rangle \tag{5.23}$$

for every $\lambda \vdash_d n-1$, $S \in \mathrm{Paths}_n(\lambda \cup a, \mathscr{A})$, $a \in \mathrm{AC}_d(\lambda)$ and for every $\mu \vdash_{d-1} n$, $T \in \mathrm{Paths}_n(\mu, \mathscr{A})$ respectively satisfy

$$1 \geqslant g_\mu \geqslant 0, \qquad 1 \geqslant g_{\lambda,a} \geqslant 0. \tag{5.24}$$

In particular, the POVM $E^{\text{☆}}$ of dPBT corresponds to $G = I$, i.e. $\psi_\Lambda(G) = I$ for every $\Lambda \in \widehat{\mathcal{A}}_{n,1}^d$, and the standard PGM E corresponds to

$$\psi_\Lambda(G) = \begin{cases} 0 & \text{if } \Lambda = (\mu, \square) \text{ where } \mu \vdash_{d-1} n, \\ I & \text{if } \Lambda = (\lambda, \varnothing) \text{ where } \lambda \vdash_d n-1. \end{cases} \tag{5.25}$$

POVMs for probabilistic PBT

The optimal pPBT measurement for optimised resource state turns out to be equal to the standard PGM E from Eqs. (5.4) and (5.17), see [SSMH17].[3]

[3] Note that the statements regarding optimal POVMs for PBT protocols with optimised resource states in the original papers [SSMH17; MSSH18] refer to so-called "dressed" effect operators, not the true effects $E_i^\star$.

In contrast, the optimal measurement for pPBT with EPR resource state is not the standard PGM E, but it is still closely related. According to [SSMH17], the optimal POVM for pPBT with EPR resource state corresponds to the POVM $E^\star$ from Eq. (5.20) with the operator $G \in \mathcal{A}^d_{n,1}$ defined as

$$\psi_\Lambda(G) := \begin{cases} 0 & \text{if } \Lambda = (\mu, \square) \text{ where } \mu \vdash_{d-1} n, \\ \dfrac{\psi_{(\lambda,\varnothing)}(\rho)}{d+\lambda_1} & \text{if } \Lambda = (\lambda, \varnothing) \text{ where } \lambda \vdash_d n-1, \end{cases} \tag{5.26}$$

where $\psi_\Lambda(\rho)$ is given in Eq. (5.7). In other words, the matrix $\psi_\Lambda(G)$ is diagonal for every $\Lambda \in \widehat{\mathcal{A}}^d_{n,1}$ and its diagonal entries corresponding to Eq. (5.21) can be written as

$$g_{\lambda,a} = \frac{d + \mathrm{cont}(a)}{d+\lambda_1}, \qquad g_\mu = 0. \tag{5.27}$$

Note that λ_1 is the highest possible content among $a \in \mathrm{AC}_d(\lambda)$, so Eq. (5.24) is satisfied.

5.2.4 Naimark dilations and implementation of measurements

In this section, we state some facts about projection-valued measures, which we will need in the later sections to work with *Naimark dilations* of PBT POVMs. Naimark dilation is a realisation of a given POVM as a projection-valued measure in a larger, so-called *dilated*, Hilbert space. In principle, that is possible for any POVM due to Naimark's dilation theorem [Wat18]. However, in general it is not obvious how to achieve a conceptually simple dilation that can be efficiently implemented. An easy example of a Naimark dilation, which we will need later to implement the measurement for dPBT.

5.2.1. Lemma. *Let $E := \{E_i\}_{i=1}^n$ be a POMV on a Hilbert space $\mathcal{H}$ such that $E_i = \frac{I_\mathcal{H}}{n}$ for every $i \in n$. Then its dilation on the Hilbert space $\hat{\mathcal{H}} := \mathbb{C}^n \otimes \mathcal{H}$ is given by $\Pi_i = |i\rangle\langle i| \otimes I_\mathcal{H}$ and isometry $V : \mathcal{H} \to \hat{\mathcal{H}}$ defined as $V|\psi\rangle = |+\rangle \otimes |\psi\rangle$, where $|+\rangle = \frac{1}{\sqrt{n}} \sum_{i=1}^n |i\rangle$.*

Proof:
The isometry $V : |\psi\rangle \mapsto |+\rangle \otimes |\psi\rangle$ means that the input density matrix on $\mathcal{H}$ is embedded in $\hat{\mathcal{H}}$ as $\rho \otimes |+\rangle\langle+|$. It is easy to see that $\mathrm{Tr}[(\rho \otimes |+\rangle\langle+|)\Pi_i] = \mathrm{Tr}[\rho E_i]$. □

Now assume that for a certain POVM with $n+1$ outcomes $k \in \{0, 1, \ldots, n\}$ we managed to dilate outcomes $k \in [n]$ to some PVM Π. The next lemma explains how to dilate a "leftover" POVM E, related to Π in a certain way. This result will be used in Section 5.4.3.

5.2.2. Lemma. *Let $\Pi := \{\Pi_i\}_{i=1}^n$ be a PVM on a Hilbert space $\mathcal{H}$ and let G be a positive semidefinite operator on $\mathcal{H}$ such that $G \preceq I_\mathcal{H}$. Suppose that there is also a POVM $E := \{E_i\}_{i=0}^n$ on $\mathcal{H}$ defined as*

$$E_i := \sqrt{G}\,\Pi_i \sqrt{G} \text{ for every } i \in [n], \qquad E_0 := I_\mathcal{H} - G. \tag{5.28}$$

Then one can dilate the POVM E on $\mathcal{H}$ to a PVM $\hat{\Pi} := \{\hat{\Pi}_i\}_{i=0}^n$ on $\hat{\mathcal{H}} := \mathbb{C}^2 \otimes \mathcal{H}$ via isometric embedding $|\psi\rangle \mapsto |0\rangle \otimes |\psi\rangle$ as follows:

$$\hat{\Pi}_i := \begin{pmatrix} \sqrt{G}\,\Pi_i\sqrt{G} & -\sqrt{G}\,\Pi_i\sqrt{I_\mathcal{H} - G} \\ -\sqrt{I_\mathcal{H} - G}\,\Pi_i\sqrt{G} & \sqrt{I_\mathcal{H} - G}\,\Pi_i\sqrt{I_\mathcal{H} - G} \end{pmatrix} \quad \forall\, i \in [n], \tag{5.29}$$

$$\hat{\Pi}_0 := \begin{pmatrix} I_\mathcal{H} - G & \sqrt{G}\sqrt{I_\mathcal{H} - G} \\ \sqrt{G}\sqrt{I_\mathcal{H} - G} & G \end{pmatrix}. \tag{5.30}$$

Proof:
It is easy to see that the dilated PVM $\{\hat{\Pi}_i\}_{i=0}^n$ on $\hat{\mathcal{H}}$ has the form

$$\hat{\Pi}_i = U \begin{pmatrix} \Pi_i & 0 \\ 0 & 0 \end{pmatrix} U^\dagger \quad \forall\, i \in [n], \text{ and } \hat{\Pi}_0 = U \begin{pmatrix} 0 & 0 \\ 0 & I_{\mathcal{H}} \end{pmatrix} U^\dagger, \tag{5.31}$$

where the unitary U is defined as

$$U := \begin{pmatrix} \sqrt{G} & -\sqrt{I_{\mathcal{H}} - G} \\ \sqrt{I_{\mathcal{H}} - G} & \sqrt{G} \end{pmatrix}. \tag{5.32}$$

It is easy to see that $\hat{\Pi}_i^2 = \hat{\Pi}_i = \hat{\Pi}_i^\dagger$ for every i and $\sum_{i=0}^n \hat{\Pi}_i = I_{\hat{\mathcal{H}}}$. Therefore $\hat{\Pi}$ is indeed a PVM on $\hat{\mathcal{H}}$. This PVM manifestly acts on vectors $|0\rangle \otimes |\psi\rangle \in \hat{\mathcal{H}}$ in the same way as the POVM E acts on $|\psi\rangle \in \mathcal{H}$, so it is indeed a Naimark's dilation of the POVM E. □

Now we explain how to implement a PVM of a certain form, which we will later use in Section 5.4.1, assuming one can efficiently implement unitaries which define this PVM. Namely, assume that we have a PVM $\Pi = \{\Pi_k\}_{k=0}^n$ on $\mathcal{H} := \mathcal{H}_1 \otimes \mathcal{H}_2$ for some Hilbert spaces $\mathcal{H}_1, \mathcal{H}_2$ such that

$$\begin{aligned} \Pi_k &:= U_k \Pi_n U_k^\dagger \text{ for every } k \in [n], \\ \Pi_n &:= I_{\mathcal{H}_1} \otimes \left(W|0\rangle\langle 0|W^\dagger\right)_{\mathcal{H}_2}, \\ \Pi_0 &= I_{\mathcal{H}} - \sum_{k=1}^n \Pi_k \end{aligned} \tag{5.33}$$

where $U_n := I_{\mathcal{H}}$, and we assume that all U_k are some easy-to-implement unitaries on $\mathcal{H} = \mathcal{H}_1 \otimes \mathcal{H}_2$, W is some easy-to-implement unitary on $\mathcal{H}_2$ and $|0\rangle$ is a computational basis vector on $\mathcal{H}_2$. We can implement the PVM Π as follows:

- Define a unitary V on $\mathcal{H}$ as

$$V := \sum_{k=0}^n \omega_{n+1}^k \Pi_k, \tag{5.34}$$

  where ω_{n+1} is root of unity of order $n+1$. Observe, that we can implement the unitary V efficiently thanks to our assumptions via the following circuit on $\mathcal{H} = \mathcal{H}_1 \otimes \mathcal{H}_2$:

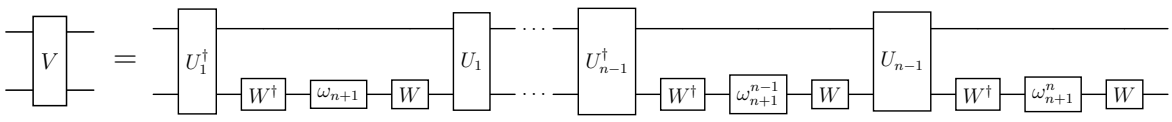

  The gate $\boxed{\omega_{n+1}^k}$ represents the operator $\omega_{n+1}^k |0\rangle\langle 0| + (I - |0\rangle\langle 0|)$ on $\mathcal{H}_2$. We also used $U_n = I_{\mathcal{H}}$.

- Note that implementing V^i is also easy:

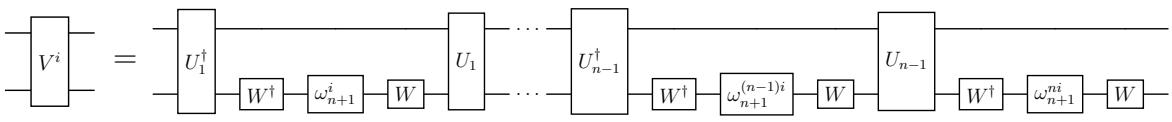

- Now we can run the phase estimation circuit to measure a given state $|\psi\rangle \in \mathcal{H}$ with the PVM Π:

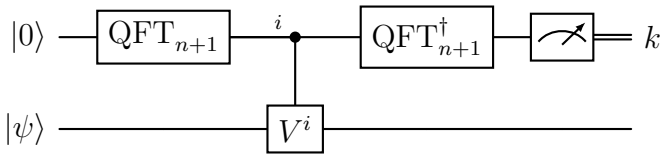

Indeed, this circuit implements the following unitary evolution for every input state $|\psi\rangle \in \mathcal{H}$:

$$\begin{aligned}|\psi\rangle|0\rangle \mapsto \sum_{i=0}^{n} \tfrac{1}{\sqrt{n+1}}|\psi\rangle|i\rangle \mapsto \sum_{i=0}^{n} \tfrac{1}{\sqrt{n+1}} V^i|\psi\rangle|i\rangle \\ = \sum_{i=0}^{n} \tfrac{1}{\sqrt{n+1}} \sum_{k=0}^{n} \omega_{n+1}^{ik} \Pi_k|\psi\rangle|i\rangle \\ = \sum_{k=0}^{n} \Pi_k|\psi\rangle \sum_{i=0}^{n} \tfrac{\omega_{n+1}^{ik}}{\sqrt{n+1}}|i\rangle \mapsto \sum_{k=0}^{n} \Pi_k|\psi\rangle|k\rangle,\end{aligned} \tag{5.35}$$

so measuring k returns the projected state $\frac{\Pi_k|\psi\rangle}{\|\Pi_k|\psi\rangle\|}$ according to the Born rule.

5.3 Naimark's dilation of the standard PGM

Before presenting our circuits, we need to explain how to dilate the POVM E from Eq. (5.4) to a projective measurement Π. We first explain how to construct such dilation explicitly, and then in Section 5.4.1 present an efficient circuit for E.

Recall from Chapter 2 that the Bratteli diagram $\mathscr{Y}$ of the symmetric group is the Young lattice (see Fig. 2.1) , and the following identity holds for every $\lambda \vdash n-1$ [Sag13] in the Young lattice:

$$n \cdot d_\lambda = \sum_{a \in \mathrm{AC}(\lambda)} d_{\lambda \cup a}, \tag{5.36}$$

where the notation $\lambda \cup a$ denotes the Young diagram in the Young lattice obtained by adding a box a to λ, and d_λ is the dimension of the symmetric group irrep λ.[4]

The main observation of this section is that for a Young diagram $\lambda \vdash n-1$, we have $\mathrm{AC}_d(\lambda) = \mathrm{AC}(\lambda)$ if $\lambda_d = 0$ and $\mathrm{AC}_d(\lambda) \neq \mathrm{AC}(\lambda)$ if $\lambda_d > 0$. In particular, when $\lambda_d = 0$ this implies that

$$\||w_{S,\lambda}\rangle\|^2 = \sum_{a \in \mathrm{AC}_d(\lambda)} \frac{d_{\lambda \cup a}}{n \cdot d_\lambda} = \sum_{a \in \mathrm{AC}(\lambda)} \frac{d_{\lambda \cup a}}{n \cdot d_\lambda} = 1, \tag{5.37}$$

so $\psi_{(\lambda,\varnothing)}(E_n)$ is an orthogonal projector. Since the cyclic shift π acts unitarily, all $\psi_{(\lambda,\varnothing)}(E_i)$ are orthogonal projectors as well. Because E provides a resolution of the identity in the irreducible representation $(\lambda, \varnothing) \in \widehat{\mathcal{A}}^d_{n,1}$, the POVM E restricted to the irreducible representation $(\lambda, \varnothing)$ with $\lambda_d = 0$ is actually a PVM there. We will replace $\psi_{(\lambda,\varnothing)}(E_n)$ by $\psi_{(\lambda,\varnothing)}(\Pi_n)$ from now on to indicate that E is actually a PVM on $(\lambda, \varnothing) \in \widehat{\mathcal{A}}^d_{n,1}$.

However, for the irreps λ with $\lambda_d > 0$ the POVM E^λ is not a PVM because $\mathrm{AC}(\lambda) = \mathrm{AC}_d(\lambda) \sqcup \{(d+1, 1)\}$ and the vectors $|w_{S,\lambda}\rangle$ are not normalised anymore:

$$\||w_{S,\lambda}\rangle\|^2 = \sum_{a \in \mathrm{AC}_d(\lambda)} \frac{d_{\lambda \cup a}}{n \cdot d_\lambda} = \left(\sum_{a \in \mathrm{AC}(\lambda)} \frac{d_{\lambda \cup a}}{n \cdot d_\lambda} \right) - \frac{d_{\lambda \cup (d+1,1)}}{n \cdot d_\lambda} = 1 - \frac{d_{\lambda \cup (d+1,1)}}{n \cdot d_\lambda} < 1, \tag{5.38}$$

[4] The dimension d_λ can be both understood as the number of paths from the root to a vertex λ in the Young lattice as well as in the Bratteli diagram $\mathscr{A}$ of $\mathcal{A}^d_{n,1}$, since up to level n the Bratteli diagram is a subset of the full Young lattice and the procedure of adding a cell is monotonic with respect to the number of rows in λ along a given path in the Young lattice.

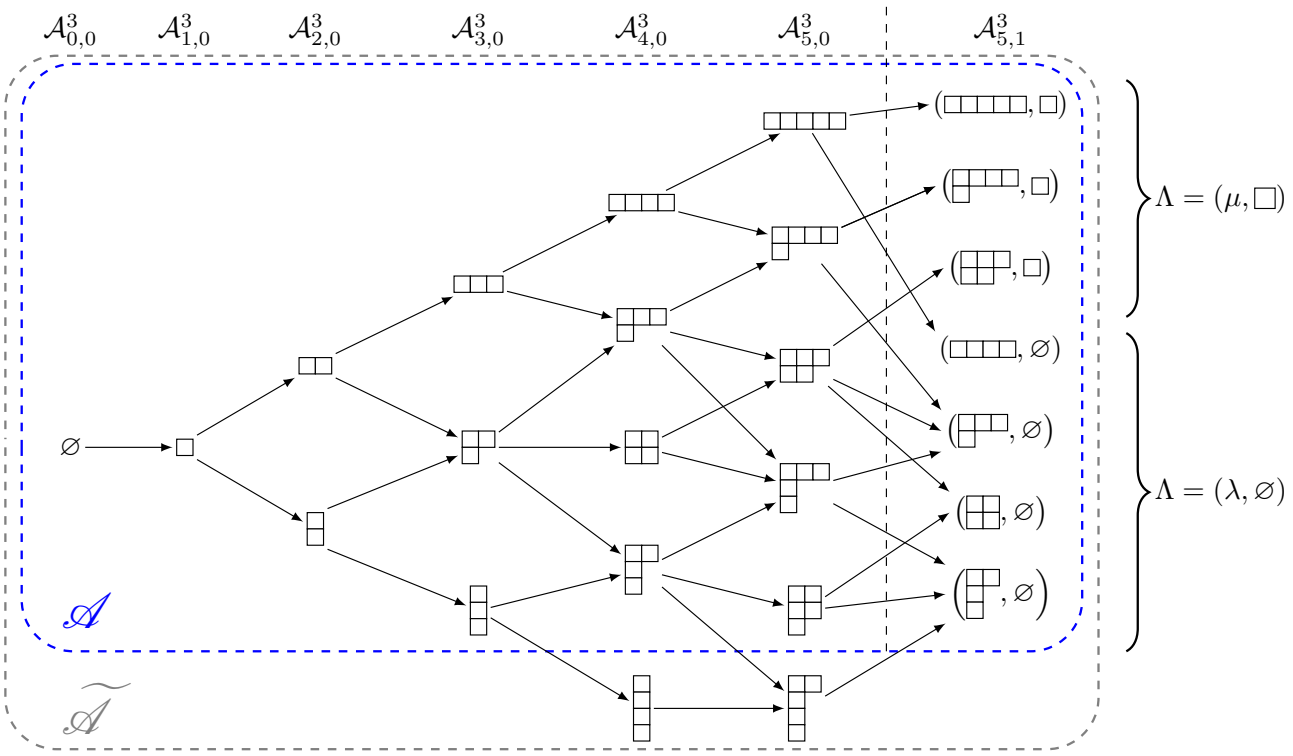

Figure 5.2: The Bratteli diagram $\mathscr{A}$ and the extended Bratteli diagram $\widetilde{\mathscr{A}}$ associated with the algebra $\mathcal{A}^3_{5,1}$. The extension of $\mathscr{A}$ to $\widetilde{\mathscr{A}}$ allows the implementation of optimal POVMs as PVMs, see Section 5.3. Vertices in the last column correspond to the set $\widehat{\mathcal{A}}^3_{5,1}$ of irreducible representations of $\mathcal{A}^3_{5,1}$. A vector space corresponding to an irrep $\Lambda \in \widehat{\mathcal{A}}^3_{5,1}$ is spanned by $\mathrm{Paths}(\Lambda, \mathscr{A})$ the set of all paths terminating at Λ, Eqs. (3.72) and (3.73) describe the action of the generators σ_i of the algebra $\mathcal{A}^3_{5,1}$ in corresponding irrep. Irreps $\Lambda \in \widehat{\mathcal{A}}^3_{5,1}$ are of two different types: either $\Lambda = (\lambda, \varnothing)$, or $\Lambda = (\mu, \square)$. Effects of POVMs implementing optimal measurements for PBT protocols corresponding to successful teleportation outcomes are supported only on irreps corresponding to $\Lambda = (\lambda, \varnothing)$.

where $\lambda \cup (d+1, 1)$ denotes the Young diagram obtained from λ by adding a cell with coordinates $(d+1, 1)$, so that $\ell(\lambda \cup (d+1, 1)) = d+1$. The vertex corresponding to this Young diagram does not exist in the Bratteli diagram $\mathscr{A}$. Fortunately, Eq. (5.38) suggests immediately how to construct a Naimark's dilation Π^λ of E^λ for λ with $\lambda_d > 0$. For this construction, one needs to modify the Bratteli diagram $\mathscr{A}$ by adding vertices to each level smaller or equal than n. Then the set of all paths in this modified Bratteli diagram will define a new basis for the Naimark dilated Hilbert space.

More concretely, to each level $k \leqslant n$ of the Bratteli diagram $\mathscr{A}$ we add all possible vertices labelled by all Young diagrams $\nu \vdash k$ such that $\nu_{d+1} = 1$. An edge between a pair of Young diagrams in two consecutive levels is added if the latter diagram can be obtained by adding a cell to the previous one. This procedure ensures that all the levels up to n of the new Bratteli diagram form a subset of the Young lattice, such that for every vertex at level n the irrep dimensions still satisfy Eq. (5.36). We call the new Bratteli diagram $\widetilde{\mathscr{A}}$. The basis for the Naimark dilated Hilbert space for the irrep $\Lambda \in \widehat{\mathcal{A}}^d_{n,1}$ consists of all paths from the root to the leaf Λ in this modified Bratteli diagram, which we denote by $\mathrm{Paths}(\Lambda, \widetilde{\mathscr{A}})$. Formally, for every $\Lambda \in \widehat{\mathcal{A}}^d_{n,1}$, if $\Lambda = (\lambda, \varnothing)$ for $\lambda \vdash n-1$, $\ell(\lambda) \geqslant d$ we define

$$\mathrm{Paths}(\Lambda, \widetilde{\mathscr{A}}) := \left\{ T = (T^0, T^1, \ldots, T^n, \Lambda) \in \widehat{\mathcal{A}}^{d+1}_{1,0} \times \cdots \times \widehat{\mathcal{A}}^{d+1}_{n,0} \times \widehat{\mathcal{A}}^{d}_{n,1} \mid T \text{ satisfies Eq. (5.40)} \right\}, \tag{5.39}$$

where

$$T^k_{d+1} \leqslant 1 \ \forall k \in [n], \text{ and } T^{k-1} \to T^k \ \forall k \in [n], \text{ and } T^n = \lambda \cup a \text{ for some } a \in \mathrm{AC}(\lambda). \tag{5.40}$$

If $\Lambda_r \neq \varnothing$ then

$$\mathrm{Paths}(\Lambda, \widetilde{\mathscr{A}}) := \mathrm{Paths}(\Lambda, \mathscr{A}). \tag{5.41}$$

This extension of the Bratteli diagram is illustrated in Fig. 5.2.

The action $\widetilde{\psi}_\Lambda$ of the transposition generators $\sigma_1, \ldots, \sigma_{n-1}$ of $\mathcal{A}^d_{n,1}$ in this dilated Bratteli diagram $\widetilde{\mathscr{A}}$ is given by the generalisation of Eq. (2.75) to all paths in $\mathrm{Paths}(\Lambda, \widetilde{\mathscr{A}})$, i.e. for every $T \in \mathrm{Paths}(\Lambda, \widetilde{\mathscr{A}})$ and every $i \in [n-1]$ we define:

$$\widetilde{\psi}_\Lambda(\sigma_i)\,|T\rangle = \frac{1}{r_i(T)}\,|T\rangle + \sqrt{1 - \frac{1}{r_i(T)^2}}\,|\sigma_i T\rangle \qquad \text{for } i \neq n. \tag{5.42}$$

For this new Bratteli diagram $\widetilde{\mathscr{A}}$, we define the dilated versions $|\widetilde{w}_{S,\lambda}\rangle$ of vectors $|w_{S,\lambda}\rangle$ for $S \in \mathrm{Paths}_{n-1}(\lambda, \widetilde{\mathscr{A}})$ as

$$|\widetilde{w}_{S,\lambda}\rangle := \sum_{a \in \mathrm{AC}(\lambda)} \sqrt{\frac{d_{\lambda \cup a}}{n \cdot d_\lambda}} |S \to (\lambda \cup a) \to (\lambda, \varnothing)\rangle. \tag{5.43}$$

Therefore in the dilated space since Eq. (5.36) holds we have

$$\| |\widetilde{w}_{S,\lambda}\rangle \|^2 = \sum_{a \in \mathrm{AC}(\lambda)} \frac{d_{\lambda \cup a}}{n \cdot d_\lambda} = 1. \tag{5.44}$$

More importantly, we have the following

5.3.1. Lemma. *For every $\Lambda = (\lambda, \varnothing)$ in the dilated Hilbert space spanned by $\mathrm{Paths}(\Lambda, \widetilde{\mathscr{A}})$ we have*

$$\sum_{k=1}^{n} \sum_{S \in \mathrm{Paths}_{n-1}(\lambda, \widetilde{\mathscr{A}})} \widetilde{\psi}_\Lambda(\pi^k) |\widetilde{w}_{S,\lambda}\rangle\langle\widetilde{w}_{S,\lambda}| \widetilde{\psi}_\Lambda(\pi^{-k}) = I \tag{5.45}$$

Proof:
Denote

$$A := \sum_{k=1}^{n} \sum_{S \in \mathrm{Paths}_{n-1}(\lambda, \widetilde{\mathscr{A}})} \widetilde{\psi}_\Lambda(\pi^k) |\widetilde{w}_{S,\lambda}\rangle\langle\widetilde{w}_{S,\lambda}| \widetilde{\psi}_\Lambda(\pi^{-k}). \tag{5.46}$$

Note that by construction Eq. (5.42) any $\sigma \in \mathrm{S}_{n-1}$ (we think of σ as an element of the algebra $\mathcal{A}^d_{n-1,0}$) commutes with the following element:

$$\sum_{S \in \mathrm{Paths}_{n-1}(\lambda, \widetilde{\mathscr{A}})} |\widetilde{w}_{S,\lambda}\rangle\langle\widetilde{w}_{S,\lambda}| \widetilde{\psi}_\Lambda(\sigma) = \widetilde{\psi}_\Lambda(\sigma) \sum_{S \in \mathrm{Paths}_{n-1}(\lambda, \widetilde{\mathscr{A}})} |\widetilde{w}_{S,\lambda}\rangle\langle\widetilde{w}_{S,\lambda}|, \tag{5.47}$$

since the above element acts as identity on $\mathrm{Paths}_{n-1}(\lambda, \widetilde{\mathscr{A}})$. Therefore A must commute with $\mathcal{A}^d_{n,0}$ since π^k are transversals for cosets of $\mathcal{A}^d_{n,0}$ over $\mathcal{A}^d_{n-1,0}$:

$$A = \frac{1}{(n-1)!} \sum_{\sigma \in \mathrm{S}_{n-1}} \sum_{k=1}^{n} \sum_{S \in \mathrm{Paths}_{n-1}(\lambda, \widetilde{\mathscr{A}})} \widetilde{\psi}_\Lambda(\pi^k \sigma) |\widetilde{w}_{S,\lambda}\rangle\langle\widetilde{w}_{S,\lambda}| \widetilde{\psi}_\Lambda((\pi^k \sigma)^{-1}) \tag{5.48}$$

$$= \frac{1}{(n-1)!} \sum_{\sigma \in \mathrm{S}_n} \sum_{S \in \mathrm{Paths}_{n-1}(\lambda, \widetilde{\mathscr{A}})} \widetilde{\psi}_\Lambda(\sigma) |\widetilde{w}_{S,\lambda}\rangle\langle\widetilde{w}_{S,\lambda}| \widetilde{\psi}_\Lambda(\sigma^{-1}). \tag{5.49}$$

This means that A is a diagonal matrix and $\langle T|A|T\rangle$ depends only on T^n, so for every $a \in \mathrm{AC}(\lambda)$ and every $T \in \mathrm{Paths}(\Lambda, \widetilde{\mathscr{A}})$ with $T^n = \lambda \cup a$ we can write

$$\langle T|A|T\rangle = \frac{1}{d_{\lambda\cup a}} \sum_{\substack{T\in\mathrm{Paths}(\Lambda,\widetilde{\mathscr{A}})\\ T^n=\lambda\cup a}} \langle T|A|T\rangle \tag{5.50}$$

$$= \frac{1}{d_{\lambda\cup a}(n-1)!} \sum_{\substack{S\in\mathrm{Paths}_{n-1}(\lambda,\widetilde{\mathscr{A}})\\ T\in\mathrm{Paths}(\Lambda,\widetilde{\mathscr{A}})\\ T^n=\lambda\cup a}} \sum_{\sigma\in\mathrm{S}_n} \langle \widetilde{w}_{S,\lambda}|\widetilde{\psi}_\Lambda(\sigma^{-1})|T\rangle\langle T|\widetilde{\psi}_\Lambda(\sigma)|\widetilde{w}_{S,\lambda}\rangle, \tag{5.51}$$

but in the above formula $\widetilde{\psi}_\Lambda(\sigma)$ commutes with $\sum_T |T\rangle\langle T|$, so

$$\langle T|A|T\rangle = \frac{1}{d_{\lambda\cup a}(n-1)!} \sum_{S\in\mathrm{Paths}_{n-1}(\lambda,\widetilde{\mathscr{A}})} \sum_{\sigma\in\mathrm{S}_n} \langle \widetilde{w}_{S,\lambda}|\widetilde{\psi}_\Lambda(\sigma^{-1})\Big(\sum_{\substack{T\in\mathrm{Paths}(\Lambda,\widetilde{\mathscr{A}})\\ T^n=\lambda\cup a}} |T\rangle\langle T|\Big)\widetilde{\psi}_\Lambda(\sigma)|\widetilde{w}_{S,\lambda}\rangle$$

$$= \frac{1}{d_{\lambda\cup a}(n-1)!} \sum_{S\in\mathrm{Paths}_{n-1}(\lambda,\widetilde{\mathscr{A}})} \sum_{\sigma\in\mathrm{S}_n} \langle \widetilde{w}_{S,\lambda}|\widetilde{\psi}_\Lambda(\sigma^{-1})\widetilde{\psi}_\Lambda(\sigma)\Big(\sum_{\substack{T\in\mathrm{Paths}(\Lambda,\widetilde{\mathscr{A}})\\ T^n=\lambda\cup a}} |T\rangle\langle T|\Big)|\widetilde{w}_{S,\lambda}\rangle$$

$$= \frac{1}{d_{\lambda\cup a}(n-1)!} \sum_{S\in\mathrm{Paths}_{n-1}(\lambda,\widetilde{\mathscr{A}})} \sum_{\sigma\in\mathrm{S}_n} \langle \widetilde{w}_{S,\lambda}|\Big(\sum_{\substack{T\in\mathrm{Paths}(\Lambda,\widetilde{\mathscr{A}})\\ T^n=\lambda\cup a}} |T\rangle\langle T|\Big)|\widetilde{w}_{S,\lambda}\rangle. \tag{5.52}$$

Therefore,

$$\langle T|A|T\rangle = \frac{1}{d_{\lambda\cup a}(n-1)!} \sum_{\sigma\in\mathrm{S}_n} \sum_{\substack{S\in\mathrm{Paths}_{n-1}(\lambda,\widetilde{\mathscr{A}})\\ T\in\mathrm{Paths}(\Lambda,\widetilde{\mathscr{A}})\\ T^n=\lambda\cup a}} |\langle T|\widetilde{w}_{S,\lambda}\rangle|^2 = \frac{n\cdot d_\lambda}{d_{\lambda\cup a}} \frac{d_{\lambda\cup a}}{n\cdot d_\lambda} = 1. \tag{5.53}$$

Since every diagonal element of A is 1, so $A = I$. □

Consequently, in the dilated space our POVM E becomes a PVM, which we denote by Π. From now on assume that we work in the dilated Gelfand–Tsetlin basis spanned by $T \in \mathrm{Paths}(\Lambda, \widetilde{\mathscr{A}})$ and we want to implement the PVM $\Pi = \{\Pi_k\}_{k=0}^n$, where for every $k \in [n]$:

$$\Pi_k := \pi^k \Pi_n \pi^{-k}, \qquad \Pi_0 = I - \sum_{k=1}^n \Pi_k, \qquad \widetilde{\psi}_{(\lambda,\varnothing)}(\Pi_n) = \sum_{S\in\mathrm{Paths}_{n-1}(\lambda,\widetilde{\mathscr{A}})} |\widetilde{w}_{S,\lambda}\rangle\langle\widetilde{w}_{S,\lambda}| \tag{5.54}$$

5.4 Efficient quantum circuits for PBT in standard encoding

5.4.1 Standard PGM

Using the results of Section 5.3, our task now is to implement the PVM Π from Eq. (5.54). We embed $\mathrm{Paths}(\mathscr{A})$ in a Hilbert space with appropriate tensor product structure dictated by the mixed quantum Schur transform. Mixed quantum Schur transform can be implemented using two different encodings for the Gelfand–Tsetlin basis of $\mathcal{A}^d_{n,1}$: the *standard* encoding or the *Yamanouchi* encoding, see Chapter 4. In this section, we discuss how to implement Π with the standard encoding. The Yamanouchi encoding implementation is explained in Section 5.5.

Before presenting our circuit for Π, we need to define a unitary $\widetilde{W}$ acting on registers T^{n-1}, T^n, T^{n+1}, which can be used to prepare the states $|\widetilde{w}_{S,\lambda}\rangle := |S\rangle|\widetilde{w}_\lambda\rangle$ for every $(\lambda, \varnothing) \in \widehat{\mathcal{A}}^d_{n,1}$ and $S \in \mathrm{Paths}(\Lambda, \widetilde{\mathscr{A}})$. Namely, we first define

$$\begin{aligned} \widetilde{W}_\lambda|0\rangle &:= |\widetilde{w}_\lambda\rangle, \\ |\widetilde{w}_\lambda\rangle &:= \sum_{a\in \mathrm{AC}(\lambda)} \sqrt{\frac{d_{\lambda\cup a}}{n\cdot d_\lambda}}|\lambda\cup a\rangle, \end{aligned} \tag{5.55}$$

where $\widetilde{W}_\lambda$ is a unitary matrix of size at most $(d+1)\times(d+1)$ with easy-to-compute entries $|\widetilde{w}_\lambda\rangle$ in its first column. Now we define $\widetilde{W}$, a controlled version of $\widetilde{W}_\lambda$, as a unitary which prepares $|\widetilde{w}_\lambda\rangle$ conditioned on λ:

$$\widetilde{W} := \sum_{\lambda\vdash_d n-1} \left(\left(\sum_{\substack{\lambda'\neq\lambda \\ \lambda'\vdash_d n-1}} |\lambda'\rangle\langle\lambda'| \right) \otimes I + |\lambda\rangle\langle\lambda| \otimes \widetilde{W}_\lambda \right) \otimes |(\lambda,\varnothing)\rangle\langle(\lambda,\varnothing)| + \sum_{\mu\vdash_{d-1} n} I\otimes I\otimes |(\mu,\square)\rangle\langle(\mu,\square)|. \tag{5.56}$$

This transformation can be implemented via a sequence of Givens rotations. Similarly to Eq. (5.55), we can define a unitary W_λ which prepares the normalised version of $|w_\lambda\rangle$:

$$\begin{aligned} W_\lambda|0\rangle &:= \frac{|w_\lambda\rangle}{\||w_\lambda\rangle\|}, \\ |w_\lambda\rangle &= \sum_{a\in \mathrm{AC}_d(\lambda)} \sqrt{\frac{d_{\lambda\cup a}}{n\cdot d_\lambda}}|\lambda\cup a\rangle. \end{aligned} \tag{5.57}$$

The gate W is now defined for Eq. (5.57) in the same way as $\widetilde{W}$ in Eq. (5.56).

Assume the initial state is $|S\rangle|0\rangle|\lambda\rangle := |S^2\rangle\ldots|S^{n-2}\rangle|\lambda\rangle|0\rangle|(\lambda,\varnothing)\rangle$ for arbitrary path $S \in \mathrm{Paths}_{n-1}(\lambda, \widetilde{\mathscr{A}})$, where $|0\rangle$ is some basis state of the register, corresponding to the n-th level of the dilated Bratteli diagram $\widetilde{\mathscr{A}}$. Then we can prepare a state $|S\rangle|\widetilde{w}_\lambda\rangle|(\lambda,\varnothing)\rangle$ as follows:

$$\left(I\otimes\widetilde{W}\right)|S\rangle|0\rangle|\lambda\rangle = |S\rangle|\widetilde{w}_\lambda\rangle|\lambda\rangle, \tag{5.58}$$

where identity I acts on the registers $|S^2\rangle\ldots|S^{n-2}\rangle$. Moreover, note that the amplitudes of the state $|\widetilde{w}_\lambda\rangle$ are easy to calculate on a classical computer in time $\widetilde{O}(d)$ due to Lemma 3.7.5, which we restate here for convenience.

5.4.1. Lemma ([Kos03]). *For every $\lambda \vdash n-1$ and $a \in \mathrm{AC}(\lambda)$ there holds*

$$\frac{\prod_{c\in \mathrm{RC}(\lambda)}(\mathrm{cont}(a)-\mathrm{cont}(c))}{\prod_{c\in \mathrm{AC}(\lambda)\setminus a}(\mathrm{cont}(a)-\mathrm{cont}(c))} = \frac{d_{\lambda\cup a}}{n\cdot d_\lambda}. \tag{5.59}$$

Each $\widetilde{W}_\lambda$ gate can be implemented as a sequence of simple controlled R_i gates, as shown in Fig. 5.7, which we define as

$$\begin{aligned} \mathrm{R}_i|0\rangle &:= \sqrt{\frac{1-\sum_{j=1}^{i}\eta_j}{1-\sum_{j=1}^{i-1}\eta_j}}\,|0\rangle + \sqrt{\frac{\eta_i}{1-\sum_{j=1}^{i-1}\eta_j}}\,|1\rangle, \\ \eta_j &:= \frac{d_{\lambda\cup a_j}}{n\cdot d_\lambda} \end{aligned} \tag{5.60}$$

where the cell $a_j \in \mathrm{AC}(\lambda)$ is located in the j-th row of λ. If for a given j there is no such cell then the control on R_i in Fig. 5.7 is not triggered. In other words, R_i is triggered only when $\lambda_{i-1} > \lambda_i$ (R_1 is always triggered). Note that due to Lemma 5.4.1 the amplitudes in Eq. (5.60) are easy to compute classically in time $\widetilde{O}(d)$.

Following the prescription outlined above, we construct in Fig. 5.5 an efficient circuit for the PGM E dilated as Π. The circuit mainly acts on the dilated space spanned by $(T^0, T^1, T^2, \ldots, T^n, T^{n+1}) \in \mathrm{Paths}(\widetilde{\mathscr{A}})$, which form the Gelfand–Tsetlin basis. The ancilla registers are used implicitly in the circuit (see Lemma 4.4.2 and Fig. 4.9).

First, a mixed quantum Schur transform maps the computational basis to the mixed Schur basis which is usually labelled by $|M_{[d-1]}, T\rangle$, where M is a Gelfand–Tsetlin pattern and T is a path in $\mathscr{A}$. We assume a tensor product structure for different vertices T^i of the path $T \in \mathrm{Paths}(\mathscr{A})$ and we use the standard encoding for $|T\rangle$. Moreover, all registers $T^2, \ldots, T^n$ are assumed to be dilated, according to the procedure explained in Section 5.3. Since T^0 and T^1 can only have one possible value, we omit those registers from the diagram since they are one-dimensional. The last level T^{n+1} of the path T is labelled by λ and indicates an irreducible representation. The cyclic permutation gate $\pi = (12\ldots n) = \sigma_1\sigma_2\cdots\sigma_{n-1}$ acts only on $n-1$ wires of the dilated Gelfand–Tsetlin basis, and each of the transpositions σ_i acts only locally on the registers T^{i-1}, T^i, T^{i+1} (σ_1 acts only on T^2, and σ_2 acts only on T^2, T^3). $\widetilde{W}$ prepares the state $|\widetilde{w}_\lambda\rangle$ conditioned on λ, i.e., $\widetilde{W}_\lambda|0\rangle = |\widetilde{w}_\lambda\rangle$ where $\widetilde{W}_\lambda$ is controlled on λ. The phase gates ω_{n+1}^{ki} act non-trivially only on $|0\rangle$ in the register T^n, and are controlled on the condition $T^{n-1} = T^{n+1} = \lambda$. Finally, the measurement outcome $k = 0$ corresponds to the failure of the protocol, otherwise $k \in [n]$ indicates the port where Bob can find the teleported state $|\psi\rangle$ of dimension d.

Gate complexity

We now argue that the gate complexity of our circuit in Fig. 5.5 is $\widetilde{O}(nd^4)$:

1. The complexity of implementing the mixed quantum Schur transform $U_{\mathrm{Sch}(n,1)}$ is $\widetilde{O}(nd^4)$, see Theorem 4.3.1, Chapter 4.

2. The complexity of implementing $\pi = \sigma_1\sigma_2\ldots\sigma_{n-1}$ based on Fig. 5.3 is $\widetilde{O}(nd^2)$. The factor n comes from the number of transpositions σ_i in π. Each transposition σ_i is 3-local: it acts only on registers T^{i-1}, T^i, T^{i+1}. More specifically, σ_i is a 2×2 rotation on T^i controlled by T^{i-1} and T^{i+1}. According to Fig. 5.6, each σ_i can be implemented with $\widetilde{O}(d^2)$ gates, each of which decompose into $\widetilde{O}(1)$ elementary gates. In particular, each of the $\mathrm{R}_{j,k}$ gates

$$\mathrm{R}_{j,k} := \begin{pmatrix} \frac{1}{r_{j,k}} & \sqrt{1-\frac{1}{r_{j,k}^2}} \\ \sqrt{1-\frac{1}{r_{j,k}^2}} & -\frac{1}{r_{j,k}} \end{pmatrix}, \qquad r_{j,k} := \lambda_j - \lambda_k + k - j \tag{5.61}$$

appearing in Fig. 5.6 can be implemented with $\widetilde{O}(1)$ elementary gates and $\widetilde{O}(1)$ auxiliary qubits for computation of rotation parameters $r_{j,k}$.

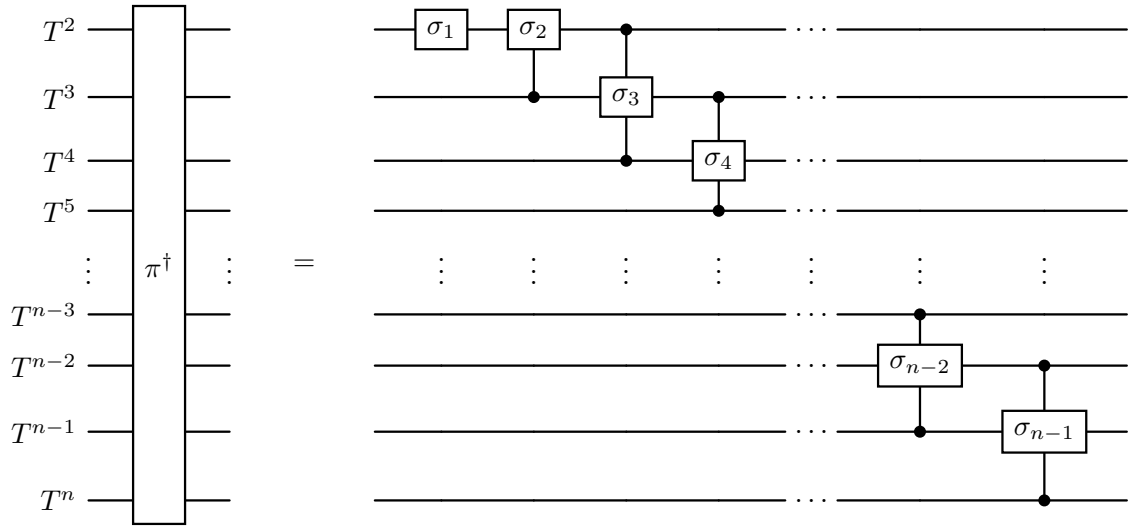

Figure 5.3: Circuit for the cyclic permutation $\pi^\dagger = \sigma_{n-1}\sigma_{n-2}\cdots\sigma_2\sigma_1$ in the Gelfand–Tsetlin basis. Each transposition σ_i acts locally on registers T^{i-1}, T^i, T^{i+1}, with T^{i-1} and T^{i+1} used as controls. Note, that σ_1 acts only on T^2, and σ_2 acts only on T^2, T^3 because we have dropped the registers T^0, T^1 (they are always one-dimensional).

3. The operation $\widetilde{W}$ defined in Eq. (5.56) is a λ-controlled unitary $\widetilde{W}_\lambda$ that acts non-trivially only on a $(d+1)$-dimensional subspace of the register T^n. This register consists of $d+1$ wires corresponding to $d+1$ rows of a Young diagram, see Fig. 5.7. The matrix entries of $\widetilde{W}_\lambda$ (see Eq. (5.55)) can be reversibly computed on the fly using gates R_i, $i \in [d+1]$ from Eq. (5.60) in classical time $\widetilde{O}(d)$, which must be implemented in a quantum circuit coherently. Therefore, implementing $\widetilde{W}$ would have the gate complexity $\widetilde{O}(d^2)$.

4. ω_{n+1}^{ki} denotes the gate $\omega_{n+1}^{ki}|0\rangle\langle 0| + (I - |0\rangle\langle 0|)$ on register T^n conditioned on the registers $T^{n-1} = \lambda$, $T^{n+1} = \Lambda = (\lambda, \varnothing)$. This has complexity $\widetilde{O}(1)$.

5. The complexity of the Quantum Fourier Transform QFT_{n+1} is $\widetilde{O}(1)$.

6. One can optionally implement the correction gate Corr together with inverse mixed Schur transform at the end to get the right post-measurement state (according to the definition of PGM E from Eq. (5.4)). For that one needs to uncompute the gates π^k for $k \in [n]$ and $\widetilde{W}_\lambda$, and instead run the gate W_λ from Eq. (5.56) followed by π^k. The complexity of implementing the correction gate does not change both the total gate and time complexities of the full circuit, adding only a constant factor overhead.

7. Now we are ready to count the total gate and time complexity. For that, notice that each gate $\pi^\dagger$ in Fig. 5.5 consisting of local gates σ_i as in Fig. 5.3 can be pushed to the left of the circuit. This will reduce the naive complexity $\widetilde{O}(n^2d^2)$ of implementing n sequential gates $\pi^\dagger$ to just $\widetilde{O}(nd^2)$. Counting everything together gives $\widetilde{O}(nd^4)$ total time complexity. The gate complexity is $\widetilde{O}(n^2d^4)$.

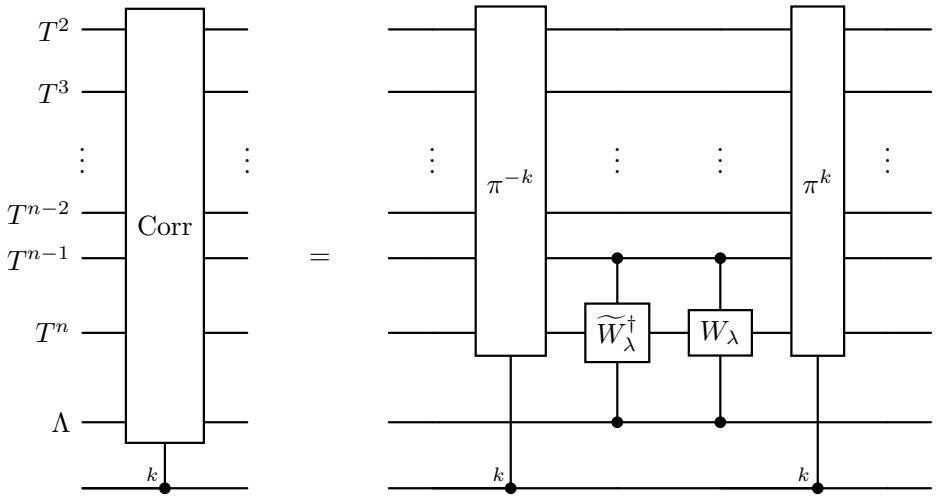

Figure 5.4: Circuit for the correction operation Corr. W_λ gate is defined in Eq. (5.56) and its implementation is completely analogous to $\widetilde{W}_\lambda$ from Fig. 5.7.

Space complexity

Similarly, we can count the number of auxiliary qubits needed to implement our circuit Fig. 5.5 in the standard encoding. However, we must be careful with the precision of implementing each gate. If the total target precision is ϵ then if the circuit has $\mathrm{poly}(n,d)$ gates it implies the precision per each gate must be $\epsilon_g := \epsilon/\,\mathrm{poly}(n,d)$. This will translate into the size of auxiliary registers for classical computation of matrix entries of the unitaries which need to be implemented coherently (see Lemma 4.4.2): the number of qubits needed for such computations will scale as $\log(1/\epsilon_g) = O(\log(1/\epsilon) + \log(n) + \log(d))$. Keeping that in mind and using Lemma 4.4.2, we can summarize the total space complexity:

1. The number of auxiliary qubits needed to implement the mixed Schur transform isometry in the standard encoding (see Theorem 4.3.1) and create a Naimark dilation from Section 5.3 after the mixed Schur transform is $(n+d)d\,\mathrm{polylog}(d,n,1/\epsilon)$.

2. The number of auxiliary qubits needed to implement each gate σ_i from Fig. 5.6 inside $\pi^\dagger$ gate from Fig. 5.3 is $\mathrm{polylog}(d,n,1/\epsilon)$. However, when $O(n)$ gates σ_i are implemented in parallel with the shift trick of $\pi^\dagger$ gates we need to have $n\,\mathrm{polylog}(d,n,1/\epsilon)$ auxiliary qubits available.

3. The gates $\widetilde{W}_\lambda$ and W_λ require $d^2\,\mathrm{polylog}(d,n,1/\epsilon)$ qubits to implement gates R_i, see Fig. 5.7.

4. Overall, the total number of auxiliary qubits needed is $(n+d)d\,\mathrm{polylog}(d,n,1/\epsilon)$.

The above analysis completes the proof of the first statement of Theorem 5.1.1 for standard PGM. In the next section, we describe how to extend the construction for standard PGM for generic PBT measurements, including the measurement needed to implement pPBT with the EPR resource state.

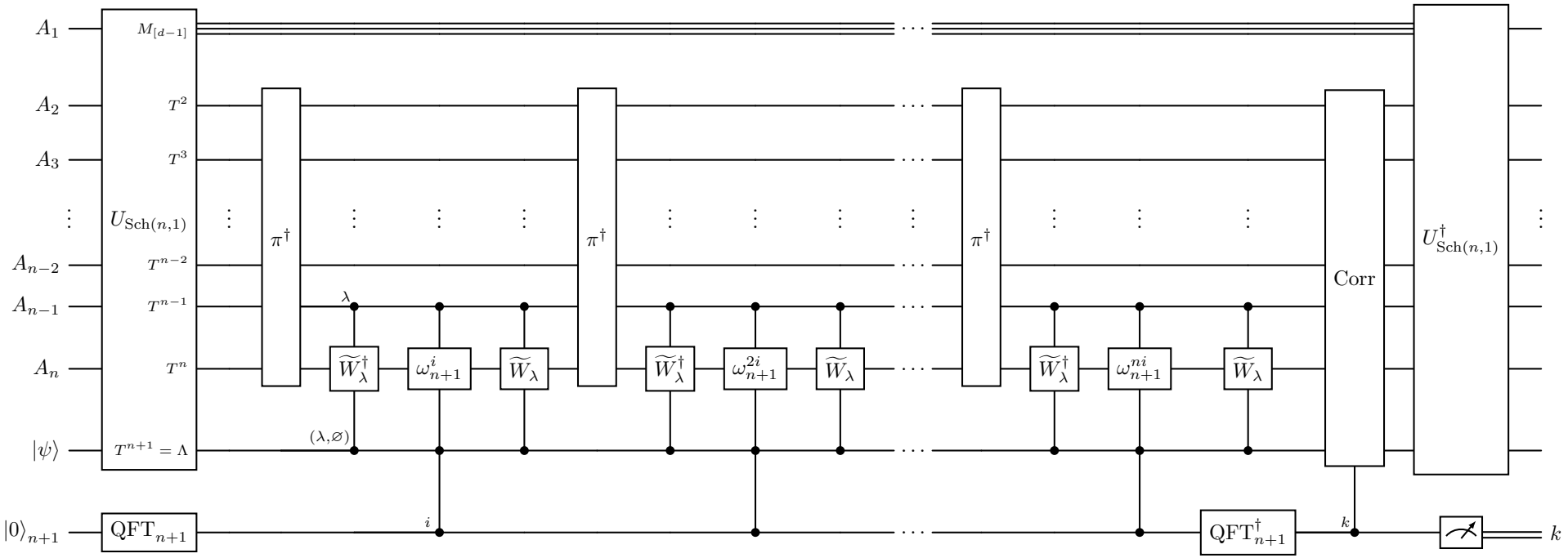

Figure 5.5: The circuit implementation of the PGM E from Eqs. (5.4) and (5.17) in standard encoding. The registers $T^2, T^3, \ldots, T^n$ are dilated as per Section 5.3. The correction gate Corr together with $U^\dagger_{\mathrm{Sch}(n,1)}$ transform is optional: it is used to bring the post-measurement state to the form defined by the original PGM measurement E.

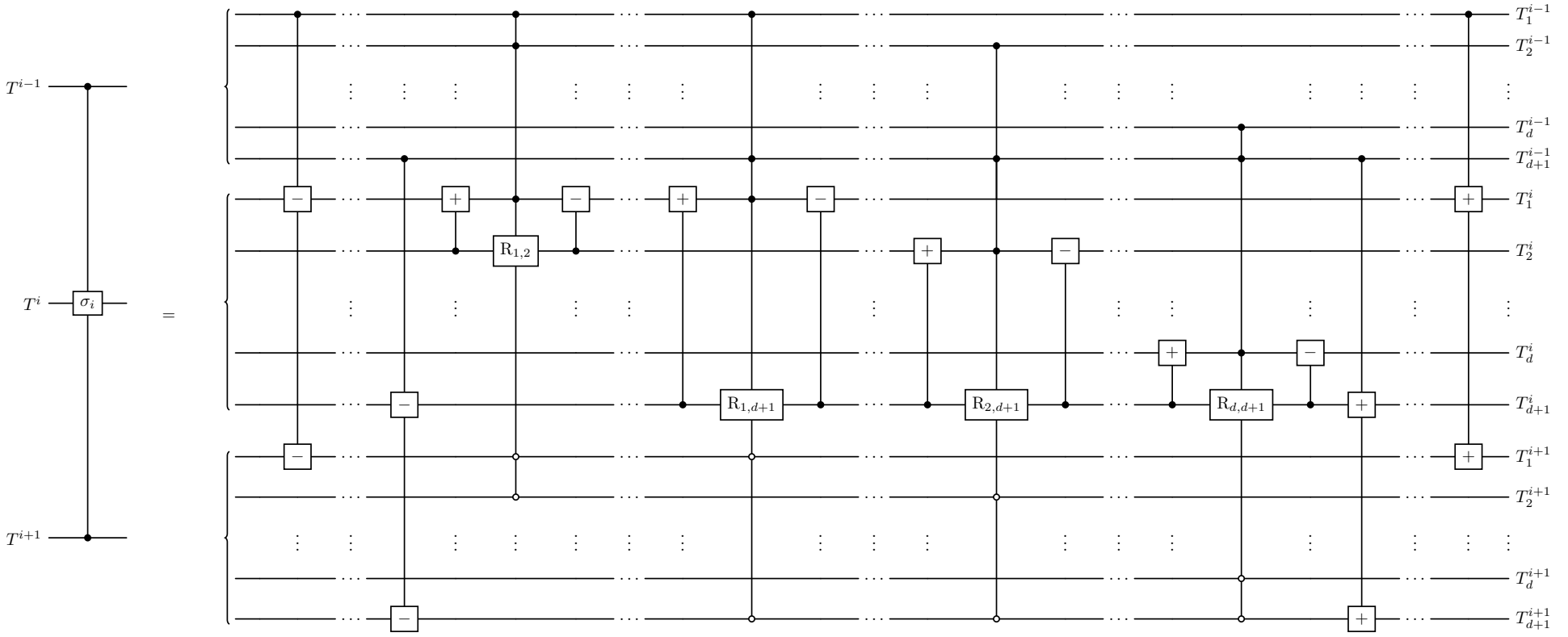

Figure 5.6: Quantum circuit for implementing the transposition σ_i in the Gelfand–Tsetlin basis. The controlled "$\pm$" gates perform arithmetic operations that add / subtract the control register from the target registers. For each j, k such that $1 \leqslant j < k \leqslant d$, the corresponding $\mathrm{R}_{j,k}$ gate defined in Eq. (5.61) acts on the k-th register of T^i and has five controls: the j-th and k-th registers of T^{i-1} and T^{i+1}, and the j-th register of T^i. At this level of abstraction, the implementation of σ_i contains $\widetilde{O}(d^2)$ gates.

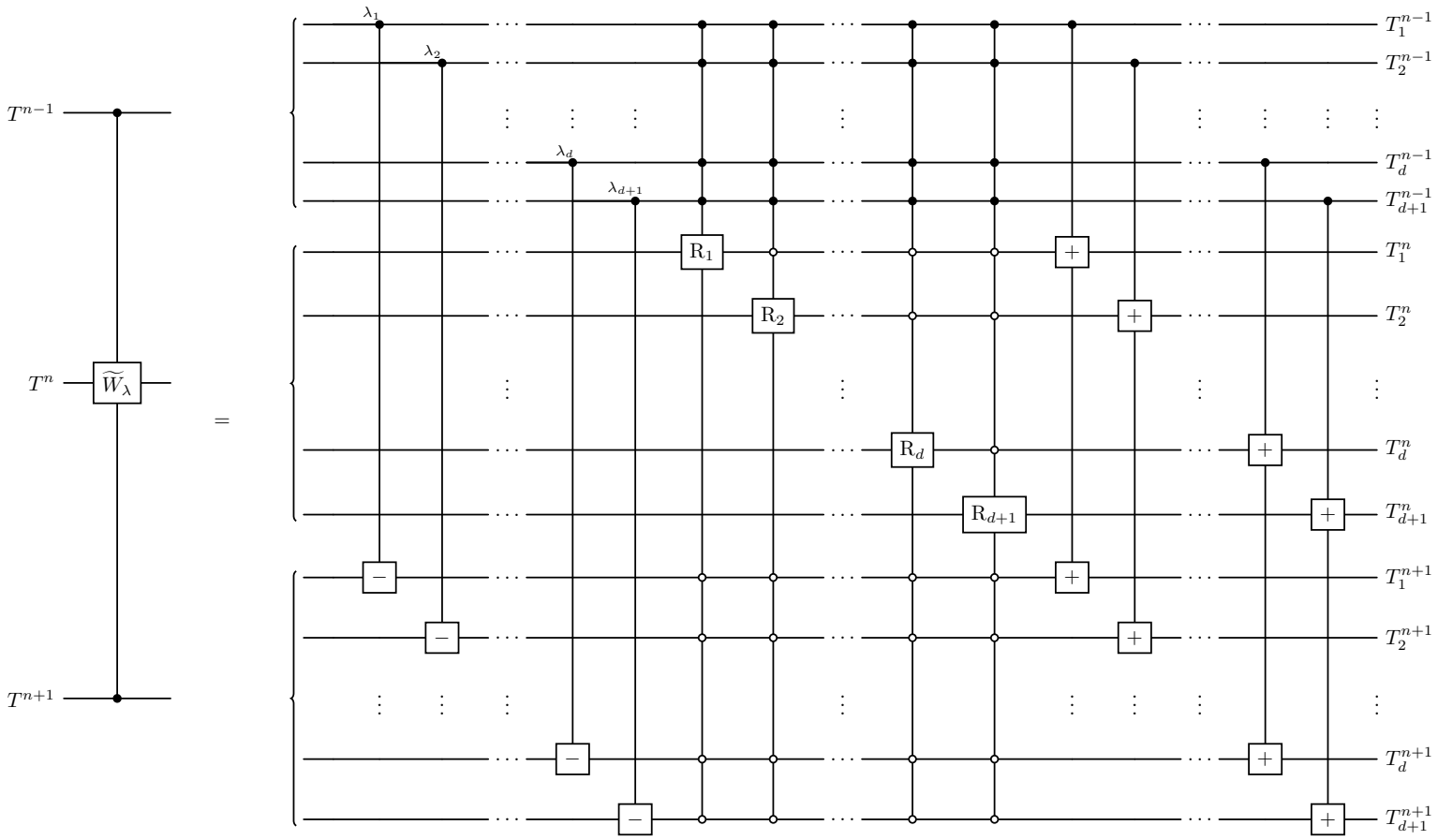

Figure 5.7: Quantum circuit for implementing the unitary $\widetilde{W}$ defined by (5.56) in the Gelfand–Tsetlin basis. The controlled "$\pm$" gates perform arithmetic operations that add / subtract the control register from the target registers, just as on Fig. 5.6. Eq. (5.61) defines rotation gates R_j that are controlled on $2(d+1+j)$ registers in total: all registers of T^{i-1} and T^{i+1} and first $(j-1)$ registers of T^i. The overall gate complexity of $\widetilde{W}$ is $\widetilde{O}(d^2)$.

5.4.2 Deterministic PBT measurement

Using the quantum circuit for the standard PGM E Fig. 5.5 we can easily implement the POVM $E^{\star}$ for the dPBT protocols from Eqs. (5.18) and (5.19). For that, we need to use Lemma 5.2.1, which tells us to use one additional auxiliary qudit of dimension n, prepared in the state $|+\rangle_n = \sum_{i=0}^{n-1} \frac{1}{\sqrt{n}}|i\rangle$. The resulting circuit is presented in Fig. 5.9. Notice that the circuit is almost the same as the one for the standard PGM E presented in Fig. 5.5. The only difference is an additional register of dimension n and a controlled Pauli gate $Z := \sum_{i=0}^{n-1} \omega_n^i |i\rangle\langle i|$.

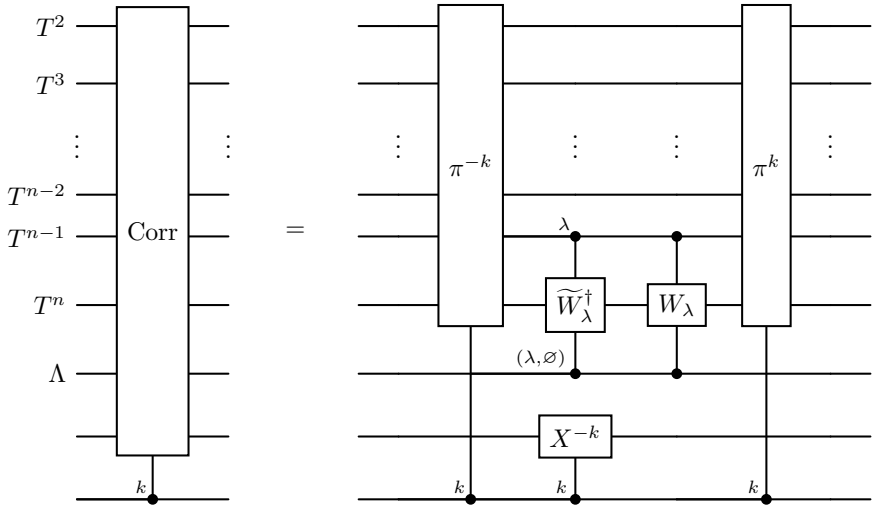

Figure 5.8: Circuit for the correction gate Corr from Fig. 5.9. It is a slight modification of the correction gate for standard PGM from Fig. 5.4.

5.4.3 Probabilistic PBT measurement with EPR resource state

The measurement for optimised resource state pPBT is the standard PGM E from Fig. 5.5. For EPR state case, it is straightforward now to extend the quantum circuit for the standard PGM to a quantum circuit for pPBT POVM defined via Eq. (5.26). For that, we can employ Lemma 5.2.2 for each irrep $(\lambda, \varnothing) \in \widehat{\mathcal{A}}_{n,1}^d$, where $\widetilde{\psi}_{(\lambda,\varnothing)}(U)$ is determined by the corresponding diagonal matrix G from Eq. (5.26) extended to Naimark dilated space as $\langle T|\widetilde{\psi}_{(\lambda,\varnothing)}(G)|T\rangle = 0$ for all $T \in \mathrm{Paths}(\Lambda, \widetilde{\mathscr{A}}) \setminus \mathrm{Paths}(\Lambda, \mathscr{A})$. We introduce an additional qubit on which we would act with a unitary $U_{\lambda,a}$ depending on the irrep $(\lambda, \varnothing) \in \widehat{\mathcal{A}}_{n,1}^d$ and $a \in \mathrm{AC}(\lambda)$:

$$U_{\lambda,a} = \begin{pmatrix} \sqrt{g_{\lambda,a}} & -\sqrt{1-g_{\lambda,a}} \\ \sqrt{1-g_{\lambda,a}} & \sqrt{g_{\lambda,a}} \end{pmatrix}, \tag{5.62}$$

where $g_{\lambda,a}$ are defined in Eq. (5.27) for pPBT with EPR resource state. The resulting circuit Fig. 5.10 is almost the same as Fig. 5.5. The only difference is an additional register and a controlled rotation matrix (5.62).

The complexity of computing $g_{\lambda,a}$ classically is $\widetilde{O}(1)$. Therefore the time, gate and space complexities of the circuit Fig. 5.10 are the same as for Fig. 5.5. The correction gate Corr in Fig. 5.10 is implemented in similar way as in Fig. 5.4, except one needs to uncompute $U_{\lambda,a}$ on the additional qubit register and do the uncomputation conditioned on the outcome $k = 0$.

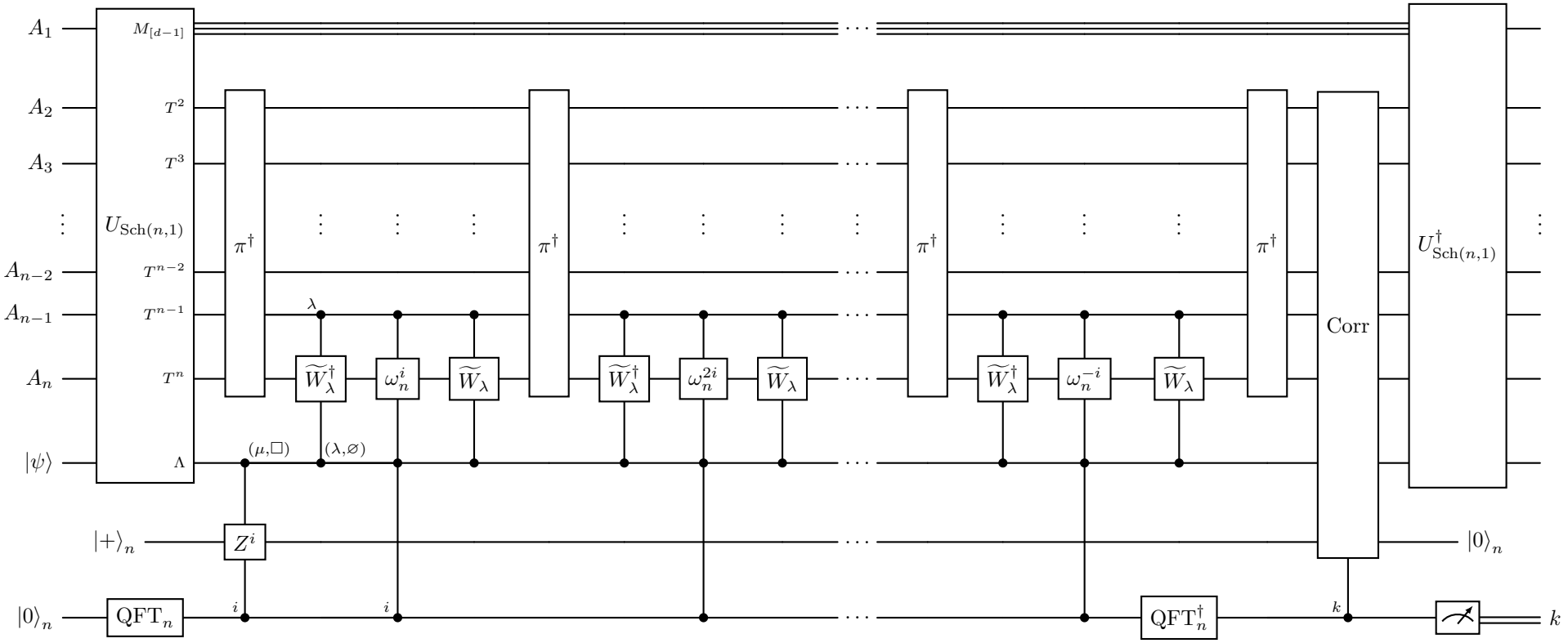

Figure 5.9: The circuit implementation of the POVM $E^{\star}$ from Eqs. (5.18) and (5.19) for dPBT in standard encoding.

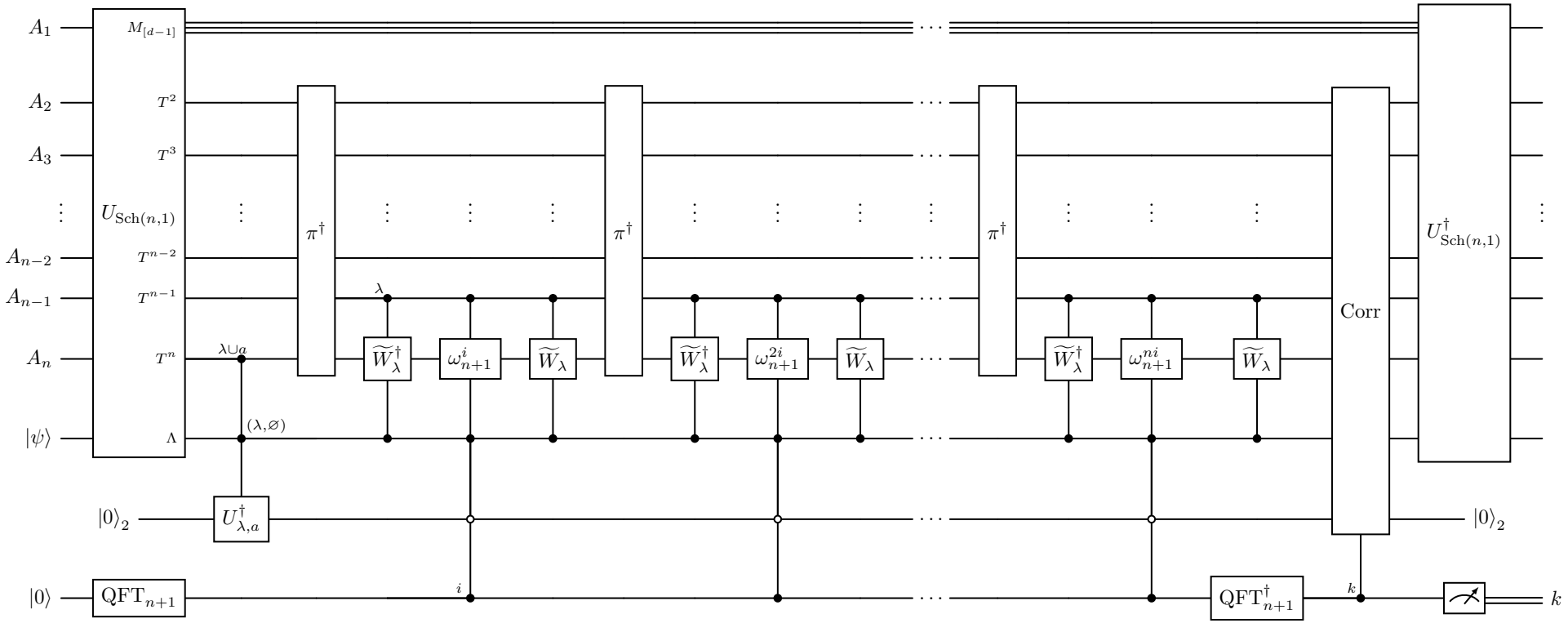

Figure 5.10: The circuit implementation of the POVM $E^\star$ for pPBT with EPR resource state defined via Eq. (5.26) in standard encoding.

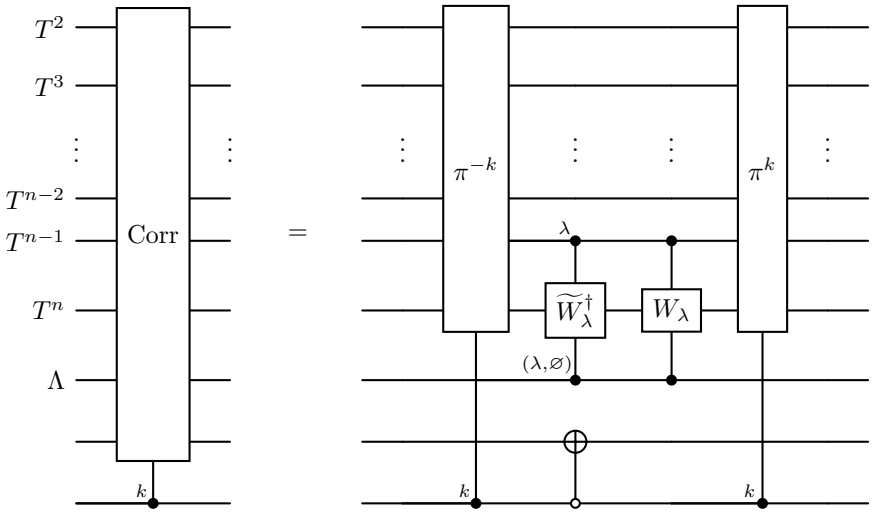

Figure 5.11: Circuit for the correction gate Corr from Fig. 5.10. It is a slight modification of the correction gate for standard PGM from Fig. 5.4.

5.4.4 Efficient quantum algorithms for generic PBT measurements

We can combine two implementations for dPBT and pPBT measurement and implement a generic measurement $E^\star$ from Eq. (5.20) defined via G operator, which is given in the Gelfand–Tsetlin basis via Eq. (5.21).

Given a phase gate $\widetilde{Z} := \sum_{i=1}^n \omega_{n+1}^i |i\rangle\langle i|$ and a unitary $U_{\Lambda,\gamma}$ acting on an auxiliary qubit defined as

$$U_{\Lambda,\gamma} = \begin{cases} R_y(g_{\lambda,a}) & \text{if } \Lambda = (\lambda,\varnothing), \gamma = \lambda \cup a, \\ R_y(g_\mu) & \text{if } \Lambda = (\mu,\square), \gamma = \mu\ , \end{cases} \qquad R_y(g) := \begin{pmatrix} \sqrt{g} & -\sqrt{1-g} \\ \sqrt{1-g} & \sqrt{g} \end{pmatrix}. \tag{5.63}$$

we can implement POVM $E^\star$ as in Fig. 5.13.

Note that our construction works for any diagonal matrix $\psi_\Lambda(G)$ as long as its diagonal entries $g_{\lambda,a}, g_\mu$ are efficiently classically computable. The correction gate Corr in Fig. 5.13 is implemented in a similar way as in Figs. 5.4, 5.8 and 5.11.

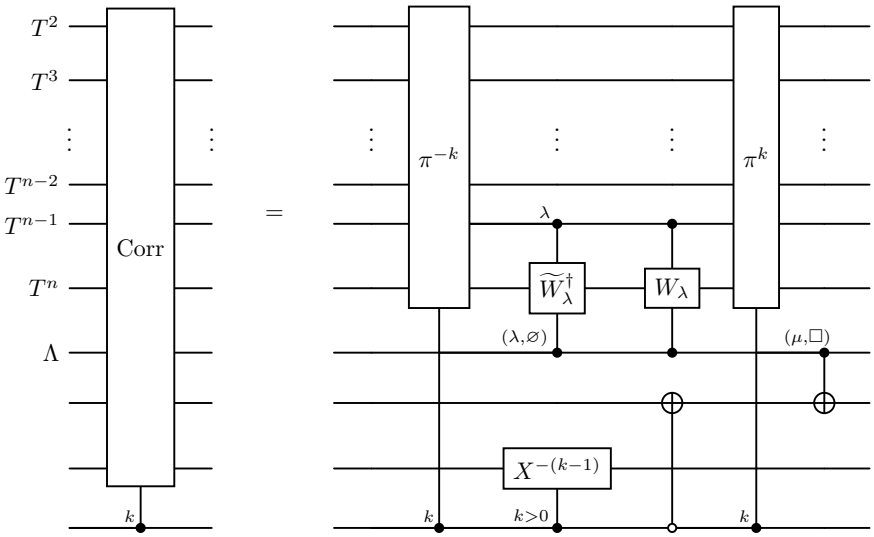

Figure 5.12: Circuit for the correction gate Corr from Fig. 5.13.

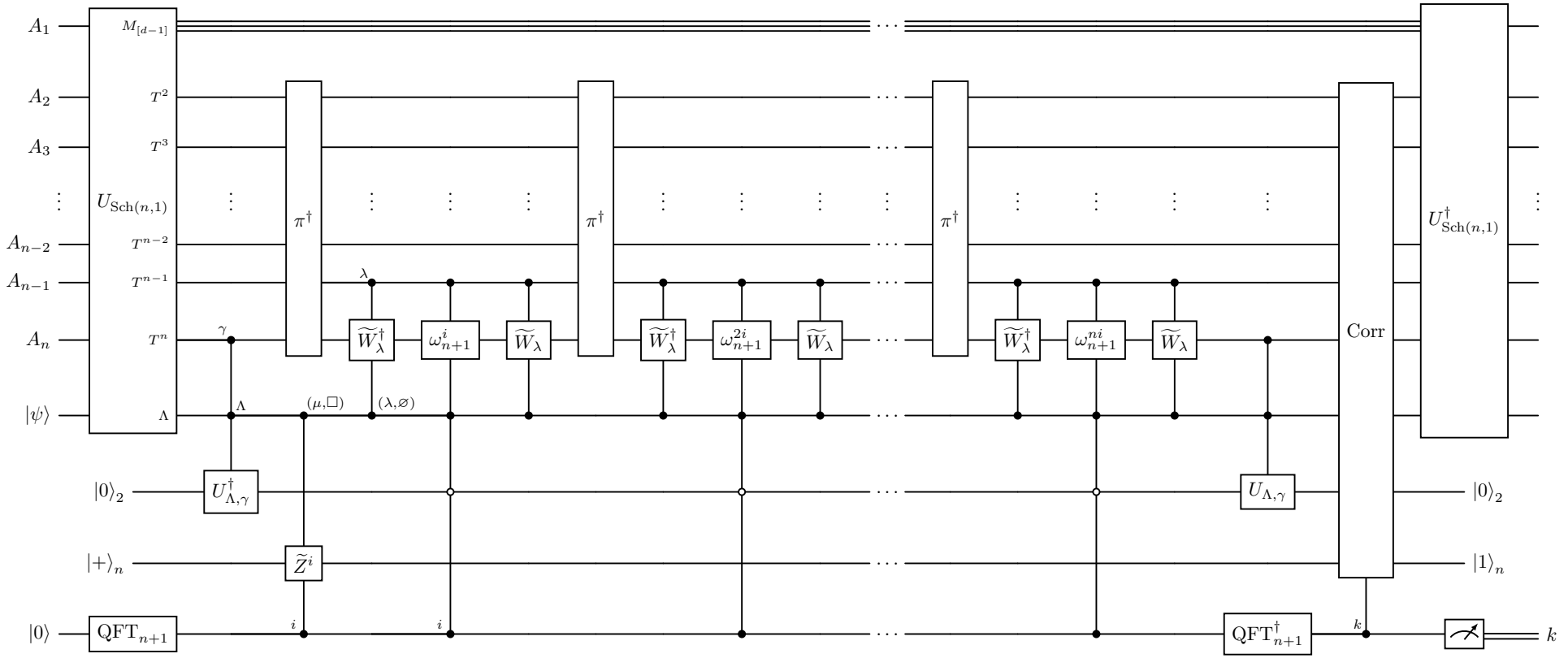

Figure 5.13: The circuit implementation of a generic POVM $E^\star$ for PBT from Eq. (5.20) in standard encoding.

5.5 PBT via Yamanouchi encoding

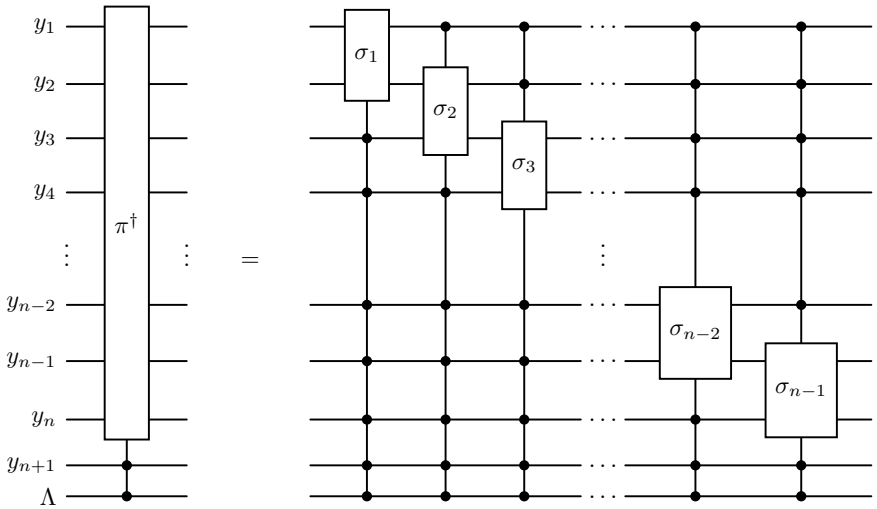

Figure 5.14: Quantum circuit for the cyclic permutation $\pi^\dagger = \sigma_{n-1}\sigma_{n-2}\cdots\sigma_2\sigma_1$ in the Yamanouchi encoding. Each transposition σ_i acts locally on registers y_i and y_{i+1}, while being controlled on all other registers y_i and Λ. Note that in standard encoding, σ_i was controlled only on two registers, compare with Fig. 5.3. Fig. 5.15 presents the exact form of a transposition σ_i gate in Yamanouchi encoding.

Using the Yamanouchi encoding possibility of the mixed quantum Schur transform (see Theorem 4.3.1), it is possible to reduce the space complexity of the constructions presented in Section 5.4.1 from $\widetilde{O}(n)$ to $\widetilde{O}(1)$. The resulting circuits for generic PBT measurements $E^\star$, including standard PGM E, dPBT POVM $E^{\star\!\!\star}$ and the POVM for EPR pPBT, are presented in Fig. 5.17. They look essentially the same as Fig. 5.13 except for the differences in implementation of gates $\pi^\dagger$, σ_i and $\widetilde{W}_\lambda$ which stem from the different type of encoding.

Similarly to Section 5.4.1 we can count the total gate and time complexities in Fig. 5.17 as follows:

1. The complexity of implementing the mixed quantum Schur transform $U_{\mathrm{Sch}(n,1)}$ in Yamanouchi encoding is $\widetilde{O}(nd^4)$, see Chapter 4.

2. The complexity of implementing $\pi = \sigma_1\sigma_2\ldots\sigma_{n-1}$ based on Fig. 5.14 is $\widetilde{O}(nd^2)$. The factor n comes from the number of transpositions σ_i in π, which are implemented sequentially.

3. Each transposition σ_i is more tricky in Yamanouchi encoding, see Figs. 5.15 and 5.16. More specifically, to implement σ_i we need to obtain the full information about the Young diagram T^{i-1} by using an auxiliary space and recording the description of T^{i-1} sequentially from registers y_k for $k < i$ via a $\mathrm{Rec_k}$ gates, see Fig. 5.15. Now, according to Fig. 5.16, each σ_i can be implemented with $\widetilde{O}(d^2)$ gates $\mathrm{R}_{i,j}$ from Eq. (5.61), acting on wires y_i, y_{i+1} each of which decompose into $\widetilde{O}(1)$ elementary gates and $\widetilde{O}(1)$ auxiliary qubits for computation of rotation parameters $r_{j,k}$.

4. The operation $\widetilde{W}$ defined in Eq. (5.56) is implemented similarly to Fig. 5.7 and the recording procedure described in Fig. 5.15. The time and gate complexities for that are $\widetilde{O}(nd^2)$.

5. The implementation of ω_{n+1}^{ki} has complexity $\widetilde{O}(n)$.

6. The complexity of the Quantum Fourier Transform QFT_{n+1} is $\widetilde{O}(1)$.

7. One can optionally implement the correction gate Corr together with inverse mixed Schur transform at the end to get the right post-measurement state as in Fig. 5.13. The complexity of implementing this does not change both the total gate and time complexities of the full circuit, adding only a constant factor overhead.

8. Overall, counting everything together gives $\widetilde{O}(n^2d^4)$ for both total gate and time complexities in Yamanouchi encoding: essentially all nontrivial operations run sequentially.

Similarly, we can count the number of auxiliary qubits needed to implement our circuit Fig. 5.5 in the Yamanouchi encoding similarly to Section 5.4.1:

1. The number of auxiliary qubits needed to implement the mixed Schur transform isometry in the Yamanouchi encoding and create a Naimark's dilation from Section 5.3 after the the mixed Schur transform is $d^2\,\mathrm{polylog}(d, n, 1/\epsilon)$, see Theorem 4.3.1. One important technical remark regarding Figs. 5.14 to 5.17 is that we do not depict an additional qudit of dimension $n+1$ which is needed to extend the Bratteli diagram from $\mathscr{A}$ to $\widetilde{\mathscr{A}}$ according to Section 5.3: it extends the space of Yamanouchi words on alphabet $[d]$ to the space of Yamanouchi words with at most one symbol $d+1$ among $y_1, \ldots, y_n$ by encoding the location i of the value $d+1$ among $y_1, \ldots, y_n$ (if there exist i such that $y_i = d+1$ then it also must be $y_{n+1} = d+1$). Incorporation of this qubit is trivial and it does not change the time and gate complexities, however, it is not convenient to draw it, so we omit it from the figures.

2. The number of auxiliary qubits needed for each σ_i from Fig. 5.16 is $\mathrm{polylog}(d, n, 1/\epsilon)$. We implement all gates σ_i sequentially in the Yamanouchi encoding so we can reuse $\mathrm{polylog}(d, n, 1/\epsilon)$ auxiliary qubits for each gate.

3. The gates $\widetilde{W}_\lambda$ and W_λ require $d^2\,\mathrm{polylog}(d, n, 1/\epsilon)$ qubits to implement gates R_i, see Fig. 5.7.

4. Overall, the total number of auxiliary qubits needed is $d^2\,\mathrm{polylog}(d, n, 1/\epsilon)$.

The above analysis finishes the proof of the second statement of Theorem 5.1.1.

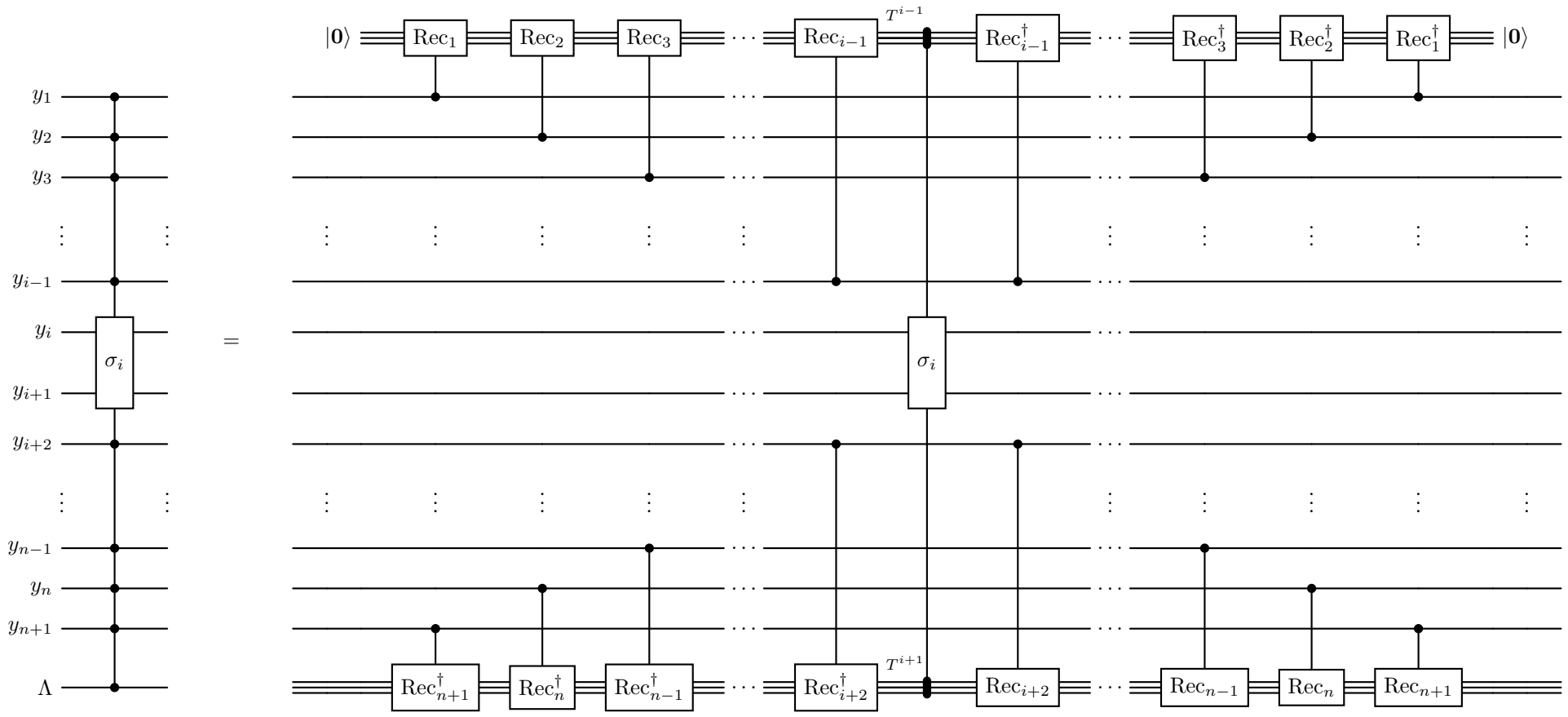

Figure 5.15: Quantum circuit for implementing a transposition σ_i in the Yamanouchi encoding. To correctly compute the rotation angles, we shall recover the information about parts T^{i-1} and T^{i+1} of a path T from its form in Yamanouchi encoding. This is achieved by a sequence of recording gates Rec_i performed on two auxiliary registers and controlled on y_i register. After recovering information about T^{i-1} and T^{i+1}, transpoition σ_i can be simply performed as presented on Fig. 5.16.

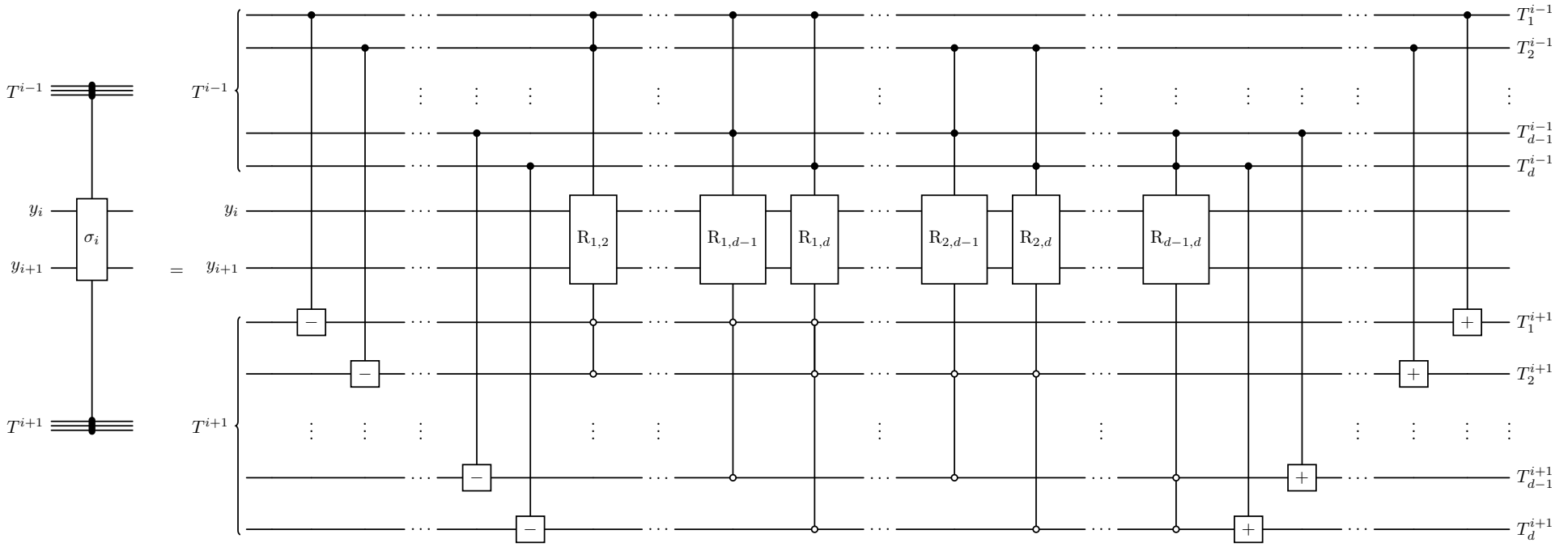

Figure 5.16: Quantum circuit implementing the transposition σ_i in the Yamanouchi encoding is similar to the circuit in the standard encoding, see Fig. 5.6. Controlled "$\pm$" gates and rotation $\mathrm{R}_{j,k}$ gates are exactly the same as on Fig. 5.6.

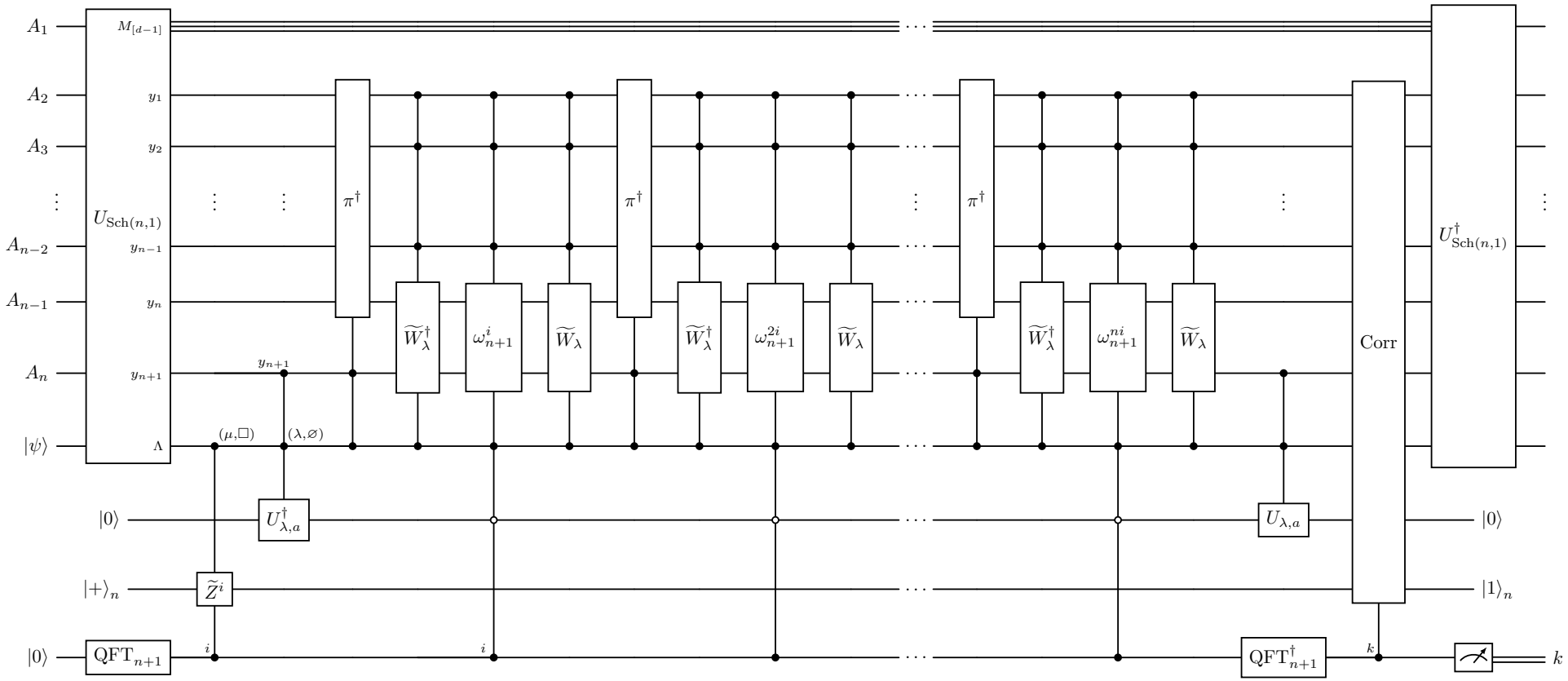

Figure 5.17: The circuit implementation of generic POVM $E^\star$ in Yamanouchi encoding. Notice that the structure of the circuit is exactly the same as with standard encoding, see Fig. 5.13, except that wires $T^2, \ldots, T^n$ containing information about path $T = (T^0, \ldots, T^n)$ via standard encoding are replaced by wires $y_1, \ldots, y_{n+1}$ which contain the same information via Yamanouchi encoding. This is obtained by another form of mixed Schur isometry, see Theorem 4.3.1. This requires reformulation for all subsequent gates from the standard to Yamanouchi encoding, which we present on Figs. 5.14 to 5.16.

5.6 Quantum circuits for optimised resource states

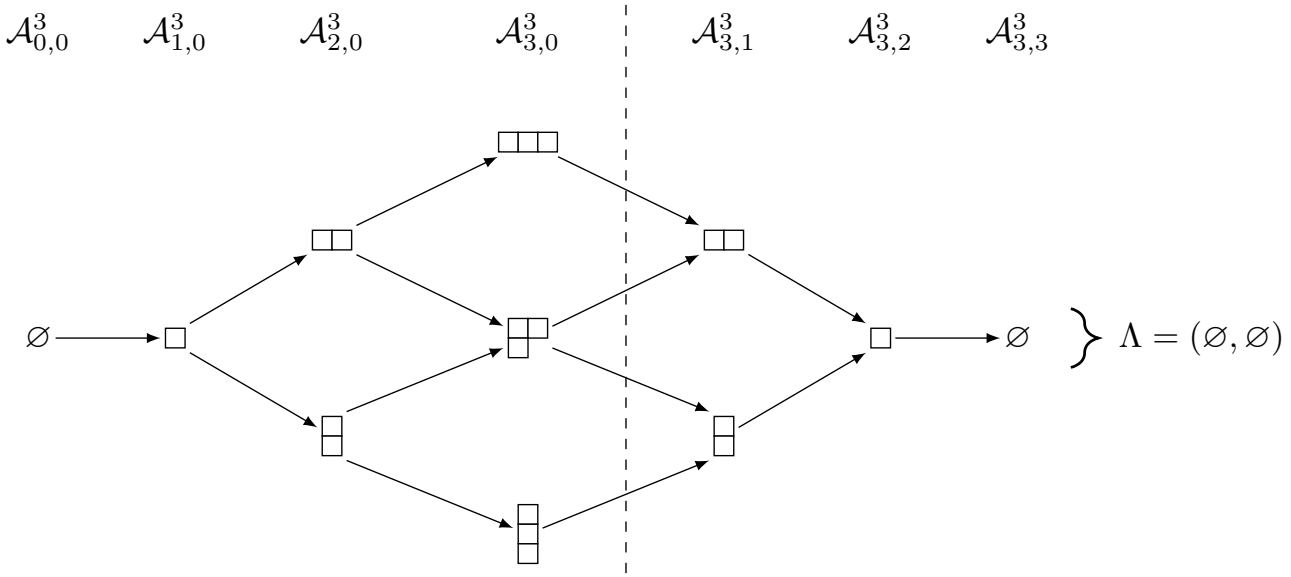

Figure 5.18: A part of the full Bratteli diagram $\hat{\mathscr{A}}$ corresponding to an irrep $\Lambda = (\varnothing, \varnothing)$ of algebra $\mathcal{A}^3_{3,3}$. The set of paths starting at the root and terminating at the end span the Gelfand–Tsetlin basis of $\Lambda = (\varnothing, \varnothing)$. A tensor product of n copies of EPR states shared between the first and second half of the systems is fully supported in irrep $\Lambda = (\varnothing, \varnothing)$ in the mixed Schur basis. In fact, it corresponds to a uniform superposition of all symmetric paths in the Gelfand–Tsetlin basis, see Eqs. (5.66) and (5.67). Similarly, the optimised resource state for PBT protocols can be expressed as a weighted superposition of symmetric paths in the Gelfand–Tsetlin basis. In particular, for pPBT the exact formula for the weights might be computed in $\widetilde{O}(d)$ time, see Eq. (5.74), while for dPBT, weights are the result of non-trivial optimisation procedure, see Eq. (5.75).

In this section, we describe efficient quantum circuits for preparing optimised resource states for the pPBT protocol. To write and present such circuits in a unified way, we shall introduce another variant of mixed Schur transform $U_{\mathrm{Sch}(n,n)}$ corresponding to the matrix algebra $\mathcal{A}^d_{n,n}$ of partially transposed permutations acting on $n+n$ qudits, each of local dimension d. The matrix algebra $\mathcal{A}^d_{n,n}$ acts on $(\mathbb{C}^d)^{\otimes n+n}$ and its irreducible representations are labelled by the following pairs of Young diagrams:

$$\widehat{\mathcal{A}}^d_{n,n} := \Big\{ (\lambda, \mu) \;\Big|\; \lambda \vdash n-k,\ \mu \vdash n-k,\ \ell(\lambda) + \ell(\mu) \leqslant d,\ \text{for } k \in [n] \Big\}. \tag{5.64}$$

Furthermore, its Bratteli diagram $\hat{\mathscr{A}}$ is adapted for the sequence of algebras $\mathcal{A}^d_{0,0} \hookrightarrow \mathcal{A}^d_{1,0} \hookrightarrow \cdots \hookrightarrow \mathcal{A}^d_{n,0} \hookrightarrow \mathcal{A}^d_{n,1} \hookrightarrow \cdots \hookrightarrow \mathcal{A}^d_{n,n}$. For our purpose it is enough to present only one special irrep $\Lambda = (\varnothing, \varnothing) \in \widehat{\mathcal{A}}^d_{n,n}$. The set of paths

$$\mathrm{Paths}((\varnothing, \varnothing), \hat{\mathscr{A}}) := \Big\{ (T^0, \ldots, T^n, T^{n+1}, \ldots, T^{2n}) \;\Big|\; T^k, T^{2n-k} \vdash k \text{ for } k \leqslant n, \text{ and } T^{i-1} \to T^i, T^{2n-i+1} \to T^{2n-i} \text{ for } i \in [n] \Big\} \tag{5.65}$$

span the Gelfand–Tsetlin basis $\{|T\rangle \mid T \in \mathrm{Paths}(\Lambda, \mathscr{A})\}$ of irreducible representation $(\varnothing, \varnothing) \in \widehat{\mathcal{A}}^d_{n,n}$, see Fig. 5.18.

Mixed Schur–Weyl duality partitions the space $(\mathbb{C}^d)^{\otimes n+n}$ into subspaces that are invariant under the natural $U^{\otimes n} \otimes \bar{U}^{\otimes n}$ action of $U \in \mathrm{U}_d$ and the action of the matrix algebra $\mathcal{A}^d_{n,n}$,

see Chapter 3 The complexity of implementing the mixed quantum Schur transform isometry $U_{\mathrm{Sch}(n,n)}$ is $\widetilde{O}(nd^4)$, see Theorem 4.3.1, Chapter 4.

A tensor product of n copies of EPR states shared between the first and second half of the systems in $(\mathbb{C}^d)^{\otimes n+n}$ has a relatively simple form in mixed Schur basis [SSMH17]. In particular, it is supported only on one irrep, namely $\Lambda = (\varnothing, \varnothing) \in \widehat{\mathcal{A}}^d_{n,n}$. Notice that the unitary group representation corresponding to $\Lambda = (\varnothing, \varnothing)$ is one dimensional. With a small abuse of notation (we supress the unitary irrep register), we have

$$U_{\mathrm{Sch}(n,n)} \left(\bigotimes_{i=1}^{n} |\Phi^+\rangle_{A_i B_i} \right) = \sum_{\mu \vdash_d n} \sqrt{\frac{d_\mu m_\mu}{d^n}} \, |\mathrm{EPR}_\mu^{[n-1]}\rangle \, |\mu\rangle_{T^n}, \tag{5.66}$$

where

$$|\mathrm{EPR}_\mu^{[n-1]}\rangle := \sum_{S \in \mathrm{Paths}_n(\mu, \hat{\mathscr{A}})} \sqrt{\frac{1}{d_\mu}} |S_0\rangle_{T^0} \cdots |S_{n-1}\rangle_{T^{n-1}} |S_{n-1}\rangle_{T^{n+1}} \cdots |S_0\rangle_{T^{2n}} \tag{5.67}$$

and $|\Phi^+\rangle_{A_i B_i} := \frac{1}{\sqrt{d}} \sum_{k=1}^{d} |k\rangle_{A_i} |k\rangle_{B_i}$ is an EPR pair shared between Alice's register i and Bob's register i. Notice that all paths present in the formula above are symmetric with respect to the middle vertex. The analytical expressions for optimised resource states in dPBT and pPBT protocols were developed in Ref [SSMH17; MSSH18; Chr+21], and in a mixed Schur basis have a similar form to n copies of EPR pairs (5.66). Indeed, in both cases, they are of the following form

$$|\Psi\rangle_T = \sum_{\mu \vdash_d n} \sqrt{f_\mu} \, |\mathrm{EPR}_\mu^{[n-1]}\rangle \, |\mu\rangle_{T^n}, \tag{5.68}$$

where $\{f_\mu\}_{\mu \vdash_d n}$ is some probability distribution satisfying $\sum_{\mu \vdash_d n} f_\mu = 1$.[5] Furthermore, we can rewrite this expression as

$$|\Psi\rangle_T = \sum_{\lambda \vdash_d n-1} \sqrt{f_\lambda} |\mathrm{EPR}_\lambda^{[n-2]}\rangle |\lambda\rangle_{T^{n-1}} |\lambda\rangle_{T^{n+1}} \left(\sum_{a \in \mathrm{AC}_d(\lambda)} \sqrt{\frac{f_{\lambda \cup a}}{f_\lambda} \frac{d_\lambda}{d_{\lambda \cup a}}} |\lambda \cup a\rangle_{T^n} \right), \tag{5.69}$$

$$|\mathrm{EPR}_\lambda^{[n-2]}\rangle := \sum_{S \in \mathrm{Paths}_{n-1}(\lambda, \hat{\mathscr{A}})} \sqrt{\frac{1}{d_\lambda}} |S_0\rangle_{T^0} \cdots |S_{n-2}\rangle_{T^{n-2}} |S_{n-2}\rangle_{T^{n+2}} \cdots |S_0\rangle_{T^{2n}}, \tag{5.70}$$

where f_λ are defined in such a way that the state $\sum_{a \in \mathrm{AC}_d(\lambda)} \sqrt{\frac{f_{\lambda \cup a}}{f_\lambda} \frac{d_\lambda}{d_{\lambda \cup a}}} |\lambda \cup a\rangle_{T^n}$ is normalised, namely

$$\frac{f_\lambda}{d_\lambda} := \sum_{a \in \mathrm{AC}_d(\lambda)} \frac{f_{\lambda \cup a}}{d_{\lambda \cup a}}. \tag{5.71}$$

We continue doing this rewriting recursively. That leads to the circuit for the preparation of $|\Psi\rangle_T$ presented in Fig. 5.19, where gates F_i prepare the following states controlled on T^{i-1}:

$$\mathrm{F}_i |\nu\rangle_{T^{i-1}} |0\rangle_{T^i} = |\nu\rangle_{T^{i-1}} \left(\sum_{a \in \mathrm{AC}_d(\nu)} \sqrt{\frac{f_{\nu \cup a}}{f_\nu} \frac{d_\nu}{d_{\nu \cup a}}} |\nu \cup a\rangle_{T^i} \right) \tag{5.72}$$

In particular, for pPBT [SSMH17] the formulas for f_ν for every $\nu \vdash_d k$ turn out to be as follows:

$$f_\nu = \frac{m_\nu^2}{\sum_{\chi \vdash_d k} m_\chi^2} \tag{5.73}$$

[5] In the PBT literature sometimes a different parametrisation is used: $f_\mu = \frac{c_\mu d_\mu m_\mu}{d^n}$ where c_μ are variables. The EPR resource state corresponds to the choice $c_\mu = 1$ for every $\mu \vdash_d n$.

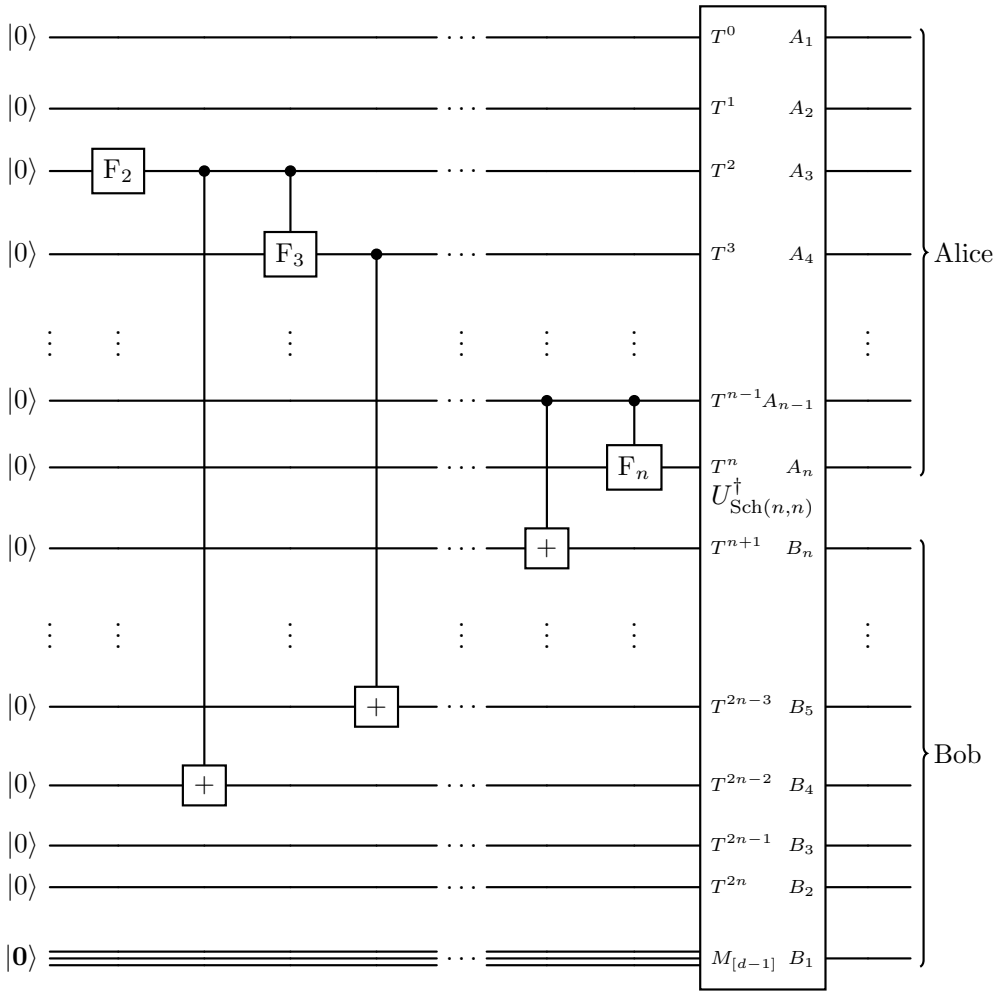

Figure 5.19: Circuit for the preparation of the resource state $|\Psi\rangle_T|0\rangle_{M_{[d-1]}}$ from Eq. (5.68). Gates F_i are defined in Eq. (5.72) via Eqs. (5.73) and (5.74).

Therefore due to [SSMH17, Proposition 25] and Eq. (5.12) the amplitudes in Eq. (5.72) for every $a \in \mathrm{AC}_d(\nu)$ and $\nu \vdash k$ can be computed efficiently in time $\widetilde{O}(d)$:

$$\frac{f_{\nu\cup a}}{f_\nu}\frac{d_\nu}{d_{\nu\cup a}} = \frac{d+\mathrm{cont}(a)}{d^2+k}\frac{m_{\nu\cup a}}{m_\nu} = \frac{d+\mathrm{cont}(a)}{d^2+k}\left(\prod_{\substack{i\,:\,i\neq r\\ 1\leqslant i\leqslant d}}\frac{\nu_r-\nu_i+i-r+1}{\nu_r-\nu_i+i-r}\right), \tag{5.74}$$

where the last equality is due to the Weyl dimension formula and r denotes the row number where the box a was added to Young diagram ν.

However, we cannot do the same analysis for the dPBT protocol [MSSH18; Led22] since f_μ for $\mu \vdash_d n$ are defined via non-trivial optimisation problem [Led22, Equation 6.3]:

$$\{f_\mu\}_{\mu\vdash_d n} = \operatorname*{arg\,max}_{\sum_\mu f_\mu=1} \sum_{\lambda\vdash_d n-1}\left(\sum_{a\in\mathrm{AC}_d(\lambda)}\sqrt{f_{\lambda\cup a}}\right)^2. \tag{5.75}$$

We leave it as an open question for future work to understand how to efficiently compute the amplitudes in Eq. (5.72) for dPBT.

5.7 Discussion

In this chapter, we used the representation theory of partially transposed permutation matrix algebras and mixed Schur–Weyl duality (see Chapters 3 and 4) to solve a long-standing open problem: finding a construction of efficient quantum circuits for both deterministic and probabilistic port-based teleportation in arbitrary local dimension. Our achievement relies on the efficient construction of the mixed quantum Schur transform (see Theorem 4.3.1). Additionally, our constructions are realised in two distinct encodings: the standard encoding and the Yamanouchi encoding, which offer a concrete trade-off between the space and time complexities of our constructions. We also presented efficient quantum circuits for preparing optimised resource states for probabilistic port-based teleportation.

Finally, we outline two immediate, yet significant, consequences of our efficient port-based teleportation constructions.

Exponentially improved lower bound for non-local quantum computation

Port-based teleportation has interesting applications in holography and non-local quantum computation. See [May19; May22], where it was argued that the complexity of the local operation controls the amount of entanglement needed to implement it non-locally, using ideas from AdS/CFT correspondence. In particular, it was derived in [May22, Lemma 9] that port-based teleportation can be used to lower bound the amount of entanglement needed to implement a given channel (from a large class of one-sided quantum channels) non-locally in terms of the so-called *interaction-class circuit complexity* [May22, Definition 3] denoted by $\mathcal{C}$:

$$\Omega(\log\log\mathcal{C}) \leqslant E_c, \tag{5.76}$$

where E_c is the entanglement cost needed to implement non-locally a unitary with complexity $\mathcal{C}$, see [May22, Equation 29]. Port-based teleportation can also be used to find an upper bound [BK11; Spe16; May22]. The derivation of the lower bound uses a trivial upper bound $\exp(O(p))$ for the complexity of the port-based teleportation in terms of the number of ports n, see [May22, Equation 47]. It is already pointed out in [May22, page 28] that a better implementation of the port-based teleportation protocol would lead to a better lower bound. Complexities of our implementations of PBT protocols are $\widetilde{O}(nd^4)$, therefore this immediately translates, according to [May22, Lemma 9], to a better lower bound:

$$\Omega(\log\mathcal{C}) \leqslant E_c, \tag{5.77}$$

thus improving exponentially upon the previous known bound.

Deterministic PBT as an optimal approximate quantum processor

Deterministic port-based teleportation was intially presented as an example of approximate universal quantum processor [IH08]. Our work provides first explicit efficient construction of such universal quantum processor for all local dimensions d, which is not based on unitary estimation procedures [YRC20; HKOT23].

However, as explained in Section 5.6, we were not able to find an efficient algorithm to produce optimal resource states for dPBT. We suspect that a suboptimal choice for dPBT resource states, described in [Chr+21, Section B], could be implementable via our scheme presented in Section 5.6. Moreover, in light of the recent work, which connected port-based teleportation with unitary estimation [YKSQM24], we also conjecture that it should be possible to construct optimal states achieving asymptotically optimal entanglement fidelity, based on the construction of optimal probe states used in unitary estimation protocol from [YRC20].

Chapter 6

Unitary-equivariant linear and semidefinite programming

Unitary equivariance is a natural symmetry that occurs in many contexts in physics and mathematics. Optimisation problems with such symmetry can often be formulated as semidefinite programs (SDPs) for a d^{n+m}-dimensional matrix variable that commutes with $U^{\otimes n} \otimes \bar{U}^{\otimes m}$, for all $U \in \mathrm{U}_d$. Solving such problems naively can be prohibitively expensive even if $n+m$ is small but the local dimension d is large. We show that, under additional symmetry assumptions, this problem reduces to a linear program that can be solved in time that does not scale in d, and we provide a general framework to execute this reduction under different types of symmetries. The key ingredient of our method is a compact parametrisation of the solution space by linear combinations of walled Brauer algebra diagrams. This parametrisation requires the idempotents of a Gelfand–Tsetlin basis, which we obtained in Section 3.6. Moreover, using results on mixed Schur–Weyl duality which we obtained in Sections 3.7 and 4.2, we can conduct a symmetry reduction of a given unitary-equivariant SDP yielding a simpler SDP with less variables. To illustrate potential applications of our framework, we use several examples from quantum information: deciding the principal eigenvalue of a quantum state, quantum majority vote, asymmetric cloning and transposition of a black-box unitary.

This chapter is based on [GO24; GBO23a]. Moreover, Section 6.5.4 is partially based on work in progress with Satoshi Yoshida, Mio Murao and Maris Ozols.

6.1 Introduction

Taking the symmetry of the problem into account is a good idea for almost any problem, including optimisation problems, since this can significantly reduce the number of parameters. In particular, this is the case for semidefinite optimisation [BGSV12; RMB21]. Given the wide range of problems in quantum information with local unitary equivariance symmetry [SC23], the main focus of our work is on linear and semidefinite optimisation under a local (n, m) unitary equivariance constraint, which naturally sits within the mixed Schur–Weyl duality framework. Typically, this means optimising over unitary-equivariant quantum channels or other tensors with this symmetry.

An early example of using $U \otimes \bar{U}$ symmetry to reduce a semidefinite optimisation problem to a linear one is the work of Rains [Rai01] on entanglement distillation under completely positive partial transpose preserving operations. He characterises the optimal distillation fidelity by a semidefinite program and then exploits the symmetry

$$(U \otimes \bar{U}) \sum_i |i\rangle \otimes |i\rangle = \sum_i |i\rangle \otimes |i\rangle \tag{6.1}$$

of the canonical maximally entangled state to reduce this to a linear program (see Example 3.4.2 for more details). This work has inspired a long sequence of results [APE03; LM15; Wan18; WW20; HSW23].

The closely related $U \otimes U$ symmetry appears in the so-called *quantum max cut* problem that has recently received significant attention [AGM20; HNPTW23; PT21; KP22; PT22; Lee22; Kin23; Tak+23; WCEHK24; LP24]. This problem is concerned with approximating the ground state and ground energy of a local Hamiltonian on a graph whose vertices are qubits and edges are assigned the projector $|\psi^-\rangle\langle\psi^-|$ onto the singlet state $|\psi^-\rangle := (|01\rangle - |10\rangle)/\sqrt{2}$. The $U \otimes U$ symmetry of $|\psi^-\rangle$ is one of the basic cases captured by our framework, and the general case of $U^{\otimes n}$ is captured by the Schur–Weyl duality (see Section 2.10).

Other instances of semidefinite optimisation problems with $U^{\otimes n} \otimes \bar{U}^{\otimes m}$ symmetry appearing in quantum computing are quantum majority vote and basis-independent evaluation of Boolean functions [BLMMO22], black-box transformations of quantum gates [QDSSM19b; QDSSM19a; QE21; YSM23b; YSM23a; Ebl+23], asymmetric cloning [NPR21; NPR23], and entanglement witnesses [HKMV22].

Previously, most of these problems have been approached individually and by ad hoc methods that work only for restricted choices of n, m, d, such as $n = 1$, $m = 1$, or $d = 2$. Our goal is to provide a general framework for solving unitary-equivariant semidefinite optimisation problems for a wide range of values of n, m, d. More specifically, our aim is to answer the following two questions.

1. *How to efficiently eliminate the irrelevant degrees of freedom from a* U_d*-equivariant optimisation problem?*

2. *Can a* U_d*-equivariant optimisation problem be solved in time that does not scale in* d*?*

We provide answers to these questions using representation-theoretic and diagrammatic methods.

Summary of our results

Consider the following general semidefinite program (SDP) for a Hermitian matrix variable X:

$$\begin{aligned} \max_X \quad & \operatorname{Tr}(CX) \\ \text{s.t.} \quad & \operatorname{Tr}(A_k X) \leqslant b_k, && \forall\, k \in [m_1], \\ & \operatorname{Tr}_{S_k}(X) = D_k, && \forall\, k \in [m_2], \\ & \left[X, U^{\otimes n} \otimes \bar{U}^{\otimes m}\right] = 0, && \forall\, U \in \mathrm{U}_d, \\ & X \succeq 0, \end{aligned} \tag{6.2}$$

where C, A_k, D_k are fixed Hermitian matrices, $b_k \in \mathbb{R}$ are fixed scalars, m_1 and m_2 denote the number of constraints that involve full trace and partial trace, and $S_k \subseteq [n+m]$ denote subsets of systems that are traced out.

Note that all matrices in Eq. (6.2) are of size $d^{n+m} \times d^{n+m}$. For this problem to have an efficient description, we assume that C, A_k, D_k are s-sparse, i.e., can be specified as a linear combination of at most s walled Brauer algebra diagrams (see Section 3.2) and elementary rank-1 matrices $|i\rangle\langle j|$ where $i, j \in [d]^{n+m}$. Our main result, Theorem 6.3.4, provides an efficient way of converting the above semidefinite program to an equivalent linear program (LP) when the matrix variable X is subject to one of the following additional symmetries: $\mathrm{S}_n \times \mathrm{S}_m$ symmetry, walled Brauer algebra symmetry, or Gelfand–Tsetlin symmetry (see Section 6.3.1 for more details).

6.1.1. Theorem (Informal). *Assuming one of the above additional symmetries on X, the SDP (6.2) can be converted to an equivalent LP with $\tilde{N} \leqslant N$ variables and $m_1 + m_2 N + \tilde{N}$ constraints where $N := (n+m)!$.*

Our approach has the advantage that d can be arbitrary[1] and the computational resources are tied only to the value of $n+m$. For example, let $(n,m) = (2,3)$ be small constants and $d = 1000$ be very large. In this regime, naively solving the above SDP is impossible in practice, since it has $d^{2(n+m)} = 1000^{10} = 10^{30}$ scalar variables. However, the complexity of our method scales only in the parameter $N = (n+m)!$, which in this case is $(2+3)! = 5! = 120$.

Our method can also provide an advantage when d is small. For example, if $d = 2$ then $d^{2(n+m)} = 2^{2(2+3)} = 2^{10} = 1024$ variables are needed naively, while only 42 suffices with our method (see Table 6.7 in Section 6.A.3).

Although our method provides a significant improvement in terms of d, its complexity still scales as $(n+m)!$, so in practice we can only deal with relatively small values of n and m. However, numerical solutions to small problem instances are still valuable, as they may reveal structures that can help tackle larger instances. For example, numerical insights can lead to a refined ansatz with fewer parameters that scales up more easily. Good ansatz, even if suboptimal, can still be used to obtain numerical bounds. If the ansatz is sufficiently simple, it might even be amenable to analytic methods. In this way, our method can potentially be used to bootstrap from small problem instances to much larger ones.

To illustrate potential applications of our method, in Section 6.5 we provide several examples from quantum information: deciding the principal eigenvalue of a quantum state, quantum majority vote, and asymmetric cloning.

Our second result does not assume additional symmetries and works as a general framework from reducing general unitary-equivariant SDPs to simpler forms.

Intuition

The main idea behind our result is as follows. While the naive semidefinite program (6.2) has $d^{2(n+m)}$ scalar variables, the unitary equivariance condition alone reduces this down to $\dim(\mathcal{A}^d_{n,m})$, where $\mathcal{A}^d_{n,m}$ is the matrix algebra of partially transposed permutations. This observation already gives us a d-independent upper bound on the number of parameters since $\dim(\mathcal{A}^d_{n,m}) \leqslant (n+m)!$. While generally this bound is loose for small d, it saturates when $d \geqslant n+m$.

This reduction in the number of parameters occurs due to mixed Schur–Weyl duality (see Chapter 3). Together with Schur's lemma, this duality implies that any unitary-equivariant matrix variable X can be written in mixed Schur basis as

$$U_{\mathrm{Sch}(n,m)} X U^\dagger_{\mathrm{Sch}(n,m)} = \bigoplus_{\lambda \in \widehat{\mathcal{A}}^d_{n,m}} X_\lambda \otimes I_{m_\lambda} \tag{6.3}$$

in some basis, where the size of each block X_λ is independent of d. The main difficulty then lies in obtaining an ansatz that captures all relevant degrees of freedom for such X, in a way that does not scale in the local dimension d. In particular, we cannot afford to simply apply the mixed Schur transform that implements the basis change in Eq. (6.3) since the underlying space has dimension d^{n+m}.

For simplicity, in Section 6.3, we only consider the special case where each X_λ is diagonal. This assumption is justified when X is subject to some additional symmetry (see Section 6.3.1 for more details). For example, under certain symmetry X is diagonal in the so-called Gelfand–Tsetlin basis and can thus be written as a linear combination of primitive idempotents of the

[1] In fact, d can even be symbolic!

partially transposed permutation algebra $\mathcal{A}^d_{n,m}$ from Section 3.6. Since the elements of $\mathcal{A}^d_{n,m}$ can be lifted from $\mathcal{B}^d_{n,m}$, this allows us to perform the entire computation within the walled Brauer algebra $\mathcal{B}^d_{n,m}$. In contrast to $\mathcal{A}^d_{n,m}$, $\mathcal{B}^d_{n,m}$ is diagrammatic, and hence we do not need to manipulate any matrices of size d^{n+m}. This is precisely why the complexity of our approach does not scale in d. In particular, we do not require explicit knowledge of the mixed Schur transform.

Our second approach, presented in Section 6.4, works with general matrix units $E_{S,T}$ for the algebra $\mathcal{A}^d_{n,m}$, so we do not assume that X_λ is diagonal. We use the properties of these matrix units and their representation in mixed Schur basis to simplify general SDPs of a form similar to Eq. (6.2) to smaller SDPs without assuming additional symmetries. This provides a concrete tool for obtaining numerical insights for small instances of previously practically unsolvable SDPs.

6.2 Preliminaries

Unitary equivariance

Our main motivating problem is the optimisation of a linear function over unitary-equivariant quantum channels. For this chapter, we define $V_{\text{in}} := (\mathbb{C}^d)^{\otimes n}$ and $V_{\text{out}} := (\mathbb{C}^d)^{\otimes m}$.

6.2.1. Definition. We say that $\Phi\colon \mathrm{End}(V_{\text{in}}) \to \mathrm{End}(V_{\text{out}})$ is a $n \to m$ *channel*. Such a channel is *locally* U_d*-equivariant* or simply *unitary-equivariant* if

$$\Phi\big(U^{\otimes n}\,\rho\,U^{\dagger\otimes n}\big) = U^{\otimes m}\,\Phi(\rho)\,U^{\dagger\otimes m} \tag{6.4}$$

for every $U \in \mathrm{U}_d$ and $\rho \in \mathrm{D}(V_{\text{in}})$.

To optimise over such channels, we need to understand their structure or, equivalently, the structure of the associated Choi matrices. The following is a well-known characterisation of the unitary equivariance of Φ in terms of its Choi matrix.

6.2.2. Proposition. *Let $X^\Phi \in \mathrm{End}(V_{in} \otimes V_{out})$ be the Choi matrix of a $n \to m$ channel Φ. Then Φ is unitary-equivariant if and only if*

$$\big[X^\Phi, U^{\otimes n} \otimes \bar{U}^{\otimes m}\big] = 0, \qquad \forall U \in \mathrm{U}_d\,. \tag{6.5}$$

Proof:
Using the definition of the Choi matrix Eq. (2.2) we get

$$\begin{aligned}\Phi\big(U^{\otimes n}\,\rho\,U^{\dagger\otimes n}\big) &= \mathrm{Tr}_{V_{\text{in}}}\big[X^\Phi((U^{\otimes n}\rho U^{\dagger\otimes n})^{\mathsf{T}} \otimes I_{\text{out}})\big] &(6.6)\\ &= \mathrm{Tr}_{V_{\text{in}}}\big[((U^{\mathsf{T}})^{\otimes n} \otimes I_{\text{out}})X^\Phi(\bar{U}^{\otimes n} \otimes I_{\text{out}})(\rho^{\mathsf{T}} \otimes I_{\text{out}})\big], &(6.7)\end{aligned}$$

so unitary equivariance of Φ gives for every $U \in \mathrm{U}_d$

$$\begin{aligned}\Phi(\rho) &= \mathrm{Tr}_{V_{\text{in}}}\big[X^\Phi(\rho^{\mathsf{T}} \otimes I_{\text{out}})\big] &(6.8)\\ &= U^{\dagger\otimes m}\Phi\big(U^{\otimes n}\,\rho\,U^{\dagger\otimes n}\big)U^{\otimes m} &(6.9)\\ &= \mathrm{Tr}_{V_{\text{in}}}\big[((U^{\mathsf{T}})^{\otimes n} \otimes U^{\dagger\otimes m})X^\Phi(\bar{U}^{\otimes n} \otimes U^{\otimes m})(\rho^{\mathsf{T}} \otimes I_{\text{out}})\big]. &(6.10)\end{aligned}$$

Since the above relation holds for every $U \in \mathrm{U}_d$, we can switch $\bar{U} \to U$, so we get

$$\big[X^\Phi, U^{\otimes n} \otimes \bar{U}^{\otimes m}\big] = 0, \tag{6.11}$$

i.e. our convention is that the last m registers of X^Φ are subject to the dual action of U_d. □

Motivating problem

Consider the following motivating semidefinite optimisation problem. Fix a quantum state $\rho \in \mathrm{D}(V_{\mathrm{in}})$ and an arbitrary Hermitian matrix $H \in \mathrm{End}(V_{\mathrm{out}})$, and assume that we want to find a unitary-equivariant $n \to m$ channel Φ that maximises the linear function $\mathrm{Tr}[\Phi(\rho)H]$. For example, if $H = |\psi\rangle\langle\psi|$ for some pure state $|\psi\rangle \in V_{\mathrm{out}}$ then $\mathrm{Tr}[\Phi(\rho)H] = \langle\psi|\Phi(\rho)|\psi\rangle$ is the fidelity between the output state $\Phi(\rho)$ and the desired target state $|\psi\rangle$.

According to Eq. (2.2), $\mathrm{Tr}[\Phi(\rho)H] = \mathrm{Tr}\big[X^\Phi(\rho^\mathsf{T} \otimes H)\big]$, so the constraints on X^Φ from Eq. (2.3) give us the following SDP:

$$\max_{X^\Phi \in \mathrm{End}(V_{\mathrm{in}} \otimes V_{\mathrm{out}})} \mathrm{Tr}\big[X^\Phi(\rho^\mathsf{T} \otimes H)\big], \quad \mathrm{Tr}_{V_{\mathrm{out}}}(X^\Phi) = I_{V_{\mathrm{in}}}, \quad X^\Phi \succeq 0. \tag{6.12}$$

This problem has a trivial solution—a channel that ignores its input ρ and prepares the principal eigenvector of H as output. To make the problem non-trivial, consider instead a collection of n pairs (ρ_i, H_i), with the goal of maximising the smallest value of $\mathrm{Tr}[\Phi(\rho_i)H_i]$, $i = 1, \ldots, n$. This is captured by the following SDP:

$$\max_{\substack{X^\Phi \in \mathrm{End}(V_{\mathrm{in}} \otimes V_{\mathrm{out}}) \\ c \in \mathbb{R}}} c, \quad \forall i\colon \mathrm{Tr}\big[X^\Phi(\rho_i^\mathsf{T} \otimes H_i)\big] \geqslant c, \quad \mathrm{Tr}_{V_{\mathrm{out}}}(X^\Phi) = I_{V_{\mathrm{in}}}, \quad X^\Phi \succeq 0. \tag{6.13}$$

This problem no longer admits a trivial solution where Φ ignores the input state.

Motivated by applications to problems mentioned in Section 6.1, we would like to incorporate the unitary-equivariance constraint (6.4) on the channel Φ in the SDPs (6.12) and (6.13). Note that using Proposition 6.2.2 in a naive way would result in an optimisation problem with an uncountable number of linear constraints and a matrix variable of dimension d^{n+m} that scales badly in d even for constant n and m. Our main contribution is an efficient method that can deal with both of these issues simultaneously. Under additional symmetry assumptions, it reduces the above SDPs to finite linear programs whose size does not scale in d. We further describe how to remove the symmetry assumption with two different methods, in Section 6.4 and in Section 6.A.2.

Optimisation under unitary equivariance

Symmetry is a powerful tool for simplifying almost any type of problem, including problems in semidefinite optimisation [BGSV12; RMB21]. Our goal is to investigate semidefinite optimisation for a matrix variable subject to a unitary equivariance constraint. To simplify the problem even further, we assume one of several additional symmetries that reduce the semidefinite program to a linear program.

A naive way of imposing unitary equivariance on Φ in our motivating problem in Eq. (6.13) is by including Eq. (6.5) as an extra linear constraint. However, this technically constitutes an uncountably infinite set of constraints. To get around this issue, we could instead demand that

$$\int_{U \in \mathrm{U}_d} \big(U^{\otimes n} \otimes \bar{U}^{\otimes m}\big) X^\Phi \big(U^{\otimes n} \otimes \bar{U}^{\otimes m}\big)^\dagger dU = X^\Phi \tag{6.14}$$

where dU denotes the Haar measure on U_d. This integral can in principle be evaluated using Weingarten calculus [CMN21; CŚ06], producing a single linear constraint on X^Φ. The resulting SDP has finite size and can be supplied to a standard solver.

However, there is another serious issue that can prevent the SDP from being solvable in practice. Namely, X^Φ is a matrix of size $d^{n+m} \times d^{n+m}$. Since each matrix entry of X^Φ is represented by a separate scalar variable in the SDP, the total number of variables is $d^{2(n+m)}$, which is prohibitive even for moderate values of d.

Motivated by this issue, our main goal is to understand whether optimisation problems with a U_d-equivariance constraint can be solved in time that does not scale in d. In this work, we focus on linear programming as a special case of semidefinite programming and answer the above question in the affirmative (see Theorem 6.3.4 for our main result).

In the context of unitary-equivariant channels, linear programs occur naturally when additional symmetries are imposed on Φ. Indeed, appropriately chosen symmetries guarantee that the Choi matrix X^Φ is diagonal in a certain basis, allowing the semidefinite constraint $X^\Phi \succeq 0$ to be replaced by scalar inequalities.

Additional symmetries

One natural example of additional $n \to m$ channel symmetries is invariance under permutations of the n input and m output systems, where each type of system is permuted separately.

Recall that the symmetric group S_n on n elements acts naturally on n qudits by permuting them. This is captured by a representation $\psi_n^d \colon \mathrm{S}_n \to \mathrm{End}(V_{\mathrm{in}})$ defined on standard basis vectors $|i_1\rangle \otimes \cdots \otimes |i_n\rangle$ with $x_1, \ldots, x_n \in \{1, \ldots, d\}$ as

$$\psi_n^d(\pi)\big(|x_1\rangle \otimes \cdots \otimes |x_n\rangle\big) := |x_{\pi^{-1}(1)}\rangle \otimes \cdots \otimes |x_{\pi^{-1}(n)}\rangle, \tag{6.15}$$

for all $\pi \in \mathrm{S}_n$, and extended linearly to all vectors in V_{in}.

6.2.3. Definition. A $n \to m$ channel Φ is *input-symmetric* if $\Phi\big(\psi_n^d(\pi)\,\rho\,\psi_n^d(\pi)^\dagger\big) = \Phi(\rho)$, for every $\rho \in \mathrm{D}(V_{\mathrm{in}})$ and $\pi \in \mathrm{S}_n$. Similarly, Φ is *output-symmetric* if $\Phi(\rho) = \psi_m^d(\sigma)\,\Phi(\rho)\,\psi_m^d(\sigma)^\dagger$, for every $\rho \in \mathrm{D}(V_{\mathrm{in}})$ and $\sigma \in \mathrm{S}_m$. We call Φ *symmetric* if it is both input- and output-symmetric:

$$\Phi\big(\psi_n^d(\pi)\,\rho\,\psi_n^d(\pi)^\dagger\big) = \psi_m^d(\sigma)\,\Phi(\rho)\,\psi_m^d(\sigma)^\dagger. \tag{6.16}$$

if for every $\rho \in \mathrm{D}(V_{\mathrm{in}})$ and every pair of permutations $(\pi, \sigma) \in \mathrm{S}_n \times \mathrm{S}_m$.

Similarly to Proposition 6.2.2, this symmetry of Φ can also be expressed in terms of its Choi matrix X^Φ.

6.2.4. Proposition. *A $n \to m$ channel Φ is symmetric if and only if its Choi matrix X^Φ satisfies*

$$\big[X^\Phi, \psi_n^d(\pi) \otimes \psi_m^d(\sigma)\big] = 0, \qquad \forall (\pi, \sigma) \in \mathrm{S}_n \times \mathrm{S}_m. \tag{6.17}$$

In Section 6.3.1 we consider two additional types of symmetries and discuss when a unitary-equivariant SDP reduces to an LP under such symmetries.

The structure of unitary-equivariant quantum channels can be described using a generalisation of Schur–Weyl duality to mixed tensor products, i.e., mixed Schur–Weyl duality from Chapter 3.

6.3 Reducing unitary-equivariant SDPs to LPs

In this section, we derive one of the main results—a pre-processing algorithm for LP solvers which accepts a sparse SDP with a U_d-equivariant constraint as input. Our algorithm also requests one of several additional symmetries (see Section 6.3.1) that guarantee that the provided SDP reduces to an LP. Although the input problem has a compact representation due to all involved matrices being sparse, naively solving it might be impossible in practice due to prohibitively large d (the SDP matrix variable has dimension d^{n+m}). Our algorithm converts the implicit input LP to an explicit smaller LP whose naive representation has size that no

longer depends on d. Although it may generally not be sparse, this LP is much smaller and can thus be further supplied as input to any standard LP solver.

In Section 6.3.1 we list the additional symmetries our algorithm requires, in Section 6.3.2 we specify the input format of our algorithm, and in Section 6.3.3 we state and prove our main result.

6.3.1 Types of symmetries

To achieve a reduction from SDP to LP, the SDP matrix variable X needs some additional symmetry in addition to unitary equivariance. For example, one option is the $\mathrm{S}_n \times \mathrm{S}_m$ permutational symmetry, which is natural in the context of $n \to m$ quantum channels, see Proposition 6.2.4. We show in Section 6.3.1 that an SDP with such symmetry reduces to an LP when $\min(n, m) \leqslant 2$. The full list of possible symmetries we consider for the SDP variable X is as follows.

6.3.1. Definition. A matrix $X \in \mathrm{End}((\mathbb{C}^d)^{\otimes n+m})$ possesses

- the $\mathrm{S}_n \times \mathrm{S}_m$ *permutational symmetry* if for every $\sigma \in \mathbb{C}(\mathrm{S}_n \times \mathrm{S}_m) \subset \mathcal{B}^d_{n,m}$

$$\left[X, \psi^d_{n,m}(\sigma)\right] = 0, \tag{6.18}$$

  or equivalently $X \in \mathcal{Z}_{\psi^d_{n,m}(\mathbb{C}(\mathrm{S}_n \times \mathrm{S}_m))}(\mathcal{A}^d_{n,m})$;

- the *walled Brauer algebra symmetry* if for every $\sigma \in \mathcal{B}^d_{n,m}$, see Section 3.2,

$$\left[X, \psi^d_{n,m}(\sigma)\right] = 0, \tag{6.19}$$

  or equivalently $X \in \mathcal{Z}(\mathcal{A}^d_{n,m})$;

- the *Gelfand–Tsetlin symmetry* if for every $A \in \mathcal{X}^{\mathcal{A}}_{n+m}$, see Eq. (3.48),

$$[X, A] = 0, \tag{6.20}$$

  or equivalently $X \in \mathcal{X}^{\mathcal{A}}_{n+m}$ since $\mathcal{X}^{\mathcal{A}}_{n+m}$ is the maximal commutative subalgebra of $\mathcal{A}^d_{n,m}$ (see Section 3.6).

The last two symmetries have an intuitive interpretation in Schur basis. Recall from Theorem 3.4.1 that there exists a mixed Schur transform $U_{\mathrm{Sch}(n,m)}$ that block-diagonalises any unitary-equivariant X:

$$U_{\mathrm{Sch}(n,m)}\, X\, U^\dagger_{\mathrm{Sch}(n,m)} = \bigoplus_{\lambda \in \widehat{\mathcal{A}}^d_{n,m}} X_\lambda \otimes I_{m_\lambda}. \tag{6.21}$$

We will assume that $U_{\mathrm{Sch}(n,m)}$ is adapted to the Gelfand–Tsetlin basis, meaning that each X_λ is expressed in this basis. Each symmetry from Definition 6.3.1 results in some simplification of the matrix variable X as each block X_λ assumes a special form. We discuss this in more detail in the following sections.

Full walled Brauer algebra symmetry

The maximal possible symmetry that can be assumed is the full *walled Brauer algebra symmetry*, which means that each X_λ in Eq. (6.21) is proportional to the identity matrix, i.e.,

$$X_\lambda = v_\lambda I_{d_\lambda} \tag{6.22}$$

for some scalar $v_\lambda \in \mathbb{R}$. In this case, the semidefinite constraint $X_\lambda \succeq 0$ reduces to $v_\lambda \geqslant 0$, thus simplifying the problem from an SDP to an LP with variables $\{v_\lambda \mid \lambda \in \widehat{\mathcal{A}}^d_{n,m}\}$. The total number of variables in the LP is

$$N^d_{n,m}(\mathrm{WB}) := \left|\widehat{\mathcal{A}}^d_{n,m}\right| = \sum_{k=0}^{\min(n,m)} f^d_{n-k,m-k}, \tag{6.23}$$

where $f^d_{n-k,m-k}$ is the number of pairs (λ_l, λ_r) of Young diagrams such that $\lambda_l \vdash n-k$, $\lambda_r \vdash m-k$ and $\ell(\lambda_l) + \ell(\lambda_r) \leqslant d$. In this case, we can write X as a linear combination of the primitive central idempotents from Eq. (3.64):

$$X = \sum_{\lambda \in \widehat{\mathcal{A}}^d_{n,m}} v_\lambda \varepsilon^{\mathcal{A}}(\lambda). \tag{6.24}$$

Gelfand–Tsetlin symmetry

A minimal symmetry that can be assumed is the *Gelfand–Tsetlin symmetry*, which means that each X_λ is diagonal in the Gelfand–Tsetlin basis, i.e.,

$$X_\lambda = \sum_{i=1}^{d_\lambda} v_{\lambda,i} |i\rangle\langle i| \tag{6.25}$$

for some scalars $v_{\lambda,i} \in \mathbb{R}$ that become the variables of the LP. The $X \succeq 0$ constraint then reduces to $v_{\lambda,i} \geqslant 0$ for all $\lambda \in \widehat{\mathcal{A}}^d_{n,m}$ and $i \in [d_\lambda]$. The total number of LP variables in this case is

$$N^d_{n,m}(\mathrm{GT}) := \sum_{\lambda \in \widehat{\mathcal{A}}^d_{n,m}} d_\lambda, \tag{6.26}$$

where $d_\lambda = \dim(V_\lambda)$ is the dimension of the corresponding simple module of $\mathcal{A}^d_{n,m}$. In this case, we can write X as a linear combination of the canonical primitive idempotents from Eq. (3.65):

$$X = \sum_{T \in \mathrm{Paths}(\mathscr{A})} v_T \varepsilon^{\mathcal{A}}_T. \tag{6.27}$$

$\mathrm{S}_n \times \mathrm{S}_m$ permutational symmetry

A somewhat intermediate symmetry that can be assumed is the $\mathrm{S}_n \times \mathrm{S}_m$ *permutational symmetry*. This symmetry allows us to simplify X_λ to

$$X_\lambda \cong \bigoplus_{\substack{\mu \vdash_d n \\ \nu \vdash_d m}} (I_\mu \otimes I_\nu) \otimes \tilde{X}^\lambda_{\mu,\nu} \tag{6.28}$$

where $\tilde{X}^\lambda_{\mu,\nu}$ is a Hermitian matrix of dimension $m^\lambda_{\mu,\nu}(d)$, see Eq. (6.126) in Section 6.A.1, and a priori we do not know the basis on the right-hand side.

There are two cases when this symmetry leads to a reduction from SDP to LP. We show in Lemmas 6.A.1 and 6.A.2 that $m^\lambda_{\mu,\nu}(d) \in \{0,1\}$ when $\min(n,m) \leqslant 2$ or $d = 2$, meaning that the corresponding term in Eq. (6.28) either drops out or $\tilde{X}^\lambda_{\mu,\nu}$ becomes a scalar $\tilde{x}^\lambda_{\mu,\nu} \in \mathbb{R}$:

$$X_\lambda \cong \bigoplus_{\substack{\mu \vdash_d n \\ \nu \vdash_d m \\ m^\lambda_{\mu,\nu}(d)=1}} \tilde{x}^\lambda_{\mu,\nu} (I_\mu \otimes I_\nu). \tag{6.29}$$

We show in Proposition 6.3.2 that when $\min(n,m) = 1$ each block X_λ becomes diagonal specifically in the Gelfand–Tsetlin basis. In contrast to Eq. (6.25), some of the diagonal entries of X_λ must be equal in this case. In the following proposition we assume $m = 1$. The argument is completely analogous when $n = 1$ since one just has to use a different sequence $\mathcal{A}$ of algebras $\mathbb{C} \hookrightarrow \mathcal{A}^d_{0,1} \hookrightarrow \cdots \hookrightarrow \mathcal{A}^d_{0,m} \hookrightarrow \mathcal{A}^d_{1,m}$ when constructing the Bratteli diagram $\mathscr{A}$ and the corresponding Gelfand–Tsetlin basis.

6.3.2. Proposition. *Fix $d \geqslant 2$ and $n \geqslant 1$, and let $X \in \mathrm{End}((\mathbb{C}^d)^{\otimes n+1})$ be a Hermitian matrix with unitary equivariance and $\mathrm{S}_n \times \mathrm{S}_1$ symmetry:*

$$\big[X, U^{\otimes n} \otimes \bar{U}\big] = 0, \qquad \forall U \in \mathrm{U}_d, \tag{6.30}$$

$$\big[X, \psi^d_n(\pi) \otimes I_d\big] = 0, \qquad \forall \pi \in \mathrm{S}_n. \tag{6.31}$$

Then X can be written as

$$X = \sum_{T \in \mathrm{Paths}(\mathscr{A})} v_{T^n, T^{n+1}} \varepsilon^{\mathcal{A}}_T, \tag{6.32}$$

where $v_{T^n,T^{n+1}} \in \mathbb{R}$ depends only on the last edge of path T.

Proof:
Let us first understand in what way the $\mathrm{S}_n \times \mathrm{S}_1$ symmetry is special among general $\mathrm{S}_n \times \mathrm{S}_m$ symmetries. Since the group S_1 is trivial, $\mathbb{C}(\mathrm{S}_n \otimes \mathrm{S}_1) \cong \mathbb{C}\mathrm{S}_n$. Moreover, $\psi^d_{n,1}(\pi \times e) = \psi^d_n(\pi) \otimes I_d$ for any $\pi \in \mathrm{S}_n$, where $e \in \mathrm{S}_1$ denotes the identity permutation. Hence

$$\psi^d_{n,1}\big(\mathbb{C}(\mathrm{S}_n \otimes \mathrm{S}_1)\big) = \psi^d_n(\mathbb{C}\mathrm{S}_n) \otimes I_d = \mathcal{A}^d_{n,0} \hookrightarrow \mathcal{A}^d_{n,1}, \tag{6.33}$$

so the algebra $\mathcal{A}^d_{n,0}$ generated by the $\mathrm{S}_n \times \mathrm{S}_1$ symmetry appears in the multiplicity-free family $\mathbb{C} \hookrightarrow \mathcal{A}^d_{1,0} \hookrightarrow \cdots \hookrightarrow \mathcal{A}^d_{n,0} \hookrightarrow \mathcal{A}^d_{n,1}$.

We can use this observation to get a better grip on the matrix X. Thanks to the mixed Schur–Weyl duality (Theorem 3.4.1), Eq. (6.30) implies that $X \in \mathcal{A}^d_{n,1}$. Also, notice from Eq. (6.33) that Eq. (6.31) is equivalent to $[X, \mathcal{A}^d_{n,0}] = 0$. By combining these two observations we see that $X \in \mathcal{Z}_{\mathcal{A}^d_{n,0}}(\mathcal{A}^d_{n,1})$.

Writing any $A \in \mathcal{A}^d_{n,1}$ in Schur basis we get

$$U_{\mathrm{Sch}(n,1)}\, A\, U^\dagger_{\mathrm{Sch}(n,1)} = \bigoplus_{\lambda \in \widehat{\mathcal{A}}^d_{n,1}} A_\lambda \otimes I_{m_\lambda} \tag{6.34}$$

where the blocks A_λ are expressed in the Gelfand–Tsetlin basis. If we instead take $A \in \mathcal{A}^d_{n,0}$ then, thanks to how the Gelfand–Tsetlin basis is recursively constructed from paths in the Bratteli diagram, the A_λ in Eq. (6.34) are block-diagonal. That is, $A_\lambda = \bigoplus_\mu A_{\lambda,\mu}$ (there are no multiplicities here since the embedding $\mathcal{A}^d_{n,0} \hookrightarrow \mathcal{A}^d_{n,1}$ is part of a multiplicity-free family).

Since $[X, A] = 0$ for all $A \in \mathcal{A}^d_{n,0}$, the blocks X_λ of X are of the form $X_\lambda = \bigoplus_\mu c_{\lambda,\mu} I_{\lambda,\mu}$ for some $c_{\lambda,\mu} \in \mathbb{R}$. In particular, they are diagonal in the Gelfand–Tsetlin basis, so $X = \sum_{T \in \mathrm{Paths}(\mathscr{A})} v_T \varepsilon^{\mathcal{A}}_T$ for some $v_T \in \mathbb{R}$ for each path T. Moreover, all variables v_T that correspond

Symmetry	Ansatz for X	Formula for $N^d_{n,m}$	Values of $N^d_{n,m}$
Full walled Brauer algebra	Eq. (6.24)	Eq. (6.23)	Table 6.4
$\mathrm{S}_n \times \mathrm{S}_m$	Eq. (6.32)	Eq. (6.35)	Table 6.6
Gelfand–Tsetlin	Eq. (6.27)	Eq. (6.26)	Table 6.5
Only unitary equivariance	Eq. (6.21)	$\dim(\mathcal{A}^d_{n,m})$	Table 6.7

Table 6.1: Summary of symmetries from Definition 6.3.1. For each symmetry, we provide pointers to the corresponding ansatz for X, the number of variables $N^d_{n,m}$ in this ansatz, and tables for numerical values of $N^d_{n,m}$. Note that the ansatz (6.32) of X in case of the $\mathrm{S}_n \times \mathrm{S}_m$ symmetry is valid only when $m = 1$; a similar formula can also be obtained for $n = 1$ as explained just before Proposition 6.3.2.

to paths T that go through a fixed vertex at level n of the Bratteli diagram have the same value (this vertex labels a simple $\mathcal{A}^d_{n,0}$-module). Formally this means that $v_T = v_{\mathrm{S}}$ for every $T, \mathrm{S} \in \mathrm{Paths}(\mathscr{A})$ such that the paths T and S in the Bratteli diagram of $\mathcal{A}^d_{n,1}$ share the same last edge, i.e., $(T^n, T^{n+1}) = (\mathrm{S}^n, \mathrm{S}^{n+1})$. In particular, if $(T^n, T^{n+1}) = (\mu, \lambda)$ then $v_T = c_{\lambda,\mu}$. □

The number of variables in this case is

$$N^d_{n,m}(\mathrm{S}_n \times \mathrm{S}_m) := \sum_{\substack{\lambda \in \widehat{\mathcal{A}}^d_{n,m} \\ \mu \vdash_d n \\ \nu \vdash_d m}} \left(m^\lambda_{\mu,\nu}(d)\right)^2. \tag{6.35}$$

This number can be easily calculated numerically using the results of Section 6.A.1. The results of this calculation for small d, n, m can be found in Section 6.A.3.

Summary

The chosen symmetry, together with unitary equivariance, guarantees that X can be expressed as a linear combination of idempotents of the algebra $\mathcal{A}^d_{n,m}$, see Eqs. (6.24), (6.27) and (6.32):

$$X = \sum_{i=1}^{n} v_i \varepsilon_i^{\mathcal{A}}, \tag{6.36}$$

where the number of terms n is given by Eqs. (6.23), (6.26) and (6.35), respectively (see Table 6.1 for a summary). Since we effectively know the basis in which X is diagonal, the SDP reduces to an LP. In particular, the scalars $v_1, \ldots, v_n \in \mathbb{R}$ in Eq. (6.36) will be the variables of the output LP produced by our algorithm. The number of variables n varies dramatically depending on the chosen symmetry type, see Section 6.A.3.

6.3.2 Input specification

Our algorithm accepts a sparse SDP composed of the following objects:

1. $n, m \geqslant 0$ – the number of input and output systems,
2. $d \geqslant 2$ – the local dimension of $(\mathbb{C}^d)^{\otimes n+m} = V_{\mathrm{in}} \otimes V_{\mathrm{out}}$,
3. $X \succeq 0$ – a Hermitian matrix variable acting on $(\mathbb{C}^d)^{\otimes n+m}$ that has to obey the U_d-equivariance condition in Eq. (6.5),
4. (in)equality constraints that involve constant sparse matrices,

5. a desired additional type of symmetry (see Section 6.3.1 for possible options) which guarantees that the problem reduces to an LP.

Our algorithm outputs an explicit LP, equivalent to the input one, whose size does not depend on d and which can be further fed as an input to a standard LP solver. We are concerned only with this pre-processing step and its complexity.

The input to our algorithm is an SDP in the following form:

$$\begin{aligned} \max_X \quad & \operatorname{Tr}(CX) \\ \text{s.t.} \quad & \operatorname{Tr}(A_k X) \leqslant b_k, && \forall k \in [m_1], \\ & \operatorname{Tr}_{S_k}(X) = D_k, && \forall k \in [m_2], \\ & \left[X, U^{\otimes n} \otimes \bar{U}^{\otimes m}\right] = 0, && \forall U \in \mathrm{U}_d, \\ & X \succeq 0, \end{aligned} \tag{6.37}$$

where m_1 and m_2 denote the number of constraints that involve full trace and partial trace, respectively. Recall from Eq. (6.5) that the penultimate condition is equivalent to unitary-equivariance of the superoperator associated to X.

The Hermitian matrices C and A_k in Eq. (6.37) are constant and *s-sparse*, meaning that they can be written as a linear combination of at most s terms, where each term is either $\psi^d_{n,m}(\sigma)$ for some diagram σ of the walled Brauer algebra $\mathcal{B}^d_{n,m}$ or an elementary standard basis matrix whose all entries are 0 and only one entry is 1, i.e., $|i\rangle\langle j|$ for some $i, j \in [d]^{n+m}$. Each D_k is a Hermitian linear combination of at most s diagrams from the walled Brauer algebra $\mathcal{B}^d_{n_k,m_k}$ obtained by removing the nodes $S_k \subseteq [n+m]$ from $\mathcal{B}^d_{n,m}$. The remaining number of nodes on each side of the wall of $\mathcal{B}^d_{n_k,m_k}$ is $n_k := n - |S_k \cap [n]|$ and $m_k := m - |(S_k - n) \cap [m]|$. The total size of the input SDP in terms of the number of scalars needed to specify the matrices C, A_k, D_k is [2]

$$(1 + m_1 + m_2)s. \tag{6.38}$$

The SDP may contain additional scalar variables that need not obey the unitary equivariance condition. Such variables do not require any pre-processing by our algorithm, so they do not incur additional costs in our setting.

If the input SDP contains partial trace constraints, our algorithm has the following technical restriction: we require the local dimension d to be sufficiently large, namely

$$d \geqslant n + m - \min_k |S_k|. \tag{6.39}$$

In particular, if X is a Choi matrix of a $n \to m$ channel and we include the partial trace constraint $\operatorname{Tr}_{V_{\text{out}}}(X) = I_{V_{\text{in}}}$ to capture trace preservation, we require that $d \geqslant n$. Due to this, for example, we cannot apply our formalism to the setting of [BLMMO22] where $d = 2$ and n is large. To remove this restriction, one would have to know the kernel of the map $\psi^d_{n,m}$ in order to correctly process the partial trace constraints in the SDP (see Example 2.8.2 for an instance where the kernel is non-trivial).

6.3.3. Remark. As outlined in Section 6.A.2, one way to obtain the kernel of $\psi^d_{n,m}$ is by using the primitive idempotents $\varepsilon^{\mathcal{A}}_T$ to compute the blocks of $\psi^d_{n,m}\left(\sum_{j=1}^{(n+m)!} b_j \sigma_j\right)$ where b_j are symbolic variables and σ_j are walled Brauer diagrams. Equating these blocks to zero produces linear equations in b_j that reveal the linear dependencies among the matrices $\psi^d_{n,m}(\sigma_j)$. We can store this information in a database and use it to reduce the complexity of multiplication in the diagrammatic algebra $\mathcal{B}^d_{n,m}$, i.e., the preimage of $\mathcal{A}^d_{n,m}$ under $\psi^d_{n,m}$. This can lead to an improved complexity in our main result Theorem 6.3.4 since the complexity parameter N can be lowered from $(n+m)!$ to $\dim(\mathcal{A}^d_{n,m})$.

[2] For simplicity, we do not count the m_2 additional parameters needed to specify the scalars b_k and the additional information needed to specify the subsets S_k in Eq. (6.37).

6.3.3 Main result

The input to our algorithm is an SDP of the form (6.37) which involves a unitary-equivariant constraint and has the following parameters:

- n and m – number of input and output systems,
- d – local dimension of each system,
- s – sparsity of matrices C, A_k, D_k,
- m_1 – number of inequality constraints,
- m_2 – number of equality constraints with partial trace.

We assume that n and m are small constants while d may generally be large. The complexity of our algorithm will scale in $(n+m)!$ but not d. This is in contrast to the naive approach of solving an SDP with a matrix variable X of dimension d^{n+m}. While the naive approach quickly becomes impractical as d grows, our method does not suffer from this problem. In fact, it even offers performance improvements for small d such as $d = 2$. Our algorithm requires assuming that X has one of the symmetries listed in Section 6.3.1, which guarantees that the SDP reduces to an LP.

The following is a formal statement of our main result.

6.3.4. Theorem. *Any SDP of the form (6.37), where X has one of the symmetries listed in Definition 6.3.1, can be converted to an equivalent LP with $\tilde{N}$ variables and $m_1 + m_2 N + \tilde{N}$ constraints. The number of variables $\tilde{N} := N^d_{n,m}(sym)$, which depends on n, m, d and the chosen symmetry sym (see Table 6.1), can always be bounded as*

$$N^d_{n,m}(sym) \leqslant \dim(\mathcal{A}^d_{n,m}) \leqslant (n+m)! =: N. \tag{6.40}$$

The algorithm consists of two parts:

1. *an input-independent pre-computation that needs to be done only once for each set of parameters n, m, d, and whose complexity does not scale in d,*
2. *and SDP-to-LP conversion that takes time*

$$(1 + m_1 + m_2)s \cdot \tilde{N} N \tag{6.41}$$

where $(1 + m_1 + m_2)s$ is the size of the input SDP.

If $d \geqslant n+m$, the run-time of the pre-computation does not scale in d, while for small $d < n+m$ additional speedup is gained. If the SDP contains partial trace constraints, i.e., $m_2 > 0$, we require that $d \geqslant n + m - \min_k |S_k|$.

6.3.5. Remark. For the sake of simplicity we will ignore various details in our analysis. In particular, we will assume that the following operations take constant time: multiplying two walled Brauer algebra diagrams, contracting a diagram with a rank-1 matrix, or computing the (partial) trace of a diagram. In reality the complexity of these operations scales with $n+m$, which is small compared to our yardstick $N = (n+m)!$. Similarly, we will ignore the fact that the input size scales as $2(n+m)\log_2 d$ when the SDP contains rank-1 matrices. Finally, we will also ignore the fact that storing the value $d^{\text{loops}(\sigma)}$ requires $(n+m)\log_2 d$ bits.

Proof:
Our algorithm consists of two parts: (1) pre-computation of a database of $\mathcal{A}^d_{n,m}$ idempotents and (2) processing the input SDP to an LP.

The pre-computation of a database of $\mathcal{A}^d_{n,m}$ idempotents can be done upfront since it depends only on the parameters n, m, d but not the input SDP. The type of idempotents needed depends on the specified symmetry type *sym* (see Section 6.3.1). In either case, they can be computed diagrammatically using the DLS algorithm from Section 3.6. It produces a list of preimages $\varepsilon_1, \ldots, \varepsilon_n \in \mathcal{B}^d_{n,m}$ of $\mathcal{A}^d_{n,m}$ idempotents, with each ε_i expressed as a linear combination of walled Brauer algebra diagrams σ_j[3]:

$$\varepsilon_i = \sum_{j=1}^{(n+m)!} \alpha_{ij} \sigma_j. \tag{6.42}$$

The resulting $\tilde{N} \times (n+m)!$ coefficient matrix α is the output of the pre-computation step. By construction, its entries are rational.

The second part of the algorithm requires a U_d-equivariant SDP as input and reduces it to an explicit LP whose size is d-independent. The main idea of this algorithm is that we can evaluate all traces appearing in Eq. (6.37) diagrammatically without ever explicitly computing any of the $d^{n+m} \times d^{n+m}$ matrices involved (see Section 3.A.1). Let us discuss this step in more detail.

Due to unitary equivariance and the additional symmetry *sym*, we can express the matrix variable X as a linear combination of idempotents $\psi^d_{n,m}(\varepsilon_i)$ with unknown coefficients $v_i \in \mathbb{R}$ as in Eq. (6.36):

$$X = \sum_{i=1}^{\tilde{N}} v_i \psi^d_{n,m}(\varepsilon_i). \tag{6.43}$$

These coefficients will be the variables of the output LP. The number $\tilde{N} = N^d_{n,m}(sym)$ of variables v_i and idempotent preimages ε_i depends on the type of symmetry (see Table 6.1 in Section 6.3.1). Since $\psi^d_{n,m}(\varepsilon_i) \succeq 0$ and these idempotents are mutually orthogonal for different i, the positive semidefinite constraint $X \succeq 0$ reduces to

$$v_i \geqslant 0, \quad \forall i = 1, \ldots, \tilde{N}. \tag{6.44}$$

For the target function and each of the constraints in Eq. (6.37), we can evaluate the corresponding trace via diagram contraction. The main idea is to expand X as a linear combination of $\psi^d_{n,m}(\sigma_j)$ using Eqs. (6.42) and (6.43):

$$X = \sum_{i=1}^{\tilde{N}} v_i \sum_{j=1}^{(n+m)!} \alpha_{ij} \psi^d_{n,m}(\sigma_j). \tag{6.45}$$

Since the constant matrices C and A_k in Eq. (6.37) are s-sparse, they are already provided to us as linear combinations of diagrams and elementary rank-1 matrices. Using these expansions together with Eq. (6.45), we can diagrammatically evaluate all traces in Eq. (6.37) by linearity (see Section 3.A.1 for more details).

In particular, the objective function can be written in terms of the LP variables v_i as follows:

$$\mathrm{Tr}(CX) = \sum_{i=1}^{\tilde{N}} v_i \sum_{j=1}^{(n+m)!} \alpha_{ij} \mathrm{Tr}\big(C \psi^d_{n,m}(\sigma_j)\big) = \sum_{i=1}^{\tilde{N}} v_i c_i = c^{\mathsf{T}} v \tag{6.46}$$

[3]By knowing the kernel of $\psi^d_{n,m}$, we can express each ε_i more economically as $\varepsilon_i = \sum_{j=1}^{m} \alpha_{ij} \sigma_j$ where $m = \dim(\mathcal{A}^d_{n,m}) \leqslant (n+m)!$.

where $c \in \mathbb{R}^{\tilde{N}}$ is a vector with entries

$$c_i := \sum_{j=1}^{(n+m)!} \alpha_{ij} \operatorname{Tr}\big(C\psi^d_{n,m}(\sigma_j)\big). \tag{6.47}$$

Since C is s-sparse, we can use Proposition 3.A.1 in Section 3.A.1 to evaluate the trace. The total time it takes to compute the vector c is

$$\#i \cdot \#j \cdot s = \tilde{N}Ns. \tag{6.48}$$

Similarly, the k-th inequality constraint can be expressed as

$$\operatorname{Tr}(A_k X) = a_k^{\mathsf{T}} v \leqslant b_k \tag{6.49}$$

where each $a_k \in \mathbb{R}^{\tilde{N}}$ is a vector with entries

$$(a_k)_i := \sum_{j=1}^{(n+m)!} \alpha_{ij} \operatorname{Tr}\big(A_k\psi^d_{n,m}(\sigma_j)\big). \tag{6.50}$$

The total time it takes to compute the tensor a is

$$\#k \cdot \#i \cdot \#j \cdot s = m_1\tilde{N}Ns. \tag{6.51}$$

Next, let us fix k and deal with the k-th partial trace equality constraint. First, we expand the partial trace $\operatorname{Tr}_{S_k}(X)$ by linearity:

$$\operatorname{Tr}_{S_k}(X) = \sum_{i=1}^{\tilde{N}} v_i \sum_{j=1}^{(n+m)!} \alpha_{ij} \operatorname{Tr}_{S_k}\big(\psi^d_{n,m}(\sigma_j)\big). \tag{6.52}$$

If $\sigma_j^{S_k}$ denotes the diagram σ_j with pairs of nodes in the set S_k that are opposite to each other contracted, then the matrix corresponding to σ_j has partial trace

$$\operatorname{Tr}_{S_k}\big(\psi^d_{n,m}(\sigma_j)\big) = d^{\operatorname{loops}_{S_k}(\sigma_j)}\psi^d_{n_k,m_k}(\sigma_j^{S_k}) \tag{6.53}$$

where $\operatorname{loops}_{S_k}(\sigma_j)$ is the number of loops formed and (n_k, m_k) is the remaining number of systems on each side of the wall, see Proposition 3.A.2 in Section 3.A.1. Substituting this into Eq. (6.52),

$$\operatorname{Tr}_{S_k}(X) = \sum_{i=1}^{\tilde{N}} v_i \sum_{j=1}^{(n+m)!} \alpha_{ij} d^{\operatorname{loops}_{S_k}(\sigma_j)}\psi^d_{n_k,m_k}(\sigma_j^{S_k}). \tag{6.54}$$

We need to compare this to D_k and derive a set of linear constraints.

Since D_k is a linear combination of diagrams,

$$D_k = \sum_{l=1}^{(n_k+m_k)!} e_{kl}\, \psi^d_{n_k,m_k}(\rho_l) \tag{6.55}$$

for some coefficients $e_{kl} \in \mathbb{R}$, where $\rho_l \in \mathcal{B}^d_{n_k,m_k}$ ranges over all walled Brauer algebra diagrams on $n_k + m_k = n + m - |S_k|$ nodes. Since $\sigma_j^{S_k}$ is a diagram in $\mathcal{B}^d_{n_k,m_k}$,

$$\psi^d_{n_k,m_k}(\sigma_j^{S_k}) = \sum_{l=1}^{(n_k+m_k)!} \delta(\sigma_j^{S_k}, \rho_l)\, \psi^d_{n_k,m_k}(\rho_l) \tag{6.56}$$

where δ denotes the Kronecker delta function. Substituting this in Eq. (6.54),

$$\mathrm{Tr}_{S_k}(X) = \sum_{l=1}^{(n_k+m_k)!} \sum_{i=1}^{\tilde{N}} v_i \sum_{j=1}^{(n+m)!} \alpha_{ij} d^{\mathrm{loops}_{S_k}(\sigma_j)} \delta(\sigma_j^{S_k}, \rho_l)\, \psi^d_{n_k,m_k}(\rho_l). \tag{6.57}$$

Because of the assumption (6.39) that $d \geqslant n+m-\min_k |S_k|$, the representation $\psi^d_{n_k,m_k}$ is faithful due to Theorem 3.4.1, and hence the matrices $\psi^d_{n_k,m_k}(\rho_l)$ are linearly independent. Comparing the coefficients at $\psi^d_{n_k,m_k}(\rho_l)$ in Eqs. (6.55) and (6.57), we conclude that

$$\sum_{i=1}^{\tilde{N}} v_i \sum_{j=1}^{(n+m)!} \alpha_{ij} d^{\mathrm{loops}_{S_k}(\sigma_j)} \delta(\sigma_j^{S_k}, \rho_l) = e_{kl}. \tag{6.58}$$

In other words, for every $1 \leqslant l \leqslant (n_k + m_k)!$ we get a linear constraint

$$\sum_{i=1}^{n} v_i (d_{kl})_i = d_{kl}^{\mathsf{T}} v = e_{kl} \tag{6.59}$$

where each $d_{kl} \in \mathbb{R}^{\tilde{N}}$ is a vector with entries

$$(d_{kl})_i := \sum_{j=1}^{(n+m)!} \alpha_{ij} d^{\mathrm{loops}_{S_k}(\sigma_j)} \delta(\sigma_j^{S_k}, \rho_l). \tag{6.60}$$

To compute all entries d_{kli} of the above tensor, we can fix k and i and then evaluate the sum over j. For each j, we determine l such that $\sigma_j^{S_k} = \rho_l$ and add the contribution $\alpha_{ij} d^{\mathrm{loops}_{S_k}(\sigma_j)}$ to the corresponding entry d_{kli}. The total time it takes to perform this computation is

$$\#k \cdot \#i \cdot \#j = m_2 \cdot \tilde{N} \cdot (n+m)! = m_2 \tilde{N} N. \tag{6.61}$$

Combining everything together, the output of our algorithm is the following LP:

$$\begin{aligned} \max_{v} \quad & c^{\mathsf{T}} v \\ \text{s.t.} \quad & a_k^{\mathsf{T}} v \leqslant b_k, \quad && \forall k \in [m_1], \\ & d_{kl}^{\mathsf{T}} v = e_{kl}, \quad && \forall k \in [m_2], l \in \big[(n_k+m_k)!\big], \\ & v_i \geqslant 0, && \forall i \in [\tilde{N}]. \end{aligned} \tag{6.62}$$

It has $\tilde{N} \leqslant N$ variables v_i and

$$m_1 + \sum_{k=1}^{m_2} (n_k+m_k)! + \tilde{N} \leqslant m_1 + m_2 N + \tilde{N} \tag{6.63}$$

constraints. The total number of scalar constants needed to specify the tensors c, a, d appearing[4] in this LP is

$$(1 + m_1 + m_2 N)\tilde{N}. \tag{6.64}$$

The total amount of time it takes to compute these tensors is obtained by adding together Eqs. (6.48), (6.51) and (6.61):

$$\tilde{N} N s + m_1 \tilde{N} N s + m_2 \tilde{N} N \leqslant (1 + m_1 + m_2) \tilde{N} N s. \tag{6.65}$$

This completes the description and complexity analysis of our algorithm. □

[4] The tensor e defined in Eq. (6.55) is already given to us as part of the input.

6.3.6. Remark. Our proof did not use the assumption that the input matrices D_k are s-sparse. This assumption only helps to keep the input SDP more compact and makes it easier to compare its size to that of the output LP. The size of the problem description grows by a factor of $\tilde{N}N$ during the conversion.

6.3.7. Remark. Our framework can be straightforwardly generalised from SDPs of the form (6.37) to the following slightly more general form:

$$\begin{aligned} \max_{X,x_1,\ldots,x_M} \quad & c_1x_1 + \cdots + c_Mx_M \\ \text{s.t.} \quad & \operatorname{Tr}(A_kX) \leqslant x_1a_{k1} + \cdots + x_Ma_{kM} + b_k, && \forall k \in [m_1], \\ & \operatorname{Tr}_{S_k}(\tilde{A}_kX) = D_k, && \forall k \in [m_2], \\ & \left[X, U^{\otimes n} \otimes \bar{U}^{\otimes m}\right] = 0, && \forall U \in \mathrm{U}_d, \\ & X \succeq 0, \end{aligned} \tag{6.66}$$

where A_k are constant s-sparse matrices that are provided as a linear combination of diagrams and elementary rank-1 matrices, and $\tilde{A}_k, D_k$ are linear combinations of at most s walled Brauer diagrams on registers that are left after tracing out systems S_k. We use this more general form of SDPs in Section 6.5.2.

6.4 Simplifying unitary-equivariant SDPs

In this section, we make a step towards removing symmetry assumptions described in Section 6.2 and simplify the SDP defined in Eq. (6.2) directly to a smaller SDP. The key ingredient here is trace calculations of *matrix units* (see Section 2.7.6) for the $\mathcal{A}^d_{n,m}$ algebra. Namely, the matrix units $E_{T,S}$ that can be defined for a pair of paths $T, S \in \operatorname{Paths}(\lambda, \mathscr{A})$ via mixed Schur transform (see Chapter 3) as follows:

$$E_{T,S} := U^\dagger_{\mathrm{Sch}(n,m)} \left(\bigoplus_{\mu \in \widehat{\mathcal{A}}^d_{n,m}} \delta_{\lambda\mu} |T\rangle\langle S| \otimes I_{m_\lambda} \right) U_{\mathrm{Sch}(n,m)}, \tag{6.67}$$

where m_λ is the dimension of the Weyl module λ of U_d, $I_{m_\lambda} = \sum_{M \in \mathrm{GT}(\lambda,d)} |M\rangle\langle M|$ is the identity matrix on the unitary irrep register for irrep λ. These matrix units form a basis of $\mathcal{A}^d_{n,m}$ and span the whole algebra:

$$\mathcal{A}^d_{n,m} = \operatorname{span}_{\mathbb{C}} \left\{ E_{T,S} \;\middle|\; \lambda \in \widehat{\mathcal{A}}^d_{n,m},\ S, T \in \operatorname{Paths}(\lambda, \mathscr{A}) \right\}. \tag{6.68}$$

One can think about matrix units as tensor networks obtained from the matrix product state representation of mixed Schur basis vectors from Lemma 4.2.1, see Fig. 6.1. Notice that the trace of a matrix unit for $T, S \in \operatorname{Paths}(\lambda, \mathscr{A})$ is

$$\operatorname{Tr}(E_{T,S}) = \delta_{T,S} m_\lambda, \tag{6.69}$$

and their product satisfies

$$E_{S,T} \cdot E_{T'S'} = \delta_{T,T'} E_{S,S'}. \tag{6.70}$$

Thanks to mixed Schur–Weyl duality (see Chapter 3), the unitary equivariance constraint on a matrix $X \in \operatorname{End}((\mathbb{C}^d)^{\otimes n+m})$ implies that it can be written as a linear combination of the matrix units of the matrix algebra $\mathcal{A}^d_{n,m}$, i.e.,

$$X = \sum_{\lambda \in \widehat{\mathcal{A}}^d_{n,m}} \sum_{S,T \in \operatorname{Paths}(\lambda,\mathscr{A})} x_{S,T} E_{S,T} \tag{6.71}$$

for some coefficients $x_{S,T} \in \mathbb{C}$.

Therefore, to simplify the full and partial trace constraints in Eq. (6.37) we need to understand how to compute traces of matrix units.

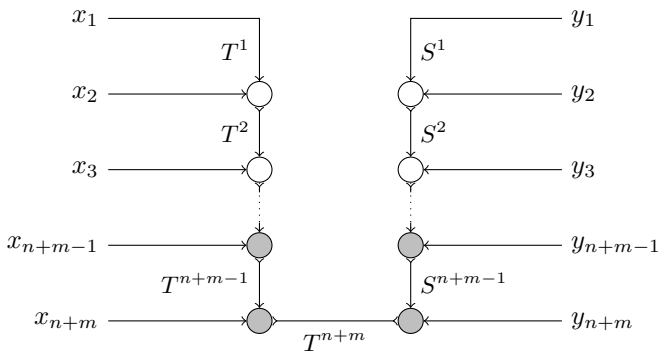

Figure 6.1: Pictorial representation of the matrix unit $E_{T,S}$ from Eq. (6.67) as a tensor network, where $T, S \in \mathrm{Paths}(\lambda, \mathscr{A})$ for some $\lambda \in \widehat{\mathcal{A}}^d_{n,m}$. The strings $x_1, \ldots, x_{n+m} \in [d]$ and $y_1, \ldots, y_{n+m} \in [d]$ index rows and columns of E_{TS} as a matrix in the standard computational basis of $(\mathbb{C}^d)^{\otimes n+m}$.

6.4.1 Full trace

In this section, we present methods to efficiently compute the trace $\mathrm{Tr}(YX)$ of the product of two matrices X and Y, where X is of the form (6.71) and Y is assumed to be of one of three special forms: it is either a matrix unit $E_{S,T}$ of $\mathcal{A}^d_{n,m}$, a matrix unit $|I\rangle\langle J|$ of $\mathrm{End}((\mathbb{C}^d)^{n+m})$, or $\psi^d_{n,m}(\pi)$, where π is a walled Brauer diagram.

First, consider the case when the matrix Y is a matrix unit, i.e. $Y = E_{S,T}$ for some $S, T \in \mathrm{Paths}(\lambda, \mathscr{A})$. As the matrix X is of the form (6.71), by elementary properties of matrix units,

$$\mathrm{Tr}(YX) = \sum_{T',S'} x_{T',S'} \,\mathrm{Tr}(E_{S,T} E_{T',S'}) = x_{T,S} \cdot m_\lambda. \tag{6.72}$$

Next, consider the case when the matrix Y is written in the computational basis and has only a single non-zero entry, i.e. $Y = |I\rangle\langle J|$ for some strings $I = (i_1, \ldots, i_{n+m}) \in [d]^{n+m}$ and $J = (j_1, \ldots, j_{n+m}) \in [d]^{n+m}$. To compute the trace $\mathrm{Tr}(YX)$, we need to rewrite the entries of the matrix X from (6.71) in the computational basis by applying mixed Schur transform:

$$\begin{aligned}\mathrm{Tr}(|I\rangle\langle J|X) &= \langle J|X|I\rangle \\ &= \sum_{\lambda \in \widehat{\mathcal{A}}^d_{n,m}} \sum_{S,T \in \mathrm{Paths}(\lambda,\mathscr{A})} x_{TS} \sum_{M \in \mathrm{GT}(\lambda,d)} \langle J|U^\dagger_{\mathrm{Sch}(n,m)}|(T,M)\rangle\langle (S,M)|U_{\mathrm{Sch}(n,m)}|I\rangle. \end{aligned} \tag{6.73}$$

Using previously derived form of mixed Schur transform in Eq. (4.17), the computation of $\langle (T,M)|U_{\mathrm{Sch}(n,m)}|I\rangle = \langle I|U^\dagger_{\mathrm{Sch}(n,m)}|(T,M)\rangle$ is reduced to the multiplication of Clebsch–Gordan matrices:

$$\langle I|U^\dagger_{\mathrm{Sch}(n,m)}|(T,M)\rangle = \begin{cases} \langle M|C^{i_{n+m}, w(i_{n+m-1},\ldots,i_1)}_{T^{n+m}T^{n+m-1}} \cdots C^{i_2}_{T^2T^1}|i_1\rangle & w(I) = w(M), \\ 0 & w(I) \neq w(M), \end{cases} \tag{6.74}$$

where $|M\rangle$ is a Gelfand–Tsetlin basis vector for the Weyl module λ and the Clebsch–Gordan matrices were defined in Eqs. (4.16) and (4.17). Notice that $\sum_{M \in \mathrm{GT}(\lambda,d)} |M\rangle\langle M| = I_{m_\lambda}$, hence we can rewrite Eq. (6.73) as

$$\langle J|X|I\rangle = \sum_{S,T} x_{S,T} \langle j_1| \left(C^{i_2}_{S^2S^1}\right)^\dagger \cdots \left(C^{j_{n+m}, w(j_{n+m-1},\ldots,j_1)}_{S^{n+m}S^{n+m-1}}\right)^\dagger C^{i_{n+m}, w(i_{n+m-1},\ldots,i_1)}_{T^{n+m}T^{n+m-1}} \cdots C^{i_2}_{T^2T^1}|i_1\rangle \tag{6.75}$$

when the weights of the strings I, J are the same, i.e. $w(I) = w(J)$; when $w(I) \neq w(J)$ then $\langle J|X|I\rangle = 0$. As it we demonstrated in Section 4.2.1, the Clebsch–Gordan matrices in the

above equations have dimensions given the by Kostka numbers $K_{T^{(k)},w(i_k,\dots,i_1)}$ and $K_{S^{(k)},w(j_k,\dots,j_1)}$ respectively, and the complexity of computing the coefficients in Eq. (6.75) is $(n+m)^{O(d^2)}$.

Finally, consider the case when the matrix Y is an image of a single Brauer diagram $\pi \in \mathcal{B}^d_{n,m}$, i.e. $Y = \psi^d_{n,m}(\pi) \in \mathcal{A}^d_{n,m}$. In order to compute the trace $\mathrm{Tr}(\psi^d_{n,m}(\pi)X)$, we shall compute the matrix entries of $\psi^d_{n,m}(\pi)$ in the Gelfand–Tsetlin basis of all irreducible representations of $\mathcal{A}^d_{n,m}$. For this purpose, we shall present the diagram $\pi \in \mathcal{B}^d_{n,m}$ in terms of the generators $\sigma_i \in \mathcal{B}^d_{n,m}$ of the walled Brauer algebra $\mathcal{B}^d_{n,m}$. Assume that the diagram π has exactly k contractions. By applying certain permutations $\sigma^u_l, \sigma^d_l \in \mathrm{S}_n$ and $\sigma^u_r, \sigma^d_r \in \mathrm{S}_m$ acting on the left and rights sides of the diagram π, it can be represented as

$$\pi = (\sigma^u_l \times \sigma^u_r)\tau_k(\sigma^d_l \times \sigma^d_r) \tag{6.76}$$

where τ_k is defined in Eqs. (3.15) and (3.16).

As $\sigma^u_l, \sigma^d_l \in \mathrm{S}_n$, they might be written as a product of at most n^2 transposition generators σ_i of the algebra $\mathcal{B}^d_{n,m}$, and similarly $\sigma^u_r, \sigma^d_r \in \mathrm{S}_m$ can be written as a product of m^2 transposition generators. Furthermore, the diagram τ_k can be decomposed into the generators σ_i of the algebra $\mathcal{B}^d_{n,m}$ as follows:

$$\tau_k = (\sigma_n\sigma_{n+1}\cdots\sigma_{n-k+1}\cdots\sigma_{n-1}\sigma_{n+k-1})\cdots(\sigma_n\sigma_{n+1}\sigma_{n+2}\sigma_{n-1}\sigma_{n-2})(\sigma_n\sigma_{n+1}\sigma_{n-1})\sigma_n \tag{6.77}$$

which is of length k^2. Altogether, the decomposition of an arbitrary diagram π into generators of the algebra $\mathcal{B}^d_{n,m}$ requires $O((n+m)^2)$ multiplications of these generators. We shall multiply these generators separately in the Gelfand–Tsetlin basis for each irreducible representation related to $\lambda \in \widehat{\mathcal{A}}^d_{n,m}$. Such multiplication has a complexity $O(d^3_\lambda)$, where d_λ is the dimension of the irreducible representation of $\mathcal{A}^d_{n,m}$ corresponding to λ. Since

$$\dim \mathcal{A}^d_{n,m} = \sum_{\lambda \in \widehat{\mathcal{A}}^d_{n,m}} d^2_\lambda, \tag{6.78}$$

the complexity of computing the aforementioned product of generators is $O\big(\big(\dim \mathcal{A}^d_{n,m}\big)^{3/2}\big)$.

Combining everything together, the total complexity of computing all matrix elements of $\psi^d_{n,m}(\pi)$, i.e. computing $\langle S|\psi_\lambda(\pi)|T\rangle$ for all $\lambda \in \widehat{\mathcal{A}}^d_{n,m}$ and $S, T \in \mathrm{Paths}(\lambda, \mathscr{A})$, is

$$O\Big((n+m)^2\big(\dim \mathcal{A}^d_{n,m}\big)^{3/2}\Big).$$

Note that having the matrix elements $\langle S|\psi_\lambda(\pi)|T\rangle$ allows us to write

$$\begin{aligned}
\mathrm{Tr}(YX) &= \mathrm{Tr}\big(\psi^d_{n,m}(\pi)X\big) && (6.79)\\
&= \sum_{\lambda \in \widehat{\mathcal{A}}^d_{n,m}} \sum_{S,T \in \mathrm{Paths}(\lambda)} \langle S|\psi_\lambda(\pi)|T\rangle \,\mathrm{Tr}(E_{S,T}X) && (6.80)\\
&= \sum_{\lambda \in \widehat{\mathcal{A}}^d_{n,m}} \sum_{S,T \in \mathrm{Paths}(\lambda)} \langle S|\psi_\lambda(\pi)|T\rangle \cdot x_{T,S} \cdot m_\lambda. && (6.81)
\end{aligned}$$

6.4.2 Partial trace

In this section, we present methods to efficiently compute the partial trace $\mathrm{Tr}_S(XY)$ of a product of two matrices where X is presented as a linear combination of the matrix units (6.71), and Y is also of one of the special forms mentioned in Section 6.4.1. For simplicity, we assume that the traced-out systems are always the last systems, i.e. we compute $\mathrm{Tr}_{S_k}(X)$ for sets $S_k := \{k+1, \dots, n+m\}$ for arbitrary k such that $1 \leqslant k \leqslant n+m-1$. In this case, we

can use the following general result by Ram and Wenzl [RW92], which we adopt to our setting of algebras $\mathcal{A}^d_{n,m}$ [5].

6.4.1. Lemma ([RW92]). *Consider any irreducible representation $\lambda \in \mathcal{A}^d_{n,m}$, two paths $S, T \in \mathrm{Paths}(\lambda, \mathscr{A})$ and the corresponding matrix unit $E_{S,T}$. One can decompose the paths S, T with respect to the last system, i.e. write $S = \bar{S} \to \lambda$ and $T = \bar{T} \to \lambda$, where $\bar{S} \in \mathrm{Paths}_{n+m-1}(\mu, \mathscr{A})$ and $\bar{T} \in \mathrm{Paths}_{n+m-1}(\mu', \mathscr{A})$ where $S^{n+m-1} = \mu$ and $T^{n+m-1} = \mu'$. Then the partial trace of the last system for the matrix unit $E_{S,T}$ is*

$$\mathrm{Tr}_{n+m} E_{S,T} = \begin{cases} \frac{m_\lambda}{m_\mu} E_{\bar{S},\bar{T}} & \mu = \mu', \\ 0 & \mu \neq \mu', \end{cases} \tag{6.82}$$

where m_λ, m_μ are dimensions of the corresponding Weyl modules.

For simplicity of notation, in this subsection, we rewrite the sequence of inclusions among the algebras $\mathcal{A}^d_k$ defined in Eq. (3.47) in the following way:

$$\mathcal{A}^d_0 \hookrightarrow \mathcal{A}^d_1 \hookrightarrow \cdots \hookrightarrow \mathcal{A}^d_{n+m-1} \hookrightarrow \mathcal{A}^d_{n+m}, \tag{6.83}$$

i.e. $\mathcal{A}^d_k := \mathcal{A}^d_{k,0}$ for $k \leqslant n$ and $\mathcal{A}^d_k := \mathcal{A}^d_{n,k-n}$ for $k \geqslant n$.

First, consider the case when $Y = I$ is the identity matrix. Applying Lemma 6.4.1 recursively, we have

$$\mathrm{Tr}_{S_k}(X) = \sum_{\lambda \in \widehat{\mathcal{A}}^d_{n,m}} \sum_{S,T \in \mathrm{Paths}(\lambda)} x_{S,T} \,\mathrm{Tr}_k \,\mathrm{Tr}_{k+1} \ldots \mathrm{Tr}_{n+m} E_{S,T} \tag{6.84}$$

$$= \sum_{\mu \in \widehat{\mathcal{A}}^d_k} \sum_{\lambda \in \widehat{\mathcal{A}}^d_{n,m}} \sum_{\substack{S,T \in \mathrm{Paths}(\lambda) \\ S^k = T^k = \mu \\ \forall i \geqslant k : S^i = T^i}} x_{S,T} \frac{m_\lambda}{m_\mu} E_{\bar{S},\bar{T}}, \tag{6.85}$$

where $\bar{S}, \bar{T} \in \mathrm{Paths}_k(\mu)$ are truncations of $S, T \in \mathrm{Paths}(\lambda)$ to the first k levels of the Bratteli diagram $\mathscr{A}$.

Second, consider the case when the matrix $Y = E_{S',T'}$ is a matrix unit for some $S', T' \in \mathrm{Paths}(\lambda, \mathscr{A})$. By elementary properties of matrix units and by applying Lemma 6.4.1 recursively, we have

$$\mathrm{Tr}_{S_k}(E_{S',T'} X) = \sum_{T \in \mathrm{Paths}(\lambda)} x_{T',T} \,\mathrm{Tr}_{S_k}(E_{S',T}) = \sum_{\mu \in \widehat{\mathcal{A}}^d_k} \sum_{\substack{T \in \mathrm{Paths}(\lambda) \\ T^k = \mu \\ \forall i \geqslant k : T^i = S'^i}} x_{T',T} \frac{m_\lambda}{m_\mu} E_{\bar{S}',\bar{T}} \tag{6.86}$$

where $\bar{S}', \bar{T} \in \mathrm{Paths}_k(\mu, \mathscr{A})$ are truncations of $S', T \in \mathrm{Paths}(\lambda, \mathscr{A})$ respectively to the first k levels of the Bratteli diagram $\mathscr{A}$.

Finally, consider the case where the matrix Y is the image of a single Brauer diagram $\pi \in \mathcal{B}^d_{n,m}$, i.e. $Y = \psi^d_{n,m}(\pi) \in \mathcal{A}^d_{n,m}$. In Section 6.4.1 we showed how to compute all matrix entries of $\psi^d_{n,m}(\pi)$ in all irreducible representations, i.e., how to compute $\langle S|\psi_\lambda(\pi)|T\rangle$ in time $O\big((n+m)^2 \big(\dim \mathcal{A}^d_{n,m}\big)^{3/2}\big)$. Having done so, we can use the same method as in Section 6.4.2

[5] In fact, it should be possible to adapt the same result for computing the partial trace over all types of subsystems $S \subset [n+m]$. Indeed, one can "SWAP" any two given subsystems using the so-called $6j$-*symbol*. In this way, the desired subsystems of S can be effectively swapped to the last positions.

to compute the partial trace:

$$\operatorname{Tr}_{S_k}(YX) = \operatorname{Tr}_{S_k}(\psi^d_{n,m}(\pi)X) = \sum_{\lambda\in\widehat{\mathcal{A}}^d_{n,m}} \sum_{S,T\in\mathrm{Paths}(\lambda)} \langle S|\psi_\lambda(\pi)|T\rangle \operatorname{Tr}_{S_k}(E_{S,T}X) \tag{6.87}$$

$$= \sum_{\lambda\in\widehat{\mathcal{A}}^d_{n,m}} \sum_{S,T\in\mathrm{Paths}(\lambda)} \langle S|\psi_\lambda(\pi)|T\rangle \sum_{\mu\in\widehat{\mathcal{A}}^d_k} \sum_{\substack{T'\in\mathrm{Paths}(\lambda)\\ S^k=T'^k=\mu\\ \forall i\geqslant k\,:\,T'^i=S^i}} x_{T,T'}\frac{m_\lambda}{m_\mu}E_{\bar{S},\bar{T}'} \tag{6.88}$$

$$= \sum_{\mu\in\widehat{\mathcal{A}}^d_k} \sum_{\lambda\in\widehat{\mathcal{A}}^d_{n,m}} \sum_{S,T\in\mathrm{Paths}(\lambda)} \sum_{\substack{T'\in\mathrm{Paths}(\lambda)\\ S^k=T'^k=\mu\\ \forall i\geqslant k\,:\,T'^i=S^i}} x_{T,T'}\langle S|\psi_\lambda(\pi)|T\rangle\frac{m_\lambda}{m_\mu}E_{\bar{S},\bar{T}'}. \tag{6.89}$$

6.4.3 Main result

Now we are ready to state the main result of the section. Consider the following class of SDPs, which is a slightly modified version of Eq. (6.37):

$$\begin{aligned} \max_X \quad & \operatorname{Tr}(CX) \\ \text{s.t.} \quad & \operatorname{Tr}(A_kX) \leqslant b_k, && \forall k\in[m_1], \\ & \operatorname{Tr}_{S_{i_k}}(D_kX) = B_k, && \forall k\in[m_2], \\ & \left[X, U^{\otimes n}\otimes\bar{U}^{\otimes m}\right] = 0, && \forall U\in\mathrm{U}_d, \\ & X\succeq 0, \end{aligned} \tag{6.90}$$

The matrices A_k, D_k, C are Hermitian, and we consider only a specific choice of the sets S_{i_k}, namely $S_{i_k} := \{i_k,\ldots,n+m\}$. In order to make the optimisation problem tractable, we make some additional assumptions on the form and sparseness of matrices A_k, C, D_k, B_k in the original problem. Hence, we analyse some particular cases in which the aforementioned matrices are given in one of the following forms:

1. they are arbitrary linear combinations of matrix units of $\mathcal{A}^d_{n,m}$,
2. they are sparse linear combinations of computational basis matrix units,
3. they are sparse linear combinations of diagrams that span $\mathcal{B}^d_{n,m}$.

The main result of this section (Theorem 6.4.2) characterises the complexity of rewriting the constraints in (6.90) into the mixed Schur basis, which allows to translate the input problem in Eq. (6.90) into the following equivalent SDP problem:

$$\begin{aligned} \max_{\{x_{S,T}\}} \quad & f_C(\{x_{S,T}\}) \\ \text{s.t.} \quad & f_{A_k}(\{x_{S,T}\}) \leqslant b_k, && \forall k\in[m_1], \\ & g^{Q,R}_{D_k,B_k}(\{x_{S,T}\}) = 0, && \forall k\in[m_2],\ \forall\mu\in\widehat{\mathcal{A}}^d_{i_k},\ \forall Q,R\in\mathrm{Paths}_{i_k}(\mu,\mathscr{A}) \\ & X_\lambda\succeq 0, \end{aligned} \tag{6.91}$$

where $X_\lambda := \sum_{S,T\in\mathrm{Paths}(\lambda,\mathscr{A})} x_{S,T}E_{S,T}$ is an λ irrep block of X, and f_C, f_{A_k}, $g^{Q,R}_{D_k,B_k}$ are some affine functions depending on indicated matrices and paths $Q,R\in\mathrm{Paths}_{i_k}(\mu,\mathscr{A})$. The above optimisation problem has $\dim(\mathcal{A}^d_{n,m}) = \sum_{\lambda\in\widehat{\mathcal{A}}^d_{n,m}} d_\lambda^2$ degrees of freedom. For comparison, the original optimisation problem has $d^{2(n+m)}$ degrees of freedom.

First, notice that if all matrices C, A_k, D_k, B_k are written as linear combinations of matrix units $E_{S,T}$, the optimisation problem (6.37) can be rewritten to the form (6.91) trivially. Furthermore, we can use the methods presented in Sections 6.4.1 and 6.4.2 to efficiently compute full and partial traces of products of matrices of different forms. Indeed, summarising the results from Sections 6.4.1 and 6.4.2, we obtain the following easy generalisation of Theorem 6.3.4:

6.4.2. THEOREM. *The computational complexity of rewriting the input SDP (6.37) with $O(d^{2(n+m)})$ variables to the reduced SDP (6.91) with $O(\dim(\mathcal{A}^d_{n,m}))$ variables is*

- $\mathrm{poly}(s, m_1, m_2, \dim \mathcal{A}^d_{n,m})$ *if C, A_k, D_k, B_k are given as s-sparse linear combinations of matrix units $E_{S,T}$ of $\mathcal{A}^d_{n,m}$, or are the identity matrix,*
- $\mathrm{poly}(s, m_1, m_2, (n+m)^{d(d+1)/2}, \dim \mathcal{A}^d_{n,m})$ *if C, A_k are given as s-sparse linear combinations of computational basis matrix units, while the matrices D_k, B_k are s-sparse linear combinations of matrix units $E_{S,T}$,*
- $\mathrm{poly}(s, m_1, m_2, n+m, \dim \mathcal{A}^d_{n,m})$ *if C, A_k, D_k are s-sparse linear combinations of diagrams in $\mathcal{B}^d_{n,m}$ and B_k is s-sparse linear combination of diagrams in $\mathcal{B}^d_{i_k}$, see Eq. (3.46).*

The proof of this theorem is essentially identical to Theorem 6.3.4: we expand the full and partial trace constraints in Eq. (6.90) by linearity according to Sections 6.4.1 and 6.4.2 and use the derived complexities to evaluate the respective coefficients in the linear constraints of Eq. (6.91). In all cases, the complexity scales polynomially with the total system size $n+m$ when the local dimension d is constant. However, since the complexities scale with $\dim(\mathcal{A}^d_{n,m})$, it implies that the scaling in the parameter $n+m$ would be superpolynomial, as $\dim(\mathcal{A}^d_{n,m})$ scales superpolynomially in $n+m$ for constant d. On the other hand, because the complexities depend on $\dim(\mathcal{A}^d_{n,m})$ rather than $\dim(\mathcal{B}^d_{n,m}) = (n+m)!$, this can make a significant difference for small values of the local dimension d. Note that the difference in scaling between $\dim(\mathcal{A}^d_{n,m})$ and $\dim(\mathcal{B}^d_{n,m})$ arises from expressing the matrix variable as a formal linear combination of matrix units $E_{S,T}$ instead of walled Brauer algebra diagrams.

The purpose of Theorem 6.4.2 is to show that there are certain regimes where this reformulation is feasible and could lead to numerical solutions of SDPs that were previously impossible to solve. We illustrate the potential of our results (Theorems 6.3.4 and 6.4.2) with several example applications in Section 6.5.

6.5 Applications

In this section, we discuss several applications of our framework, focussing on four natural unitary-equivariant problems in quantum information theory: deciding the principal eigenvalue of a quantum state, quantum majority vote, asymmetric cloning, and transposition of a black-box unitary operation (they are inspired by [KW01a], [BLMMO22], [NPR21], and [QE21], respectively). These are only meant as toy examples that illustrate how our framework can be easily applied to a variety of problems, and hence we do not attempt to derive full analytical solutions. Similarly, this list of applications is by no means exhaustive. Other potential applications (within quantum information) include entanglement witness construction [BSH24], and quantum error-correction [KL22] and machine learning [QE21; ZLLSK23]. The four main applications mentioned above are discussed in separate sections below.

6.5.1 Deciding the principal eigenvalue

This application is inspired by the problem of estimating the spectrum of a given quantum state [KW01a]. Let ρ be a d-dimensional quantum state that is picked from some unitary-invariant

measure. Given $\rho^{\otimes n}$ and a threshold value $c \in [1/d, 1]$, the problem is to decide whether $\lambda_{\max} < c$ or $\lambda_{\max} \geqslant c$, where $\lambda_{\max}$ is the principal eigenvalue of ρ.

For concreteness, we assume that ρ is produced by choosing a uniformly random pure state in $\mathbb{C}^d \otimes \mathbb{C}^k$ and discarding the ancillary k-dimensional system. This guarantees that ρ has a unitary-invariant measure. Moreover, the eigenvalues $\lambda = (\lambda_1, \ldots, \lambda_d)$ of such ρ have the same probability density as those of a normalised Wishart matrix [Nec07, Proposition 4]:

$$\mu_{d,k}(\lambda_1, \ldots, \lambda_d) := \frac{1}{\sqrt{d}} C_{d,k} V(\lambda)^2 \prod_{i=1}^{d} \lambda_i^{k-d} \tag{6.92}$$

where $C_{d,k}$ is a normalisation constant and $V(\lambda)$ is the Vandermonde determinant:

$$C_{d,k} := \frac{\Gamma(dk)}{\prod_{j=0}^{d-1} \Gamma(d+1-j)\Gamma(k-j)}, \qquad V(\lambda) := \prod_{1 \leqslant i < j \leqslant d} (\lambda_i - \lambda_j). \tag{6.93}$$

The $1/\sqrt{d}$ factor in Eq. (6.92) accounts for the fact that (unlike in [Nec07]) we treat all $\lambda_1, \ldots, \lambda_d$ as independent variables. The density $\mu_{d,k}$ is normalised to 1 on the standard probability simplex

$$\Delta_{d-1} := \{(\lambda_1, \ldots, \lambda_d) : \lambda_1 + \cdots + \lambda_d = 1, \lambda_1, \ldots, \lambda_d \geqslant 0\}. \tag{6.94}$$

Any strategy for this problem can be described by a two-outcome measurement with operators $P, Q \succeq 0$ such that $P + Q = I_{d^n}$, where P and Q correspond to outcomes $\lambda_{\max} < c$ and $\lambda_{\max} \geqslant c$, respectively. The optimal probability of distinguishing the two cases correctly is

$$p^n_{d,k}(c) = \min_{U \in \mathrm{U}_d} \max_{\substack{P,Q \succeq 0 \\ P+Q=I}} \tag{6.95}$$
$$\left(\int_{\lambda \in \Delta_{d-1}} \mu_{d,k}(\lambda) \operatorname{Tr}\Big[\rho(\lambda, U)^{\otimes n} \Big(\delta\big(\tfrac{1}{d} \leqslant \lambda_{\max} < c\big) P + \delta(c \leqslant \lambda_{\max} \leqslant 1) Q \Big) \Big] \right),$$

where $\rho(\lambda, U) := U \operatorname{diag}(\lambda) U^\dagger$ and δ denotes the indicator function for the corresponding subregion of Δ_{d-1}.

To simplify this expression, we focus on the trace. Using the cyclic property, we can move the unitary dependence from ρ onto P and Q:

$$\operatorname{Tr}\Big[\operatorname{diag}(\lambda)^{\otimes n} \Big(\delta\big(\tfrac{1}{d} \leqslant \lambda_{\max} < c\big) U^{\dagger \otimes n} P U^{\otimes n} + \delta(c \leqslant \lambda_{\max} \leqslant 1) U^{\dagger \otimes n} Q U^{\otimes n} \Big) \Big]. \tag{6.96}$$

Then, by twirling over U_d, we can turn the worst case probability into the average case and thus remove the minimisation over U in Eq. (6.95) altogether. Hence, without loss of generality $P, Q \in \mathcal{A}^d_{n,0}$ in an optimal strategy, i.e., they can be written as linear combinations of n-qudit permutations. Moreover, since $\rho(\lambda, U)^{\otimes n}$ is invariant under qudit permutations, we can also twirl P and Q over S_n. Hence, we can write P as a non-negative linear combination of primitive central idempotents of $\mathcal{A}^d_{n,0}$, see Eq. (6.36), and set $Q = I_{d^n} - P$.

With these simplifications, we can evaluate the trace in Eq. (6.96) diagrammatically, giving us a polynomial in the eigenvalues λ_i. Plugging this back into Eq. (6.95) allows us to evaluate the integral over λ. The resulting expression depends only on the decomposition of P into idempotents. This reduces the problem from an SDP to an LP, where we only need to optimise the weights in the decomposition of P. The following example provides an explicit formula for $p^n_{d,k}(c)$, for a specific combination of parameters, obtained using this procedure.

6.5.1. Example ($n = 3$, $d = 2$, $k = 2$). An exact formula for the success probability as a function of the threshold value c in this case is given by

$$p^3_{2,2}(c) := \begin{cases} 2(1-c)(4c^2-2c+1) & \text{if } c \in [1/2, c_1], \\ \frac{7}{5} - \frac{6}{5}c(16c^4 - 40c^3 + 40c^2 - 20c + 5) & \text{if } c \in [c_1, c_2], \\ (2c-1)^3 & \text{if } c \in [c_2, 1], \end{cases} \tag{6.97}$$

where $c_1 \approx 0.821569391$ and $c_2 \approx 0.913830846$ are roots of the polynomials $96x^5 - 240x^4 + 200x^3 - 60x^2 + 3$ and $24x^5 - 60x^4 + 70x^3 - 45x^2 + 15x - 3$, respectively. A plot of the function $p^3_{2,2}(c)$ is shown in Fig. 6.2. Note that $p^3_{2,2}(1/2) = p^3_{2,2}(1) = 1$ since the problem of deciding the largest eigenvalue becomes trivial for extreme values of c. The success probability $p^3_{2,2}(c)$ is always at least $p^3_{2,2}(c_2) \approx 0.566968020$ and never below the trivial $n = 1$ lower bound

$$p^1_{2,2}(c) := \max\{2(1-c)(4c^2-2c+1), (2c-1)^3\} \tag{6.98}$$

whose minimum is $1/2$ at $c = \frac{1}{2} + \frac{1}{2^{4/3}}$. Using the same procedure, we also obtained explicit expressions for $p^n_{2,2}(c)$ with $n = 1, \ldots, 8$. Their plots are shown in Fig. 6.3.

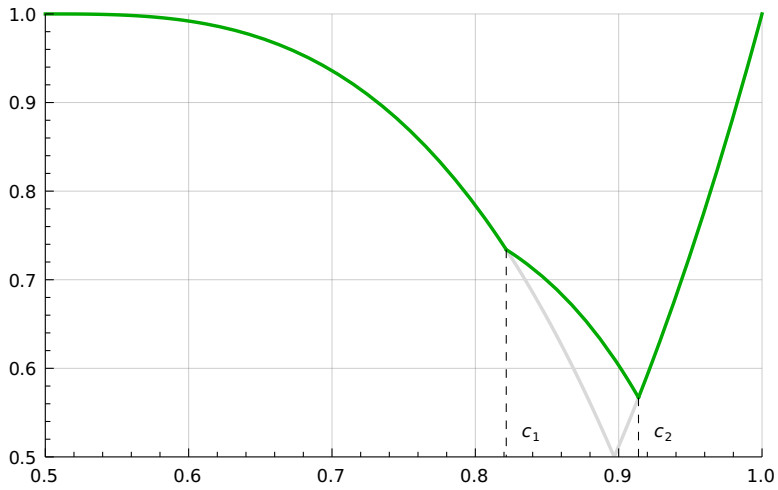

Figure 6.2: Plot of the success probability $p^3_{2,2}(c)$ from Eq. (6.97) as a function of $c \in [1/2, 1]$. The gray curves represent the trivial lower bound from Eq. (6.98) obtained by setting $n = 1$.

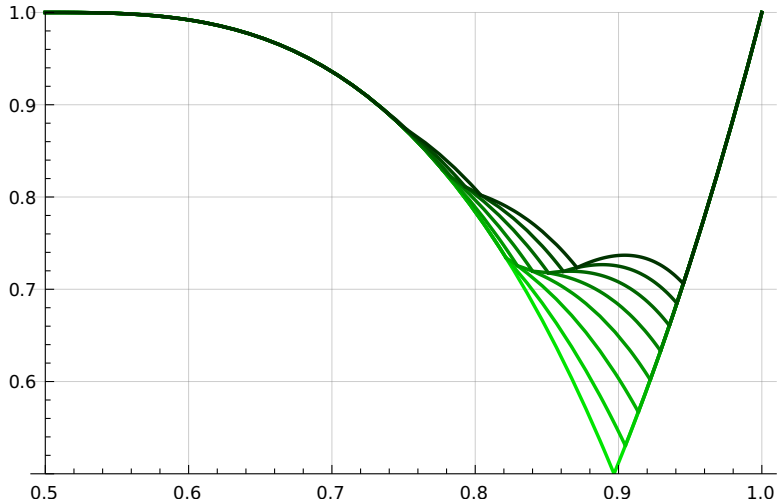

Figure 6.3: Plots of $p^n_{2,2}(c)$ for $n = 1, \ldots, 8$ (darker lines correspond to larger values of n). As n gets larger, the curves move upwards and the number of their segments increases.

6.5.2 Quantum majority vote

This application of our framework is inspired by the work of [BLMMO22] on optimal unitary-equivariant quantum channels for evaluating permutation-equivariant and symmetric Boolean functions.

As usual, let $n, m \geqslant 0$ denote the number of inputs and outputs, and let $d \geqslant 2$ denote their dimension. We are interested in functions of the form $f\colon [d]^n \to [d]^m$, or more generally in multi-valued functions or relations $f \subseteq [d]^n \times [d]^m$.

We call f *equivariant* with respect to the symmetric group S_d on the alphabet $[d]$ if $f(\pi \cdot x) = \pi \cdot f(x)$ for every $\pi \in \mathrm{S}_d$, where $\pi \cdot (x_1, \ldots, x_n) := (\pi(x_1), \ldots, \pi(x_n))$ for all $x_1, \ldots, x_n \in [d]$ (this is a classical analogue of Definition 6.2.1). We say that f is *symmetric* if its inputs and outputs have $\mathrm{S}_n \times \mathrm{S}_m$ permutation symmetry, i.e., if $f(\pi \circ x) = \sigma \circ f(x)$ for every $(\pi, \sigma) \in \mathrm{S}_n \times \mathrm{S}_m$, where $\pi \circ x := (x_{\pi^{-1}(1)}, \ldots, x_{\pi^{-1}(n)})$ and $\sigma \circ f(x)$ is defined similarly (this is a classical analogue of Definition 6.2.3).

The most important example of an equivariant and symmetric function is the *majority vote* function $f\colon [d]^n \to [d]$ that outputs the most frequently occurring input symbol. Since, in general, this symbol may not be unique, we prefer to think of $f \subseteq [d]^n \times [d]$ as a relation. One can also consider generalisations with $m \geqslant 1$ where the m most popular symbols must be output in any order.

A natural quantum generalisation of an equivariant function f is a unitary-equivariant map $\Psi_f\colon \mathrm{End}(V_{\mathrm{in}}) \to \mathrm{End}(V_{\mathrm{out}})$ such that $\Psi_f(|x\rangle\langle x|) = |f(x)\rangle\langle f(x)|$ for all $x \in [d]^n$. In case of a multi-valued function f, the ideal quantum map can be taken as $\Psi_f(|x\rangle\langle x|) = \Pi_{f(x)}$, where $\Pi_{f(x)} := \sum_{y \in f(x)} |y\rangle\langle y|$ is the rank-$|f(x)|$ orthogonal standard basis projector on all valid output states. Note that the ideal map Ψ_f may not be a quantum channel in general.

Given a classical S_d-equivariant and $\mathrm{S}_n \times \mathrm{S}_m$ symmetric relation $f \subseteq [d]^n \times [d]^m$, we would like to find a unitary-equivariant $n \to m$ quantum channel Φ_f that approximates the ideal functionality. Namely, one that maximises the worst-case fidelity

$$\min_{x \in [d]^n} \mathrm{Tr}\big(\Phi_f(|x\rangle\langle x|)\, \Pi_{f(x)}\big). \tag{6.99}$$

We can formulate this as an SDP for computing the worst-case fidelity $F \in \mathbb{R}$ of an optimal quantum channel represented by its Choi matrix $X \in \mathrm{End}((\mathbb{C}^d)^{\otimes n+m})$:

$$\begin{aligned} \max_{X,F} \quad & F \\ \text{s.t.} \quad & \mathrm{Tr}\Big(X\big(|x\rangle\langle x| \otimes \Pi_{f(x)}\big)\Big) \geqslant F, \quad \forall x \in [d]^n, \\ & \mathrm{Tr}_{V_{\mathrm{out}}}(X) = I_{V_{\mathrm{in}}}, \\ & \big[X, U^{\otimes n} \otimes \bar{U}^{\otimes m}\big] = 0, \qquad \forall U \in \mathrm{U}_d, \\ & X \succeq 0. \end{aligned} \tag{6.100}$$

As a generalisation of [BLMMO22], we consider the majority relation on any alphabet $[d]$ with $d \geqslant 3$. For simplicity, we restrict ourselves to the case of $n = 3$ inputs (and $m = 1$ outputs). In this case the majority relation for any $d \geqslant 3$ is fully defined by

$$\begin{aligned} 111 &\mapsto 1, \\ 112 &\mapsto 1, \\ 123 &\mapsto 1, 2, 3, \end{aligned} \tag{6.101}$$

which are extended to the whole domain using symmetry and equivariance. These rules cover three distinct cases: when all three inputs are equal, when one of them is different, and when

all three are different. Since there is no clear majority in the last case, the relation can output any of the three symbols.

For quantum majority vote with $n = 3$, $m = 1$, and $d \geqslant 3$ the symmetries of the Choi matrix X of the optimal quantum channel Φ_f allow us to reduce the SDP (6.100) to an LP using the ansatz (6.36) for X:

$$X = \sum_{i=1}^{N(d)} v_i \varepsilon_{T_i}^{\mathcal{A}}, \tag{6.102}$$

where ε_{T_i} are primitive idempotents that correspond to distinct root-leaf paths T_i in the Bratteli diagram of $\mathcal{A}_{3,1}^d$, and $N(d) := N_{3,1}^d(\mathrm{GT})$ is the total number of such paths, see Eq. (6.26). Based on Eq. (6.101), which defines the majority relation on three symbols, the resulting LP for any $d \geqslant 3$ has the following form:

$$\begin{aligned}
\max_{F, v_1, \ldots, v_{N(d)}} \quad & F \\
\text{s.t.} \quad & \sum_{i=1}^{N(d)} v_i \langle 111, 1 | \varepsilon_{T_i}^{\mathcal{A}} | 111, 1 \rangle \geqslant F, \\
& \sum_{i=1}^{N(d)} v_i \langle 112, 1 | \varepsilon_{T_i}^{\mathcal{A}} | 112, 1 \rangle \geqslant F, \\
& \sum_{i=1}^{N(d)} v_i \sum_{y=1}^{3} \langle 123, y | \varepsilon_{T_i}^{\mathcal{A}} | 123, y \rangle \geqslant F, \\
& \sum_{i=1}^{N(d)} v_i \operatorname{Tr}_{V_{\mathrm{out}}} \varepsilon_{T_i}^{\mathcal{A}} = I_{V_{\mathrm{in}}}, \\
& v_i \geqslant 0, \quad \forall i \in [N(d)], \\
& v_i = v_j \text{ whenever } T_i \text{ and } T_j \text{ share the same last edge.}
\end{aligned} \tag{6.103}$$

The last condition is a consequence of Proposition 6.3.2 and ensures $\mathrm{S}_n \times \mathrm{S}_1$ symmetry of the majority relation. Enforcing this symmetry effectively decreases the number of variables in the LP (6.103) from $N(d)$, which corresponds to the Gelfand–Tsetlin symmetry, to the smaller value of $N_{3,1}^d(\mathrm{S}_3 \times \mathrm{S}_1)$ (see Eq. (6.35)) that corresponds to the $\mathrm{S}_3 \times \mathrm{S}_1$ symmetry. Explicit values of these numbers can be found in Tables 6.5 and 6.6 in Section 6.A.3.

The LP (6.103) can be solved exactly and the optimal fidelity turns out to be $F = 8/9$ for all $d \geqslant 2$, thus extending the $d = 2$ result of [BLMMO22].

6.5.3 Asymmetric cloning

In this section, we provide an example of how our approach based on primitive idempotents can be used to solve a general unitary-equivariant SDP that does not reduce to an LP. This example is based on the problem of asymmetric cloning from [NPR21; NPR23]. The problem is to find a $1 \to m$ quantum channel $\Phi\colon \mathrm{End}(\mathbb{C}^d) \to \mathrm{End}(V_{\mathrm{out}})$ whose marginals $\Phi_i := \mathrm{Tr}_{[m]\setminus\{i\}} \circ \Phi$ satisfy

$$\Phi_i(\rho) = p_i \rho + (1 - p_i) \frac{I}{d} \tag{6.104}$$

for all $i \in [m]$ and states $\rho \in \mathrm{D}(V)$ where $V = \mathbb{C}^d$. We consider the case $m = 3$ with $d = 2$ and $d = 3$, and plot the set of triples (p_1, p_2, p_3) in Eq. (6.104) that are physically realizable. Note that this set is invariant under permutations of p_i.

According to [NPR21], the Choi matrix X^Φ of the channel Φ is a linear combination of partially transposed permutation matrices, i.e., $X^\Phi \in \mathcal{A}^d_{1,m}$. We can use the primitive idempotents from Eq. (3.65) to construct the blocks X^Φ_λ without explicitly computing the Schur transform $U_{\mathrm{Sch}(n,m)}$, see Section 6.A.2 for more details. The resulting blocks are then subject to positive semidefinite and trace constraints. In this way we can formulate the question of physical realizability of the channel Φ as a semidefinite feasibility problem.

Two examples of SDPs resulting from this procedure are given below. They characterise asymmetric $1 \to 3$ cloning in dimensions $d = 2$ and $d = 3$. Here we denote for brevity $X^i := X^\Phi_{\lambda_i}$ for every $\lambda_i \in \widehat{\mathcal{A}}^d_{1,m}$.

6.5.2. Example ($m = 3$ and $d = 2$). Positive semidefinite constraints:

$$\left(X^1_{1,1}\right) \succeq 0, \qquad \begin{pmatrix} X^2_{1,1} & X^2_{1,2} \\ X^2_{2,1} & X^2_{2,2} \end{pmatrix} \succeq 0, \qquad \begin{pmatrix} X^3_{1,1} & X^3_{1,2} & X^3_{1,3} \\ X^3_{2,1} & X^3_{2,2} & X^3_{2,3} \\ X^3_{3,1} & X^3_{3,2} & X^3_{3,3} \end{pmatrix} \succeq 0. \tag{6.105}$$

Trace constraint:

$$5X^1_{1,1} + X^2_{1,1} + X^2_{2,2} + 3X^3_{1,1} + 3X^3_{2,2} + 3X^3_{3,3} = 2. \tag{6.106}$$

Expressions for realizable triples (p_1, p_2, p_3):

$$p_1 = \frac{1}{3}\left(3X^3_{1,1} + X^2_{1,1} + 5X^1_{1,1} + 3X^3_{2,2} + 9X^3_{3,3} + 3X^2_{2,2} - 3\right), \tag{6.107}$$

$$\begin{aligned} p_2 = \frac{1}{6}\Big(&6X^3_{1,1} + 5X^2_{1,1} + 10X^1_{1,1} + 15X^3_{2,2} + 3\sqrt{3}X^3_{2,3} + 3\sqrt{3}X^3_{3,2} \\ &+ 9X^3_{3,3} + \sqrt{3}X^2_{1,2} + \sqrt{3}X^2_{2,1} + 3X^2_{2,2} - 6\Big), \end{aligned} \tag{6.108}$$

$$\begin{aligned} p_3 = \frac{1}{6}\Big(&14X^3_{1,1} + 5X^2_{1,1} + 10X^1_{1,1} + 2\sqrt{2}X^3_{1,2} + 2\sqrt{2}X^3_{2,1} + 7X^3_{2,2} \\ &+ 9X^3_{3,3} + 2\sqrt{6}X^3_{1,3} + 2\sqrt{6}X^3_{3,1} + \sqrt{3}X^3_{2,3} + \sqrt{3}X^3_{3,2} - \sqrt{3}X^2_{1,2} \\ &- \sqrt{3}X^2_{2,1} + 3X^2_{2,2} - 6\Big). \end{aligned} \tag{6.109}$$

The feasible region for (p_1, p_2, p_3) is shown in Fig. 6.4.

6.5.3. Example ($m = 3$ and $d = 3$). Positive semidefinite constraints: $\left(X^1_{1,1}\right) \succeq 0$,

$$\begin{pmatrix} X^2_{1,1} & X^2_{1,2} \\ X^2_{2,1} & X^2_{2,2} \end{pmatrix} \succeq 0, \qquad \begin{pmatrix} X^3_{1,1} & X^3_{1,2} & X^3_{1,3} \\ X^3_{2,1} & X^3_{2,2} & X^3_{2,3} \\ X^3_{3,1} & X^3_{3,2} & X^3_{3,3} \end{pmatrix} \succeq 0, \qquad \begin{pmatrix} X^4_{1,1} & X^4_{1,2} & X^4_{1,3} \\ X^4_{2,1} & X^4_{2,2} & X^4_{2,3} \\ X^4_{3,1} & X^4_{3,2} & X^4_{3,3} \end{pmatrix} \succeq 0. \tag{6.110}$$

Trace constraint:

$$X^4_{1,1} + 2X^3_{1,1} + 5X^2_{1,1} + 8X^1_{1,1} + X^4_{2,2} + X^4_{3,3} + 2X^3_{2,2} + 2X^3_{3,3} + 5X^2_{2,2} = 1. \tag{6.111}$$

Expressions for realizable triples (p_1, p_2, p_3):

$$p_1 = \frac{1}{8}\big(3X_{1,1}^4 + 6X_{1,1}^3 + 15X_{1,1}^2 + 24X_{1,1}^1 + 3X_{2,2}^4 \tag{6.112}$$
$$+ 12X_{3,3}^4 + 6X_{2,2}^3 + 24X_{3,3}^3 + 15X_{2,2}^2 - 4\big)\,,$$
$$p_2 = \frac{1}{8}\Big(3X_{1,1}^4 + 6X_{1,1}^3 + 15X_{1,1}^2 + 24X_{1,1}^1 + 11X_{2,2}^4 + 2\sqrt{2}X_{2,3}^4 + 2\sqrt{2}X_{3,2}^4 \tag{6.113}$$
$$+ 4X_{3,3}^4 + 22X_{2,2}^3 + 4\sqrt{2}X_{2,3}^3 + 4\sqrt{2}X_{3,2}^3 + 8X_{3,3}^3 + 15X_{2,2}^2 - 4\Big)\,,$$
$$p_3 = \frac{1}{8}\big(9X_{1,1}^4 + 21X_{1,1}^3 + 15X_{1,1}^2 + 24X_{1,1}^1 + 8X_{3,3}^3 + 15X_{2,2}^2 \tag{6.114}$$
$$+ 5X_{2,2}^4 + 7X_{2,2}^3 + 4X_{3,3}^4 + 2\sqrt{3}X_{1,2}^4 + 2\sqrt{3}X_{2,1}^4 - 4$$
$$- \sqrt{2}X_{2,3}^4 - \sqrt{2}X_{3,2}^4 - \sqrt{6}X_{3,1}^4 - \sqrt{6}X_{1,3}^4 + \sqrt{15}X_{1,2}^3$$
$$+ \sqrt{15}X_{2,1}^3 + \sqrt{30}X_{3,1}^3 + \sqrt{30}X_{1,3}^3 + \sqrt{2}X_{2,3}^3 + \sqrt{2}X_{3,2}^3\big)\,.$$

The feasible region for (p_1, p_2, p_3) is shown on th right in Fig. 6.4.

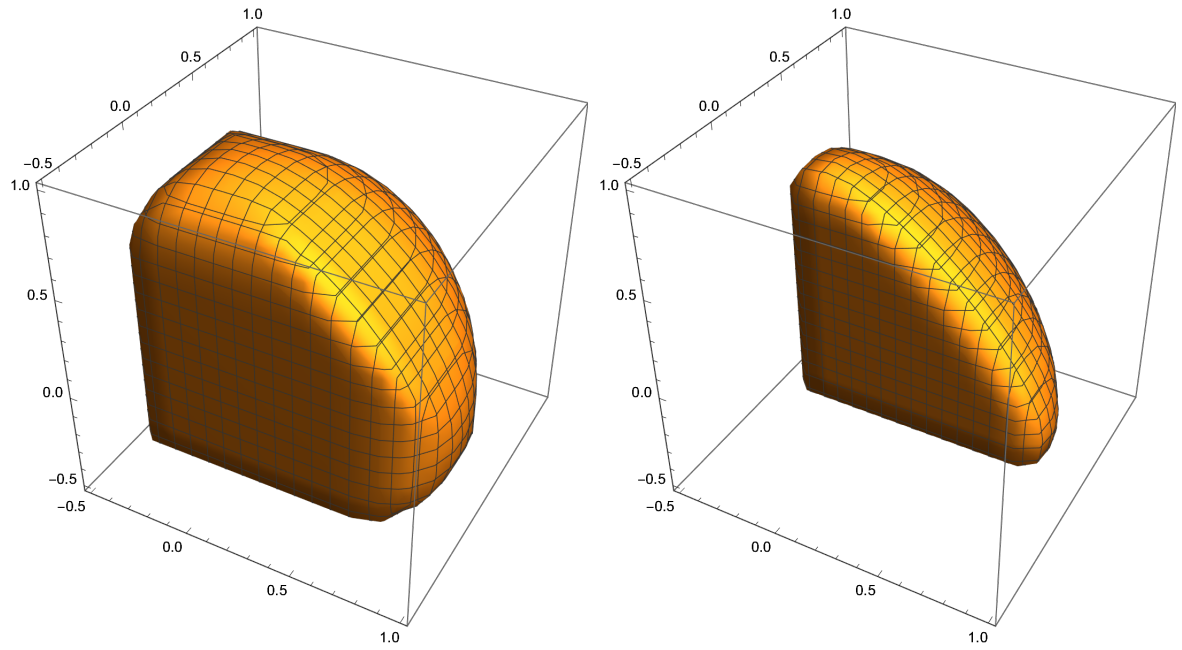

Figure 6.4: Plot of the feasible region for (p_1, p_2, p_3) in the asymmetric cloning SDP for $m = 3$, $d = 2$ (left) and $m = 3$, $d = 3$ (right).

6.5.4 Universal transposition of unitaries

Following the work of [QE21] and others [QDSSM19b; QDSSM19a; YSM23b; YSM23a; Ebl+23], we present another application of our method—transforming a black-box unitary operation. Consider the following general problem: given n copies of an unknown d-dimensional unitary U, the task is to find a universal protocol that implements $f(U)$, where f is some function of U. This protocol can be either *deterministic* or *probabilistic*, depending on whether it always succeeds or not, and either *exact* or *non-exact*, depending on the channel fidelity between the ideal channel and the one implemented by the protocol. In particular, we focus on the deterministic case where $f(U) = U^\mathsf{T}$. Our main result in this section is the existence of an exact and deterministic protocol which transforms 4 copies of a black-box single-qubit unitary U into $f(U) = U^\mathsf{T}$. This result is similar to the work [YSM23a], which proves the same claim for

the function $f(U) = U^{-1}$. For more detailed background on this topic, we refer the reader to [QE21; YSM23a]; here we only introduce the necessary ingredients needed to describe our approach.

Following previous work, we use the formalism of quantum superchannels. We search for a deterministic sequential protocol accomplishing our task by expressing it as a quantum sequential superchannel [QE21]. A *quantum superchannel* is a linear map $\mathcal{C}\colon \bigotimes_{i=1}^{n}\big(\mathrm{End}(\mathcal{I}_i) \to \mathrm{End}(\mathcal{O}_i)\big) \to \big(\mathrm{End}(\mathcal{P}) \to \mathrm{End}(\mathcal{F})\big)$ that transforms n quantum channels into a new quantum channel. Here the spaces $\mathcal{I}_i = \mathcal{O}_i = \mathcal{P} = \mathcal{F} = \mathbb{C}^d$ correspond to the inputs $\mathcal{I}_i$ and outputs $\mathcal{O}_i$ of the i-th copy of the channel $\mathcal{U}(\rho) := U\rho U^\dagger$ associated with the unknown input unitary U, and $\mathcal{P}$ and $\mathcal{F}$ are the input and output spaces of the desired output channel $\mathcal{U}_f(\rho) := f(U)\rho f(U)^\dagger$ that represents the target unitary $f(U)$. Let $\mathcal{I}^n := \bigotimes_{i=1}^{n}\mathcal{I}_i$ and $\mathcal{O}^n := \bigotimes_{i=1}^{n}\mathcal{O}_i$. A *quantum sequential superchannel* $\mathcal{C}$ (also known as a *quantum comb*) is a quantum superchannel with certain additional constraints on its Choi matrix $C \in \mathrm{End}(\mathcal{P} \otimes \mathcal{I}^n \otimes \mathcal{O}^n \otimes \mathcal{F})$ [CDP08]:

$$C \succeq 0, \tag{6.115}$$

$$\mathrm{Tr}\, C = 1, \tag{6.116}$$

$$\mathrm{Tr}_{\mathcal{I}_i} C_i = C_{i-1} \otimes I_{\mathcal{O}_{i-1}}, \quad \forall i \in [n+1], \tag{6.117}$$

where $C_{n+1} := C$, $\mathcal{I}_{n+1} := \mathcal{F}$, $\mathcal{O}_0 := \mathcal{P}$ and $C_{i-1} := \frac{1}{d}\,\mathrm{Tr}_{\mathcal{I}_i\mathcal{O}_{i-1}} C_i$.

Finding a deterministic sequential superchannel $\mathcal{C}$ which implements the operation $\mathcal{C}(\mathcal{U}^{\otimes n}) = \mathcal{U}^{\mathsf{T}}$ with highest possible average channel fidelity is equivalent to solving the following SDP for the Choi matrix C of $\mathcal{C}$ [QE21]:

$$\begin{aligned} \max_{C} \quad & \mathrm{Tr}(C\Omega_{n,d}) \\ \text{s.t.} \quad & C \text{ satisfies (6.115)–(6.117)}, \end{aligned} \tag{6.118}$$

where $\Omega_{n,d}$ is given by

$$\Omega_{n,d} := \frac{1}{d^2} \sum_{\lambda,\mu \in \widehat{\mathcal{A}}^d_{n,1}} \sum_{T,T' \in \mathrm{Paths}(\lambda,\mathscr{A})} \frac{(E^\lambda_{T,T'})_{\mathcal{I}^n\mathcal{F}} \otimes (E^\lambda_{T,T'})_{\mathcal{O}^n\mathcal{P}}}{m_\lambda}, \tag{6.119}$$

where $E^\lambda_{T,T'}$ are matrix units for the Gelfand–Tsetlin basis of $\mathcal{A}^d_{n,1}$, adapted to the sequence $\mathcal{A}^d_{0,0} \hookrightarrow \mathcal{A}^d_{1,0} \hookrightarrow \ldots \hookrightarrow \mathcal{A}^d_{n,0} \hookrightarrow \mathcal{A}^d_{n,1}$, and $\mathscr{A}$ is the Bratteli diagram corresponding to this sequence of algebras. Notice that $\Omega_{n,d}$ has the mixed unitary symmetry:

$$\left[\Omega_{n,d}, V^{\otimes n}_{\mathcal{I}^n} \otimes \bar{V}_{\mathcal{F}} \otimes U^{\otimes n}_{\mathcal{O}^n} \otimes \bar{U}_{\mathcal{P}}\right] = 0, \qquad \forall U, V \in \mathrm{U}_d\,. \tag{6.120}$$

Therefore without loss of generality the optimal solution of the SDP (6.118) also has the same symmetry:

$$\left[C, V^{\otimes n}_{\mathcal{I}^n} \otimes \bar{V}_{\mathcal{F}} \otimes U^{\otimes n}_{\mathcal{O}^n} \otimes \bar{U}_{\mathcal{P}}\right] = 0, \qquad \forall U, V \in \mathrm{U}_d, \tag{6.121}$$

which allows us to use the following ansatz for C:

$$C = \sum_{\lambda,\mu \in \widehat{\mathcal{A}}^d_{n,1}} \sum_{S,S' \in \mathrm{Paths}(\lambda,\mathscr{A})} \sum_{Q,Q' \in \mathrm{Paths}(\mu,\tilde{\mathscr{A}})} c^{\lambda\mu}_{SS'QQ'} (E^\lambda_{S,S'})_{\mathcal{I}^n\mathcal{F}} \otimes (\tilde{E}^\mu_{Q,Q'})_{\mathcal{P}\mathcal{O}^n}, \tag{6.122}$$

where $\tilde{E}^\lambda_{Q,Q'}$ are matrix units for the Gelfand–Tsetlin basis of $\mathcal{A}^d_{n,1}$, adapted to a different sequence $\mathcal{A}^d_{0,0} \hookrightarrow \mathcal{A}^d_{0,1} \hookrightarrow \mathcal{A}^d_{1,1} \hookrightarrow \ldots \hookrightarrow \mathcal{A}^d_{n,1}$, and $\tilde{\mathscr{A}}$ is the Bratteli diagram corresponding to it. The reason we choose a different Gelfand–Tsetlin basis on the systems $\mathcal{P}\mathcal{O}^n$ is that this choice is more suitable to apply Lemma 6.4.1 for simplification of partial trace constraints in Eq. (6.117).

$f(U)$	d \ n	1	2	3	4
U^T	2	0.500000	0.750000	0.933013	1.000000
	3	0.222222	0.407407	0.626597	0.799250
	4	0.125000	0.218750	0.362903	0.544148
	5	0.080000	0.136000	0.214954	0.331871
U^{-1}	2	0.500000	0.750000	0.933013	1.000000
	3	0.222222	0.333333	0.444444	0.555556
	4	0.125000	0.187500	0.250000	0.312500
	5	0.080000	0.120000	0.160000	0.200000

Table 6.2: Optimal values of the SDP (6.118). The column $f(U)$ indicates the task, for which we want to find a deterministic sequential superchannel $\mathcal{C}$.

Note that the semidefinite constraint (6.115) becomes

$$C \succeq 0 \qquad \Leftrightarrow \qquad \left[c^{\lambda\mu}_{SS'QQ'}\right]_{(SQ),(S'Q')} \succeq 0, \quad \forall \lambda, \mu \in \widehat{\mathcal{A}}^d_{n,1}, \tag{6.123}$$

where we think of $\left[c^{\lambda\mu}_{SS'QQ'}\right]_{(SQ),(S'Q')} \in \mathrm{End}(\mathbb{C}^{d_\lambda} \otimes \mathbb{C}^{d_\mu})$ as matrices.

Using Eqs. (6.119) and (6.122) we can rewrite the objective function as

$$\mathrm{Tr}(C\Omega_{n,d}) = \frac{1}{d^2} \sum_{\lambda,\mu \in \widehat{\mathcal{A}}^d_{n,1}} \sum_{\substack{T,T' \in \mathrm{Paths}(\lambda,\mathscr{A}) \\ Q,Q' \in \mathrm{Paths}(\mu,\tilde{\mathscr{A}})}} \frac{c^{\lambda,\mu}_{T'TQQ'}}{m_\lambda m_\mu} \mathrm{Tr}(\psi^d_{n+1}(\pi) E^\lambda_{TT'} \psi^d_{n+1}(\pi^{-1}) \tilde{E}^\mu_{TT'}), \tag{6.124}$$

where $\psi^d_{n+1}(\pi)$ is the tensor representation of the full cyclic permutation on $(\mathbb{C}^d)^{n+1}$. The coefficients $\mathrm{Tr}(\psi^d_{n+1}(\pi) E^\lambda_{TT'} \psi^d_{n+1}(\pi^{-1}) \tilde{E}^\mu_{TT'})$ could be computed numerically using tensor network representation of matrix units (see Fig. 6.1). Finally, we can rewrite constraints of the SDP (6.118) using our methods from Section 6.4 and solve the new simplified SDP numerically. Our numerical results are summarised in Table 6.2.

We can also solve a similar problem for the function $f(U) = U^{-1}$ and verify the results obtained in [YSM23a]. In that case, the SDP (6.118) has the same form, except that the matrices C and $\Omega_{n,d}$ posses a different symmetry: they commute with $U^{\otimes n+1}_{\mathcal{O}^n\mathcal{P}} \otimes V^{\otimes n+1}_{\mathcal{I}^n\mathcal{F}}$ for every $U, V \in \mathrm{U}_d$. This corresponds to the case $m = 0$ in the formalism of mixed Schur–Weyl duality.

In both tasks we successfully reproduce the known results from [QE21; YSM23a], while obtaining a range of new values for the transposition task.

6.6 Discussion

We have described how symmetry reduction can be utilised for unitary-equivariant SDPs, which commonly arise in quantum information theory. Nevertheless, our work raises several interesting open questions that we have not yet been able to resolve:

1. Derive an explicit basis in which our ansatz for X is diagonal under the $\mathrm{S}_n \times \mathrm{S}_m$ symmetry when $d = 2$ or $\min(n, m) = 2$.

2. Characterise the kernel of the map $\psi^d_{n,m}$ that embeds the walled Brauer algebra $\mathcal{B}^d_{n,m}$ into the partially-transposed permutation matrix algebra $\mathcal{A}^d_{n,m}$. This would allow removing the technical restriction (6.39) in Theorem 6.3.4 that d must be sufficiently large. Moreover, this could also provide additional speed-ups for small d since all calculations could be

performed using a linearly independent diagram basis of size much smaller than $(n+m)!$. One possible method for computing $\ker \psi^d_{n,m}$ is sketched in Remark 6.3.3.

3. The number of variables $N^d_{n,m}$ in Tables 6.5 and 6.7 does not depend on $n+m$. Could we prove it?

4. It should be possible to treat the local dimension d symbolically and deduce the asymptotic scaling of the solution as $d \to \infty$.

Moreover, our SDP reduction procedures could be made faster by applying the Fast Fourier transform (FFT). Indeed, FFT was successfully adapted to the setting of finite groups and some finite-dimensional semisimple algebras [MRW18a; MRW18b] and could be easily adapted for the full walled Brauer algebra $\mathcal{B}^d_{n,m}$, when it is semisimple. However, for the algebra of partially transposed permutations $\mathcal{A}^d_{n,m}$, it is not clear to us how to present the set of vectors which span the entire algebra $\mathcal{A}^d_{n,m}$. The non-triviality of the ideal $\ker(\psi^d_{n,m})$ makes the adaptation of [MRW18a; MRW18b] highly non-trivial, so we leave it for future work.

The applications provided in Section 6.5 are only for illustrative purposes. We expect that one should be able to go much further by bearing the full weight of our method. For example, concerning the application in Section 6.5.4, we would like to find, for any given d, how many copies of a black-box unitary U are needed to implement $f(U)$ exactly and deterministically via a sequential superchannel.

Our approach is an example of the general philosophy outlined in [BGSV12] for solving SDPs with $*$-matrix algebra symmetries. Other instances of this setting are also useful in quantum information [GNW21] and hence worth investigating.

Finally, given a solution X of a unitary-equivariant SDP that describes a Choi matrix, it is interesting to find an efficient quantum circuit that implements the corresponding quantum channel. Note that [BLMMO22] achieves this when $d = 2$, $n = 2k+1$ and $m = 1$. Recently, some work has been done in that direction: [Ngu23] described some classes instances where construction of efficient circuits is possible. This approach is based on the mixed Schur transform $U_{\mathrm{Sch}(n,m)}$ for general values of n, m, d. Could there be more examples which were not considered in [Ngu23]?

6.A Appendix

6.A.1 Restriction to $\mathrm{S}_n \times \mathrm{S}_m$ permutational symmetry

In this appendix we describe how the simple module V_λ of $\mathcal{A}^d_{n,m}$ restricts to the algebra $\psi^d_{n,m}(\mathbb{C}(\mathrm{S}_n \times \mathrm{S}_m))$. This question was first answered in [Kin70; Kin71]. It also follows from [Koi89, Proposition 2.2, Corollary 2.3.1] and [Hal96, Theorem 1.7] that a general formula for this restriction is

$$\mathrm{Res}^{\mathcal{A}^d_{n,m}}_{\mathrm{S}_n\times\mathrm{S}_m} V_\lambda \cong \bigoplus_{\substack{\mu\vdash_d n\\ \nu\vdash_d m}} (S^\mu \otimes S^\nu)^{\oplus m^\lambda_{\mu,\nu}(d)} \tag{6.125}$$

where S^μ and S^ν are simple modules of $\mathbb{C}\mathrm{S}_n$ and $\mathbb{C}\mathrm{S}_m$, respectively. For $\lambda = (\lambda^l, \lambda^r) \in \widehat{\mathcal{A}}^d_{n,m}$ with $\ell(\lambda^l) + \ell(\lambda^r) \leqslant d$ and $\mu \vdash n, \nu \vdash m$ with $\ell(\mu), \ell(\nu) \leqslant d$ the multiplicity $m^\lambda_{\mu,\nu}(d)$ is given by the following formula:

$$m^\lambda_{\mu,\nu}(d) := \sum_{\substack{\tilde\lambda: f(\tilde\lambda,d)=\lambda\\ \ell(\tilde\lambda^l)\leqslant d\\ \ell(\tilde\lambda^r)\leqslant d}} g(\tilde\lambda, d) \sum_{\gamma\vdash k(\tilde\lambda)} c^\mu_{\gamma\tilde\lambda^l} c^\nu_{\gamma\tilde\lambda^r} \tag{6.126}$$

where $\tilde\lambda = (\tilde\lambda^l, \tilde\lambda^r)$ is a pair of partitions $\tilde\lambda^l \vdash n - k(\tilde\lambda)$ and $\tilde\lambda^r \vdash m - k(\tilde\lambda)$ for some integer $k(\tilde\lambda) \geqslant 0$, and $c^\mu_{\gamma\tilde\lambda^r}$, $c^\nu_{\gamma\tilde\lambda^l}$ are the Littlewood–Richardson coefficients. The numbers $g(\tilde\lambda, d) \in \{-1, 0, 1\}$ and the bipartitions $f(\tilde\lambda, d)$ are defined as follows. If $\ell(\tilde\lambda^l) + \ell(\tilde\lambda^r) \leqslant d$ then $f(\tilde\lambda, d) := \tilde\lambda$ and $g(\tilde\lambda, d) := 1$. If $\ell(\tilde\lambda^l) + \ell(\tilde\lambda^r) > d$ then $f(\tilde\lambda, d)$ and $g(\tilde\lambda, d)$ are obtained via the following procedure (here μ' denotes the transpose of the Young diagram μ):

- If $d - \tilde\lambda^{r\prime}_i - \tilde\lambda^r_1 + i = \tilde\lambda^{l\prime}_j - \tilde\lambda^r_1 - j + 1$ for some $i \in [\tilde\lambda^r_1]$ and $j \in [\tilde\lambda^l_1]$, then $g(\tilde\lambda, d) := 0$ and $f(\tilde\lambda, d)$ is left undefined.
- Otherwise, sort the (distinct) numbers

$$\big(d - \tilde\lambda^{r\prime}_i - \tilde\lambda^r_1 + i : i = \tilde\lambda^r_1, \dots, 1\big) \cup \big(\tilde\lambda^{l\prime}_j - \tilde\lambda^r_1 - j + 1 : j = 1, \dots, \tilde\lambda^l_1\big) \tag{6.127}$$

  in decreasing order and denote the resulting list by $(k_1, \dots, k_{\tilde\lambda^r_1 + \tilde\lambda^l_1})$. Denote the permutation that achieves this sorting by π and let $g(\tilde\lambda, d) := \mathrm{sgn}(\pi)$. The bipartition $f(\tilde\lambda, d) = \big(f(\tilde\lambda, d)^l, f(\tilde\lambda, d)^r\big)$ is then defined via its transpose as follows:

$$f(\tilde\lambda, d)^{l\prime} := \big(d - k_i - i + 1 : i = \tilde\lambda^r_1, \dots, 1\big), \tag{6.128}$$
$$f(\tilde\lambda, d)^{r\prime} := \big(k_{\tilde\lambda^r_1 + j} + \tilde\lambda^r_1 + j - 1 : j = 1, \dots, \tilde\lambda^l_1\big). \tag{6.129}$$

Using a more geometric understanding of this procedure from [Kin71, eq. (2.18)] we arrive at the following multiplicity-free results.

6.A.1. Lemma. *If* $\min(n, m) \leqslant 2$ *then the multiplicity* $m^\lambda_{\mu,\nu}(d)$ *defined in Eq.* (6.126) *is either* 0 *or* 1 *for any valid* λ, μ, ν, d.

Proof:
Fix a valid combination of λ, μ, ν, d, i.e., $\mu \vdash n$, $\nu \vdash m$ with $\ell(\mu), \ell(\nu) \leqslant d$ and $\lambda = (\lambda^l, \lambda^r)$ with $n - |\lambda^l| = m - |\lambda^r| \geqslant 0$ and $\ell(\lambda^l) + \ell(\lambda^r) \leqslant d$. Assume that $\tilde\lambda = (\tilde\lambda^l, \tilde\lambda^r)$ is a pair of partitions $\tilde\lambda^l \vdash n - k(\tilde\lambda)$ and $\tilde\lambda^r \vdash m - k(\tilde\lambda)$ for some integer $k(\tilde\lambda) \geqslant 0$. Without loss of generality it is enough to consider only the $m = 1$ and $m = 2$ cases.

Case $m = 1$. Assume that $\ell(\tilde{\lambda}^l) \leqslant d$ and $\ell(\tilde{\lambda}^r) = 1$. Then according to [Kin71] we have that

$$g(\tilde{\lambda}, d) = \begin{cases} 1 & \text{if } \ell(\tilde{\lambda}^l) + \ell(\tilde{\lambda}^r) \leqslant d, \\ 0 & \text{if } \ell(\tilde{\lambda}^l) + \ell(\tilde{\lambda}^r) = d+1. \end{cases} \tag{6.130}$$

The set $\{\tilde{\lambda} : f(\tilde{\lambda}, d) = \lambda\}$ contains at most two elements corresponding to $\ell(\tilde{\lambda}^l) + \ell(\tilde{\lambda}^r) \leqslant d$ and $\ell(\tilde{\lambda}^l) + \ell(\tilde{\lambda}^r) = d+1$. Moreover, there is only one term in the sum $\sum_{\gamma \vdash k(\tilde{\lambda})} c^{\mu}_{\gamma\tilde{\lambda}^l} c^{\nu}_{\gamma\tilde{\lambda}^r}$ in Eq. (6.126) corresponding to either the empty partition $\gamma = \varnothing$ or $\gamma = (1)$. Each of these Littlewood–Richardson coefficients is either zero or one due to the Pieri rule [Mac98], which is a special case of the Littlewood–Richardson rule [BZ88; RS98; Gas98; Ste02]. Therefore $m^{\lambda}_{\mu,\nu}(d) \in \{0, 1\}$.

Case $m = 2$. Assume that $\ell(\tilde{\lambda}^l) \leqslant d$ and $\ell(\tilde{\lambda}^r) \leqslant 2$. Analogously, from [Kin71] it follows that

$$g(\tilde{\lambda}, d) = \begin{cases} 1 & \text{if } \ell(\tilde{\lambda}^l) + \ell(\tilde{\lambda}^r) \leqslant d, \\ -1 & \text{if } \ell(\tilde{\lambda}^l) = d \text{ and } \ell(\tilde{\lambda}^r) = 2 \text{ and } \tilde{\lambda}^l_1 > \tilde{\lambda}^l_2, \\ 0 & \text{otherwise.} \end{cases} \tag{6.131}$$

There are three possible cases depending on the value of $k(\tilde{\lambda}) \in \{0, 1, 2\}$:

- If $k(\tilde{\lambda}) = 0$ then the only term in the sum $\sum_{\gamma \vdash k(\tilde{\lambda})} c^{\mu}_{\gamma\tilde{\lambda}^l} c^{\nu}_{\gamma\tilde{\lambda}^r}$ corresponds to $\gamma = \varnothing$ and each Littlewood–Richardson coefficient is either zero or one, which implies that $\sum_{\gamma \vdash k(\tilde{\lambda})} c^{\mu}_{\gamma\tilde{\lambda}^l} c^{\nu}_{\gamma\tilde{\lambda}^r} \in \{0, 1\}$.

- If $k(\tilde{\lambda}) = 1$ then $\tilde{\lambda}^r = (1)$ and the only term in the sum $\sum_{\gamma \vdash k(\tilde{\lambda})} c^{\mu}_{\gamma\tilde{\lambda}^l} c^{\nu}_{\gamma\tilde{\lambda}^r}$ corresponds to $\gamma = (1)$, which means that $\sum_{\gamma \vdash k(\tilde{\lambda})} c^{\mu}_{\gamma\tilde{\lambda}^l} c^{\nu}_{\gamma\tilde{\lambda}^r} \in \{0, 1\}$.

- If $k(\tilde{\lambda}) = 2$ then $\tilde{\lambda}^r = \varnothing$ and therefore

$$\sum_{\gamma \vdash k(\tilde{\lambda})} c^{\mu}_{\gamma\tilde{\lambda}^l} c^{\nu}_{\gamma\tilde{\lambda}^r} = \sum_{\gamma \vdash k(\tilde{\lambda})} c^{\mu}_{\gamma\tilde{\lambda}^l} \delta_{\nu,\gamma} = c^{\mu}_{\nu\tilde{\lambda}^l} \in \{0, 1\}, \tag{6.132}$$

  where the conclusion follows from $\nu \vdash 2$ and the Pieri rule.

Moreover, for any valid λ there is either exactly one $\tilde{\lambda}$ for which $f(\tilde{\lambda}, d) = \lambda$ (namely $\tilde{\lambda} = \lambda$) or exactly two different $\tilde{\lambda}_1, \tilde{\lambda}_2$ with $g(\tilde{\lambda}_1, d) = -1$ and $g(\tilde{\lambda}_2, d) = 1$. Therefore $m^{\lambda}_{\mu,\nu}(d) \in \{0, 1\}$. □

6.A.2. Lemma. *If* $d = 2$ *then the multiplicity* $m^{\lambda}_{\mu,\nu}(d)$ *defined in Eq.* (6.126) *is either* 0 *or* 1 *for any valid* λ, μ, ν.

Proof:
Fix a valid combination of λ, μ, ν, i.e., $\mu \vdash n$, $\nu \vdash m$ with $\ell(\mu), \ell(\nu) \leqslant 2$ and $\lambda = (\lambda^l, \lambda^r)$ with $k := n - |\lambda^l| = m - |\lambda^r| \geqslant 0$ and $\ell(\lambda^l) + \ell(\lambda^r) \leqslant d$. Assume that $\tilde{\lambda} = (\tilde{\lambda}^l, \tilde{\lambda}^r)$ is a pair of partitions $\tilde{\lambda}^l \vdash n - k(\tilde{\lambda})$ and $\tilde{\lambda}^r \vdash m - k(\tilde{\lambda})$ for some integer $k(\tilde{\lambda}) \geqslant 0$ with $\ell(\tilde{\lambda}^l) \leqslant 2$ and $\ell(\tilde{\lambda}^r) \leqslant 2$. Again, we use a result of [Kin71] stating that for $d = 2$,

$$g(\tilde{\lambda}, 2) = \begin{cases} 1 & \text{if } \ell(\tilde{\lambda}^l) + \ell(\tilde{\lambda}^r) \leqslant 2, \\ -1 & \text{if } \ell(\tilde{\lambda}^l) = \ell(\tilde{\lambda}^r) = 2 \text{ and } \tilde{\lambda}^l_1 > \tilde{\lambda}^l_2 \text{ and } \tilde{\lambda}^{r\prime}_1 > \tilde{\lambda}^{r\prime}_2, \\ 0 & \text{otherwise.} \end{cases} \tag{6.133}$$

We need to consider only two different cases.

Case $k = \min(n, m)$. Without loss of generality assume $k = m$, i.e., $\lambda^r = \varnothing$. Then according to Eq. (6.133) the first sum in Eq. (6.126) contains only one term corresponding to $\tilde{\lambda} = \lambda$:

$$m^{\lambda}_{\mu,\nu}(2) = \sum_{\gamma \vdash k} c^{\mu}_{\gamma\lambda^l} c^{\nu}_{\gamma\varnothing} = \sum_{\gamma \vdash k} c^{\mu}_{\gamma\lambda^l} \delta_{\nu,\gamma} = c^{\mu}_{\nu\lambda^l}. \tag{6.134}$$

Since $\ell(\mu), \ell(\nu), \ell(\lambda^l) \leqslant 2$, it follows from the Littlewood–Richardson rule that $m^{\lambda}_{\mu,\nu}(2) = c^{\mu}_{\nu\lambda^l} \in \{0, 1\}$.

Case $k < \min(n, m)$. In this case λ^l, λ^r are non-empty Young diagrams with only one row, i.e., $\ell(\lambda^l) = \ell(\lambda^r) = 1$. According to Eq. (6.133) there are now two $\tilde{\lambda}$ such that $f(\tilde{\lambda}, 2) = \lambda$ and $g(\tilde{\lambda}, 2) \neq 0$, namely $\tilde{\lambda} = \lambda$ which corresponds to $g(\tilde{\lambda}, 2) = 1$ and $\tilde{\lambda} = (\tilde{\lambda}^l, \tilde{\lambda}^r) = ((\lambda^l_1, 1), (\lambda^r_1, 1))$ which corresponds to $g(\tilde{\lambda}, 2) = -1$. Therefore

$$m^{\lambda}_{\mu,\nu}(2) = \sum_{\gamma \vdash k} c^{\mu}_{\gamma\lambda^l} c^{\nu}_{\gamma\lambda^r} - \sum_{\gamma \vdash k-1} c^{\mu}_{\gamma(\lambda^l_1,1)} c^{\nu}_{\gamma(\lambda^r_1,1)}. \tag{6.135}$$

Since $\ell(\lambda^l) = \ell(\lambda^r) = 1$ and $\ell(\mu), \ell(\nu) \leqslant 2$ we can use the Pieri rule to deduce $c^{\mu}_{\gamma\lambda^l}, c^{\nu}_{\gamma\lambda^r} \in \{0, 1\}$ and calculate

$$\begin{aligned} c^{\mu}_{\gamma\lambda^l} \neq 0 \text{ iff } \gamma \vdash k \text{ and } \ell(\gamma) \leqslant 2 \text{ and } \mu_2 \leqslant \gamma_1 \leqslant \mu_1 \text{ and } \gamma_2 \leqslant \mu_2, \\ c^{\nu}_{\gamma\lambda^r} \neq 0 \text{ iff } \gamma \vdash k \text{ and } \ell(\gamma) \leqslant 2 \text{ and } \nu_2 \leqslant \gamma_1 \leqslant \nu_1 \text{ and } \gamma_2 \leqslant \nu_2. \end{aligned}$$

Therefore the first sum in Eq. (6.135) becomes

$$\begin{aligned} &|\{(\gamma_1, \gamma_2) \vdash k : \max(\mu_2, \nu_2) \leqslant \gamma_1 \leqslant \min(\mu_1, \nu_1), \gamma_2 \leqslant \min(\mu_2, \nu_2)\}| = \\ &\quad = \left| \left\{ \gamma_2 \in \mathbb{Z} : \max(0, k - \mu_1, k - \nu_1) \leqslant \gamma_2 \leqslant \min\left(\left\lfloor \frac{k}{2} \right\rfloor, k - \mu_2, k - \nu_2, \mu_2, \nu_2 \right) \right\} \right|. \end{aligned} \tag{6.136}$$

It can be rewritten as

$$\sum_{\gamma \vdash k} c^{\mu}_{\gamma\lambda^l} c^{\nu}_{\gamma\lambda^r} = \max\left(\min\left(\left\lfloor \frac{k}{2} \right\rfloor, k - \mu_2, k - \nu_2, \mu_2, \nu_2 \right) - \max(0, k - \mu_1, k - \nu_1) + 1, 0 \right). \tag{6.137}$$

Similarly, the Littlewood–Richardson rule implies that $c^{\mu}_{\gamma(\lambda^l_1,1)}, c^{\nu}_{\gamma(\lambda^r_1,1)} \in \{0, 1\}$. Furthermore,

$$\begin{aligned} c^{\mu}_{\gamma(\lambda^l_1,1)} \neq 0 \text{ iff } \gamma \vdash k - 1 \text{ and } \ell(\gamma) \leqslant 2 \text{ and } \mu_2 \leqslant \gamma_1 + 1 \leqslant \mu_1 \text{ and } \gamma_2 \leqslant \mu_2 - 1, \\ c^{\nu}_{\gamma(\lambda^r_1,1)} \neq 0 \text{ iff } \gamma \vdash k - 1 \text{ and } \ell(\gamma) \leqslant 2 \text{ and } \nu_2 \leqslant \gamma_1 + 1 \leqslant \nu_1 \text{ and } \gamma_2 \leqslant \nu_2 - 1. \end{aligned}$$

The second sum in Eq. (6.135) now becomes

$$\begin{aligned} &|\{(\gamma_1, \gamma_2) \vdash k - 1 : \max(\mu_2, \nu_2) \leqslant \gamma_1 + 1 \leqslant \min(\mu_1, \nu_1), \gamma_2 \leqslant \min(\mu_2, \nu_2) - 1\}| = \\ &= \left| \left\{ \gamma_2 \in \mathbb{Z} : \max(0, k - \mu_1, k - \nu_1) \leqslant \gamma_2 \leqslant \min\left(\left\lfloor \frac{k-1}{2} \right\rfloor, k - \mu_2, k - \nu_2, \mu_2 - 1, \nu_2 - 1 \right) \right\} \right|. \end{aligned} \tag{6.138}$$

It can be rewritten as

$$\begin{aligned} &\sum_{\gamma \vdash k-1} c^{\mu}_{\gamma(\lambda^l_1,1)} c^{\nu}_{\gamma(\lambda^r_1,1)} = \\ &\quad = \max\left(\min\left(\left\lfloor \frac{k-1}{2} \right\rfloor, k - \mu_2, k - \nu_2, \mu_2 - 1, \nu_2 - 1 \right) - \max(0, k - \mu_1, k - \nu_1) + 1, 0 \right). \end{aligned} \tag{6.139}$$

From Eqs. (6.135), (6.137) and (6.139) we clearly see that $m^{\lambda}_{\mu,\nu}(2) \in \{0, 1\}$. □

6.A.2 Computing the blocks of $\mathcal{A}^d_{n,m}$ in the Gelfand–Tsetlin basis

Here we propose an algorithm for computing the blocks of an arbitrary $\mathcal{A}^d_{n,m}$ algebra element in the Gelfand–Tsetlin basis. In line with our philosophy, the algorithm is fully diagrammatic, namely, all computation takes place in $\mathcal{B}^d_{n,m}$ instead of $\mathcal{A}^d_{n,m}$. Here we only sketch the reasoning behind the algorithm, and we leave it to future work to establish its correctness formally. This paves one possible route for removing the additional symmetry assumption in Theorem 6.3.4 and thus extending our framework from linear to general semidefinite unitary-equivariant programs, alongside with other approach described in Section 6.4.

The natural $*$-algebra structure of $\mathcal{B}^d_{n,m}$ is the important ingredient in this section. Consider a random hermitian (with respect to the natural $*$-algebra structure) element of $\mathcal{B}^d_{n,m}$ given as a linear combination of diagrams with random real coefficients b_i:

$$B := \sum_{i=1}^{(n+m)!} b_i \sigma_i. \tag{6.140}$$

Throughout this section we fix $\lambda \in \widehat{\mathcal{A}}^d_{n,m}$ and choose an arbitrary ordering $i \in [d_\lambda]$ of all paths in $\mathrm{Paths}(\lambda)$. Let B_{ij} denote the (i,j)-th entry of block λ when the matrix $\psi^d_{n,m}(B) \in \mathcal{A}^d_{n,m}$ is expressed in the Gelfand–Tsetlin basis. That is, let $B_{ij} := (A_\lambda)_{ij}$ for all $i,j \in [d_\lambda]$, where A_λ is a matrix of size $d_\lambda \times d_\lambda$ that appears in the first register of the decomposition:

$$U_{\mathrm{Sch}(n,m)}\, \psi^d_{n,m}(B)\, U^\dagger_{\mathrm{Sch}(n,m)} = \bigoplus_{\lambda \in \widehat{\mathcal{A}}^d_{n,m}} [A_\lambda \otimes I_{m_\lambda}]. \tag{6.141}$$

Note from Eq. (6.140) that B_{ij} is a linear combination of the variables b_k. Our goal is to determine B_{ij} for all choices of $\lambda \in \widehat{\mathcal{A}}^d_{n,m}$ and $i,j \in [d_\lambda]$.

Let $T = \lambda_0 \to \cdots \to \lambda_{n+m}$ be the i-th path in the Bratteli diagram of $\mathcal{B}^d_{n,m}$ that goes from the root to the leaf λ. Let us denote the preimage of $\varepsilon^{\mathcal{A}}_T$ under $\psi^d_{n,m}$ by

$$\varepsilon_i := \prod_{k=1}^{n+m} \prod_{\mu : \lambda_{k-1} \to \mu \neq \lambda_k} \frac{J^{\mathcal{B}}_k - c_{\lambda_{k-1}\to\mu}}{c_{\lambda_{k-1}\to\lambda_k} - c_{\lambda_{k-1}\to\mu}} \in \mathcal{B}^d_{n,m}, \tag{6.142}$$

where, in contrast to Eq. (3.65), the second product runs over edges in the Bratteli diagram of the family $\mathcal{B}$ instead of $\mathcal{A}$. By construction, the block λ of ε_i is equal to $|i\rangle\langle i|$ while all other blocks vanish:

$$U_{\mathrm{Sch}(n,m)}\, \psi^d_{n,m}(\varepsilon_i)\, U^\dagger_{\mathrm{Sch}(n,m)} = \bigoplus_{\mu \in \widehat{\mathcal{A}}^d_{n,m}} \big[\delta_{\lambda,\mu} |i\rangle\langle i| \otimes I_{m_\mu}\big]. \tag{6.143}$$

Since $\psi^d_{n,m}(\varepsilon_i B \varepsilon_i) = B_{ii} \cdot \psi^d_{n,m}(\varepsilon_i)$, knowing ε_i allows us to diagrammatically extract B_{ii} by computing

$$B_{ii} = \frac{\mathrm{Tr}(B\varepsilon_i)}{\mathrm{Tr}(\varepsilon_i)}, \tag{6.144}$$

where $\mathrm{Tr}(\varepsilon_i) = m_\lambda$ for every $i \in [d_\lambda]$.

To extract the off-diagonal entries B_{ij}, we would like to have operators ε_{ij} that are analogous to ε_i but instead of $|i\rangle\langle i|$ have $|i\rangle\langle j|$, for any $i,j \in [d_\lambda]$, in block λ of Eq. (6.143). While we do not have an expression for ε_{ij}, knowing ε_i and ε_j is enough to diagrammatically extract B_{ij}. This can be done via the following algorithm:

1. For every $i \in [d_\lambda]$, diagrammatically compute $\varepsilon_1 B \varepsilon_i$ and $\varepsilon_i B \varepsilon_1$. Since

$$\psi^d_{n,m}(\varepsilon_1 B \varepsilon_i) \cdot \psi^d_{n,m}(\varepsilon_i B \varepsilon_1) = B_{1i} B_{i1} \cdot \psi^d_{n,m}(\varepsilon_1), \tag{6.145}$$

we can diagrammatically compute

$$B_{1i}B_{i1} = \frac{\mathrm{Tr}\big((\varepsilon_1 B \varepsilon_i)\cdot(\varepsilon_i B \varepsilon_1)\big)}{\mathrm{Tr}(\varepsilon_1)}. \tag{6.146}$$

2. Since the element B is hermitian with real coefficients, $B_{1i} = B_{i1}$ as real numbers. From Eq. (6.146) we can set

$$B_{1i} = B_{i1} := \sqrt{\frac{\mathrm{Tr}\big((\varepsilon_1 B \varepsilon_i)\cdot(\varepsilon_i B \varepsilon_1)\big)}{\mathrm{Tr}(\varepsilon_1)}} \tag{6.147}$$

3. For every $i \in [d_\lambda]$ we set

$$\varepsilon_{1i} := \frac{\varepsilon_1 B \varepsilon_i}{B_{1i}}, \qquad \varepsilon_{i1} := \frac{\varepsilon_i B \varepsilon_1}{B_{i1}}. \tag{6.148}$$

4. Once we know all of the ε_{1i} and ε_{i1}, we can diagrammatically compute

$$B_{ij} = \frac{\mathrm{Tr}\big(\varepsilon_{1i} B \varepsilon_{j1}\big)}{\mathrm{Tr}(\varepsilon_1)} \tag{6.149}$$

for every $i, j \in [d_\lambda]$. We can also compute $\varepsilon_{ij} = \varepsilon_{i1}\varepsilon_{1j}$ for every $i, j \in [d_\lambda]$.

Since the multiplication of two arbitrary linear combinations of diagrams has complexity $O\big(\dim(\mathcal{B}^d_{n,m})^2\big)$, the complexity $O\big(\dim(\mathcal{B}^d_{n,m})^2 \dim(\mathcal{A}^d_{n,m})\big)$ of the above algorithm does not depend on d asymptotically since

$$O\big(((n+m)!)^2 \dim(\mathcal{A}^d_{n,m})\big) \leqslant O\big(((n+m)!)^3\big), \tag{6.150}$$

where we used $\dim(\mathcal{A}^d_{n,m}) \leqslant \dim(\mathcal{B}^d_{n,m}) = (n+m)!$ (that is quite crude bound for small d).

6.A.3 Numerical values for the number of variables $N^d_{n,m}$

$n+m$		2	3	4	5	6	7	8	9	10
d	2	1.20	1.81	2.41	3.01	3.61	4.21	4.82	5.42	6.02
	3	1.91	2.86	3.82	4.77	5.73	6.68	7.63	8.59	9.54
	4	2.41	3.61	4.82	6.02	7.22	8.43	9.63	10.84	12.04
	5	2.80	4.19	5.59	6.99	8.39	9.79	11.18	12.58	13.98
	6	3.11	4.67	6.23	7.78	9.34	10.89	12.45	14.01	15.56
	7	3.38	5.07	6.76	8.45	10.14	11.83	13.52	15.21	16.90
	8	3.61	5.42	7.22	9.03	10.84	12.64	14.45	16.26	18.06
	9	3.82	5.73	7.63	9.54	11.45	13.36	15.27	17.18	19.08
	10	4.00	6.00	8.00	10.00	12.00	14.00	16.00	18.00	20.00

Table 6.3: The logarithm of the number of variables $\log_{10}(d^{2(n+m)})$ in a naive implementation of the SDP (6.37).

n	m	d								
		2	3	4	5	6	7	8	9	10
1	1	2								
1	2	2	3							
1	3	3	4	5						
2	2	3	5	6						
1	4	3	6	7	8					
2	3	3	6	8	9					
1	5	4	7	10	11	12				
2	4	4	8	12	14	15				
3	3	4	8	12	14	15				
1	6	4	9	13	16	17	18			
2	5	4	10	15	19	21	22			
3	4	4	10	16	21	23	24			
1	7	5	11	17	21	24	25	26		
2	6	5	12	21	27	31	33	34		
3	5	5	12	21	28	33	35	36		
4	4	5	13	23	31	37	39	40		
1	8	5	13	21	28	32	35	36	37	
2	7	5	14	25	35	41	45	47	48	
3	6	5	15	27	39	47	52	54	55	
4	5	5	15	28	41	50	56	58	59	
1	9	6	15	27	36	43	47	50	51	52
2	8	6	17	32	46	57	63	67	69	70
3	7	6	17	34	50	63	71	76	78	79
4	6	6	18	37	56	72	82	88	90	91
5	5	6	18	36	54	70	80	86	88	89

Table 6.4: The number of variables $N^d_{n,m}$ in a unitary-equivariant LP with full walled Brauer algebra symmetry, see Eq. (6.23).

$n+m$		2	3	4	5	6	7	8	9	10
d	2	2	3	6	10	20	35	70	126	252
	3		4	9	21	51	127	323	835	2,188
	4			10	25	70	196	588	1,764	5,544
	5				26	75	225	715	2,347	7,990
	6					76	231	756	2,556	9,096
	7						232	763	2,611	9,415
	8							764	2,619	9,486
	9								2,620	9,495
	10									9,496

Table 6.5: The number of variables $N^d_{n,m}$ in a unitary-equivariant LP with Gelfand–Tsetlin symmetry, see Eq. (6.26).

n	m	d								
		2	3	4	5	6	7	8	9	10
1	1	2								
1	2	3	4							
1	3	4	6	7						
2	2	6	9	10						
1	4	5	9	11	12					
2	3	7	14	17	18					
1	5	6	12	16	18	19				
2	4	10	22	30	33	34				
3	3	10	25	34	37	38				
1	6	7	16	23	27	29	30			
2	5	11	30	44	52	55	56			
3	4	13	39	60	70	73	74			
1	7	8	20	31	38	42	44	45		
2	6	14	41	67	82	90	93	94		
3	5	16	56	96	119	129	132	133		
4	4	19	66	116	143	154	157	158		
1	8	9	25	41	53	60	64	66	67	
2	7	15	52	91	119	134	142	145	146	
3	6	19	79	148	195	219	229	232	233	
4	5	22	97	189	253	282	293	296	297	
1	9	10	30	53	71	83	90	94	96	97
2	8	18	66	126	172	201	216	224	227	228
3	7	22	102	213	298	347	371	381	384	385
4	6	28	139	306	434	505	535	546	549	550
5	5	28	149	332	478	556	587	598	601	602

Table 6.6: The number of variables $N^d_{n,m}$ in a unitary-equivariant SDP with an $\mathrm{S}_n \times \mathrm{S}_m$ symmetry, see Eq. (6.35). Such SDP reduces to an LP when $\min(n, m) \leqslant 2$ or $d = 2$, see Section 6.A.1. These cases are highlighted in grey.

$n+m$		2	3	4	5	6	7	8	9	10
d	2	2	5	14	42	132	429	1,430	4,862	16,796
	3		6	23	103	513	2,761	15,767	94,359	586,590
	4			24	119	694	4,582	33,324	261,808	2,190,688
	5				120	719	5,003	39,429	344,837	3,291,590
	6					720	5,039	40,270	361,302	3,587,916
	7						5,040	40,319	362,815	3,626,197
	8							40,320	362,879	3,628,718
	9								362,880	3,628,799
	10									3,628,800

Table 6.7: The number of variables $N^d_{n,m} = \dim(\mathcal{A}^d_{n,m})$ in a unitary-equivariant SDP with no additional symmetry.

Chapter 7

Monogamy of highly symmetric states

In this chapter, we go a little bit beyond the standard setting of mixed Schur–Weyl duality and explore another version of Schur–Weyl duality involving the orthogonal group. The specific problem we focus on is *quantum state extendibility*. More precisely, we investigate the extent to which two particles can be maximally entangled when they are similarly entangled also with other particles on the complete graph, specifically focusing on Werner, isotropic, and Brauer states. We approach the problem by formalising it as a semidefinite program (SDP), which we solve analytically using tools from representation theory of symmetric, unitary and orthogonal groups, and the Brauer algebra.

This chapter is based on [All+23].

7.1 Introduction

Monogamy of entanglement is a fundamental feature of quantum theory [Ter04; KW04]. Intuitively, it states that if two quantum systems are entangled with each other, they cannot be too entangled with other systems. Incarnations of monogamy include the so-called *quantum de Finetti theorem*, allowing, for example, security proofs of quantum cryptography [Ren08], SDP relaxations for bilinear optimisation [BBFS22], and ground energy approximations of local Hamiltonians via product states [BH13]. Studying monogamy in full generally is equivalent to the so-called *quantum marginal problem* [WDGC13; Sch15; Kly04; Kly06], which is a notoriously difficult problem. Restricted versions of the quantum marginal problem known as *state extension* or *state extendibility* problems [Wer89a; Doh14] are fundamental in quantum information. The main idea behind state extension is to certify or find a suitable global state on several quantum systems such that certain subsystems are in a fixed specified state.

In this chapter, we formalize state extension by introducing the concept of G-*extendibility* for arbitrary graphs G, and study it analytically for several important classes of symmetric states widely used in quantum information on clique graphs $G = K_n$.

More concretely, a bipartite symmetric quantum state σ is G-*extendible* for a graph G if there exists a global state ρ, on the vertices of G, such that for all edges e of G the reduced state ρ_e is equal to σ. Our graph extendibility approach, which can be viewed as a continuation of the work described in [WVC03], not only generalises existing concepts but also serves as a unifying framework for various problems in quantum information theory.

Consider the scenario where the graph G is a *star graph* $K_{1,n}$. In this case, our $K_{1,n}$-*extendibility* is equivalent to the established notion of n-*extendibility* of a bipartite quantum state, which was first used to formalize the intuition behind *monogamy of entanglement* [Ter04]. It states that if a bipartite state is n-*extendible* for every n, it must be a separable state of the form $\sum_i p_i \rho_i \otimes \sigma_i$ [FLV88; RW88; DPS04].

In the instance where the graph G is a *complete bipartite graph* $K_{n,m}$, then our $K_{n,m}$-*extendibility* correspond to the n, m-*extendibility*, also known as *symmetric extendibility* [TDS03]. Moreover, a bipartite state is n, m-*extendible* for all n, m, if and only if it is n-*extendible* for all n [JV13].

In the case where the graph G equals a *complete graph* K_n, then our K_n-*extendibility* is equivalent to the n-*exchangeability* of a bipartite symmetric quantum state. This notion is related to the celebrated *quantum de Finetti theorem*. It asserts that if a bipartite state is n-*exchangeable* for every n, then it is a convex combination of product states of the form $\sum_i p_i \rho_i \otimes \rho_i$ [HM76; CFS02; KR05; CKMR07].

All these notions have a lot of applications. For example, the $K_{1,n}$-extendibility of isotropic states is intrinsically related to $1 \to n$ quantum cloning problem [Wer98; KW99; NPR23]. One approach to obtaining the optimal $1 \to n$ symmetric quantum cloning map is to exploit Choi–Jamiołkowski's isomorphism to translate a $K_{1,n}$-extendible isotropic state into a quantum channel. Furthermore, extendibility on *circle graphs* has direct implications for quantum cryptography in the context of quantum position verification [Buh+14; KMS11; Unr14]. Our framework is also suitable for quantum network applications, notably in generating multiple EPR-pairs from an n-party resource state [BSSW24].

In quantum information, it is common to consider classes of symmetric states, such as the one-parameter families of *Werner* and *isotropic states* [Wer89b; HH99]. They admit a two-parameter generalisation to what we call *Brauer states* [VW01; PJPY24], which are defined through the *Schur–Weyl duality* of the *orthogonal group* [Bra37]. Brauer states can be seen as a generalisation of Choi states of quantum channels commonly known as *Werner–Holevo channels*.

In this work, we focus on understanding the monogamy of entanglement of such states. In particular, we determine the exact possible maximum values of the projection to the maximally entangled state and antisymmetric Werner state. Before our work, the exact values in arbitrary local dimensions for the projection overlap in the case of Werner, and isotropic states were known only in the context of the monogamy theorem, namely for $K_{1,n}$-extendibility [VW01] and for *complete bipartite graph* $K_{n,m}$-extendibility [JSZ22]. Some aspects of K_n-extendibility were also studied in [JSZ18; JZ21; Jak22].

Understanding the properties of the mentioned symmetric states is important in quantum information. Examples of applications of these symmetries can be found in recent work focusing on developing approximation algorithms for local Hamiltonians, notably the quantum Max-Cut problem [Tak+23; WCEHK24]. In these applications, the analytical values that we derive are crucial for understanding this model, as they provide insights beyond what can be obtained by asymptotic approximations. In the context of constructing approximation algorithms to quantum Max-Cut problem, exact $K_{1,n}$-extendibility value played a crucial role in obtaining better approximation ratios beyond product state approximations [AGM20; PT21; Lee22; Kin23; LP24]. We expect our results to be similarly helpful for obtaining better approximation values for such optimisation problems.

Summary of our results

We informally summarize our results here. We shall consider the n-exchangeability of the three distinct families of symmetric quantum states: Werner, Brauer, and isotropic. We provide analytical solutions of maximum values of the projection onto the antisymmetric state in the Werner case, as well as into the maximally entangled state in the Brauer and isotropic case. We call these values $q_W(n, d), p_B(n, d)$ and $p_I(n, d)$, respectively.

7.1.1. THEOREM (Summary of Theorems 7.4.1, 7.4.2, 7.4.10 and Lemma 7.4.9). *The maximum values of the above projections are:*

$$\textbf{\textit{Werner:}}\ q_W(n,d) = \frac{d-1}{2d}\frac{(n+k+d)(n-k)}{n(n-1)} + \frac{k(k-1)}{n(n-1)},\ \textit{where } k = n \bmod d,$$

$$\textbf{\textit{Brauer:}}\ p_B(n,d) = \frac{1}{d} + \left(1-\frac{1}{d}\right)\frac{1}{n+n \bmod 2 - 1},$$
$$q_B(n,d) = q_W(n,d),$$

$$\textbf{\textit{Isotropic:}}\ p_I(n,d) = \begin{cases} \frac{1}{d^2} + \left(1-\frac{1}{d^2}\right)\frac{1}{n+n \bmod 2-1} & \textit{if } d > n \textit{ or either } d \textit{ or } n \textit{ is even,} \\ \frac{1}{d^2} + \left(1-\frac{1}{d^2}\right)\min\left\{\frac{2d+1}{2dn+1}, \frac{1}{n-1}\right\} & \textit{if } n \geqslant d \textit{ and both } d \textit{ and } n \textit{ are odd.} \end{cases}$$

As a corollary, if we parametrize the Werner and isotropic states with a parameter p, and the Brauer states with two parameters p and q (see Section 7.2.2), we can summarize in the following table the parameter values for which these families of states are $K_{1,n}$-extendible (n-extendible) and K_n-extendible (n-exchangeable) for all n:

	$K_{1,n}$-extendibility	K_n-extendibility
Werner	$q \leqslant \frac{1}{2}$	$q \leqslant \frac{d-1}{2d}$
Brauer	$p \leqslant \frac{1}{d} \wedge q \leqslant \frac{1}{2}$	$p \leqslant \frac{1}{d} \wedge q \leqslant f(p)$
isotropic	$p \leqslant \frac{1}{d}$	$p = \frac{1}{d^2}$

where $f(p)$ is some unknown function such that it is upper bounded as $f(p) \leqslant \frac{d-1}{2d}$, see Conjecture 7.5.1. However, for qubits the whole Brauer (p,q)-extendibility region can be obtained analytically for all n:

7.1.2. THEOREM (Theorem 7.4.15). *For $d = 2$ and all $n \geqslant 2$ the maximal value $q(p)$ for every $p \in [0,1]$ equals to*

$$q(p) = \begin{cases} \frac{\lceil n/2\rceil+1}{\lceil n/2\rceil-1}p & \textit{if } p < \frac{\lceil n/2\rceil-1}{2(2\lceil n/2\rceil-1)}, \\ \frac{\lceil n/2\rceil}{2\lceil n/2\rceil-1} - p & \textit{if } \frac{\lceil n/2\rceil}{2\lceil n/2\rceil-1} \geqslant p \geqslant \frac{\lceil n/2\rceil-1}{2(2\lceil n/2\rceil-1)}, \\ 0 & \textit{otherwise.} \end{cases} \tag{7.1}$$

In particular, this theorem implies $f(p) = 1/4 - |1/4 - p|$ for qubits, see Fig. 7.6.

The chapter is organised as follows. In Section 7.2 we recall some basic definitions and known representation theory results. In Section 7.3, we set up the problems through primal and dual SDP formulations. Section 7.4 contains the main results of the chapter, namely, the solution of the problems in the case of the complete graph for the above three families of symmetric states.

7.2 Preliminaries

In this chapter, the term *graph* refers to an undirected, simple graph that has no self-loops. A graph $G = (V, E)$ has vertex set V, edge set $E \subset V \times V$, and its number of vertices is equal to $n := |V|$. We denote by $\mathrm{Aut}(G)$ the *automorphism group* of the graph G. The *complete graph* K_n with n vertices includes all possible edges, i.e. $(u,v) \in E$ for each distinct pair of vertices u and v in V (e.g., see Fig. 7.1a). This graph has $n(n-1)/2$ edges, which is the maximum number

of edges in an n-vertex graph. The *star graph* $K_{1,n}$ on $n+1$ vertices has a distinct central vertex $v \in V$ that is connected to each of the remaining n vertices, i.e. $E = \{(u, v) \mid u \in V, u \neq v\}$ (e.g., see Fig. 7.1b). An *edge-transitive* graph is a graph G such that for any two edges e_1 and e_2 in E, there exists an automorphism of G that maps e_1 to e_2 [Big93]. Equivalently, a graph G is edge-transitive if and only if $G \setminus e_1 \simeq G \setminus e_2$ for all $e_1, e_2 \in E$ [ADSV92]. Both the complete graphs and the star graphs are edge-transitive. An example of a non edge-transitive graph is given in the *path graph* P_5 Fig. 7.1c.

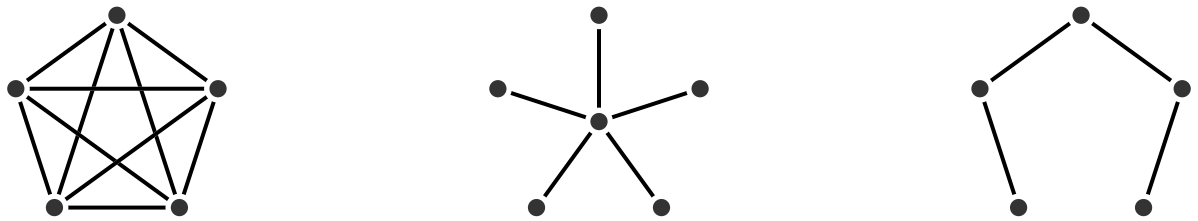

(a) K_5 (b) $K_{1,5}$ (c) P_5

Figure 7.1: The complete graph K_5 with $\mathrm{Aut}(K_5) \simeq S_5$, the star graph $K_{1,5}$ with $\mathrm{Aut}(K_{1,5}) \simeq S_5$, and the path graph P_5 with $\mathrm{Aut}(P_5) \simeq \mathbb{Z}_2$.

Let $\mathcal{H} := \mathbb{C}^d$ denote a complex Hilbert space of finite dimension $d \geqslant 2$. For any graph G, we will associate a separate copy of $\mathcal{H}$ to each vertex of G (we will refer to $d = \dim \mathcal{H}$ as *local dimension*). The combined space associated to V is then the n-fold tensor power $\mathcal{H}^{\otimes n}$. If ρ is a quantum state on $\mathcal{H}^{\otimes n}$ and $e = (u, v) \in E$ an edge, we will denote by ρ_e the *reduced state* on systems u and v:

$$\rho_e := \mathrm{Tr}_{V \setminus \{u,v\}} \rho. \tag{7.2}$$

In quantum information literature, a bipartite quantum state ρ on $\mathcal{H}_A \otimes \mathcal{H}_B$ is called n-*extendible* with respect to $\mathcal{H}_B$ if there exists a quantum state σ on $\mathcal{H}_A \otimes \mathcal{H}_B^{\otimes n}$, invariant under any permutation of the $\mathcal{H}_B$ subsystems, such that

$$\rho = \mathrm{Tr}_{B^{\otimes n-1}} \sigma. \tag{7.3}$$

We can express this concept as a *marginal problem* within the context of the star graph $K_{1,n}$, where the central vertex corresponds to the system $\mathcal{H}_A$, and the leaves represent the subsystems $\mathcal{H}_B$. A quantum state ρ is n-extendible if and only if there exists a state on $K_{1,n}$ with reduced states along all edges equal ρ. Therefore, in the current chapter, we refer to n-*extendibility* as $K_{1,n}$-*extendibility*.

Let $\mathrm{W}, \mathrm{I}, \mathrm{F} \in \mathrm{Herm}(\mathcal{H} \otimes \mathcal{H})$ denote the unnormalised *maximally entangled* and *maximally mixed* states, and the *flip* operator on two systems:

$$\mathrm{W} := \sum_{i,j=1}^{d} |ii\rangle\langle jj|, \quad \mathrm{I} := \sum_{i,j=1}^{d} |ij\rangle\langle ij| \quad \text{and} \quad \mathrm{F} := \sum_{i,j=1}^{d} |ij\rangle\langle ji|. \tag{7.4}$$

Note that $\mathrm{Tr}\,\mathrm{W} = d$, $\mathrm{Tr}\,\mathrm{I} = d^2$ and $\mathrm{Tr}\,\mathrm{F} = d$.

7.2.1 Schur–Weyl duality for the orthogonal group

For this chapter, in addition to Schur–Weyl duality for the symmetric group (see Section 2.10), we also need a similar result for the orthogonal group. This Schur–Weyl duality result was discovered by Richard Brauer for *orthogonal* and *symplectic groups* [Bra37]. In the following, we only focus on the complex orthogonal group O_d. Brauer's variant of Schur–Weyl duality states that the commutant of the diagonal action of the complex orthogonal group O_d on the

space $(\mathbb{C}^d)^{\otimes n}$ is the image of the *Brauer algebra* Br_n^d. More precisely, using the same diagonal action ϕ_n^d from Eq. (2.108) for the subgroup $\mathrm{O}_d \subset \mathrm{GL}_d$

$$\phi_n^d(g)(|x_1\rangle \otimes |x_2\rangle \otimes \cdots \otimes |x_n\rangle) = g|x_1\rangle \otimes g|x_2\rangle \otimes \cdots \otimes g|x_n\rangle \tag{7.5}$$

for every $g \in \mathrm{O}_d$, we define the matrix algebra

$$\mathcal{O}_n^d := \mathrm{span}_{\mathbb{C}}\{\phi_n^d(g) \mid g \in \mathrm{O}_d\}. \tag{7.6}$$

The commutant of $\mathcal{O}_n^d$ will turn out to be the image of the Brauer algebra Br_n^d which we define now.

A *Brauer diagram* is a diagram with two columns of n vertices which are paired up in an arbitrary way, i.e. it is a pairing on a set of $2n$ elements. The set of all Brauer diagrams is denoted Br_n. For example, a diagram from Br_5 may look like

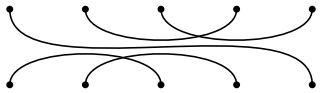

(7.7)

The Brauer algebra Br_n^d for any $d \in \mathbb{C}$ is defined as the complex vector space spanned by all Brauer diagrams $\pi \in \mathrm{Br}_n$, i.e. $\mathrm{Br}_n^d := \mathrm{span}_{\mathbb{C}}\{\pi \in \mathrm{Br}_n\}$. The multiplication in Br_n^d is defined by concatenation of such diagrams, counting the number of loops formed, erasing them and multiplying the result by a factor of $d^{\#\mathrm{loops}}$. This exactly identital to the walled Brauer algebra, see Section 3.2. Note that the symmetric group algebra $\mathbb{C}\mathrm{S}_n$, is a subalgebra of the Brauer algebra, $\mathbb{C}\mathrm{S}_n \subset \mathrm{Br}_n^d$, consisting only of diagrams which do not have vertical pairings on the same side of the diagram.

The Brauer algebra Br_n^d admits an action on $(\mathbb{C}^d)^{\otimes n}$ defined via a linear map $\psi_n^d : \mathrm{Br}_n^d \to (\mathbb{C}^d)^{\otimes n}$, such that for every diagram $\pi \in \mathrm{Br}_n^d$ and $x_{\bar{1}}, \ldots, x_{\bar{n}}, x_1, \ldots, x_n \in [d]$,

$$\big(\langle x_{\bar{1}}| \otimes \cdots \otimes \langle x_{\bar{n}}|\big)\psi_n^d(\pi)\big(|x_1\rangle \otimes \cdots \otimes |x_n\rangle\big) := \begin{cases} 1 & \text{if } x_k = x_l \text{ for all vertices } k \text{ and } l \text{ connected in } \pi, \\ 0 & \text{otherwise,} \end{cases} \tag{7.8}$$

which is exactly analogous to Eq. (3.17). The image $\psi_n^d(\mathrm{Br}_n^d)$ of the diagram algebra Br_n^d is a matrix representation of Br_n^d which we will denote by

$$\mathcal{B}_n^d := \mathrm{span}_{\mathbb{C}}\{\psi_n^d(\pi) \mid \pi \in \mathrm{Br}_n^d\}. \tag{7.9}$$

Note that, in contrary to Eq. (3.46), in this chapter $\mathcal{B}_n^d$ refers to the matrix representation of the Brauer algebra and not to the walled Brauer algebra. The matrix algebra $\mathcal{B}_n^d$ is always semisimple, while the diagram algebra Br_n^d is not for small integers d [Wen88; DWH99; Rui05; RS06; AST17]. The irreducible representations of $\mathcal{B}_n^d$ are labelled using the following set [Oka16]:

$$\widehat{\mathcal{B}}_n^d := \left\{ \lambda \vdash n - 2r \;\middle|\; r \in \left\{0, \ldots, \left\lfloor \frac{n}{2} \right\rfloor\right\} \text{ and } \lambda'_1 + \lambda'_2 \leqslant d \right\}. \tag{7.10}$$

We will denote by $V_\lambda^{\mathcal{B}_n^d}$ and $W_\lambda^{\mathcal{O}_n^d}$ the spaces on which the corresponding irreducible representations of $\mathcal{B}_n^d$ and $\mathcal{O}_n^d$ act. Now we are ready to state the version of Schur–Weyl duality discovered by Brauer.

7.2.1. Theorem (Brauer). *The matrix algebras $\mathcal{B}_n^d$ and $\mathcal{O}_n^d$ are mutual commutants of each other. Equivalently, the space $(\mathbb{C}^d)^{\otimes n}$ decomposes into isotypic sectors labelled by $\lambda \in \widehat{\mathcal{B}}_n^d$ consisting of tensor product of irreducible representations of $\mathcal{B}_n^d$ and $\mathcal{O}_n^d$:*

$$(\mathbb{C}^d)^{\otimes n} \simeq \bigoplus_{\lambda \in \widehat{\mathcal{B}}_n^d} V_\lambda^{\mathcal{B}_n^d} \otimes W_\lambda^{\mathcal{O}_n^d}. \tag{7.11}$$

7.2.2 Werner, isotropic and Brauer states

In this chapter, we consider three classes of symmetric bipartite states ρ_{AB} based on different commutation relations:

1. a *Werner state* ρ_{AB} commutes with $U \otimes U$, i.e., $\left[\rho, U \otimes U\right] = 0$ for every $U \in \mathrm{U}_d$,
2. an *isotropic state* ρ_{AB} commutes with $\bar{U} \otimes U$, i.e., $\left[\rho, \bar{U} \otimes U\right] = 0$ for every $U \in \mathrm{U}_d$,
3. a *Brauer state*[1] ρ_{AB} commutes with $O \otimes O$, i.e., $\left[\rho, O \otimes O\right] = 0$ for every $O \in \mathrm{O}_d$.

Using the Schur–Weyl dualities from Sections 2.10 and 7.2.1, we can observe that these states are just linear combinations of the operators I, F, W. For our purposes, it will be better to parameterize them in terms of the projectors onto irreducible representations of the Brauer algebra $\mathcal{B}_2^d$:

$$\Pi_{\varnothing} := \frac{\mathrm{W}}{d}, \quad \Pi_{\ydiagram{2}} := \frac{\mathrm{I} - \mathrm{F}}{2}, \quad \Pi_{\ydiagram{1,1}} := \frac{\mathrm{I} + \mathrm{F}}{2} - \frac{\mathrm{W}}{d}, \tag{7.12}$$

and the projectors onto the irreducible representations of $\mathcal{S}_2^d$, known as antisymmetric and symmetric subspaces, are

$$\varepsilon_{\ydiagram{2}} := \frac{\mathrm{I} - \mathrm{F}}{2}, \quad \varepsilon_{\ydiagram{1,1}} := \frac{\mathrm{I} + \mathrm{F}}{2}. \tag{7.13}$$

These projectors are primitive central idempotents, see Section 2.7.5. More generally, we can define a primitive central idempotent ε_λ known as *Young symmetriser* which corresponds to an irreducible representation λ of $\mathcal{S}_n^d$. We also call ε_λ an *isotypic projector* onto the relevant sector λ in the classical Schur–Weyl duality, see Section 2.10. Note that

$$\Pi_{\varnothing} + \Pi_{\ydiagram{2}} + \Pi_{\ydiagram{1,1}} = \mathrm{I}, \quad \varepsilon_{\ydiagram{2}} = \Pi_{\ydiagram{2}}, \quad \varepsilon_{\ydiagram{1,1}} = \mathrm{I} - \Pi_{\ydiagram{2}} = \Pi_{\ydiagram{1,1}} + \Pi_{\varnothing}, \tag{7.14}$$

and

$$\operatorname{Tr} \Pi_{\varnothing} = 1, \quad \operatorname{Tr} \Pi_{\ydiagram{2}} = \frac{d(d-1)}{2}, \quad \operatorname{Tr} \Pi_{\ydiagram{1,1}} = \frac{d(d+1)}{2} - 1. \tag{7.15}$$

The three classes of states can then be parameterised as follows:

1. The Werner states form a one-parameter family, parameterised by $q \in [0, 1]$, given by a convex combination of the normalised *antisymmetric* and *symmetric* projectors:

$$q \cdot \frac{\Pi_{\ydiagram{2}}}{\operatorname{Tr} \Pi_{\ydiagram{2}}} + (1 - q) \cdot \frac{\mathrm{I} - \Pi_{\ydiagram{2}}}{\operatorname{Tr}(\mathrm{I} - \Pi_{\ydiagram{2}})}. \tag{7.16}$$

2. The isotropic states form a one-parameter family, parameterised by $p \in [0, 1]$, given by a convex combination of the *maximally entangled state* and the normalised projection onto its orthogonal complement:

$$p \cdot \Pi_{\varnothing} + (1 - p) \cdot \frac{\mathrm{I} - \Pi_{\varnothing}}{\operatorname{Tr}(\mathrm{I} - \Pi_{\varnothing})}. \tag{7.17}$$

3. The Brauer states form a two-parameter family, parameterised by $p, q \in [0, 1]$ with $p + q \leqslant 1$, given by a convex combination of all three normalised orthogonal projectors:

$$p \cdot \Pi_{\varnothing} + q \cdot \frac{\Pi_{\ydiagram{2}}}{\operatorname{Tr} \Pi_{\ydiagram{2}}} + (1 - p - q) \cdot \frac{\Pi_{\ydiagram{1,1}}}{\operatorname{Tr} \Pi_{\ydiagram{1,1}}}. \tag{7.18}$$

A Werner state ρ_{AB} is separable if and only if $q \leqslant \frac{1}{2}$ [Wer89b], an isotropic state ρ_{AB} is separable if and only if $p \leqslant \frac{1}{d}$ [HH99], and a Brauer state ρ_{AB} is separable if and only if $q \leqslant \frac{1}{2}$ and $p \leqslant \frac{1}{d}$ (see Section 7.A.5).

[1] More precisely, we are talking about *orthogonal Brauer* states. In the case of the symplectic group, the commutant is also a Brauer algebra, so the corresponding states would be called *symplectic Brauer* states.

7.2.3 Jucys–Murphy elements

Special elements of the symmetric group algebra $\mathbb{C}\mathrm{S}_n$ and the Brauer algebra Br_n^d, called *Jucys–Murphy elements*, generate maximal commutative subalgebras inside the matrix algebras $\mathcal{A}_n^d$ and $\mathcal{B}_n^d$, respectively. They allow us, in principle, to build a representation theory of these algebras starting purely from the knowledge of their spectrum (see Section 2.7).

Recall from Eq. (2.73) that for $\mathbb{C}\mathrm{S}_n$ the Jucys–Murphy elements J_k^{S} are defined as $J_1^{\mathrm{S}} := 0$ and for every $k \in \{2, \dots, n\}$

$$J_k^{\mathrm{S}} := \sum_{i=1}^{k-1} (i, k), \tag{7.19}$$

where (i, k) is the transposition of i and k. Similarly, for the Brauer algebra Br_n^d the Jucys–Murphy elements J_k^{Br} are defined as $J_1^{\mathrm{Br}} := 0$ and, for every $k \in \{2, \dots, n\}$,

$$J_k^{\mathrm{Br}} := \sum_{i=1}^{k-1} (i, k) - \overline{(i, k)}, \tag{7.20}$$

where $\overline{(i, k)}$ is the vertical pairing vertices i and k. The sum of all Jucys–Murphy elements is central in the corresponding matrix algebra. Its spectrum is well-known and summarised in the next two lemmas which we adapt to our notation from [DLS18].

7.2.2. Lemma. *Consider the following element of the matrix algebra $\mathcal{A}_n^d$:*

$$J_{\mathcal{S}} := \sum_{k=1}^{n} \psi_n^d\big(J_k^{\mathrm{S}}\big) = \sum_{1 \leqslant i < j \leqslant n} \mathrm{F}_{i,j}. \tag{7.21}$$

Then, for any irreducible representation $\mu \in \widehat{\mathcal{A}}_n^d$, the element $J_{\mathcal{S}}$ acts on the irrep μ as a multiple of the identity:

$$\psi_\mu(J_{\mathcal{S}}) = \mathrm{cont}(\mu) \cdot I. \tag{7.22}$$

7.2.3. Lemma. *Consider the following element of the matrix algebra $\mathcal{B}_n^d$:*

$$J_{\mathcal{B}} := \sum_{k=1}^{n} \psi_n^d\big(J_k^{\mathrm{Br}}\big) = \sum_{1 \leqslant i < j \leqslant n} (\mathrm{F}_{i,j} - \mathrm{W}_{i,j}). \tag{7.23}$$

Then, for any irreducible representation $\lambda \in \widehat{\mathcal{B}}_n^d$, the element $J_{\mathcal{B}}$ acts on the irrep λ as a multiple of the identity:

$$\psi_\lambda(J_{\mathcal{B}}) = \left(\mathrm{cont}(\lambda) - \frac{n - |\lambda|}{2}(d - 1)\right) \cdot I, \tag{7.24}$$

where ψ_λ is irreducible representation of the algebra $\mathcal{B}_n^d$.

7.2.4. Remark. The commutation relation $[J_{\mathcal{S}}, J_{\mathcal{B}}] = 0$ holds for all n and d. This implies in particular that $J_{\mathcal{S}}$ and $J_{\mathcal{B}}$ share a common eigenbasis and can be simultaneously diagonalised.

7.2.4 Restrictions of Brauer algebra representations

We saw in Section 7.2.1 that under the action of the Brauer algebra Br_n^d, the space $\big(\mathbb{C}^d\big)^{\otimes n}$ decomposes into irreducible representations as

$$\big(\mathbb{C}^d\big)^{\otimes n} \simeq \bigoplus_{\lambda \in \widehat{\mathcal{B}}_n^d} V_\lambda^{\mathcal{B}_n^d} \otimes W_\lambda^{\mathcal{O}_n^d}. \tag{7.25}$$

By *restricting* the irreducible representations $V^{\mathcal{B}_n^d}$ of the algebra $\mathcal{B}_n^d$ to the algebra $\mathcal{A}_n^d$, the space $\left(\mathbb{C}^d\right)^{\otimes n}$ decomposes further as

$$\left(\mathbb{C}^d\right)^{\otimes n} \simeq \bigoplus_{\lambda\in\widehat{\mathcal{B}}_n^d} \mathrm{Res}^{\mathcal{B}_n^d}_{\mathcal{A}_n^d}\left(V_\lambda^{\mathcal{B}_n^d}\right) \otimes W_\lambda^{\mathcal{O}_n^d} \tag{7.26}$$

$$\simeq \bigoplus_{\lambda\in\widehat{\mathcal{B}}_n^d}\left(\bigoplus_{\mu\in\widehat{\mathcal{A}}_n^d} V_\mu^{\mathcal{A}_n^d}\otimes\mathbb{C}^{m_{\lambda,\mu}}\right)\otimes W_\lambda^{\mathcal{O}_n^d} \tag{7.27}$$

$$\simeq \bigoplus_{\mu\in\widehat{\mathcal{A}}_n^d} V_\mu^{\mathcal{A}_n^d}\otimes\left(\bigoplus_{\lambda\in\widehat{\mathcal{B}}_n^d} W_\lambda^{\mathcal{O}_n^d}\otimes\mathbb{C}^{m_{\lambda,\mu}}\right). \tag{7.28}$$

The multiplicities $m_{\lambda,\mu}$ have no known concise formula. Even the set

$$\Omega_{n,d} := \left\{(\lambda,\mu)\in\widehat{\mathcal{B}}_n^d\times\widehat{\mathcal{A}}_n^d \mid m_{\lambda,\mu}\neq 0\right\} \tag{7.29}$$

is still unknown analytically. However, Okada characterises it through an algorithm [Oka16, Proposition 2.5]. He finds a relatively simple subset $\Gamma_{n,d}\subset\Omega_{n,d}$ [Oka16, Theorem 5.4] defined as

$$\Gamma_{n,d} := \left\{(\lambda,\mu)\in\widehat{\mathcal{B}}_n^d\times\widehat{\mathcal{A}}_n^d \mid \lambda=(1^m),\, r(\mu)=m \text{ for some } m\in\{0,\dots,d\}\right\}, \tag{7.30}$$

where $r(\mu)$ is the number of rows with odd size in the Young diagram μ and $(1^0) := \varnothing$ is the empty partition.

The algorithm from [Oka16, Proposition 2.5, Proposition 2.6, Theorem 5.4] gives an analytical characterisation of some subsets of the set $\Omega_{n,d}$ in the following three easy cases:

1. if $\lambda=(1^m)$ for some $m\in\{0,\dots,d\}$, then $(\lambda,\mu)\in\Omega_{n,d}$ if and only if $r(\mu)=m$, i.e., $(\lambda,\mu)\in\Gamma_{n,d}$,
2. if $\lambda\vdash n$, then $(\lambda,\mu)\in\Omega_{n,d}$ if and only if $\mu=\lambda$,
3. if $\mu=(n)$, then $(\lambda,\mu)\in\Omega_{n,d}$ if and only if $\lambda=(n-2r)$ for some $r\in\{0,\dots,\lfloor\frac{n}{2}\rfloor\}$.

7.2.5. Remark. When the dimension d is 2, a complete and simple characterisation of positive multiplicities $m_{\lambda,\mu}$ can be found from the Okada algorithm [Oka16, Proposition 2.5] (see also [Rya, Proposition 6.6]): $(\lambda,\mu)\in\Omega_{n,2}$ if and only if $\lambda_1\leqslant\mu_1-\mu_2$, with the exceptions of $\lambda=\varnothing$, in which case both rows of μ must be even, and $\lambda=(1,1)$, in which case both rows of μ must be odd.

7.3 General formalisation of the problem

In this section, we formalize our problem. We quantify the monogamy of our highly symmetric entangled states via the following general semidefinite programs (SDPs). Let $\Pi\in\mathrm{Herm}(\mathcal{H}\otimes\mathcal{H})$ be any *flip-invariant* two-qudit projector, i.e., $\mathrm{F}\Pi\mathrm{F}^\dagger=\Pi$. Later Π will be either $\Pi_\varnothing$ or $\Pi_\boxplus$, and one should think about these projectors as the ones which select the entangled subspace of interest of the total Hilbert space. Now we want to solve the following SDPs for different choices of graph $G=(V,E)$ and projectors Π:

$$\tilde{p}^w_\Pi(G,d) := \max_{\rho,p}\ p \qquad \text{s.t.}\quad \mathrm{Tr}[\Pi_e\rho]\geqslant p\quad\forall e\in E,\quad \mathrm{Tr}[\rho]=1,\quad \rho\succeq 0, \tag{7.31}$$

$$p^w_\Pi(G,d) := \max_{\rho,p}\ p \qquad \text{s.t.}\quad \mathrm{Tr}[\Pi_e\rho]=p\quad\forall e\in E,\quad \mathrm{Tr}[\rho]=1,\quad \rho\succeq 0, \tag{7.32}$$

$$p^{avg}_\Pi(G,d) := \max_{\rho}\ \frac{1}{|E|}\sum_{e\in E}\mathrm{Tr}[\Pi_e\rho] \qquad \text{s.t.}\quad \mathrm{Tr}[\rho]=1,\quad \rho\succeq 0, \tag{7.33}$$

where Π_e is defined for every edge $e \in E$ as $\Pi_e := \Pi \otimes I_{\bar{e}}$, and $I_{\bar{e}}$ is the identity on all vertices except those of e. Note that $p_\Pi^{avg}(G,d)$ is just the largest eigenvalue of the Hamiltonian $\frac{1}{|E|}\sum_{e\in E}\Pi_e$:

$$p_\Pi^{avg}(G,d) = \lambda_{\max}\left(\sum_{e\in E}\frac{1}{|E|}\Pi_e\right). \tag{7.34}$$

We can also formalize our intuition from Section 7.1 a bit differently. Namely, given a one-parameter family of bipartite states $\sigma(p)$ and a graph G, we want to maximize p by finding a global state ρ such that $\rho_e = \sigma(p)$ for every edge $e \in E$:

$$p_\sigma(G,d) := \max_{\rho,p}\ p \qquad \text{s.t.} \quad \rho_e = \sigma(p) \quad \forall e \in E, \quad \mathrm{Tr}[\rho] = 1, \quad \rho \succeq 0, \tag{7.35}$$

The parameter p should be understood as some measure of entanglement. We focus on the cases, where σ states are Werner, Brauer or isotropic with p being the overlap onto the relevant projector Π defined as $p = \mathrm{Tr}[\Pi\sigma(p)]$.

7.3.1 Dual SDP approach

The *Lagrangian* [BV04] associated with the optimisation problem (7.31) is defined as

$$L\big(p,\rho,Z,(x_e)_e,y\big) := p + y\big(\mathrm{Tr}[\rho]-1\big) + \sum_{e\in E} x_e\big(\mathrm{Tr}[\Pi_e\rho]-p\big) + \big\langle Z,\rho\big\rangle, \tag{7.36}$$

where $y \in \mathbb{R}$ and $(x_e \in \mathbb{R})_e$ are real *Lagrange multipliers*, $Z \in \mathrm{Herm}\big((\mathbb{C}^d)^{\otimes n}\big)$ and $\langle\cdot,\cdot\rangle$ denotes the *Frobenius inner product*

$$\big\langle A,B\big\rangle := \mathrm{Tr}\left[A^*B\right]. \tag{7.37}$$

The *Min-Max principle* states that

$$\max_{p,\rho\succeq 0}\ \min_{\substack{y,x_e\geqslant 0\\ Z\succeq 0}}\ L\big(p,\rho,Z,(x_e)_e,y\big) \leqslant \min_{\substack{y,x_e\geqslant 0\\ Z\succeq 0}}\ \max_{p,\rho\succeq 0}\ L\big(p,\rho,Z,(x_e)_e,y\big). \tag{7.38}$$

In fact, *Slater's condition* holds true for our SDP (take $\rho = \frac{1}{d^n}\cdot \mathrm{I}^{\otimes n}$ and $p = 0$) and we have the equality. Rewriting the Lagrangian gives

$$L\big(p,\rho,Z,(x_e)_e,y\big) = -y + p\left(1-\sum_{e\in E}x_e\right) + \big\langle H+Z+yI,\rho\big\rangle, \tag{7.39}$$

where $H := \sum_{e\in E} x_e\Pi_e$. Making the constraints of the Lagrangian explicit, that is,

$$\max_{p,\rho\succeq 0}\ L\big(p,\rho,Z,(x_e)_e,y\big) = \begin{cases} -y & \text{if } \sum_{e\in E}x_e = 1 \text{ and } 0 \succeq H+Z+yI \\ \infty & \text{otherwise} \end{cases} \tag{7.40}$$

after substitution $y \mapsto -y$ the dual SDP of Eq. (7.32) becomes

$$\tilde{p}_\Pi^w(G,d) = \min_{(x_e)_e,y,Z}\ y \qquad \text{s.t.} \quad \sum_{e\in E}x_e = 1, \quad x_e \geqslant 0 \quad \forall e\in E, \quad 0 \succeq H+Z-yI, \quad Z\succeq 0. \tag{7.41}$$

Recall that for any Hermitian matrix M the smallest $\lambda \in \mathbb{R}$ such that $\lambda I \succeq M$ is equal to the largest eigenvalue $\lambda_{\max}(M)$. Then Eq. (7.41) can be, after simplifying the variable Z, rewritten as

$$\tilde{p}_\Pi^w(G,d) = \min_{\substack{\sum_{e\in E}x_e=1\\ x_e\geqslant 0,\,\forall e\in E}} \lambda_{\max}\left(\sum_{e\in E}x_e\Pi_e\right). \tag{7.42}$$

A similar calculation for $p^w_\Pi(G,d)$ from Eq. (7.31) shows that

$$p^w_\Pi(G,d) = \min_{\sum_{e\in E} x_e = 1} \lambda_{\max}\left(\sum_{e\in E} x_e \Pi_e\right). \tag{7.43}$$

We conjecture that $\tilde{p}^w_\Pi(G,d) = p^w_\Pi(G,d)$, and even more generally that:

7.3.1. Conjecture. *For any graph G and a flip-invariant orthogonal projection Π,*

$$\min_{\sum_{e\in E} x_e = 1} \lambda_{\max}\left(\sum_{e\in E} x_e \Pi_e\right) = \min_{\substack{\sum_{e\in E} x_e = 1 \\ x_e \geqslant 0,\, \forall e\in E}} \lambda_{\max}\left(\sum_{e\in E} x_e \Pi_e\right). \tag{7.44}$$

7.3.2 Automorphism group action and edge-transitive graphs

Let ρ be an optimal solution of the primal SDP (7.32) for a given graph $G = (V,E)$ with objective value p, and let us twirl it using the symmetries of G:

$$\tilde{\rho} = \frac{1}{|\mathrm{Aut}(G)|} \sum_{\pi\in \mathrm{Aut}(G)} \psi^d_n(\pi)\rho\psi^d_n(\pi^{-1}), \tag{7.45}$$

where $\mathrm{Aut}(G)$ is the automorphism group of G. Let $o(e)$ denote the orbit of edge $e \in E$ under this action. Note that $\tilde{\rho}$ still satisfies the inequality constraints of SDP (7.31):

$$\mathrm{Tr}[\Pi_e \tilde{\rho}] = \frac{1}{|o(e)|} \sum_{e'\in o(e)} p_{e'} \geqslant p, \tag{7.46}$$

where $p_e := \mathrm{Tr}[\Pi_e \rho]$ and we used that $p_e \geqslant p$ for the feasible solution ρ. That means that we can always restrict the set of feasible solutions only to those that are invariant under the action of the automorphism group of the graph G. This observation simplifies the dual SDP (7.42):

$$\tilde{p}^w_\Pi(G,d) = \min_{\substack{\sum_{o\in O(G)} x_o = 1 \\ x_o \geqslant 0,\, \forall o\in O(G)}} \lambda_{\max}\left(\sum_{o\in O(G)} x_o \sum_{e\in o} \frac{1}{|o|}\Pi_e\right), \tag{7.47}$$

where o denotes an orbit in the set of all orbits $O(G)$ of the induced automorphism group $\mathrm{Aut}(G)$ action on the set of edges E. An edge-transitive graph G has only one orbit, so the condition $x_o \geqslant 0$ naturally holds for Eq. (7.32) and Eq. (7.47) simplifies to

$$\tilde{p}^w_\Pi(G,d) = \lambda_{\max}\left(\sum_{e\in E} \frac{1}{|E|}\Pi_e\right) = p^{avg}_\Pi(G,d) = p^w_\Pi(G,d). \tag{7.48}$$

In the following sections, we will focus on understanding the values $p^w_\Pi(G,d)$ for the complete graph $G = K_n$ for the following choices of Π:

$$q_W(n,d) := p^w_\Pi(K_n,d) \text{ for } \Pi := \Pi_{\boxplus}, \tag{7.49}$$

$$p_B(n,d) := p^w_\Pi(K_n,d) \text{ for } \Pi := \Pi_{\oslash}. \tag{7.50}$$

We will also formulate a similar problem for isotropic states (which form a subset of Brauer states). In that case, we will refer to the optimised value by $p_I(n,d)$, see Section 7.4.2.

7.4 K_n-Extendibility

7.4.1 Werner states

Let us first consider in detail the case where the reduced two-body state is a Werner state, i.e., $\Pi = \Pi_{\boxplus} = \frac{\mathrm{I}-\mathrm{F}}{2}$. One can, in principle, directly solve Eq. (7.32) using techniques from [CKMR07], see Section 7.A.1. In this section, we will show how Jucys–Murphy elements help to solve the dual SDP in a simpler manner. It is easy to see that

$$q_W(n,d) = \lambda_{\max}(H_{K_n}) = \frac{1}{2}\left(1 - \frac{\lambda_{\min}(J_{\mathrm{S}})}{|E|}\right), \tag{7.51}$$

where $J_{\mathrm{S}} = \sum_{i=1}^{n} J_i$ and J_i are Jucys–Murphy elements for symmetric group S_n. The spectrum for Jucys–Murphy elements is well known, see Section 7.2.3, so we can write:

$$\lambda_{\min}(J_{\mathrm{S}}) = \min_{\substack{\lambda \vdash n \\ l(\lambda) \leqslant d}} \mathrm{cont}(\lambda), \tag{7.52}$$

with $\mathrm{cont}(\lambda)$ the content of the Young diagram $\lambda \vdash n$. The optimal Young diagram λ^* that achieves the minimum is the tallest one with the constraint that the number of rows is less than or equal to d, i.e. the most rectangular shape possible:

$$\lambda_1^* = \cdots = \lambda_k^* = \frac{n-k}{d} + 1, \quad \lambda_{k+1}^* = \cdots = \lambda_d^* = \frac{n-k}{d}, \tag{7.53}$$

where $k := n \bmod d$. Therefore we can write

$$\begin{aligned}
\lambda_{\min}(J) = &\sum_{i=0}^{k-1}\left(-\left(\frac{n-k}{d}+1\right)i + \frac{n-k}{2d}\left(\frac{n-k}{d}+1\right)\right) \\
&\qquad + \sum_{i=k}^{d-1}\left(-\frac{n-k}{d}i + \frac{n-k}{2d}\left(\frac{n-k}{d}-1\right)\right) &(7.54)\\
= &\left(\frac{n-k}{d}+1\right)\left(\frac{k(n-k)}{2d} - \frac{k(k-1)}{2}\right) \\
&\qquad + \frac{n-k}{d}\left(\frac{d-k}{2}\left(\frac{n-k}{d}-1\right) - \frac{(d-k)(d+k-1)}{2}\right) &(7.55)\\
= &\frac{k(d-k)(d+1)}{2d} + \frac{n(n-d^2)}{2d}. &(7.56)
\end{aligned}$$

The above argument gives a proof for the following theorem.

7.4.1. Theorem. *The optimisation problem Eq. (7.49) has the optimal value*

$$q_W(n,d) = \frac{d-1}{2d}\frac{(n+k+d)(n-k)}{n(n-1)} + \frac{k(k-1)}{n(n-1)}, \tag{7.57}$$

where $k = n \bmod d$.

7.4.2 Isotropic states

Another important class of bipartite states with symmetries are isotropic states of the form Eq. (7.17), which form a subset of Brauer states. A convenient way to write an isotropic state is using as a linear combination of $\frac{\mathrm{W}}{d}$ and $\frac{\mathrm{I}}{d^2}$:

$$p' \cdot \frac{\mathrm{W}}{d} + (1-p') \cdot \frac{\mathrm{I}}{d^2}. \tag{7.58}$$

d \ n	2	3	4	5	6	7	8	9
2	1	$1/2$	$1/2$	$2/5$	$2/5$	$5/14$	$5/14$	$1/3$
3	1	1	$2/3$	$3/5$	$3/5$	$11/21$	$1/2$	$1/2$
4	1	1	1	$3/4$	$2/3$	$9/14$	$9/14$	$7/12$
5	1	1	1	1	$4/5$	$5/7$	$19/28$	$2/3$
6	1	1	1	1	1	$5/6$	$3/4$	$17/24$
7	1	1	1	1	1	1	$6/7$	$7/9$
8	1	1	1	1	1	1	1	$7/8$
9	1	1	1	1	1	1	1	1

Figure 7.2: The first values of $q_W(n,d)$. The values of $q_W(n,d)$, for which the Werner states ρ_e are separable (i.e. $q \leqslant 1/2$), are in grey.

When $\frac{-1}{d^2-1} \leqslant p' \leqslant 1$, the state ρ is positive semidefinite and unit trace, and hence a quantum state. The parameters p of Eq. (7.17) and p' of Eq. (7.58) are related via

$$p' = p + \frac{p-1}{d^2-1} = p\frac{d^2}{d^2-1} - \frac{1}{d^2-1}, \qquad p = \frac{1}{d^2} + \left(1 - \frac{1}{d^2}\right)p' \tag{7.59}$$

and an isotropic state ρ becomes separable if and only if $p' \leqslant \frac{1}{d+1}$.

If we want to formulate an optimisation problem similar to that in Eq. (7.32) for isotropic states, then one should add additional constraints $[\rho_e, U \otimes \bar{U}] = 0$ for every edge $e \in E(K_n)$ and arbitrary unitary $U \in \mathrm{U}_d$, to the optimisation problem (7.32). Equivalently, we can formulate the problem Eq. (7.35) for isotropic states as the following SDP:

$$p'_I(n,d) := \max_{\rho,p'} \quad p' \qquad \text{s.t.} \quad \rho_e = \frac{p'}{d} \cdot \mathrm{W} + \frac{1-p'}{d^2} \cdot \mathrm{I} \quad \forall e \in E, \quad \mathrm{Tr}[\rho] = 1, \quad \rho \succeq 0. \tag{7.60}$$

This problem depends on the number of quantum systems n and their dimension d. The aim is to find a state on a complete graph such that the reduced states between each pair of vertices are as maximally entangled as possible. Note that in the previous SDP (7.60), the condition $\mathrm{Tr}[\rho] = 1$ is superfluous, and the optimisation problem reduces to:

$$p'_I(n,d) = \max_{\rho,p'} \quad p' \qquad \text{s.t.} \quad \rho_e = \frac{p'}{d} \cdot \mathrm{W} + \frac{1-p'}{d^2} \cdot \mathrm{I} \quad \forall e \in E, \quad \rho \succeq 0. \tag{7.61}$$

It turns out that the dual problem can written as follows (see Section 7.A.2 for the derivation):

$$p'_I(n,d) = \min_{x \in \mathbb{R}} \lambda_{\max}\left(\sum_{e \in E}\left(\left(\frac{1}{|E|(1-d)} - x\right)(\mathrm{I}_e - d \cdot \mathrm{F}_e) + x(\mathrm{F}_e - \mathrm{W}_e)\right)\right). \tag{7.62}$$

We can find the value Eq. (7.62) analytically, which is one of the main results of this chapter:

7.4.2. Theorem. *The optimisation problem Eq. (7.62) has the optimal value*

$$p'_I(n,d) = \begin{cases} \frac{1}{n+n \bmod 2-1} & \text{if } d > n \text{ or either } d \text{ or } n \text{ is even} \\ \min\left\{\frac{2d+1}{2dn+1}, \frac{1}{n-1}\right\} & \text{if } n \geqslant d \text{ and both } d \text{ and } n \text{ are odd.} \end{cases} \tag{7.63}$$

The corresponding value $p_I(n,d)$ can be obtained from the relation Eq. (7.59):

$$p_I(n,d) = \begin{cases} \frac{1}{d^2} + \left(1 - \frac{1}{d^2}\right)\frac{1}{n+n \bmod 2-1} & \text{if } d > n \text{ or either } d \text{ or } n \text{ is even} \\ \frac{1}{d^2} + \left(1 - \frac{1}{d^2}\right)\min\left\{\frac{2d+1}{2dn+1}, \frac{1}{n-1}\right\} & \text{if } n \geqslant d \text{ and both } d \text{ and } n \text{ are odd.} \end{cases} \tag{7.64}$$

d \ n	2	3	4	5	6	7	8	9
2	1	$1/3$	$1/3$	$1/5$	$1/5$	$1/7$	$1/7$	$1/9$
3	1	$7/19$	$1/3$	$7/31$	$1/5$	$7/43$	$1/7$	$1/8$
4	1	$1/3$	$1/3$	$1/5$	$1/5$	$1/7$	$1/7$	$1/9$
5	1	$1/3$	$1/3$	$11/51$	$1/5$	$11/71$	$1/7$	$11/91$
6	1	$1/3$	$1/3$	$1/5$	$1/5$	$1/7$	$1/7$	$1/9$
7	1	$1/3$	$1/3$	$1/5$	$1/5$	$5/33$	$1/7$	$15/127$
8	1	$1/3$	$1/3$	$1/5$	$1/5$	$1/7$	$1/7$	$1/9$
9	1	$1/3$	$1/3$	$1/5$	$1/5$	$1/7$	$1/7$	$19/163$

(a) The first values of $p'_I(n, d)$.

d \ n	2	3	4	5	6	7	8	9
2	1	$1/2$	$1/2$	$2/5$	$2/5$	$5/14$	$5/14$	$1/3$
3	1	$25/57$	$11/27$	$29/93$	$13/45$	$11/43$	$5/21$	$2/9$
4	1	$3/8$	$3/8$	$1/4$	$1/4$	$11/56$	$11/56$	$1/6$
5	1	$9/25$	$9/25$	$21/85$	$29/125$	$67/355$	$31/175$	$71/455$
6	1	$19/54$	$19/54$	$2/9$	$2/9$	$1/6$	$1/6$	$11/81$
7	1	$17/49$	$17/49$	$53/245$	$53/245$	$13/77$	$55/343$	$121/889$
8	1	$11/32$	$11/32$	$17/80$	$17/80$	$5/32$	$5/32$	$1/8$
9	1	$83/243$	$83/243$	$17/81$	$17/81$	$29/189$	$29/189$	$187/1467$

(b) The first values of $p_I(n, d)$.

Figure 7.3: The first values of $p'_I(n, d)$ and $p_I(n, d)$. The values for which the isotropic states ρ_e are separable (i.e. $p \leqslant 1/d$), are in grey. Note that they decrease with respect to n, but are not monotonic with respect to d.

The proof of this theorem is provided in the next sections. Our strategy is to prove the theorem in the two cases separately:

- when $d > n$ or d is even or n is even,
- when $d \leqslant n$ and d is odd and n is odd,

by combining Theorem 7.4.5 and Theorem 7.4.8. We begin by establishing a simple lower bound using the notion of perfect matching of a graph.

Lower bound

We can get a simple lower bound on $p'_I(n, d)$ by looking at a set of perfect matchings on the complete graph. A perfect matching on a graph is a set of edges, such that every vertex is contained in exactly one of those edges.

7.4.3. Proposition. *There are* $(2n-1)!!$ *perfect matchings on* K_{2n}*, and if* e *is an edge on* K_{2n}*, then there are* $(2n-3)!!$ *perfect matchings on* K_{2n} *containing* e*.*

Proof:
Let a_n be the number of perfect matching on K_{2n}; clearly $a_1 = 1$. Now assume $n > 1$ and let

v be a vertex in V. This vertex can be matched with $2n-1$ other vertices, let $u \in V$ be such other vertex matched with v. Remove u and v from K_{2n}, the resulting graph $K_{2n} \setminus \{u, v\}$ is the complete graph $K_{2(n-1)}$. Thus, by induction on n, the number of perfect matchings on K_{2n} satisfies the recursive relation:

$$a_n = (2n-1)a_{n-1} \quad \Longrightarrow \quad a_n = (2n-1)!!. \tag{7.65}$$

Assume $e = (u, v)$ in E, thus the number of perfect matchings containing e is the number of perfect matchings on $K_{2n} \setminus \{u, v\}$, that is $(2n-3)!!$. □

A lower bound on the optimisation problem in Eq. (7.60) can be written as follows. For even n, let $E_1, \ldots, E_{(n-1)!!}$ be all the perfect matchings on K_n, and for each perfect matching E_k, define the quantum state $\rho^{(k)}$ on K_n by,

$$\rho^{(k)} := \prod_{e \in E_k} \frac{\mathrm{W}_e}{d}. \tag{7.66}$$

For odd n, let v be a vertex in V, and let $E_{v,1}, \ldots, E_{v,(n-2)!!}$ be all the perfect matchings on $K_n \setminus \{v\}$. Define the quantum state $\rho^{(v,k)}$ on K_n by,

$$\rho^{(v,k)} := \frac{\mathrm{I}_v}{d^2} \cdot \prod_{e \in E_{v,k}} \frac{\mathrm{W}_e}{d}. \tag{7.67}$$

That is a quantum state maximally entangled on the perfect matching edges, and a maximally mixed state $\frac{\mathrm{I}_v}{d^2}$ on the remaining vertex v in the odd case. For example, on K_6 the quantum state constructed from the perfect matching $\big\{(1,2),(3,4),(5,6)\big\}$ is equal to

$$\frac{\mathrm{W}}{d} \otimes \frac{\mathrm{W}}{d} \otimes \frac{\mathrm{W}}{d}, \tag{7.68}$$

and on K_7 the quantum state constructed from the perfect matching $\big\{(2,3),(4,5),(6,7)\big\}$ of $K_7 \setminus \{1\}$ is equal to

$$\frac{\mathrm{I}}{d} \otimes \frac{\mathrm{W}}{d} \otimes \frac{\mathrm{W}}{d} \otimes \frac{\mathrm{W}}{d}. \tag{7.69}$$

Let ρ be the quantum state defined on K_n, as a uniform combination of the previously constructed states $\rho^{(k)}$ and $\rho^{(v,k)}$:

$$(n \text{ even}) \qquad \rho := \frac{1}{(n-1)!!} \sum_{1 \leqslant k \leqslant (n-1)!!} \rho^{(k)}$$

$$(n \text{ odd}) \qquad \rho := \frac{1}{n(n-2)!!} \sum_{\substack{v \in K_n \\ 1 \leqslant k \leqslant (n-2)!!}} \rho^{(v,k)},$$

Then for all edges e in K_n, the reduced quantum state ρ_e is

$$\rho_e = \begin{cases} \frac{1}{n-1}\frac{1}{d} \cdot \mathrm{W} + \frac{n-2}{n-1}\frac{1}{d^2} \cdot \mathrm{I} & n \text{ even} \\ \frac{1}{n}\frac{1}{d} \cdot \mathrm{W} + \frac{n-1}{n}\frac{1}{d^2} \cdot \mathrm{I} & n \text{ odd}, \end{cases} \tag{7.70}$$

where the corresponding normalisation factors can be found using Proposition 7.4.3. The lower bound becomes

$$p'_I(n,d) \geqslant \begin{cases} \frac{1}{n-1} & n \text{ even} \\ \frac{1}{n} & n \text{ odd}. \end{cases} \tag{7.71}$$

In particular, the lower bound is independent of the dimension d.

Proof of Theorem 7.4.2

Using Lemmas 7.2.2 and 7.2.3, the decomposition of the vector space $\left(\mathbb{C}^d\right)^{\otimes n}$ under the action of the Brauer algebra $\mathcal{B}_n^d$, and under the decomposition of the restriction of the irreducible representations of the Brauer algebra $\mathcal{B}_n^d$ to the symmetric group S_n, we can write

$$f(x) := \lambda_{\max}\left(\sum_{e\in E}\left(\left(\frac{1}{|E|(1-d)} - x\right)(\mathrm{I}_e - d\,\mathrm{F}_e) + x(\mathrm{F}_e - \mathrm{W}_e)\right)\right) = \max_{(\lambda,\mu)\in\Omega_{n,d}} f_{\mu,\lambda}(x), \quad (7.72)$$

for affine functions $f_{\mu,\lambda}(x)$ defined as

$$f_{\mu,\lambda}(x) := \frac{1}{d-1}\left(\frac{d\ \mathrm{cont}(\mu)}{|E|} - 1\right) + x\big(\mathrm{cont}(\lambda) + d\ \mathrm{cont}(\mu) - r(d-1) - |E|\big), \quad (7.73)$$

with $|\lambda| = n - 2r$. The dual optimisation problem is then the minimum value of the max over a set of affine functions, i.e.,

$$p'_I(n,d) = \min_{x\in\mathbb{R}} \max_{(\lambda,\mu)\in\Omega_{n,d}} f_{\mu,\lambda}(x). \quad (7.74)$$

Case when $d > n$ or d is even or n is even.

A feasible solution for our dual problem Eq. (7.74) (i.e., an upper bound for the SDP Eq. (7.60)) can be made by setting $x = \frac{1}{|E|(1-d)}$. Note that in this case $x < 0$, since $d \geqslant 2$. Then Eq. (7.74) becomes

$$p'_I(n,d) \leqslant \min_{\lambda\in\widehat{\mathcal{B}}_n^d} \frac{2}{n(n-1)(1-d)}\big(\mathrm{cont}(\lambda) - r(d-1)\big). \quad (7.75)$$

7.4.4. Lemma. *If $d > n$, or either d or n is even, then,*

$$p'_I(n,d) \leqslant \begin{cases} \frac{1}{n} & \text{if } n \text{ is odd} \\ \frac{1}{n-1} & \text{if } n \text{ is even.} \end{cases} \quad (7.76)$$

Proof:
It is enough to prove that

$$\min_{\lambda\in\widehat{\mathcal{B}}_n^d} \mathrm{cont}(\lambda) - r(d-1) \leqslant \begin{cases} \frac{(1-d)(n-1)}{2} & \text{if } n \text{ is odd} \\ \frac{(1-d)n}{2} & \text{if } n \text{ is even,} \end{cases} \quad (7.77)$$

If $d > n$, the minimisation can be restricted to only single-column partitions $\lambda := \left(1^{(n-2r)}\right)$, for all $r \in \{0,\ldots,\lfloor\frac{n}{2}\rfloor\}$, which is always possible when $d > n$. Let $|\lambda| := n - 2r$, then

$$\min_{\lambda\in\widehat{\mathcal{B}}_n^d} \mathrm{cont}(\lambda) - r(d-1) \leqslant \min_{r\in\{0,\ldots,\lfloor\frac{n}{2}\rfloor\}} \mathrm{cont}\left(1^{(n-2r)}\right) - r(d-1) \quad (7.78)$$

$$= \min_{r\in\{0,\ldots,\lfloor\frac{n}{2}\rfloor\}} -\frac{|\lambda|\big(|\lambda|-1\big)}{2} - (d-1)\frac{n-|\lambda|}{2} \quad (7.79)$$

$$= \begin{cases} \frac{(1-d)(n-1)}{2} & \text{if } n \text{ is odd} \\ \frac{(1-d)n}{2} & \text{if } n \text{ is even.} \end{cases} \quad (7.80)$$

Otherwise, if d is even, let $r^* = \lceil \frac{n}{2} \rceil - \frac{d}{2}$. Then the single-column partition $\lambda := \left(1^{(n-2(r+r^*))}\right)$ satisfies $\lambda'_1 + \lambda'_2 \leqslant d$ for all $r \in \{0, \ldots, \lfloor \frac{n}{2} \rfloor - r^*\}$, and,

$$\min_{\lambda \in \widehat{\mathcal{B}}_n^d} \operatorname{cont}(\lambda) - r(d-1) \leqslant \min_{r \in \{0,\ldots,\lfloor \frac{n}{2} \rfloor - r^*\}} \operatorname{cont}\left(1^{(n-2r)}\right) - (r + r^*)(d-1) \tag{7.81}$$

$$= \begin{cases} \frac{(1-d)(n-1)}{2} & \text{if } n \text{ is odd} \\ \frac{(1-d)n}{2} & \text{if } n \text{ is even.} \end{cases} \tag{7.82}$$

The same result holds if n is even. □

7.4.5. Theorem. *If $d > n$, or either d or n is even, then,*

$$p'_I(n,d) = \begin{cases} \frac{1}{n} & \text{if } n \text{ is odd} \\ \frac{1}{n-1} & \text{if } n \text{ is even.} \end{cases} \tag{7.83}$$

Proof:
Using construction from Section 7.4.2 and Lemma 7.4.4, the dual optimisation problem is lower and upper bounded by $\frac{1}{n}$ if n is odd and $\frac{1}{n-1}$ if n is even. □

Case when $d \leqslant n$ and d is odd and n is odd.

Let us evaluate the affine functions $f_{\mu,\lambda}$ of Eq. (7.73) at the negative coordinate $\tilde{x} := \frac{1}{|E|(1-d)}$:

$$f_{\mu,\lambda}(\tilde{x}) = \frac{1}{d-1}\left(\frac{d \operatorname{cont}(\mu)}{|E|} - 1\right) + \tilde{x}(\operatorname{cont}(\lambda) + d \operatorname{cont}(\mu) - r(d-1) - |E|) \tag{7.84}$$

$$= \frac{1}{n-1} + \tilde{x} \cdot h(\lambda), \tag{7.85}$$

where $h(\lambda)$ is defined by $h(\lambda) := \frac{1}{2}\sum_{i=0}^{\lambda_1} \lambda'_i(d - \lambda'_i + 2(i-1))$. At this coordinate the affine functions do not depend on μ anymore, so we define

$$g(\lambda) := f_{\mu,\lambda}(\tilde{x}). \tag{7.86}$$

The offsets of the affine functions do not depend on λ either, therefore we define

$$a(\mu) := \frac{1}{d-1}\left(\frac{d \operatorname{cont}(\mu)}{|E|} - 1\right). \tag{7.87}$$

Let $n \geqslant d$ and $k := \lfloor \frac{n-d}{2}/d \rfloor$ and $m := \frac{n-d}{2} \bmod d$. Then we can define two partitions λ_1, λ_2 in $\widehat{\mathcal{B}}_n^d$ and three partitions $\mu_1, \mu_2, \widetilde{\mu}_2$[2] in $\widehat{\mathcal{A}}_n^d$:

$$\begin{aligned} \lambda_1 &:= (1^d) & \mu_1 &:= (n) \\ \lambda_2 &:= (1) & \mu_2 &:= (n-d+1, 1^{d-1}) \\ & & \widetilde{\mu}'_2 &:= (d^{2k+1}, m^2). \end{aligned} \tag{7.88}$$

[2]In the definition above, $\widetilde{\mu}_2$ is given using the column notation $\widetilde{\mu}'_2$. Using the row notation it becomes $\widetilde{\mu}_2 = \left((2k+3)^m, (2k+1)^{d-m}\right)$: m rows of size $(2k+3)$ and $d-m$ rows of size $(2k+1)$. For example, see Fig. 7.4, where $\widetilde{\mu}_2$ of the current proof corresponds to μ_4 on the plot.

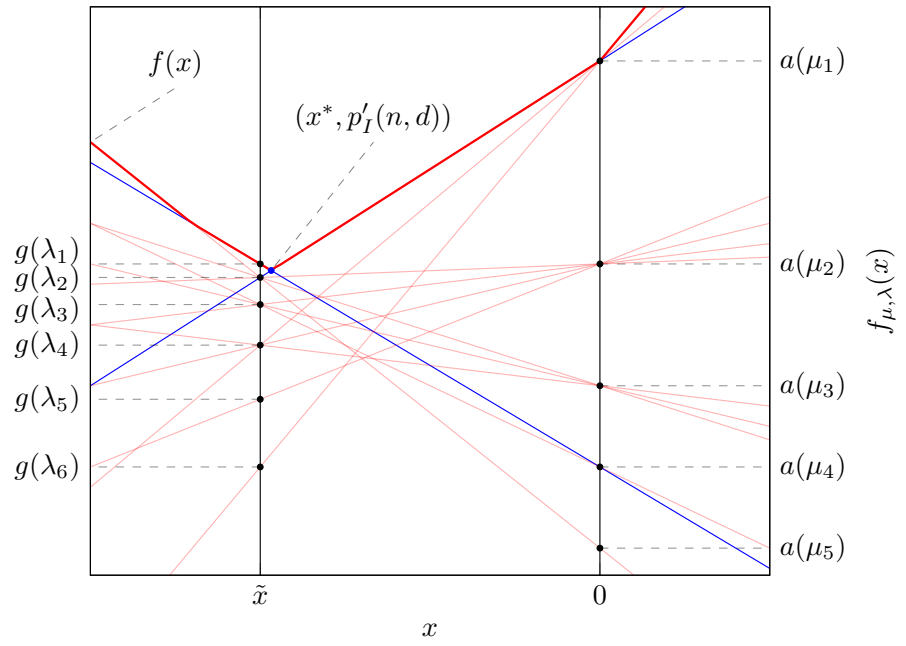

Figure 7.4: A typical behavior of the spectrum $f_{\mu,\lambda}(x)$ (thin red lines; $f(x)$ is in bold red) for all $(\lambda,\mu) \in \Omega_{n,d}$ when d is odd, n is odd and $d \leqslant n \leqslant 2d+1$. The coordinate $x = x^*$ corresponds to the optimal value $f(x^*) = p'_I(n,d)$. The plot corresponds to the parameters $n = 5$ and $d = 3$. The partitions λ corresponding to the points $(\tilde{x}, g(\lambda))$ are $\lambda_1 = (1^3)$, $\lambda_2 = (1)$, $\lambda_3 = (2,1)$, $\lambda_4 = (3)$, $\lambda_5 = (4,1)$, $\lambda_6 = (5)$. The partitions μ characterising the offsets $a(\mu)$ for the functions $f_{\mu,\lambda}(x)$ are $\mu_1 = (5)$, $\mu_2 = (4,1)$, $\mu_3 = (3,2)$, $\mu_4 = (3,1,1)$, $\mu_5 = (2,2,1)$. Some other values in that case are $\tilde{x} = 1/20$, $g(\lambda_1) = 1/4$, $x^* = -3/62$, $p'(n,d) = 7/31$.

7.4.6. Lemma. *Let d and n odd, $n \geqslant d$, and λ_1, μ_2 from Eq. (7.88), then*

$$g(\lambda_1) - a(\mu_2) = \frac{2d+2-n}{n-1}. \tag{7.89}$$

In particular $g(\lambda_1) < a(\mu_2)$ if $n \geqslant 2d+3$, and $g(\lambda_1) > a(\mu_2)$ if $n \leqslant 2d+1$.

Proof:
The content of μ_2 is $\frac{(n-d+1)(n-d)}{2} - \frac{d(d-1)}{2}$. Also $h(\lambda_1) = 0$, so $g(\lambda_1) = \frac{1}{n-1}$. Then

$$g(\lambda_1) - a(\mu_2) = \frac{1}{n-1} - \frac{1}{d-1}\left(\frac{d\,\mathrm{cont}(\mu_2)}{|E|} - 1\right) \tag{7.90}$$

$$= -d\frac{(n-d+1)(n-d) - d(d-1)}{n(n-1)(d-1)} + \frac{1}{d-1} + \frac{1}{n-1} \tag{7.91}$$

$$= \frac{2d+2-n}{n-1}. \tag{7.92}$$

□

7.4.7. Lemma. *Let d and n odd, $n \geqslant d$, and the partitions defined in Eq. (7.88), then for all i and j we have $(\lambda_i, \mu_j) \in S$, and the relations*

$$g(\lambda) \leqslant g(\lambda_2) \leqslant g(\lambda_1) \quad \text{and} \quad a(\mu) \leqslant a(\mu_1), \tag{7.93}$$

for all $\lambda \neq \lambda_1$ in $\widehat{\mathcal{B}}_n^d$ and all $\mu \neq \mu_1$ in $\widehat{\mathcal{A}}_n^d$. Moreover for all $(\lambda_1, \mu) \in \Omega_{n,d}$ we have

$$a(\mu) \leqslant a(\mu_2). \tag{7.94}$$

Proof:
By definition of S, we have $(\lambda_i, \mu_j) \in S$ for all i and j. Let λ in $\widehat{\mathcal{B}}_n^d$ then

$$g(\lambda) = \frac{1}{n-1} + \tilde{x}h(\lambda), \tag{7.95}$$

with $\tilde{x} < 0$ and $h(\lambda) = \frac{1}{2}\sum_{i=0}^{\lambda_1} \lambda_i'(d - \lambda_i' + 2(i-1))$. But since $\lambda_1' \leqslant d$ holds for all λ in $\widehat{\mathcal{B}}_n^d$, then $h(\lambda) \geqslant 0$. In particular, $h(\lambda_2) = \frac{d-1}{2}$, and $h(\lambda) = 0$ iff $\lambda = \lambda_1$. Assume there exists λ in $\widehat{\mathcal{B}}_n^d$ such that

$$g(\lambda_2) \leqslant g(\lambda) \leqslant g(\lambda_1), \tag{7.96}$$

then necessarily the first term of $h(\lambda)$ is either $h(\lambda_1)$ or $h(\lambda_2)$, since it minimised for the columns (1) and (1^d). But since all the terms in $h(\lambda)$ are positive, then either $g(\lambda) = g(\lambda_1)$ or $g(\lambda) = g(\lambda_2)$.

Because μ_1 is the n-box Young diagram that maximises the content function, then

$$a(\mu) \leqslant a(\mu_1), \tag{7.97}$$

for all $\mu \neq \mu_1$ in $\widehat{\mathcal{A}}_n^d$.

Assume there exists μ such that $(\lambda_1, \mu) \in \Omega_{n,d}$ and

$$a(\mu_2) \leqslant a(\mu) \leqslant a(\mu_1). \tag{7.98}$$

Since $\big((1^d), \mu\big) \in S$ implies $\big((1^d), \mu\big) \in \Omega_{n,d}$, then $(\lambda_1, \mu) \in S$, and by definition $r(\mu) = d$. Thus necessarily $\mathrm{cont}(\mu_2) \leqslant \mathrm{cont}(\mu)$, which implies that the first row of μ_2 is of size at most $n-d+1$. But the content of a Young diagram is a non-decreasing function of the first row's size, i.e. for all Young diagrams $\nu \vdash n$ and $\mu \vdash n$ with the same number of boxes n such that $\nu_1 \leqslant \mu_1$ we have $\mathrm{cont}(\nu) \leqslant \mathrm{cont}(\mu)$. Then μ_2 and μ share the same first row, and $\mu_2 = \mu$. □

7.4.8. Theorem. *When d is odd, n is odd and $n \geqslant d$, the value $p_I'(n,d)$ is*

$$p_I'(n,d) = \min\left(\frac{2d+1}{2dn+1}, \frac{1}{n-1}\right). \tag{7.99}$$

Proof:
Let λ_1, λ_2 and $\mu_1, \mu_2, \widetilde{\mu}_2$ as in Eq. (7.88), and let us prove that the optimal solution of the dual problem is $p_I'(n,d) = g(\lambda_1)$ when $n \geqslant 2d+3$, and lies at intersection of the affine functions f_{μ_1,λ_2} and f_{μ_2,λ_1}, when $n \leqslant 2d+1$. Now since

$$\begin{aligned}\mathrm{cont}(\widetilde{\mu}_2) &= \sum_{i=1}^{2k+1}\left(-\frac{d(d-1)}{2} + (i-1)d\right) + \sum_{i=2k+2}^{2k+3}\left(-\frac{m(m-1)}{2} + (i-1)m\right) \\ &= \frac{d(2k+1)(2k+1-d)}{2} + m(4k+4-m),\end{aligned} \tag{7.100}$$

and $n - d = 2kd + 2m$ with $m \in \{0, \ldots, d-1\}$, we can write

$$g(\lambda_1) - a(\widetilde{\mu}_2) = \frac{1}{n-1} - \frac{1}{d-1}\left(\frac{d\ \mathrm{cont}(\widetilde{\mu}_2)}{|E|} - 1\right) \tag{7.101}$$

$$= \frac{n(d+n-2) - 2d\ \mathrm{cont}(\widetilde{\mu}_2)}{n(n-1)(d-1)} \tag{7.102}$$

$$= \frac{(d+2)(2m^2 - 2dm - n + dn)}{n(n-1)(d-1)} \tag{7.103}$$

$$\geqslant \frac{(d+2)\big(-(d-1)(d+1)/2 + d(d-1)\big)}{n(n-1)(d-1)} \tag{7.104}$$

$$= \frac{(d+2)(d-1)}{2n(n-1)} > 0, \tag{7.105}$$

where in the first inequality we used $n \geqslant d$ and that the minimum of $2m^2 - 2dm$ on the domain $m \in \{0, \ldots, d-1\}$ is achieved for $m = (d-1)/2$. Geometrically this means that the point $(0, a(\widetilde{\mu}_2))$ is always lower than $(\tilde{x}, g(\lambda_1))$.

Suppose that $n \geqslant 2d+3$, then the relation

$$g(\lambda_1) < a(\mu_2), \tag{7.106}$$

holds by Lemma 7.4.6. Therefore $p'_I(n,d) \geqslant g(\lambda_1)$ since the optimal point should be above the intersection of the affine functions f_{μ_2,λ_1} and $f_{\widetilde{\mu}_2,\lambda_1}$ that is, above $g(\lambda_1)$. But since $g(\lambda) \leqslant g(\lambda_1)$ for all λ in $\widehat{\mathcal{B}}_n^d$ by Lemma 7.4.7, it must be $p'_I(n,d) = g(\lambda_1)$.

Suppose that $n \leqslant 2d+1$, then the relation

$$a(\mu) \leqslant a(\mu_2), \tag{7.107}$$

holds for all $(\lambda_1, \mu) \in \Omega_{n,d}$, by Lemma 7.4.7. Then $p'_I(n,d)$ lies above the affine function f_{μ_2,λ_1}. But $g(\lambda) \leqslant g(\lambda_1)$ for all λ in $\widehat{\mathcal{B}}_n^d$, by Lemma 7.4.7, then $p'_I(n,d)$ must lie on the affine function f_{μ_2,λ_1}, at the intersection with another affine function $f_{\mu,\lambda}$ with $g(\lambda) \leqslant a(\mu)$. Among all such affine functions there are no functions with $\lambda = \lambda_1$ due to Lemma 7.4.7. Because $g(\lambda) \leqslant g(\lambda_2)$ for all $\lambda \neq \lambda_1$ in $\widehat{\mathcal{B}}_n^d$ and $a(\mu) \leqslant a(\mu_1)$ for all $\mu \in \widehat{\mathcal{A}}_n^d$, by Lemma 7.4.7, it must be that this function is f_{μ_1,λ_2}. Therefore $p'_I(n,d)$ lies at intersection of the affine functions f_{μ_1,λ_2} and f_{μ_2,λ_1}.

In order to find the intersection of f_{μ_1,λ_2} and f_{μ_2,λ_1} we need to solve $p'_I(n,d) := f_{\mu_1,\lambda_2}(x^*) = f_{\mu_2,\lambda_1}(x^*)$, which gives $x^* = \frac{4d}{(d-1)(n-1)(2dn+1)}$ and $p'_I(n,d) = \frac{2d+1}{2dn+1}$.

In conclusion, when $n \geqslant 2d+3$ then $p'_I(n,d) = \frac{1}{n-1}$, and when $n \leqslant 2d+1$ then $p'(n,d) = \frac{2d+1}{2dn+1}$, which is equivalent to the statement of the theorem. □

7.4.3 Brauer states

Understanding the K_n-extendibility in full generality in the case of Brauer states

$$p \cdot \Pi_{\varnothing} + q \cdot \frac{\Pi_{\ydiagram{1}}}{\operatorname{Tr} \Pi_{\ydiagram{1}}} + (1-p-q) \cdot \frac{\Pi_{\ydiagram{2}}}{\operatorname{Tr} \Pi_{\ydiagram{2}}} \tag{7.108}$$

means to find the full 2D region of allowed (p,q) values for arbitrary n and d. As a first step to solve this general problem, this section aims to determine the maximum values of q and p, denoted $q_B(n,d)$ and $p_B(n,d)$, for the K_n-extendibility of Brauer states, as well as the complete K_n-extendibility polytope of qubit Brauer states.

Maximising the $q_B(n,d)$

We define $q_B(n,d)$ formally as follows:

$$\begin{aligned} q_B(n,d) := \max_{\rho,q,p} \quad & q \\ \text{s.t.} \quad & \rho_e = p \cdot \Pi_{\varnothing} + q \cdot \frac{\Pi_{\ydiagram{1}}}{\operatorname{Tr} \Pi_{\ydiagram{1}}} + (1-p-q) \cdot \frac{\Pi_{\ydiagram{2}}}{\operatorname{Tr} \Pi_{\ydiagram{2}}} \quad \forall e \in E, \\ & \operatorname{Tr}[\rho] = 1, \quad \rho \succeq 0. \end{aligned} \tag{7.109}$$

It turns out that this value is the same as the corresponding value for the Werner state case.

7.4.9. Lemma. *For every n and d the following relation holds*

$$q_B(n,d) = q_W(n,d). \tag{7.110}$$

d \ n	2	3	4	5	6	7	8	9
2	1	$2/3$	$2/3$	$3/5$	$3/5$	$4/7$	$4/7$	$5/9$
3	1	$5/9$	$5/9$	$7/15$	$7/15$	$3/7$	$3/7$	$11/27$
4	1	$1/2$	$1/2$	$2/5$	$2/5$	$5/14$	$5/14$	$1/3$
5	1	$7/15$	$7/15$	$9/25$	$9/25$	$11/35$	$11/35$	$13/45$
6	1	$4/9$	$4/9$	$1/3$	$1/3$	$2/7$	$2/7$	$7/27$
7	1	$3/7$	$3/7$	$11/35$	$11/35$	$13/49$	$13/49$	$5/21$
8	1	$5/12$	$5/12$	$3/10$	$3/10$	$1/4$	$1/4$	$2/9$
9	1	$11/27$	$11/27$	$13/45$	$13/45$	$5/21$	$5/21$	$17/81$

Figure 7.5: The first largest values of $p_B(n,d)$ of the K_n-extendible Brauer states. All 2-body Brauer states corresponding to these values are entangled due to Corollary 7.4.11, in contrast to Fig. 7.2.

Proof:
Given any solution ρ to the optimisation problem (7.109), we can twirl it over unitary group action $U^{\otimes n}$ without changing the value of the optimisation problem since $\Pi_{\boxplus}$ is invariant under $U^{\otimes 2}$ action. It means that 2-body marginals of the twirled ρ are Werner states, and we reduced the problem of calculating $q_B(n,d)$ to calculating $q_W(n,d)$. □

Now, we move to the more complicated case of understanding the value $p_B(n,d)$.

Maximising the $p_B(n,d)$

Consider now Eq. (7.32) for the projector onto maximally entangled state $\Pi := \frac{\mathrm{W}}{d}$ on the complete graph K_n. We have due to Eq. (7.48):

$$p_B(n,d) = \frac{1}{d\cdot|E|}\lambda_{\max}\left(\sum_{e\in E}\mathrm{W}_e\right), \tag{7.111}$$

and with the help of Jucys–Murphy elements we can get the spectrum of the Hamiltonian $H_B := \sum_{e\in E}\mathrm{W}_e$. Just note that the sum of Jucys–Murphy elements for the symmetric group algebra and the Brauer algebra commute. It means that we can subtract the corresponding spectra to get

$$\operatorname{spec}(H_B) = \left\{ g(\mu,\lambda) \,\middle|\, \mu\in\widehat{\mathcal{A}}_n^d,\ \lambda\in\widehat{\mathcal{B}}_n^d,\ (\lambda,\mu)\in\Omega_{n,d}\right\}, \tag{7.112}$$

where $\Omega_{n,d}$ is defined in Eq. (7.29) and

$$g(\mu,\lambda) := \operatorname{cont}(\mu) - \operatorname{cont}(\lambda) + \frac{(n-|\lambda|)(d-1)}{2}. \tag{7.113}$$

Therefore

$$p_B(n,d) = \frac{1}{d\cdot|E|}\max_{(\mu,\lambda)\in\Omega_{n,d}} g(\mu,\lambda). \tag{7.114}$$

7.4.10. Theorem. *The optimisation problem Eq. (7.50) has the optimal value*

$$p_B(n,d) = \frac{1}{d} + \left(1-\frac{1}{d}\right)\frac{1}{n+n \bmod 2 - 1}. \tag{7.115}$$

Proof:
Let $\lambda \vdash n-2r$, $\lambda \in \widehat{\mathcal{B}}_n^d$ for some fixed r and define

$$f(\lambda) := -\operatorname{cont}(\lambda) + \frac{(n-|\lambda|)(d-1)}{2}. \tag{7.116}$$

Since the content of a Young diagram λ is a non-decreasing function of the first row's size (when the number of boxes is fixed), then in order to maximize $f(\lambda)$ we can assume that λ takes the most rectangular shape possible in order to minimize $\operatorname{cont}(\lambda)$. Namely, $f(\lambda^*) \geqslant f(\lambda)$ where $\lambda^* \vdash n-2r$

$$\lambda_1^* = \ldots = \lambda_k^* = \frac{n-2r-k}{d} + 1, \quad \lambda_{k+1}^* = \ldots = \lambda_d^* = \frac{n-2r-k}{d}, \tag{7.117}$$

and $k := n-2r \bmod d$. Then, in particular, we can use our calculation from Eq. (7.56) to write

$$f(\lambda^*) = \frac{1}{2d}\big(nd(d-1) - |\lambda^*|^2 + d|\lambda^*| - k(d-k)(d+1)\big) \tag{7.118}$$

Assume $|\lambda^*| > d$ and consider three cases:

1. $n-2r-k$ is even. Define $\tilde{r} := \frac{n-2r-k}{2}$. Then $n-2r-2\tilde{r} = k$ and we can set $\tilde{\lambda} \vdash k$ as a vertical one column Young diagram $\tilde{\lambda} := (1^k)$. Since $\tilde{k} := |\tilde{\lambda}| \bmod d = k$. We see from Eq. (7.118) that $f(\tilde{\lambda}) > f(\lambda^*)$.

2. $n-2r-k$ is odd and $k = 0$. Then also d is odd, meaning that we can set $\tilde{\lambda} \vdash d$, $\tilde{\lambda} := (1^d)$ preserving $\tilde{k} = k = 0$. Again we deduce from Eq. (7.118) that $f(\tilde{\lambda}) > f(\lambda^*)$.

3. $n-2r-k$ is odd and $k > 0$. In this case we define $\tilde{\lambda} \vdash k-1$, $\tilde{\lambda} := (1^{k-1})$. Using $|\lambda^*| \geqslant d+k$, we can estimate the difference $f(\tilde{\lambda}) - f(\lambda^*)$ as

$$\begin{aligned} 2d(f(\tilde{\lambda}) - f(\lambda^*)) &= |\lambda^*|^2 - |\tilde{\lambda}|^2 - d(|\lambda^*| - |\tilde{\lambda}|) - (k-1)(d-k+1)(d+1) + k(d-k)(d+1) \\ &= |\lambda^*|(|\lambda^*| - d) - (k-1)^2 + d(k-1) + (d+1)(1+d-2k) \\ &= |\lambda^*|(|\lambda^*| - d) + d^2 - k^2 + d - kd \\ &\geqslant (d+k)k + d^2 - k^2 + d - kd = d(d+1) > 0, \end{aligned} \tag{7.119}$$

meaning that again $f(\tilde{\lambda}) > f(\lambda^*)$.

The above analysis means that we can assume without loss of generality that the maximiser of the function $f(\lambda)$ over $\lambda \in \widehat{\mathcal{B}}_n^d$ is a Young diagram λ with one column only, i.e. $\lambda = (1^k)$ for some $k \leqslant d$. Therefore

$$\max_{(\mu,\lambda)\in\Omega_{n,d}} g(\mu,\lambda) = \max_{(\mu,\lambda)\in\Gamma_{n,d}} g(\mu,\lambda) = \begin{cases} g((n),\varnothing) & n \text{ even}, \\ g((n),(1)) & n \text{ odd}, \end{cases} \tag{7.120}$$

which gives us

$$p_B(n,d) = \frac{2}{dn(n-1)}\left(\frac{n(n-1)}{2} + \frac{(n-n \bmod 2)(d-1)}{2}\right) \tag{7.121}$$

$$= \frac{1}{d} + \frac{(n-n \bmod 2)(d-1)}{dn(n-1)}. \tag{7.122}$$

□

7.4.11. Corollary. *For all n and d, any feasible solution ρ for the optimal value $p_B(n,d)$ has entangled reduced Brauer states ρ_e.*

Proof:
Using the PPT criterion from Section 7.A.5, an element from the two-parameter (p,q) family of Brauer states for any fixed $d \geqslant 2$, is separable if and only if it lies in the region specified by

$$\begin{cases} 0 \leqslant p \leqslant \frac{1}{d} \\ 0 \leqslant q \leqslant \frac{1}{2} \end{cases} \tag{7.123}$$

But from Theorem 7.4.10, we always have $p_B(n,d) > \frac{1}{d}$ for any finite n. □

7.4.12. Theorem. *For all n and d, there exists a feasible solution ρ for the optimal value $p_B(n,d)$ such that for all edges e:*

$$\rho_e = p_B(n,d) \cdot \Pi_{\varnothing} + \big(1 - p_B(n,d)\big) \cdot \frac{\Pi_{\square\square}}{\operatorname{Tr} \Pi_{\square\square}}.$$

Proof:
We are going to solve the following optimisation problem:

$$\begin{aligned} p^*(n,d) = \max_{\rho,p} \quad & p \\ \text{s.t.} \quad & \rho_e = p \cdot \Pi_{\varnothing} + (1-p) \cdot \frac{\Pi_{\square\square}}{\operatorname{Tr} \Pi_{\square\square}} \quad \forall e \in E, \quad \operatorname{Tr}[\rho] = 1, \quad \rho \succeq 0. \end{aligned} \tag{7.124}$$

and show that, in fact, $p^*(n,d) = p_B(n,d)$. This suffices to prove the claim. In Section 7.A.3 we show that actually

$$p^*(n,d) = \min_{x \in \mathbb{R}} \max_{(\lambda,\mu) \in \Omega_{n,d}} \quad \frac{1}{d \cdot |E|} \left(\operatorname{cont}(\mu) - \operatorname{cont}(\lambda) + \frac{(n - |\lambda|)(d-1)}{2} \right) + \frac{x}{d} \left(1 - \frac{\operatorname{cont}(\mu)}{|E|} \right). \tag{7.125}$$

Equivalently, we want to minimize over $x \in \mathbb{R}$ a piecewise linear function

$$h(x) := \max_{(\lambda,\mu) \in \Omega_{n,d}} h_{\lambda,\mu}(x), \tag{7.126}$$

where we define affine functions $h_{\lambda,\mu}(x)$ as

$$h_{\lambda,\mu}(x) := \frac{1}{d \cdot |E|} \left(\operatorname{cont}(\mu) - \operatorname{cont}(\lambda) + \frac{(n - |\lambda|)(d-1)}{2} \right) + \frac{x}{d} \left(1 - \frac{\operatorname{cont}(\mu)}{|E|} \right). \tag{7.127}$$

Note that the finite optimum value $p^*(n,d)$ is always achieved at an intersection of at least two different affine functions $h_{\lambda,\mu}(x)$, and there must be at least one function among them with non-positive slope and at least one with non-negative slope. However, $\operatorname{cont}(\mu) \leqslant |E|$ so all functions $h_{\lambda,\mu}(x)$ have non-negative slopes. Moreover, the functions $h_{\lambda,\mu}(x)$ with $\mu = (n)$ are the only ones which have zero slopes (because this is the only μ which achieves $\operatorname{cont}(\mu) = |E|$). So it means that the optimum value is achieved for $\mu = (n)$ and some λ such that $(\lambda,\mu) \in \Omega_{n,d}$ with the formula

$$p^*(n,d) = \max_{(\lambda,(n)) \in \Omega_{n,d}} \frac{1}{d \cdot |E|} \left(|E| - \operatorname{cont}(\lambda) + \frac{(n - |\lambda|)(d-1)}{2} \right), \tag{7.128}$$

where we used the fact that $\operatorname{cont}(\mu) = |E|$. But we have already calculated this quantity in Theorem 7.4.10, so

$$p^*(n,d) = \frac{1}{d \cdot |E|} \max_{(\mu,\lambda) \in \Omega_{n,d}} g(\mu,\lambda) = p_B(n,d), \tag{7.129}$$

which proves the claim. □

K_n-extendibility polytope for qubits

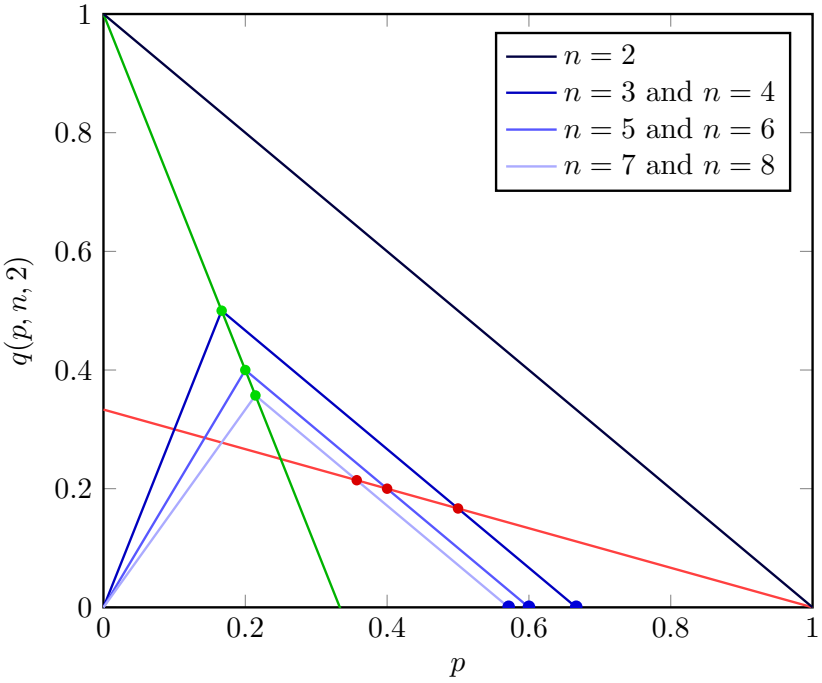

Figure 7.6: In blue, the optimal values of $q(p, n, 2)$ for $n \in \{2, \ldots, 8\}$. The K_n-extendibility for qubits Brauer states is the polytope given by the extremal points of those piecewice functions, see Theorem 7.4.15. The blues dots correspond to the optimal values of Theorem 7.4.10. The green line corresponds to the parameters (p, q) of Werner states, and the green dots to the optimal values of Theorem 7.4.1. The red line corresponds to the parameters (p, q) of isotropic states, and the red dots to the optimal values of Theorem 7.4.2.

To understand the complete K_n-extendibility for qubit Brauer states, we solve the following optimisation problem in this subsection

$$\begin{aligned} q(p, n, d) = \max_{\rho, q} \quad & q \\ \text{s.t.} \quad & \rho_e = p \cdot \Pi_{\varnothing} + q \cdot \frac{\Pi_{\boxplus}}{\operatorname{Tr} \Pi_{\boxplus}} + (1 - p - q) \cdot \frac{\Pi_{\boxplus}}{\operatorname{Tr} \Pi_{\boxplus}}, \quad \forall e \in E \\ & \rho \succeq 0, \end{aligned} \tag{7.130}$$

for all $p \in [0, 1]$, $n \geqslant 2$ and $d = 2$, i.e. the largest values of q, given a fixed p such that the Brauer state with parameter (p, q) is K_n-extendible. Note that from Section 7.4.3, the optimal solution $q(p, n, d)$ is zero when p is larger than $p_B(n, d)$.

Recall that from Remark 7.2.5, the complete set $\Omega_{n,2}$ is known: $(\lambda, \mu) \in \Omega_{n,2}$ if and only if $\lambda_1 \leqslant \mu_1 - \mu_2$, with the exceptions of $\lambda = \varnothing$, in which case both rows of μ must be even, and $\lambda = (1, 1)$, in which case both rows of μ must be odd.

In Section 7.A.4 we show that $q(p, n, 2)$ is equal to the following optimisation problem:

$$\begin{aligned} q(p, n, 2) &= \min_{x \in \mathbb{R}} \max_{(\lambda, \mu) \in \Omega_{n,2}} f_{\mu,\lambda}(p, x) \\ f_{\mu,\lambda}(p, x) &= \frac{x}{2 \cdot |E|} \left(\operatorname{cont}(\mu) - \operatorname{cont}(\lambda) + \frac{(n - |\lambda|)}{2} \right) + \frac{1}{2} \left(1 - \frac{\operatorname{cont}(\mu)}{|E|} \right) - p \cdot x. \end{aligned} \tag{7.131}$$

Similarly to the proof of the K_n-extendibility of isotropic states (see Section 7.4.2), let $\tilde{x} := 1$, and define the two functions:

$$g(p, \lambda) := f_{\mu,\lambda}(p, \tilde{x}) \quad \text{and} \quad a(\mu) := f_{\mu,\lambda}(p, 0),$$

where $f_{\mu,\lambda}(p,\tilde{x})$ does not depend on μ, and $f_{\mu,\lambda}(p,0)$ does not depend on λ nor on p.

Let μ in $\Omega_{n,2}$, then $\mu = (n-k,k)$ for some $k \in \{0,\dots,\lfloor \frac{n}{2} \rfloor\}$, and hence there are $\lfloor \frac{n}{2} \rfloor + 1$ possibilities for μ, namely:

$$(n,0), \qquad (n-1,1), \qquad (n-2,2), \quad \cdots \quad \big(n-\lfloor \tfrac{n}{2} \rfloor, \lfloor \tfrac{n}{2} \rfloor\big).$$

We will prove that for all $\mu = (n-k,k)$ there exist λ_1 and λ_2 defined by

$$\lambda_1 \coloneqq \begin{cases} (1) & \text{if } n \text{ is odd} \\ (1,1) & \text{if } n \text{ is even} \end{cases} \quad \text{and} \quad \lambda_2 \coloneqq \begin{cases} (1) & \text{if } n \text{ is odd} \\ \varnothing & \text{if } n \text{ is even,} \end{cases} \tag{7.132}$$

such that either $(\lambda_1,\mu) \in \Omega_{n,2}$ or $(\lambda_2,\mu) \in \Omega_{n,2}$

7.4.13. Lemma. *Let λ_1, λ_2 be the partitions defined by Eq. (7.132), and let $\mu = (n-k,k)$ for some $k \in \{0,\dots,\lfloor \frac{n}{2} \rfloor\}$, then:*

- *if n is odd, both (λ_1,μ) and (λ_2,μ) are in $\Omega_{n,2}$,*
- *if n is even and k is odd, $(\lambda_1,\mu) \in \Omega_{n,2}$,*
- *if n is even and k is even, $(\lambda_2,\mu) \in \Omega_{n,2}$.*

Moreover for all λ in $\Omega_{n,2}$, then

$$g(p,\lambda_1) = g(p,\lambda_2) \geqslant g(p,\lambda).$$

Proof:
The first part is a direct consequence of the Remark 7.2.5: if n is odd then $\mu_1 - \mu_2 \in \{1,\dots,n\}$ is always larger or equal to 1, otherwise both rows of μ have the same parity as k, and the result holds by the two exception rules of Remark 7.2.5.

Note that given any λ, λ' in $\Omega_{n,2}$, such that $g(0,\lambda) \geqslant g(0,\lambda')$, the inequality $g(p,\lambda) \geqslant g(p,\lambda')$ holds for any $p \in [0,1]$. Hence we will prove the second part of the Lemma for $p = 0$. We have

$$g(0,\lambda_1) = g(0,\lambda_2) = \frac{n}{2(n-1)}.$$

Using that $\lambda = (1,1)$ is the only possible vertical Young diagram (i.e. with negative content) of $\widehat{\mathcal{B}}_n^2$, since

$$\widehat{\mathcal{B}}_{2k}^2 = \{(1,1)\} \cup \{(2k-2r) \mid r \in \{0,\dots,k\}\} \tag{7.133}$$

$$\widehat{\mathcal{B}}_{2k+1}^2 = \{(2k+1-2r) \mid r \in \{0,\dots,k\}\}, \tag{7.134}$$

and given that

$$g\big(0,(n-2r)\big) = \frac{-\operatorname{cont}\big((n-2r)\big) + r}{2 \cdot |E|} + \frac{1}{2}, \tag{7.135}$$

is an increasing function of $r \in \{0,\dots,\lfloor \frac{n}{2} \rfloor\}$ with maximum at $r = \lfloor \frac{n}{2} \rfloor$, i.e. $g(0,\varnothing)$ if n is even, and $g(0,(1))$ if n is odd; we conclude that

$$g(0,\lambda_1) = g(0,\lambda_2) \geqslant g\big(0,(n-2r)\big), \tag{7.136}$$

for all $r \in \{0,\dots,\lfloor \frac{n}{2} \rfloor\}$, and thus in particular for all λ in $\Omega_{n,2}$. □

Let λ in $\Omega_{n,2}$, then either λ equals $(1,1)$ or $\varnothing$, or there exists a $r \in \{0,\dots,\lfloor \frac{n-1}{2} \rfloor\}$ such that $\lambda = (n-2r)$. We will see now which pair (μ,λ) are in $\Omega_{n,2}$ in the latter case.

7.4.14. Lemma. *Let $\lambda = (n-2r)$ for some $r \in \{0, \dots, \lfloor \frac{n-1}{2} \rfloor\}$. Then a pair (μ, λ) with $\mu = (n-k, k)$ is in $\Omega_{n,2}$ if and only if $k \in \{0, \dots, r\}$.*

Proof:
Let $\mu = (n-k, k)$ for some $k \in \{0, \dots, \lfloor \frac{n}{2} \rfloor\}$. Since λ is neither $\varnothing$ nor $\{1, 1\}$ (the two exceptions of Remark 7.2.5) we know hat $(\mu, \lambda) \in \Omega_{n,2}$ if and only if

$$n - 2r \leqslant n - 2k, \tag{7.137}$$

that is, if $r \geqslant k$. □

Let $\mu = (n-k, k)$ with $k \in \{0, \dots, \lfloor \frac{n}{2} \rfloor\}$, then the function

$$k \longmapsto a\big((n-k, k)\big) = \frac{k(n+1-k)}{n(n-1)},$$

is a positive increasing function on the interval $[0, \frac{n+1}{2}]$.

Let $\lambda = (n-2r)$ for some $r \in \{0, \dots, \lfloor \frac{n-1}{2} \rfloor\}$, and $\mu = (n-r, r)$. Then the function

$$p \longmapsto g(p, \lambda) - a(\mu) = \frac{r(n-r-1)}{n(n-1)} - p,$$

is positive for all $p \leqslant \frac{r(n-r-1)}{n(n-1)}$, i.e. the affine function $f_{\mu,\lambda}$ has positive slope. In particular, the affine function $f_{(n),(n)}$ has always a non-positive slope for $p \geqslant 0$.

Now we are ready to characterise K_n-extendibility for qubit Brauer states, which is given by the polytope in Fig. 7.6. Its boundary is described in the following theorem:

7.4.15. Theorem. *For all n, and all $p \in [0, 1]$ the optimal value $q(p, n, 2)$ is equal to*

$$q(p,n,2) = \begin{cases} \frac{\lceil n/2 \rceil + 1}{\lceil n/2 \rceil - 1} p & \text{if } p < \frac{\lceil n/2 \rceil - 1}{2(2\lceil n/2 \rceil - 1)}, \\ \frac{\lceil n/2 \rceil}{2\lceil n/2 \rceil - 1} - p & \text{if } \frac{\lceil n/2 \rceil}{2\lceil n/2 \rceil - 1} \geqslant p \geqslant \frac{\lceil n/2 \rceil - 1}{2(2\lceil n/2 \rceil - 1)}, \\ 0 & \text{otherwise.} \end{cases} \tag{7.138}$$

Proof:
From Lemma 7.4.13, we know that for all $\mu \in \widehat{\mathcal{A}}_n^d$, either (λ_1, μ) or (λ_2, μ) is in $\Omega_{n,2}$, and the function $\lambda \mapsto g(p, \lambda)$ is maximised for those two λ's. Since $a(\mu)$ is maximised for $\mu_1 := \big(n - \lfloor \frac{n}{2} \rfloor, \lfloor \frac{n}{2} \rfloor\big)$, we know that the optimal value $q(p, n, 2)$ lies at the intersection of the affine functions f_{μ_1,λ_1} or f_{μ_1,λ_2}.

If n is even, the affine functions f_{μ_1,λ_1} and f_{μ_1,λ_2} have slopes equal to

$$g\big(p, (1,1)\big) - a\big(\tfrac{n}{2}, \tfrac{n}{2}\big) = g\big(p, \varnothing\big) - a\big(\tfrac{n}{2}, \tfrac{n}{2}\big) = \frac{n-2}{4(n-1)} - p. \tag{7.139}$$

Note that in this case, only one of the two affine functions f_{μ_1,λ_1} and f_{μ_1,λ_2} are included in the optimisation problem $q(p, n, 2)$. When $n = 2$ and $p = 0$, both f_{μ_1,λ_1} and f_{μ_1,λ_2} are constant functions and optimal value $q(p, n, 2)$ equals to $f_{\mu_1,\lambda_1}(0) = f_{\mu_1,\lambda_2}(0) = 1$, as expected.

Let n even and $p \leqslant \frac{n-2}{4(n-1)}$, then f_{μ_1,λ_1} and f_{μ_1,λ_2} have non-negative slope, and the optimal value $q(p, n, 2)$ must lie at the intersection of another affine function $f_{\mu,\lambda}$ with non-positive slope. From Lemma 7.4.14 we know that for all $r \in \{0, \dots, \lfloor \frac{n-1}{2} \rfloor\}$ and all $k \in \{0, \dots, r\}$, the pair (λ_r, μ_k) with $\lambda_r = (n-2r)$ and $\mu_k = (n-k, k)$ is in $\Omega_{n,2}$. Thus if f_{μ_k,λ_r} has non-positive slope for some r and k, then given $k' \geqslant k$, the affine function $f_{\mu_{k'},\lambda_r}$ has also non-positive slope. Moreover the intersection between $f_{\mu_{k'},\lambda_r}$ and f_{μ_1,λ_1} or f_{μ_1,λ_2} is always higher than the intersection between f_{μ_k,λ_r} and f_{μ_1,λ_1} or f_{μ_1,λ_2}. Thus we can restrict the intersection problem

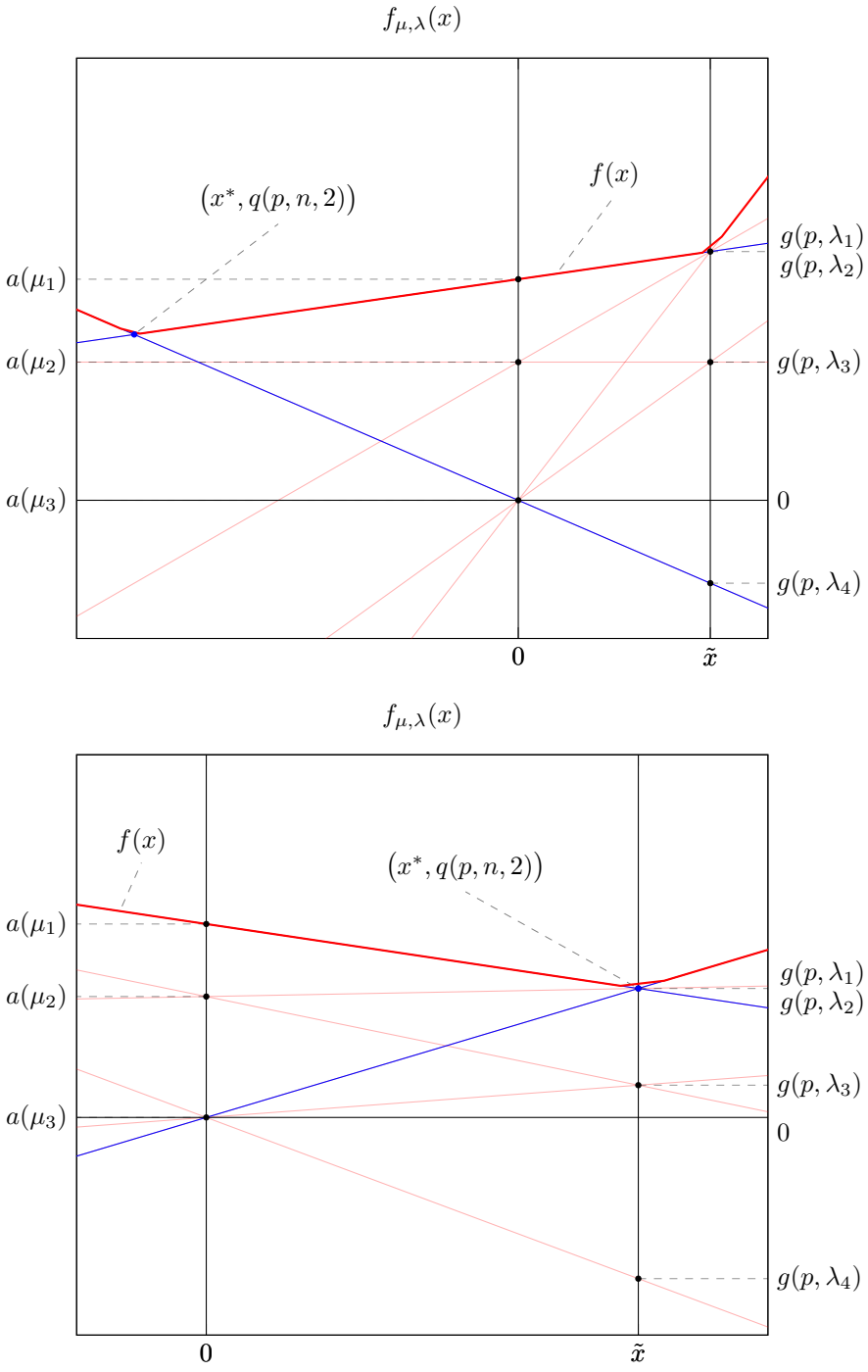

Figure 7.7: Two typical behaviors of the spectrum $f_{\mu,\lambda}(x)$ (thin red lines; $f(x)$ is in bold red) for all $(\lambda,\mu) \in \Omega_{n,2}$, for small p on the top and large p on the bottom. The coordinate $x = x^*$ corresponds to the optimal value $f(x^*) = q(p,n,2)$. The plot corresponds to the parameters $n = 5$ with $p = \frac{3}{20}$ on the top and $p = \frac{1}{3}$ on the bottom. The partitions λ corresponding to the points $(\tilde{x}, g(p,\lambda))$ are $\lambda_1 = \lambda_2 = (1)$, $\lambda_3 = (3)$, $\lambda_4 = (5)$. The partitions μ characterising the offsets $a(\mu)$ for the functions $f_{\mu,\lambda}(x)$ are $\mu_1 = (3,2)$, $\mu_2 = (4,1)$, $\mu_3 = (3,2)$, $\mu_4 = (5)$.

to affine functions f_{μ_r,λ_r} with $r \in \{0,\dots,\lfloor\frac{n-1}{2}\rfloor\}$. The affine functions f_{μ_r,λ_r} intersect f_{μ_1,λ_1} or f_{μ_1,λ_2} at

$$x_r = \frac{4}{2r-n+2} - 1 \quad \text{and} \quad y_r = \frac{4p(1-n)+n-2}{(n-1)(2r-n+2)} + \frac{1}{n-1} + p. \tag{7.140}$$

The largest value of y_r is reached at $r = 0$ and is equal to $y_0 = \frac{p(n+2)}{n-2}$. Not that since $g\big(p,(1,1)\big) - a\big(\frac{n}{2},\frac{n}{2}\big)$ and $g\big(p,\varnothing\big) - a\big(\frac{n}{2},\frac{n}{2}\big)$ are both non-negative, and from Lemma 7.4.13:

$$g(p,\lambda_1) = g(p,\lambda_2) \geqslant g(p,\lambda),$$

for all λ in $\Omega_{n,2}$, then there is no μ in $\Omega_{n,2}$ such that f_{μ,λ_1} or f_{μ,λ_2} has non-positive slope. Thus if n even and $p \leqslant \frac{n-2}{4(n-1)}$, then $q(p,n,2) = \frac{p(n+2)}{n-2}$.

Let n even and $p > \frac{n-2}{4(n-1)}$, then f_{μ_1,λ_1} and f_{μ_1,λ_2} have negative slope, and the optimal value $q(p,n,2)$ must lie at the intersection of another affine function $f_{\mu,\lambda}$ with non-negative slope. But from Lemma 7.4.13:

$$g(p,\lambda_1) = g(p,\lambda_2) \geqslant g(p,\lambda),$$

for all λ in $\Omega_{n,2}$. Thus no intersection can occur at a point higher than $g(p,\lambda_1) = g(p,\lambda_2)$. But from Lemma 7.4.13, we know that for any $\mu_k = (n-k,k)$ for some $k \in \{0,\dots,\lfloor\frac{n}{2}\rfloor\}$, either (λ_1,μ_k) or (λ_2,μ_k) is in $\Omega_{n,2}$. In particular, the affine functions f_{μ_0,λ_1} or f_{μ_0,λ_2} have non-negative slope when $g(p,\lambda_1) = g(p,\lambda_2) \geqslant 0$, that is $p \leqslant \frac{n}{2(n-1)}$, and intersect f_{μ_1,λ_1} or f_{μ_1,λ_2} identically at

$$x_0 = 1 \quad \text{and} \quad y_0 = \frac{n}{2(n-1)} - p. \tag{7.141}$$

Thus if n even and $\frac{n}{2(n-1)} \geqslant p > \frac{n-2}{4(n-1)}$, then $q(p,n,2) = \frac{n}{2(n-1)} - p$.

If n is odd, both f_{μ_1,λ_1} and f_{μ_1,λ_2} are included in the optimisation problem $q(p,n,2)$, and the two affine functions f_{μ_1,λ_1}, f_{μ_1,λ_2} coincide with slopes equal to

$$g\big(p,(1)\big) - a\big(\lceil\tfrac{n}{2}\rceil,\lfloor\tfrac{n}{2}\rfloor\big) = \frac{n-1}{4n} - p. \tag{7.142}$$

Let n be odd and $p \leqslant \frac{n-1}{4n}$, then f_{μ_1,λ_1} and f_{μ_1,λ_2} have a non-negative slope, and the optimal value $q(p,n,2)$ must be at the intersection of another affine function $f_{\mu,\lambda}$ with a non-positive slope. Following the same argument as for even n: the affine functions f_{μ_r,λ_r} intersect f_{μ_1,λ_1} or f_{μ_1,λ_2} at

$$x_r = \frac{4}{2r-n+1} - 1 \quad \text{and} \quad y_r = \frac{n-4pn-1}{n(2r-n+1)} + \frac{1}{n} + p. \tag{7.143}$$

The largest value of y_r is reached at $r = 0$, is equal to $y_0 = \frac{p(n+3)}{n-1}$, and no other intersection occurs higher. Thus if n odd and $p \leqslant \frac{n-1}{4n}$, then $q(p,n,2) = \frac{p(n+3)}{n-1}$.

Let n odd and $p > \frac{n-1}{4n}$, then f_{μ_1,λ_1} and f_{μ_1,λ_2} have negative slope, and the optimal value $q(p,n,2)$ must lie at the intersection with another affine function $f_{\mu,\lambda}$ with non-negative slope. Following the same argument as for even n: the affine functions f_{μ_0,λ_1} or f_{μ_0,λ_2} have non-negative slope when $g(p,\lambda_1) = g(p,\lambda_2) \geqslant 0$, that is $p \leqslant \frac{n+1}{2n}$, and intersect f_{μ_1,λ_1} or f_{μ_1,λ_2} identically at

$$x_0 = 1 \quad \text{and} \quad y_0 = \frac{1}{2}\left(\frac{1}{n} - 2p + 1\right). \tag{7.144}$$

Thus if n odd and $\frac{n+1}{2n} \geqslant p > \frac{n-1}{4n}$, then $q(p,n,2) = \frac{1}{2}\big(\frac{1}{n} - 2p + 1\big) = \frac{n+1}{2n} - p$.

Collecting everything together we get the following answer:

$$q(p,n,2) = \begin{cases} \frac{n+2}{n-2}p & \text{if } n \text{ even and } p < \frac{n-2}{4(n-1)}, \\ \frac{n}{2(n-1)} - p & \text{if } n \text{ even and } \frac{n}{2(n-1)} \geqslant p \geqslant \frac{n-2}{4(n-1)}, \\ \frac{n+3}{n-1}p & \text{if } n \text{ odd and } p < \frac{n-1}{4n}, \\ \frac{n+1}{2n} - p & \text{if } n \text{ odd and } \frac{n+1}{2n} \geqslant p \geqslant \frac{n-1}{4n}, \\ 0 & \text{otherwise,} \end{cases} \tag{7.145}$$

$$= \begin{cases} \frac{\lceil n/2 \rceil + 1}{\lceil n/2 \rceil - 1}p & \text{if } p < \frac{\lceil n/2 \rceil - 1}{2(2\lceil n/2 \rceil - 1)}, \\ \frac{\lceil n/2 \rceil}{2\lceil n/2 \rceil - 1} - p & \text{if } \frac{\lceil n/2 \rceil}{2\lceil n/2 \rceil - 1} \geqslant p \geqslant \frac{\lceil n/2 \rceil - 1}{2(2\lceil n/2 \rceil - 1)}, \\ 0 & \text{otherwise.} \end{cases} \tag{7.146}$$

□

7.5 Discussion

Asymptotic limits

It is interesting to analyse the asymptotic behavior of $q_W(n,d)$, $p_B(n,d)$, and $p_I(n,d)$ as the dimension d becomes large. Deriving from Theorem 7.4.1, the asymptotic behavior of the Werner case $q_W(n,d)$ is:

$$\lim_{d\to\infty} q_W(n,d) = \lim_{d\to\infty} \left(\frac{d-1}{2d} \cdot \frac{(n+k+d)(n-k)}{n(n-1)} + \frac{k(k-1)}{n(n-1)} \right) = 1, \tag{7.147}$$

with $k = n \bmod d$. Correspondingly, for the Brauer case $p_B(n,d)$, Theorem 7.4.10 yields:

$$\lim_{d\to\infty} p_B(n,d) = \lim_{d\to\infty} \left(\frac{1}{d} + \frac{1}{n + n \bmod 2 - 1} - \frac{1}{d(n + n \bmod 2 - 1)} \right) = \frac{1}{n + n \bmod 2 - 1}. \tag{7.148}$$

Lastly, the isotropic case $p'_I(n,d)$, from Theorem 7.4.2, takes the form::

$$\lim_{d\to\infty} p_I(n,d) = \lim_{d\to\infty} p'_I(n,d) = \lim_{d\to\infty} \begin{cases} \frac{1}{n+n \bmod 2-1} & \text{if } d > n \text{ or either } d \text{ or } n \text{ is even} \\ \min\left\{ \frac{2d+1}{2dn+1}, \frac{1}{n-1} \right\} & \text{if } n \geqslant d \text{ and both } d \text{ and } n \text{ are odd} \end{cases}$$
$$= \frac{1}{n + n \bmod 2 - 1}. \tag{7.149}$$

It can be observed that in large dimensions, $p_B(n,d)$ and $p_I(n,d)$ become equal.

As the number of vertices n grows, $p'_I(n,d)$ converges to zero. This implies that an isotropic state ρ is K_n-extendible for all n if and only if $\rho = \frac{\mathbb{I}}{d^2}$. For Werner and Brauer states, the limits $\lim_{n\to\infty} q_W(n,d) = \frac{d-1}{2d}$ and $\lim_{n\to\infty} p_B(n,d) = \frac{1}{d}$ hold, which makes non-trivial K_n-extendible Werner and Brauer states possible.

Moreover, due to Section 7.A.5, it is interesting to note that for a fixed d and for every $n \geqslant 2$, there exists entangled Brauer state which is K_n-extendible. However, this is not true neither for Werner nor for isotropic states.

We could not solve a general Brauer K_n-extendibility region problem. However, we are tempted to formulate the following conjecture:

7.5.1. Conjecture. *Brauer K_n-extendibility region is a polytope for all n and d. However, in the limit $n \to \infty$ it is not a polytope.*

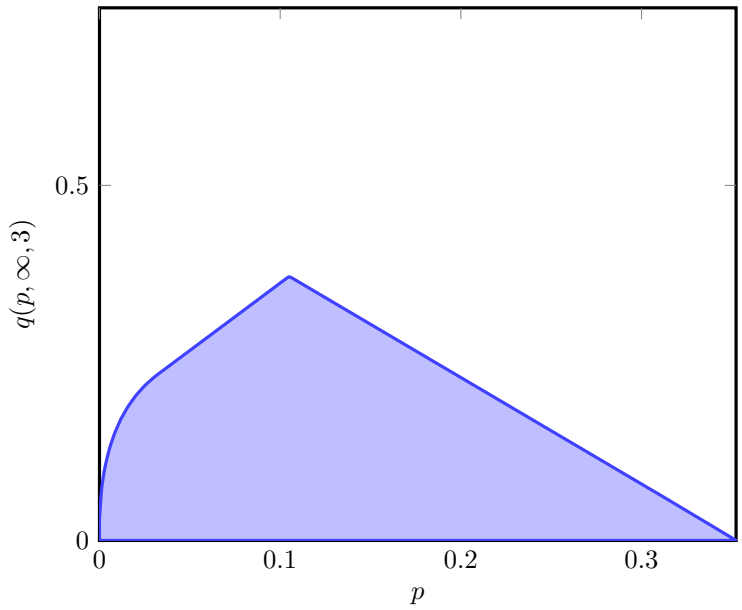

Figure 7.8: Asymptotic K_n-extendibility for qutrit Brauer states is not a polytope.

For example, one could see how the limiting shape of the Brauer K_n-extendibility region for $d = 3$ looks numerically in Fig. 7.8. Related to that example, we expect that results and methods developed in [Rya; JSZ18; Jak22] could be helpful to tackle specifically the $d = 3$ case analytically for arbitrary n.

Optimal states

The optimal state for the Werner case which achieves $q_W(n, d)$ can be easily obtained from the proof in Section 7.A.1. Namely, an optimal state ρ is the normalised projector onto the isotypic component λ:

$$\rho = \frac{\varepsilon_\lambda}{\operatorname{Tr} \varepsilon_\lambda}, \tag{7.150}$$

such that

$$\lambda_1 = \ldots = \lambda_k = \frac{n-k}{d} + 1, \quad \lambda_{k+1} = \ldots = \lambda_d = \frac{n-k}{d}, \tag{7.151}$$

where $k := n \bmod d$.

In general, it is not known which quantum state ρ gives the optimal value $p_B(n, d)$, or $p'_I(n, d)$, but using Section 7.2.1, it must be in the algebra generated by the action of the Brauer algebra into the tensor space $(\mathbb{C}^d)^{\otimes n}$. We leave it as an open problem to analyse and understand in detail the structure of the optimal states in terms of the Brauer diagrams.

$K_{n,m}$-extendibility

One can formulate optimisation problems Eqs. (7.35) and (7.48) in the setting of other edge-transitive graphs G. In particular, if G is a complete bipartite graph $K_{n,m}$, then the relevant optimisation problems were solved in [JSZ22] for Werner and isotropic states. For example, the optimal values $p_I(K_{n,m}, d)$ and $p_B(K_{n,m}, d)$ are:

$$p_I(K_{n,m}, d) = p_B(K_{n,m}, d) = \frac{1}{d} + \left(1 - \frac{1}{d}\right) \frac{1}{\max(n, m)}. \tag{7.152}$$

Note, that in the case of a complete bipartite graph $K_{n,m}$ the value $p_B(K_{n,m}, d)$ of the Brauer state optimisation problem Eq. (7.48) coincides with the value $p_I(K_{n,m}, d)$ above due

to symmetries of the graph $K_{n,m}$: one can twirl the solution of the Brauer state optimisation problem with $U\otimes\bar{U}$ to get the isotropic solution without changing the optimal value $p_B(K_{n,m}, d)$.

Notably, $q_W(K_{n,m}, d)$ does not have a nice expression for general d [JSZ22], so it is currently an open problem to find one. In the special case $m = 1$, the formula for $q_W(K_{n,1}, d)$ was found in [JV13]:

$$q_W(K_{n,1}, d) = \min\left(\frac{n+d-1}{2n}, 1\right). \tag{7.153}$$

In general, it is interesting to understand the values $q_W(G, d)$, $p_I(G, d)$, $p_B(G, d)$ as well as the full (p, q) extendibility region for arbitrary edge-transitive graphs.

7.A Appendix

7.A.1 K_n-Extendibility of Werner states via primal SDP

Let $n \geqslant 1$ be the number of systems and $d \geqslant 2$ the local dimension of each system. We want to solve the optimisation problem Eq. (7.32) for $\Pi = \frac{\mathrm{I}-\mathrm{F}}{2}$, i.e. our goal is to determine $q_W(n,d)$. Given an optimal ρ, we can assume without loss of generality that it has $U^{\otimes n}$ and S_n symmetry. This means, that we want to find an n-qudit density matrix ρ whose any two-body marginal corresponding to an edge e in the graph K_n is

$$\rho_e = p\rho_{\ydiagram{2}} + (1-p)\rho_{\ydiagram{1,1}} \tag{7.154}$$

where $p \in [0,1]$ and

$$\rho_{\ydiagram{2}} := \frac{\varepsilon_{\ydiagram{2}}}{\operatorname{Tr}\varepsilon_{\ydiagram{2}}}, \quad \rho_{\ydiagram{1,1}} := \frac{\varepsilon_{\ydiagram{1,1}}}{\operatorname{Tr}\varepsilon_{\ydiagram{1,1}}}, \tag{7.155}$$

with ranks $\operatorname{Tr}\varepsilon_{\ydiagram{2}} = \frac{d(d-1)}{2}$ and $\operatorname{Tr}\varepsilon_{\ydiagram{1,1}} = \frac{d(d+1)}{2}$.

Since the solution ρ has $U^{\otimes n}$ and S_n symmetry, then we can assume

$$\rho = \sum_{\substack{\lambda\vdash n \\ l(\lambda)\leqslant d}} \beta_\lambda \rho_\lambda, \tag{7.156}$$

where β_λ is some probability distribution $\{\beta_\lambda \,|\, \lambda\vdash n\}$ and ρ_λ are normalised isotypical projectors ε_λ onto the subspace λ in the Schur–Weyl duality:

$$\rho_\lambda := \frac{\varepsilon_\lambda}{\operatorname{Tr}\varepsilon_\lambda} = \frac{\varepsilon_\lambda}{d_\lambda m_\lambda}. \tag{7.157}$$

Their ranks $\operatorname{Tr}\varepsilon_\lambda = d_\lambda m_\lambda$ are given by dimensions of symmetric and unitary group irreps, see Eqs. (2.40) and (2.47). The key result which allows us to find $q_W(n,d)$ is the following lemma.

7.A.1. Lemma ([CKMR07]). $\operatorname{Tr}_{[n]\setminus e}\rho_\lambda = \alpha^\lambda_{\ydiagram{2}}\varepsilon_{\ydiagram{2}} + \alpha^\lambda_{\ydiagram{1,1}}\varepsilon_{\ydiagram{1,1}}$ *where*

$$\alpha^\lambda_{\ydiagram{2}} = \frac{s^*_{\ydiagram{2}}(\lambda)}{m_{\ydiagram{2}} n(n-1)}, \tag{7.158}$$

where $s^*_\mu(\lambda)$ is the shifted Schur function s^*_μ evaluated for the partition λ, see [OO97].

Therefore, if we compute for every edge e the reduced density matrix ρ_e then we get

$$\begin{aligned}\rho_e = \operatorname{Tr}_{[n]\setminus e}\rho &= \sum_{\substack{\lambda\vdash n \\ l(\lambda)\leqslant d}} \beta_\lambda \operatorname{Tr}_{[n]\setminus e}\rho_\lambda = \sum_{\substack{\lambda\vdash n \\ l(\lambda)\leqslant d}} \beta_\lambda(\alpha^\lambda_{\ydiagram{2}}\varepsilon_{\ydiagram{2}} + \alpha^\lambda_{\ydiagram{1,1}}\varepsilon_{\ydiagram{1,1}}) \\ &= \Bigg(\sum_{\substack{\lambda\vdash n \\ l(\lambda)\leqslant d}} \beta_\lambda \alpha^\lambda_{\ydiagram{2}} \operatorname{Tr}\varepsilon_{\ydiagram{2}}\Bigg)\rho_{\ydiagram{2}} + \Bigg(\sum_{\substack{\lambda\vdash n \\ l(\lambda)\leqslant d}} \beta_\lambda \alpha^\lambda_{\ydiagram{1,1}} \operatorname{Tr}\varepsilon_{\ydiagram{1,1}}\Bigg)\rho_{\ydiagram{1,1}},\end{aligned} \tag{7.159}$$

which means that

$$p = \sum_{\substack{\lambda\vdash n \\ l(\lambda)\leqslant d}} \beta_\lambda \frac{d_{\ydiagram{2}} s^*_{\ydiagram{2}}(\lambda)}{n(n-1)}. \tag{7.160}$$

So after using a formula for the shifted Schur function [OO97] we get the following solution to our optimisation problem:

$$q_W(n,d) = \max_{\substack{\lambda\vdash n \\ l(\lambda)\leqslant d}} \frac{d_{\ydiagram{2}} s^*_{\ydiagram{2}}(\lambda)}{n(n-1)} = \max_{\substack{\lambda\vdash n \\ l(\lambda)\leqslant d}} \frac{\sum_{d\geqslant i>j\geqslant 1}\lambda_i(\lambda_j+1)}{n(n-1)} \tag{7.161}$$

7.A.2. Example. When $d = 2$, the general formula for α is

$$\frac{\lambda_2(\lambda_1 + 1)}{n(n-1)}. \tag{7.162}$$

We want to maximize this subject to $n \geqslant \lambda_1 \geqslant \lambda_2 \geqslant 0$ and $\lambda_1 + \lambda_2 = n$. The optimal value is

$$\alpha = \begin{cases} \frac{1}{4} + \frac{3}{4n} & \text{if } n \text{ is odd,} \\ \frac{1}{4} + \frac{3}{4(n-1)} & \text{if } n \text{ is even.} \end{cases} \tag{7.163}$$

7.A.3. Theorem. *The general answer to Eq. (7.161) is*

$$q_W(n,d) = \frac{d-1}{2d} \cdot \frac{(n+k+d)(n-k)}{n(n-1)} + \frac{k(k-1)}{n(n-1)} \tag{7.164}$$

where $k = n \bmod d$.

Proof:
We will guess the optimal solution for the Young diagram λ and prove that it is not possible to improve on it. The conjectured optimal solution:

$$\lambda_1 = \ldots = \lambda_k = \frac{n-k}{d} + 1, \quad \lambda_{k+1} = \ldots = \lambda_d = \frac{n-k}{d} \tag{7.165}$$

Consider an arbitrary Young diagram $\mu = \lambda + \Delta$, which you get by a perturbation Δ, i.e. $\Delta := (\Delta_1, \ldots, \Delta_d)$ with the properties $\sum_{i=1}^{d} \Delta_i = 0$ and $\sum_{i=1}^{j} \Delta_i \geqslant 0$ for all $j \in \{1, \ldots, d\}$. Then we can estimate the difference between shifted Schur functions as

$$\begin{aligned}
\frac{s^*_{\boxplus}(\mu) - s^*_{\boxplus}(\lambda)}{d_{\boxplus}} &= \sum_{d \geqslant i > j \geqslant 1} \big((\lambda_i + \Delta_i)(\lambda_j + \Delta_j + 1) - \lambda_i(\lambda_j + 1)\big) \\
&= \sum_{d \geqslant i > j \geqslant 1} (\Delta_i \lambda_j + \lambda_i \Delta_j + \Delta_i + \Delta_i \Delta_j) \\
&= \sum_{i=2}^{d} \Delta_i \sum_{j=1}^{i-1} \lambda_j + \sum_{i=1}^{d-1} \Delta_i \sum_{j=i+1}^{d} \lambda_j + \sum_{i=2}^{d} \Delta_i (i-1) - \frac{1}{2} \sum_{i=1}^{d} \Delta_i^2 \\
&= \Delta_d \sum_{j=1}^{d-1} \lambda_j + \Delta_1 \sum_{j=2}^{d} \lambda_j + \sum_{i=2}^{d-1} \Delta_i \sum_{j=1}^{d} \lambda_j - \sum_{i=2}^{d-1} \Delta_i \lambda_i + \sum_{j=2}^{d-1} \sum_{i=j}^{d} \Delta_i - \frac{1}{2} \sum_{i=1}^{d} \Delta_i^2 \\
&= \Delta_d (n - \lambda_d) + \Delta_1 (n - \lambda_1) - n(\Delta_d + \Delta_1) - \sum_{i=2}^{d-1} \Delta_i \lambda_i - \sum_{j=2}^{d-1} \sum_{i=1}^{j-1} \Delta_i - \frac{1}{2} \sum_{i=1}^{d} \Delta_i^2 \\
&= - \sum_{i=1}^{d} \Delta_i \lambda_i - \sum_{j=2}^{d-1} \sum_{i=1}^{j-1} \Delta_i - \frac{1}{2} \sum_{i=1}^{d} \Delta_i^2 \\
&= - \sum_{i=1}^{k} \Delta_i \left(\frac{n-k}{d} + 1 \right) - \sum_{i=k+1}^{d} \Delta_i \frac{n-k}{d} - \sum_{j=2}^{d-1} \sum_{i=1}^{j-1} \Delta_i - \frac{1}{2} \sum_{i=1}^{d} \Delta_i^2 \\
&= - \sum_{i=1}^{k} \Delta_i - \sum_{j=2}^{d-1} \sum_{i=1}^{j-1} \Delta_i - \frac{1}{2} \sum_{i=1}^{d} \Delta_i^2 \leqslant 0,
\end{aligned}$$

which shows that λ is actually the optimal solution. Evaluating the shifted Schur function at λ gives the answer. □

7.A.2 The dual SDP: Isotropic states

In this section we are going to solve the optimisation problem Eq. (7.61):

$$p'_I(n,d) = \max_{\rho,p'} \quad p' \qquad \text{s.t.} \quad \rho_e = \frac{p'}{d}\cdot \mathrm{W} + \frac{1-p'}{d^2}\cdot \mathrm{I} \quad \forall e \in E, \quad \rho \succeq 0.$$

The Lagrangian [BV04] associated with it is defined as,

$$L\big(p,\rho,(h_e)_e,Z\big) := p + \sum_{e\in E}\Big\langle h_e, \rho_e - \frac{p}{d}\mathrm{W} - \frac{(1-p)}{d^2}\mathrm{I}\Big\rangle + \big\langle Z,\rho\big\rangle, \tag{7.166}$$

where $(h_e)_e$ is a family of Hermitian matrices acting on $\big(\mathbb{C}^d\big)^{\otimes 2}$, Z is a Hermitian matrix acting on $\big(\mathbb{C}^d\big)^{\otimes n}$ and $\langle\cdot,\cdot\rangle$ denotes the Frobenius inner product. The Min-Max principle states that

$$\max_{\rho,p} \quad \min_{\substack{Z,(h_e)_e\\ Z\succeq 0}} \quad L\big(p,\rho,Z,(h_e)_e\big) \leqslant \min_{\substack{Z,(h_e)_e\\ Z\succeq 0}} \quad \max_{\rho,p} \quad L\big(p,\rho,Z,(h_e)_e\big).$$

In fact, Slater's condition holds for our SDP (take $\rho = \frac{1}{d^n}\cdot \mathrm{I}^{\otimes n}$ and $p=0$) and we have the equality. Rewriting the Lagrangian gives,

$$L\big(p,\rho,(h_e)_e,Z\big) = -\frac{\mathrm{Tr}[H]}{d^n} + p\bigg(1 - \sum_{e\in E}\Big\langle h_e, \frac{\mathrm{W}}{d} - \frac{\mathrm{I}}{d^2}\Big\rangle\bigg) + \big\langle H+Z,\rho\big\rangle,$$

where $H := \sum_{e\in E}(h_e \otimes I_{\bar{e}})$ and $I_{\bar{e}}$ is the identity on all vertices except those of e. Therefore the dual SDP of Eq. (7.61) is

$$p'_I(n,d) = \min_{(h_e)_e,Z} \quad -\frac{\mathrm{Tr}[H]}{d^n} \quad \text{s.t.} \quad \sum_{e\in E}\Big\langle h_e, \frac{\mathrm{W}}{d} - \frac{\mathrm{I}}{d^2}\Big\rangle = 1, \quad H+Z=0, \quad Z\succeq 0. \tag{7.167}$$

Recall that for any Hermitian matrix M the smallest $\lambda\in\mathbb{R}$ such that $\lambda I \succeq M$ is equal to the largest eigenvalue of M, denoted $\lambda_{\max}(M)$. Then using the substitution $(h_e - \frac{\mathrm{Tr}[h_e]}{d^2} I_e) \mapsto h_e$ the Eq. (7.167) can be rewritten as

$$p'_I = \min_{(h_e)_e} \quad \lambda_{\max}\bigg(\sum_{e\in E} h_e \otimes I_{\bar{e}}\bigg) \quad \text{s.t.} \quad \sum_{e\in E}\Big\langle h_e, \frac{\mathrm{W}}{d}\Big\rangle = 1, \quad \mathrm{Tr}[h_e]=0 \quad \forall e\in E. \tag{7.168}$$

We can simplify Eq. (7.168) even further, using the commutation relation of the isotropic states, i.e

$$[\rho, \bar{U}\otimes U] = [\rho, O\otimes O] = 0, \qquad \forall U\in \mathrm{U}_d,\ \forall O\in \mathrm{O}_d, \tag{7.169}$$

by twirling the operator H with respect to the orthogonal group. Let $(h_e^*)_e = \arg\ p'_I(n,d)$ be a family of Hermitian matrices acting on $\big(\mathbb{C}^d\big)^{\otimes 2}$ optimal for the dual problem $p'_I(n,d)$. For all edges $e\in E$, define the twirling of h_e^* as follows:

$$\widetilde{h_e^*} := \int_{\mathrm{O}_d} O^{\otimes 2} h_e^* \big(O^*\big)^{\otimes 2}\,\mathrm{d}\,O, \tag{7.170}$$

where the integral is taken with respect to the normalised Haar measure on the orthogonal group. Twirling in the same fashion the operator H^* we get $\widetilde{H^*}$. Then by the convexity of $\lambda_{\max}$,

$$\lambda_{\max}(H^*) \geqslant \lambda_{\max}\big(\widetilde{H^*}\big).$$

The constraints of the Eq. (7.168) are also satisfied with $\left(\widetilde{h_e^*}\right)_e$ by the cyclic property of the trace, and hence we can restrict the dual problem to twirled $\left(\widetilde{h_e}\right)_e$.

Since each $\widetilde{h_e}$ commutes with the action of the orthogonal group, we can write (see Section 7.2.1),

$$\widetilde{h_e} = \alpha_e \mathrm{I}_e + \beta_e \mathrm{W}_e + \gamma_e \mathrm{F}_e, \tag{7.171}$$

where $\mathrm{F} := \sum_{i,j=1}^{d} |ij\rangle\langle ji|$ is the flip operator. Note that condition $\mathrm{Tr}[\widetilde{h_e}] = 0$ is equivalent to $\alpha_e = -\frac{\beta_e+\gamma_e}{d}$. Then Eq. (7.168) becomes

$$\begin{aligned} p'_I(n,d) = \min_{(\beta_e,\gamma_e)_e} \quad & \lambda_{\max}\left(\sum_{e\in E}\left(-\frac{\beta_e+\gamma_e}{d}\mathrm{I}_e + \beta_e \mathrm{W}_e + \gamma_e \mathrm{F}_e\right) \otimes I_{\bar{e}}\right) \\ \text{s.t.} \quad & (d^2-1)\left(\sum_{e\in E}\beta_e\right) + (d-1)\left(\sum_{e\in E}\gamma_e\right) = d. \end{aligned} \tag{7.172}$$

Similarly, using the commutation relation

$$[\rho, \psi_n^d(\pi)] = 0, \qquad \forall \pi \in \mathrm{S}_n, \tag{7.173}$$

we get that for all edges $e \in E$ the values of β_e and γ_e are equal, i.e. we can write for some $\beta \in \mathbb{R}$ and $\gamma \in \mathbb{R}$:

$$\forall e \in E: \quad \beta_e = \beta \quad \text{and} \quad \gamma_e = \gamma. \tag{7.174}$$

Therefore we can rewrite Eq. (7.172) as follows:

$$\begin{aligned} p'_I(n,d) = \min_{\beta,\gamma} \quad & \lambda_{\max}\left(\sum_{e\in E}\left(-\frac{\beta+\gamma}{d}\mathrm{I}_e + \beta \mathrm{W}_e + \gamma \mathrm{F}_e\right) \otimes I_{\bar{e}}\right) \\ \text{s.t.} \quad & (d^2-1)|E|\beta + (d-1)|E|\gamma = d. \end{aligned} \tag{7.175}$$

Using the constraint $(d^2-1)|E|\beta+(d-1)|E|\gamma = d$ to eliminate γ, and by the change of variable $-\beta \mapsto x$ and rewriting

$$f(x) := \lambda_{\max}(H(x)), \qquad H(x) := \sum_{e\in E}\left(\left(\frac{1}{|E|(1-d)} - x\right)(\mathrm{I}_e - d\,\mathrm{F}_e) + x(\mathrm{F}_e - \mathrm{W}_e)\right) \otimes I_{\bar{e}}, \tag{7.176}$$

we reformulate Eq. (7.175) as

$$p'_I(n,d) = \min_{x\in\mathbb{R}} f(x). \tag{7.177}$$

7.A.3 The dual SDP: Brauer states when $q = 0$

In this section, we are going to solve the following optimisation problem:

$$p^*(n,d) = \max_{\rho,p} \quad p \qquad \text{s.t.} \quad \rho_e = p \cdot \Pi_\varnothing + (1-p)\cdot \frac{\Pi_{\square\square}}{\mathrm{Tr}\,\Pi_{\square\square}} \quad \forall e \in E, \quad \rho \succeq 0. \tag{7.178}$$

Similarly to Section 7.A.2, the Slater's condition holds for our SDP: take $\lambda = (n)$, and set $p = \frac{1}{1+\mathrm{Tr}\,\Pi_{\square\square}}$ and $\rho = \frac{\varepsilon_\lambda}{\mathrm{Tr}\,\varepsilon_\lambda}$ is a normalised projector onto the symmetric subspace of n qudits. Therefore, we get the following dual SDP:

$$p^*(n,d) = \min_{(h_e)_e, Z} \quad -\sum_{e\in E}\left\langle h_e, \frac{\Pi_{\square\square}}{\mathrm{Tr}\,\Pi_{\square\square}}\right\rangle \quad \text{s.t.} \quad \sum_{e\in E}\left\langle h_e, \Pi_\varnothing - \frac{\Pi_{\square\square}}{\mathrm{Tr}\,\Pi_{\square\square}}\right\rangle = 1, \quad H + Z = 0, \quad Z \succeq 0. \tag{7.179}$$

This SDP has orthogonal symmetry and S_n of the complete graph K_n, therefore similarly to Section 7.A.2, we can assume that $h_e = \alpha \mathrm{I}_e + \beta \mathrm{W}_e + \gamma \mathrm{F}_e$ for every $e \in E$. In the end, this leads to the following simplification of Eq. (7.179):

$$p^*(n,d) = \min_{x \in \mathbb{R}} \quad \frac{1}{d \cdot |E|} \lambda_{\max} \left(\sum_{e \in E} \mathrm{W}_e - x \cdot \mathrm{F}_e \right) + \frac{x}{d}. \tag{7.180}$$

But the spectrum of the Hamiltonian $\sum_{e \in E} \mathrm{W}_e - x \cdot \mathrm{F}_e$ can be easily obtained, see Section 7.2.3. Therefore we can simplify Eq. (7.180) to

$$p^*(n,d) = \min_{x \in \mathbb{R}} \max_{(\lambda,\mu) \in \Omega_{n,d}} \quad \frac{1}{d \cdot |E|} \left(\mathrm{cont}(\mu) - \mathrm{cont}(\lambda) + \frac{(n - |\lambda|)(d-1)}{2} \right) + \frac{x}{d} \left(1 - \frac{\mathrm{cont}(\mu)}{|E|} \right). \tag{7.181}$$

7.A.4 The dual SDP: Brauer states with fixed p

In this section, we are going to solve the following optimisation problem:

$$\begin{aligned} q(p,n,d) = \max_{\rho, q} \quad & q \\ \text{s.t.} \quad & \rho_e = p \cdot \Pi_\varnothing + q \cdot \tfrac{\Pi_{\square}}{\operatorname{Tr} \Pi_{\square}} + (1 - p - q) \cdot \tfrac{\Pi_{\square\square}}{\operatorname{Tr} \Pi_{\square\square}}, \quad \forall e \in E \\ & \rho \succeq 0. \end{aligned} \tag{7.182}$$

Slater's condition holds for our SDP as in Section 7.A.2. Therefore the dual SDP of Eq. (7.178) is

$$\begin{aligned} q(p,n,d) = \min_{(h_e)_e, Z} \quad & - \sum_{e \in E} \left\langle h_e, p \cdot \Pi_\varnothing + (1-p) \cdot \tfrac{\Pi_{\square\square}}{\operatorname{Tr} \Pi_{\square\square}} \right\rangle \\ \text{s.t.} \quad & \sum_{e \in E} \left\langle h_e, \tfrac{\Pi_{\square}}{\operatorname{Tr} \Pi_{\square}} - \tfrac{\Pi_{\square\square}}{\operatorname{Tr} \Pi_{\square\square}} \right\rangle = 1, \; H + Z = 0, \; Z \succeq 0. \end{aligned} \tag{7.183}$$

Similarly to Section 7.A.3, we can assume that $h_e = \alpha \mathrm{I}_e + \beta \mathrm{W}_e + \gamma \mathrm{F}_e$ for every $e \in E$. This leads to the following simplification of Eq. (7.183):

$$q(p,n,d) = \min_{x \in \mathbb{R}} \frac{1}{|E|} \lambda_{\max} \left(\sum_{e \in E} x \frac{\mathrm{W}_e}{d} - \frac{\mathrm{F}_e}{2} \right) + \frac{1}{2} - p \cdot x. \tag{7.184}$$

But the spectrum of the Hamiltonian $\sum_{e \in E} x \frac{\mathrm{W}_e}{d} - \frac{\mathrm{F}_e}{2}$ can be easily obtained, see Section 7.2.3. Therefore we can simplify Eq. (7.183) to

$$q(p,n,d) = \min_{x \in \mathbb{R}} \max_{(\lambda,\mu) \in \Omega_{n,d}} \frac{x}{d \cdot |E|} \left(\mathrm{cont}(\mu) - \mathrm{cont}(\lambda) + \frac{(n - |\lambda|)(d-1)}{2} \right) + \\ + \frac{1}{2} \left(1 - \frac{\mathrm{cont}(\mu)}{|E|} \right) - p \cdot x. \tag{7.185}$$

7.A.5 PPT criterion for Brauer states

The two-parameter (p, q) family of Brauer states, given by Eq. (7.18) as a sum of orthogonal projectors, is positive semidefinite if and only if $p \geqslant 0, q \geqslant 0$ and $p + q \leqslant 1$. This family of states can be alternatively parametrised as:

$$p' \cdot \frac{\mathrm{W}}{d} + q' \cdot \frac{\mathrm{F}}{d} + (1 - p' - q') \cdot \frac{\mathrm{I}}{d^2}. \tag{7.186}$$

The parameters (p, q) of Eq. (7.18) and (p', q') of Eq. (7.186) are related via

$$\begin{cases} p' = p - \frac{2(1-p-q)}{d(d+1)-2} \\ q' = \frac{-q}{d-1} + \frac{d(1-p-q)}{d(d+1)-2} \end{cases} \quad \text{and} \quad \begin{cases} p = \frac{p'(d^2-1)+q'(d-1)+1}{d^2} \\ q = -\frac{p'(d-1)+q'(d^2-1)-d+1}{2d}, \end{cases} \tag{7.187}$$

such that Eq. (7.186) is positive semidefinite if and only if the following holds

$$\begin{cases} p'(d^2-1) + q'(d-1) + 1 \geqslant 0 \\ -p' - q'(d+1) + 1 \geqslant 0 \\ 2 - d + d^2 + p'(d^2+d-2) - q'(d^3-3d+2) \leqslant 2d^2. \end{cases} \tag{7.188}$$

A bipartite state satisfies the PPT criterion (or simply is PPT) if its partial transpose is positive semidefinite. Consequently, the set of PPT states contains the set of separable states. In the context of the two-parameter family of Brauer states, the PPT criterion is equivalent to the separability [VW01; PJPY24]. The partial transpose of a Brauer state of the form Eq. (7.186) becomes

$$p' \cdot \frac{\mathrm{F}}{d} + q' \cdot \frac{\mathrm{W}}{d} + (1 - p' - q') \cdot \frac{\mathrm{I}}{d^2}, \tag{7.189}$$

i.e. it is just the change of variable: $(p', q') \mapsto (q', p')$. A Brauer state's separability (or equivalently PPT) is determined by the intersection of the region defined by:

$$\begin{cases} q'(d^2-1) + p'(d-1) + 1 \geqslant 0 \\ -q' - p'(d+1) + 1 \geqslant 0 \\ 2 - d + d^2 + q'(d^2+d-2) - p'(d^3-3d+2) \leqslant 2d^2, \end{cases} \tag{7.190}$$

and Eq. (7.188).Alternatively, using the relations Eq. (7.187) a Brauer state for any fixed $d \geqslant 2$ is separable if and only if

$$\begin{cases} 0 \leqslant q \leqslant \frac{1}{2} \\ 0 \leqslant p \leqslant \frac{1}{d}. \end{cases} \tag{7.191}$$

Bibliography

[ABMSL23] Rene Allerstorfer, Harry Buhrman, Alex May, Florian Speelman, and Philip Verduyn Lunel. "Relating non-local quantum computation to information theoretic cryptography". *arXiv preprint* (2023). arXiv: 2306.16462.

[ABSL22] Rene Allerstorfer, Harry Buhrman, Florian Speelman, and Philip Verduyn Lunel. "On the Role of Quantum Communication and Loss in Attacks on Quantum Position Verification". *arXiv preprint* (2022). arXiv: 2208.04341.

[ADSV92] Lars Døvling Andersen, Songkang Ding, Gert Sabidussi, and Preben Dahl Vestergaard. "Edge orbits and edge-deleted subgraphs". *Graphs and Combinatorics* 8 (1992). DOI: 10.1007/BF01271706.

[AGKH24] Mirko Arienzo, Dmitry Grinko, Martin Kliesch, and Markus Heinrich. "Bosonic randomized benchmarking with passive transformations". *arXiv preprint* (2024). arXiv: 2408.11111.

[AGM20] Anurag Anshu, David Gosset, and Karen Morenz. "Beyond product state approximations for a quantum analogue of Max Cut". *15th Conference on the Theory of Quantum Computation, Communication and Cryptography (TQC 2020)*. Vol. 158. Leibniz International Proceedings in Informatics (LIPIcs). 2020. DOI: 10.4230/LIPIcs.TQC.2020.7. arXiv: 2003.14394.

[AH21] Sam Armon and Tom Halverson. "Transition Matrices Between Young's Natural and Seminormal Representations". *The Electronic Journal of Combinatorics* 28.3 (2021). DOI: 10.37236/10081. arXiv: 2012.03828.

[AISW20] Jayadev Acharya, Ibrahim Issa, Nirmal V. Shende, and Aaron B. Wagner. "Estimating quantum entropy". *IEEE Journal on Selected Areas in Information Theory* 1.2 (2020). DOI: 10.1109/JSAIT.2020.3015235.

[All+23] Rene Allerstorfer, Matthias Christandl, Dmitry Grinko, Ion Nechita, Maris Ozols, Denis Rochette, and Philip Verduyn Lunel. "Monogamy of highly symmetric states". *arXiv preprint* (2023). arXiv: 2309.16655.

[APE03] Koenraad Audenaert, Martin B. Plenio, and Jens Eisert. "Entanglement cost under positive-partial-transpose-preserving operations". *Phys. Rev. Lett.* 90.2 (2003). DOI: 10.1103/PhysRevLett.90.027901. arXiv: quant-ph/0207146.

[AST17] Henning Haahr Andersen, Catharina Stroppel, and Daniel Tubbenhauer. "Semisimplicity of Hecke and (walled) Brauer algebras". *Journal of the Australian Mathematical Society* 103.1 (2017). DOI: 10.1017/S1446788716000392. arXiv: 1507.07676.

[Aub18] Guillaume Aubrun. *Schur-Weyl Duality*. 2018. URL: https://math.univ-lyon1.fr/~aubrun/recherche/schur-weyl.pdf.

[BBCV21] Michael M. Bronstein, Joan Bruna, Taco Cohen, and Petar Veličković. "Geometric deep learning: grids, groups, graphs, geodesics, and gauges". *arXiv preprint* (2021). arXiv: 2104.13478.

[BBFS22] Mario Berta, Francesco Borderi, Omar Fawzi, and Volkher B. Scholz. "Semidefinite programming hierarchies for constrained bilinear optimization". *Mathematical Programming* 194.1 (2022). DOI: 10.1007/s10107-021-01650-1. arXiv: 1810.12197.

[BCH06] Dave Bacon, Isaac L. Chuang, and Aram W. Harrow. "Efficient quantum circuits for Schur and Clebsch–Gordan transforms". *Physical Review Letters* 97.17 (2006). DOI: 10.1103/physrevlett.97.170502. arXiv: quant-ph/0407082.

[BCS20] Ivan Bardet, Benoît Collins, and Gunjan Sapra. "Characterization of equivariant maps and application to entanglement detection". *Annales Henri Poincaré* 21.10 (2020). DOI: 10.1007/s00023-020-00941-1. arXiv: 1811.08193.

[Ben+93] Charles H. Bennett, Gilles Brassard, Claude Crépeau, Richard Jozsa, Asher Peres, and William K. Wootters. "Teleporting an unknown quantum state via dual classical and Einstein-Podolsky-Rosen channels". *Physical review letters* 70.13 (1993). DOI: 10.1103/PhysRevLett.70.1895.

[Ben+94] Georgia Benkart, Manish Chakrabarti, Thomas Halverson, Robert Leduc, Chanyoung Y. Lee, and Jeffrey Stroomer. "Tensor product representations of general linear groups and their connections with Brauer algebras". *Journal of Algebra* 166.3 (1994). DOI: 10.1006/jabr.1994.1166.

[Ben96] Georgia Benkart. "Commuting actions—A tale of two groups". *Lie Algebras and Their Representations*. Vol. 194. Contemporary Mathematics. American Mathematical Society, 1996. DOI: 10.1090/conm/194/02387.

[Ber12] Sonya Berg. "A quantum algorithm for the quantum Schur–Weyl transform". PhD thesis. University of California, Davis, 2012. arXiv: 1205.3928.

[BGLW24] Harry Buhrman, Dmitry Grinko, Philip Verduyn Lunel, and Jordi Weggemans. "Permutation tests for quantum state identity". *arXiv preprint* (2024). arXiv: 2405.09626.

[BGSV12] Christine Bachoc, Dion C. Gijswijt, Alexander Schrijver, and Frank Vallentin. "Invariant semidefinite programs". *Handbook on Semidefinite, Conic and Polynomial Optimization*. Springer, 2012. DOI: 10.1007/978-1-4614-0769-0_9. arXiv: 1007.2905.

[BH13] Fernando G.S.L. Brandao and Aram W. Harrow. "Product-state approximations to quantum ground states". *Proceedings of the forty-fifth annual ACM symposium on Theory of computing*. 2013. DOI: 10.1145/2488608.2488719. arXiv: 1310.0017.

[Big93] Norman Biggs. *Algebraic graph theory*. Cambridge university press, 1993. DOI: 10.1017/CBO9780511608704.

[BK11] Salman Beigi and Robert König. "Simplified instantaneous non-local quantum computation with applications to position-based cryptography". *New Journal of Physics* 13.9 (2011). DOI: 10.1088/1367-2630/13/9/093036. arXiv: 1101.1065.

[BL68] Lawrence C. Biedenharn and James D. Louck. "A pattern calculus for tensor operators in the unitary groups". *Communications in Mathematical Physics* 8.2 (1968). DOI: 10.1007/BF01645800.

[BLMMO22] Harry Buhrman, Noah Linden, Laura Mančinska, Ashley Montanaro, and Maris Ozols. "Quantum majority vote". *arXiv preprint* (2022). arXiv: 2211.11729.

[BO20] Daria V. Bulgakova and Oleg Ogievetsky. "Fusion procedure for the walled Brauer algebra". *Journal of Geometry and Physics* 149 (2020). DOI: 10.1016/j.geomphys.2019.103580. arXiv: 1911.10537.

[Bot16] Alonso Botero. "Quantum information and the representation theory of the symmetric group". *Revista Colombiana de Matemáticas* 50.2 (2016). DOI: 10.15446/recolma.v50n2.62210.

[Bra37] Richard Brauer. "On algebras which are connected with the semisimple continuous groups". *Annals of Mathematics* 38.4 (1937). DOI: 10.2307/1968843.

[Bra72] Ola Bratteli. "Inductive limits of finite dimensional C^*-algebras". *Transactions of the American Mathematical Society* 171 (1972). DOI: 10.1090/S0002-9947-1972-0312282-2.

[BRR23] Jakob E. Björnberg, Hjalmar Rosengren, and Kieran Ryan. "Heisenberg models and Schur–Weyl duality". *Advances in Applied Mathematics* 151 (2023). DOI: 10.1016/j.aam.2023.102572. arXiv: 2201.10209.

[BS12] Jonathan Brundan and Catharina Stroppel. "Gradings on walled Brauer algebras and Khovanov's arc algebra". *Advances in Mathematics* 231.2 (2012). DOI: 10.1016/j.aim.2012.05.016. arXiv: 1107.0999.

[BSH24] Maria Balanzó-Juandó, Michał Studziński, and Felix Huber. "Positive maps from the walled Brauer algebra". *Journal of Physics A: Mathematical and Theoretical* 57.11 (2024). DOI: 10.1088/1751-8121/ad2b86. arXiv: 2112.12738.

[BSSW24] Sergey Bravyi, Yash Sharma, Mario Szegedy, and Ronald de Wolf. "Generating k EPR-pairs from an n-party resource state". *Quantum* 8 (2024). DOI: 10.22331/q-2024-05-14-1348. arXiv: 2211.06497.

[Buh+14] Harry Buhrman, Nishanth Chandran, Serge Fehr, Ran Gelles, Vipul Goyal, Rafail Ostrovsky, and Christian Schaffner. "Position-based quantum cryptography: Impossibility and constructions". *SIAM Journal on Computing* 43.1 (2014). DOI: 10.1007/978-3-642-22792-9_24.

[Buh+16] Harry Buhrman, Łukasz Czekaj, Andrzej Grudka, Michał Horodecki, Paweł Horodecki, Marcin Markiewicz, Florian Speelman, and Sergii Strelchuk. "Quantum communication complexity advantage implies violation of a Bell inequality". *Proceedings of the National Academy of Sciences* 113.12 (2016). DOI: 10.1073/pnas.1507647113. arXiv: 1502.01058.

[Bul20] Daria V. Bulgakova. "Some aspects of representation theory of walled Brauer algebras". PhD thesis. Aix Marseille Université, 2020.

[BV04] Stephen P. Boyd and Lieven Vandenberghe. *Convex optimization*. Cambridge university press, 2004. DOI: 10.1145/2020408.2020410.

[BZ88] Arkady Berenshtein and Andrei Zelevinskii. "Involutions on Gel'fand–Tsetlin schemes and multiplicities in skew GL_n-modules". *Doklady Akademii Nauk*. Vol. 300. 6. Russian Academy of Sciences. 1988.

[Can11] Constantin Candu. "The continuum limit of gl(M|N) spin chains". *Journal of High Energy Physics* 2011.7 (2011). DOI: 10.1007/JHEP07(2011)069. arXiv: 1012.0050.

[CDDM08] Anton Cox, Maud De Visscher, Stephen Doty, and Paul Martin. "On the blocks of the walled Brauer algebra". *Journal of Algebra* 320.1 (2008). DOI: 10.1016/j.jalgebra.2008.01.026. arXiv: 0709.0851.

[CDP08] Giulio Chiribella, G. Mauro D'Ariano, and Paolo Perinotti. "Quantum circuit architecture". *Physical Review Letters* 101.6 (2008). DOI: 10.1103/PhysRevLett.101.060401. arXiv: 0712.1325.

[Cer00] Nicolas J. Cerf. "Asymmetric quantum cloning in any dimension". *Journal of Modern Optics* 47.2-3 (2000). DOI: 10.1080/09500340008244036. arXiv: quant-ph/9805024.

[CFS02] Carlton M. Caves, Christopher A. Fuchs, and Rüdiger Schack. "Unknown quantum states: the quantum de Finetti representation". *Journal of Mathematical Physics* 43.9 (2002). DOI: 10.1063/1.1494475. arXiv: quant-ph/0104088.

[Chr+21] Matthias Christandl, Felix Leditzky, Christian Majenz, Graeme Smith, Florian Speelman, and Michael Walter. "Asymptotic performance of port-based teleportation". *Communications in Mathematical Physics* 381.1 (2021). DOI: 10.1007/s00220-020-03884-0. arXiv: 1809.10751.

[CHW07] Andrew M. Childs, Aram W. Harrow, and Paweł Wocjan. "Weak Fourier-Schur sampling, the hidden subgroup problem, and the quantum collision problem". *STACS 2007*. Springer, 2007. DOI: 10.1007/978-3-540-70918-3_51. arXiv: quant-ph/0609110.

[CKMR07] Matthias Christandl, Robert König, Graeme Mitchison, and Renato Renner. "One-and-a-Half Quantum de Finetti Theorems". *Communications in Mathematical Physics* 273.2 (2007). DOI: 10.1007/s00220-007-0189-3. arXiv: quant-ph/0602130.

[CL96] William Y.C. Chen and James D. Louck. "Interpolation for symmetric functions". *Advances in mathematics* 117.1 (1996). DOI: 10.1006/aima.1996.0004.

[CM23] Enrique Cervero and Laura Mančinska. "Weak Schur sampling with logarithmic quantum memory". *arXiv preprint* (2023). arXiv: 2309.11947.

[CMN21] Benoit Collins, Sho Matsumoto, and Jonathan Novak. "The Weingarten calculus". *arXiv preprint* (2021). arXiv: 2109.14890.

[Coh21] Taco S. Cohen. "Equivariant convolutional networks". PhD thesis. University of Amsterdam, 2021.

[COS18] Benoît Collins, Hiroyuki Osaka, and Gunjan Sapra. "On a family of linear maps from $M_n(\mathbb{C})$ to $M_{n^2}(\mathbb{C})$". *Linear Algebra and its Applications* 555 (2018). DOI: 10.1016/j.laa.2018.06.011. arXiv: 1802.07553.

[Cox12] Anton Cox. *Representation theory of finite dimensional algebras*. 2012.

[CR62] Charles W. Curtis and Irving Reiner. *Representation Theory of Finite Groups and Associative Algebras*. AMS Chelsea Publishing Series. Interscience Publishers, 1962.

[CŚ06] Benoît Collins and Piotr Śniady. "Integration with respect to the Haar measure on unitary, orthogonal and symplectic group". *Communications in Mathematical Physics* 264.3 (2006). DOI: 10.1007/s00220-006-1554-3. arXiv: math-ph/0402073.

[CST10] T. Ceccherini-Silberstein, F. Scarabotti, and F. Tolli. *Representation Theory of the Symmetric Groups: The Okounkov-Vershik Approach, Character Formulas, and Partition Algebras*. Cambridge Studies in Advanced Mathematics. Cambridge University Press, 2010.

[CW16] Taco Cohen and Max Welling. "Group equivariant convolutional networks". *Proceedings of The 33rd International Conference on Machine Learning*. Vol. 48. Proceedings of Machine Learning Research. New York, New York, USA: PMLR, 2016. arXiv: 1602.07576.

[DJR04] Thomas Decker, Dominik Janzing, and Martin Rötteler. "Implementation of group-covariant positive operator valued measures by orthogonal measurements". *Journal of Mathematical Physics* 46.1 (2004). DOI: 10.1063/1.1827924. arXiv: quant-ph/0407054.

[DK12] Yurj A. Drozd and Vladimir V. Kirichenko. *Finite Dimensional Algebras*. Springer, 2012.

[DLS18] Stephen Doty, Aaron Lauve, and George H. Seelinger. "Canonical idempotents of multiplicity-free families of algebras". *L'Enseignement Mathématique* 64.1/2 (2018). DOI: 10.4171/LEM/64-1/2-2. arXiv: 1606.08900.

[Doh14] Andrew C. Doherty. "Entanglement and the shareability of quantum states". *Journal of Physics A: Mathematical and Theoretical* 47.42 (2014). DOI: 10.1088/1751-8113/47/42/424004.

[Dot08] Stephen Doty. "New versions of Schur–Weyl duality". *Finite Groups 2003: Proceedings of the Gainesville Conference on Finite Groups, March 6–12, 2003*. De Gruyter, 2008. DOI: 10.1515/9783110198126.59. arXiv: 0704.1877.

[DPS04] Andrew C. Doherty, Pablo A. Parrilo, and Federico M. Spedalieri. "Complete family of separability criteria". *Physical Review A* 69.2 (2004). DOI: 10.1103/PhysRevA.69.022308.

[DS23] Piotr Dulian and Adam Sawicki. "Matrix concentration inequalities and efficiency of random universal sets of quantum gates". *Quantum* 7 (2023). DOI: 10.22331/q-2023-04-20-983. arXiv: 2202.05371.

[DWH99] William F. Doran IV, David B. Wales, and Philip J. Hanlon. "On the semisimplicity of the Brauer centralizer algebras". *Journal of Algebra* 211.2 (1999). DOI: 10.1006/jabr.1998.7592.

[Ebl+23] Daniel Ebler, Michał Horodecki, Marcin Marciniak, Tomasz Młynik, Marco Túlio Quintino, and Michał Studziński. "Optimal universal quantum circuits for unitary complex conjugation". *IEEE Transactions on Information Theory* 69.8 (2023). DOI: 10.1109/TIT.2023.3263771. arXiv: 2206.00107.

[EK09] Bryan Eastin and Emanuel Knill. "Restrictions on transversal encoded quantum gate sets". *Phys. Rev. Lett.* 102.11 (2009). DOI: 10.1103/PhysRevLett.102.110502. arXiv: 0811.4262.

[Eti+11] Pavel Etingof, Oleg Golberg, Sebastian Hensel, Tiankai Liu, Alex Schwendner, Dmitry Vaintrob, and Elena Yudovina. *Introduction to Representation Theory*. Vol. 59. Student mathematical library. American Mathematical Society, 2011. arXiv: 0901.0827.

[EW01] Tilo Eggeling and Reinhard F. Werner. "Separability properties of tripartite states with $U \otimes U \otimes U$ symmetry". *Phys. Rev. A* 63.4 (2001). DOI: 10.1103/PhysRevA.63.042111. arXiv: quant-ph/0010096.

[Fai+20] Philippe Faist, Sepehr Nezami, Victor V. Albert, Grant Salton, Fernando Pastawski, Patrick Hayden, and John Preskill. "Continuous symmetries and approximate quantum error correction". *Phys. Rev. X* 10.4 (2020). DOI: 10.1103/PhysRevX.10.041018. arXiv: 1902.07714.

[Fan+14] Heng Fan, Yi-Nan Wang, Li Jing, Jie-Dong Yue, Han-Duo Shi, Yong-Liang Zhang, and Liang-Zhu Mu. "Quantum cloning machines and the applications". *Physics Reports* 544.3 (2014). DOI: 10.1016/j.physrep.2014.06.004. arXiv: 1301.2956.

[FH91] William Fulton and Joe Harris. *Representation Theory: A First Course*. Vol. 129. Graduate Texts in Mathematics. Springer Science & Business Media, 1991.

[FLV88] Mark Fannes, John T. Lewis, and André Verbeure. "Symmetric states of composite systems". *Letters in Mathematical Physics* 15 (1988). DOI: 10.1007/BF00398595.

[FTH23] Jiani Fei, Sydney Timmerman, and Patrick Hayden. "Efficient Quantum Algorithm for Port-based Teleportation". *arXiv preprint* (2023). arXiv: 2310.01637.

[Gas98] Vesselin Gasharov. "A short proof of the Littlewood-Richardson rule". *European Journal of Combinatorics* 19.4 (1998). DOI: 10.1006/eujc.1998.0212.

[GBO23a] Dmitry Grinko, Adam Burchardt, and Maris Ozols. "Gelfand–Tsetlin basis for partially transposed permutations, with applications to quantum information". *arXiv preprint* (2023). arXiv: 2310.02252.

[GBO23b] Dmitry Grinko, Adam Burchardt, and Maris Ozols. "Efficient quantum circuits for port-based teleportation". *arXiv preprint* (2023). arXiv: 2312.03188.

[GBW21] Martina Gschwendtner, Andreas Bluhm, and Andreas Winter. "Programmability of covariant quantum channels". *Quantum* 5 (2021). DOI: 10.22331/q-2021-06-29-488. arXiv: 2012.00717.

[GNW21] David Gross, Sepehr Nezami, and Michael Walter. "Schur–Weyl duality for the Clifford group with applications: property testing, a robust Hudson theorem, and de Finetti representations". *Communications in Mathematical Physics* 385.3 (2021). DOI: 10.1007/s00220-021-04118-7. arXiv: 1712.08628.

[GO24] Dmitry Grinko and Maris Ozols. "Linear programming with unitary-equivariant constraints". *Communications in Mathematical Physics* 405.12 (2024). DOI: 10.1007/s00220-024-05108-1. arXiv: 2207.05713.

[GT50] Israel M. Gelfand and Michael L. Tsetlin. "Finite-dimensional representations of the group of unimodular matrices". *Dokl. Akad. Nauk SSSR*. Vol. 71. 8. 1950.

[GU24] Dmitry Grinko and Roope Uola. "On compatibility of binary qubit measurements". *arXiv preprint* (2024). arXiv: 2407.07711.

[GW21] Martina Gschwendtner and Andreas Winter. "Infinite-dimensional programmable quantum processors". *PRX Quantum* 2.3 (2021). DOI: 10.1103/prxquantum.2.030308. arXiv: 2012.00736.

[GW98] Roe Goodman and Nolan R. Wallach. *Representations and Invariants of the Classical Groups*. Cambridge University Press, 1998.

[Hal96] Thomas Halverson. "Characters of the centralizer algebras of mixed tensor representations of $GL(r, \mathbb{C})$ and the quantum group $\mathcal{U}_q(gl(r, \mathbb{C}))$". *Pacific Journal of Mathematics* 174.2 (1996). DOI: 10.2140/pjm.1996.174.359.

[Har05] Aram W. Harrow. "Applications of coherent classical communication and the Schur transform to quantum information theory". PhD thesis. MIT, 2005. arXiv: quant-ph/0512255.

[Hei25] Werner Heisenberg. "Über quantentheoretische Umdeutung kinematischer und mechanischer Beziehungen". *Zeitschrift für Physik* (1925).

[HH99] Michał Horodecki and Paweł Horodecki. "Reduction criterion of separability and limits for a class of distillation protocols". *Physical Review A* 59.6 (1999). DOI: 10.1103/PhysRevA.59.4206.

[HHJWY17] Jeongwan Haah, Aram W. Harrow, Zhengfeng Ji, Xiaodi Wu, and Nengkun Yu. "Sample-optimal tomography of quantum states". *IEEE Transactions on Information Theory* 63.9 (2017). DOI: 10.1109/tit.2017.2719044. arXiv: 1508.01797.

[HKMV22] Felix Huber, Igor Klep, Victor Magron, and Jurij Volčič. "Dimension-free entanglement detection in multipartite Werner states". *Communications in Mathematical Physics* 396.3 (2022). DOI: 10.1007/s00220-022-04485-9. arXiv: 2108.08720.

[HKOT23] Jeongwan Haah, Robin Kothari, Ryan O'Donnell, and Ewin Tang. "Query-optimal estimation of unitary channels in diamond distance". *2023 IEEE 64th Annual Symposium on Foundations of Computer Science (FOCS)*. IEEE. 2023. DOI: 10.1109/FOCS57990.2023.00028. arXiv: 2302.14066.

[HLM21] Austin Hulse, Hanqing Liu, and Iman Marvian. "Qudit circuits with SU(d) symmetry: Locality imposes additional conservation laws". *arXiv preprint* (2021). arXiv: 2105.12877.

[HM76] Robin L. Hudson and Graham R. Moody. "Locally normal symmetric states and an analogue of de Finetti's theorem". *Zeitschrift für Wahrscheinlichkeitstheorie und verwandte Gebiete* 33.4 (1976). DOI: 10.1007/BF00534784.

[HNPS21] Patrick Hayden, Sepehr Nezami, Sandu Popescu, and Grant Salton. "Error correction of quantum reference frame information". *PRX Quantum* 2.1 (2021). DOI: 10.1103/PRXQuantum.2.010326. arXiv: 1709.04471.

[HNPTW23] Yeongwoo Hwang, Joe Neeman, Ojas Parekh, Kevin Thompson, and John Wright. "Unique Games hardness of Quantum Max-Cut, and a conjectured vector-valued Borell's inequality". *Proceedings of the 2023 Annual ACM-SIAM Symposium on Discrete Algorithms (SODA)*. SIAM. 2023. DOI: 10.1137/1.9781611977554.ch48. arXiv: 2111.01254.

[How22] R.M. Howe. *An Invitation to Representation Theory: Polynomial Representations of the Symmetric Group*. Springer Undergraduate Mathematics Series. Springer International Publishing, 2022.

[HSW23] Tharon Holdsworth, Vishal Singh, and Mark M Wilde. "Quantifying the performance of approximate teleportation and quantum error correction via symmetric 2-PPT-extendible channels". *Physical Review A* 107.1 (2023). DOI: 10.1103/PhysRevA.107.012428. arXiv: 2207.06931.

[Hub21] Felix Huber. "Positive maps and trace polynomials from the symmetric group". *Journal of Mathematical Physics* 62.2 (2021). DOI: 10.1063/5.0028856. arXiv: 2002.12887.

[HW94] Paul Hausladen and William K. Wootters. "A 'pretty good' measurement for distinguishing quantum states". *Journal of Modern Optics* 41.12 (1994). DOI: 10.1080/09500349414552221.

[IH08] Satoshi Ishizaka and Tohya Hiroshima. "Asymptotic teleportation scheme as a universal programmable quantum processor". *Phys. Rev. Lett.* 101.24 (2008). DOI: 10.1103/PhysRevLett.101.240501. arXiv: 0807.4568.

[IH09] Satoshi Ishizaka and Tohya Hiroshima. "Quantum teleportation scheme by selecting one of multiple output ports". *Physical Review A* 79.4 (2009). DOI: 10.1103/PhysRevA.79.042306. arXiv: 0901.2975.

[Ish15] Satoshi Ishizaka. "Some remarks on port-based teleportation". *arXiv preprint* (2015). arXiv: 1506.01555.

[Jak22] Dávid Jakab. "The Interplay of Unitary and Permutation Symmetries in Composite Quantum Systems". PhD thesis. 2022.

[JK20] Ji Hye Jung and Myungho Kim. "Supersymmetric polynomials and the center of the walled Brauer algebra". *Algebras and Representation Theory* 23.5 (2020). DOI: 10.1007/s10468-019-09922-3. arXiv: 1508.06469.

[Jor09] Stephen P. Jordan. "Permutational quantum computing". *arXiv preprint* (2009). arXiv: 0906.2508.

[JSZ18] Dávid Jakab, Gergely Szirmai, and Zoltán Zimborás. "The bilinear-biquadratic model on the complete graph". *Journal of Physics A: Mathematical and Theoretical* 51.10 (9, 2018). DOI: 10.1088/1751-8121/aaa92b. arXiv: 1709.06602.

[JSZ22] Dávid Jakab, Adrián Solymos, and Zoltán Zimborás. "Extendibility of Werner states". *arXiv preprint* (2022). arXiv: 2208.13743.

[Juc74] Algimantas Adolfas Jucys. "Symmetric polynomials and the center of the symmetric group ring". *Reports on Mathematical Physics* 5.1 (1974). DOI: 10.1016/0034-4877(74)90019-6.

[JV13] Peter D. Johnson and Lorenza Viola. "Compatible quantum correlations: Extension problems for Werner and isotropic states". *Phys. Rev. A* 88.3 (2013). DOI: 10.1103/PhysRevA.88.032323. arXiv: 1305.1342.

[JZ21] Dávid Jakab and Zoltán Zimborás. "Quantum phases of collective SU(3) spin systems with bipartite symmetry". *Physical Review B* 103.21 (28, 2021). DOI: 10.1103/PhysRevB.103.214448. arXiv: 2001.08310.

[Key02] Michael Keyl. "Fundamentals of quantum information theory". *Physics Reports* 369.5 (2002). DOI: 10.1016/S0370-1573(02)00266-1. arXiv: quant-ph/0202122.

[Key06] Michael Keyl. "Quantum state estimation and large deviations". *Reviews in Mathematical Physics* 18.01 (2006). DOI: 10.1142/S0129055X06002565. arXiv: quant-ph/0412053.

[Kin23] Robbie King. "An improved approximation algorithm for quantum max-cut on triangle-free graphs". *Quantum* 7 (2023). DOI: 10.22331/q-2023-11-09-1180. arXiv: 2209.02589.

[Kin70] Ronald C. King. "Generalized Young tableaux and the general linear group". *Journal of Mathematical Physics* 11.1 (1970). DOI: 10.1063/1.1665059.

[Kin71] Ronald C. King. "Modification rules and products of irreducible representations of the unitary, orthogonal, and symplectic groups". *Journal of Mathematical Physics* 12.8 (1971). DOI: 10.1063/1.1665778.

[Kir08] Alexander A. Kirillov. *An introduction to Lie groups and Lie algebras*. Vol. 113. Cambridge University Press, 2008. DOI: 10.1017/CBO9780511755156.

[KL21] Linghang Kong and Zi-Wen Liu. "Charge-conserving unitaries typically generate optimal covariant quantum error-correcting codes". *arXiv preprint* (2021). arXiv: 2102.11835.

[KL22] Linghang Kong and Zi-Wen Liu. "Near-optimal covariant quantum error-correcting codes from random unitaries with symmetries". *PRX Quantum* 3.2 (2022). DOI: 10.1103/PRXQuantum.3.020314. arXiv: 2112.01498.

[Kly04] Alexander A. Klyachko. "Quantum marginal problem and representations of the symmetric group". *arXiv preprint* (2004). arXiv: quant-ph/0409113.

[Kly06] Alexander A. Klyachko. "Quantum marginal problem and N-representability". *Journal of Physics: Conference Series* 36 (2006). DOI: 10.1088/1742-6596/36/1/014.

[KMS11] Adrian Kent, William J. Munro, and Timothy P. Spiller. "Quantum tagging: Authenticating location via quantum information and relativistic signaling constraints". *Physical Review A* 84.1 (2011). DOI: 10.1103/PhysRevA.84.012326. arXiv: 1008.2147.

[KMSH21] Piotr Kopszak, Marek Mozrzymas, Michał Studziński, and Michał Horodecki. "Multiport based teleportation – transmission of a large amount of quantum information". *Quantum* 5 (2021). DOI: 10.22331/q-2021-11-11-576. arXiv: 2008.00856.

[Koe08] Steffen Koenig. "A panorama of diagram algebras". *Trends in Representation Theory of Algebras and Related Topics*. EMS Series of Congress Reports. European Mathematical Society, 2008. DOI: 10.4171/062-1/12.

[Koi89] Kazuhiko Koike. "On the decomposition of tensor products of the representations of the classical groups: by means of the universal characters". *Advances in Mathematics* 74.1 (1989). DOI: 10.1016/0001-8708(89)90004-2.

[Kos03] Masashi Kosuda. "A new proof for some relations among axial distances and hook-lengths". *Tokyo Journal of Mathematics* 26.1 (2003).

[KP22] John Kallaugher and Ojas Parekh. "The quantum and classical streaming complexity of quantum and classical max-cut". *2022 IEEE 63rd Annual Symposium on Foundations of Computer Science (FOCS)*. IEEE. 2022. DOI: 10.1109/FOCS54457.2022.00054. arXiv: 2206.00213.

[KR05] Robert König and Renato Renner. "A de Finetti representation for finite symmetric quantum states". *Journal of Mathematical physics* 46.12 (2005). DOI: 10.1063/1.2146188. arXiv: quant-ph/0410229.

[KR07] Yusuke Kimura and Sanjaye Ramgoolam. "Branes, anti-branes and Brauer algebras in gauge-gravity duality". *Journal of High Energy Physics* 2007.11 (2007). DOI: 10.1088/1126-6708/2007/11/078. arXiv: 0709.2158.

[Kro19] Hari Krovi. "An efficient high dimensional quantum Schur transform". *Quantum* 3 (2019). DOI: 10.22331/q-2019-02-14-122. arXiv: 1804.00055.

[KS18] William M. Kirby and Frederick W. Strauch. "A practical quantum algorithm for the Schur transform". *Quantum Information & Computation* 18.9&10 (2018). DOI: 10.26421/QIC18.9-10-1. arXiv: 1709.07119.

[KW01a] Michael Keyl and Reinhard F. Werner. "Estimating the spectrum of a density operator". *Physical Review A* 64.5 (2001). DOI: 10.1103/PhysRevA.64.052311. arXiv: quant-ph/0102027.

[KW01b] Michael Keyl and Reinhard F. Werner. "The rate of optimal purification procedures". *Annales Henri Poincaré* 2.1 (2001). DOI: 10.1007/PL00001027. arXiv: quant-ph/9910124.

[KW04] Masato Koashi and Andreas Winter. "Monogamy of quantum entanglement and other correlations". *Physical Review A* 69.2 (2004). DOI: 10.1103/PhysRevA.69.022309. arXiv: quant-ph/0310037.

[KW99] Michael Keyl and Reinhard F. Werner. "Optimal cloning of pure states, testing single clones". *Journal of Mathematical Physics* 40.7 (1999). DOI: 10.1063/1.532887. arXiv: quant-ph/9807010.

[Lar+22] Martín Larocca, Frédéric Sauvage, Faris M Sbahi, Guillaume Verdon, Patrick J Coles, and Marco Cerezo. "Group-invariant quantum machine learning". *PRX Quantum* 3.3 (2022). DOI: 10.1103/PRXQuantum.3.030341. arXiv: 2205.02261.

[LB70] James D. Louck and Lawrence C. Biedenharn. "Canonical unit adjoint tensor operators in $U(n)$". *Journal of Mathematical Physics* 11.8 (1970). DOI: 10.1063/1.1665404.

[Led22] Felix Leditzky. "Optimality of the pretty good measurement for port-based teleportation". *Letters in Mathematical Physics* 112.5 (2022). DOI: 10.1007/s11005-022-01592-5. arXiv: 2008.11194.

[Lee22] Eunou Lee. "Optimizing quantum circuit parameters via SDP". *arXiv preprint* (2022). arXiv: 2209.00789.

[LM15] Debbie Leung and William Matthews. "On the power of PPT-preserving and non-signalling codes". *IEEE Transactions on Information Theory* 61.8 (2015). DOI: 10.1109/TIT.2015.2439953. arXiv: 1406.7142.

[Lou08] James D. Louck. *Unitary Symmetry and Combinatorics*. World Scientific Publishing Company, 2008. DOI: 10.1142/6863.

[LP24] Eunou Lee and Ojas Parekh. "An improved Quantum Max Cut approximation via matching". *arXiv preprint* (2024). arXiv: 2401.03616.

[LR04] Victor Lomonosov and Peter Rosenthal. "The simplest proof of Burnside's theorem on matrix algebras". *Linear Algebra and its Applications* 383 (2004). DOI: 10.1016/j.laa.2003.08.012.

[Mac98] Ian Grant Macdonald. *Symmetric functions and Hall polynomials*. Oxford University Press, 1998.

[Mar22] Iman Marvian. "Restrictions on realizable unitary operations imposed by symmetry and locality". *Nature Physics* 18.3 (2022). DOI: 10.1038/s41567-021-01464-0. arXiv: 2003.05524.

[May19] Alex May. "Quantum tasks in holography". *Journal of High Energy Physics* 2019.10 (2019). DOI: 10.1007/JHEP10(2019)233. arXiv: 1902.06845.

[May22] Alex May. "Complexity and entanglement in non-local computation and holography". *Quantum* 6 (2022). DOI: 10.22331/q-2022-11-28-864. arXiv: 2204.00908.

[Mey+23] Johannes Jakob Meyer, Marian Mularski, Elies Gil-Fuster, Antonio Anna Mele, Francesco Arzani, Alissa Wilms, and Jens Eisert. "Exploiting symmetry in variational quantum machine learning". *PRX Quantum* 4.1 (2023). DOI: 10.1103/PRXQuantum.4.010328. arXiv: 2205.06217.

[MHS14] Marek Mozrzymas, Michał Horodecki, and Michał Studziński. "Structure and properties of the algebra of partially transposed permutation operators". *Journal of Mathematical Physics* 55.3 (2014). DOI: doi.org/10.1063/1.4869027. arXiv: 1308.2653.

[MLH24] Iman Marvian, Hanqing Liu, and Austin Hulse. "Rotationally invariant circuits: Universality with the exchange interaction and two ancilla qubits". *Physical Review Letters* 132.13 (2024). DOI: 10.1103/PhysRevLett.132.130201. arXiv: 2202.01963.

[MRW18a] David Maslen, Daniel N. Rockmore, and Sarah Wolff. "Separation of Variables and the Computation of Fourier Transforms on Finite Groups, II". *Journal of Fourier Analysis and Applications* 24.1 (2018). DOI: 10.1007/s00041-016-9516-4. arXiv: 1512.02445.

[MRW18b] David Maslen, Daniel N. Rockmore, and Sarah Wolff. "The efficient computation of Fourier transforms on semisimple algebras". *Journal of Fourier Analysis and Applications* 24 (2018). DOI: 10.1007/s00041-017-9555-5. arXiv: 1609.02634.

[MS14] Iman Marvian and Robert W. Spekkens. "A generalization of Schur–Weyl duality with applications in quantum estimation". *Communications in Mathematical Physics* 331.2 (2014). DOI: 10.1007/s00220-014-2059-0. arXiv: 1112.0638.

[MSD17] Marek Mozrzymas, Michał Studziński, and Nilanjana Datta. "Structure of irreducibly covariant quantum channels for finite groups". *Journal of Mathematical Physics* 58.5 (2017). DOI: 10.1063/1.4983710. arXiv: 1610.05657.

[MSH18] Marek Mozrzymas, Michał Studziński, and Michał Horodecki. "A simplified formalism of the algebra of partially transposed permutation operators with applications". *Journal of Physics A: Mathematical and Theoretical* 51.12 (2018). DOI: 10.1088/1751-8121/aaad15. arXiv: 1708.02434.

[MSK21] Marek Mozrzymas, Michał Studziński, and Piotr Kopszak. "Optimal multi-port-based teleportation schemes". *Quantum* 5 (2021). DOI: 10.22331/q-2021-06-17-477. arXiv: 2011.09256.

[MSSH18] Marek Mozrzymas, Michał Studziński, Sergii Strelchuk, and Michał Horodecki. "Optimal port-based teleportation". *New Journal of Physics* 20.5 (2018). DOI: 10.1088/1367-2630/aab8e7. arXiv: 1707.08456.

[Mur81] G. Eugene Murphy. "A new construction of Young's seminormal representation of the symmetric groups". *Journal of Algebra* 69.2 (1981). DOI: 10.1016/0021-8693(81)90205-2.

[Naz96] Maxim Nazarov. "Young's orthogonal form for Brauer's centralizer algebra". *Journal of Algebra* 182.3 (1996). DOI: 10.1006/jabr.1996.0195.

[NC10] Michael A. Nielsen and Isaac L. Chuang. *Quantum computation and quantum information*. Cambridge university press, 2010. DOI: 10.1017/CBO9780511976667.

[NC97] Michael A. Nielsen and Isaac L. Chuang. "Programmable quantum gate arrays". *Physical Review Letters* 79.2 (1997). DOI: 10.1103/PhysRevLett.79.321. arXiv: quant-ph/9703032.

[Nec07] Ion Nechita. "Asymptotics of random density matrices". *Annales Henri Poincaré* 8.8 (2007). DOI: 10.1007/s00023-007-0345-5. arXiv: quant-ph/0702154.

[Ngu23] Quynh T. Nguyen. "The mixed Schur transform: efficient quantum circuit and applications". *arXiv preprint* (2023). arXiv: 2310.01613.

[Nik07] Pavel P. Nikitin. "The centralizer algebra of the diagonal action of the group $GL_n(\mathbb{C})$ in a mixed tensor space". *Journal of Mathematical Sciences* 141.4 (2007). DOI: 10.1007/s10958-007-0053-1.

[NPR21] Ion Nechita, Clément Pellegrini, and Denis Rochette. "A geometrical description of the universal $1 \to 2$ asymmetric quantum cloning region". *Quantum Information Processing* 20.10 (2021). DOI: 10.1007/s11128-021-03258-y. arXiv: 2106.09655.

[NPR23] Ion Nechita, Clément Pellegrini, and Denis Rochette. "The asymmetric quantum cloning region". *Letters in Mathematical Physics* 113.3 (2023). DOI: 10.1007/s11005-023-01694-8. arXiv: 2209.11999.

[Oka16] Soichi Okada. "Pieri Rules for Classical Groups and Equinumeration between Generalized Oscillating Tableaux and Semistandard Tableaux". *Electron. J. Comb.* 23 (2016). DOI: 10.37236/6214. arXiv: 1606.02375.

[OO97] Andrei Okounkov and Grigori Olshanski. "Shifted Schur functions". *Algebra i Analiz* 9.2 (1997). arXiv: q-alg/9605042.

[OV96] Andrei Okounkov and Anatoly Vershik. "A new approach to representation theory of symmetric groups". *Selecta Mathematica, New Series* 2.4 (1996). DOI: 10.1007/BF02433451.

[OW15] Ryan O'Donnell and John Wright. "Quantum spectrum testing". *Proceedings of the forty-seventh annual ACM symposium on Theory of computing*. 2015. DOI: 10.1145/2746539.2746582. arXiv: 1501.05028.

[OW16] Ryan O'Donnell and John Wright. "Efficient quantum tomography". *Proceedings of the Forty-Eighth Annual ACM Symposium on Theory of Computing*. STOC'16. New York, NY, USA: Association for Computing Machinery, 2016. DOI: 10.1145/2897518.2897544. arXiv: 1508.01907.

[OW17] Ryan O'Donnell and John Wright. "Efficient quantum tomography II". *Proceedings of the 49th Annual ACM Symposium on Theory of Computing*. STOC'17. New York, NY, USA: Association for Computing Machinery, 2017. DOI: 10.1145/3055399.3055454. arXiv: 1612.00034.

[PBP21] Jason Pereira, Leonardo Banchi, and Stefano Pirandola. "Characterising port-based teleportation as universal simulator of qubit channels". *Journal of Physics A: Mathematical and Theoretical* 54.20 (2021). DOI: 10.1088/1751-8121/abe67a. arXiv: 1912.10374.

[PJPY24] Sang-Jun Park, Yeong-Gwang Jung, Jeongeun Park, and Sang-Gyun Youn. "A universal framework for entanglement detection under group symmetry". *Journal of Physics A: Mathematical and Theoretical* 57.32 (2024). DOI: 10.1088/1751-8121/ad6413. arXiv: 2301.03849.

[PLLP19] Stefano Pirandola, Riccardo Laurenza, Cosmo Lupo, and Jason L. Pereira. "Fundamental limits to quantum channel discrimination". *npj Quantum Information* 5.1 (2019). DOI: 10.1038/s41534-019-0162-y. arXiv: 1803.02834.

[PT21] Ojas Parekh and Kevin Thompson. "Application of the level-2 quantum Lasserre hierarchy in quantum approximation algorithms". *48th International Colloquium on Automata, Languages, and Programming (ICALP 2021)*. Vol. 198. Leibniz International Proceedings in Informatics (LIPIcs). 2021. DOI: 10.4230/LIPIcs.ICALP.2021.102. arXiv: 2105.05698.

[PT22] Ojas Parekh and Kevin Thompson. "An optimal product-state approximation for 2-local quantum Hamiltonians with positive terms". *arXiv preprint* (2022). arXiv: 2206.08342.

[QDSSM19a] Marco Túlio Quintino, Qingxiuxiong Dong, Atsushi Shimbo, Akihito Soeda, and Mio Murao. "Probabilistic exact universal quantum circuits for transforming unitary operations". *Physical Review A* 100.6 (2019). DOI: 10.1103/PhysRevA.100.062339. arXiv: 1909.01366.

[QDSSM19b] Marco Túlio Quintino, Qingxiuxiong Dong, Atsushi Shimbo, Akihito Soeda, and Mio Murao. "Reversing unknown quantum transformations: Universal quantum circuit for inverting general unitary operations". *Phys. Rev. Lett.* 123.21 (2019). DOI: 10.1103/PhysRevLett.123.210502. arXiv: 1810.06944.

[QE21] Marco Túlio Quintino and Daniel Ebler. "Deterministic transformations between unitary operations: Exponential advantage with adaptive quantum circuits and the power of indefinite causality". *Quantum* 6 (2021). DOI: 10.22331/q-2022-03-31-679. eprint: 2109.08202.

[Qia+22] Zhuoran Qiao, Anders S. Christensen, Matthew Welborn, Frederick R. Manby, Anima Anandkumar, and Thomas F. Miller III. "Informing geometric deep learning with electronic interactions to accelerate quantum chemistry". *Proceedings of the National Academy of Sciences* 119.31 (2022). arXiv: 2105.14655.

[Rai01] Eric M. Rains. "A semidefinite program for distillable entanglement". *IEEE Transactions on Information Theory* 47.7 (2001). DOI: 10.1109/18.959270. arXiv: quant-ph/0008047.

[Ren08] Renato Renner. "Security of quantum key distribution". *International Journal of Quantum Information* (2008). arXiv: quant-ph/0512258.

[RMB21] Denis Rosset, Felipe Montealegre-Mora, and Jean-Daniel Bancal. "RepLAB: A computational / numerical approach to representation theory". *Quantum Theory and Symmetries*. Springer, 2021. DOI: 10.1007/978-3-030-55777-5_60. arXiv: 1911.09154.

[RS06] Hebing Rui and Mei Si. "A criterion on the semisimple Brauer algebras II". *Journal of Combinatorial Theory, Series A* 113.6 (2006). DOI: 10.1016/j.jcta.2005.09.005.

[RS98] Jeffrey B. Remmel and Mark Shimozono. "A simple proof of the Littlewood–Richardson rule and applications". *Discrete Mathematics* 193.1–3 (1998). DOI: 10.1016/S0012-365X(98)00145-9.

[Rui05] Hebing Rui. "A criterion on the semisimple Brauer algebras". *Journal of Combinatorial Theory, Series A* 111.1 (2005). DOI: 10.1016/j.jcta.2004.11.009.

[Rut48] Daniel Edwin Rutherford. *Substitutional analysis*. Edinburgh University Press, 1948.

[RW88] Guido A. Raggio and Reinhard F. Werner. "Quantum statistical mechanics of general mean field systems". *Helv. Phys. Acta* 62 (1988).

[RW92] Arun Ram and Hans Wenzl. "Matrix units for centralizer algebras". *Journal of Algebra* 145.2 (1992). DOI: 10.1016/0021-8693(92)90109-Y.

[Rya] Kieran Ryan. "On a Class of Orthogonal-Invariant Quantum Spin Systems on the Complete Graph". *International Mathematics Research Notices* 2023.7 (). DOI: 10.1093/imrn/rnac034. arXiv: 2011.07007.

[Rya21] Kieran Ryan. "Representation-theoretic approaches to several problems in probability". PhD thesis. Queen Mary University of London, 2021.

[Sag13] Bruce E. Sagan. *The symmetric group: representations, combinatorial algorithms, and symmetric functions*. Graduate Texts in Mathematics. Springer New York, 2013. DOI: 10.1007/978-1-4757-6804-6.

[SC23] Paul Skrzypczyk and Daniel Cavalcanti. *Semidefinite Programming in Quantum Information Science*. IOP Publishing, 2023.

[Sch15] Christian Schilling. "The quantum marginal problem". *Mathematical Results in Quantum Mechanics: Proceedings of the QMath12 Conference*. World Scientific. 2015. arXiv: 1404.1085.

[Sch27] Issai Schur. "Über die rationalen Darstellungen der allgemeinen linearen Gruppe". German. *Sitzungsberichte der Preussischen Akademie der Wissenschaften* (1927).

[SGSV24] Eddie Schoute, Dmitry Grinko, Yiğit Subaşı, and Tyler Volkoff. "Quantum programmable reflections". *arXiv preprint* (2024). arXiv: 2411.03648.

[SHM13] Michał Studziński, Michał Horodecki, and Marek Mozrzymas. "Commutant structure of $U^{\otimes(n-1)} \otimes U^*$ transformations". *Journal of Physics A: Mathematical and Theoretical* 46.39 (2013). DOI: 10.1088/1751-8113/46/39/395303. arXiv: 1305.6183.

[SIGA05] Valerio Scarani, Sofyan Iblisdir, Nicolas Gisin, and Antonio Acín. "Quantum cloning". *Rev. Mod. Phys.* 77.4 (2005). DOI: 10.1103/RevModPhys.77.1225. arXiv: quant-ph/0511088.

[SMK22] Michał Studziński, Marek Mozrzymas, and Piotr Kopszak. "Square-root measurements and degradation of the resource state in port-based teleportation scheme". *Journal of Physics A: Mathematical and Theoretical* 55.37 (2022). DOI: 10.1088/1751-8121/ac8530. arXiv: 2105.14886.

[SMKH22] Michał Studziński, Marek Mozrzymas, Piotr Kopszak, and Michał Horodecki. "Efficient multi port-based teleportation schemes". *IEEE Transactions on Information Theory* (2022). DOI: 10.1109/TIT.2022.3187852. arXiv: 2008.00984.

[SMZ22] Adam Sawicki, Lorenzo Mattioli, and Zoltán Zimborás. "Universality verification for a set of quantum gates". *Phys. Rev. A* 105.5 (2022). DOI: 10.1103/PhysRevA.105.052602. arXiv: 2111.03862.

[Spe16] Florian Speelman. "Instantaneous non-local computation of low T-depth quantum circuits". *11th Conference on the Theory of Quantum Computation, Communication and Cryptography (TQC 2016)*. Vol. 61. Leibniz International Proceedings in Informatics (LIPIcs). Dagstuhl, Germany: Schloss Dagstuhl–Leibniz-Zentrum fuer Informatik, 2016. DOI: 10.4230/LIPIcs.TQC.2016.9. arXiv: 1511.02839.

[SS15] Antonio Sartori and Catharina Stroppel. "Walled Brauer algebras as idempotent truncations of level 2 cyclotomic quotients". *Journal of Algebra* 440 (2015). DOI: 10.1016/j.jalgebra.2015.06.018. arXiv: 1411.2771.

[SS23a] Oskar Słowik and Adam Sawicki. "Calculable lower bounds on the efficiency of universal sets of quantum gates". *Journal of Physics A: Mathematical and Theoretical* 56.11 (2023). DOI: 10.1088/1751-8121/acbd24. arXiv: 2201.11774.

[SS23b] Sergii Strelchuk and Michał Studziński. "Minimal port-based teleportation". *New Journal of Physics* 25.6 (2023). DOI: 10.1088/1367-2630/acdab4. arXiv: 2111.05499.

[SSMH17] Michał Studziński, Sergii Strelchuk, Marek Mozrzymas, and Michał Horodecki. "Port-based teleportation in arbitrary dimension". *Scientific reports* 7.1 (2017). DOI: 10.1038/s41598-017-10051-4. arXiv: 1612.09260.

[ST17] Alexei M. Semikhatov and Ilya Yu. Tipunin. "Quantum walled Brauer algebra: commuting families, baxterization, and representations". *Journal of Physics A: Mathematical and Theoretical* 50.6 (2017). DOI: 10.1088/1751-8121/50/6/065202. arXiv: 1512.06994.

[ST22] Vikesh Siddhu and Sridhar Tayur. "Five starter pieces: Quantum information science via semidefinite programs". *Tutorials in Operations Research: Emerging and Impactful Topics in Operations*. INFORMS, 2022. arXiv: 2112.08276.

[Ste02] John Stembridge. "A concise proof of the Littlewood–Richardson rule". *The Electronic Journal of Combinatorics* (2002). DOI: 10.37236/1666.

[Ste87] John Stembridge. "Rational tableaux and the tensor algebra of $\mathfrak{gl}_n$". *Journal of Combinatorial Theory, Series A* 46.1 (1987). DOI: 10.1016/0097-3165(87)90077-X.

[Tak+23] Jun Takahashi, Chaithanya Rayudu, Cunlu Zhou, Robbie King, Kevin Thompson, and Ojas Parekh. "An SU(2)-symmetric Semidefinite Programming Hierarchy for Quantum Max Cut". *arXiv preprint* (2023). arXiv: 2307.15688.

[TDS03] Barbara Terhal, Andrew Doherty, and David Schwab. "Symmetric extensions of quantum states and local hidden variable theories". *Physical review letters* 90.15 (2003). DOI: 10.1103/PhysRevLett.90.157903.

[Ter04] Barbara Terhal. "Is entanglement monogamous?" *IBM Journal of Research and Development* 48.1 (2004). DOI: 10.1147/rd.481.0071.

[Tur89] Vladimir G. Turaev. "Operator invariants of tangles, and R-matrices". *Izvestiya Rossiiskoi Akademii Nauk. Seriya Matematicheskaya* 53.5 (1989). DOI: 10.1070/IM1990v035n02ABEH000711.

[Unr14] Dominique Unruh. "Quantum position verification in the random oracle model". *Advances in Cryptology–CRYPTO 2014: 34th Annual Cryptology Conference, Santa Barbara, CA, USA, August 17-21, 2014, Proceedings, Part II 34*. Springer. 2014. DOI: 10.1007/978-3-662-44381-1_1.

[VK92] Naum Ya. Vilenkin and Anatoli U. Klimyk. "Representations in the Gel'fand-Tsetlin Basis and Special Functions". *Representation of Lie Groups and Special Functions: Volume 3: Classical and Quantum Groups and Special Functions*. Dordrecht: Springer Netherlands, 1992. DOI: 10.1007/978-94-017-2881-2_5.

[VK95] Naum Ya. Vilenkin and Anatoliy U. Klimyk. *Representation of Lie Groups and Special Functions: Recent Advances*. Springer Science & Business Media, 1995. DOI: 10.1007/978-94-017-2885-0.

[VO05] Anatoly Vershik and Andrei Okounkov. "A new approach to the representation theory of the symmetric groups. II". *Journal of Mathematical Sciences* 131 (2005). DOI: 10.1007/s10958-005-0421-7. arXiv: math/0503040.

[VW01] Karl Gerd H. Vollbrecht and Reinhard F. Werner. "Entanglement measures under symmetry". *Physical Review A* 64.6 (2001). DOI: 10.1103/PhysRevA.64.062307.

[Wan18] Xin Wang. "Semidefinite optimization for quantum information". PhD thesis. University of Technology Sydney, 2018.

[War79] Edward Waring. "Problems concerning interpolations". *Philosophical transactions of the Royal Society of London* 69 (1779).

[Wat18] John Watrous. *The Theory of Quantum Information*. Cambridge University Press, 2018.

[WCEHK24] Adam Bene Watts, Anirban Chowdhury, Aidan Epperly, J William Helton, and Igor Klep. "Relaxations and exact solutions to quantum Max Cut via the algebraic structure of swap operators". *Quantum* 8 (2024). arXiv: 2307.15661.

[WDGC13] Michael Walter, Brent Doran, David Gross, and Matthias Christandl. "Entanglement polytopes: multiparticle entanglement from single-particle information". *Science* 340.6137 (2013). DOI: 10.1126/science.1232957. arXiv: 1208.0365.

[Wen88] Hans Wenzl. "On the structure of Brauer's centralizer algebras". *Annals of Mathematics* 128.1 (1988). DOI: 10.2307/1971466.

[Wer89a] Reinhard F. Werner. "An application of Bell's inequalities to a quantum state extension problem". *Letters in Mathematical Physics* 17.4 (1, 1989). DOI: 10.1007/BF00399761.

[Wer89b] Reinhard F. Werner. "Quantum states with Einstein-Podolsky-Rosen correlations admitting a hidden-variable model". *Physical Review A* 40.8 (1989). DOI: 10.1103/PhysRevA.40.4277.

[Wer98] Reinhard F. Werner. "Optimal cloning of pure states". *Physical Review A* 58.3 (1998). DOI: 10.1103/PhysRevA.58.1827. arXiv: quant-ph/9804001.

[Wey46] Hermann Weyl. *The Classical Groups: Their Invariants and Representations*. Princeton university press, 1946.

[WFVW21] Maurice Weiler, Patrick Forré, Erik Verlinde, and Max Welling. "Coordinate independent convolutional networks – Isometry and gauge equivariant convolutions on Riemannian manifolds". *arXiv preprint* (2021). arXiv: 2106.06020.

[WHS23] Adam Wills, Min-Hsiu Hsieh, and Sergii Strelchuk. "Efficient Algorithms for All Port-Based Teleportation Protocols". *arXiv preprint* (2023). arXiv: 2311.12012.

[Wri16] John Wright. "How to learn a quantum state". PhD thesis. Carnegie Mellon University, 2016.

[WS23] Adam Wills and Sergii Strelchuk. "Generalised Coupling and An Elementary Algorithm for the Quantum Schur Transform". *arXiv preprint* (2023). arXiv: 2305.04069.

[WSV12] Henry Wolkowicz, Romesh Saigal, and Lieven Vandenberghe. *Handbook of Semidefinite Programming: Theory, Algorithms, and Applications*. International Series in Operations Research & Management Science. Springer, 2012. DOI: 10.1007/978-1-4615-4381-7.

[WVC03] Michael M. Wolf, Frank Verstraete, and Ignacio Cirac. "Entanglement and frustration in ordered systems". *International Journal of Quantum Information* 1.04 (2003). DOI: 10.1142/S021974990300036X. arXiv: quant-ph/0311051.

[WW20] Xin Wang and Mark M. Wilde. "Cost of quantum entanglement simplified". *Phys. Rev. Lett.* 125.4 (2020). DOI: 10.1103/PhysRevLett.125.040502. arXiv: 2007.14270.

[YKSQM24] Satoshi Yoshida, Yuki Koizumi, Michał Studziński, Marco Túlio Quintino, and Mio Murao. "One-to-one Correspondence between Deterministic Port-Based Teleportation and Unitary Estimation". *arXiv preprint* (2024). arXiv: 2408.11902.

[YMRCW22] Yuxiang Yang, Yin Mo, Joseph M. Renes, Giulio Chiribella, and Mischa P. Woods. "Optimal universal quantum error correction via bounded reference frames". *Phys. Rev. Research* (2022). DOI: 10.1103/PhysRevResearch.4.023107. arXiv: 2007.09154.

[YRC20] Yuxiang Yang, Renato Renner, and Giulio Chiribella. "Optimal Universal Programming of Unitary Gates". *Phys. Rev. Lett.* 125 (21 2020). DOI: 10.1103/PhysRevLett.125.210501. arXiv: 2007.10363.

[YSM23a] Satoshi Yoshida, Akihito Soeda, and Mio Murao. "Reversing Unknown Qubit-Unitary Operation, Deterministically and Exactly". *Phys. Rev. Lett.* 131 (12 2023). DOI: 10.1103/PhysRevLett.131.120602. arXiv: 2209.02907.

[YSM23b] Satoshi Yoshida, Akihito Soeda, and Mio Murao. "Universal construction of decoders from encoding black boxes". *Quantum* 7 (2023). DOI: 10.22331/q-2023-03-20-957. arXiv: 2110.00258.

[ZKW07] Yong Zhang, Louis H Kauffman, and Reinhard F Werner. "Permutation and its partial transpose". *International Journal of Quantum Information* 05.04 (2007). DOI: 10.1142/S021974990700302X. arXiv: quant-ph/0606005.

[ZLLSK23] Han Zheng, Zimu Li, Junyu Liu, Sergii Strelchuk, and Risi Kondor. "Speeding up learning quantum states through group equivariant convolutional quantum ansätze". *PRX Quantum* 4.2 (2023). DOI: 10.1103/PRXQuantum.4.020327. arXiv: 2112.07611.

Abstract

Mixed Schur–Weyl duality in quantum information. In this thesis, we explore the interplay between representation theory and quantum information. We focus on mixed Schur–Weyl duality, which is a generalisation of Schur–Weyl duality that considers the action of $U^{\otimes n} \otimes \bar{U}^{\otimes m}$ on the space $(\mathbb{C}^d)^{\otimes n+m}$. This setting naturally arises in quantum information tasks involving unitary-equivariant channels, such as port-based teleportation, quantum majority vote, and universal transposition of unitary operators.

A key contribution of this thesis is explicit derivation of action of the generators of the partially transposed permutation matrix algebra in the Gelfand–Tsetlin basis. This algebra is the commutant of the mixed unitary action described above. We also provide constructions of primitive and primitive central idempotents for this algebra.

As another key result of this thesis, we develop efficient quantum circuits for the mixed quantum Schur transform, a novel primitive in quantum information. The key ingredient of our construction is new efficient quantum circuits for the dual Clebsch–Gordan transform of the unitary group.

A significant application of our findings is the construction of efficient quantum algorithms for port-based teleportation, a variant of quantum teleportation that eliminates the need for corrective operations. Efficient constructions of port-based teleportation protocols were not known before our work. This highlights the importance of the mathematical tools developed in this thesis, which can deal with mixed Schur–Weyl duality in quantum information tasks.

We also explore the use of mixed Schur–Weyl duality for symmetry reduction of semidefinite optimisation problems with unitary equivariance symmetry. By exploiting these symmetries, we show how to reduce certain semidefinite programs to linear programs of significantly smaller size.

Finally, we also study some aspects of monogamy of entanglement. Specifically, we study the extendibility of quantum states possessing unitary, mixed unitary, or orthogonal symmetry on the complete graph. This involves studying constraints on bipartite entanglement of a global state when its two-party marginals are identical and belong to a specific symmetry class. We obtain analytically the exact maximum values for projections onto the maximally entangled state and the antisymmetric state for each of the three symmetry classes.

This thesis establishes a solid mathematical foundation for mixed Schur–Weyl duality and demonstrates its usefulness in quantum information and computing. We expect that our tools and algorithms will also help addressing other problems in other areas of quantum information processing, such as quantum communication, quantum cryptography, and quantum simulation.

Samenvatting

Gemengde Schur–Weyl-dualiteit in quantuminformatie. In dit proefschrift onderzoeken we de wisselwerking tussen representatietheorie en quantuminformatie. We richten ons op gemengde Schur–Weyl-dualiteit, een generalisatie van Schur–Weyl-dualiteit die de werking van $U^{\otimes n} \otimes \bar{U}^{\otimes m}$ op de ruimte $(\mathbb{C}^d)^{\otimes n+m}$ beschouwt. Deze context komt op natuurlijke wijze voor bij quantuminformatietaken die gebruikmaken van unitaire-equivariante kanalen, zoals port-based teleportatie, quantummeerderheidsstemming en universele transpositie van unitaire operatoren.

Een belangrijke bijdrage van dit proefschrift is de expliciete afleiding van de werking van de generatoren van de gedeeltelijk getransponeerde permutatiematrix-algebra in de Gelfand–Tsetlin-basis. Deze algebra is de commutant van de hierboven beschreven gemengde unitaire werking. We geven ook constructies van primitieve en primitieve centrale idempotenten voor deze algebra.

Als een andere belangrijke bijdrage van dit proefschrift ontwikkelen we efficiënte quantumcircuits voor de gemengde quantum-Schur-transformatie, een nieuw primitief in quantuminformatie. Het kernonderdeel van onze constructie bestaat uit nieuwe efficiënte quantumcircuits voor de duale Clebsch–Gordan-transformatie van de unitaire groep.

Een belangrijke toepassing van onze bevindingen is de constructie van efficiënte quantumalgoritmen voor port-based teleportatie, een variant van quantumteleportatie die geen correctieve operaties vereist. Voor ons werk waren efficiënte constructies van port-based teleportatieprotocollen niet bekend. Dit onderstreept het belang van de wiskundige technieken die in dit proefschrift zijn ontwikkeld en die gemengde Schur–Weyl-dualiteit kunnen toepassen in quantuminformatietaken.

We onderzoeken ook het gebruik van de gemengde Schur–Weyl-dualiteit voor symmetrische reductie van semidefiniete optimalisatieproblemen met unitaire equivariantie-symmetrie. Door gebruik te maken van deze symmetrieën laten we zien hoe bepaalde semidefiniete programma's kunnen worden gereduceerd tot lineaire programma's van aanzienlijk kleinere omvang.

Tot slot bestuderen we enkele aspecten van de monogamie van quantumverstrengeling. Specifiek onderzoeken we de extensie van quantumtoestanden met unitaire, gemengde unitaire of orthogonale symmetrie op de volledige graaf. Dit omvat het bestuderen van beperkingen op bipartiete verstrengeling van een globale toestand wanneer de twee-partijen marginalen identiek zijn en tot een specifieke symmetrieklasse behoren. We laten analytisch de exacte maximale waarden voor projecties op de maximaal verstrengelde toestand en de antisymmetrische toestand voor elk van de drie symmetrieklassen zien.

Dit proefschrift biedt een solide wiskundige basis voor gemengde Schur–Weyl-dualiteit en toont de bruikbaarheid ervan aan in quantuminformatie en quantumcomputing. We verwachten dat onze technieken en algoritmen zullen bijdragen aan het aanpakken van andere problemen in andere gebieden van quantuminformatie, zoals quantumcommunicatie, quantumcryptografie en quantumsimulatie.

Titles in the ILLC Dissertation Series:

ILLC DS-2020-08: **Philip Schulz**
Latent Variable Models for Machine Translation and How to Learn Them

ILLC DS-2020-09: **Jasmijn Bastings**
A Tale of Two Sequences: Interpretable and Linguistically-Informed Deep Learning for Natural Language Processing

ILLC DS-2020-10: **Arnold Kochari**
Perceiving and communicating magnitudes: Behavioral and electrophysiological studies

ILLC DS-2020-11: **Marco Del Tredici**
Linguistic Variation in Online Communities: A Computational Perspective

ILLC DS-2020-12: **Bastiaan van der Weij**
Experienced listeners: Modeling the influence of long-term musical exposure on rhythm perception

ILLC DS-2020-13: **Thom van Gessel**
Questions in Context

ILLC DS-2020-14: **Gianluca Grilletti**
Questions & Quantification: A study of first order inquisitive logic

ILLC DS-2020-15: **Tom Schoonen**
Tales of Similarity and Imagination. A modest epistemology of possibility

ILLC DS-2020-16: **Ilaria Canavotto**
Where Responsibility Takes You: Logics of Agency, Counterfactuals and Norms

ILLC DS-2020-17: **Francesca Zaffora Blando**
Patterns and Probabilities: A Study in Algorithmic Randomness and Computable Learning

ILLC DS-2021-01: **Yfke Dulek**
Delegated and Distributed Quantum Computation

ILLC DS-2021-02: **Elbert J. Booij**
The Things Before Us: On What it Is to Be an Object

ILLC DS-2021-03: **Seyyed Hadi Hashemi**
Modeling Users Interacting with Smart Devices

ILLC DS-2021-04: **Sophie Arnoult**
Adjunction in Hierarchical Phrase-Based Translation

ILLC DS-2021-05: **Cian Guilfoyle Chartier**
A Pragmatic Defense of Logical Pluralism

ILLC DS-2021-06: **Zoi Terzopoulou**
Collective Decisions with Incomplete Individual Opinions

ILLC DS-2021-07: **Anthia Solaki**
Logical Models for Bounded Reasoners

ILLC DS-2021-08: **Michael Sejr Schlichtkrull**
Incorporating Structure into Neural Models for Language Processing

ILLC DS-2021-09: **Taichi Uemura**
Abstract and Concrete Type Theories

ILLC DS-2021-10: **Levin Hornischer**
Dynamical Systems via Domains: Toward a Unified Foundation of Symbolic and Non-symbolic Computation

ILLC DS-2021-11: **Sirin Botan**
Strategyproof Social Choice for Restricted Domains

ILLC DS-2021-12: **Michael Cohen**
Dynamic Introspection

ILLC DS-2021-13: **Dazhu Li**
Formal Threads in the Social Fabric: Studies in the Logical Dynamics of Multi-Agent Interaction

ILLC DS-2021-14: **Álvaro Piedrafita**
On Span Programs and Quantum Algorithms

ILLC DS-2022-01: **Anna Bellomo**
Sums, Numbers and Infinity: Collections in Bolzano's Mathematics and Philosophy

ILLC DS-2022-02: **Jan Czajkowski**
Post-Quantum Security of Hash Functions

ILLC DS-2022-03: **Sonia Ramotowska**
Quantifying quantifier representations: Experimental studies, computational modeling, and individual differences

ILLC DS-2022-04: **Ruben Brokkelkamp**
How Close Does It Get?: From Near-Optimal Network Algorithms to Suboptimal Equilibrium Outcomes

ILLC DS-2022-05: **Lwenn Bussière-Carae**
No means No! Speech Acts in Conflict

ILLC DS-2022-06: **Emma Mojet**
Observing Disciplines: Data Practices In and Between Disciplines in the 19th and Early 20th Centuries

ILLC DS-2022-07: **Freek Gerrit Witteveen**
Quantum information theory and many-body physics

ILLC DS-2023-01: **Subhasree Patro**
Quantum Fine-Grained Complexity

ILLC DS-2023-02: **Arjan Cornelissen**
Quantum multivariate estimation and span program algorithms

ILLC DS-2023-03: **Robert Paßmann**
Logical Structure of Constructive Set Theories

ILLC DS-2023-04: **Samira Abnar**
Inductive Biases for Learning Natural Language

ILLC DS-2023-05: **Dean McHugh**
Causation and Modality: Models and Meanings

ILLC DS-2023-06: **Jialiang Yan**
Monotonicity in Intensional Contexts: Weakening and: Pragmatic Effects under Modals and Attitudes

ILLC DS-2023-07: **Yiyan Wang**
Collective Agency: From Philosophical and Logical Perspectives

ILLC DS-2023-08: **Lei Li**
Games, Boards and Play: A Logical Perspective

ILLC DS-2023-09: **Simon Rey**
Variations on Participatory Budgeting

ILLC DS-2023-10: **Mario Giulianelli**
Neural Models of Language Use: Studies of Language Comprehension and Production in Context

ILLC DS-2023-11: **Guillermo Menéndez Turata**
Cyclic Proof Systems for Modal Fixpoint Logics

ILLC DS-2023-12: **Ned J.H. Wontner**
Views From a Peak: Generalisations and Descriptive Set Theory

ILLC DS-2024-01: **Jan Rooduijn**
Fragments and Frame Classes: Towards a Uniform Proof Theory for Modal Fixed Point Logics

ILLC DS-2024-02: **Bas Cornelissen**
Measuring musics: Notes on modes, motifs, and melodies

ILLC DS-2024-03: **Nicola De Cao**
Entity Centric Neural Models for Natural Language Processing

ILLC DS-2024-04: **Ece Takmaz**
Visual and Linguistic Processes in Deep Neural Networks: A Cognitive Perspective

ILLC DS-2024-05: **Fatemeh Seifan**
Coalgebraic fixpoint logic Expressivity and completeness result

ILLC DS-2024-06: **Jana Sotáková**
Isogenies and Cryptography

ILLC DS-2024-07: **Marco Degano**
Indefinites and their values

ILLC DS-2024-08: **Philip Verduyn Lunel**
Quantum Position Verification: Loss-tolerant Protocols and Fundamental Limits

ILLC DS-2024-09: **Rene Allerstorfer**
Position-based Quantum Cryptography: From Theory towards Practice

ILLC DS-2024-10: **Willem Feijen**
Fast, Right, or Best? Algorithms for Practical Optimization Problems

ILLC DS-2024-11: **Daira Pinto Prieto**
Combining Uncertain Evidence: Logic and Complexity

ILLC DS-2024-12: **Yanlin Chen**
On Quantum Algorithms and Limitations for Convex Optimization and Lattice Problems

ILLC DS-2024-13: **Jaap Jumelet**
Finding Structure in Language Models

ILLC DS-2025-01: **Julian Chingoma**
On Proportionality in Complex Domains

ILLC DS-2025-02: **Dmitry Grinko**
Mixed Schur–Weyl duality in quantum information